



# Synthesis, structural elucidation and biological evaluation of Pipecolidepsin A and Phakellistatin 19

Marta Pelay Gimeno

**ADVERTIMENT.** La consulta d'aquesta tesi queda condicionada a l'acceptació de les següents condicions d'ús: La difusió d'aquesta tesi per mitjà del servei TDX ([www.tdx.cat](http://www.tdx.cat)) ha estat autoritzada pels titulars dels drets de propietat intel·lectual únicament per a usos privats emmarcats en activitats d'investigació i docència. No s'autoritza la seva reproducció amb finalitats de lucre ni la seva difusió i posada a disposició des d'un lloc aliè al servei TDX. No s'autoritza la presentació del seu contingut en una finestra o marc aliè a TDX (framing). Aquesta reserva de drets afecta tant al resum de presentació de la tesi com als seus continguts. En la utilització o cita de parts de la tesi és obligat indicar el nom de la persona autora.

**ADVERTENCIA.** La consulta de esta tesis queda condicionada a la aceptación de las siguientes condiciones de uso: La difusión de esta tesis por medio del servicio TDR ([www.tdx.cat](http://www.tdx.cat)) ha sido autorizada por los titulares de los derechos de propiedad intelectual únicamente para usos privados enmarcados en actividades de investigación y docencia. No se autoriza su reproducción con finalidades de lucro ni su difusión y puesta a disposición desde un sitio ajeno al servicio TDR. No se autoriza la presentación de su contenido en una ventana o marco ajeno a TDR (framing). Esta reserva de derechos afecta tanto al resumen de presentación de la tesis como a sus contenidos. En la utilización o cita de partes de la tesis es obligado indicar el nombre de la persona autora.

**WARNING.** On having consulted this thesis you're accepting the following use conditions: Spreading this thesis by the TDX ([www.tdx.cat](http://www.tdx.cat)) service has been authorized by the titular of the intellectual property rights only for private uses placed in investigation and teaching activities. Reproduction with lucrative aims is not authorized neither its spreading and availability from a site foreign to the TDX service. Introducing its content in a window or frame foreign to the TDX service is not authorized (framing). This rights affect to the presentation summary of the thesis as well as to its contents. In the using or citation of parts of the thesis it's obliged to indicate the name of the author.

Programa de Química Orgànica

Tesi Doctoral

# **Synthesis, structural elucidation and biological evaluation of Pipecolidepsin A and Phakellistatin 19**

Marta Pelay Gimeno

Dirigida i revisada per:

Dr. Fernando Albericio  
(Universitat de Barcelona)

Dra. Judit Tulla Puche  
(Institut de Recerca Biomèdica Barcelona)

Barcelona, 2013



Tesi Doctoral

# Synthesis, structural elucidation and biological evaluation of Pipecolidepsin A and Phakellistatin 19

Marta Pelay Gimeno



UNIVERSITAT DE BARCELONA



IRB  
BARCELONA

INSTITUTE  
FOR RESEARCH  
IN BIOMEDICINE

Departament de Química Orgànica

Facultat de Química

Universitat de Barcelona

2013



# **CONTENTS**







1.5.2.2. Second strategy: diMe-Gln + ester. Incorporation of the last two moieties as a single unit	68
1.5.3. Solid-phase synthesis of Pipecolidepsin A	71
1.5.3.1. First strategy: AHDMHA + ester	71
1.5.3.2. Second strategy: diMe-Gln + ester	77
1.5.3.3. Third strategy: change of resin	87
1.5.3.4. Fourth strategy: DADHOHA + ester	90
1.5.3.5. HPLC-PDA monitoring of Pipecolidepsin A large scale synthesis	91
1.5.4. Solid-phase synthesis of Pipecolidepsin A'	94
1.5.4.1. First strategy: diMe-Gln + ester. Stepwise elongation	94
1.5.4.2. HPLC-PDA monitoring of Pipecolidepsin A' large scale synthesis	96
1.5.5. Validation of synthetic Pipecolidepsin A' and Pipecolidepsin A	99
1.5.5.1. Chemical validation	99
1.5.5.2. Spectral validation	100
1.5.5.3. Biological validation	102
References	104

## **Chapter 2. Synthesis, structural elucidation and biological evaluation of**

<b>Phakellistatin 19</b>	<b>113</b>
2.1. Introduction: Phakellistatins	115
2.2. Solid-phase synthesis of Phakellistatin 19	122
2.3. Synthesis of a small library of Phakellistatin 19 analogs	128
2.4. Validation of synthetic Phakellistatin 19	128
2.4.1. Chemical validation	128
2.4.2. Spectral validation	129
2.4.3. Biological validation	130
2.5. Structural elucidation	132
2.5.1. Chemical shifts: <sup>1</sup> H and <sup>13</sup> C assignment	132
2.5.2. Chemical shifts and temperature: temperature coefficients	133
2.5.3. NOE cross peaks	134
2.5.3.1. Qualitative analysis	135

---

2.5.3.2. Quantitative analysis	136
2.5.3. Coupling constants: dihedral angles	139
2.6. Finding an explanation for biological activity discrepancies between synthetic and natural Phakellistatin 19.	139
2.6.1. An epimer being responsible of the biological activity?	139
2.6.2. <i>Cis-trans</i> isomerism at the Pro linkages responsible of the activity?	144
2.6.2.1. Thermodynamic studies of the <i>cis-trans</i> equilibrium at the Pro linkages: Biological evaluation	144
2.6.2.2. Thermodynamic studies of the <i>cis-trans</i> equilibrium at the Pro linkages: Structural study	145
2.6.3. Enhancing the <i>cis</i> isomerism: Pro replacement by $\Psi^{\text{Me,Me}}$ Pro	147
2.6.3.1. Synthesis of a small library of $\Psi^{\text{Me,Me}}$ Pro-containing Phakellistatin 19 analogs	147
2.6.3.2. Biological evaluation of a small library of $\Psi^{\text{Me,Me}}$ Pro-containing Phakellistatin 19 analogs	152
2.6.3.3. Structural study of a small library of $\Psi^{\text{Me,Me}}$ Pro-containing Phakellistatin 19 analogs	153
References	160
<b>Conclusions</b>	<b>163</b>
<b>Materials and methods</b>	<b>169</b>
References	240
<b>Resum</b>	<b>241</b>



# **ABBREVIATIONS AND ANNEXES**



## Annex I. Abbreviations and Acronyms

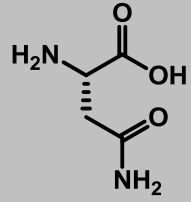
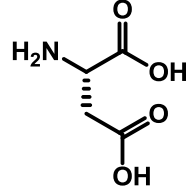
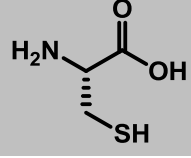
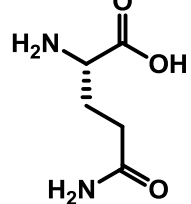
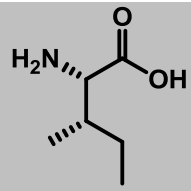
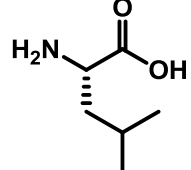
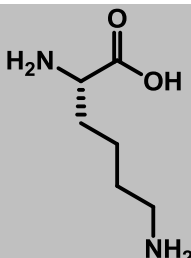
AB	3-(4-Hydroxymethylphenoxy)propionic acid
AD	Asymmetric dihydroxylation
ACN	Acetonitrile
AcOH	Acetic acid
ALCL	Anaplastic large cell lymphoma
Alloc	Allyloxycarbonyl
AM	Amino methyl resin
Boc	<i>tert</i> -Butyloxycarbonyl
BTC	Bis-(trichloromethyl)carbonate
COMU	1-[(1-(Cyano-2-ethoxy-2-oxoethylideneaminoxy)-dimethylamino-morpholinomethylene)]methanaminium hexafluorophosphate
2-CTC	2-Chlorotrityl chloride resin
Cl-HOBt	6-Chloro-1-hydroxybenzotriazole
$\delta$	Chemical shifts
DAST	Diethylaminosulfur trifluoride
DCC	<i>N,N'</i> -Dicyclohexylcarbodiimide
DCM	Dichloromethane
DIEA	<i>N,N</i> -Diisopropylethylamine
DIPCDI	<i>N,N'</i> -Diisopropylcarbodiimide
DIPA	Diisopropylamine
DKP	Diketopiperazine
DMAP	4-Dimethylaminopyridine
DMF	Dimethylformamide
DMSO	Dimethyl sulfoxide
ED <sub>50</sub>	Effective dose
EDC	1-Ethyl-3-(3-dimethylaminopropyl)carbodiimide
EMA	European Medicines Agency
EtOAc	Ethyl acetate
Et <sub>2</sub> O	Diethyl ether
EtOH	Ethanol
FDA	Food and Drug Administration
Fmoc	9-Fluorenylmethyloxycarbonyl
Fmoc-Cl	9-Fluorenylmethyloxycarbonyl chloride
Fmoc-OSu	9-Fluorenylmethyl succinimidyl carbonate
COSY	Correlation Spectroscopy
HATU	<i>N</i> -[(Dimethylamino)-1 <i>H</i> -1,2,3-triazolo[4,5- <i>b</i> ]pyridin-1-yl-methylene)- <i>N</i> -methylmethanaminium hexafluorophosphate <i>N</i> -oxide
HBTU	<i>N</i> -[(1 <i>H</i> -Benzotriazol-1-yl)-(dimethylamino)methylene] <i>N</i> -methylmethanaminium hexafluorophosphate <i>N</i> -oxide

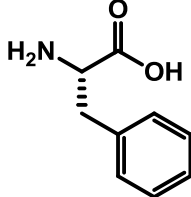
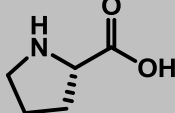
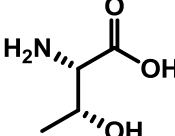
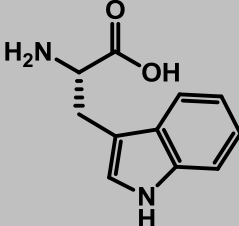
HCTU	<i>N</i> -[(6-Chloro-1 <i>H</i> -benzotriazol-1-yl)- (dimethylamino)methylene] <i>N</i> -methylmethanaminium hexafluorophosphate <i>N</i> -oxide
HFA	Hexafluoroacetone
HIV	Human immunodeficiency virus
HMBC	Heteronuclear multiple-bond correlation spectroscopy
HMQC	Heteronuclear multiple-quantum correlation
HOAt	1-Hydroxy-7-azabenzotriazole
HOBt	Hydroxybenzotriazole
HPLC-PDA	High-performance liquid chromatography-photo diode array
HPLC-MS	High-performance liquid chromatography-mass spectrometry
HRMS	High-resolution mass spectrometry
HSQC	Heteronuclear single quantum coherence
HTS	High throughput screening
Hz	Hertz
GI <sub>50</sub>	Compound concentration that produces 50% of cell growth inhibition, as compared to control cultures
ISPA	Isolation spin pair approximation
<i>J</i>	Coupling constant
LAB	Lithium amidotrihydroborate
LC <sub>50</sub>	Compound concentration that produces 50% of net cell killing (cytotoxic effect)
LDA	Lithium diisopropylamide
MALDI	Matrix-assisted laser desorption/ionization
MeOH	Methanol
MRSA	Methicillin-resistant <i>Staphylococcus aureus</i>
MS	Mass spectrometry
MS-MS	Tandem mass spectrometry
MSNT	1-(2-Mesitylenesulfonyl)-3-nitro-1 <i>H</i> -1,2,4-triazole
MTT	3-(4,5-Dimethylthiazol-2-yl)-2,5-diphenyltetrazolium bromide
MW	Molecular weight
NanoESI	Nano-electrospray ionization mass spectrometry
NCE	New chemical entity
n.d.	Non-determined
NMO	<i>N</i> -Methylmorpholine <i>N</i> -oxide
NMR	Nuclear magnetic resonance
NOE	Nuclear overhauser effect
NOESY	Nuclear overhauser enhancement spectroscopy
ppm	Parts-per-million
PPTS	Pyridinium <i>p</i> -toluenesulfonate
PAL	Peptide amide linker resin
PyAOP	Azabenzotriazol-1-yl- <i>N</i> -oxy-tris(pyrrolidino)phosphonium hexafluorophosphate
PyBOP	Benzotriazol-1-yl- <i>N</i> -oxy-tris(pyrrolidino)phosphonium hexafluorophosphate

ROE	Rotating-frame overhauser effect
ROESY	Rotational nuclear overhauser effect spectroscopy
SA	Simulated annealing
SARs	Structure-activity relationships
SPE	Solid phase extraction
SPPS	Solid phase peptide synthesis
SRB	Sulforhodamine B
TBAF	Tetrabutylammonium fluoride
<sup>t</sup> Bu	<i>tert</i> -Butyl
$\tau_c$	Correlation time
TCA	Trichloroacetic acid
TCFH	<i>N,N,N',N'</i> -Tetramethylchloroformamidinium hexafluorophosphate
TFA	Trifluoroacetic acid
TGI	Total cell growth inhibition (cytostatic effect)
THF	Tetrahydrofuran
Thz	Thiazolidine
TIS	Triisopropylsilane
TLC	Thin layer chromatography
Tmob	8-2,4,6-Trimethoxybenzyl
TPAP	Tetrapropylammonium perruthenate
TOCSY	Total correlated spectroscopy
$t_R$	Retention time
Tris	Tris(hydroxymethyl)aminomethane
UV	Ultraviolet
VRE	Vancomycin-resistant <i>Enterococci</i>



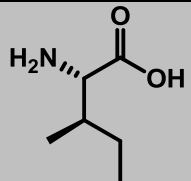
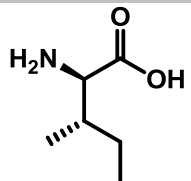
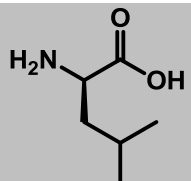
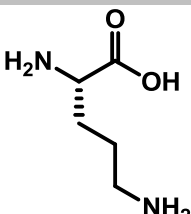
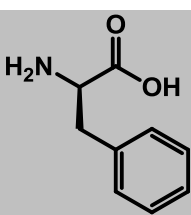
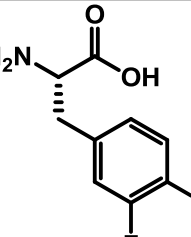
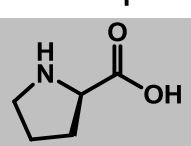
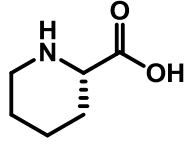
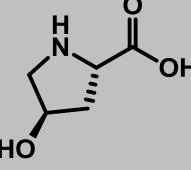
## Annex II. Natural amino acids

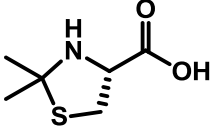
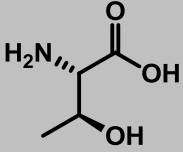
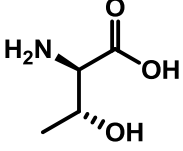
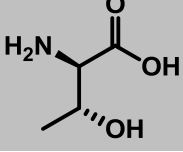
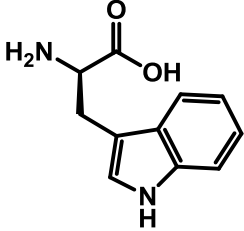
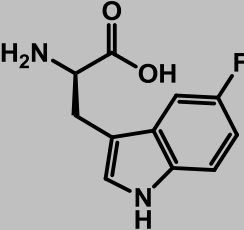
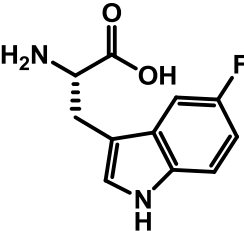
Amino acid	Code	Structure
L-Asparagine	Asn, N	
L-Aspartic acid	Asp, D	
L-Cysteine	Cys, C	
L-Glutamine	Gln, Q	
L-Isoleucine	Ile, I	
L-Leucine	Leu, L	
L-Lysine	Lys, K	

L-Phenylalanine	Phe, F	
L-Proline	Pro, P	
L-Threonine	Thr, T	
L-Tryptophan	Trp, W	

## Annex III. Non-proteinogenic amino acids

Amino acid	Code	Structure
(2 <i>R</i> ,3 <i>R</i> ,4 <i>R</i> )-2-Amino-3-hydroxy-4,5-dimethylhexanoic acid	AHDMHA	
D-Asparagine	D-Asn, n*	
<i>threo</i> -β-EtO-Asparagine	<i>threo</i> -β-EtO-Asn	
D-Aspartic acid	D-Asp, d*	
(2 <i>R</i> ,3 <i>R</i> ,4 <i>S</i> )- 4,7-Diamino-2,3-dihydroxy-7-oxoheptanoic acid	DADHOHA	
(3 <i>S</i> ,4 <i>R</i> )-3,4-Dimethyl-L-glutamine	DiMe-Gln	
NMe-Glutamine	NMe-Gln	
NMe-Glutamic acid	NMe-Glu	

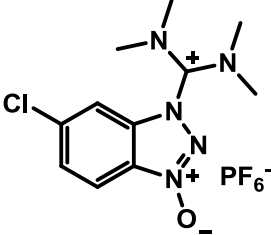
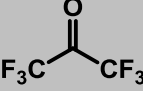
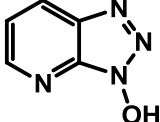
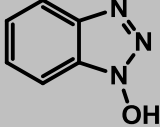
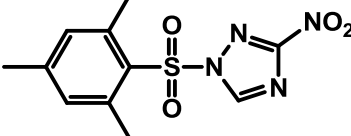
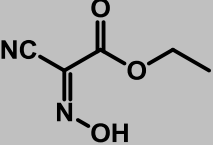
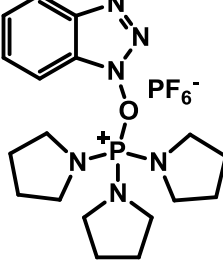
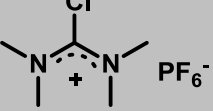
<i>allo</i> -Isoleucine	<i>allo</i> -Ile	
D-Isoleucine	D-Ile, i*	
D-Leucine	D-Leu, l*	
L-Ornithine	Orn	
D-Phenylalanine	D-Phe, f*	
3,4-Difluoro-L-Phenylalanine	Phe-(3,4-F <sub>2</sub> )	
D-Proline	D-Pro, p*	
Homoproline or Pipecolic acid	HomoPro, Pip	
4-Hydroxy-L-Proline	4-HO-Pro	

<b>2,2-Dimethyl-1,3-thiazolidine-4-carboxylic acid</b>	$\Psi^{\text{Me,Me}}\text{Pro, Thz}$	
<i>allo</i> -Threonine	<i>allo</i> -Thr	
<i>D-allo</i> -Threonine	<i>D-allo</i> -Thr	
<i>D</i> -Threonine	<i>D</i> -Thr, t*	
<i>D</i> -Tryptophan	<i>D</i> -Trp, w*	
5-Fluoro- <i>D</i> -Tryptophane	<i>D</i> -Trp-(5-F)	
5-Fluoro- <i>L</i> -Tryptophane	Trp-(5-F)	

\* In this table, lower case letters describe D-aa.

## Annex IV. Coupling reagents

Coupling reagent/additive	Symbol	Structure
Bis-(trichloromethyl)carbonate	BTC	
6-Chloro-1-hydroxybenzotriazole	Cl-HOBt	
1-[(1-(Cyano-2-ethoxy-2-oxoethylideneaminoxy)-dimethylamino-morpholinomethylene)]methanaminium hexafluorophosphate	COMU	
<i>N,N'</i> -Dicyclohexylcarbodiimide	DCC	
<i>N,N</i> -Diisopropylethylamine	DIEA	
<i>N,N'</i> -Diisopropylcarbodiimide	DIPCDI	
1-Ethyl-3-(3-dimethylaminopropyl)carbodiimide	EDC	
<i>N</i> -[(Dimethylamino)-1 <i>H</i> -1,2,3-triazolo[4,5- <i>b</i> ]pyridin-1-yl-methylene]- <i>N</i> -methylmethanaminium hexafluorophosphate <i>N</i> -oxide	HATU	
<i>N</i> -[(1 <i>H</i> -Benzotriazol-1-yl-(dimethylamino)methylene)] <i>N</i> -methylmethanaminium hexafluorophosphate <i>N</i> -oxide	HBTU	

<i>N</i> -[(6-Chloro-1 <i>H</i> -benzotriazol-1-yl)-(dimethylamino)methylene] <i>N</i> -methylmethanaminium hexafluorophosphate <i>N</i> -oxide	HCTU	
Hexafluoroacetone	HFA	
1-Hydroxy-7-azabenzotriazole	HOAt	
Hydroxybenzotriazole	HOBt	
1-(2-Mesitylenesulfonyl)-3-nitro-1 <i>H</i> -1,2,4-triazole	MSNT	
2-Cyano-2-(hydroxyimino)acetate	Oxyma	
Benzotriazol-1-yl- <i>N</i> -oxytris(pyrrolidino)phosphonium hexafluorophosphate	PyBOP	
<i>N,N,N',N'</i> -Tetramethylchloroformamidinium hexafluorophosphate	TCFH	

# **INTRODUCTION AND OBJECTIVES**





## Introduction

Since ancient times the human being has used natural products as therapeutic agents to treat nearly every human condition.<sup>1</sup> Furthermore, for the last few decades, they have also been employed as biochemical tools for the better comprehension of the targets and pathways involved in the disease process. Their structural complexity, chemical diversity and biological specificity are matchless. Thus, they represent a different region of the chemical space compared to the synthetic compounds which cannot be easily replaced.<sup>2</sup>

However, the use of natural products as the main source for drug discovery has also some severe intrinsic problems: labor-intensive and time-consuming procedures to obtain the quantities required for pre-clinical studies; a extremely high structural complexity that represents a synthetic challenge and a considerable drawback for the development of analogs; re-discovery of already known compounds; and a time-line exceeding the standards of the pharmaceutical companies.<sup>3</sup>

In the early 1990s, the development of High-throughput screening (HTS) together with the introduction of combinatorial chemistry pushed the natural product research programs into the background.<sup>4</sup> The higher capacity to produce large libraries of new synthetic compounds in a short period of time by means of combinatorial chemistry, and the dramatic increase in the biological evaluation speed thanks to HTS refinement, represented unbeatable improvements with respect to the disadvantaged screening of natural products. As a result, pharmaceutical companies significantly reduced their drug discovery programs based on natural products.<sup>5</sup>

However, to date only one single *de novo* combinatorial NCE has been approved by the FDA: the kinase inhibitor sorafenib for renal carcinoma.<sup>6,7</sup> Thus, the failure of the large synthetic libraries in the race of finding first-in-class drugs combined with several improvements in the screening of natural products, have enabled a small renaissance of the natural products in the drug discovery programs during the last few years.

Simultaneously, the so-called chemistry of natural products has been transformed by the new methodologies and technological advances developed during the last years, enabling a re-establishment of natural products as the main source for drug development. Thus, the combination of HPLC and SPE (solid phase extraction) techniques with NMR and MS technologies, and the implementation of bioassay-guided fractionation have substantially decreased the time needed for dereplication, isolation and structure elucidation, making more efficient and straightforward the screening process for natural products.

Furthermore, several advances in synthetic organic methodologies have occurred during the last years: the development of the semi-synthetic approach, consisting in the generation of analogs by synthetically modifying natural products<sup>8,9</sup>; the introduction of the chemoenzymatic approach, that uses not only chemical tools, but also enzymes to transform natural products<sup>10,11</sup>; the application of diverted total synthesis<sup>12</sup>; the use of the combinatorial chemistry tools to create libraries based on natural product scaffolds<sup>2,13,14</sup>; and the combinatorial biosynthesis that uses the genetic engineering to create libraries based on natural products<sup>15,16</sup>, have enabled the chemist to access a raising structural complexity difficult to imagine several years ago.

Moreover, advances in microbial genomics may represent a revolution in the discovery of new natural products.<sup>17</sup> This new technology has enabled the rapid identification of genes encoding novel secondary metabolites (most of them would have probably gone unnoticed by traditional screening methods) and the computational prediction of chemical structures on the basis of genomic sequences. Furthermore and more important, it is possible to find specific fermentation conditions to express genes encoding a particular natural product.<sup>18,19</sup>

In this new drug discovery outlook, the use of marine actinomycetes, fungi and myxobacteria as source of natural products could represent a more prolific approach for the development of new drugs based in natural structures, limiting the chances to find already known compounds.<sup>20,21,22</sup>

In this sense, we have to consider that marine ecosystem occupies the 70% of the earth's surface and holds a huge biodiversity, which is subjected to a higher evolutionary pressure and a smaller impact of the human being than the terrestrial ecosystem. Thus, it represents a vast source of natural compounds owning unprecedented, highly diverse and extremely complex structures, displaying interesting and assorted biological activities.<sup>23</sup> And only 30 years ago, it was still to be explored.

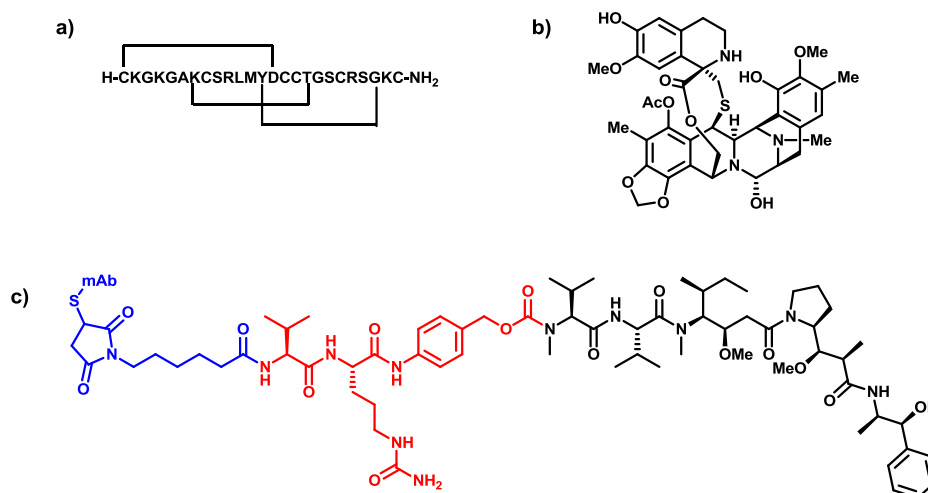
The technological improvements occurred in scuba diving and harvest procedures; together with the development of more accurate and precise chromatographic techniques, which enable the identification and biological evaluation of new natural compounds using smaller amounts of products, have facilitate a more exhaustive exploration of the marine environment in search of new compounds candidates to drugs. Thus, since the 1970s, more than 15000 natural products displaying different bioactivities have been isolated from marine microbes, algae and invertebrates.<sup>24</sup>

Marine life has adapted and survived to the most extreme conditions: fierce interspecies competition over limited resources, frozen temperatures, almost complete lack of oxygen and light, etc. Moreover, most of the marine organisms are not provided with physical defenses to protect themselves from predators, to feed and to safeguard their own space. Hence, they have developed highly efficient and sophisticated chemical tools that act as an "immune" system. By excreting these chemicals to the environment, they protect themselves from external aggressions. The "dilution effect", occurred when these secondary metabolites

are poured into the sea water, guarantees the survival of only the most effective chemicals, turning them into the most attractive natural compounds to enter biomedical programs.

Marine natural compounds own really interesting and diversified biological profiles including bioactive properties such as anti-tumor, anti-cancer, anti-microtubule, anti-proliferative, anti-hypertensive, anti-inflammatory, anti-virus, antifungal, cytotoxic as well as antibiotic properties.<sup>25</sup> Furthermore, the biodiversity found in the marine environment exceeds the one of the terrestrial environment which, on the top of that, has been far exploited since the beginning of the human being history.

All the efforts put on drug development from marine sources have started to bear fruit. Thus, in December 2004 Ziconotide (known under the trade name of Prialt and developed by Elan Pharmaceuticals) was the first drug derived from a marine natural product approved in the USA for the treatment of pain. It is the synthetic form of  $\omega$ -conotoxin MVIIA, a linear 25 amino acids peptide isolated from the venom of a tropical marine cone snail, and shows a well-defined three-dimensional structure stabilized by the presence of three disulphide bridges. Moreover, Trabectedin (known under the trade name Yondelis and developed by PharmaMar)<sup>26</sup> became the first marine anticancer drug to receive approval in the EU in October 2007. It is an alkaloid isolated with extremely poor yields from extracts of the Caribbean tunicate *Ecteinascidia turbinata*, and accessed by means of a semi-synthetic approach from the multi-kilogram scale available antibiotic cyanosfracin B. Finally, Brentuximab vedotin (known under the trade name Adcetris and developed by Seattle Genetics)<sup>27</sup> was approved by the FDA in August 2011 for the treatment of Hodgkin's lymphoma and systemic anaplastic large cell lymphoma (ALCL). From a structural perspective, it consists of three components: a specific antibody for human CD30 (chimeric immunoglobulin G1 mAb cAC10) covalently linked to a synthetic analog of the marine natural product Dolastatin 10 (the microtubule-disrupting agent MMAE) through a protease-cleavable linker (Figure 1).



**Figure 1:** Chemical structures of a) Ziconotide; b) Trabectedin; and c) Brentuximab vedotin. They illustrate the chemical diversity found in the sea.

The role and the potential of natural products in the drug discovery game are reaffirmed by the following figures published this year. Data from the last 30 years (01/01/1981-12/31/2010) show that from all the approved drugs, 60% are either natural products or based in natural structures. Moreover, when specifically referred to anticancer drugs, this percentage is increased up to a 70%.<sup>28</sup> These data together with the significant number of drugs derived from natural products that are currently undergoing evaluation in clinical trials,<sup>29</sup> illustrates the importance of natural sources for the development of new drugs, even when a large number of research programs in natural product discovery run by pharmaceutical companies have been terminated.

Marine natural products are from very diverse chemical nature: phenols, alkaloids, terpenoids, polyesters, peptides and other secondary metabolites produced by different marine organisms such as sponges, bacteria, dinoflagellate and seaweed. In the present thesis, the attention will be focused in the synthesis of marine cyclopeptides displaying interesting cytotoxicities against several cancer cell lines.

## Objectives

1. Development of a robust and efficient synthetic route for Pipecolidepsin A, a cyclodepsipeptide isolated from a *Homophymia* marine sponge which has been shown to display promising cytotoxic activity.
2. Synthesis of *L-threo*- $\beta$ -EtO-Asn and DADHOHA, two non natural amino acids present in the Pipecolidepsin A structure.
3. Validation of the chemical structure proposed for Pipecolidepsin A: facing all structural uncertainties.
4. Set up of a synthetic strategy to access Phakellistatin 19, a homodetic cyclopeptide from marine origin that has been shown interesting anticancer properties.
5. Synthesis of a Phakellistatin 19 analogs' library. Establishment of structure-activity relationships (SARs) and development of related peptides with improved bioactivities.

## References

- (1) Dias, D. a.; Urban, S.; Roessner, U. *Metabolites* **2012**, *2*, 303–336.
- (2) Takagi, M.; Shin-Ya, K. *The Journal of antibiotics* **2012**, *65*, 443–7.
- (3) Lam, K. S. *Trends in Microbiol.* **2007**, *15*, 279–289.
- (4) Baltz, R. H. *Journal of industrial microbiology & biotechnology* **2006**, *33*, 507–513.
- (5) von Nussbaum, F.; Anlauf, S.; Benet-Buchholz, J.; Häbich, D.; Köbberling, J.; Musza, L.; Telser, J.; Rübsamen-Waigmann, H.; Brunner, N. a *Angew. Chem. Int. Ed.* **2007**, *46*, 2039–2042.
- (6) Llovet, J. M.; Ricci, S.; Mazzaferro, V.; Hilgard, P.; Gane, E.; Blanc, J.; Oliveira, A. C. D.; Santoro, A.; Raoul, J.; Forner, A.; Schwartz, M.; Porta, C.; Zeuzem, S.; Bolondi, L.; Greten, T. F.; Galle, P. R.; Seitz, J.; Borbath, I.; Häussinger, D.; Giannaris, T.; Sc, B.; Shan, M.; Ph, D.; Moscovici, M.; Voliotis, D.; Bruix, J. *N. Engl. J. Med.* **2008**, *359*, 378–390.
- (7) Coriat, R.; Nicco, C.; Chéreau, C.; Mir, O.; Alexandre, J.; Ropert, S.; Weill, B.; Chaussade, S.; Goldwasser, F.; Batteux, F. *Mol. Cancer Ther.* **2012**, *11*, 2284–2293.
- (8) Leeds, J. a; Schmitt, E. K.; Krastel, P. *Expert Opin. Invest. Drugs* **2006**, *15*, 211–226.
- (9) Butler, M. S.; Buss, A. D. *Biochem. Pharmacol.* **2006**, *71*, 919–929.
- (10) Müller, M. *Curr. Opin. Biotech.* **2004**, *15*, 591–598.
- (11) Lamb, S. S.; Wright, G. D. *P. Natl. Acad. Sci. USA* **2005**, *102*, 519–520.
- (12) Paterson, I.; Anderson, E. A. *Science* **2005**, *310*, 451–453.
- (13) Ortholand, J.-Y.; Ganesan, A. *Curr. Opin. Chem. Biol.* **2004**, *8*, 271–280.
- (14) Ganesan, A. *Curr. Opin. Biotech.* **2004**, *15*, 584–590.
- (15) Sánchez, C.; Zhu, L.; Braña, A. F.; Salas, A. P.; Rohr, J.; Méndez, C.; Salas, J. A. *P. Natl. Acad. Sci. USA* **2005**, *102*, 461–466.
- (16) Floss, H. G. *J. Biotechnol.* **2006**, *124*, 242–257.
- (17) Baltz, R. H. *Nat. Biotechnol.* **2006**, *24*, 1533–1540.
- (18) Bode, H. B.; Bethe, B.; Höfs, R.; Zeeck, A. *Chem. Bio. Chem.* **2002**, *3*, 619–627.
- (19) Kegler, C.; Gerth, K.; Müller, R. *J. Biotechnol.* **2006**, *121*, 201–212.



- (20) Marris, E. *Nature* **2006**, *443*, 904–905.
- (21) Newman, D. J.; Cragg, G. M. *Curr. Drug Targets* **2006**, *7*, 279–304.
- (22) Zotchev, S. B. *J. Biotechnol.* **2012**, *158*, 168–175.
- (23) Hill, R. A. *Annu. Rep. Prog. Chem. B* **2012**, *108*, 131–146.
- (24) Cuevas, C.; Pérez, M.; Martín, M. J.; Chicharro, J. L.; Fernández-Rivas, C.; Flores, M.; Francesch, A.; Gallego, P.; Zarzuelo, M.; de La Calle, F.; García, J.; Polanco, C.; Rodríguez, I.; Manzanares, I. *Org. Lett.* **2000**, *2*, 2545–2548.
- (25) Salomon, C. E.; Magarvey, N. A.; Sherman, D. H. *Nat. Prod. Rep.* **2004**, *21*, 105–121.
- (26) Molinski, T. F.; Dalisay, D. S.; Lievens, S. L.; Saludes, J. P. *Nat. Rev. Drug Discov.* **2009**, *8*, 69–85.
- (27) Younes, A.; Yasothan, U.; Kirkpatrick, P. *Nat. Rev. Drug Discov.* **2012**, *11*, 19–20.
- (28) Newman, D. J.; Cragg, G. M. *J. Nat. Prod.* **2012**, *75*, 311–335.
- (29) Butler, M. S. *Nat. Prod. Rep.* **2005**, *22*, 162–195.

# **CHAPTER 1**

**Synthesis, structural elucidation and  
biological evaluation of Pipecolidepsin A**



### **1.1. Introduction: “Head-to-side-chain” cyclodepsipeptides**

A peptide is an oligomer of up to 60 amino acids. When at least one of the amide bonds from a peptide is replaced by an ester bond, we talk about depsipeptides. They have proven to be highly promising candidates to pharmaceutical agents as they own a huge structural diversity and display a broad spectrum of biological activities: antiplasmodial, antiviral, antimicrobial, insecticidal, cytotoxic, antiproliferative and anticancer activities, as well as exhibit ionophoric and anthelmintic properties. Most of the bioactive peptides have been mainly extracted from tunicates, bacteria, sponges and mollusks.

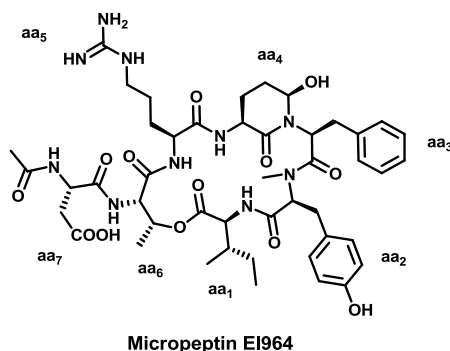
The presence of several unique residues and the complex structural features shown by marine depsipeptides, turns its structural elucidation into a challenge only boosted by their interesting therapeutic profiles. Thus, research in this field has thrived over the last years and several depsipeptides are now undergoing evaluation in clinical trials.

Since the early 90's, the bibliography has been enriched with a number of depsipeptides that belong to a new family of peptides: “head-to-side-chain” cyclodepsipeptides. These peptides present a unique structural arrangement: a macrocyclic region closed through an ester bond between the C-terminus and a  $\beta$ -hydroxyl group,

terminated with a polyketide moiety or a more simple branched aliphatic acid. This structural pattern, the presence of unique and complex residues and interesting bioactivities are the main features shared by all the members of this new class of depsipeptides.

### 1.1.1. Families of “head-to-side-chain” cyclodepsipeptides

Marine cyanobacteria are an extremely prolific source of natural compounds bearing a wide range of structures and biological profiles. Among all the secondary metabolites produced by these organisms, we would like to point out the **3-amino-6-hydroxypiperidone (Ahp)-containing cyclic depsipeptides**. Micropeptins,<sup>1,2</sup> cyanopeptolins,<sup>3,4</sup> oscillapeptins,<sup>5,6</sup> nostopeptins,<sup>7,8</sup> aeruginopeptins,<sup>9,10</sup> largamides,<sup>11</sup> lyngbyastatins<sup>12,13</sup> etc. are cyclodepsipeptides with serine protease inhibitory activity sharing the same structural scaffold: a “head-to-side-chain” macrocyclic region, mostly comprising six residues, closed through an ester bond with the hydroxyl group of a L-Thr, and terminated with a more mutable linear fragment, often blocked by hydrophobic acids. Micropeptin EI964 perfectly illustrates this family of cyclodepsipeptides (Figure 2).



**Figure 2:** Chemical structure of Micropeptin EI964.

Commonly aa<sub>1</sub> is L-Ile, L-Val or L-Leu (all hydrophobic residues); aa<sub>2</sub> is NMe-L-Tyr that can present different substitution patterns (halogenated, NMe-L-Tyr(OMe)...) or NMe-L-Phe; aa<sub>3</sub> accepts a higher variability and can be a hydrophobic residue such as L-Ile, L-Phe, L-Val and L-Leu or a polar uncharged amino acid such as L-Thr; aa<sub>4</sub> is always Ahp or its methylated version Amp; and aa<sub>5</sub> is the residue showing the highest diversity as it can be L-Leu, Abu, L-Arg, L-Tyr, L-HomoTyr, L-Lys, L-Gln, L-HcAla, L-Trp... The macrolactone framework represents a potent inhibitor prototype in which aa<sub>5</sub> binds the S1 specificity pocket of the enzymes blocking the interaction of proteases with their substrates.<sup>14,15</sup> Thus, the nature of this residue is crucial in terms of selectivity and explains its variability. Trypsin prefers basic residues (Arg and Lys)

while chymotrypsin prefers large hydrophobic residues (Tyr, Phe, Trp).<sup>14,16,17,18,19</sup> Abu enhances selectivity for elastase.<sup>13</sup> The *O* from the hydroxyl group of Ahp/Amp participates in an intramolecular hydrogen bond with the NH of aa<sub>1</sub> and the *N*Me-Tyr or *N*Me-Phe facilitates the formation of a *cis* peptide bond. These structural features make the cycle very rigid<sup>14,17,18</sup> protecting this class of cyclodepsipeptides from the proteases activity and providing a clearly-defined 3D structure. The presence of unnatural amino acids in their structure also provides resistance against enzymatic hydrolysis.

The L-Thr residue at the branching position plays a crucial structural role and has been described to occupy the subsite S2 of the protease. Only some nostopeptins present a different amino acid at this position, a 3-hydroxy-4-methylproline residue, whose stereochemistry has not been assigned yet.<sup>20</sup>

The linear arm is postulated to interact with more distal regions of the proteases (S3 and S4 subsites) through hydrogen bonds.<sup>5</sup> Hence, selectivities and potencies can also be influenced by the highly diverse length and nature of the exocyclic fragment. Experimental data showed the requirement of at least a two units-long exocyclic arm for strong activity.<sup>21</sup>

From a synthetic point of view, only a few members of this huge Ahp-containing depsipeptides family have been synthesized. Thus, Somamide A<sup>22</sup> was fully synthesized in solution while a full solid phase strategy was developed for Symplocamide A.<sup>23,24</sup> The key step of Symplocamide A synthesis is the spontaneous formation of the Ahp moiety from a glutamic aldehyde generated once the linear precursor is totally assembled. The ester bond is formed after incorporation of the two exocyclic moieties using DIPCDI-DMAP (10:1). The peptidic chain is elongated through the ester bond using Boc chemistry to avoid possible DKP at the ester level and the macrolactamization step was performed on solid-phase.

Also produced by bacteria and sharing an analogous “head-to-side-chain” framework, we find two cyclodepsipeptides displaying interesting *in vitro* and *in vivo* antibiotic activity against aerobic and anaerobic Gram-positive bacteria, especially against methicillin-resistant *Staphylococcus aureus* (MRSA) and vancomycin-resistant *enterococci* (VRE). **Katanosin A** and **Katanosin B** (also known as **Lysobactin**) (Figure 3) were isolated from the culture broth of a strain related *Cytophaga*.

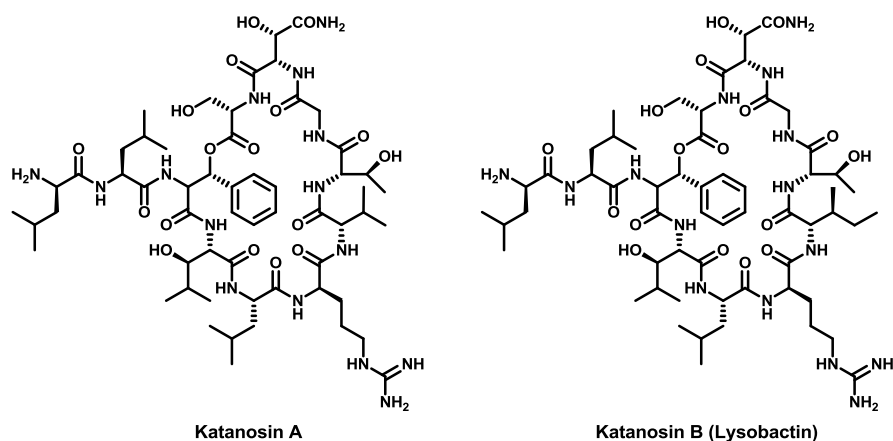


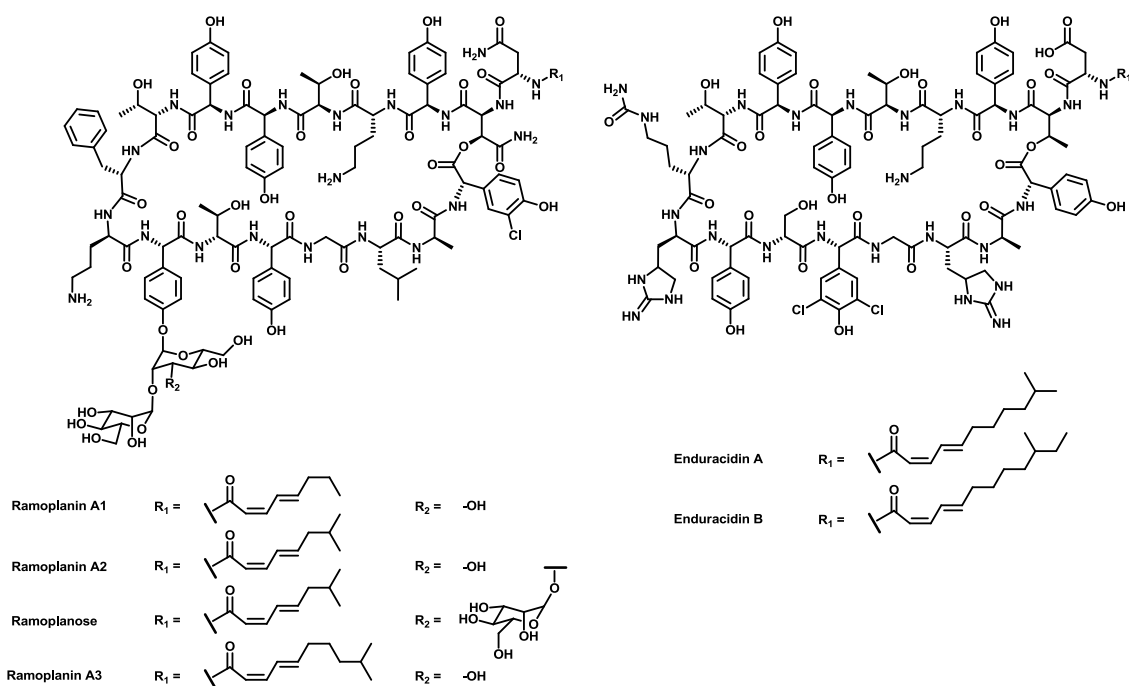
Figure 3: Chemical structures of Katanosin A and B.

The absence of the Ahp-moiety; the free *N*-terminus; a bigger macrocyclic ring (9 residues); the occurrence of different uncommon amino acids ( $\beta$ -HO-Leu or  $\beta$ -HO-Asn); the presence of both L- and D- configurations; and a more bulky and hydrophobic residue at the branching position (L-HO-Phe) are some of the more significant structural differences with regard to the Ahp-containing cyclodepsipeptides family.

Two different syntheses in solution<sup>25,26</sup> and one on solid phase<sup>27</sup> have been described so far for Katanosin B (Lysobactin). The solid phase approach represents a more straightforward strategy to rapidly access structural analogs in order to identify the key moieties responsible of the interesting bioactivity. Epimerization and  $\beta$ -elimination (especially favored by the aromatic nature of the residue at the branching position) while forming the ester bond represent the bottleneck of Lysobactin synthesis. After exhaustive study of conditions, it was determined that *N* <sup>$\alpha$</sup>  Alloc-protected Ser, DIPCDI and DMAP at 37 °C were the optimal conditions to overcome these severe side reactions. The residues of the exocyclic arm were already assembled when the ester was constructed. No DKP formation at the ester level was detected. The final cyclization step was carried out in solution.

Displaying promising activity against several resistant Gram-positive bacteria (also including vancomycin-resistant *Enterococcus faecium* (VRE) and methicillin-resistant *Staphylococcus aureus* (MRSA)) and sharing an analogous “head-to-side-chain” framework, **ramoplanin** (A1-A3),<sup>28,29</sup> **ramoplanose**<sup>30</sup> and two other structurally related peptides, **janiemycin**<sup>31</sup> (uncharacterized but reported to be a member of the same family) and **enduracidin** (A and B)<sup>32</sup>, were described (Figure 4). Ramoplanins and ramoplanose are 17-residue non-ribosomally produced lipoglycopeptides, while enduracidins do not own any monosaccharide moiety in their structure. Ramoplanins’ mode of action was revealed

totally different from vancomycin (2-10 times less potent). They inhibit bacterial cell-wall biosynthesis by binding and sequestering lipid intermediates I and II.



**Figure 4:** Chemical structures of Ramoplanin A1-A3, Ramoplanose and Enduracidin A and B.

In all cases, the macrocyclic region, formed by 16 residues (the largest macrolactone of all the known “head-to-side-chain” cyclodepsipeptides), is linked to an exocyclic arm formed by one single aa acylated at its *N*-terminus with a polyunsaturated fat acid. All ramoplanins and ramoplanose bear an *L*-allo- $\beta$ -HO-Asn residue at the branching position and enduracidins an *L*-Thr. Several unnatural amino acids are present in their structures such as hydroxyphenylglycine and chlorated derivatives, enduracididine, ornitine and citrulline.

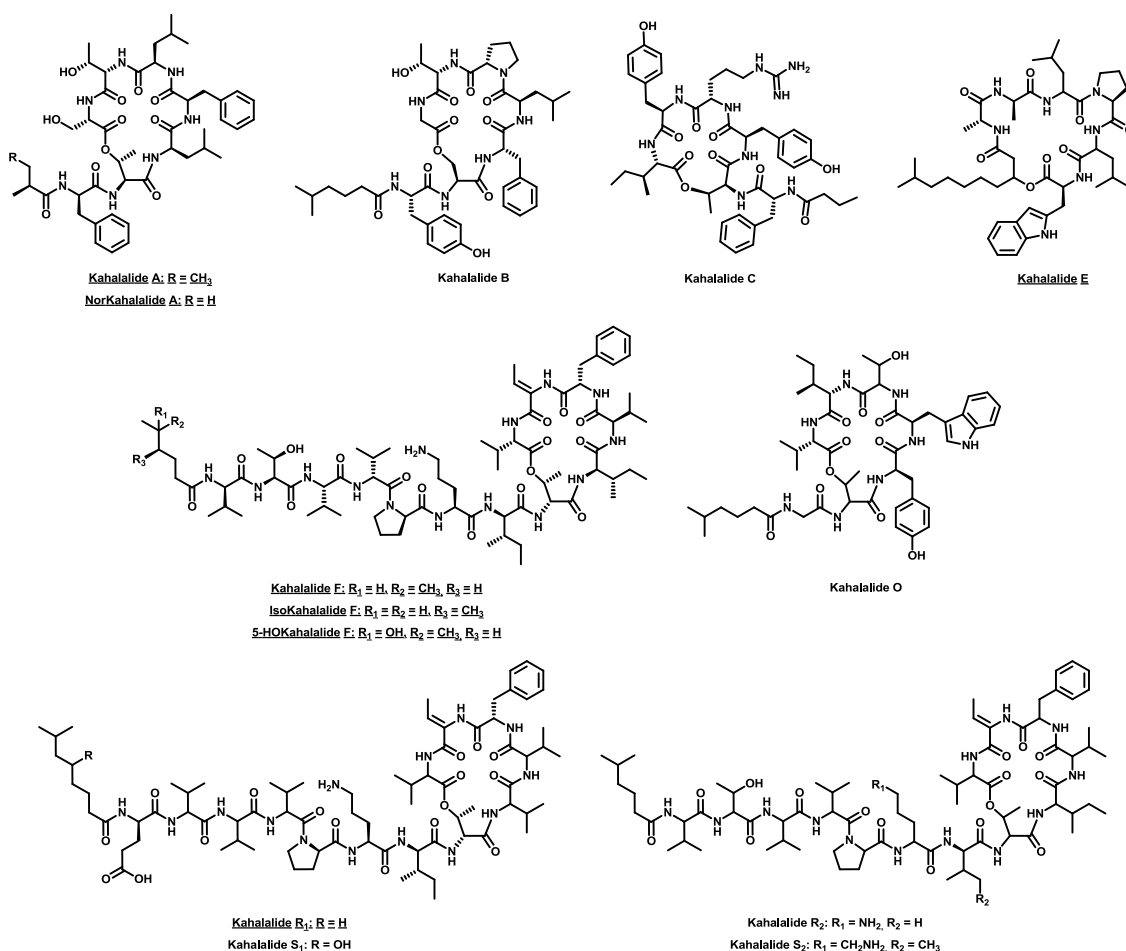
Several convergent syntheses on solution have been reported in the literature for ramoplanin A2 and ramoplanose aglycons,<sup>33,34</sup> and ramoplanin A1 and A3 aglycons.<sup>35</sup> No strategies have been developed for enduracidin A or B and no solid-phase approaches have been suggested for any peptide. However, some ramoplanin’s semisynthetic derivatives have already been obtained<sup>36</sup> and some noteworthy work on the biosynthesis of ramoplanin A2 has already been started.<sup>37</sup>

A close-related “head-to-side-chain” arrangement was also found in another family of cyclodepsipeptides. **Kahalalides**<sup>38,39,40,41</sup> were isolated from the herbivorous marine mollusks *Elysia rufescens*, *Elysia ornate* or *Elysia grandifolia* and their algal diet *Bryopsis pennata* or



*Bryopsis plumosa*. They make up a large family of marine peptides with highly variable compositions and sizes. Its members range from tripeptides to tridecapeptides, and includes homodetic linear peptides, “head-to-tail” cyclodepsipeptides and “head-to-side-chain” cyclodepsipeptides, all of them acylated at their *N*-terminus.

Among the 24 described natural members of this family, only 7 own interesting therapeutic profiles.<sup>38,39,42,43,44,45,46,47</sup> They exhibit highly diverse biological activities including cytotoxicity and antitumor, antimicrobial, antileishmanial and immunosuppressive activities. Significantly, all the active members are cyclodepsipeptides and 6 out of the 7 exhibit the uncommon “head-to-side-chain” structural arrangement closed through an ester bond (Figure 5).



**Figure 5:** Structures of “head-to-side-chain” Kahalalides plus Kahalalide E. All the Kahalalides displaying interesting biological activities appear underlined.

From a structural perspective, we are further more interested in the “head-to-side-chain” Kahalalides, meaning Kahalalide A, B, C, F, O, R<sub>1</sub>, R<sub>2</sub>, S<sub>1</sub>, S<sub>2</sub>, NorKahalalide A, IsoKahalalide F and 5-OHKahalalide F. Their macrocyclic region comprises 6 amino acids with

one single exception, Kahalalide C, which bears a 5-residues ring. Most of the amino acids found on Kahalalides are residues with hydrophobic or polar uncharged side chains having abundance of both L- and D- configurations, what represents a significant change with regard to the Ahp-containing depsipeptides family. Other differences between the two big families are: the presence of other residues such as L-Ser or D-*allo*-Thr, and not only L-Thr, at the branching position of the Kahalalides; the commercial availability of all their residues with the exception of Abu; the occurrence of a much longer exocyclic arm (up to seven residues); and the presence of a much simpler *N*-terminal acid, which is, most of the times completely aliphatic, and only in some cases a hydroxyacid.

However, as it was reported for the Ahp-containing depsipeptides, the “head-to-side-chain” structural arrangement also seems to be essential to keep the biological activity of the kahalalides with therapeutic interest.

KF shows the most complete biological activity profile of all the natural Kahalalides described so far.<sup>38,39,45,46,47</sup> It has shown selectivity against solid tumor cell lines with IC<sub>50</sub> at the low μM range (in A-549, HT-29, LOVO, P-388, KB and CV-1 cells); antiviral activity against HSV II using mink lung cells; antigungal activity with IC<sub>50</sub> values below 3.3 μM against *Candida albicans*, *Candida neoformans* and *Aspergillus fumigatus*; immunosuppressive activity; and antileishmanial activity with good to moderate IC<sub>50</sub> values against *Leishmania donovani* and *Leishmania pifanoi* (promastigotes and amastigotes). Thus, exhaustive structural, synthetic, biological, clinical and mechanistical studies have been conducted during the last 20 years.

A complete analogs program has provided valuable structure-activity relationships (SARs).<sup>46,47</sup> KF owns three different domains: domain A includes the macrocyclic region; domain B comprises the linear exocyclic arm; and domain C is formed by the *N*-terminal acid. Several changes were performed in all domains to construct up to 143 analogs. It was concluded that: the ring is crucial to keep the biological properties as the linear precursor of KF, Kahalalide G, did not display any activity; the presence of the Z-Dhb residue and several D-aa increase the resistance against enzymatic hydrolysis and provides rigidity, which is essential to keep the activity; the position occupied by L-Phe must host a highly hydrophobic residue; the absolute configuration of all residues is crucial, meaning that the peptide is more three-dimensional structured than expected; and, finally, an increase in the sterical hindrance and/or the hydrophobic nature of the side chains represents an increase in activity.

To further support the experimental data collected for Kahalalide F, a more reduced analogs program conducted also for Kahalalide A<sup>48</sup> provided similar conclusions regarding the “head-to-side-chain” arrangement. The synthesis and biological evaluation of 5 analogs, including its linear version, was performed to point out the importance of the macrolactone framework and the presence of free Ser and Thr residues to keep its activity against *Mycobacterium tuberculosis*.

From a synthetic point of view, only total synthesis of Kahalalide A, B, F and IsoKahalalide F have been published.<sup>44,48,49,50,51,52</sup> Kahalalide A was accessed by means of total synthesis on solid phase. A backbone cyclization strategy was carried out using the Kenner sulfonamide safety-catch linker. The ester bond over the L-Thr residue was built once the two moieties of the exocyclic arm were already assembled. The Fmoc-L-Ser(<sup>t</sup>Bu)-OH was incorporated following a double treatment with DIPCDI and DMAP (4:4:0.4) in THF (2 h + o/n).

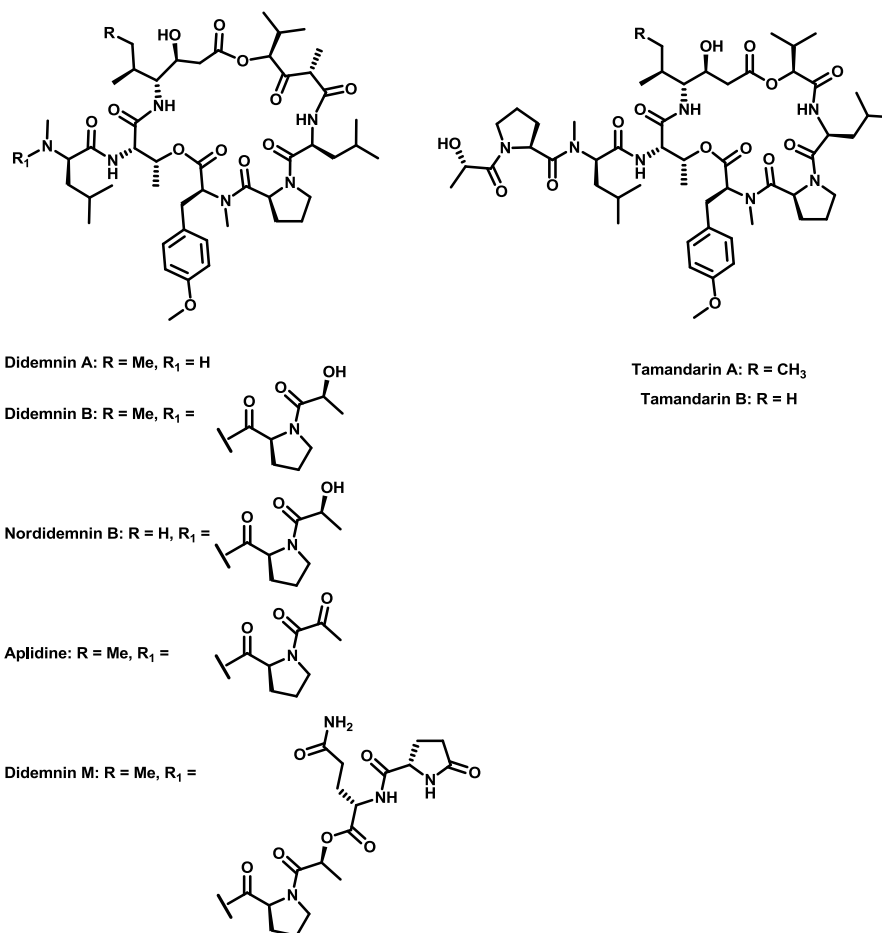
Kahalalide B was synthesized following two different synthetic strategies: complete elongation of the linear precursor on solid-phase and cyclization through i) the peptidic bond Gly-Thr or ii) the ester bond D-Ser-Gly. The first approach presents some advantages: a faster cyclization reaction; a cleaner and better yielding cleavage step; and the avoidance of a last deprotection step in solution. Cyclization through the ester bond has not been attempted for any other related cyclodepsipeptide. Only the presence of the least bulky  $\beta$ -hydroxy- $\alpha$ -amino acid at the branching position (D-Ser) enables the performance of such a synthetic approach.

A lot of effort has been put into the synthesis of the more complex Kahalalide F. Thus, not only a linear solid phase synthesis, but also convergent strategies, have been successfully developed. The synthesis of linear KF was started by anchoring Fmoc-D-Val-OH onto 2-CTC resin. The ester bond was formed before complete assembly of the exocyclic arm by means of DIPCDI-DMAP. The Z-Dhb residue could be generated on solid-phase or in solution and incorporated as a dipeptide. The final cyclization step was carried out between the residues Phe-D-Val. The convergent strategies comprise the solid phase syntheses of branched peptides using tri- and tetra-orthogonal protection schemes; their cyclization and deprotection of the *N*-terminal in solution; the synthesis on solid phase of the linear components; and the final condensation of the two fragments in solution using PyAOP-DIEA. The best approach condenses the fragments through the peptidic bond D-Pro-Orn to avoid epimerization. No DKP formation at the ester level was detected.

**Didemnins**<sup>53,54</sup> and **tamandarins**<sup>55</sup> are complex cyclodepsipeptides isolated from Caribbean and Brazilian tunicates respectively, displaying interesting antitumor, antiviral and immunosuppressive activities at low nano- and femtomolar range. Additionally, they inhibit *in vitro* protein biosynthesis and induce rapid apoptosis. They own a “head-to-side-chain”-like structural arrangement closely related to the ones described previously, but comprising two ester bonds.

From a structural perspective, Tamandarins are simplified versions of Didemnins (Figure 6). They contain a  $\gamma$ -amino acid and a  $\alpha$ -hydroxy acid (*S*-hydroxyisovaleric acid, Hiv) that forms the second ester bond in the macrocyclic region. In Didemnins the Hiv moiety is replaced with the more complex  $\alpha$ -( $\alpha$ -hydroxyisovaleryl)propionyl (HIP) unit. They contain both L- and D- amino acids and, significantly, as it happens in the Ahp-containing cyclodepsipeptides family, L-Thr occupies always the branching position.

Several total syntheses for Didemnins A, B and C and Dehydrodidemnin B and Nordidemnin B have been developed.<sup>56,57,58,59,60</sup> They all are synthetic approaches in solution mainly differing in the site of cyclization and the coupling reagents.<sup>61</sup> Furthermore, a number of total syntheses in solution of Tamandarin A,<sup>62,63</sup> Tamandarin B<sup>63,64</sup> and analogs<sup>65,66,67</sup> have also been described. Significantly, once again, structure-activity relationships of the Didemnins point out that the macrolactone framework is a crucial structural arrangement regarding to the bioactivities of the natural peptides, especially cytotoxicities and antiviral properties.<sup>68</sup>



**Figure 6:** Structures of natural Didemnins and Tamandarins.

Finally, there is a huge and varied family of cyclodepsipeptides, all produced by marine sponges, that also possess the distinctive “head-to-side-chain” structural arrangement *via* an ester bond. All of them contain a 22 or a 25-membered macrolactone that bears a  $\beta$ -hydroxy- $\alpha$ -amino acid with the *D-allo* configuration at the branching position. Furthermore, they share a number of uncommon residues described for the first time after the isolation of these natural peptides. Significantly, the same rare residue is acylating the branching position of all the isolated members. The exocyclic arm is either composed of three amino acids, one of them being a  $\gamma$ -amino acid, or four  $\alpha$ -amino acids. Its *N*-terminus is always acylated with a  $\beta$ -hydroxyacid. In the structure of these peptides, both L- and D- amino acids are found. Finally, all the cyclodepsipeptides own interesting therapeutic profiles, mostly displaying cytoprotective activity against HIV-1 infection.

In 1996 Zampella and co-workers described the first member of the **Callipeltins**. Callipeltin A<sup>69</sup> is a “head-to-side-chain” cyclic depsidecapeptide isolated from a shallow water sponge of the genus *Callipelta*, in the order *Lithistida*, collected in the waters off New

Caledonian. Its isolation enabled the description of three new and complex amino acids:  $\beta$ -methoxytyrosine, (3*S*,4*R*)-3,4-dimethyl-L-glutamine and (2*R*,3*R*,4*S*)-4-amino-7-guanidino-2,3-dihydroxyheptanoic acid. From the same marine sponge, a truncated version of Callipeltin A named Callipeltin B, and the linear peptides Callipeltins C-M were also isolated.<sup>70,71,72,73</sup> Callipeltins A and B (Figure 7) contain a *D*-allo-Thr at the branching position of a 22-membered macrolactone (6 residues), and display an interesting cytotoxicity against several cancer cell lines. Additionally, Callipeltin A was found to be active against human immunodeficiency (HIV) virus.

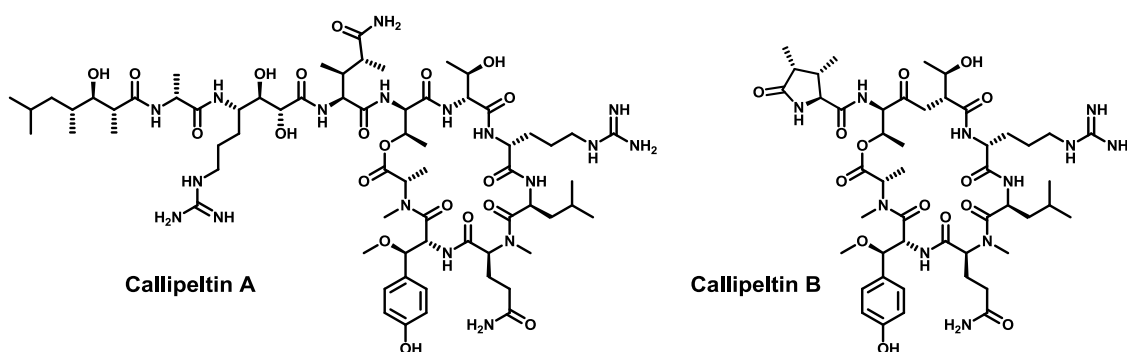


Figure 7: Chemical structures of Callipeltin A and B.

The total synthesis of Callipeltin B on solid phase was published by Lipton and co-workers.<sup>74</sup> They chose to start the linear peptide elongation by incorporating the cyclic anhydride of Fmoc-*N*-methylglutamic acid onto the Sieber resin, and to carry out the macrolactamization step at the *N*Me-Ala- $\beta$ -MeO-Tyr linkage. The ester bond was formed once the DiMePyroGlu was already coupled and using Alloc-*N*Me-Ala-OH and MSNT in conjunction with *N*-methylimidazole. Desmethoxycallipeltin B and other analogs have also been synthesized and biologically evaluated.<sup>75,76</sup>

The same new and bizarre three residues were found in other cyclodepsipeptides isolated in Papua New Guinea from the marine sponge *Neamphius huxleyi*. **Neamphamide A**,<sup>77,78</sup> **B**,<sup>79,80</sup> **C**<sup>80</sup> and **D**<sup>80</sup> (Figure 8) are depsipeptides with a 25- and a 22-membered macrolactone respectively, a *D*-allo-Thr residue at the branching point and the same terminating polyketide moiety of Callipeltin A. Neamphamide A displays a potent cytoprotective activity against HIV-1 infection, while Neamphamide B shows potent antimycobacterial activity against *Mycobacterium smegmatis* and *bovis* BCG. An outstanding structural feature and an important difference with regard to Callipeltin A is the presence in their macrocyclic region of the rare L-homoproline. No syntheses have been described so far.

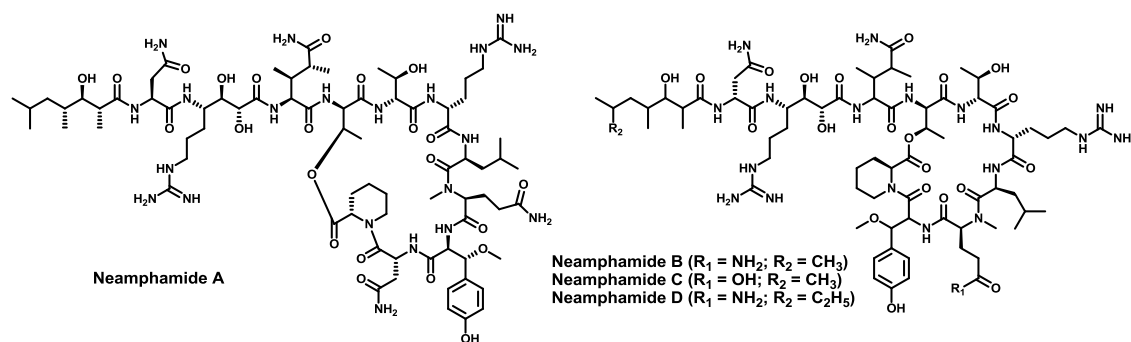


Figure 8: Chemical structures of Neamphamide A-D.

L-Homoproline,  $\beta$ -methoxytyrosine and (3*S*,4*R*)-3,4-dimethyl-L-glutamine are also contained in the **Papuaamides**,<sup>81,82</sup> isolated in 1999 in Papua New Guinea from two sponges, *Theonella mirabilis* and *Theonella swinhoei*. Moreover, they contain other strange amino acids such as L-3-methoxyalanine and D-*allo*- $\beta$ -hydroxyleucine at the branching position, as well as two previously undescribed terminating moieties: 2,3-dihydroxy-2,6,8-trimethyldeca-(4*Z*,6*E*)-dienoic acid and 3-hydroxy-2,6,8-trimethyldeca-(4*Z*,6*E*)-dienoic acid (Figure 9). Papuaamides A and B inhibited the infection of human T-lymphoblastoid cells by HIV-1<sub>RF</sub> *in vitro*. Papuaamide A also displays cytotoxic activity against a panel of human cancer cell lines. Papuaamide A synthesis in solution was published by Ma and co-workers on 2008.<sup>83</sup>

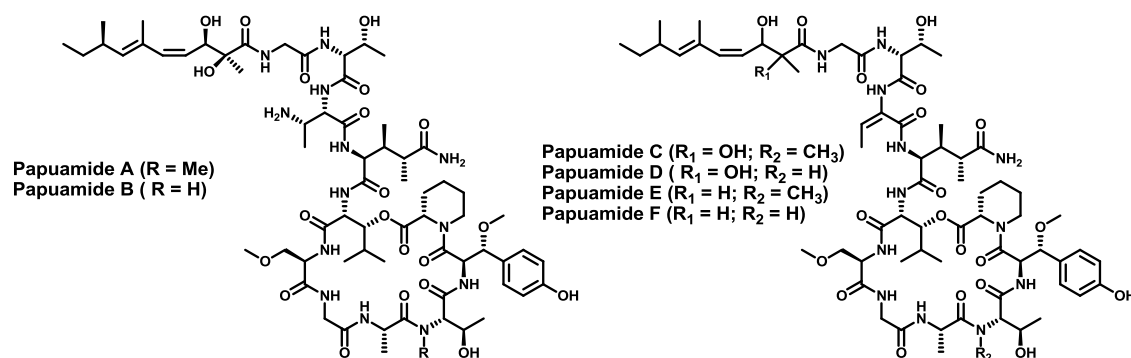


Figure 9: Chemical structures of Papuaamides A-F.

From the same *Theonella swinhoei* sponge in Papua New Guinea, another member of the “head-to-side-chain” cyclodepsipeptides family was isolated. **Theopapuaamide A**<sup>84</sup> is a cyclic depsiundecapeptide bearing a D-*allo*-Thr at the branching position and two unprecedented amino acid residues in its structure:  $\beta$ -methoxyasparagine and 4-amino-5-methyl-2,3,5-trihydroxyhexanoic acid. The 3-hydroxy-2,4,6-trimethyloctanoic acid acylates the N-terminus. Theopapuaamides B-D<sup>85</sup> were isolated from the *Siliquariaspongia mirabilis* sponge. They also contain a rare D-3-acetamido-2-aminopropanoic acid and the (3*S*,4*S*)-4-amino-2,3-

dihydroxy-5-methylhexanoic acid (Figure 10). Theopapuamides A-C are cytotoxic against human colon carcinoma (HCT-116) cells and show strong antifungal activity against wildtype and amphotericin B-resistant strains of *Candida albicans*. Furthermore, Theopapuamide A also exhibits cytotoxicity against CEM-TART cell line. No syntheses have been described so far.

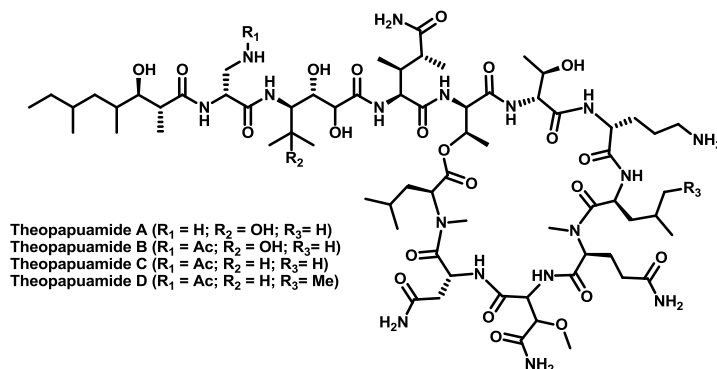


Figure 10: Chemical structures of Theopapuamides A-D.

Sharing a pretty close scaffold with Papuamides, **Mirabamides**<sup>86,87</sup> were isolated from the marine sponge *Siliquariaspongia mirabilis*, collected from Chuuk Lagoon in the Federated States of Micronesia. Mirabamides contain two new entities: a rare glycosylated amino acid  $\beta$ -methoxytyrosine 4'-*O*- $\alpha$ -L-rhamnopyranoside and the 4-chloro-L-homoproline (Figure 11). Mirabamides A, C and D inhibit HIV-1 in neutralization and fusion assays showing that their action occurs at the early stages of HIV-1 entry. Mirabamides A-C show also antimicrobial activity toward *C. albicans* and *B. subtilis*. No syntheses have been described so far.

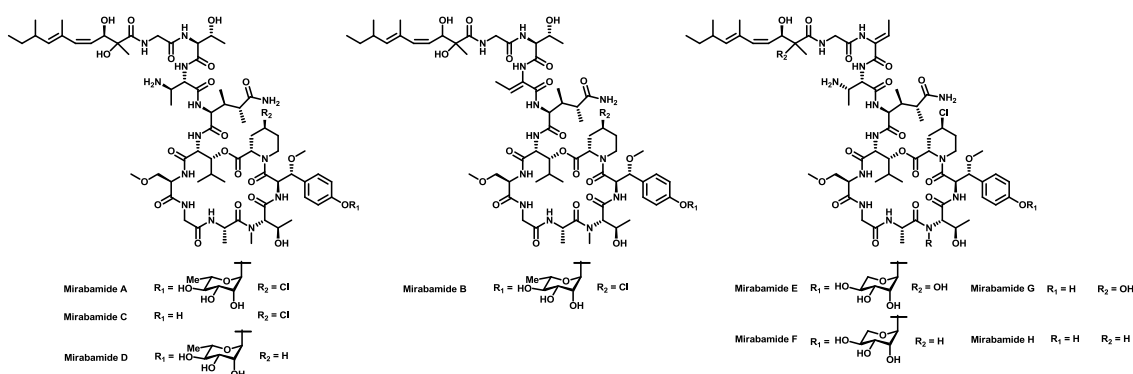
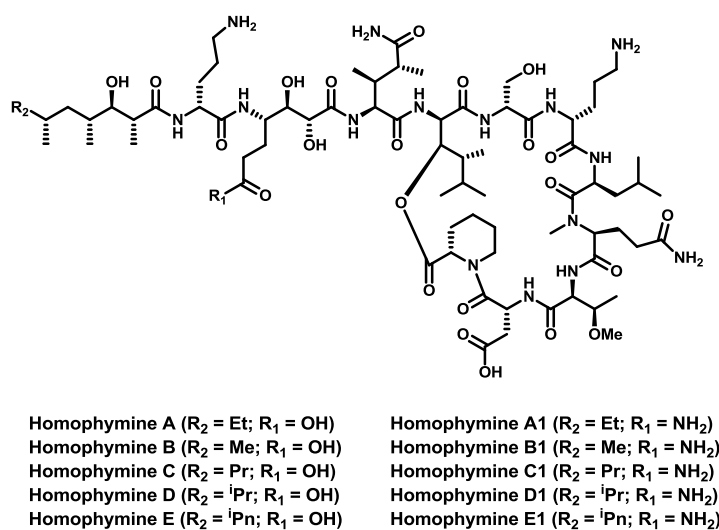


Figure 11: Chemical Structures of Mirabamides A-H.

In 2008 and 2009 Zampella and co-workers described ten new cyclodepsipeptides named **Homophymines** A-E and A1-E1<sup>88,89</sup> isolated from the marine sponge *Homophymia*, in the order *Lithistida*, collected in New Caledonian. They all are “head-to-side-chain” cyclic depsiundecapeptides that contain: a 25-membered macrolactone; the unusual residues

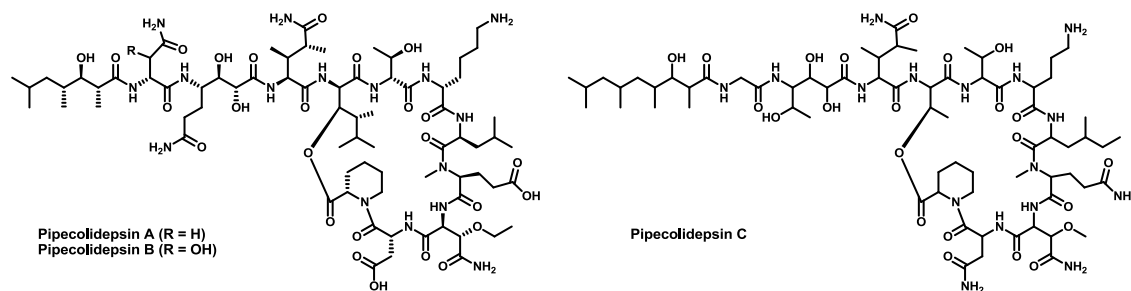


(3*S*,4*R*)-3,4-dimethyl-L-glutamine, L-ThrOMe and L-homoproline; up to five different polyketide terminating moieties; and three unprecedented amino acids, (2*R*,3*R*,4*S*)-4-amino-2,3-dihydroxy-1,7-heptandioic acid (ADHA) or (2*R*,3*R*,4*S*)-4,7-diamino-2,3-dihydroxy-7-oxoheptanoic acid (DADHOHA) and the (2*R*,3*R*,4*R*)-2-amino-3-hydroxy-4,5-dimethylhexanoic acid (*D-allo*-AHDMHA) at the branching position (Figure 12). All the members described so far exhibit a potent cytotoxic activity. Furthermore, the first isolated member Homophymine A displays as well an interesting cytoprotective activity against HIV-1 infection at very low concentrations. No syntheses have been described so far.



**Figure 12:** Chemical structures of Homophymines A-E and A1-E1.

Finally, from a *Homophymia* marine sponge collected in the coasts of Madagascar, PharmaMar isolated Pipecolidepsins A, B and C. They are “head-to-side-chain” cyclic depsipeptides also bearing a 25-membered macrolactone and containing the rare amino acids L-homoproline, L-homoisoleucine,  $\beta$ -EtO-Asn,  $\beta$ -MeO-Asn, (3*S*,4*R*)-3,4-dimethyl-L-glutamine, DADHOHA and the terminating HTMHA acid (Figure 13). Pipecolidepsins A and B have the unique (2*R*,3*R*,4*R*)-2-amino-3-hydroxy-4,5-dimethylhexanoic acid (*D-allo*-AHDMHA) at the branching position, while Pipecolidepsin C possesses a much more simple *D-allo*-Thr residue. The three depsipeptides display interesting cytotoxicities against three human cancer cell lines (Lung-NSCLC A549, Colon HT-29 and Breast MDA-MB-231) with  $GI_{50}$  around  $10^{-07}$  M. In the present thesis, the first total synthesis of Pipecolidepsin A is described. It is the first “head-to-side-chain” cyclodepsipeptide bearing the unprecedented *D-allo*-AHDMHA at the branching position whose synthesis has been achieved.



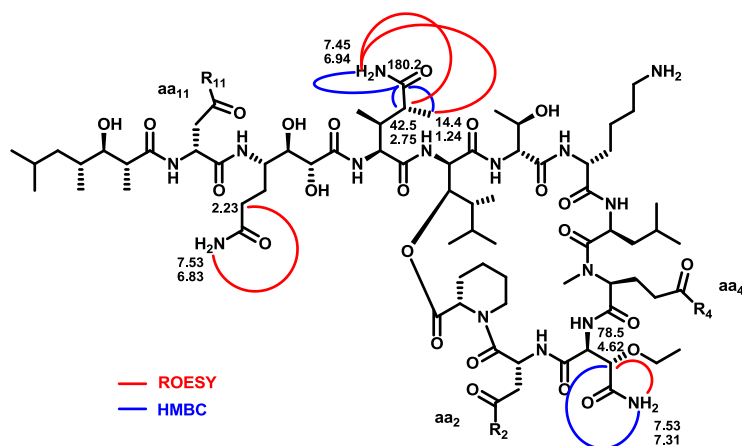
**Figure 13:** Chemical structures of Pipecolidepsin A, B and C.

## 1.2. Structure elucidation of Pipecolidepsin A

The structure of Pipecolidepsin A was determined by HPLC-MS, acid hydrolysis and exhaustive NMR analysis. A complete set of monodimensional and homonuclear and heteronuclear bidimensional NMR experiments in different solvents ( $\text{CD}_3\text{OD}$ ,  $\text{CD}_3\text{OH}$ ,  $\text{DMSO}-d_6$  and  $\text{H}_2\text{O}-\text{ACN}-d_3$  (5:1)) were recorded. The interpretation of all the spectroscopic data enabled the proposal of a preliminary structure for Pipecolidepsin A.<sup>90</sup>

However, structure elucidation of natural products is an extremely challenging task always subjected to corrections as its synthetic process goes along. Thus, the literature contains several examples of natural structures corrected after their syntheses were performed. NMR characterization and biological evaluation of the synthetic counterparts turn to be crucial for the validation of the proposed structures.<sup>49,71</sup>

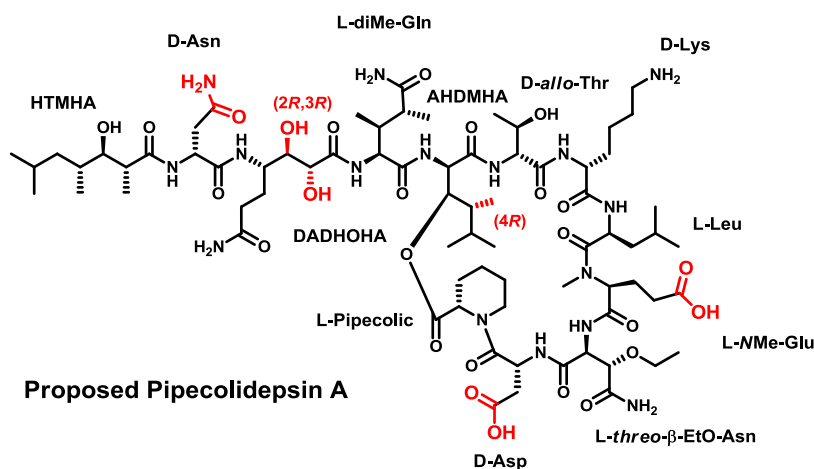
Pipecolidepsin A was not exempt from the structural uncertainty. The first NMR studies confirmed the presence of four side-chain amides, but only the placement in the peptidic sequence of three of them. Thus, the side-chain amides of diMe-Gln, *L*-threo- $\beta$ -EtO-Asn and DADHOHA residues were confirmed by heteronuclear multiple-bond correlations (HMBC) and/or through-space correlations (ROESY) (Figure 14). No correlations were found for the fourth amide.



**Figure 14:** HMBC and ROESY correlations of the side-chain amide protons of the natural Pipecolidepsin A. The non-assigned side-chain carboxylic acids and amide are shown as  $R_i$  groups.

The peptidic sequence held three positions susceptible to bear the non-assigned side-chain amide: aa<sub>2</sub>, aa<sub>4</sub> and aa<sub>11</sub>. A non-concluding MS-MS experiment supported the hypothesis of aa<sub>2</sub> = D-Asp; aa<sub>4</sub> = NMe-Glu and aa<sub>11</sub> = D-Asn.

Furthermore, the stereochemical information regarding the diol function of the unique DADHOHA residue and C4 of the unprecedented AHDMHA amino acid was not completely elucidated. A *cis* configuration of the diol was confirmed, while the absolute stereochemistry of the two hydroxyl groups remained unclear. Finally, the configurations described for similar residues in other cyclodepsipeptides published in the literature were assumed,<sup>88</sup> and a preliminary structure for Pipecolidepsin A was proposed (Figure 15). Therefore, the synthetic studies were performed on this chemical structure.

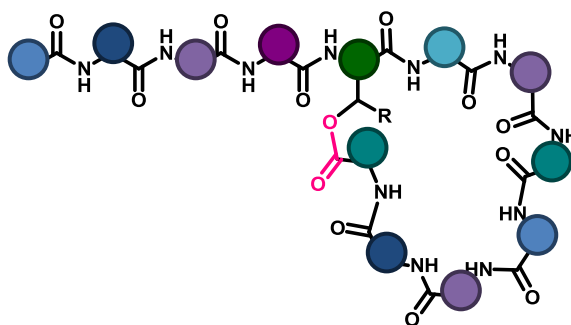


**Figure 15:** Preliminary structure proposed for Pipecolidepsin A. The structural uncertainties are highlighted in red.

### 1.3. Towards the synthesis of proposed Pipecolidepsin A

#### 1.3.1. General considerations prior to the synthetic strategy establishment

The distinctive motive of depsipeptides is the presence of, at least, one ester bond in its backbone. In the large family of heterodetic “head-to-side-chain” cyclic peptides (Figure 16), the ester bond is the linkage at the branching position. Usually, all synthetic strategies developed for this family of depsipeptides, revolve around this unit.



**Figure 16:** Model structure for the “head-to-side-chain” cyclodepsipeptides family. The ester bond is highlighted in pink.

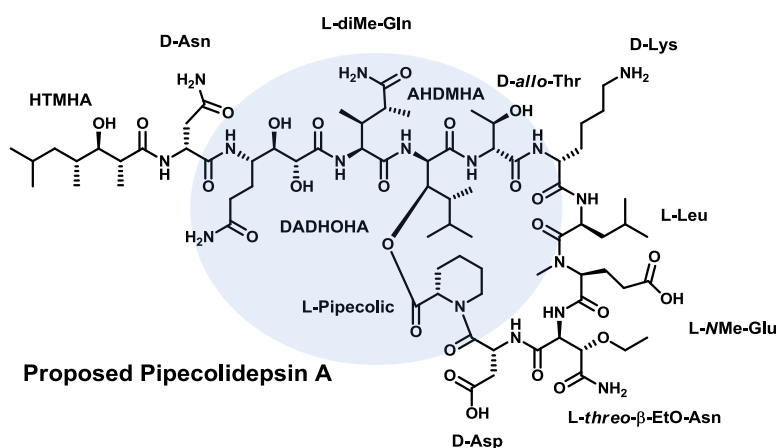
First of all, its formation represents the most challenging step in their syntheses. The hydroxyl function is less nucleophilic than the amino function hence the carboxylic acid requires a stronger activation to form an ester than to form an amide. However, this strong activation puts chiral integrity of the amino acids at risk. Finding the balance between yield and minimization of racemization, usually turns into the bottleneck of a depsipeptide synthesis.

Secondly, its presence can be associated with two severe side reactions: formation of diketopiperazines (DKP) during the handling of the second amino acid after the ester bond formation; and the  $N \rightarrow O$ -transacylation when the ester is formed before the removal of the  $N^\alpha$ -protecting group of the hydroxyl amino acid.<sup>74</sup>

In the big family of the “head-to-side-chain” cyclodepsipeptides synthesized by marine sponges, the  $\beta$ -hydroxy- $\alpha$ -amino acid placed at the branching position always has *D-allo*-configuration, being the *D-allo*-Thr the most frequent one, and the *D-allo*- $\beta$ -HO-Leu and the *D-allo*-AHDMA residues other examples. As it is well known, Thr is the most hindered of the natural amino acids, and the *D-allo*-Thr adds the extra complexity of the poor commercial availability. In terms of uniqueness and intricacy, Pipecolidepsins represents a paradigm. This family contains the *D-allo*-AHDMA residue, which in colloquial terms could be called as a

super Thr because incorporates a 2-methyl-butan-3-yl radical to the already hindered Thr. To add extra difficulty to peptcolidepsins syntheses, their unprecedented AHDMHA moiety is surrounded with another four rare and bizarre residues. Thus, AHDMHA acylates to a  $\beta$ -hydroxy- $\alpha$ -amino acid [D-*allo*-Thr(<sup>t</sup>Bu)], and is acylated by the unusual diMe-Gln, which is, in turn, acylated by the highly hindered  $\gamma$ -amino acid DADHOHA. The construction of the  $\beta$ -branched arrangement is carried out *via* esterification of the hydroxyl function of AHDMHA with the *N*-alkylated L-pipecolic acid, which in addition of its sterical hindrance, is prone to facilitate DKP formation.

The assembly of the peptidic core centered at the AHDMHA residue (Figure 17), the construction of the  $\beta$ -branched arrangement through an extremely hindered ester bond and the presence of many uncommon residues makes the preparation of proposed Pipecolidepsin A an unprecedented *tour de force*.



**Figure 17:** Preliminary structure proposed for Pipecolidepsin A. The peptidic core is highlighted in blue.

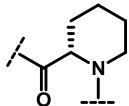
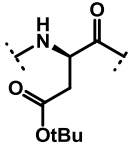
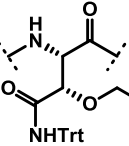
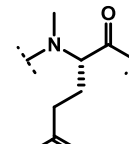
The extremely complex structure of proposed Pipecolidepsin A strongly demands a versatile synthetic approach which facilitates the attempt of many peptide chain assembly schemes, coupling conditions and cyclization strategies. In comparison with peptide synthesis in solution, the solid-phase approach offers a better flexibility and rapidness that facilitate a large number of trials, necessary to find a validated synthetic route for the target molecules. Furthermore, in a medicinal chemistry program, it will enable a more straightforward access to analogs. Thus, the SPPS was the strategy of choice to face proposed Pipecolidepsin A synthesis.

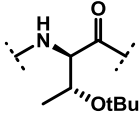
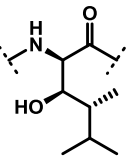
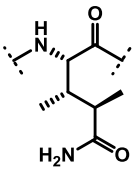
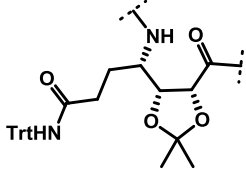
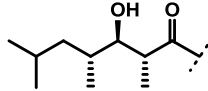
### 1.3.2. Design of proposed Pipecolidepsin A synthetic strategy

Before undertaking the design of the synthetic strategy for proposed Pipecolidepsin A, a careful analysis of the main obstacles that can be found during its synthesis was carried out. On the basis of this study, the first choices were made.

#### 1.3.2.1. Potential side reactions

A detailed description of all the secondary reactions and the main synthetic challenges to consider during proposed Pipecolidepsin A syntheses is shown in Table 1. It is important to take into account that all these side reactions, common in SPPS, can be more important in the synthesis of our desired molecule, due to the presence of extremely hindered amino acids (mostly *N*-alkyl and  $\beta$ -branched residues), which are usually in consecutive positions. This will be translated into poor acylation rates with the consequent longer reaction times, therefore facilitating the side reactions.

Residue	Potential side-reactions and synthetic challenges
	Racemization Stability of the ester in front of the synthetic conditions $\beta$ -branched arrangement
	Aspartimide formation
	Elimination of the EtO- moiety Decreased coupling rate due to the steric hindrance Non-commercial availability
	Decreased acylation rate due to the <i>N</i> Me group

	Decreased coupling rate due to steric hindrance
	Acylation of the unprotected hydroxyl group Formation of the ester bond over a secondary and extremely hindered hydroxyl group DKP formation within the chain Decreased coupling rate due to steric hindrance Non-commercial availability
	Dehydration to nitrile of the unprotected side-chain amide Intramolecular lactamization Decreased coupling rate due to steric hindrance Non-commercial availability
	Decreased coupling rate due to steric hindrance Non-commercial availability
	Acylation of the unprotected hydroxyl group Decreased coupling rate due to steric hindrance Non-commercial availability

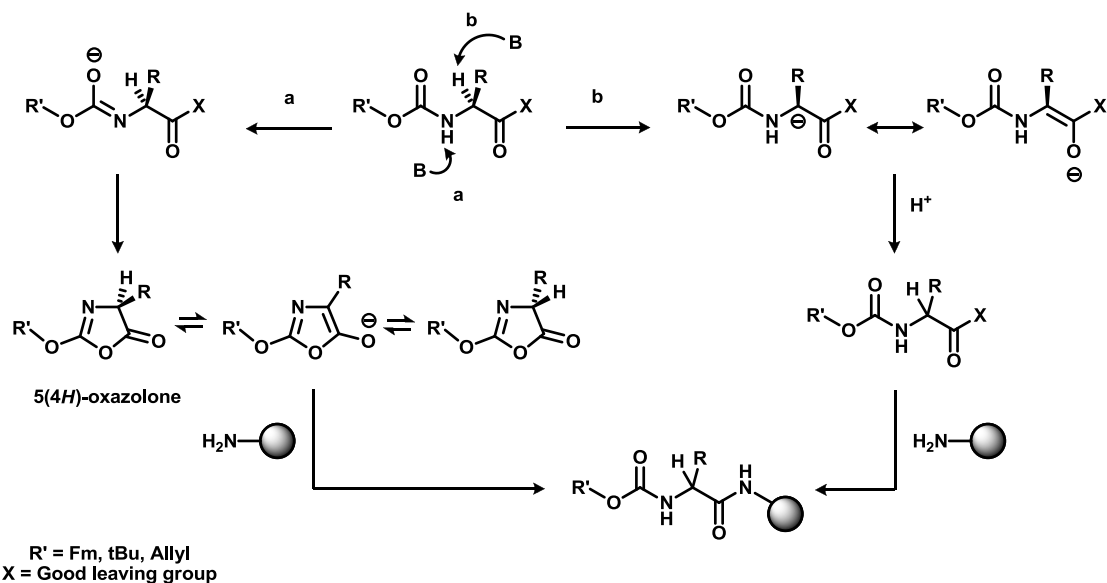
**Table 1:** All side reactions associated with Pipecolidepsin A residues.

Racemization and the formation of the DKP after  $N^\alpha$ -deprotection of the second aa coupled onto the resin must be also considered as potential side reactions.

### Racemization

Although this side reaction can take place in all coupling conditions, it is expected to be more significant during the esterification step. The ester bond will be formed *via* reaction of the hydroxyl group with the activated carboxylic acid.<sup>1</sup> The epimerization can occur *via* both direct enolization and 5(4*H*)-oxazolone formation (Scheme 1).

<sup>1</sup> Formation of the ester *via* displacement of halides or activated alcohol moieties by the carboxylic/carboxylate group has been discarded because the secondary alcohol would rather undergo an elimination side reaction.

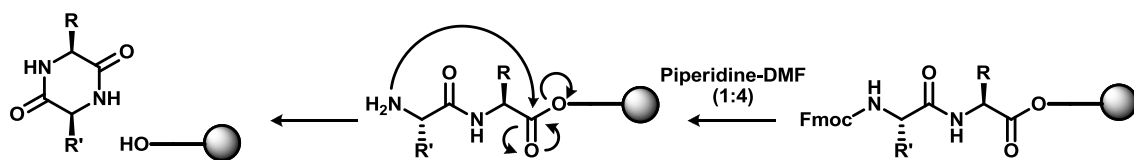


**Scheme 1:** Racemization mechanisms during activation step.

Remarkably, the ester bond links the two residues placed at the branching position of proposed Pipecolidepsin A. This feature, together with the large steric hindrance exerted by the secondary alcohol of the AHDMHA moiety, are the strongest synthetic delicacies of this ester bond. This highly impeded environment will favor racemization, so ester bond formation should be carefully monitored. Finally, the ester bond's stability in acid and basic conditions will also need to be studied.

### DKP formation

Diketopiperazines are cyclic by-products typically occurring during SPPS of peptide-acids.<sup>91</sup> Once the  $\alpha$ -amino group of the (n-1)-aa is unprotected, it can attack intramolecularly the carbonyl group of the peptide-resin linkage,<sup>92</sup> therefore furnishing these cyclic dipeptides (Scheme 2).



**Scheme 2:** Mechanism of DKP formation

The extent of this secondary reaction depends on several factors. The presence of residues, in either the first (n) or the second (n-1) position, that can easily adopt a *cis*-configuration of the amide bond, such as Gly, Pro or *N*-alkyl amino acids, specially favors DKP



formation. Furthermore, a combination of one L-aa and one D-aa, also promotes this side reaction because of stereochemical factors (Figure X). The opposite chirality of the two  $C^\alpha$  enables a favorable transition state leading to the formation of the DKP. Finally, the nature of the solid support is the most important factor. Good leaving groups or small steric hindrance at the peptide-resin linkages significantly boost this secondary reaction. Weak acids and bases catalyze the DKP formation reaction.

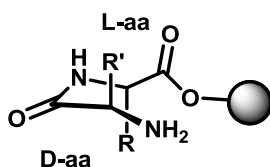
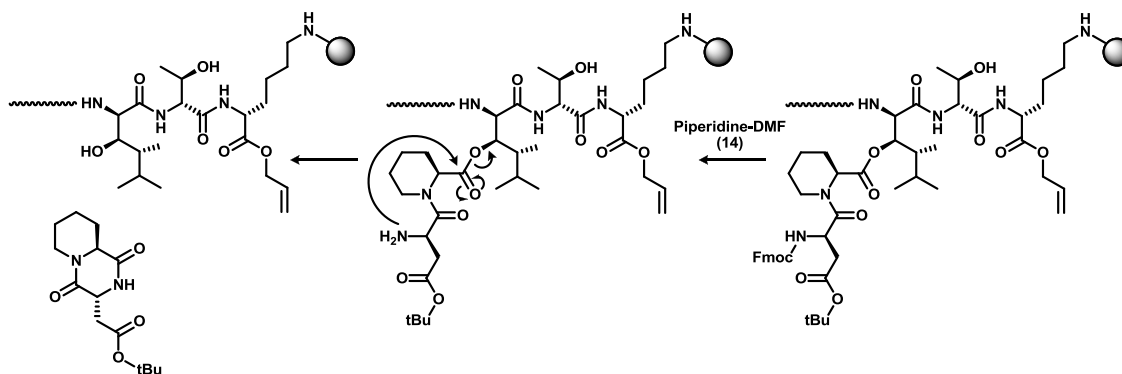


Figure 18: Favored combination L-aa and D-aa at the C-terminus

Minimization of this side reaction is achieved by careful selection of the solid support and by adoption of specific protocols according to the protection strategy. In Boc chemistry, *reverse addition*, this means adding the carbodiimide before the aa, or *in situ* neutralization of the dipeptide-resin when coupling the third aa, strongly decreases the DKP formation rates. In Fmoc chemistry, elimination of the Fmoc group using fast piperidine treatments or TBAF deprotection conditions, efficiently minimize the extent of this side reaction. Although synthetically more demanding, incorporation of the second and third amino acids as protected dipeptides is an alternative protocol useful for both protection strategies when facing the assembly of the most severe sequences.

Proposed Pipecolidepsin A has a unique structural arrangement, a “head-to-side-chain” macrocyclic region through an ester bond terminated with a polyketide moiety. The presence of both, a cyclic and a linear domain in the depsipeptide, represents an extra degree of complexity that must be considered when choosing the starting and the cyclization points. A peptide chain growing in two directions, with its protection requirements and all the additional steric hindrance, are some of the synthetic challenges of a  $\beta$ -branched arrangement. Furthermore, the peptide being elongated through the ester bond entails a DKP formation side reaction within the chain, specially favored by the presence of the pipercolic moiety at the  $n$  position (with regard to the ester bond) (Scheme 3).

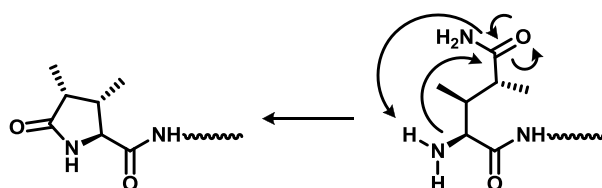


**Scheme X:** Mechanism of formation of DKP within the chain for Pipecolidepsin A.

Thus, not only DKP formation at the C-terminus but also within the chain after ester bond formation will be considered as potential side reactions when attempting Pipecolidepsin A synthesis.

#### PyrodiMeglutamic formation

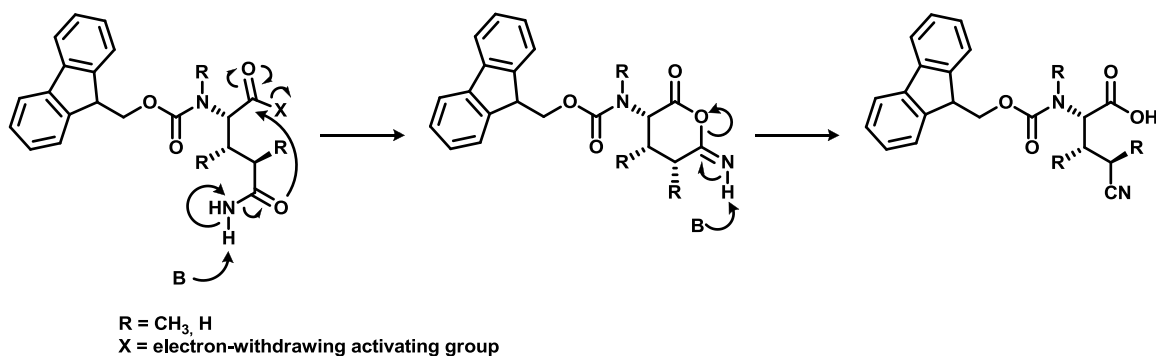
Completely unprotected Gln tends to cyclize both in acid and basic conditions as well as in the presence of metal ions. The two extra methyl substituents of the diMe-Gln moiety dramatically increase this tendency, turning the pyrodiMeglutamic derivative into the main by-product of proposed Pipecolidepsin A synthesis (Scheme 4). Sterical reasons could account for this promotion. This side reaction takes place when the  $\alpha$ -amino group of diMe-Gln is unprotected, this means, during Fmoc elimination and Fmoc-DADHOHA(acetonide, Trt)-OH coupling. Careful optimization of these two processes will be required.



**Scheme 4:** Mechanism of pyrodiMeglutamic formation

#### Dehydration of side-chain amides in Gln-related moieties

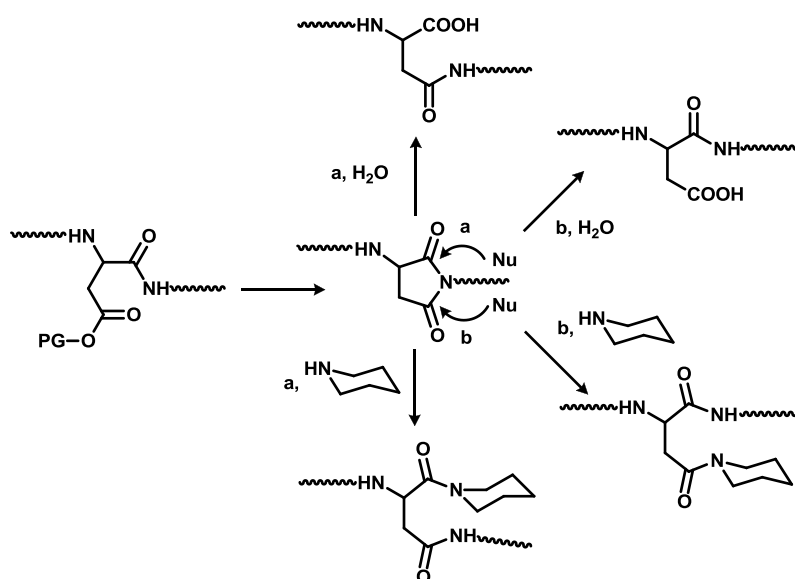
Unprotected side-chain amide of Gln typically undergoes dehydration to nitrile when the  $\alpha$ -COOH is in its activated form (Scheme 5). DiMe-Gln will also furnish the corresponding nitrile derivative. The presence of base during the activation step favors this side-reaction. Fine tuning of the coupling conditions will be carried out to minimize it. Whether or not this side reaction is promoted by the presence of two extra methyl groups will be investigated.



**Scheme 5:** Unprotected side-chain amides dehydration mechanism

### Aspartimide formation

Aspartimide formation occurs during peptide chain elongation under basic or acidic catalysis (Scheme 6). Troublesome sequences are Asp-Gly, Asp-Ala, Asp-Ser and, particularly, Asp(<sup>t</sup>Bu)-Asn(Trt). Sterically hindered protecting groups for the ω-COOH and a small percentage of HOBt in the piperidine solution used for the Fmoc elimination, minimize this secondary reaction. In proposed Pipecolidepsin A, the D-Asp is coupled to an *N*-alkylated residue (pipecolic), what completely discards the occurrence of this side-reaction.



**Scheme 6:** Mechanism of aspartimide formation

#### 1.3.2.2. Polymeric support and protection scheme

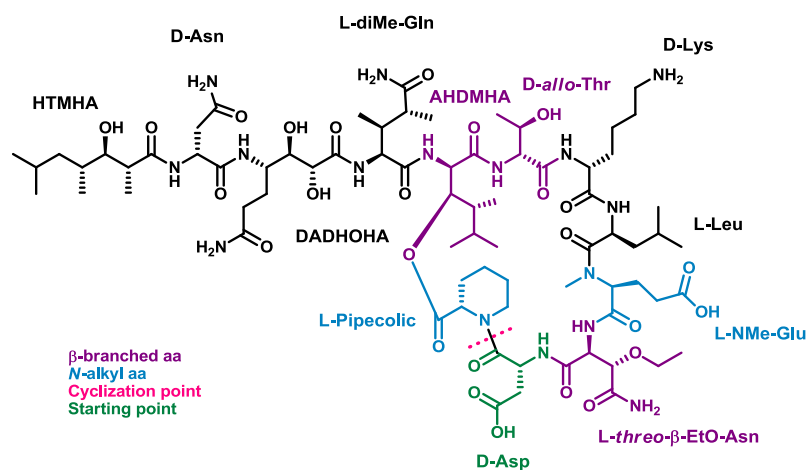
SPPS typically uses two protection strategies: Boc/Bzl and Fmoc/<sup>t</sup>Bu. The first strategy requires harsh acidic conditions for α-amino deprotection and for cleavage of the linkage peptide-resin, while the second strategy enables peptide synthesis in milder conditions. Due to the unknown stability of the ester bond and of the non-natural residues present in proposed

Pipecolidepsin A, the strategy suggested was based on the safer Fmoc chemistry. Thus, the temporary protecting group will be base-labile (Fmoc) and all side-chain protecting groups acid-labile (<sup>t</sup>Bu for acids and hydroxyls, Trt for amides, Boc for amines and acetonide for 1,2-diols). The permanent protecting group at the C-terminus will be chosen among all the polymeric supports that enable the synthesis of peptide-acids. 2-Chlorotrityl resin (2-CTC)<sup>93,94</sup> was finally chosen because it minimizes DKP formation and furnishes completely protected peptides after cleavage, enabling the performance of the key cyclization step not only on solid-phase but also in solution. This resin is quantitatively cleaved under extremely mild acid conditions (1% TFA in DCM, a mixture of AcOH and trifluoroethanol in DCM or hexafluoroisopropanol in DCM) providing a partially orthogonal protection scheme.

The “head-to-side-chain” nature of proposed Pipecolidepsin A forces the implementation of another level of orthogonality in the general protection strategy. Thus, the amino and the acid functions involved in the cyclization step will be protected with Allyl-based moieties, this means Allyl ester and Alloc group. These protecting groups are only removed in neutral reductive conditions which do not affect the rest of protecting groups.

#### 1.3.2.3. Starting and cyclization points

The efficiency of a peptide synthesis is directly affected by the choice of the starting and cyclization points. Usually, these two points concur in the same residue and their selection must be carefully undertaken, especially when the synthesis of a  $\beta$ -branched peptide is faced. All possible cyclization points in proposed Pipecolidepsin A involve  $\beta$ -branched or *N*-alkylated residues with one exception: D-Lys(Boc)-Leu. Nevertheless, choosing the D-Lys(Boc) residue as the starting point would entail the formation of the sensitive ester bond at a really early stage, the elongation of the peptide chain in two directions and the occurrence of DKP within the chain. Therefore, other possibilities were examined and the D-Asp in the cycle was finally chosen considering the following advantages: (i) possibility of carrying out the macrolactamization step both on solid phase and in solution; (ii) ester bond construction at a later stage of the peptide synthesis; (iii) minimization of the DKP formation involving both *N*-alkyl amino acids and embedded ester bonds; (iv) avoidance/minimization of peptide elongation in two directions (Figure 19).

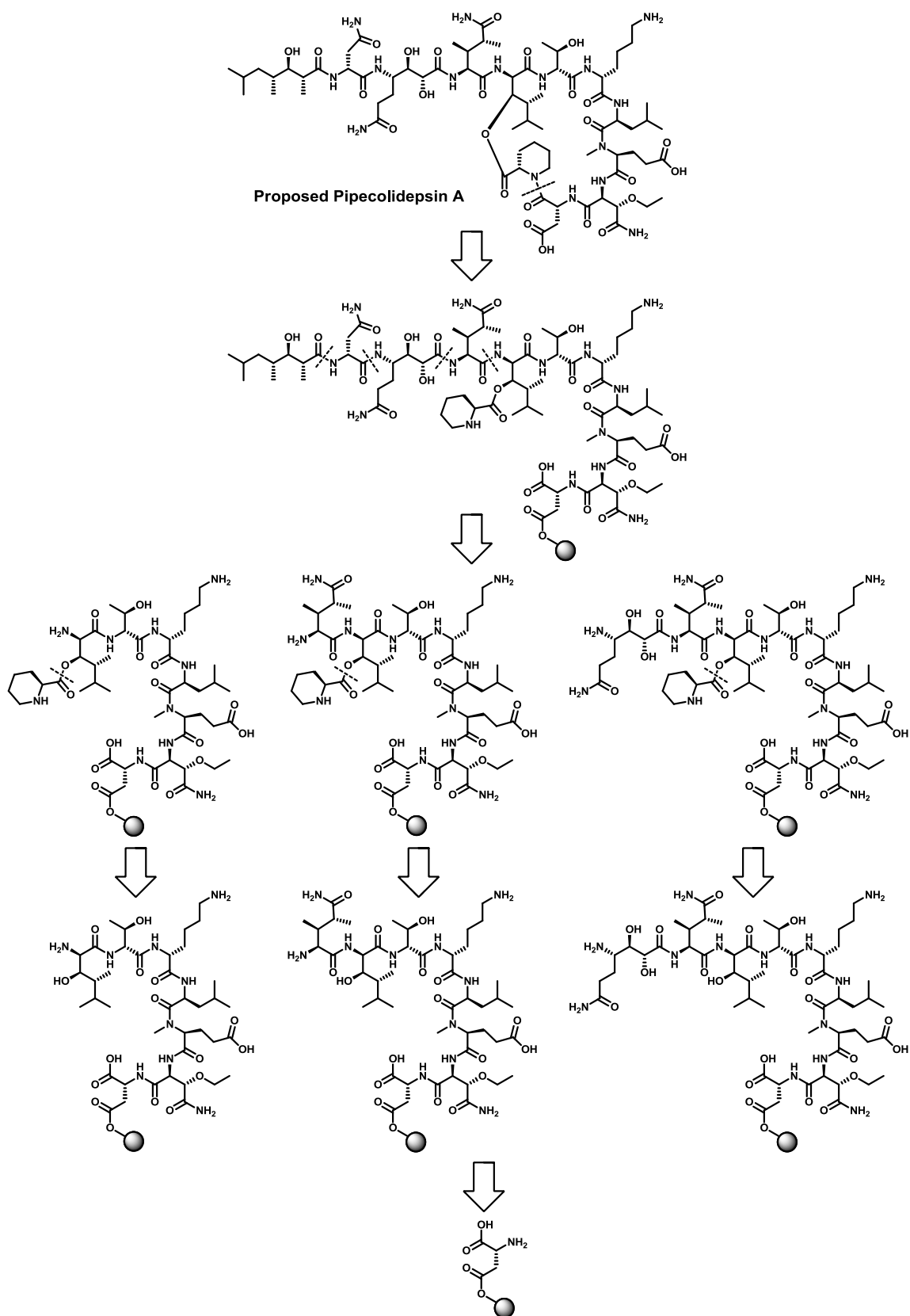


**Figure 19:** Starting and cyclization points selected for proposed Pipecolidepsin A synthesis. β-branched and N-alkylated aa within the cycle are highlighted in purple and blue respectively.

#### 1.3.2.4. Coupling conditions and peptide chain elongation

HATU-HOAt-DIEA<sup>95</sup> was adopted as the coupling system for the amide formation during proposed Pipecolidepsin A synthesis. This cyclodepsipeptide has a significant abundance of highly hindered amino acids, specially β-branched and N-alkyl residues, and comprises up to 6 synthetic moieties. These two features account for the selection of a highly efficient coupling method that will maximize coupling rates using minimum amounts of amino acids and with minimized side reactions. The uronium salt HATU, largely fulfils these synthetic demands with one main drawback, a guanidylated secondary reaction that can be minimized using reaction times below 1.5 h and a small shortage of the coupling reagent. Ester bond formation demands an exhaustive analysis of conditions that will be detailed in section 1.5.3.2.

With all these considerations in mind, the following schematic retrosynthetic analysis is proposed. Thus, the peptide chain will be elongated in the C→N terminal direction starting from side-chain anchoring of Fmoc-D-Asp(OH)-OAllyl or from direct incorporation of Fmoc-D-Asp(<sup>t</sup>Bu)-OH. The ester bond construction, as the bottleneck of the syntheses, will be evaluated at different peptide assembly stages: after incorporation of Fmoc-D-allo-AHDMHA-OH, Fmoc-diMe-Gln-OH and Fmoc-DADHOHA(acetonide, Trt)-OH (Figure 20).

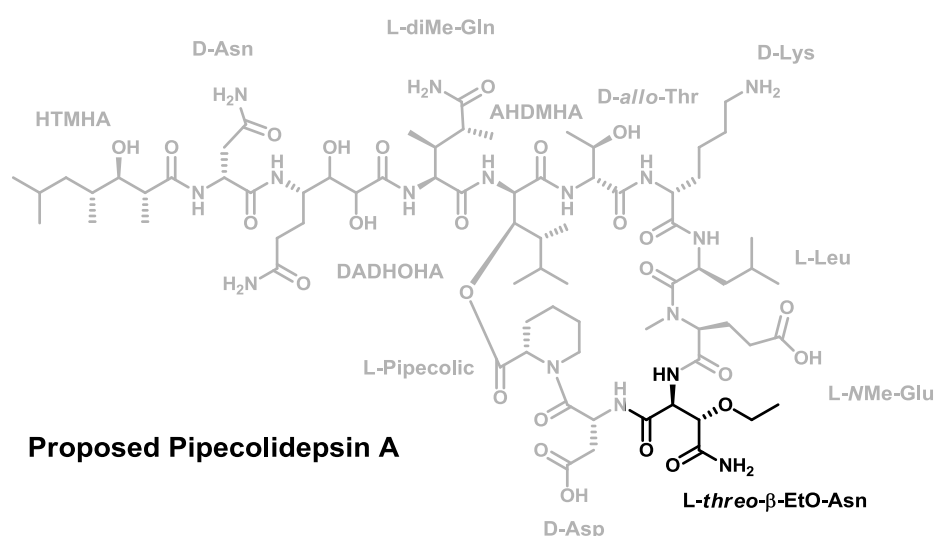


**Figure 20:** Retrosynthetic analysis of proposed Pipecolidepsin A considering solid-phase cyclization.

## 1.4. Synthesis of proposed Pipecolidepsin A's building blocks

Proposed Pipecolidepsin A contains 5 non-commercially available amino acids: *L-threo*- $\beta$ -EtO-Asn, *D-allo*-AHDMHA, *L*-diMe-Gln, DADHOHA and HTMHA. The synthesis of their suitable protected derivatives is the first step of the *tour du force* that will finally lead to synthetic Pipecolidepsin A.

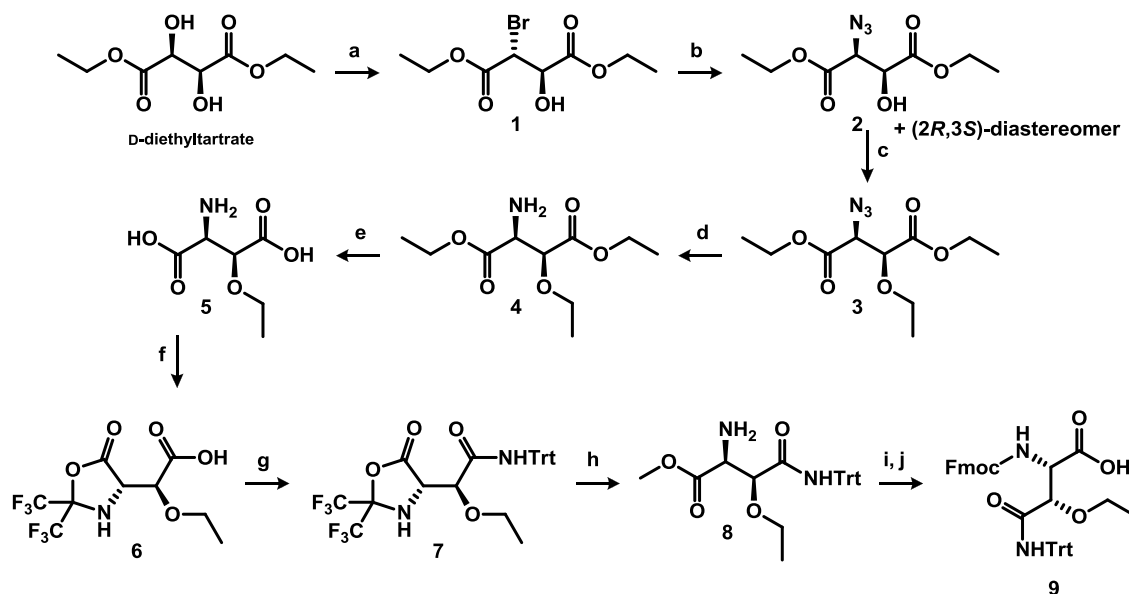
### 1.4.1. Synthesis of Fmoc-*L-threo*- $\beta$ -EtO-Asn(Trt)-OH



**Figure 21:** Preliminary structure proposed for Pipecolidepsin A. The *L-threo*- $\beta$ -EtO-Asn residue is highlighted.

*L-Threo*- $\beta$ -hydroxyasparagine is a non-proteinogenic amino acid present, at least, in two marine cyclodepsipeptides, named Ramoplanin A2<sup>28</sup> and Lysobactin [Katanosin B<sup>96</sup>], displaying interesting bioactivities. Thus, due to its pharmaceutical interest, three enantioselective synthetic approaches have been developed. Boger *et al.* suggested a strategy based on the efficient Sharpless asymmetric aminohydroxylation (AA) of a commercial available cinnamate ester to fix the required *L-threo* configuration.<sup>97</sup> Lectka and co-workers published an approach where the key step was the opening of a  $\beta$ -lactam obtained by an asymmetric [2+2] cycloaddition between a ketene and an imine, using a cinchona alkaloid as the catalyst.<sup>98</sup> Finally, VanNieuwenhze developed a third strategy based on the Cardillo's stereoselective conversion of *L*-aspartic acid into *L-threo*- $\beta$ -hydroxyaspartic acid.<sup>99</sup>

*L-Threo*- $\beta$ -ethoxyasparagine (Figure 21) is a related amino acid found in our target molecule proposed Pipecolidepsin A. An alternative route also starting from *D*-diethyltartrate was designed, validated and published (Scheme 7).<sup>100</sup>



**Scheme 7:** Synthesis of Fmoc-L-threo- $\beta$ -EtO-Asn(Trt)-OH (**9**). a) HBr (30 % in AcOH), 0  $\rightarrow$  25  $^{\circ}$ C, 12 h;  $\text{CH}_3\text{COCl}$ , EtOH, reflux, 8 h, 90%; b)  $\text{NaN}_3$ , 15-Crown-5, dry DMF, 36 h, 90%; c)  $\text{Ag}_2\text{O}/\text{EtI}$ , dry  $\text{Et}_2\text{O}$ , reflux, 15 h, 89%; d)  $\text{H}_2$ , Pd/C, EtOAc, 25  $^{\circ}$ C, 15 h, 87%; e) 5 M aqueous HCl, reflux, 5 h; propylene oxide, 25  $^{\circ}$ C, 84%; f) hexafluoroacetone, dry DMF, 25  $^{\circ}$ C, 22 h, 83%; g) oxalyl chloride, dry DMF, 25  $^{\circ}$ C, 30 min; tritylamine, dry toluene, 0  $^{\circ}$ C, 1 h, 59%; h) MeOH/4 M HCl in dry dioxane, 0  $^{\circ}$ C, 15 h, 95%; i) KOH, dioxane- $\text{H}_2\text{O}$  (2:1), 25  $^{\circ}$ C, 1 h; j) Fmoc-OSu, dioxane- $\text{H}_2\text{O}$  (2:1), pH = 9, 25  $^{\circ}$ C, 1 h, 70% (two steps).

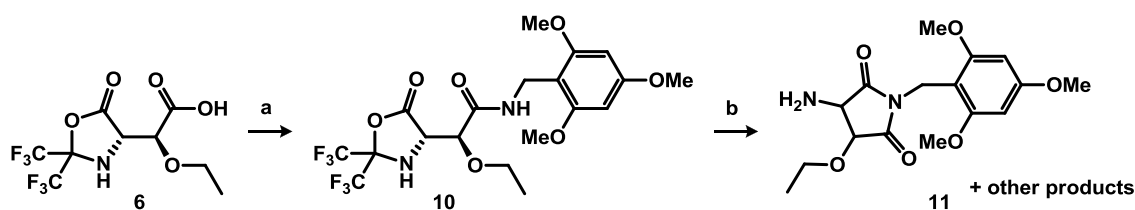
(2*S*,3*S*)-2-azido-3-hydroxysuccinate intermediate **2** was obtained as a diastereomeric mixture with up to 20% of (2*R*,3*S*)-2-azido-3-hydroxysuccinate.<sup>101,102</sup> Although this sub-product was completely eliminated during purification of intermediate **7**, the presence of the (2*R*,3*S*)-diastereomer was taken into account when choosing the reagents to form the ethyl ester. Thus, all the methods based on basic OH-deprotonation and subsequent reaction with EtI were totally discarded due to the risk of epimerization at C3.<sup>103</sup> An epimerization at this carbon would produce not only an amount of (2*S*,3*R*)-diastereomer, but also a percentage of (2*R*,3*R*)-enantiomer. Finally, a mild, non-basic procedure using  $\text{Ag}_2\text{O}/\text{EtI}$  was successfully employed.<sup>104</sup>

After azide to amine reduction, and acid hydrolysis of the ester groups, the differentiation between the two carboxylic acids was accomplished by means of the bidentate protecting/activating reagent hexafluoroacetone (HFA). As previously published by our group, HFA selectively undergoes cyclocondensation with the  $\alpha$ -amino carboxylic acid unit to give 2,2-bis(trifluoromethyl)-1,3-oxazolidin-4-ones.<sup>105</sup> The reaction proceeded with completely chemoselectivity and excellent yields for intermediate **5**.

For the conversion of the unreacted carboxylic acid of intermediate **6** into a suitable protected amide group, the use of the 2,4,6-trimethoxybenzyl-protected amide was reasoned to be easier than the trityl-amide due to its less steric hindrance and superior nucleophilicity. Its lability to acid conditions and its orthogonality to the Fmoc-group turned this protection



group into a valid option.<sup>106</sup> Reaction of intermediate **6** with EDC and 2,4,6-trimethoxybenzylamine (Scheme 8) worked successfully, while the same conditions with tritylamine failed completely. The direct use in SPPS of 2,2-bis(trifluoromethyl)-1,3-oxazolidin-4-ones, like intermediate **10**, is limited,<sup>107</sup> thus, exchange of HFA-protection group for *N*-Fmoc protection was attempted. However, mild hydrolysis of **10** afforded compound **11** *via* a major intramolecular cyclization side reaction between the activated acid and the amide group. After evaluation of the resulting reaction crude, the strategy was ruled out.

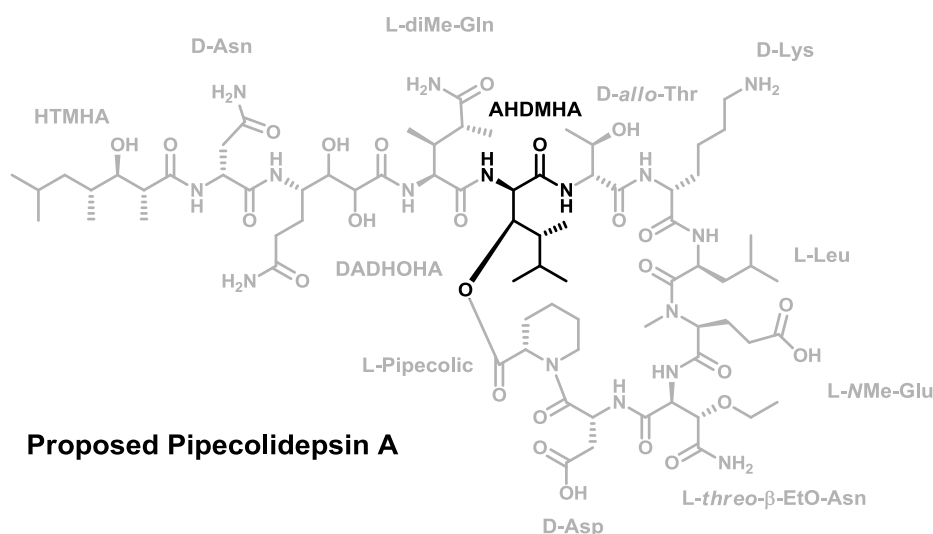


**Scheme 8:** Synthetic scheme of the Tmob-protected amide formation. a) EDC·HCl, 2,4,6-trimethoxybenzylamine, 25 °C; b) H<sub>2</sub>O, 25 °C.

Finally, generation of the trityl-protected amide was successfully achieved with diastereomeric purity by means of strong activation of the carboxylic acid moiety as an acid chloride using oxalyl chloride.

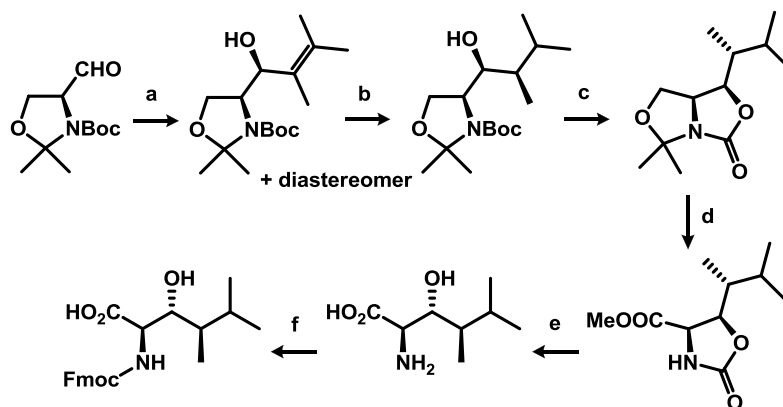
The final hydrolysis of the oxazolidine **7** proceeded very slowly. To overcome this problem, the methyl ester hydrochloride **8** intermediate was synthesized by stirring in a mixture of MeOH-4 M HCl in dioxane.

Fmoc-*L*-*threo*-β-EtO-Asn(Trt)-OH diastereomerically pure was obtained following a 10-step synthesis with an overall yield of 17%.

1.4.2. Synthesis of Fmoc-D-*allo*-AHDMHA-OH

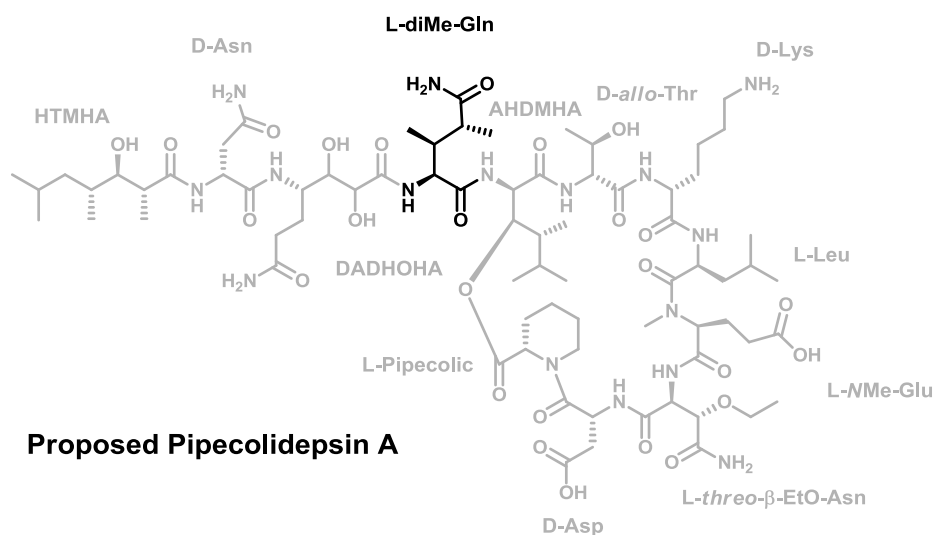
**Figure 22:** Preliminary structure proposed for Pipecolidepsin A. The D-*allo*-AHDMHA residue is highlighted.

The unprecedented residue AHDMHA (Figure 22), as the junction between the C-terminus and the peptide side-chain *via* the  $\beta$ -hydroxy group, is a key amino acid in pipecolidepsins and homophymines. Its absolute configuration was assumed to be in proposed Pipecolidepsin A as the one described for Homophymine A (2*R*,3*R*,4*R*), a hypothesis also supported by the preponderant D-*allo* isomerism of the residues, commonly Thr and  $\beta$ -HO-Leu, found at the branching point of other natural “head-to-side-chain” cyclodepsipeptides from the same family. Several synthetic approaches to  $\beta$ -hydroxy- $\alpha$ -amino acids are already reported<sup>108,109,110,111</sup> due to their importance and presence in nature, while only few examples of the more complex  $\gamma$ -branched  $\beta$ -hydroxy- $\alpha$ -amino acids are described so far.<sup>112</sup> Thus, an efficient stereoselective synthesis that allowed the access to the four possible diastereomers appropriately protected at the amino group (configuration at C2 remained fixed) has been developed by our group (Scheme 9).



**Scheme 9:** Synthesis of Fmoc-D-*allo*-AHDMHA-OH. a) i. 2-bromo-3-methyl-2-butene, <sup>t</sup>BuLi, Et<sub>2</sub>O, -78 °C, 3.3 h; ii. Garner's aldehyde, Et<sub>2</sub>O, -78 → 25 °C, 1.2 h, 34%; b) H<sub>2</sub> (4 atm), Pd(C), MeOH, -78 °C, 2 d, 78%; c) 2,6-di-*tert*-butylpyridine, Tf<sub>2</sub>O, DCM, 0 °C, 10 min, 90%; d) Jones reagent, acetone, 0 °C, 15 h, 67%; e) conc. HCl, reflux, 72 h, 100%; f) Fmoc-OSu, 0.5% Na<sub>2</sub>CO<sub>3</sub>-dioxane (1:1), 25 °C, 15 h, 91%.

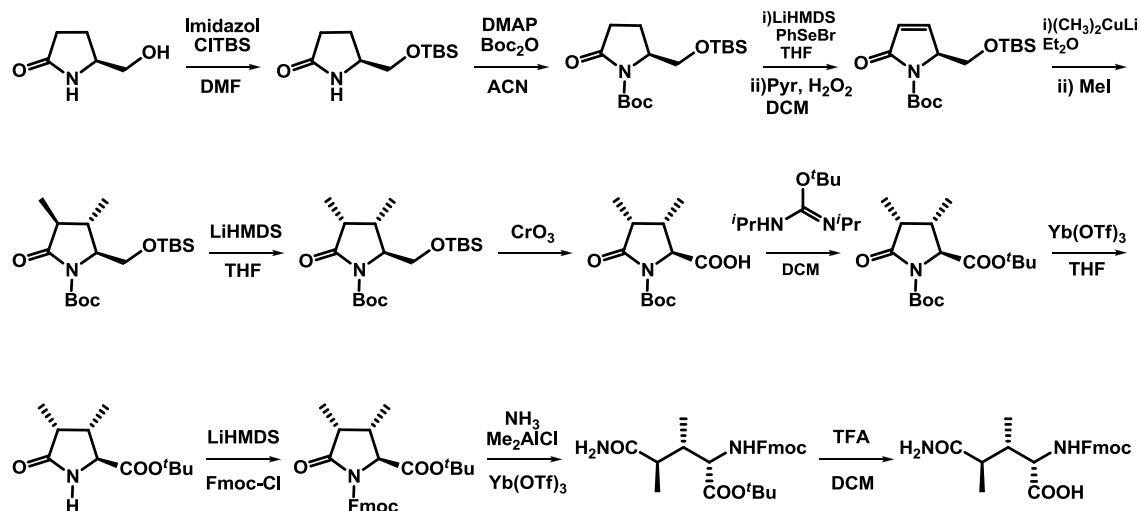
### 1.4.3. Synthesis of Fmoc-diMe-Gln-OH



**Figure 23:** Preliminary structure proposed for Pipecolidepsin A. The L-diMe-Gln residue is highlighted.

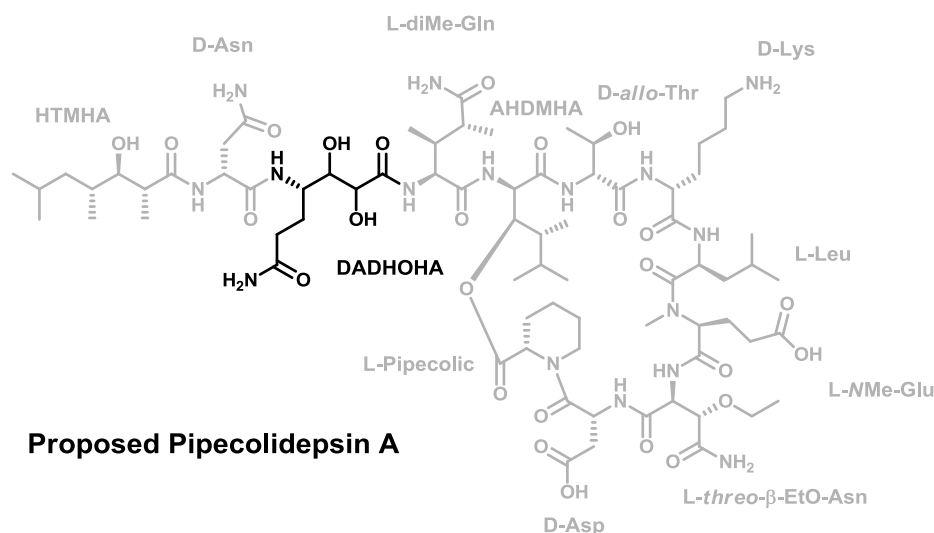
L-DiMe-Gln (Figure 23) is the only aa common to all the “head-to-side-chain” cyclodepsipeptides produced by marine sponges that have been isolated so far. Furthermore, it always acylates the residue placed at the branching position.

Considering its structural interest, several syntheses have been developed.<sup>113,114,115,116</sup> PharmaMar synthesized this building block following procedures described in the literature. Additionally, α-amino protection was carried out under standard procedures known in the literature (Scheme 10).



**Scheme 10:** Synthesis of Fmoc-diMe-Gln-OH. Synthetic scheme followed by PharmaMar.

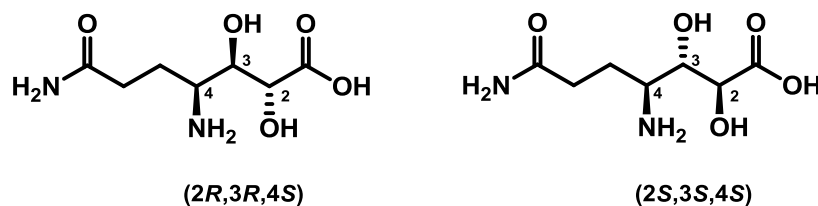
#### 1.4.4. Synthesis of Fmoc-DADHOHA(acetonide, Trt)-OH



**Figure 24:** Preliminary structure proposed for Pipecolidepsin A. The DADHOHA residue is highlighted. No stereochemistry is specified for C2 and C3.

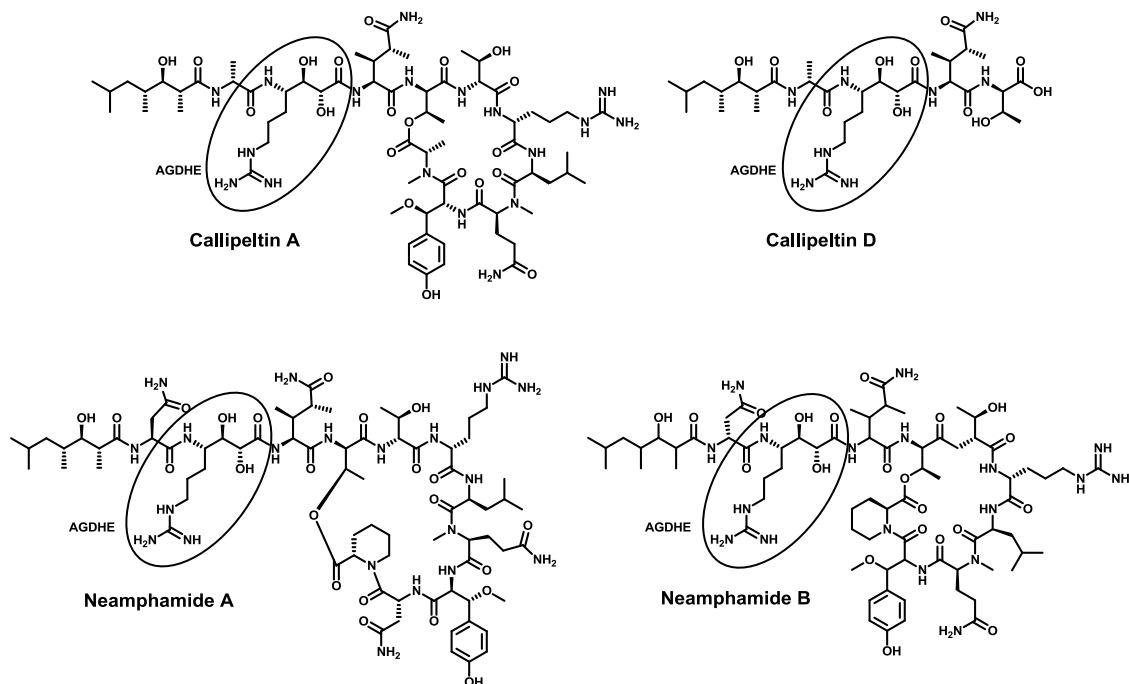
As it has been explained before (see section 1.2.), the DADHOHA (Figure 24) moiety was affected by stereochemical uncertainty. NMR data from the natural Pipecolidepsin A established *S* as the absolute configuration for C4 and strongly suggested that C2 and C3 have the same configuration. Nevertheless, no spectroscopic data provided evidence of the relative configuration between the adjacent hydroxyl and amino groups at C3 and C4 (Figure 25). Marfey's analysis confirmed *S* absolute configuration for C4 but did not shed light on C2 and C3 stereochemistry, as this fragment of the molecule was lost during the acidic hydrolysis of

natural Pipecolidepsin A. Thus, a non diastereoselective synthesis of 4,7-diamino-2,3-dihydroxy-7-oxoheptanoic acid (DADHOHA) was suggested.



**Figure 25:** Chemical structures of the two possible diastereomers of DADHOHA

The  $(2R,3R,4S)$ -4,7-diamino-2,3-dihydroxy heptanoic acid (AGDHE) is a closely-related moiety present in Callipeltin A, linear Callipeltin D and Neamphamide A and B (Figure 26).

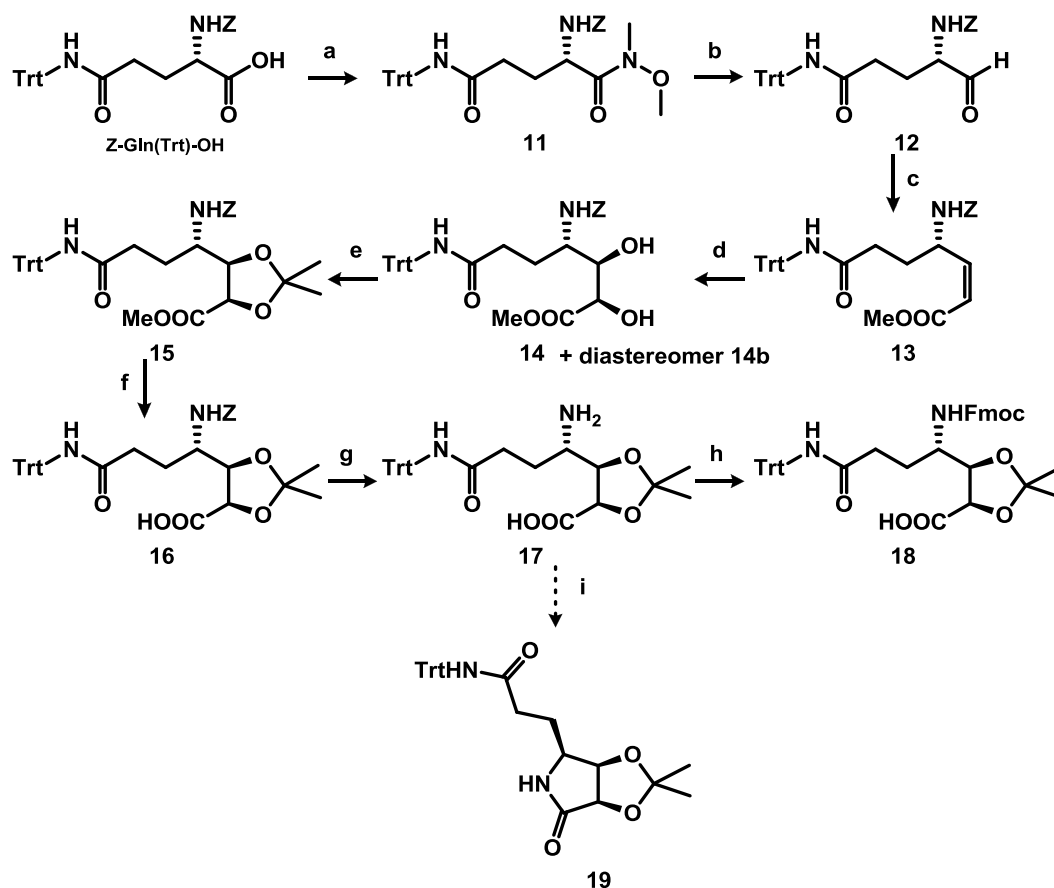


**Figure 26:** Chemical structures of Callipeltin A and D and Neamphamide A and B. The AGDHE moiety is encircled.

Several syntheses of AGDHE and of its amino derivative, in which a  $\omega$ -amino group replaces the  $\omega$ -guanidinium, have been published in the literature so far. Two different synthetic routes starting from a carbohydrate, D-glucose<sup>117</sup> or D-ribose,<sup>118</sup> have been developed. Both are stereoselective syntheses that use the sugar molecule as a chiral template and provide the  $\omega$ -amino derivative after more than 13 synthetic steps and with quite low yields. Moreover, a stereoselective synthesis of the guanide derivative using L-ascorbic acid as

a starting material was also described.<sup>117</sup> Finally, one non-stereoselective and one stereoselective syntheses from a protected L-ornithine derivative were published by Lipton<sup>119</sup> and Kim<sup>120</sup> respectively.

Keeping Lipton's synthesis in mind and starting from the commercially available Z-L-Gln(Trt)-OH, a synthetic route to obtain DADHOHA was proposed (Scheme 11). The two hydroxyl substituents having the same configuration made a *cis*-dihydroxylation mandatory.



**Scheme 11.** Synthesis of Fmoc-DADHOHA(acetonide, Trt)-OH. a) i. EDC, HOBT, dry DMF, 25 °C, 30 min; ii. *N,O*-dimethylhydroxylamine, DIEA, dry DMF, 25 °C, 3 h; 96%; b) LiAlH<sub>4</sub>, dry THF, 0 °C, 30 min, 97%; c) (CF<sub>3</sub>CH<sub>2</sub>O)<sub>2</sub>P(O)CH<sub>2</sub>COOMe, KHMDS, 18-crown-6, dry THF, -78 °C, 3 h, 67%; d) cat. OsO<sub>4</sub>, NMO, THF-H<sub>2</sub>O (9:1), 25 °C, 10 days, 75% (**14**) and 77% (diastereomer); e) (CH<sub>3</sub>)<sub>2</sub>C(OCH<sub>3</sub>)<sub>2</sub>, cat. PPTS, dry toluene, 25 → 60 °C, 36 h, 77% (**15**) and 96% (diastereomer); f) LiOH, THF-H<sub>2</sub>O (7:3), 0 °C, 2 h, 98% (**16**) and 96% (diastereomer); g) H<sub>2</sub> (1 atm), Pd-C (10%), dry MeOH, 25 °C, 5 h, 94% (**17**) and 93% (diastereomer); h) Fmoc-Cl, NaN<sub>3</sub>, dioxane-H<sub>2</sub>O (1:1), pH 9, 0 °C, 5 d, 46% (**18**) and 45% (diastereomer); i) EDC, HOBT, DMF, 25 °C, 6 h, 61% (**19**) and 52% (diastereomer).

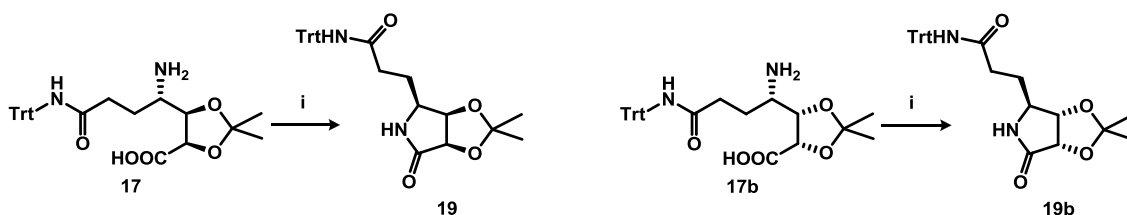
Z-L-Gln(Trt)-OH was converted into the Weinreb-amide using EDC (DCC also provided optimum yields but required an extra purification step) and HOBT and then reduced to the corresponding aldehyde with LiAlH<sub>4</sub>. At this point, a Z-stereospecific Horner-Wadsworth-Emmons olefination, using a Still-Gennari phosphonate in the presence of KHMDS, allowed the transformation of the initial  $\alpha$ -amino acid into a  $\gamma$ -amino acid. The reaction was kept at -78 °C for up to 5 h, but no significant difference in yield was detected when increasing the reaction

time. The reaction did not reach 100% conversion in any case, and no traces of E-alkene were detected in the crude. As purification of the aldehyde did not lead to higher yields, it was finally used without further purification.

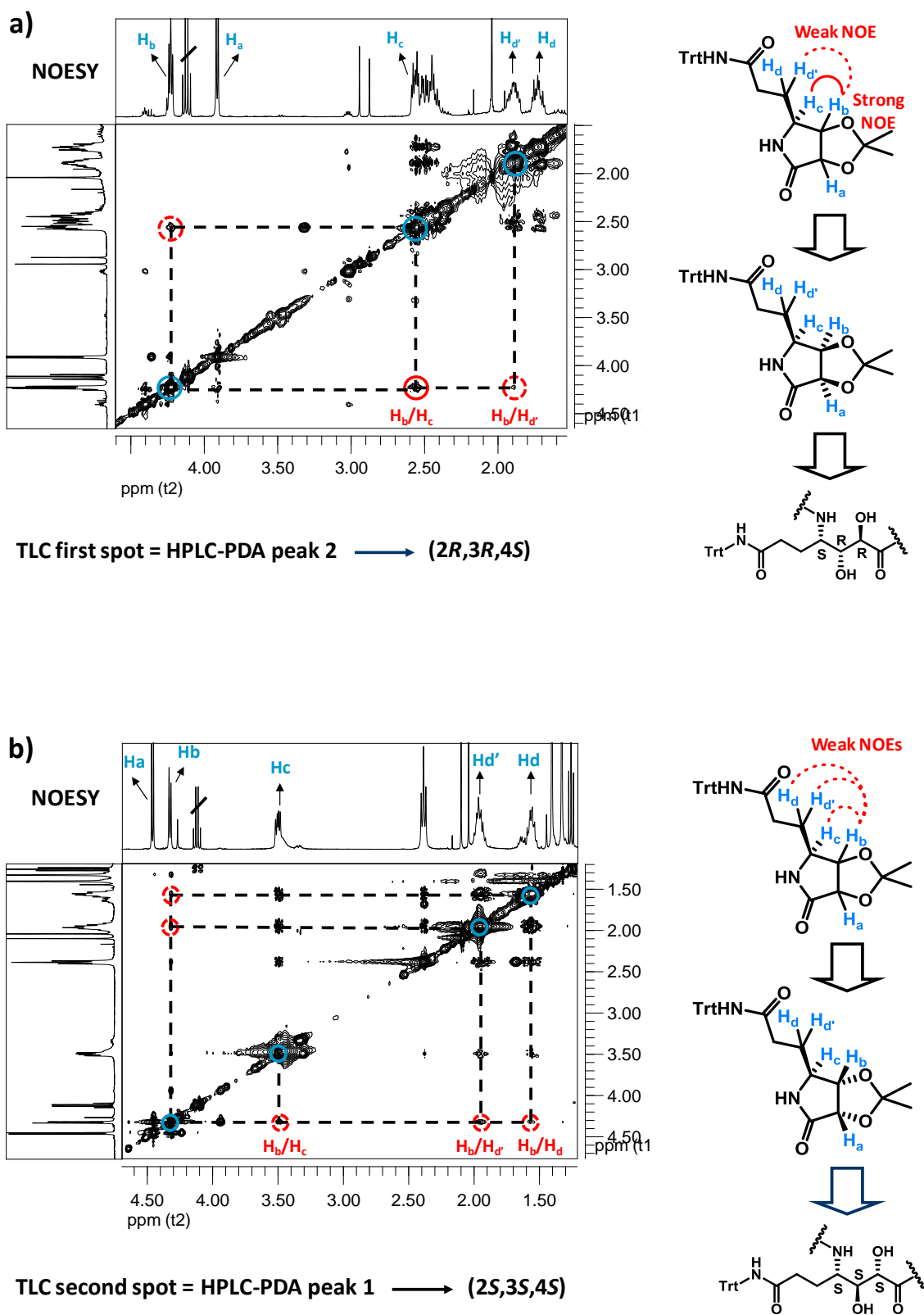
*Cis*-Disubstituted olefins are poor substrates for asymmetric dihydroxylation (AD)<sup>121</sup> being *cis*-allylic and homoallylic alcohols the exception. Some improvements have been done with cyclic *cis*-disubstituted olefins but the enantiomeric excess described for acyclic and non-conjugated olefins are not satisfactory enough.<sup>122,123</sup> Thus, alkene **13** was subjected to dihydroxylation with catalytic OsO<sub>4</sub> and stoichiometric amount of NMO as the oxidant to provide, after purification, the two diastereomeric diols with 75% and 77% yield. The reaction rate is highly dependent on the amount of OsO<sub>4</sub> catalyst and the scale of work. The addition of stoichiometric methanesulfonamide did not represent a reduction of the reaction time.

The diols were protected as pentacyclic acetals in the presence of acetone dimethyl acetal and catalytic PPTS, and then subjected to basic hydrolysis of the methyl ester and hydrogenolysis of the Z group. The last Fmoc-protection step proceeded with moderate yields due to a spontaneous intramolecular lactamization side reaction that happened to occur in all the conditions attempted (Fmoc-Cl, Fmoc-N<sub>3</sub>, Fmoc-OSu).

To accomplish the total stereochemical determination of the building block, it was required to synthesize a more rigid structure that would enable its assignment based on NOE's cross-peaks analysis. Hence, the bicyclic structure **19** was synthesized reacting intermediate **17** with EDC and HOBT (Scheme 12). NOE's cross-peaks interpretation led to univocal assignment of the absolute configuration for C2 and C3 (Figure 27).



**Scheme 12:** Formation of the bicycles *via* intramolecular lactamization of the two diastereomeric forms of the unprotected  $\gamma$ -amino acid obtained. i) EDC, HOBT, DMF, 25 °C, 6 h, 61% (**11**) and 52% (**11b**).

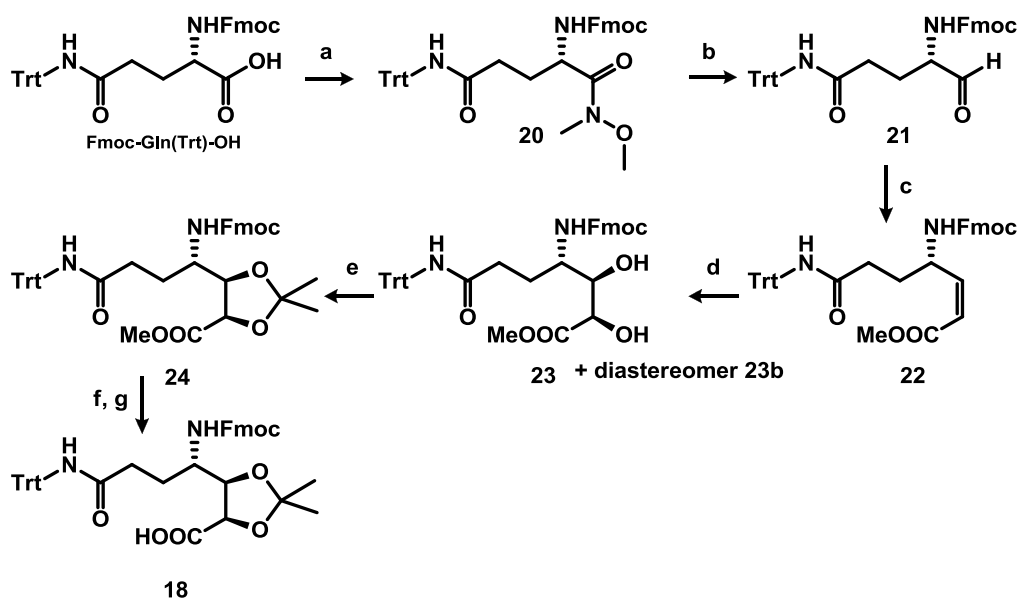


**Figure 27:** NOESY experiments of a) bicycle obtained after lactamization of the first TLC spot; b) bicycle obtained after lactamization of the second TLC spot.



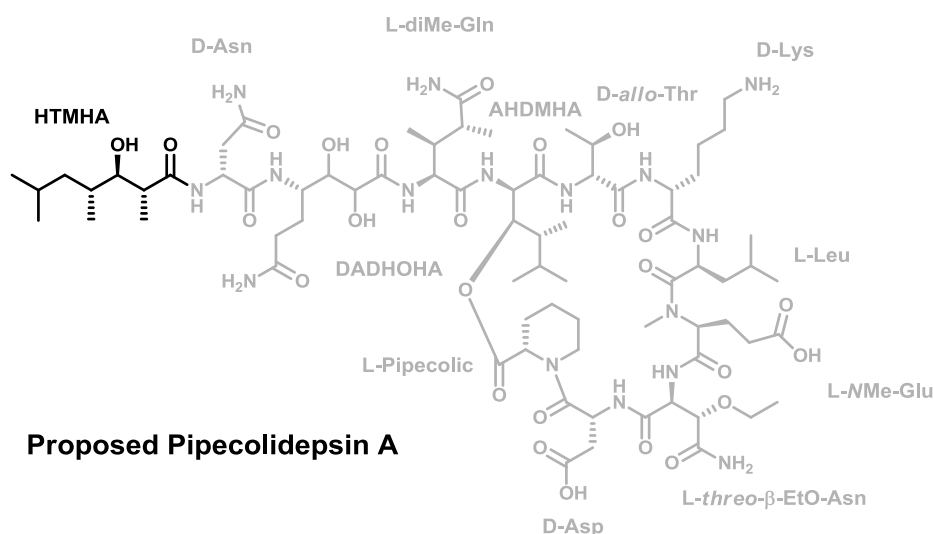
In conclusion, this strategy is a 8-step synthesis that provides the (2*R*,3*R*,4*S*)-4,7-diamino-2,3-dihydroxy-7-oxoheptanoic acid with 15% overall yield and its diastereomer (2*S*,3*S*,4*S*)-4,7-diamino-2,3-dihydroxy-7-oxoheptanoic acid with 19% overall yield.

An analogous synthetic route with a different protection scheme was also developed (Scheme 13). In this strategy, the Fmoc-L-Gln(Trt)-OH was used as the starting material. The main disadvantages of this alternative are caused by the lability of the Fmoc group to basic conditions. Thus, careful handling of the LiAlH<sub>4</sub> reagent during the reduction of the Weinreb amide to aldehyde was required. Decrease of hydride equivalents and reaction times, addition of LiAlH<sub>4</sub> on the amide solution and two different quenching reagents (5% aqueous KHSO<sub>4</sub> and saturated NH<sub>4</sub>Cl solution) did not improve the yield of the synthetic step. Finally, replacement of solid LiAlH<sub>4</sub> by a 1 M solution in dry THF, which addition was easier to control, enabled the loss of only a residual amount of protecting group. Furthermore, partial deprotection of the amino group was impossible to avoid during the basic hydrolysis of the methyl ester intermediate **24**. The use of milder basic reagents (such as LiOOH) and limited equivalents of base at low temperatures were tested, but the results were completely unsatisfactory and the amino function required Fmoc re-protection. On the contrary, this is a shorter route (6 steps) with better overall yields for both diastereomers [24% for (2*R*,3*R*,4*S*) and 30% for (2*S*,3*S*,4*S*)], and simplified purification steps (especially the alkene intermediate) due to the superior bulkyness and hydrophobicity of the Fmoc with respect to the Z group.



**Scheme 13.** Synthesis of Fmoc-DADHOHA(acetonide, Trt)-OH. a) EDC, HOBT, dry DMF, 25 °C, 30 min; *N,O*-dimethylhydroxylamine, DIEA, dry DMF, 25 °C, 3 h, 98%; b) LiAlH<sub>4</sub> (1 M in dry THF), dry THF, 0 °C, 30 min, 96%; c) (CF<sub>3</sub>CH<sub>2</sub>O)<sub>2</sub>P(O)CH<sub>2</sub>COOMe, KHMDS, 18-crown-6, dry THF, -78 °C, 3.5 h, 72%; d) cat. OsO<sub>4</sub>, NMO, THF-H<sub>2</sub>O (9:1), 25 °C, 7 days, 76% (**23**) and 70% (diastereomer **23b**); e) (CH<sub>3</sub>)<sub>2</sub>C(OCH<sub>3</sub>)<sub>2</sub>, cat. PPTS, dry toluene, 60 °C, 24 h, 77% (**24**) and quantitative (diastereomer); f) LiOH, THF-H<sub>2</sub>O (7:3), 0 °C, 2 h; g) Fmoc-OSu, THF-H<sub>2</sub>O (7:3), pH = 8, 25 °C, 12 h, 57% (**18**) and 60% (diastereomer).

### 1.4.5. Synthesis of HTMHA

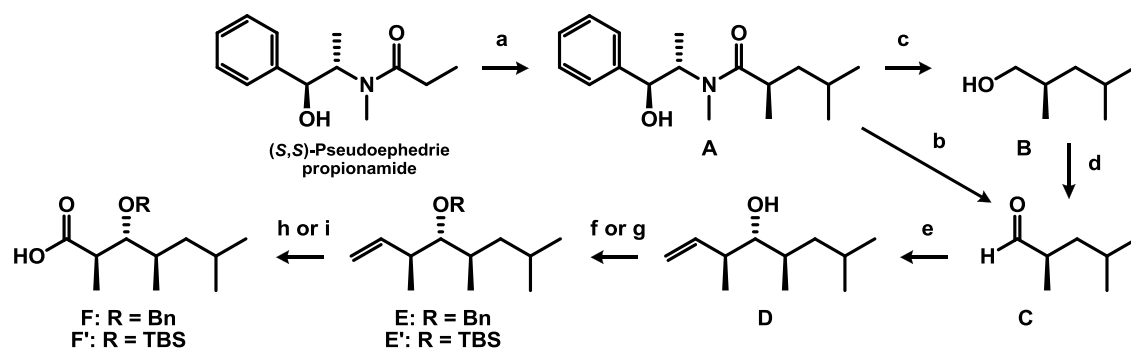


**Figure 28:** Preliminary structure for proposed Pipecolidepsin A. The HTMHA residue is highlighted.

Stereochemical uncertainty also affected the *N*-terminal moiety of Callipeltin A and linear Callipeltin D. Thus, up to three different synthetic strategies to obtain the (2*R*,3*R*,4*S*)-3-hydroxy-2,4,6-trimethylheptanoic acid can be found in the literature. Joullié *et al.* obtained the desired molecule starting from L-valine in nine steps, being the Heathcook variant of the Evans aldol reactions the key transformation.<sup>124</sup> D'Auria and colleagues, also taking advantage of the Evans' asymmetric aldol chemistry, developed an efficient and highly stereoselective 10-step route from commercially available methyl (2*S*)-2-methyl-3-hydroxypropionate.<sup>125</sup> Finally, Yadav and co-workers suggested the desymmetrization of a bicyclic precursor to obtain the same target molecule.<sup>126</sup>

However, exhaustive <sup>1</sup>H and <sup>13</sup>C NMR and optical rotation data comparison of the natural fragment from Callipeltin A with the four synthetic diastereomers (2*R*,3*R*,4*R*), (2*S*,3*R*,4*R*), (2*S*,3*R*,4*S*) and (2*R*,3*R*,4*S*), unambiguously confirmed the stereochemistry (2*R*,3*R*,4*R*) for the common acylating moiety of Callipeltin A and D, Neamphamide A, Homophymine B and B1 and Pipecolidepsin A and B.

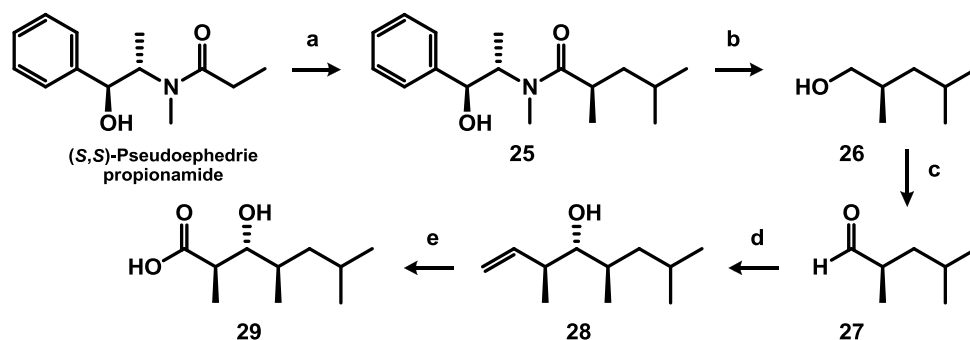
Two different stereoselective syntheses of (2*R*,3*R*,4*R*)-3-hydroxy-2,4,6-trimethylheptanoic acid (Figure 28) with a Brown's crotylboration as the key step have been published so far.<sup>127,128</sup> Thus, D'Auria asymmetrically formed the C3-C4 bond in one step employing this efficient chemistry, while Lipton stereoselectively assembled the C2-C3 bond using the same approach. We decided to reproduce Lipton's strategy, the shorter one, in order to obtain the required building block (Scheme 14).



**Scheme 14:** Lipton's synthesis of (2*R*,3*R*,4*R*)-3-hydroxy-2,4,6-trimethylheptanoic acid. a) LDA, LiCl, dry THF, -78 °C; 1-iodo-2-methylpropane, -78 °C, 98%; b) LiAlH(OEt)<sub>3</sub>, dry hexanes-THF, 0 °C; TFA, 1 M HCl, 86%; c) LAB, dry THF; d) TPAP, NMO, 4 Å MS, dry DCM, 77% (two steps); e) *t*-BuOK, *trans*-2-butene, *n*-BuLi, -78 to -57 °C; (-)-*B*-methoxydiisopinocampheylborane; BF<sub>3</sub>·Et<sub>2</sub>O, **C**, -78 °C, 75%; f) benzyl 2,2,2-trichloroacetimidate, cat. TfOH, dry cyclohexane-DCM, 96%; g) TBSCl, imidazole, dry DCM, 98%; h) cat. OsO<sub>4</sub>, NaIO<sub>4</sub>, NMO, dioxane-H<sub>2</sub>O; NaClO<sub>2</sub>, H<sub>2</sub>NSO<sub>3</sub>H, 95%; i) cat. NaIO<sub>4</sub>/RuCl<sub>3</sub>·H<sub>2</sub>O, CCl<sub>4</sub>-ACN-H<sub>2</sub>O, 98%.

The main problem when reproducing the Lipton's synthesis is the extremely high volatility of the intermediates, especially the alcohol **B**, the aldehyde **C** and the alkene **D**. Thus, chromatographic purification was reduced at the minimum and the protection of the alcohol group of intermediate **D** was considered dispensable and therefore suppressed. Some other variations were also introduced: the LDA required to perform Myers alkylation of commercially available (*S,S*)-pseudoephedrine propionamide was generated *in situ* by means of DIPA reaction with *n*-BuLi; the shorter route *via* reduction of the tertiary amide to aldehyde was discarded; instead, oxidation of the alcohol **B** to the corresponding aldehyde was performed using the efficient Dess-Martin reagent; and the key Brown's crotylboronation could only be reproduced when using new and checked chiral auxiliary (-)-*B*-methoxydiisopinocampheylborane.

Finally, the desired unprotected (2*R*,3*R*,4*R*)-3-hydroxy-2,4,6-trimethylheptanoic acid (HTMHA) was obtained following the modified Scheme 15, even though its final purity and the overall yield were not extremely high. Exhaustive HPLC-PDA purification of the final cyclodepsipeptide would make up for the low purity of the building block.



**Scheme 15:** Modified Lipton's synthesis of (2*R*,3*R*,4*R*)-3-hydroxy-2,4,6-trimethylheptanoic acid. a) DIPA, *n*-BuLi, LiCl, dry THF, -78 °C, 1 h; 1-iodo-2-methylpropane, -78 °C, 3.5 h; b) DIPA, *n*-BuLi, H<sub>3</sub>B-NH<sub>3</sub>, dry THF, -78 → 25 °C, 2 h; c) Dess-Martin, dry DCM, 25 °C, 30 min; d) *t*-BuOK, *trans*-2-butene, *n*-BuLi, -78 → -57 °C; (-)-*B*-methoxydiisopinocampheylborane; BF<sub>3</sub>·Et<sub>2</sub>O, **21**, -78 °C; e) cat. OsO<sub>4</sub>, NaIO<sub>4</sub>, NMO, dioxane-H<sub>2</sub>O, 25 °C, 3 h; NaClO<sub>2</sub>, H<sub>2</sub>NSO<sub>3</sub>H, 0 → 25 °C, 2 h.

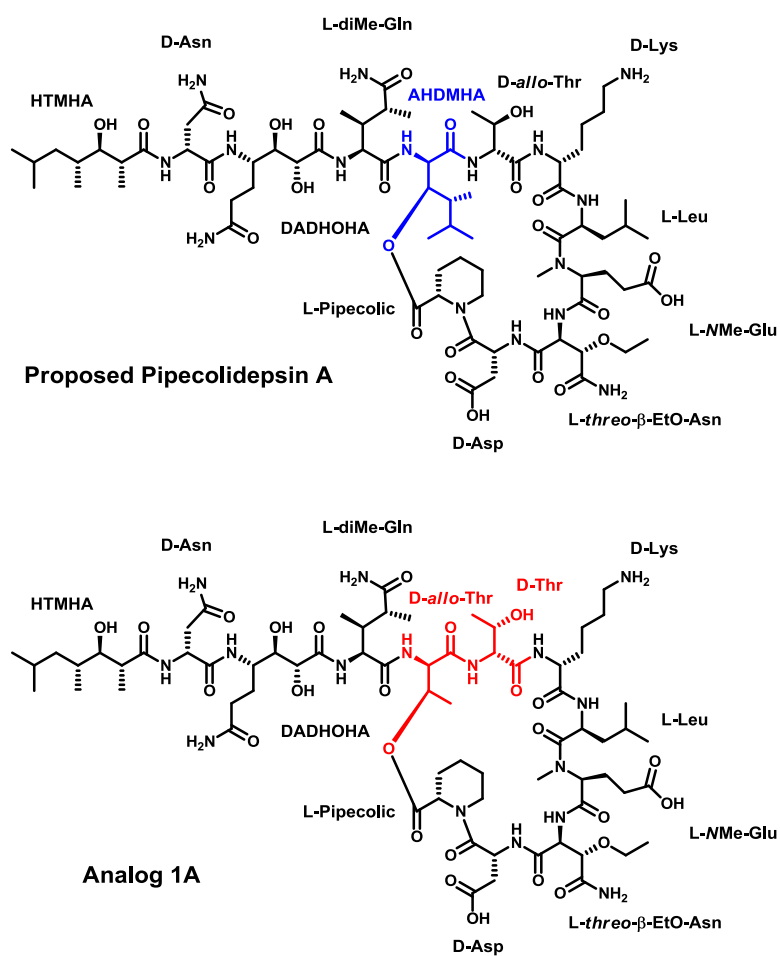
With all the building blocks in hand, the solid phase synthesis of Pipecolidepsin A was attempted.

## 1.5. Solid-phase synthesis of proposed Pipecolidepsin A

### 1.5.1. First approach: synthetic studies of Analog A1

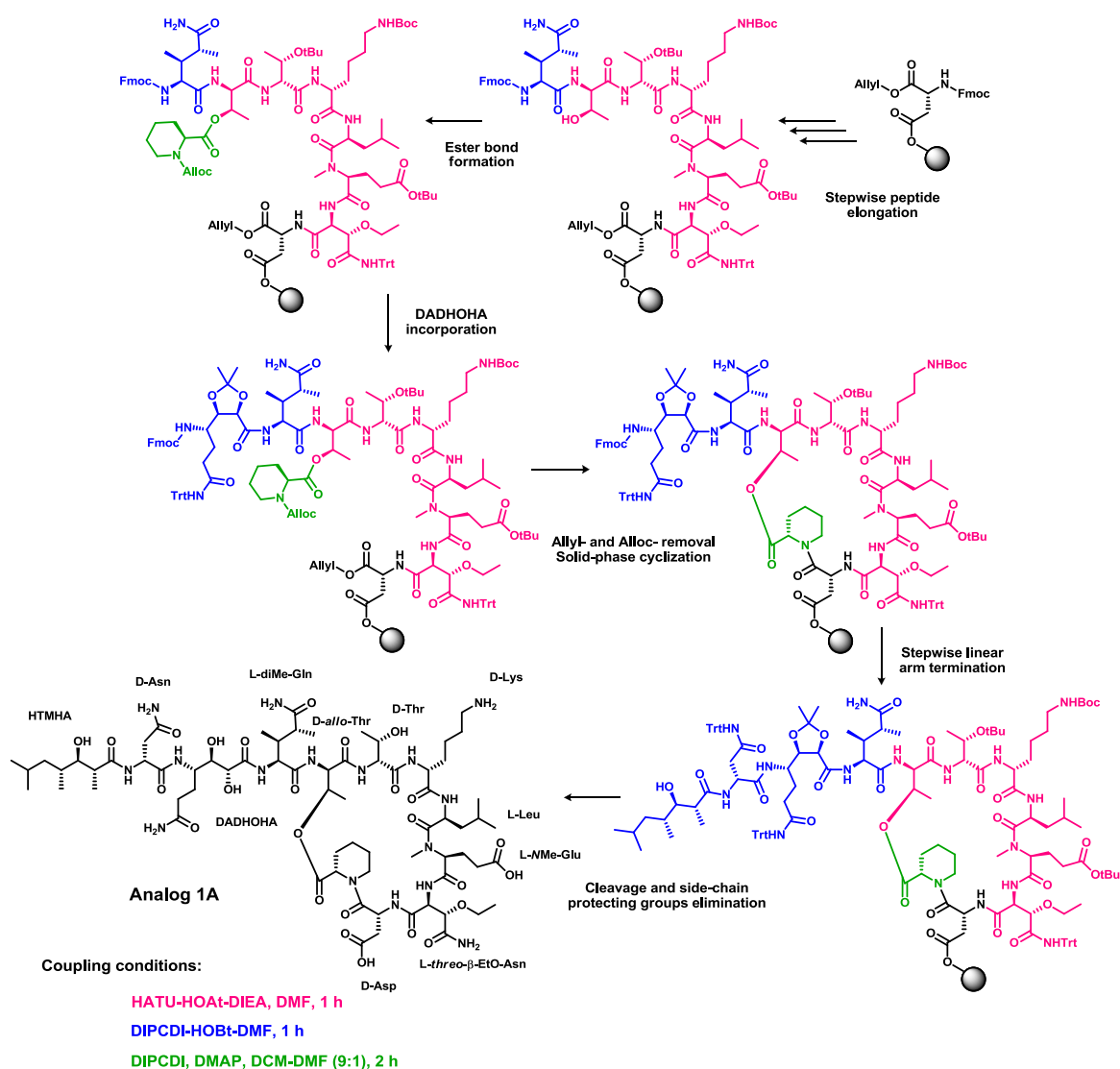
A simplified analog of proposed Pipecolidepsin A (Analog 1A, Figure 29) was designed in order to set up a validated synthetic strategy for the natural cyclodepsipeptide. With that purpose, AHDMHA and *D*-*allo*-Thr(<sup>t</sup>Bu) residues were replaced by the commercially available and less expensive *D*-*allo*-Thr and *D*-Thr(<sup>t</sup>Bu), respectively.<sup>11</sup> With the protection scheme, the polymeric support and the starting and cyclization points already chosen, the synthesis of the analog A1 was carried out paying special attention to all the possible side-reactions previously mentioned (see Section 1.3.2.).

<sup>11</sup> The smaller bulkiness of the *D*-*allo*-Thr in front of the *D*-*allo*-AHDMHA residue was taken into account for the design of the final strategy of proposed Pipecolidepsin A.



**Figure 29:** Preliminary structure proposed for Pipecolidepsin A and chemical structure of Analog 1A. Differences in peptidic sequences are shown in red. The key AHDMHA residue appears in blue.

## 1.5.1.1. First strategy: diMe-Gln + ester. Cyclization before peptide elongation



**Scheme 16:** Analog 1A first synthetic strategy: diMe-Gln incorporation + ester bond formation; cyclization before complete assembly of the linear peptide. Coupling conditions are shown in different colors.

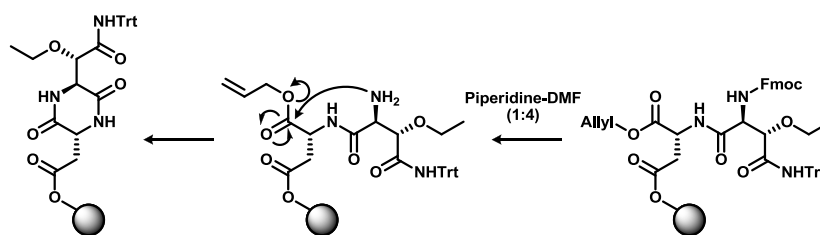
In this first strategy (Scheme 16), the linear peptide was assembled till the diMe-Gln moiety, keeping in place the last Fmoc group. Then, the ester bond was formed and, after Fmoc removal, the DADHOHA residue was incorporated. At this point, the Allyl and Alloc groups were eliminated and the cyclization step was attempted on solid-phase. Finally, the linear arm was elongated and the fully accomplished peptide cleaved from the resin. In a last step, all the side-chain protecting groups were simultaneously removed in solution.

The synthesis of Analog 1A was monitored by reversed-phase HPLC-PDA and HPLC-MS. After all key reactions, a small aliquot of the resin was cleaved under acidic conditions and the

crude analyzed in detail to study the occurrence and the extent of all the side reactions previously considered.

#### L-threo- $\beta$ -EtO-Asn(Trt): DKP formation and ethoxy- elimination

DKP formation was evaluated by Fmoc quantification when deprotecting the residues D-Asp and NMe-Glu(<sup>t</sup>Bu) and by HPLC analysis. As the first residue was incorporated into the resin through the  $\omega$ -COOH group, the corresponding DKP would remain linked to the 2-CTC resin (Scheme 17) making possible its detection by HPLC.



**Scheme 17:** Mechanism of DKP formation in proposed Pipecolidensin A.

HPLC-PDA and HPLC-MS analysis after incorporation of the Fmoc-NMe-Glu(<sup>t</sup>Bu)-OH moiety revealed the presence of one single product, the tripeptide Fmoc-NMe-Glu- $\beta$ -EtO-Asn-D-Asp-OAllyl, precluding either DKP formation or ethoxy- elimination. The loading values found after Fmoc elimination of the D-Asp and the NMe-Glu(<sup>t</sup>Bu) residues also confirmed the absence of DKP formation.

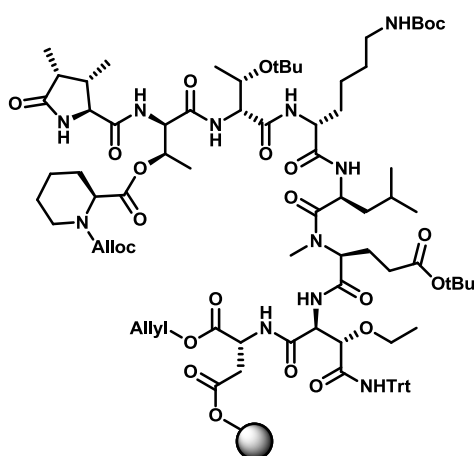
Small amounts of L-threo- $\beta$ -EtO-Asn(Trt) deletion were detected by HPLC analysis when it was incorporated under the conditions aa-HATU-HOAt-DIEA (2.3:2.3:2.3:4.6) in DMF for 1 h. Thus, to achieve quantitative conversions, at least, 2.5 equivalents of aa and highly concentrated coupling solutions in DMF should be used. Finally, the bulkiness of its  $\beta$ -branched character demands an extra 10 min Fmoc-elimination treatment to accomplish quantitative deprotection of the  $\alpha$ -amino group. Therefore, from now on, the Fmoc group from all residues of proposed Pipecolidensin A will be removed using a longer procedure: piperidine-DMF (1:4),  $2 \times 1$  min,  $2 \times 5$  min and  $1 \times 10$  min.

#### diMe-Gln and DADHOHA: dehydration to nitrile and pyrodiMeglutamic formation

The coupling of diMe-Gln residue was performed using DIPCDI-HOBt in DMF. This activation method enables working under mild and close to neutral conditions, which are required to minimize dehydration of diMe-Gln that occurs when the  $\alpha$ -COOH is activated (see section 2.3.2.1.). However, these conditions may not guarantee quantitative incorporation of

such a bulky moiety over a  $\beta$ -branched residue [*D-allo*-Thr(OH) in this analog]. Thus, some experimentation with the reaction times was carried out. A long treatment (aa-DIPCDI-HOBt, 2:2:2; DMF; 1.5 h) resulted in a high percentage of dehydration (up to 33%), while two consecutive coupling treatments (aa-DIPCDI-HOBt, 3:3:3 and 2:2:2; DMF) of 1 h ensured quantitative incorporation with minimized dehydration (down to 7%). The dehydration percentage did not increase after multiple treatments. The replacement of the *D-allo*-Thr with the more bulky AHDMHA residue in the target molecule hampers even more the Fmoc-diMe-Gln-OH incorporation. Thus, adjustment of the equivalents will be required.

Another side-reaction associated with the diMe-Gln moiety is the formation of the pyrodiMeglutamic derivative through an intramolecular lactamization (see section 2.3.2.1.). This cyclization only occurs when the  $\alpha$ -amino group is unprotected, this means, during Fmoc-diMe-Gln deprotection and Fmoc-DADHOHA(acetonide, Trt)-OH coupling. In order to minimize its formation, a 3-min Fmoc elimination treatment was implemented for the diMe-Gln residue, and several coupling conditions for the DADHOHA were examined. This residue was first assembled under the conditions aa-DIPCDI-HOBt (2:2:2, DMF, 1 h), because it remained unknown whether basic conditions, such as HATU-HOAt-DIEA, would favor or not the dehydration side-reaction of the diMe-Gln moiety. HPLC analysis after diol incorporation revealed a substantial percentage of pyrodiMeglutamic by-product (Figure 30), suggesting that the coupling of such a bulky DADHOHA residue in these mild conditions was occurring slowly, and a change in strategy was required. This by-product terminates the growing peptide chain thus decreasing the effective loading of the resin and the overall yield.



**Figure 30:** Terminated peptidic chain by the pyrodiMeglutamic derivative

In subsequent syntheses, the DADHOHA moiety is incorporated before the ester bond is formed. The absence of the ester bond could potentially help to minimize the



pyrodiMeglutamic by-product formation by causing less steric hindrance. This will be carefully examined.

No acylation of the free hydroxyl function of the *D-allo*-Thr moiety was detected by HPLC analysis after Fmoc-diMe-Gln-OH incorporation. As the AHDMHA is more hindered than the *D-allo*-Thr, it is foreseen that its hydroxyl group will not undergo acylation in the synthesis of the target molecule.

#### Pipecolic: ester bond formation

After incorporation of Fmoc-diMe-Gln-OH and before its Fmoc removal, the ester bond was constructed under the common conditions aa-DIPCDI-DMAP (8:8:0.5) in DCM:DMF (9:1). The reaction was quantitative after 2 h of treatment and no epimerization was detected by HPLC analysis. At this point, the bigger bulkiness of the AHMDHA residue can have a negative effect when the syntheses of the target molecule will be attempted. Much more experimentation will be required.

#### Macrolactamization

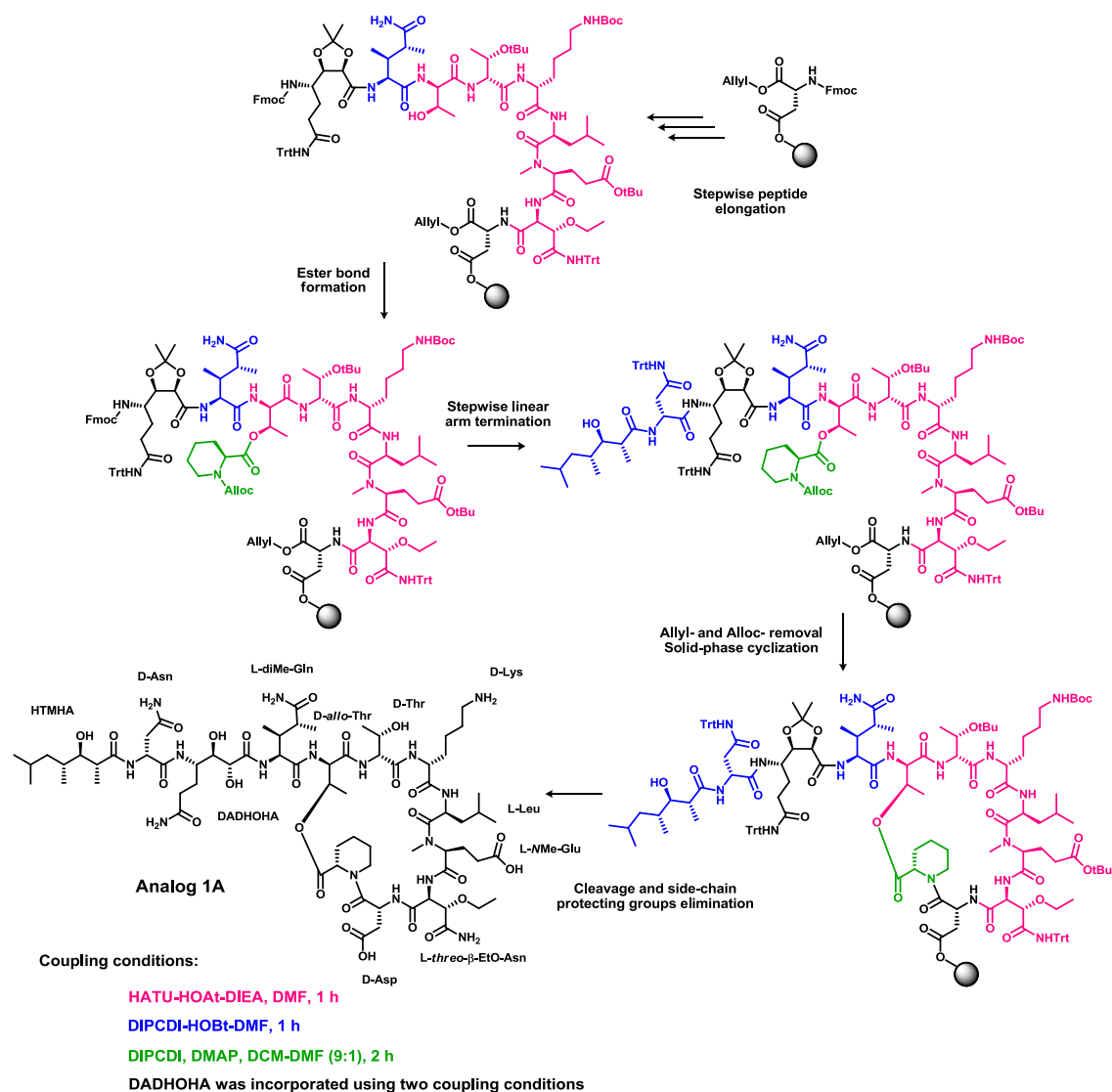
In order to evaluate the effect of the steric hindrance of the exocyclic arm on the cyclization reaction, this step was initially carried out before complete elongation of the linear peptide. After 1 h-treatment with the efficient coupling system PyBOP-HOAt-DIEA (4:4:8) in DMF, HPLC analysis revealed an extremely complex and dirty cyclization crude. No starting material was detected by HPLC-MS. In view of the complicated chromatographic profile, the synthesis was not completed. Thus, in later attempts the macrolactamization step will be faced after having finished the linear peptide assembly (see section 2.5.1.2.).

#### General considerations

Side-chain anchoring of Fmoc-D-Asp(OH)-OAllyl (0.6 mmol aa/g resin, 6 mmol DIEA/g resin, in DCM for 45 min) to the 2-CTC resin proceeded smoothly and with satisfactory loadings (0.6 mmol/g).

The efficient coupling system HATU-HOAt-DIEA overcame the steric hindrance of nearly all the Analog 1A building blocks providing quantitative couplings as judged by Kaiser test and reversed-phase HPLC-PDA and HPLC-MS analysis. Only the residue Leu was re-coupled when acylating to a *N*Me amino acid.

## 1.5.1.2. Second strategy: DADHOHA + ester



**Scheme 18:** Analog 1A second synthetic: DADHOHA incorporation + ester bond formation; cyclization after complete assembly of the linear peptide. Coupling conditions are shown in different colors.

In this second strategy (Scheme 18), two main modifications were implemented with respect to the previous one. First of all, the peptide chain was elongated until the DADHOHA moiety and then the ester bond was formed. And secondly, the exocyclic arm was fully assembled before carrying out the macrolactamization step. Moreover, the Fmoc-DADHOHA(acetonide, Trt)-OH  $\gamma$ -amino acid was incorporated using two coupling conditions and the effect of this change in the pyrodiMeglutamic formation was evaluated. The macrolactamization step was only attempted on solid-phase. Two different coupling systems were evaluated.

### DADHOHA incorporation: pyrodiMeglutamic formation

Two coupling systems were selected to incorporate the Fmoc-DADHOHA(acetonide, Trt)-OH into the growing peptide chain before the ester bond formation: a mild and close to neutral system (DIPCDI-HOBt) and a strong and basic system (HATU-HOAt-DIEA). Changing to a more efficient coupling method significantly decreases the pyrodiMeglutamic derivative formation, without the increase of basicity affecting the sensitive diMe-Gln residue. Hence, a stronger activation of the  $\alpha$ -COOH from the DADHOHA moiety favors a quicker coupling onto the diMe-Gln, reducing the lifetime of its free  $\alpha$ -amino group and, therefore, minimizing the intramolecular lactamization side reaction.

The use of the mild DIPCDI-HOBt conditions in a less hindered environment (in this second strategy the ester bond is not formed when the DADHOHA residue is incorporated) does not provide better crudes in terms of purity and yield evaluated by HPLC analysis. Thus, DIPCDI-HOBt is completely discarded to incorporate DADHOHA residue.

### Pipecolic: ester bond formation

The ester bond was constructed at a later stage of the peptide assembly. Therefore, longer treatments were needed to overcome the additional steric hindrance and to obtain similar conversions. After three consecutive treatments (2 h + o/n + 3 h) under the common conditions aa-DIPCDI-DMAP (8:8:0.5) in DCM-DMF (9:1), the ester was quantitatively formed without extra side products being detected in the crude.

When facing the synthesis of the target molecule, the ester will be formed over a more hindered hydroxyl group (from the AHDMHA residue). In this extremely hampered context, the length of the peptidic chain when forming the ester will be crucial. Thus, the shorter the linear arm is, and the less hindered the environment of the pipecolic residue is, the easier to form the challenging ester linkage is.

### HTMHA: overacylation

The polyketide moiety HTMHA is a highly substituted aliphatic  $\beta$ -hydroxy carboxylic acid and the terminating moiety of Pipecolidepsin A and analogs. Thus, the coupling of such a bulky moiety in such a highly hindered environment forces a fine tuning of the coupling method/system, equivalents and reaction times to achieve quantitative acylation rates.

In a first attempt, the polyketide moiety HTMHA was incorporated without pre-activation and using DIPCDI-HOBt (2:2:2) to avoid possible overacylations of its free hydroxyl group. Several re-couplings under these conditions were needed to obtain quantitative incorporations. The presence of overacylation or other side products were not detected according to HPLC analysis. The Kaiser test resulted unreliable at this point suggesting that the peptide could be adopting a secondary structure.

The increase of equivalents up to 4 enabled shorter reaction times (1 h) at small scale. However, at bigger scale 4 equivalents and a reaction time of 4.5 h were needed to obtain quantitative couplings.

### Macrolactamization

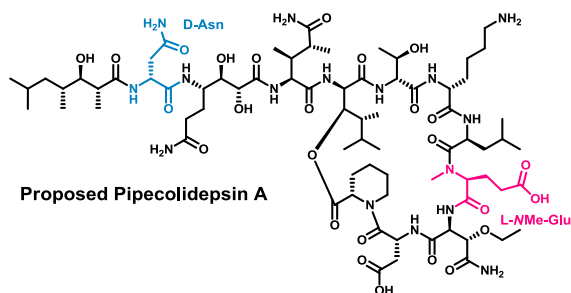
The cyclization step was undertaken using two coupling systems: PyBOP-HOAt-DIEA (4:4:8) in DMF and DIPCDI-Oxyma (4:4) in DCM-DMF (1:1). The first conditions gave better results in terms of purity, even though some starting material was still detected after a 2-h treatment. The complete assembly of the linear peptide before the cyclization step simplifies the final crude of the Analog 1A. This will be the strategy of choice from now on.

#### *1.5.1.3. Complete $^1\text{H}$ assignment of Analog 1A: revision of the preliminary structure proposed for Pipecolidepsin A*

Analog 1A was obtained with a 3.1% yield when following the second synthetic strategy. With the molecule on hand, exhaustive NMR studies were performed in  $\text{CD}_3\text{OH}$ . The analysis of the spectroscopic data revealed that all the side-chain amides present in the cyclodepsipeptide showed NOE cross-peaks with the precedent  $\text{CH}_2$  of the side-chain. In view of these results, a revision of all the NMR spectra of the natural Pipecolidepsin A was undertaken (Figure 31).

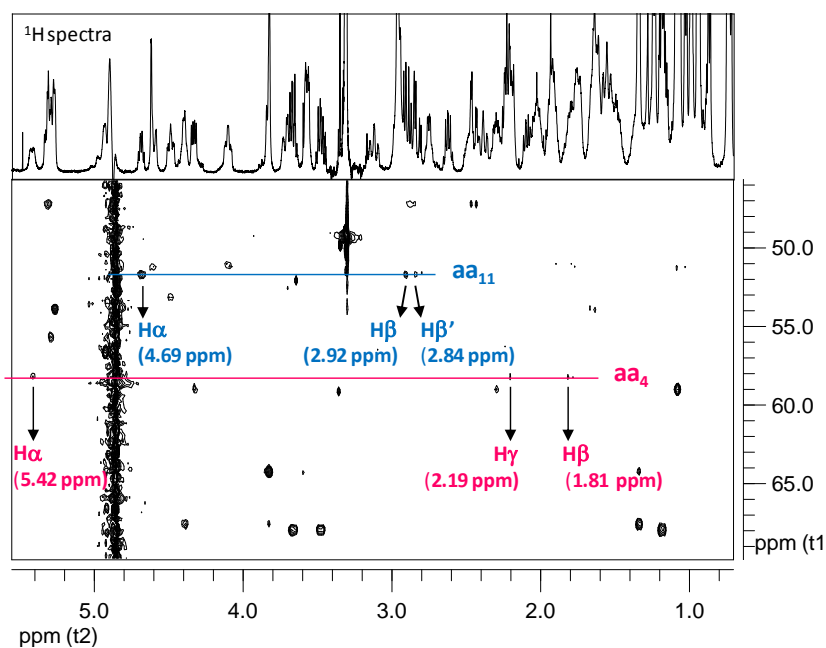
First assignment of aa<sub>4</sub> and aa<sub>11</sub>:

NMe-Glu (aa <sub>4</sub> )		D-Asn (aa <sub>11</sub> )	
NMe	2.96	NH	8.35
H $\alpha$	5.42	H $\alpha$	4.69
H $\beta$	2.46/1.81	H $\beta$	2.92/2.84
H $\gamma$	2.19/2.08	CONH <sub>2</sub>	7.21/6.75
COOH	-		

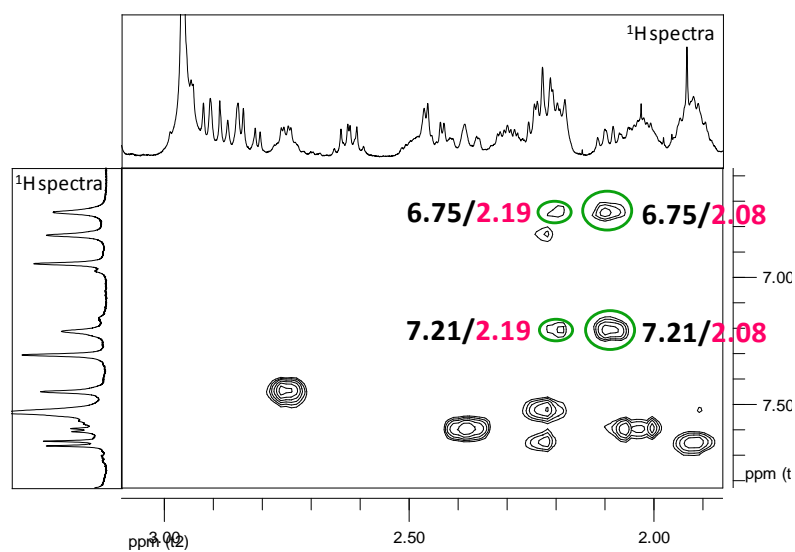


## Revision of NMR data:

## HMQC-TOCSY

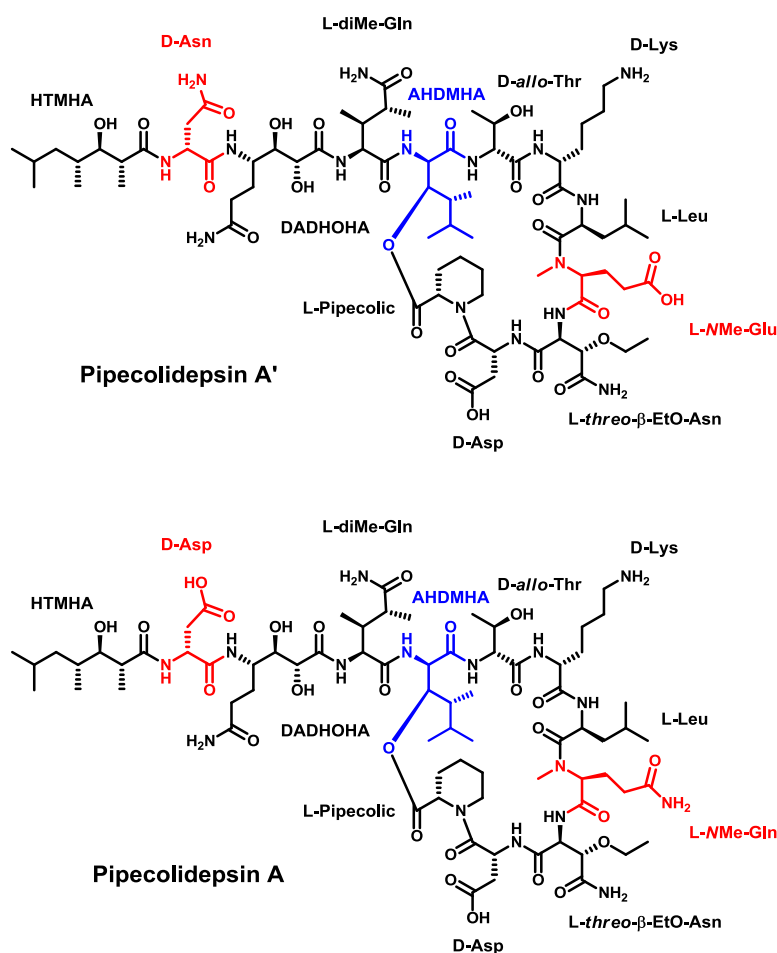


## gROESY



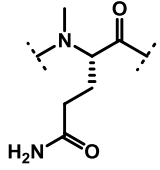
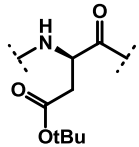
**Figure 31:** HMQC-TOCSY experiment of natural Pipecolidepsin A. The spin system of aa<sub>4</sub> is highlighted in blue and the one of aa<sub>11</sub> in red; gROESY experiment of natural Pipecolidepsin A. NOE cross-peaks between the non-assigned side-chain amide and the  $\gamma$ -CH<sub>2</sub> of aa<sub>4</sub> were detected.

The NMR spectra were revised by means of a new processing software named Mestre-C. The HMQC-TOCSY experiment enabled the identification of the two uncertain spin systems:  $\alpha$ - $\beta/\beta'$  and  $\alpha$ - $\beta/\beta'$ - $\gamma/\gamma'$  corresponding to  $aa_{11}$  and  $aa_4$  respectively. The COSY experiment provided the lacking information of  $aa_4$ 's spin system, this is  $H\beta'$  (2.46 ppm) and  $H\gamma'$  (2.09 ppm). With the verified chemical shifts in hand completely matching with the first assignment, the gROESY was carefully analyzed to find four new cross-peaks that were not detected during the first structure elucidation process. These cross-peaks correlated the two protons of the non-assigned side-chain amide with the  $CH_2$  belonging to a  $\alpha$ - $\beta/\beta'$ - $\gamma/\gamma'$  spin system, which univocally placed the side-chain amide at the  $aa_4$ . Thus, a final and corrected structure for Pipecolidepsin A was proposed (Figure 32) were  $aa_4 = NMe-Gln$  and  $aa_{11} = D-Asp$ . Therefore, from now on, the preliminary structure proposed for Pipecolidepsin A will be referred to as Pipecolidepsin A', and the final and corrected structure will be referred to as Pipecolidepsin A.



**Figure 32:** Preliminary and uncorrected structure of Pipecolidepsin A (Pipecolidepsin A') and final and corrected structure of Pipecolidepsin A (Pipecolidepsin A). The differences between the two structures are shown in red; the key AHDMA residue is highlighted in blue.

The proposal of a new structure forced the re-analysis of the potential side reactions to consider before attempting the SPPS of Pipecolidepsin A and increased the previous list (Table 2).

Residue	Extra potential side-reactions for corrected-Pipecolidepsin A
	Dehydration to nitrile of the unprotected side-chain amide Intramolecular lactamization Decreased acylation rate due to the <i>N</i> Me group Non-commercial availability
	Aspartimide formation

**Table 2:** Extra side-reactions to consider when attempting Pipecolidepsin A synthesis.

#### NMe-Gln: side-chain dehydration and intramolecular lactamization

Side-chain unprotected *N*Me-Gln is associated with two significant side reactions: dehydration to nitrile of the side-chain amide when the acid is in its activated form; and intramolecular lactamization.

*N*Me-groups increase the nucleophilic character of the *N* but also its steric hindrance. The effect of the *N*-methylation in the extent of these two secondary reactions will be carefully checked during the first synthetic approaches. The absence of the methyl groups at  $\beta$  and  $\gamma$  positions may decrease the occurrence of intramolecular lactamization with respect to the diMe-Gln residue. However, whether or not dehydration side reaction is promoted in this *N*-methylated amino acid is completely unknown.

Fmoc-*N*Me-Gln-OH was synthesized by PharmaMar following synthetic procedures already described in the literature.<sup>129</sup>

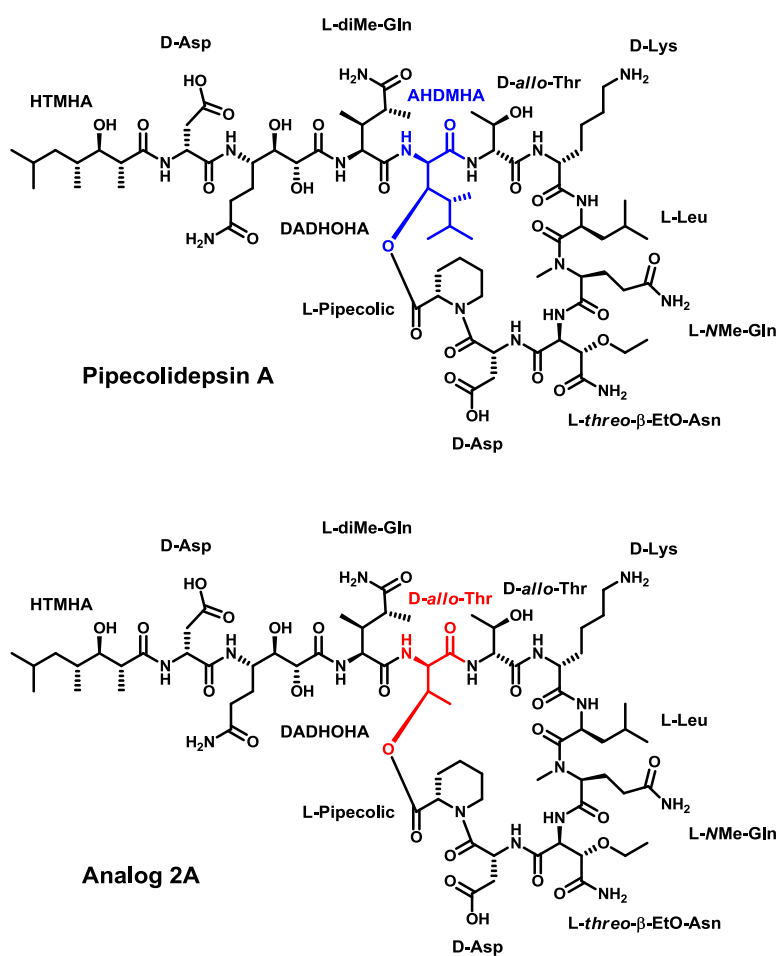
#### D-Asp(<sup>t</sup>Bu): aspartimide formation

Pipecolidepsin A contains two D-Asp residues. The D-Asp in the cycle cannot undergo aspartimide formation as it is coupled to an *N*-alkylated residue. However, this second extra D-Asp moiety located at the exocyclic arm follows the DADHOHA residue, assembly that,

somehow, remembers the sequence Asp(<sup>t</sup>Bu)-Gln(Trt), which could be prone to give aspartimides. Thus, careful monitorization when elongating the peptidic arm will be settled.

### 1.5.2. Second approach: synthetic studies of a Pipecolidepsin A analog

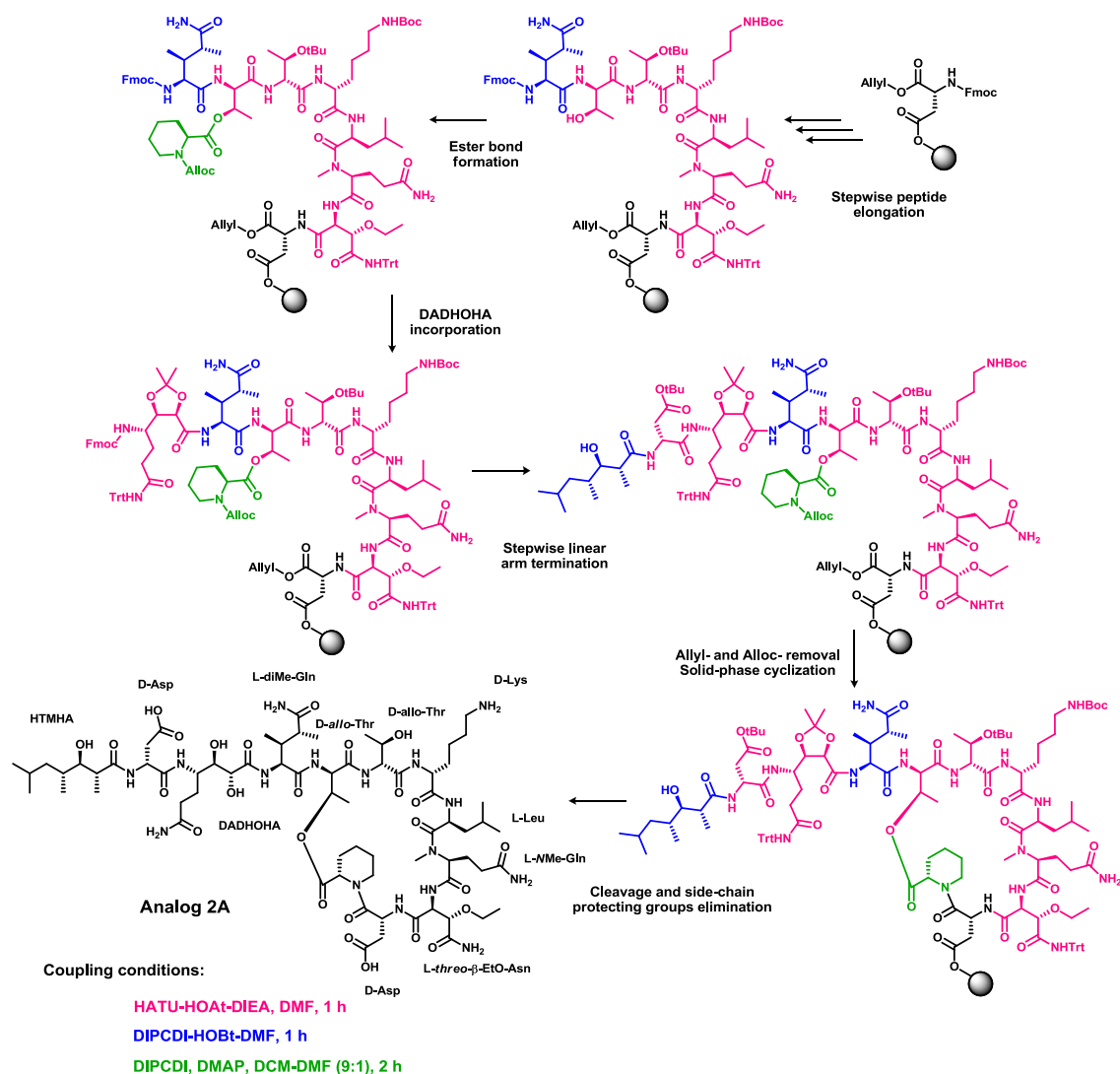
To evaluate whether the differences in the peptidic sequence between Pipecolidepsin A' and Pipecolidepsin A would have an effect on the performance of their syntheses, an analog of Pipecolidepsin A was also designed (Figure 33). Thus, the AHDMHA residue was replaced by the simpler D-*allo*-Thr and the synthesis of Analog 2A was attempted.



**Figure 33:** Chemical structures of Pipecolidepsin A and Analog 2A. Differences in the peptidic sequence are shown red. The key AHDMHA residue is highlighted in blue.



## 1.5.2.1. First strategy: diMe-Gln + ester. Stepwise arm elongation



**Scheme 19:** Analog 2A first synthetic strategy: diMe-Gln incorporation + ester bond formation; stepwise elongation of the exocyclic arm. Coupling conditions are shown in different colors.

For the synthesis of the Analog 2A (Scheme 19), the optimized strategy, previously established for Analog 1A, was implemented. Thus, the linear peptide was elongated until the diMe-Gln residue before forming the ester bond; the peptidic arm was fully assembled to finally perform the macrolactamization as the last synthetic step; the DADHOHA moiety was incorporated using the efficient coupling system HATU-HOAt-DIEA to minimize the pyrodiMeglutamic derivative formation. The synthesis of Analog 2A was carefully monitored to check whether the sequence modifications would significantly affect it.

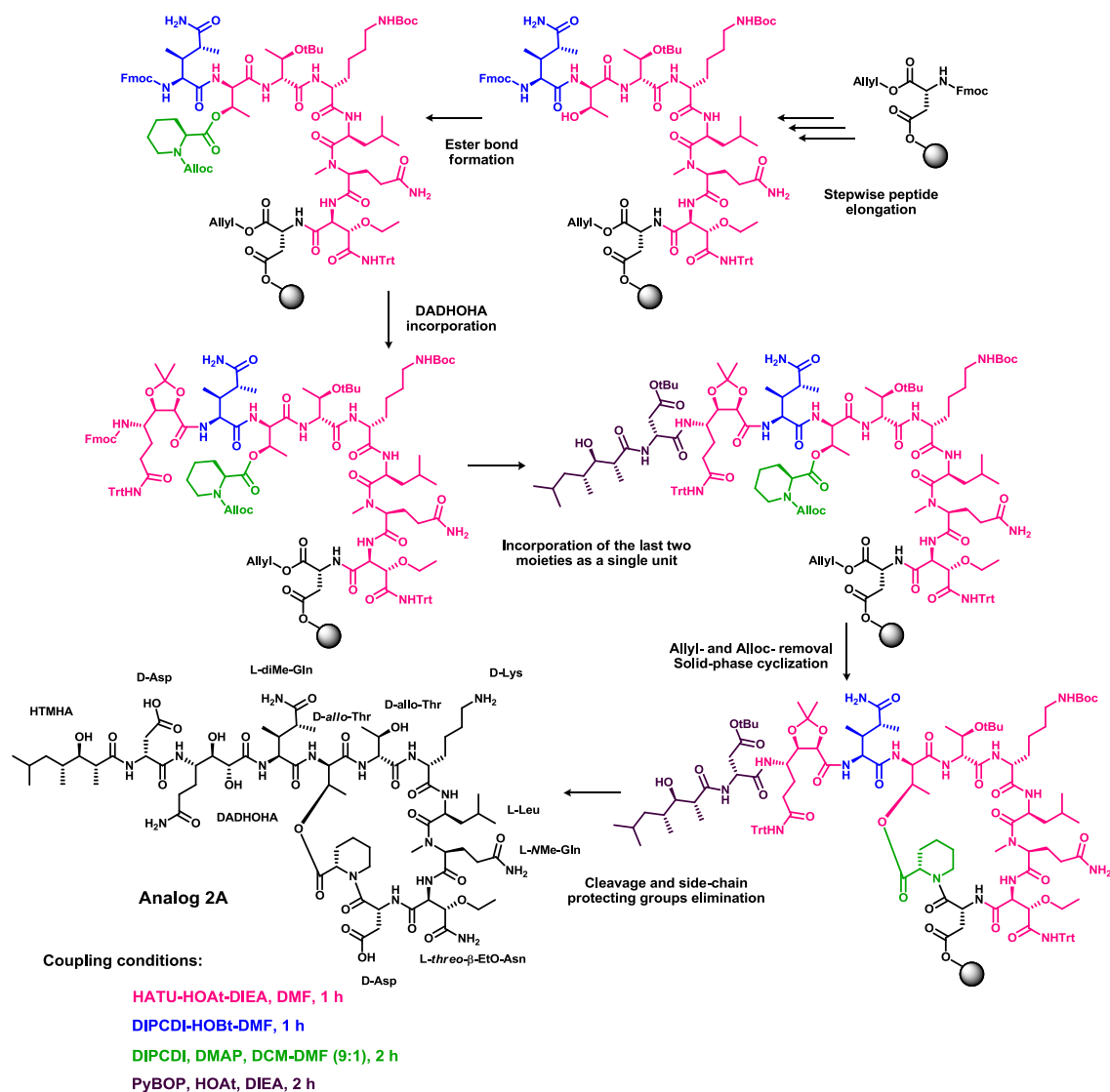
#### NMe-Gln: dehydration and pyroglutamic derivative formation

The incorporation of the residue Fmoc-NMe-Gln-OH using HATU-HOAt-DIEA entails a small percentage of the free side-chain amide dehydration to nitrile (up to 5%) that can be assumed without a change in the coupling method. However, no intramolecular lactamization was detected by HPLC analysis, suggesting that the NMe group represents a high sterical hindrance that prevents this side reaction to occur (see section 2.3.2.1.).

#### D-Asp(<sup>t</sup>Bu): aspartimide formation

The stepwise incorporation of the last two moieties from the exocyclic arm substantially decreases the purity of the peptidic crude as judged by HPLC analysis (see Figure X). The Fmoc-D-Asp(<sup>t</sup>Bu)-OH was incorporated by means of HATU-HOAt-DIEA (3:3:6, in DMF, 1 h) and the HTMHA moiety using DIPCDI-HOBt (4:4, in DMF, 1 h) without pre-activation to avoid any potential overacylation. A likely explanation for this feature would be an aspartimide formation issue (see section 2.3.2.1.). Thus, a second synthesis was performed incorporating the last two moieties as a single unit.

### 1.5.2.2. Second strategy: diMe-Gln + ester. Incorporation of the last two moieties as a single unit

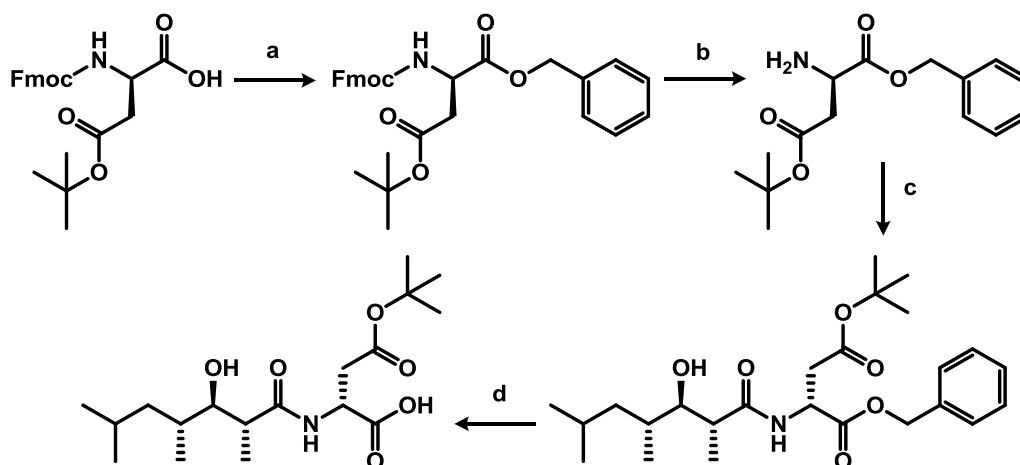


**Scheme 20:** Analog 2A second synthetic strategy: diMe-Gln incorporation + ester bond formation; coupling of the last two moieties as a single unit. Coupling conditions are shown in different colors.

In this synthesis (Scheme 20), the last two moieties instead of being incorporated stepwise, were coupled as a single unit. The purity of the resulting crude was evaluated by HPLC analysis.

#### Synthesis of the building block HTMHA-D-Asp<sup>t</sup>(Bu)-OH

The synthesis of the unit HTMHA-D-Asp<sup>t</sup>(Bu)-OH required the previous preparation of the monomer HTMHA as it has already been described in section 1.4.5.. Then, the dipeptidomimetic was accessed as follows (Scheme 21).



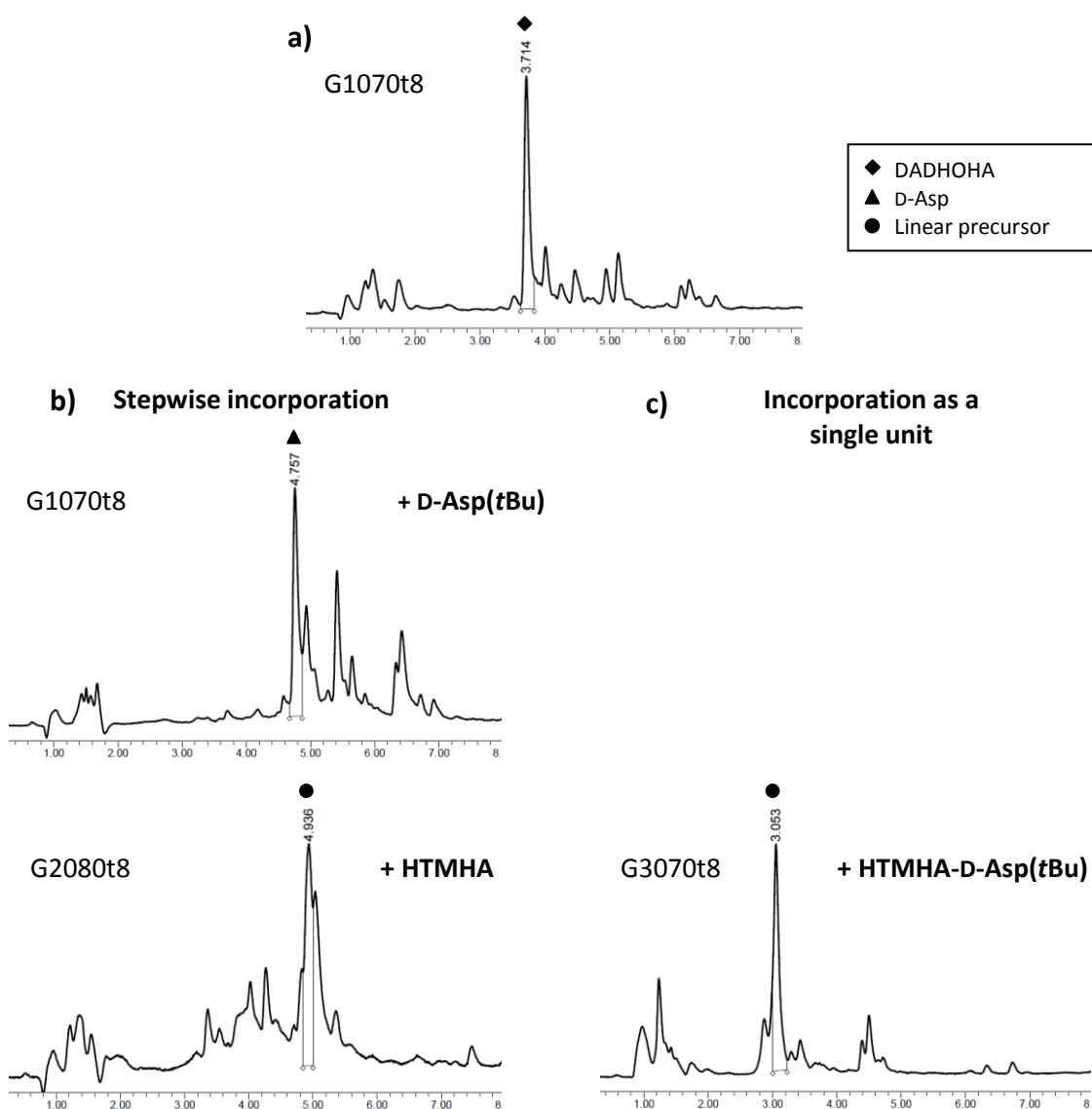
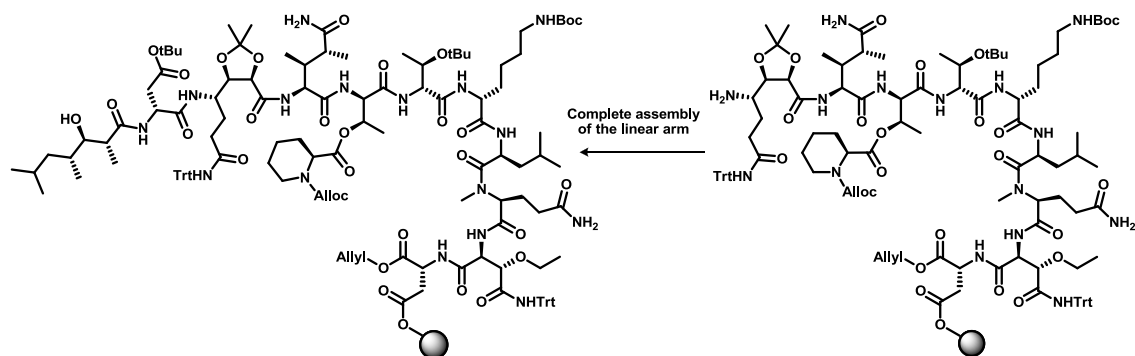
**Scheme 21:** a) i)  $\text{Cs}_2\text{CO}_3$ , dry MeOH, 25 °C, 20 min, ii) BzBr, dry DMF, 25 °C, 2 h; b) Piperidine-DCM (1:4), 25 °C, 40 min; c) HTMHA, EDC, HOBt, dry DCM-DMF (1:1), 25 °C, 8 h; d)  $\text{H}_2$  (1 atm), Pd(C), dry MeOH, 25 °C, o/n.

Thus, the  $\alpha$ -COOH of the Fmoc-D-Asp(<sup>t</sup>Bu)-OH was protected as the benzyl ester by reaction of the corresponding pre-formed Cs salt with BzBr. Then, the Fmoc was eliminated with piperidine-DCM (1:4) and the free amino group coupled to the previously synthesized HTMHA using the water soluble carbodiimide EDC. Finally, the benzyl ester was hydrogenated and the resulting acid was used without further purification even though the purity was around 60%.

#### HTMHA-D-Asp(<sup>t</sup>Bu)-OH

The incorporation of the building block HTMHA-D-Asp(<sup>t</sup>Bu)-OH onto the growing peptide chain is a more challenging process due to its poorer reactivity and solubility. A slow coupling rate combined with a more favored racemization side reaction because of the acylated amino function, required fine tuning of the coupling method to keep by-products to a minimum. Phosphonium salts together with the HOAt additive, represents an efficient coupling system that minimizes racemization at the C-terminus and allows long reaction times.

HTMHA-D-Asp(<sup>t</sup>Bu)-OH building block was coupled using PyBOP-HOAt-DIEA (5:5:10) in DMF for 2 h without pre-activation. The scaling-up of this reaction was performed with 4 equivalents and required longer reaction times up to 3.5 h. The reaction was monitored by reversed-phase HPLC analysis. No overacylation problems were detected. Compared to the stepwise incorporation of the last two moieties, this procedure provided cleaner crudes (Figure 34). The extra purification step of HTMHA-D-Asp(<sup>t</sup>Bu)-OBz intermediate together with the avoidance of the aspartimide formation account for the substantial improvement.



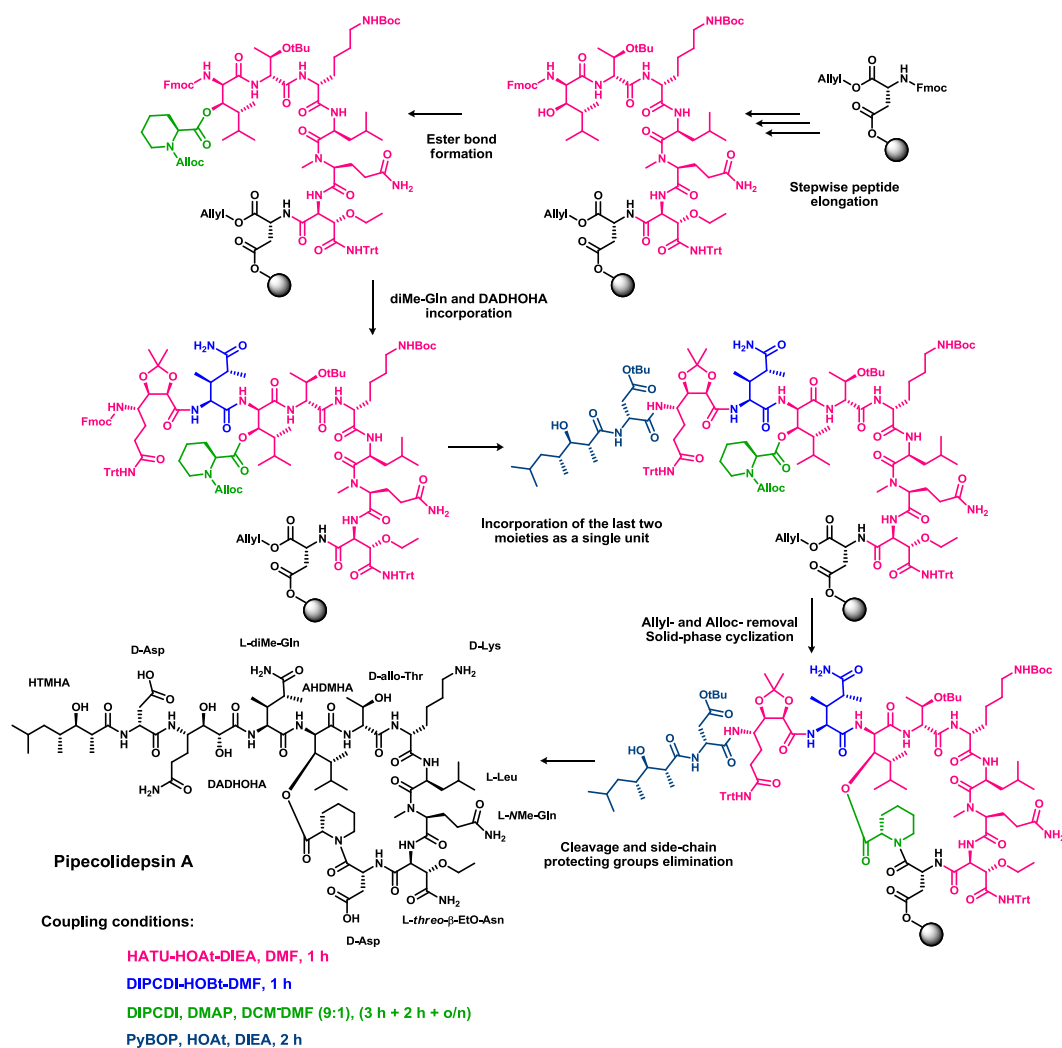
**Figure 34:** HPLC chromatograms of the complete assembly of the linear Analog 2A: a) DADHOHA; b) stepwise incorporation of the last two moieties; c) incorporation of the last two moieties as a single unit.

This new synthetic approach was implemented in the global synthetic strategy of Pipecolidepsin A.

### 1.5.3. Solid-phase synthesis of Pipecolidepsin A

The syntheses of analogs 1A and 2A were useful to evaluate the extent of most of the possible side reactions associated with the synthesis of Pipecolidepsin A' and Pipecolidepsin A; to optimize the coupling conditions of each residue; to check whether or not the starting and cyclization point was appropriate; and to prove that the synthetic approach actually enabled the access to the desired analogs. However, these first approaches did not face the bottleneck step of Pipecolidepsin A synthesis, which is the formation of the ester bond between the AHDMHA hydroxyl group and the Alloc-pipecolic-OH residue. Thus, in order to find the best approach, its construction was evaluated at different Pipecolidepsin A assembly stages: after incorporation of Fmoc-AHDMHA-OH, Fmoc-diMeGln-OH and Fmoc-DADHOHA-OH.

#### 1.5.3.1. First strategy: AHDMHA + ester



**Scheme 22:** Pipecolidepsin A first synthetic strategy: AHDMHA incorporation + ester bond formation. Coupling conditions are shown in different colors.

The occurrence of a  $N \rightarrow O$  transacylation side reaction has already been described when esterification of a  $N^\alpha$ -protected  $\beta$ -hydroxy amino acid is carried out.<sup>74</sup> However, the extraordinary bulkiness of the AHDMHA residue was believed to minimize this side reaction. Furthermore, since the esterification reaction is carried out over an extremely hindered secondary alcohol, its attempt in the least impeded environment (growing peptide chain assembled until the Fmoc-protected AHDMHA residue), remained fully justified (Scheme 22).

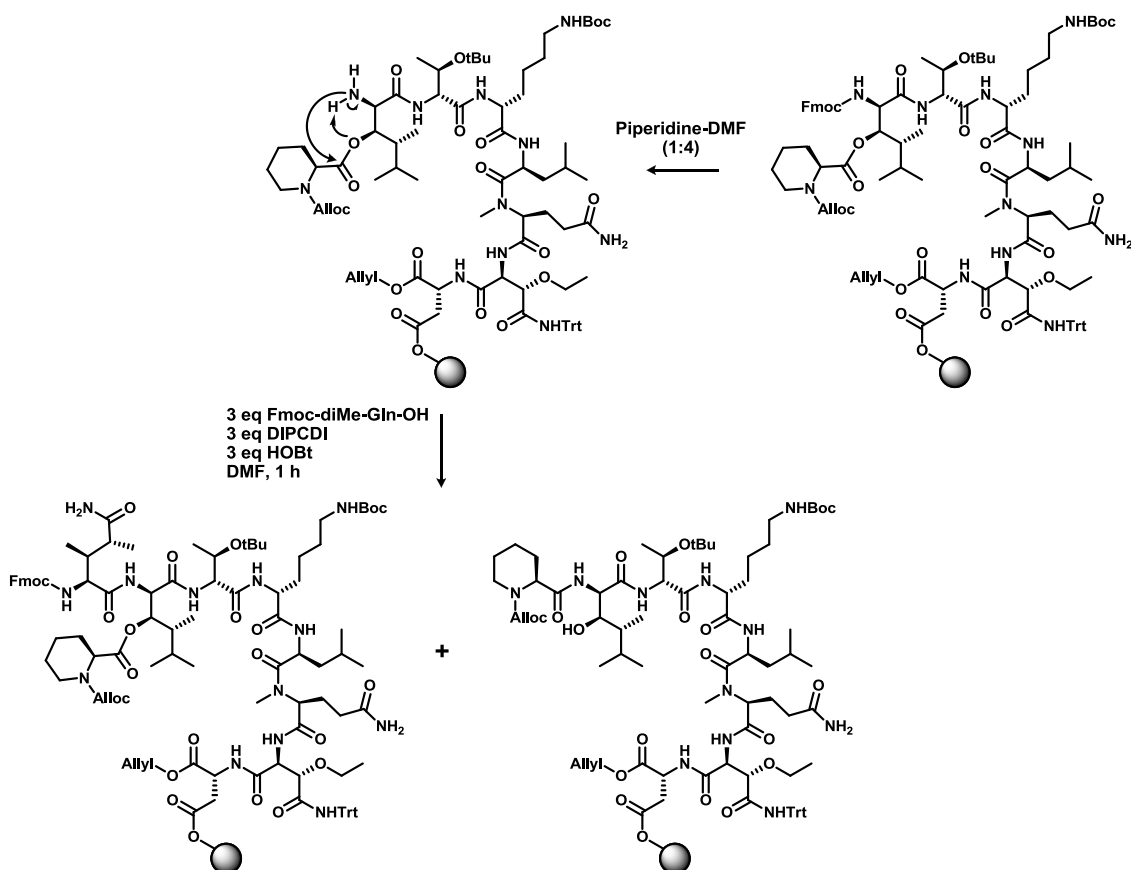
#### AHDMHA: coupling and acylation rates

The common conditions Fmoc-AHDMHA-OH-HATU-HOAt-DIEA (2.5:2.5:2.5:5) in DMF for 1 h, were appropriate to achieve quantitative coupling of this highly hindered  $\gamma$ -branched- $\beta$ -hydroxy- $\alpha$ -amino acid. However, its bulkiness did affect its acylation rate by the adjacent Fmoc-diMe-Gln-OH residue. As it was explained in section 1.5.1.1, diMe-Gln was introduced using mild and close to neutral conditions that did not ensure its quantitative coupling in less hindered peptides such as Analogs 1A and 2A. Therefore, this problem was even more significant with Pipecolidepsin A. After some experimentation, conditions with an optimized ratio between equivalents, re-couplings, dehydration and conversions were found, obtaining with a single coupling with 4.5 equivalents of Fmoc-diMe-Gln-OH, DIPCDI and HOBT the best results. Despite the insolubility of the Fmoc-protected aa in DMF, a highly concentrated reaction solution was also crucial. Other combinations involving a re-coupling (3 equivalents + 1 equivalent or 3 equivalents + 2 equivalents) were less advantageous. Dehydration was kept around 9%, only slightly higher than the one obtained with the analogs owning a *D-allo*-Thr(OH) instead of the AHDMHA residue. As expected, no overacylation of the free hydroxyl group was detected after subsequent couplings.

#### Pipecolic: ester bond formation

To obtain reasonable conversions when forming the ester bond (6% of starting material remaining as judged by HPLC analysis), the common conditions aa-DIPCDI-DMAP (8:8:0.5) in DCM-DMF (9:1) were performed for three times: 3 h + 2 h + o/n. The crude did not show extra peaks after consecutive treatments.

At this stage, the  $\alpha$ -amino group of the AHDMHA residue was deprotected following the usual procedure: piperidine-DMF (1:4) for  $2 \times 1$  min,  $2 \times 5$  min and  $1 \times 10$  min. Then, the Fmoc-diMe-Gln-OH was coupled using 3 equivalents of aa, DIPCDI and HOBT in DMF for 1 h. The Kaiser test confirmed the absence of free amino function. HPLC-PDA and HPLC-MS analysis should allow quantification of the rapid occurring  $N \rightarrow O$  transacylation side reaction (Scheme 23).

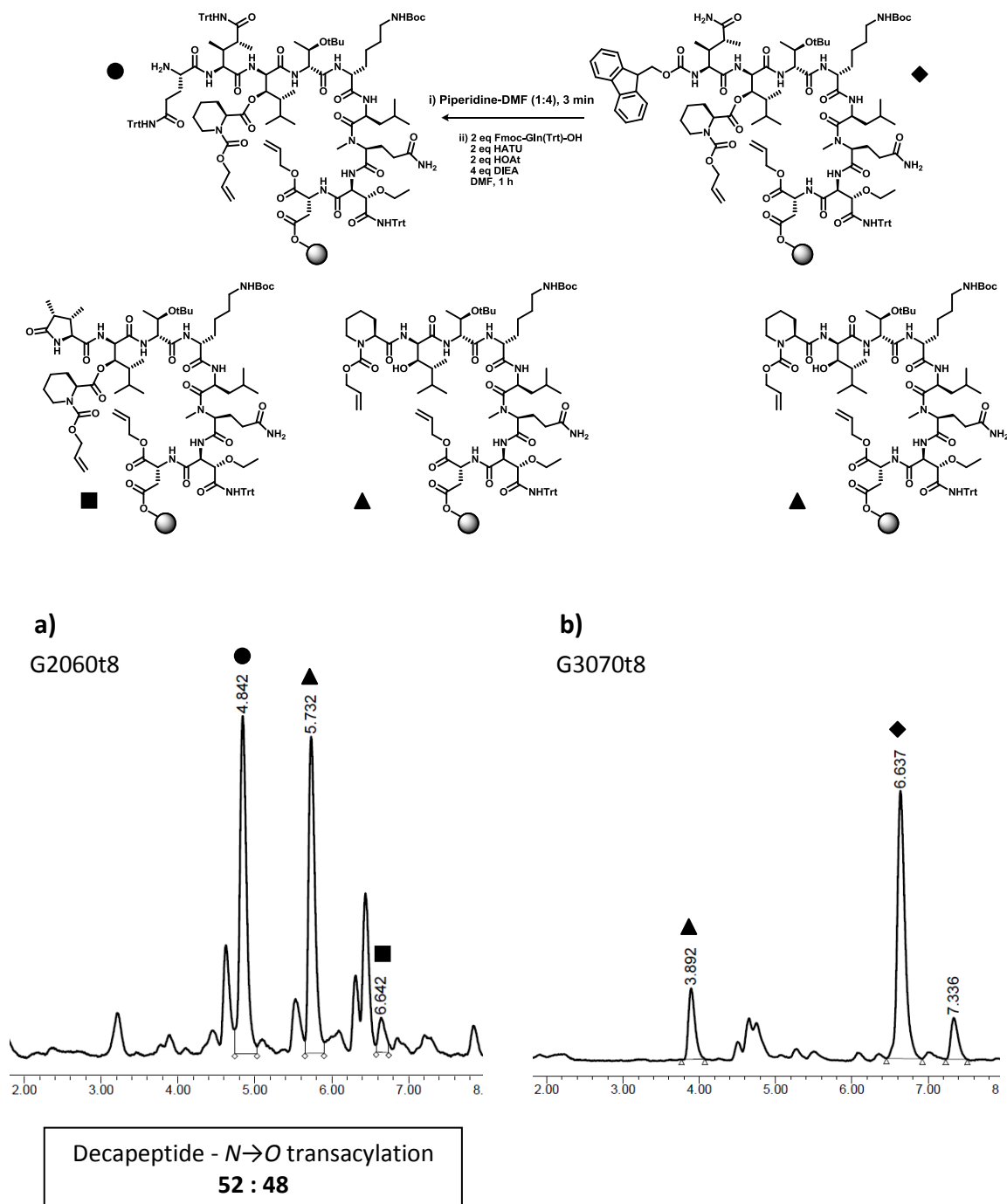


**Scheme 23:** Coupling of Fmoc-diMe-Gln-OH and associated  $N \rightarrow O$  transacylation side reaction.

The corresponding  $N \rightarrow O$  transacylated by-product was clearly identified as one of the major peaks in the HPLC-PDA chromatogram obtained after diMe-Gln incorporation. Since this was the only peak not showing the Fmoc UV profile (Figure 35 b), quantification of the  $N \rightarrow O$  transacylation extent was only feasible after coupling and subsequent Fmoc elimination of the following residue. To avoid the loss of the valuable Fmoc-DADHOHA(acetonide,Trt)-OH building block, a commercial aa [Fmoc-Gln(Trt)-OH] was coupled instead (Figure 35 a). The ratio between the  $N \rightarrow O$  transacylated by-product and the decapeptide with the Gln at the  $N$ -terminus was 1:1. The pyrodiMeglutamic derivative was a minor impurity because the coupling of a less hindered aa was more straightforward. Considering the bigger steric hindrance of the



DADHOHA residue, it is foreseen that its coupling will render a bigger percentage of pyrodiMeglutamic derivative. Thus, the application of this strategy to the corrected Pipecolidepsin A synthesis would provide an even lower amount of desired intermediate. In view of these results, optimization of this synthetic strategy was attempted.

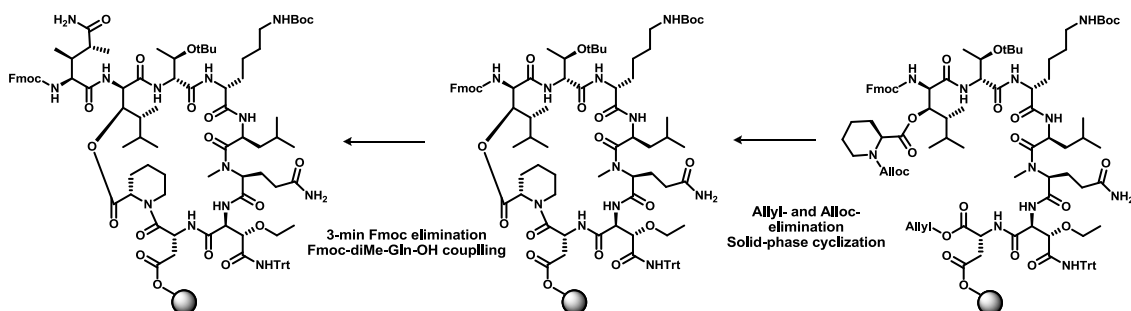


**Figure 35:** HPLC-PDA chromatograms: a) after Fmoc-Gln(Trt)-OH coupling and Fmoc elimination; b) after Fmoc-diMe-Gln-OH coupling.

Improving the first strategy: attempts to minimize the  $N \rightarrow O$  transacylation side reaction

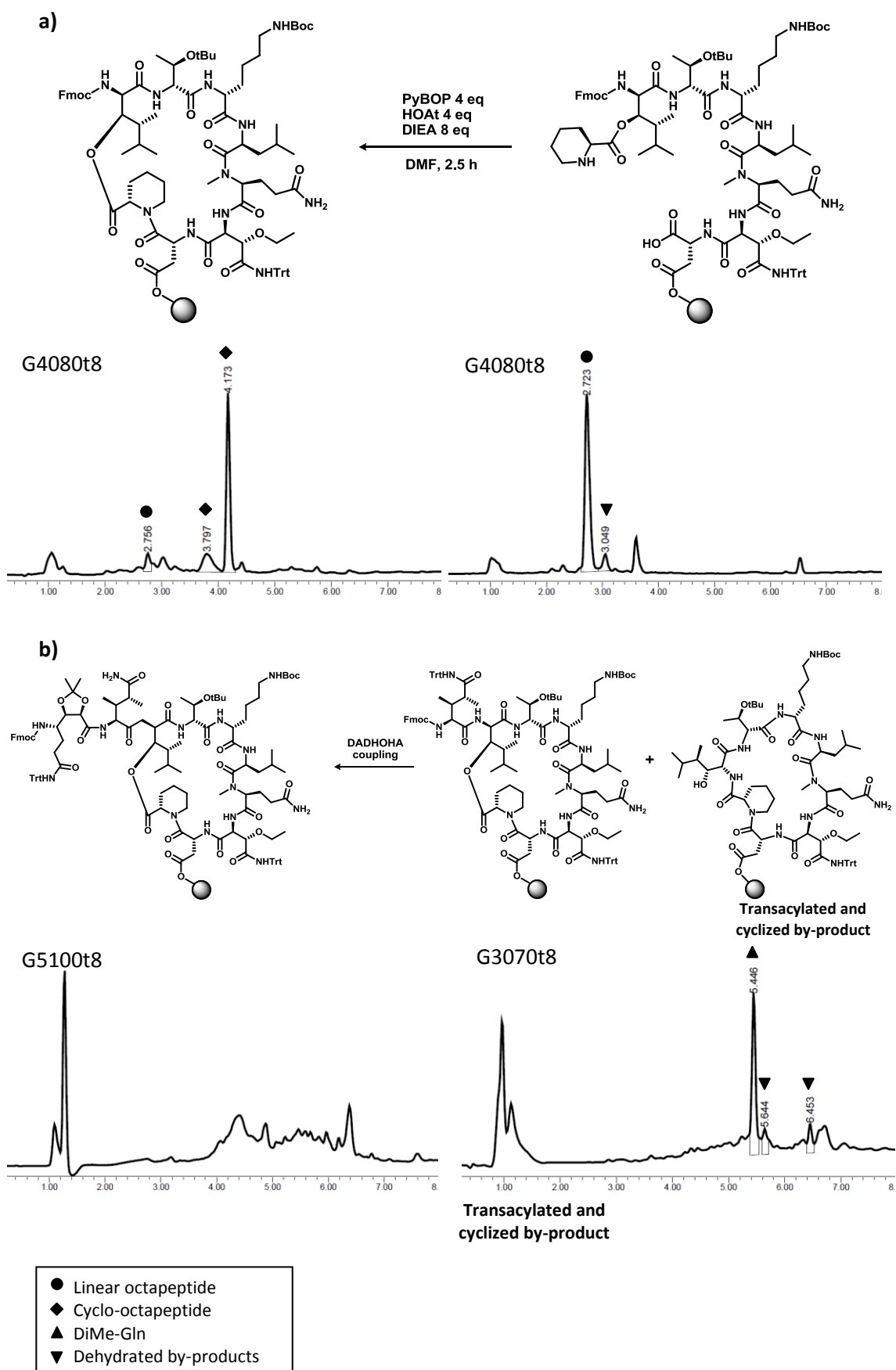
$N \rightarrow O$ -transacylation is a rapid intramolecular side reaction occurring when the  $\alpha$ -amino group from the AHDMHA residue is unprotected. Diminishing the time-life of this free amino group could affect the extent of this side reaction. Thus, the usual Fmoc-elimination procedure can be cut down to a single 3-min treatment and/or the diMe-Gln coupling can be performed under the most efficient coupling conditions. Since the dehydration to nitrile of the diMe-Gln side-chain amide occurs when the  $\alpha$ -COOH is in its activated form, highly reactive species and basic conditions promote this side reaction. Thus, changes in the already validated coupling conditions for diMe-Gln are completely discarded. A shorter Fmoc-deprotection treatment was tested with completely unsuccessful results.

Considering all these experimental data and before turning down this strategy, a last modification was attempted. A more conformational restricted environment was believed to minimize the extent of the  $N \rightarrow O$  transacylation. Thus, the strategy was revised and the cycle was assembled before the diMe-Gln was coupled (Scheme 24).



**Scheme 24:** Modification of the AHDMHA + ester strategy. The cycle was assembled before the Fmoc-diMe-Gln-OH was incorporated.

The macrolactamization proceeded smoothly when performed with PyBOP-HOAt-DIEA (4:4:8) in DMF for 2.5 h. A small percentage of starting material and two main peaks, both with the mass of the cyclized octapeptide but one much bigger than the other, were detected by HPLC analysis. The cyclic nature of the aa at the  $N$ -terminus would account for the existence of these two peaks: the *cis* and the *trans* conformers at the linkage Pipecolic-D-Asp. The Fmoc group from de AHDMHA residue was removed with a 3-min treatment of piperidine-DMF (1:4) and the Fmoc-diMe-Gln-OH was incorporated using DIPCDI and HOBT (4:4:4 and 2:2:2 in DMF, 1 h each). Then, after a 3-min Fmoc-deprotection, the DADHOHA moiety was incorporated and the Fmoc removed again. Detailed HPLC analysis of the described synthetic steps is shown in Scheme 25.

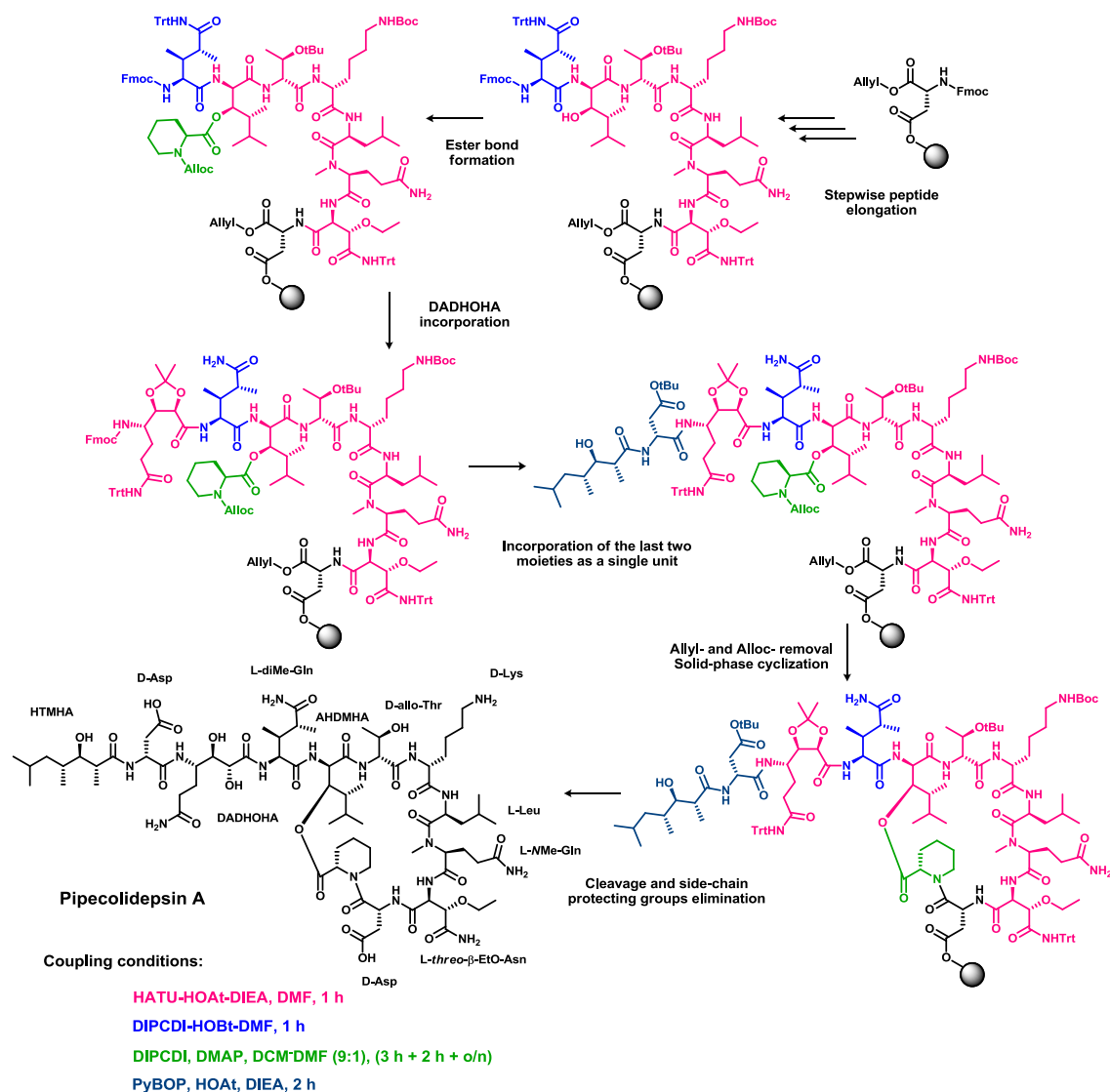


**Scheme 25:** Chromatographic profiles of the key steps of the synthetic strategy AHDMHA + ester + cyclization.

After coupling of the diMe-Gln, the HPLC-MS analysis confirmed the presence of a side product with the mass of the Fmoc-protected cyclo-octapeptide. A negative ninyhydrin test enabled its identification as the  $N \rightarrow O$  transacylated and cyclized octapeptide (Figure 25 b).

The chromatogram obtained after elimination of the DADHOHA Fmoc group was extremely complex and did not show a main peak. In basis of these results, the formation of the ester bond after incorporation of the AHDMHA residue was finally ruled out due to a  $N \rightarrow O$  transacylation side reaction that could not be minimized. The construction of the ester at a different peptide assembly stage was investigated.

### 1.5.3.2. Second strategy: diMe-Gln + ester



**Scheme 26:** Pipecolidepsin A second synthetic strategy: diMe-Gln incorporation + ester bond formation. Coupling conditions are shown in different colors.

In this second synthetic approach (Scheme 26), the peptide is assembled until the Fmoc-diMe-Gln-OH residue before forming the ester bond. This strategy ensured the avoidance of the *N*→*O*-transacylation side reaction but presented a more sterically hindered environment for the ester bond formation.

#### Pipecolic: ester bond formation

As it was justified in section 1.3.2.1., only methods of solid-phase ester formation *via* activation of the carboxylic acid were attempted. All the conditions tried are detailed in Table 3.

Entry	Coupling system	Time	T	% Ester <sup>[a]</sup>
1	aa (8 eq), DIPCDI (8 eq), DMAP (1 eq) <sup>[b]</sup>	20 h	25 °C	27
2	aa (16 eq), DIPCDI (10 eq), DMAP (1 eq) <sup>[b]</sup>	4 h	25 °C	15
3	aa (10 eq), TCFH (10 eq), HOAt (10 eq), DIEA (20 eq) <sup>[c]</sup>	2 h	25 °C	0
4	aa (10 eq), TCFH (10 eq) <sup>[c]</sup>	3 h	25 °C	0
5	aa-F (10 eq), DIEA (25 eq) <sup>[d]</sup>	4 h	25 °C	0
6	aa (5 eq), HATU (5 eq), HOAt (5 eq), DIEA (10 eq) <sup>[c]</sup>	1 h	25 °C	0
7	aa (5 eq), MSNT (5 eq), NMI (4 eq) <sup>[d]</sup>	3 h	25 °C	0
8	aa (5 eq), MSNT (5 eq), NMI (4 eq), DIEA (8 eq) <sup>[d]</sup>	3 h	25 °C	0
9	aa (5 eq), BTC (1.65 eq), collidine (14 eq) <sup>[c]</sup>	12 h	25 °C	0
10	aa (16 eq), DIPCDI (10 eq), DMAP (0.5 eq) <sup>[b]</sup>	30 h	45 °C	84
11	aa (16 eq), DIPCDI (10 eq), DMAP (0.5 eq), MW <sup>[b]</sup>	0.5 h	40 °C	27
12	aa (15 eq), DIPCDI (15 eq), DMAP (0.5 eq) <sup>[b]</sup>	2.5 h	45 °C	98

**Table 3:** Ester formation conditions; <sup>[a]</sup>respect to the starting material; <sup>[b]</sup>DCM-DMF (9:1); <sup>[c]</sup>DMF; <sup>[d]</sup>DCM.

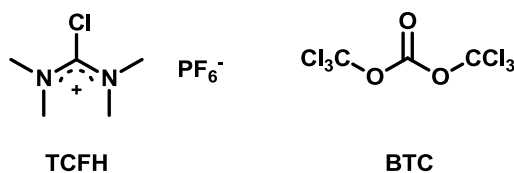
The carboxylic acid of Alloc-pipecolic-OH was activated *via* coupling reagents such as carbodiimides (entries 1-2, 10-12), uronium salts (entry 6) and arenesulfonyl derivatives (entries 7-8); and *via* isolated active species, specifically protected amino acids halides, such as acid chlorides (entries 3-4, 9) and acid fluorides (entry 5).

Phosphonium and uronium salts are highly efficient coupling reagents for amide bond formation. However, the active species formed under these conditions are the corresponding benzotriazole (OBt) or azabenzotriazole (OAt) esters, which are less reactive but stable species. Thus, they work effectively for regular peptide couplings, but turned out to be less appropriate for the formation of the more demanding ester bond. Finally, only HATU, one of the more

efficient reagents from this family, was investigated at room temperature to find that the ester bond was not formed at all.

1-(Mesitylenesulfonyl)-3-nitro-1,2,4-triazole (MSNT) was first developed as a condensing reagent for polynucleotides synthesis.<sup>130</sup> Later, it was claimed to provide quantitative anchorage of Fmoc-protected aa onto polystyrene and cellulose derived resins through an ester bond, almost without racemization and dipeptide formation.<sup>131</sup> Nowadays, MSNT is a well-known phosphorylating<sup>132,133</sup> and acylating reagent of hydroxyl functions, widely used in SPPS for anchoring Fmoc-protected aa into hydroxyl resins (because of its high yields and low racemization levels).<sup>134,135</sup> It was used to form Pipecolidepsin A ester bond with completely unsuccessful results.

Acid chlorides are highly reactive species used in SPPS for difficult couplings, ester bonds formation included. The strong activation of the carboxylic acid and the simplicity of the by-products released during the coupling reaction, are the main advantages of these activated species. However, the highly acidic conditions required to prepare these acid chlorides precludes their application in the Boc/Bzl SPPS, and restricts their use in the Fmoc/<sup>t</sup>Bu SPPS to those aa not bearing acid-sensitive side-chain protecting groups. The development of new derivatizing reagents for the *in situ* preparation of Fmoc-*N*<sup>α</sup>-protected amino acid chlorides, such as TCFH<sup>136</sup> and BTC<sup>137</sup> (Figure 36), has overcome this major disadvantage.



**Figure 36:** Structures of TCFH and BTC

The two reagents were used to prepare the corresponding Alloc-pipecolic-Cl *in situ*. It was never isolated, but poured directly into the resin without purification. TCFH was used in the presence of HOAt and DIEA or alone, recovering in any case the starting material completely intact. Neither BTC gave ester formation, but only dehydrated products: monodehydrated diMe-Gln, monodehydrated NMe-Gln and didehydrated diMe-Gln and NMe-Gln. The starting material was partially recovered.

Finally, the use of carbodiimides in the presence of catalytic amounts of DMAP gave the best results. Since the Fmoc/<sup>t</sup>Bu was the strategy of choice, DIPCDI was preferred because of the higher solubility of the derived urea in DMF-based mediums. Carbodiimides mechanism

can work through different activated species such as the *O*-acylisourea and the symmetrical anhydride, which are not efficient enough to give quantitative conversions. Thus, catalytic amounts of DMAP are added to significantly enhance the reaction rates. However, the racemization extent is also increased. By keeping the amount of DMAP to less than a 10% of the protected aa and the coupling reagent, adding it onto the resin after the reactive species are formed, and performing the coupling at 0 °C, the racemization is usually kept to a minimum.

At 25 °C, the conditions involving Alloc-pipecolic-OH-DIPCDI-DMAP (8:8:1) in DCM-DMF (9:1) worked slightly less efficiently than the symmetrical anhydride (Alloc-pipecolic-OH-DIPCDI-DMAP (16:10:1) in DCM-DMF (9:1)). Nevertheless, even when applying consecutive treatments and longer reaction times, the coupling methods were not efficient enough to obtain ester bond formation rates higher than 30%. Moreover, it was observed that, after a moderate conversion obtained in a more effective first treatment, the followings furnished conversions under 8%. Quantitative formation of the ester bond could not be achieved under these conditions.

On the basis of these results, DIPCDI-based methods were selected and more harsh conditions were implemented. At 45 °C there was a huge difference between the efficiency of the *O*-acylisourea and the symmetrical anhydride activated species. One single treatment of 2.5 h with aa-DIPCDI-DMAP (15:15:0.5) in DCM-DMF (9:1) at 45 °C was enough to obtain a 98% conversion. On the contrary, the conditions aa-DIPCDI-DMAP (16:10:0.5) in DCM-DMF at 45 °C required several consecutive treatments (12 h + 2 × 4 h + 2 × 5 h) to achieve 84% conversion. The use of the MW with the symmetrical anhydride conditions did not represent a significant improvement. After a first treatment of 30 min at 40 °C, which furnished a 27% of the ester bond, a second treatment of 2 h at 45 °C increased the conversion only a 7%.

Careful HPLC analysis of the crudes after formation of the ester bond at 45 °C allowed the identification of a second peak with the same mass of the desired intermediate. This by-product was not detected during the synthesis of Analog 2A and Analog 1A. The use of DMAP at high temperatures, even though in catalytic amounts, promotes the *C*-terminus racemization of the pipecolic residue furnishing two diastereomers of the desired intermediate. The epimerization was minimized down to 11% under the conditions aa-DIPCDI-DMAP (15:15:0.5) in DCM-DMF (9:1) for 2.3 h at 45 °C.

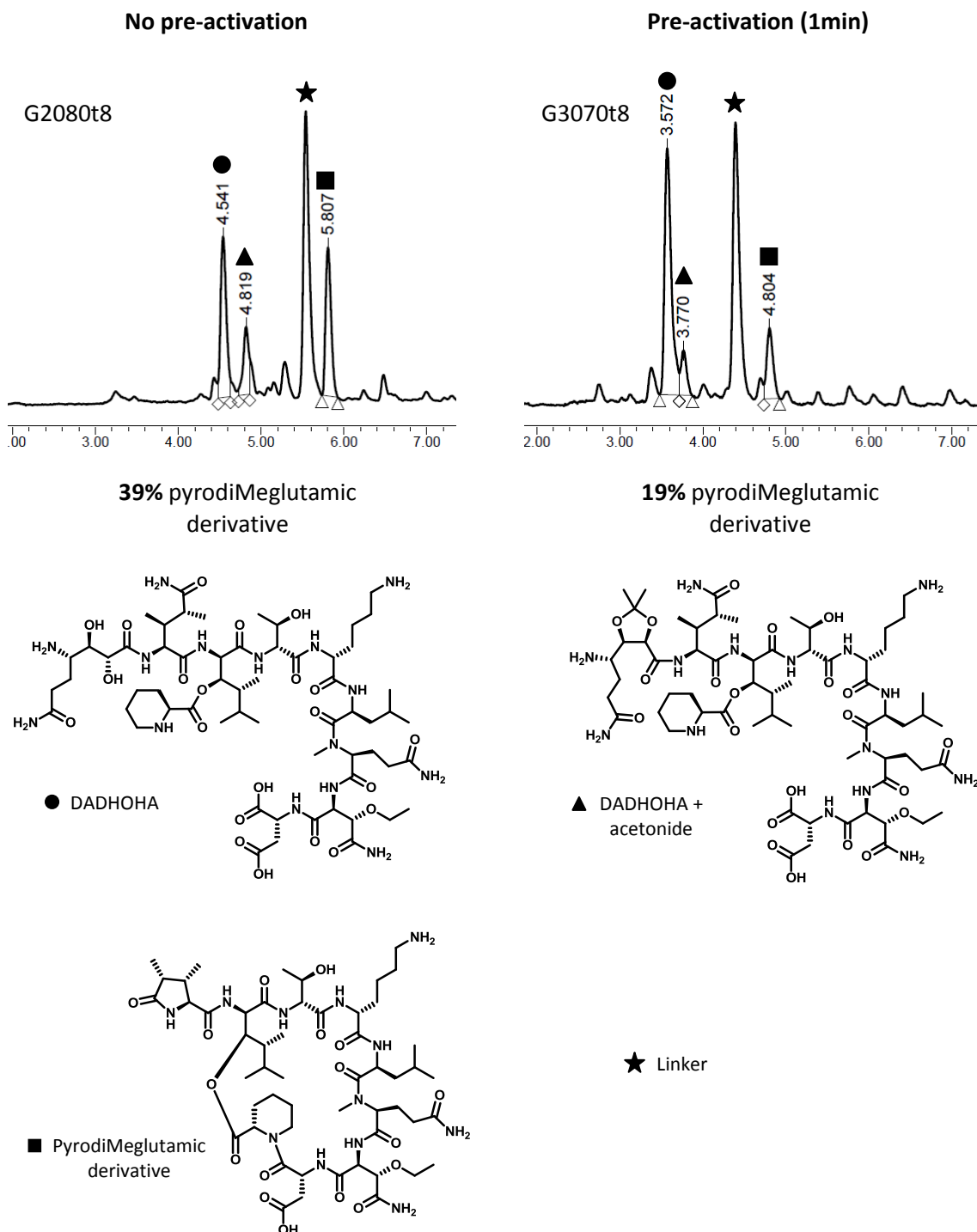
Quantitative conversions achieved after a single treatment of 2.5 h and the minimized racemization side reaction, account for the final choice of aa-DIPCDI-DMAP (15:15:0.5) at 45 °C as the coupling conditions to form the ester bond.

#### DADHOHA: pyrodiMeglutamic derivative minimization

The formation of the ester bond under harsh conditions (high temperatures in the presence of catalytic base) can promote the elimination of the Fmoc-protecting group of the diMe-Gln residue and the consequent formation of the pyrodiMeglutamic derivative. The exhaustive screening of conditions to form the ester bond revealed that the use of high temperatures is mandatory to achieve quantitative conversions. Thus, minimization of the pyrodiMeglutamic derivative while forming the ester cannot be improved. However, some more tuning of the DADHOHA incorporation can be studied. Syntheses of Analogs 1A and 2A showed the necessity of using efficient coupling methods in order to speed as much as possible the diol coupling and reduce the percentage of the pyrodiMeglutamic by-product. Hence, the reagents DIPCDI-HOBt were discarded in favour of the stronger HATU-HOAt-DIEA system. However, the steric demands of Pipecolidepsin A are higher and the need of efficiency for this coupling becomes even more imperative.

Pipecolidepsin A was attempted using HATU-HOAt-DIEA (2.5:2.5:5) in DMF for 1 h to incorporate the residue Fmoc-DADHOHA(acetonide, Trt)-OH. Two syntheses were performed, but only one implemented the pre-activation mode (1 min). One minute of pre-activation reduced 50% the percentage of pyrodiMeglutamic derivative in the final chromatogram (Figure 37).



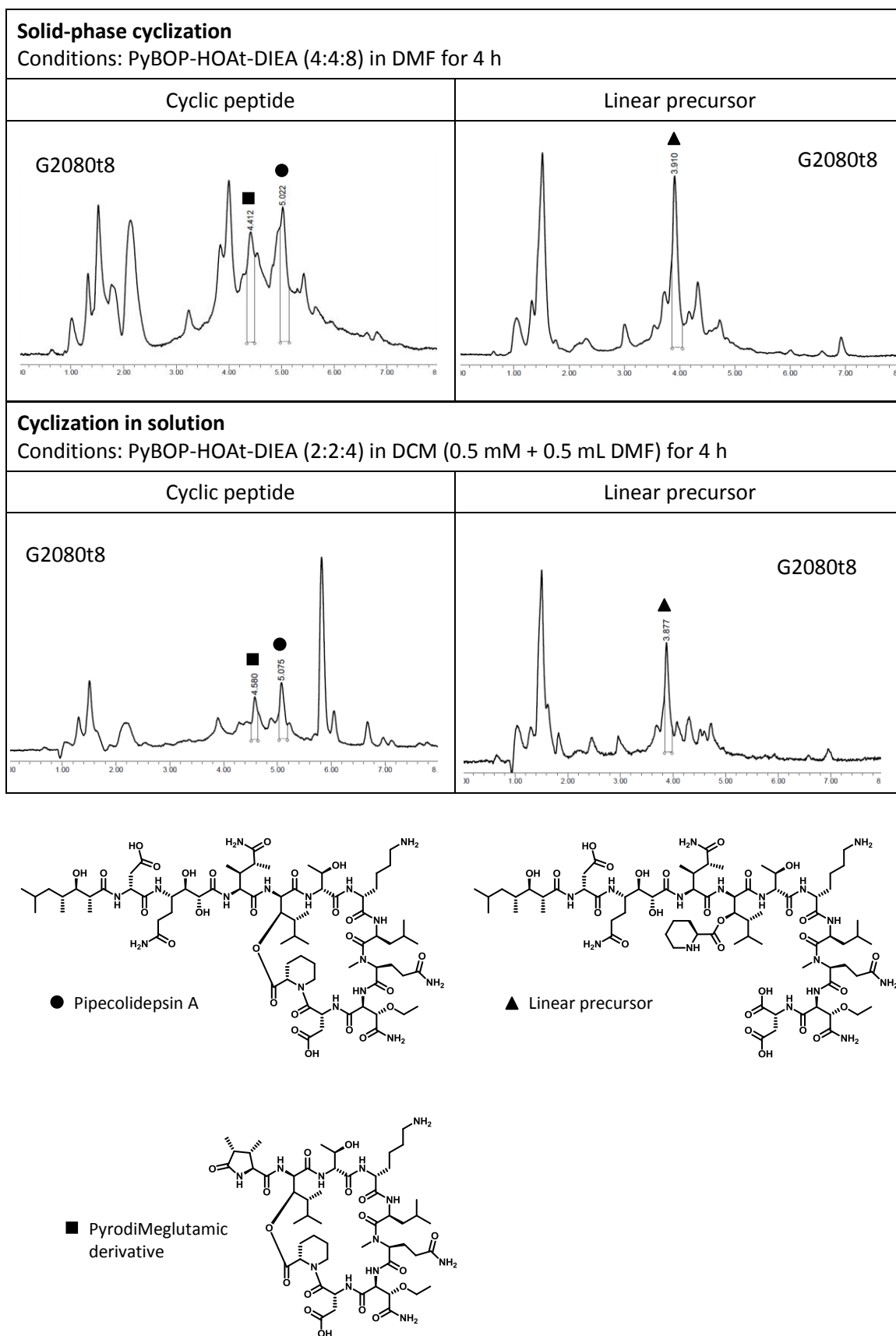


**Figure 37:** HPLC chromatograms at  $\lambda = 220$  nm after incorporation and Fmoc-elimination of the DADHOHA residue under the conditions aa-HATU-HOAt-DIEA (2.5:2.5:2.5:5) in DMF for 1 h; a) without pre-activation; b) with 1 min of pre-activation. The major peak corresponds to the linker (see section 1.5.3.3.).

Other attempts such as adding HOBt to the piperidine solution for the Fmoc elimination of diMe-Gln residue or incorporating the DADHOHA moiety with DIPCDI-Oxyma were completely unsuccessful.

### Macrolactamization: solid phase vs solution

Once a strategy to obtain the fully assembled linear peptide was validated, the macrolactamization step was subjected to evaluation. Thus, two different linear precursors were synthesized: starting by side-chain anchoring Fmoc-D-Asp(OH)-OAllyl to the resin and by incorporation through the  $\alpha$ -COOH of Fmoc-D-Asp(<sup>t</sup>Bu)-OH. Both solid-phase cyclization and cyclization in solution were performed using the coupling method PyBOP-HOAt-DIEA (Figure 38), which proved to be the best option (see section 1.5.1.2.). The macrolactamization step proceeds cleaner when it is performed in solution.



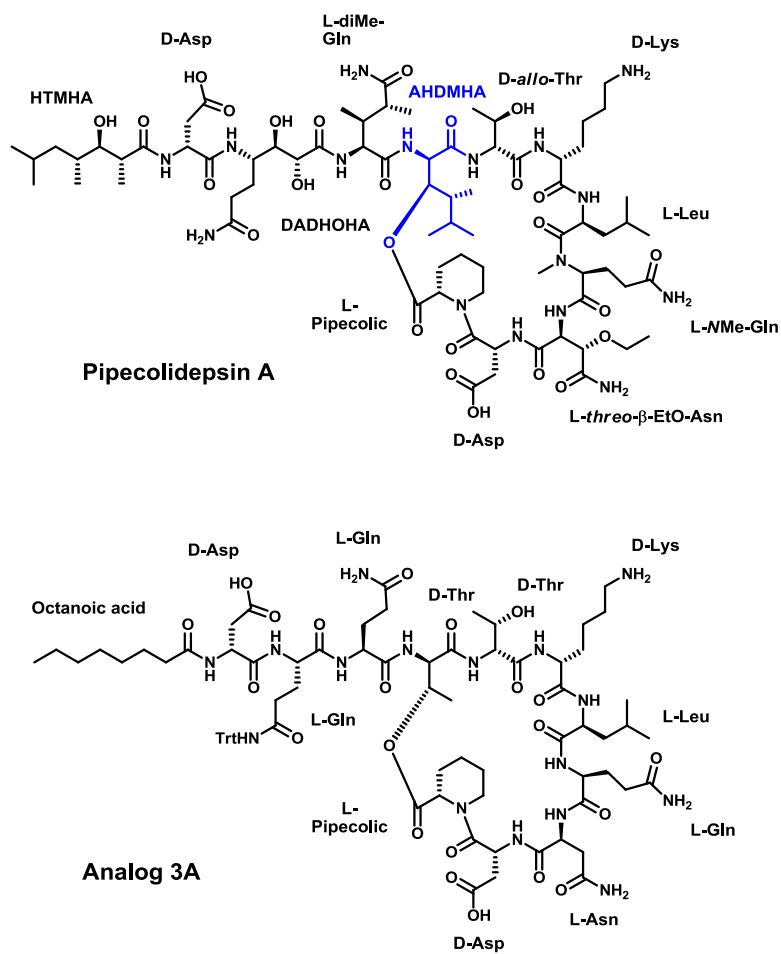
**Figure 38:** HPLC chromatograms of the linear precursors and the corresponding cyclized peptides from cyclizations on solid-phase and in solution.

### Scale up: change of resin

All the optimization of Pipecolidepsin A synthesis was performed at really small scale (less than 30 mg of 2-CTC resin). During the scaling-up (200 mg of 2-CTC resin) of the synthetic scheme, an unexpected problem appeared. HPLC analysis after the treatment to form the ester bond showed extremely low absorbances. Furthermore, a significant decrease in the resin weight was also detected after the performance of this synthetic step. These features altogether suggested that the conditions required to form the ester bond were too harsh for the labile 2-CTC resin, and that the peptide was undergoing partial cleavage during ester formation.

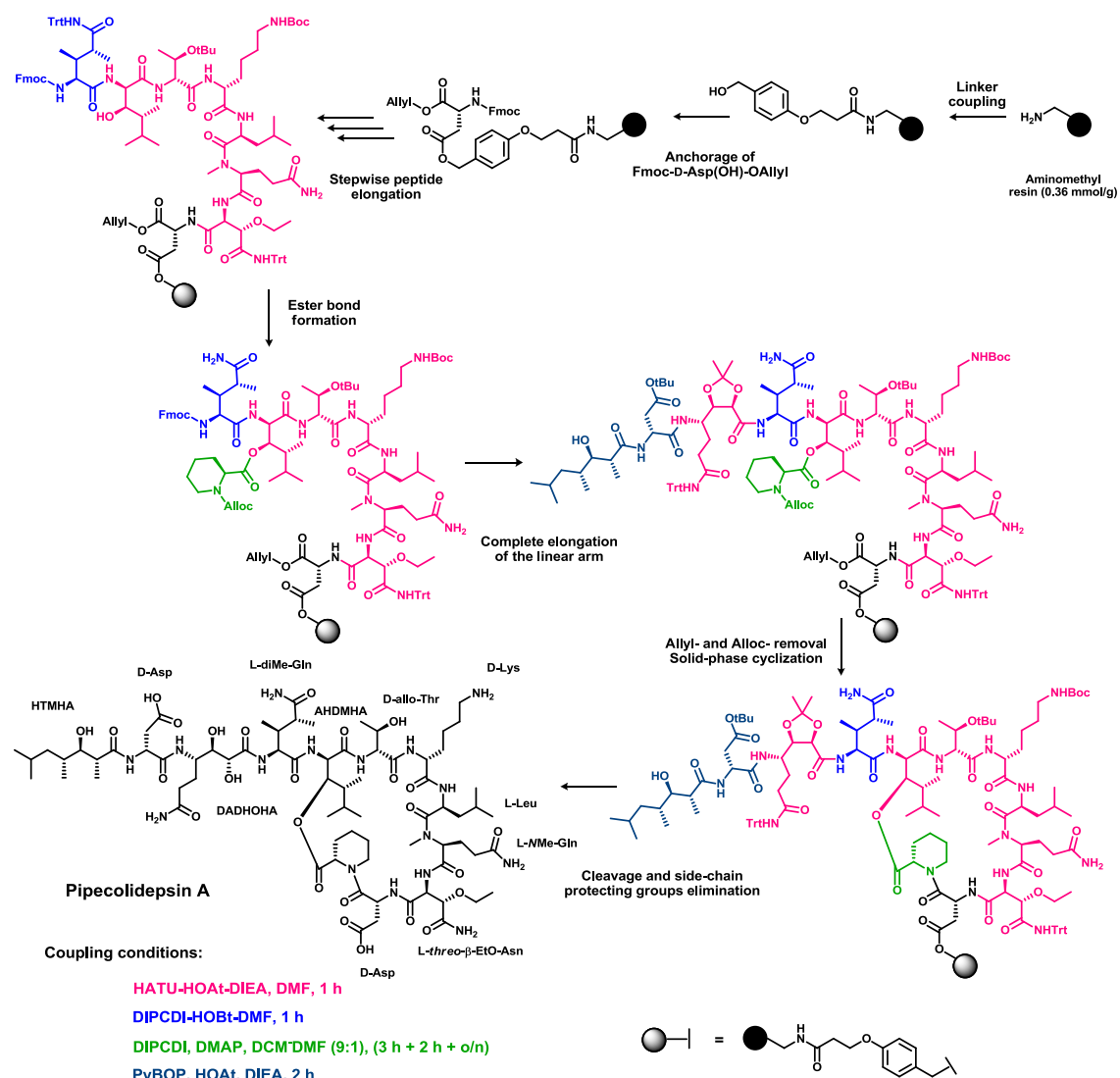
A second analog of Pipecolidepsin A (Figure 39) in which all the residues were replaced by commercially available amino acids, was synthesized at larger scale (200 mg of 2-CTC resin). We wanted to investigate whether or not the peptidic sequence was partially responsible of the loss of peptide. Since the peptide was also partially cleaved after the ester bond formation, it is foreseen that the harsh conditions used in its construction are the only responsible of the loss of the growing peptidic chain. Additionally, the symmetrical anhydride conditions were also examined to find that they enhanced cleavage of the peptide.

In order to solve this problem and considering the impossibility of changing the ester bond formation conditions, the 2-CTC resin was replaced by the more resistant Wang like resin [3-(4-hydroxymethylphenoxy)propionylaminopolystyrene]. The use of this Wang resin precludes carrying out the macrolactamization step in solution since the cleavage of the peptide from the resin, would concomitantly remove all protecting groups.



**Figure 39:** Chemical structures of Pipecolidepsin A and Analog 2D. The key AHDMHA residue is shown in blue.

## 1.5.3.3. Third strategy: change of resin



**Scheme 27:** Pipecolidepsin A third synthetic strategy: diMe-Gln incorporation + ester bond formation. Implementation of the Wang like resin. Coupling conditions are shown in different colors.

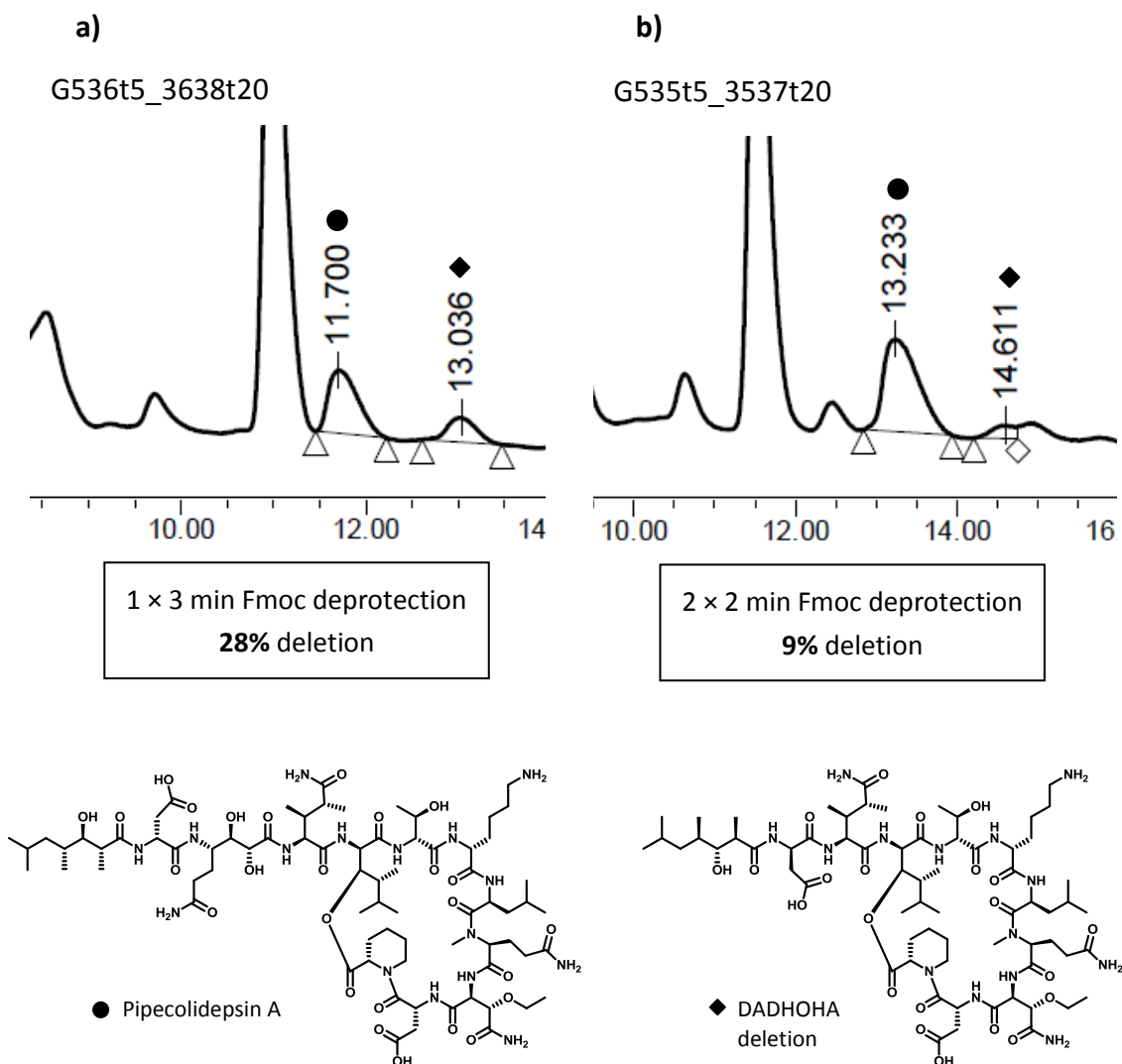
The 2-CTC resin was replaced by a Wang-like resin with a loading capacity of 0.36 mmol/g to facilitate the solid-phase macrolactamization (Scheme 27). Thus, after incorporation of the [3-(4-hydroxymethylphenoxy)propionic acid (AB linker) with HBTU-HOBt-DIEA (3:3:3) in DMF for 1.5 h, the Fmoc-D-Asp(OH)-OAllyl was side-chain anchored to the resin under the conditions aa-DIPCDI-HOBt-DMAP (5:5:5:0.5) in DCM-DMF (1.3:1) for (2 × 3 h). To terminate the excess of reactive positions, the resin was acetylated using a solution of Ac<sub>2</sub>O-DIEA (50:50) in DMF for 16 min. The peptidic chain was elongated until the AHDMHA residue by employing the coupling method HATU-HOAt-DIEA (x:x:2x) in DMF for 1 h in pre-activation mode (1 min). Only the Leu residue was re-coupled. Then, Fmoc-diMe-Gln-OH was incorporated using DIPCDI-HOBt (4.5:4.5) in DMF for 1 h without pre-activation and the ester

bond was formed under the conditions Alloc-pipecolic-OH-DIPCDI-DMAP (15:15:0.5) in DCM-DMF (9:1) at 45 °C for 2.5 h. After HPLC verification of the quantitative formation of the ester bond, the DADHOHA moiety was coupled with HATU-HOAt-DIEA (2.5:2.5:5) in DMF for 1 h in pre-activation mode (1 min). The last two moieties were incorporated as a single unit with PyBOP-HOAt-DIEA (5:5:10) in DMF for 3.5 h without pre-activation. The Fmoc group from the diMe-Gln residue was eliminated with a short treatment 2 × 2 min with piperidine-DMF (1:4) (see below). The rest of the Fmoc groups were removed using a long treatment of 2 × 1 min, 2 × 5 min and 1 × 10 min. Finally, after elimination of the Allyl and Alloc groups with catalytic [Pd(PPh<sub>3</sub>)<sub>4</sub>] in the presence of the scavenger Ph<sub>3</sub>SiH, the macrolactamization step was carried out on solid phase with PyBOP-HOAt-DIEA (4:4:8) in DMF for 3 h. The linkage peptide-resin was cleaved and the side-chain protecting groups eliminated simultaneously with a treatment of 1.5 h with a TFA-H<sub>2</sub>O-TIS (95:2.5:2.5) solution.

All the synthetic scheme established with 2-CTC worked analogously with the Wang like resin [3-(4—hydroxymethylphenoxy)propionylaminopolystyrene]. No DKP formation was detected and only a problem due to the bigger scale needed optimization.

#### diMe-Gln: short Fmoc elimination and scale up

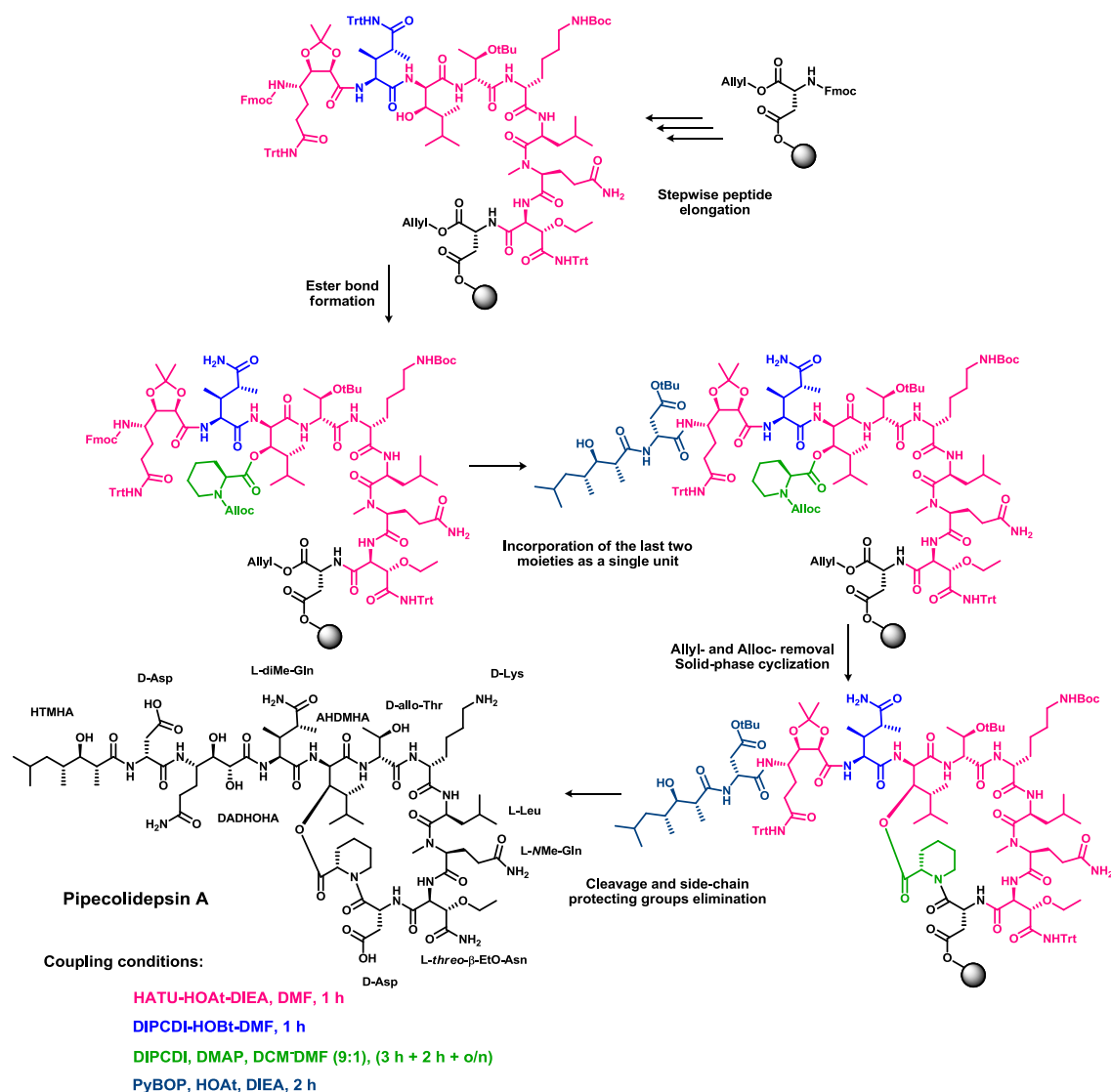
A new by-product was identified by HPLC-PDA and HPLC-MS analysis after complete assembly of the linear precursor of corrected Pipecolidepsin A during the first large scale synthesis. The mass matched with a DADHOHA deletion. However, a deletion at this position was completely unexpected because of the huge tendency of the previous residue to undergo intramolecular lactamization when its  $\alpha$ -amino group is unprotected. To confirm the identity of the new by-product, the Fmoc elimination treatment of 1 × 3 min (Figure 40 a) was replaced by a 2 × 2 min (Figure 40 b), a bit longer and involving the renewal of the piperidine solution. HPLC analysis showed a substantial decrease of the new impurity, thus supporting the initial hypothesis.



Sterical reasons would explain this phenomenon. A long piperidine treatment would remove not only all the Fmoc group from the DADHOHA residue, but also the remaining Fmoc from the diMe-Gln. Nevertheless, partial incorporation of the DADHOHA would render a more hindered environment, thus preventing the free diMe-Gln  $\alpha$ -amino from undergoing intramolecular lactamization. A longer Fmoc-deprotection treatment decreases the occurrence of the DADHOHA deletion in a 68%.



## 1.5.3.4. Fourth strategy: DADHOHA + ester



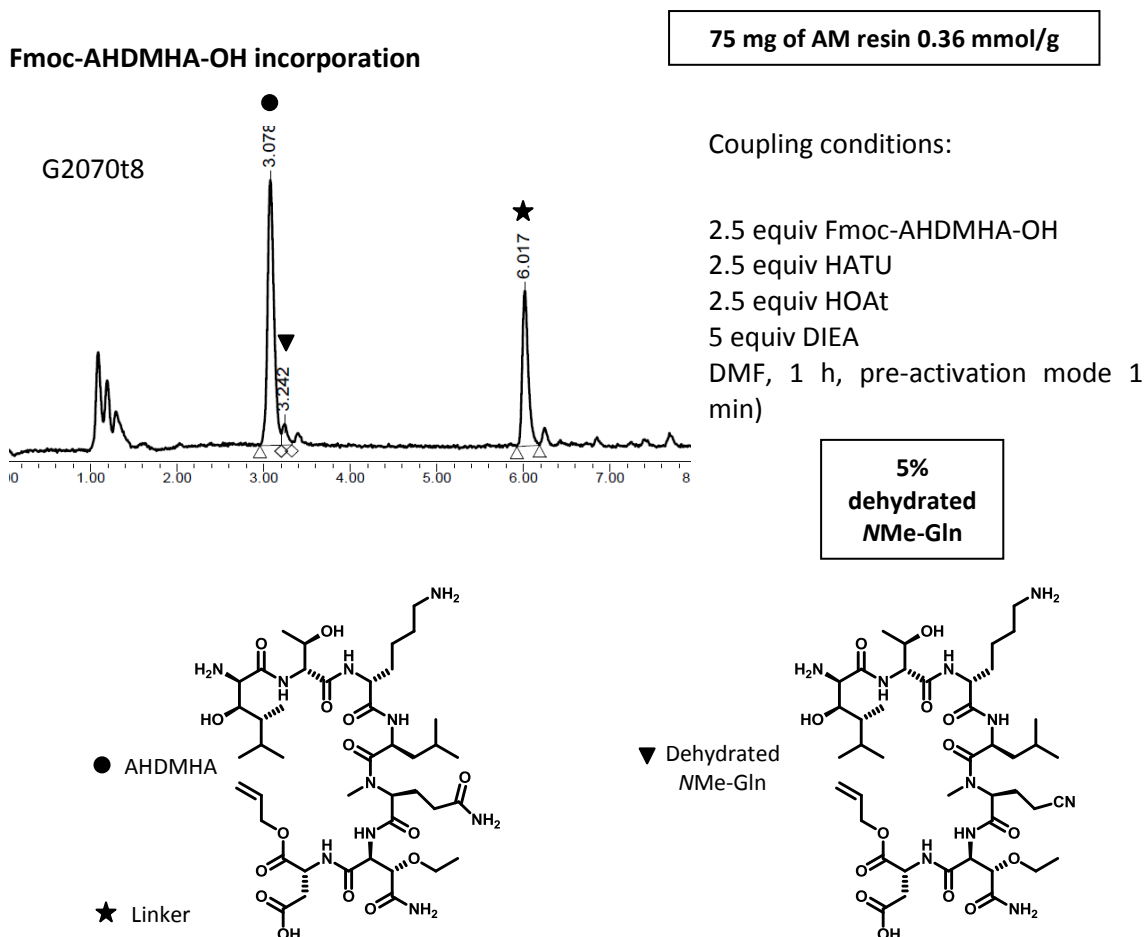
**Scheme 28:** Pipecolidepsin A fourth synthetic strategy: DADHOHA incorporation + ester bond formation. The synthesis is performed on 2-CTC resin. Coupling conditions are shown in different colors.

A last synthetic strategy examined whether or not the formation of the ester bond at a later stage of the linear peptide assembly would furnish cleaner chromatographic profiles and higher yields (Scheme 28). The incorporation of the DADHOHA residue before Alloc-pipecolic-OH entails a significant increase in the sterical hindrance around AHDMHA hydroxyl group, challenging even more the construction of an already highly demanding ester bond. This synthetic scheme claims to minimize as much as possible the formation of the prodiMeglutamic by-product. In view of the exhaustive screening of conditions to form the ester bond in a less bulky environment, it is foreseen that extremely harsh conditions will be required.

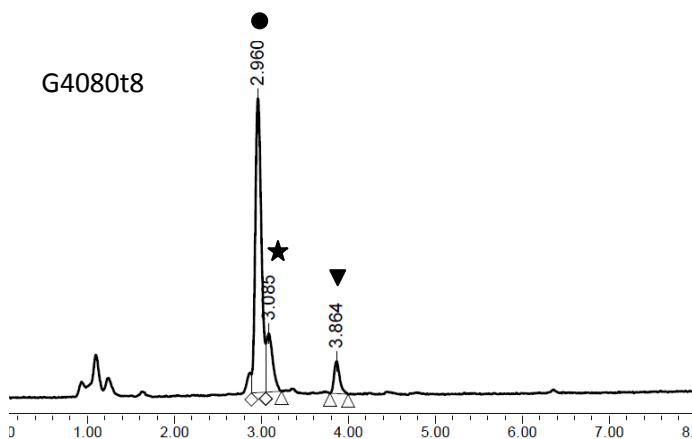
### Pipecolic: ester bond formation

The ester bond formation was attempted using the best conditions found in the previous diMe-Gln incorporation + ester bond formation strategy, but substantially increasing the temperature. Thus, after a 3 h-treatment with Alloc-pipecolic-OH-DIPCDI-DMAP (15:15:0.5) in DCM-DMF (9:1) at 75 °C, only starting material was recovered. An additional treatment of 2 h under the same conditions but using the microwave was completely unsuccessful and no starting material was identified by HPLC analysis. No more conditions were screened and the strategy was ruled out.

#### 1.5.3.5. HPLC-PDA monitoring of Pipecolidepsin A large scale synthesis



## Fmoc-diMe-Gln-OH incorporation



Coupling conditions:

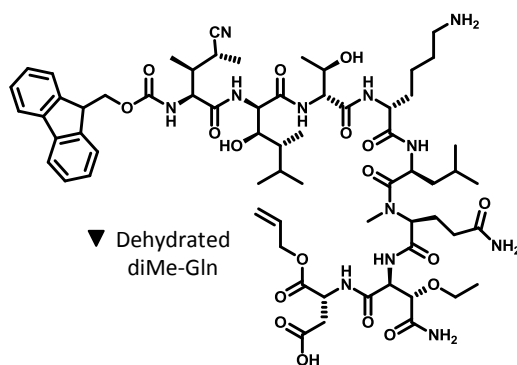
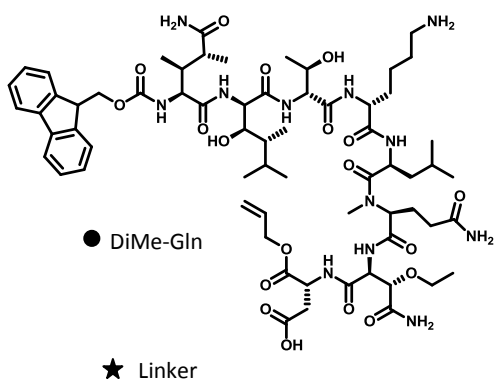
4.5 equiv Fmoc-diMe-Gln-OH

4.5 equiv DIPCDI

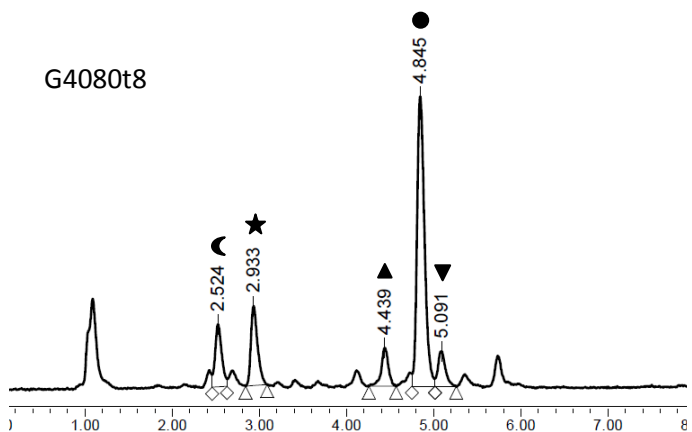
4.5 equiv HOBt

DMF, 1 h, no pre-activation mode

9%  
dehydrated  
diMe-Gln



## Ester bond formation



Coupling conditions:

15 equiv Fmoc-diMe-Gln-OH

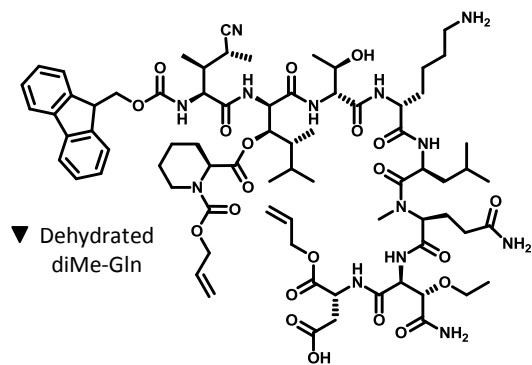
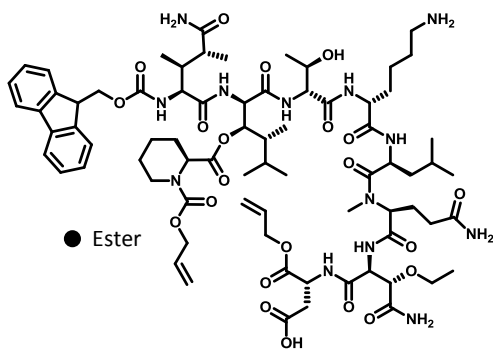
15 equiv DIPCDI

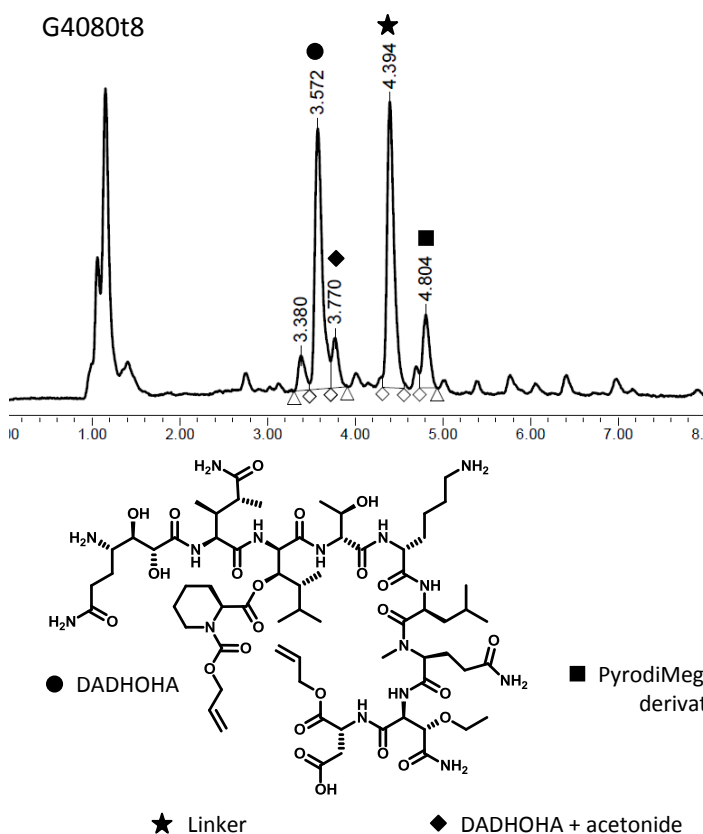
0.5 equiv DMAP

Dry DCM-DMF (9:1), 2 h, 45 °C

Another 30 min-treatment was required

Ester-epimer  
89:11

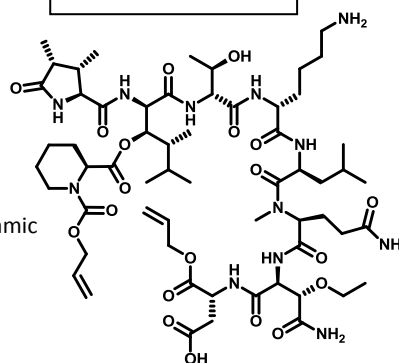
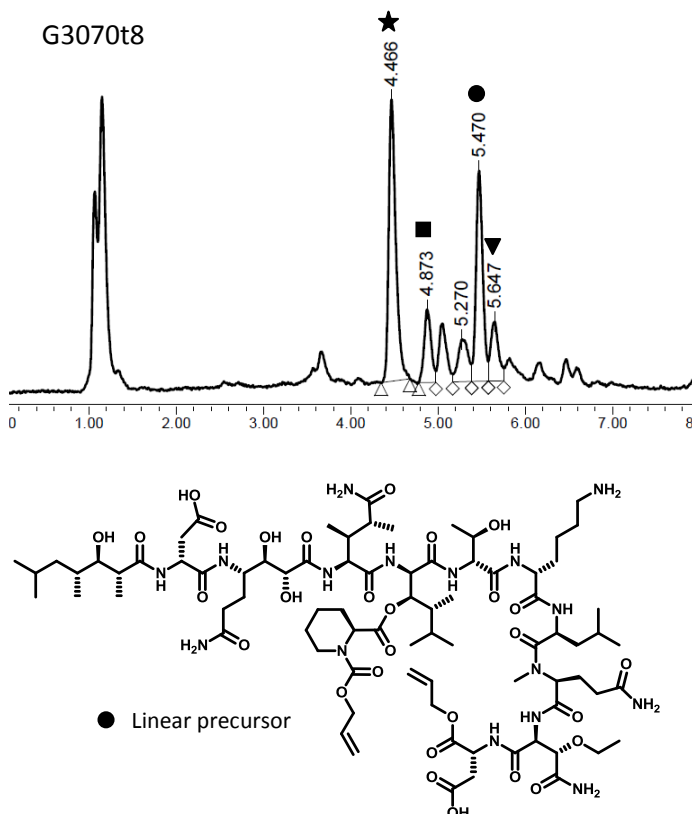


**Fmoc-DADHOHA(acetonide, Trt)-OH incorporation**


Coupling conditions:

2.5 equiv Fmoc-DADHOHA(acetonide, Trt)-OH  
 2.5 equiv HATU  
 2.5 equiv HOAt  
 5 equiv DIEA  
 DMF, 1 h, pre-activation mode (1 min)

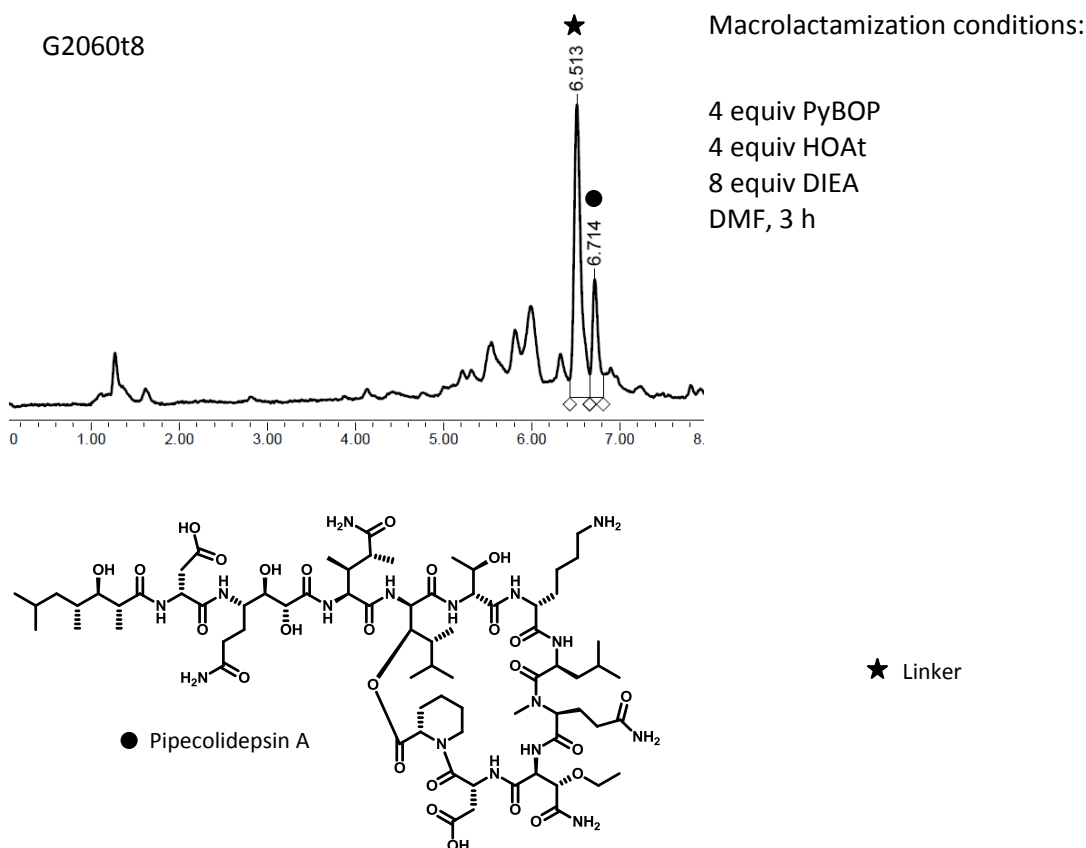
DADHOHA-  
 PyrodiMeglutamic  
 82:18


**Complete assembly of the linear precursor**


Coupling conditions:

5 equiv HTMHA-D-Asp(<sup>t</sup>Bu)-OH  
 5 equiv PyBOP  
 5 equiv HOAt  
 10 equiv DIEA  
 DMF, 3.5 h, no pre-activation mode

## Final cyclization step

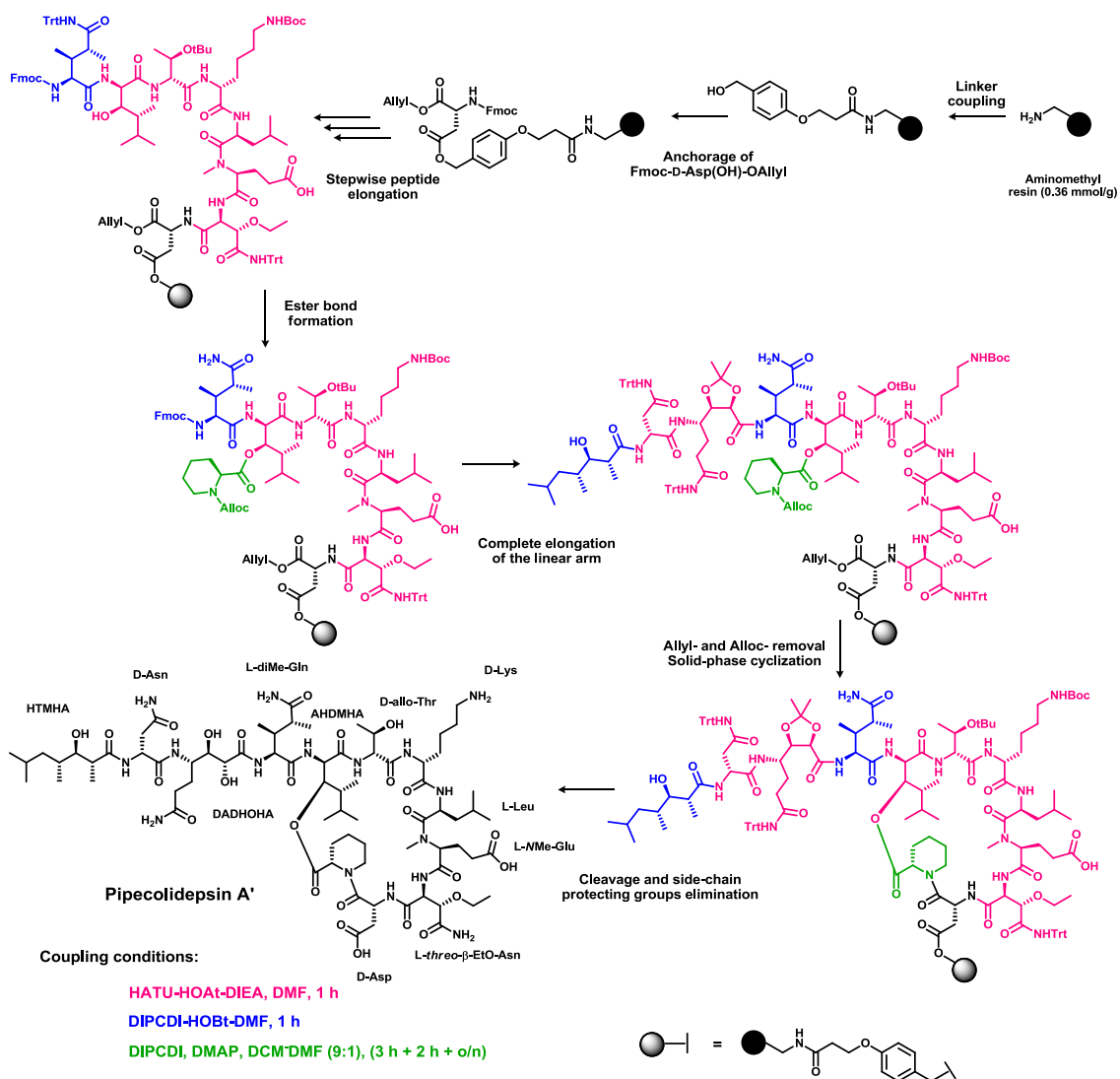


## 1.5.4. Solid-phase synthesis of Pipecolidepsin A'

Although the well-founded hypothesis that the first Pipecolidepsin A structure proposal was miss-assigned, it was decided to undertake its synthesis in order to enable its comparison with the natural product.

1.5.4.1. First strategy: *diMe-Gln + ester. Stepwise arm elongation.*

All the optimizations done during Pipecolidepsin A synthetic studies were applied to Pipecolidepsin A'. This means: resin choice; coupling conditions of building blocks; Fmoc-elimination treatments; minimization of *diMe-Gln* side-chain amide dehydration; ester bond formation; reduction of *pyrodiMe-glutamic* derivative; decrease of *DADHOHA* deletion and solid-phase macrolactamization. The main change with regard to Pipecolidepsin A synthesis was the stepwise total assembly of the linear arm due to the absence of aspartimides formation. Furthermore, the replacement of *NMe-Gln* moiety by *NMe-Glu* eliminates the side-chain dehydration by-product. Thus, Pipecolidepsin A final synthetic strategy was also applied to Pipecolidepsin A' (Scheme 30).

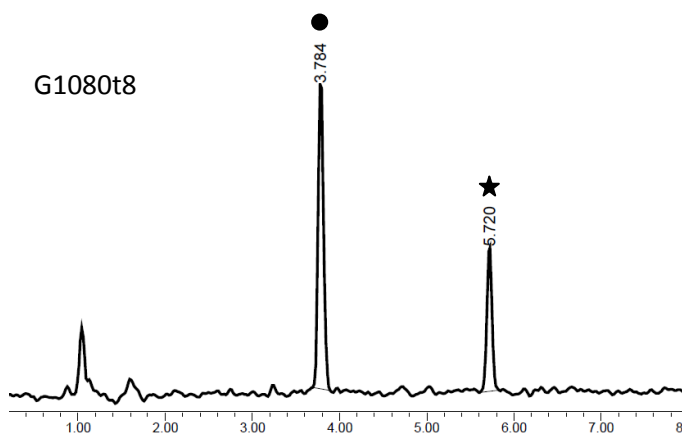


**Scheme 30:** Pipecolidepsin A' synthetic strategy: diMe-Gln incorporation + ester bond formation. Coupling conditions are shown in different colors.

1.5.4.2. HPLC-PDA monitoring of *Pipecolidepsin A'* large scale synthesis

## Fmoc-AHDMHA-OH incorporation

150 mg of AM resin 0.36 mmol/g



Coupling conditions:

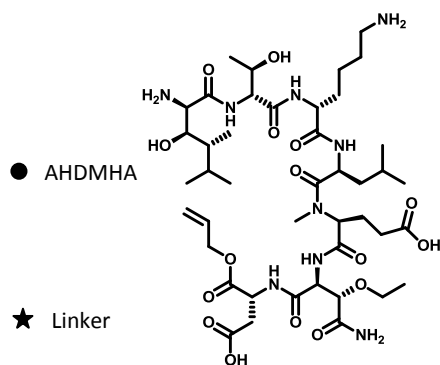
2.5 equiv Fmoc-AHDMHA-OH

2.5 equiv HATU

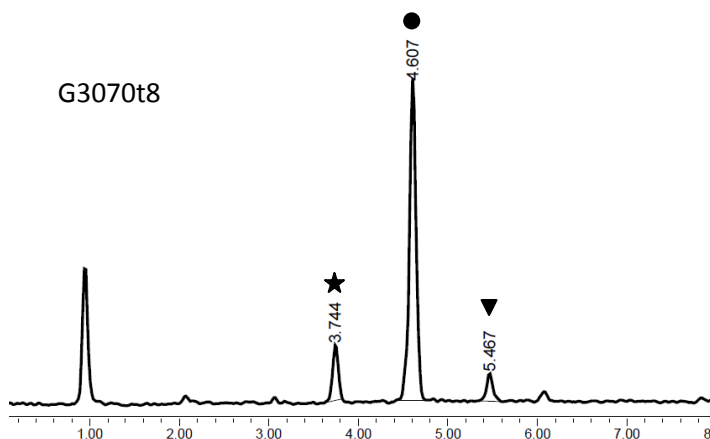
2.5 equiv HOAt

5 equiv DIEA

DMF, 1 h, pre-activation mode (1 min)



## Fmoc-diMe-Gln-OH incorporation



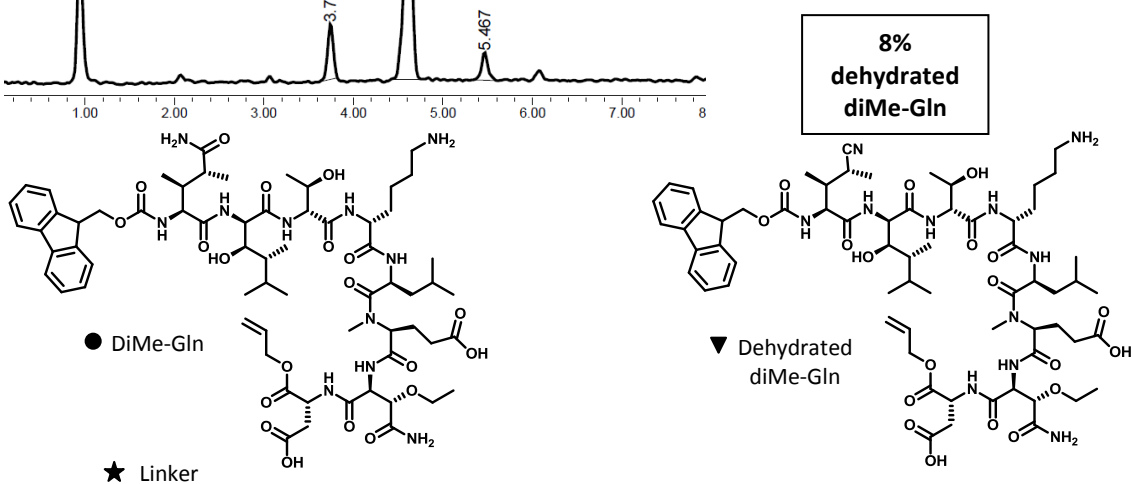
Coupling conditions:

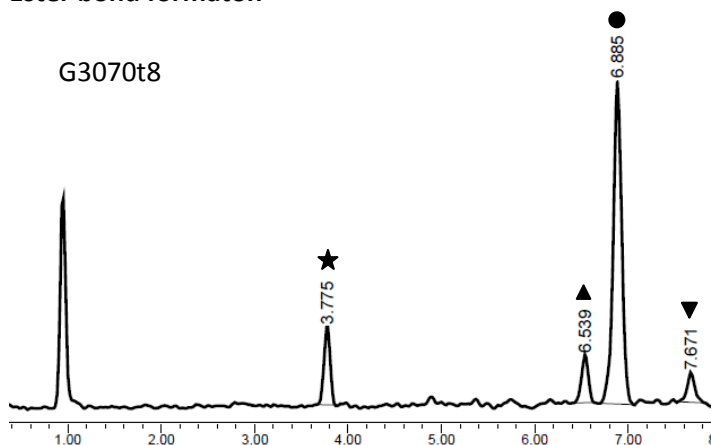
4.5 equiv Fmoc-diMe-Gln-OH

4.5 equiv DIPCDI

4.5 equiv HOBT

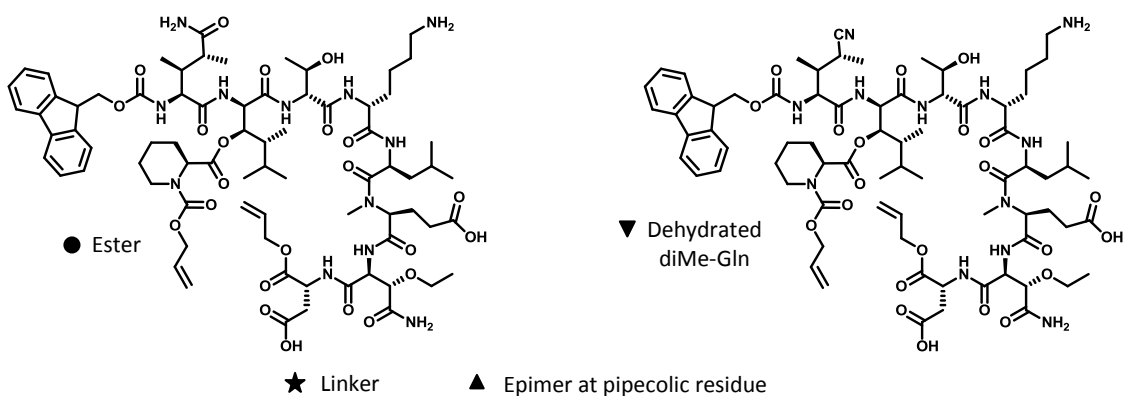
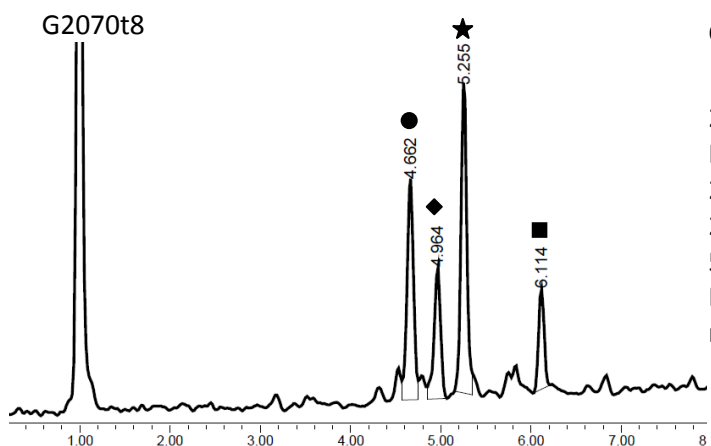
DMF, 1 h, no pre-activation mode



**Ester bond formaton**


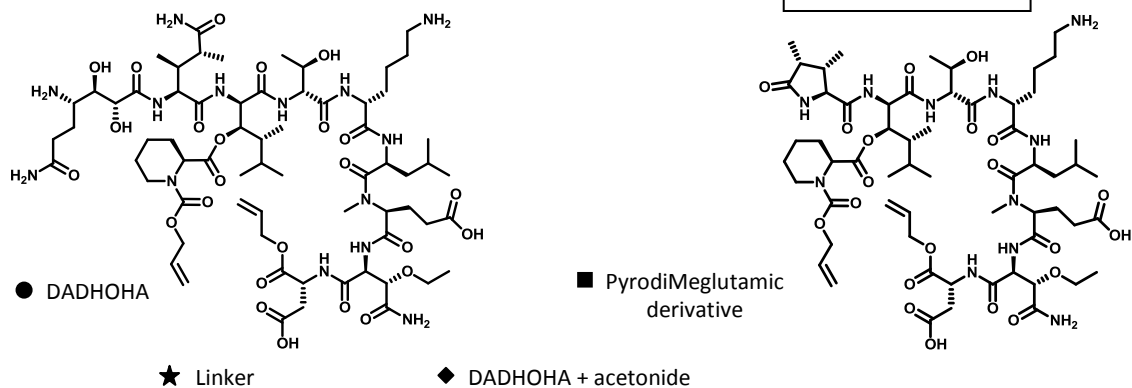
Coupling conditions:

 15 equiv Fmoc-diMe-Gln-OH  
 15 equiv DIPCDI  
 0.5 equiv DMAP  
 Dry DCM-DMF (9:1), 2 h 5 min,  
 45 °C

**Ester-epimer  
89:11**

**Fmoc-DADHOHA(acetonide, Trt)-OH incorporation**


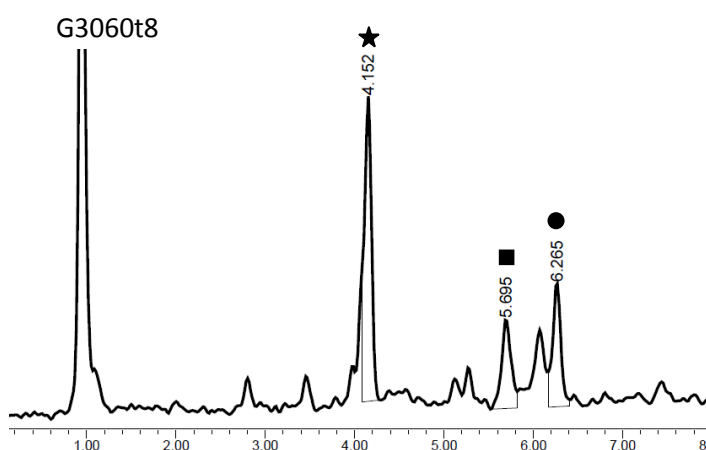
Coupling conditions:

 2.5 equiv Fmoc-DADHOHA(acetonide, Trt)-OH  
 2.5 equiv HATU  
 2.5 equiv HOAt  
 5 equiv DIEA  
 DMF, 1 h, pre-activation mode (1 min)

**DADHOHA-  
PyrodiMeglutamic  
81:19**


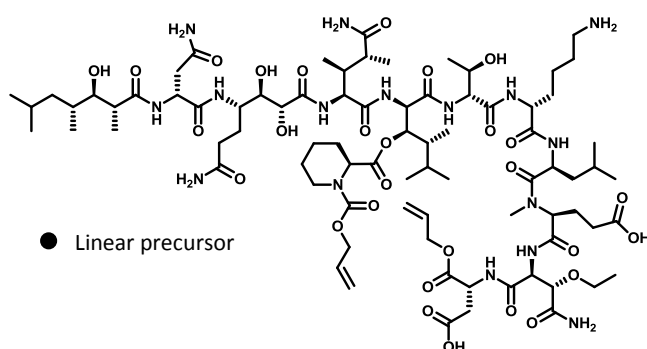


## Complete assembly of the linear precursor



Coupling conditions:

3 + 1 equiv HTMHA  
 3 + 1 equiv DIPCDI  
 3 + 1 equiv HOBt  
 DMF, 3.25 h + 1 h, no pre-activation mode

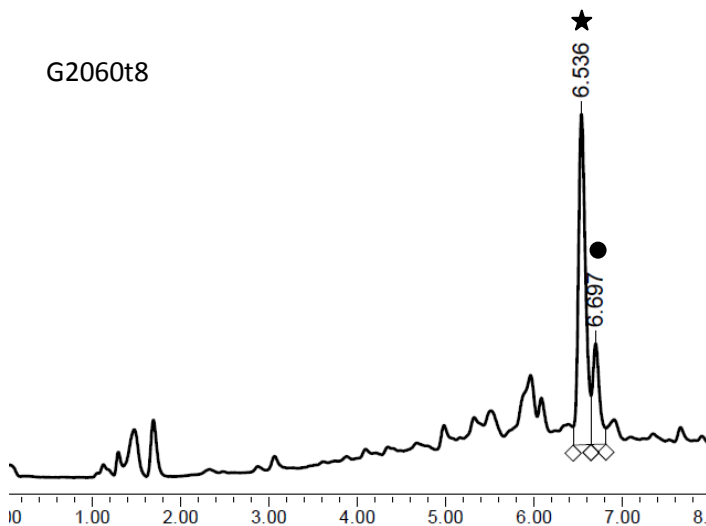


★ Linker

■ PyrodiMeglutamic derivative

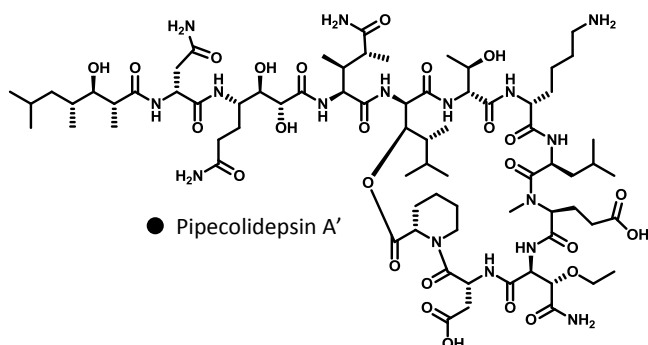
● Linear precursor

## Final cyclization step



Macrolactamization conditions:

4 equiv PyBOP  
 4 equiv HOAt  
 8 equiv DIEA  
 DMF, 3 h



★ Linker

● Pipecolidepsin A'

The extents of the side reactions occurring during Pipecolidepsin A large scale synthesis are completely reproducible during Pipecolidepsin A' synthesis. Thus, no more optimizations were done with the new peptide.

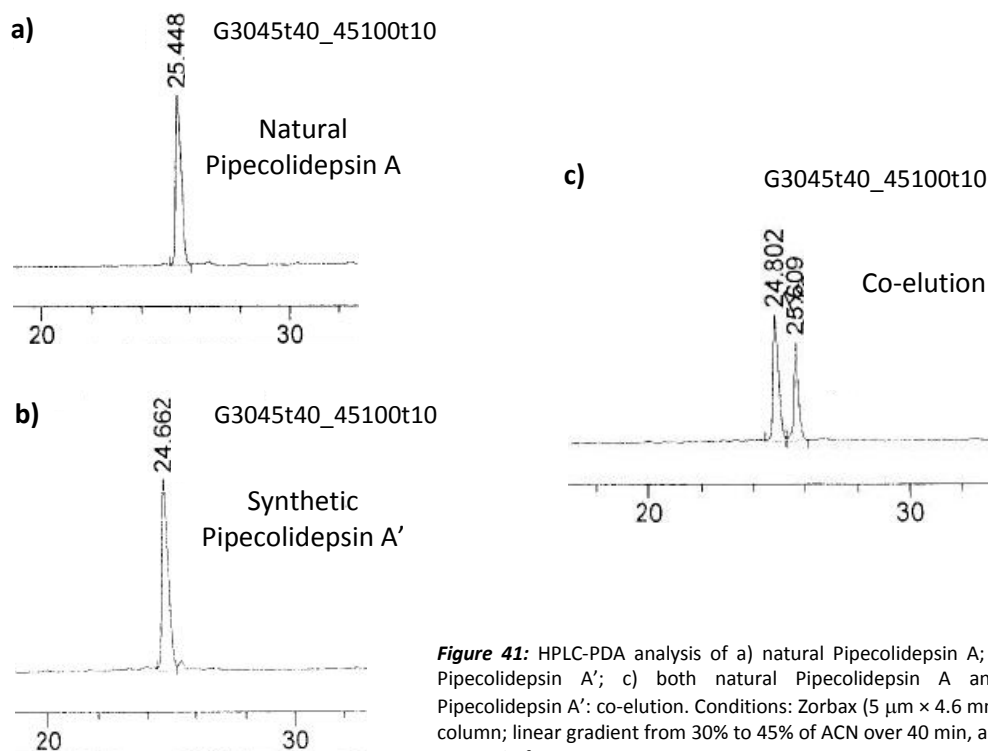
### 1.5.5. Validation of synthetic Pipecolidepsin A' and Pipecolidepsin A

The validation of the proposed structure for a natural product is always a crucial and decisive step when synthesizing natural compounds. Regarding to our targeted molecule, this validation step should allow settling the doubt over the placement of the fourth side-chain amide. Thus, a series of chemical, spectral and biological validations were undertaken in order to unequivocally assign one of the two proposed structures to natural Pipecolidepsin A.

#### 1.5.5.1. Chemical validation

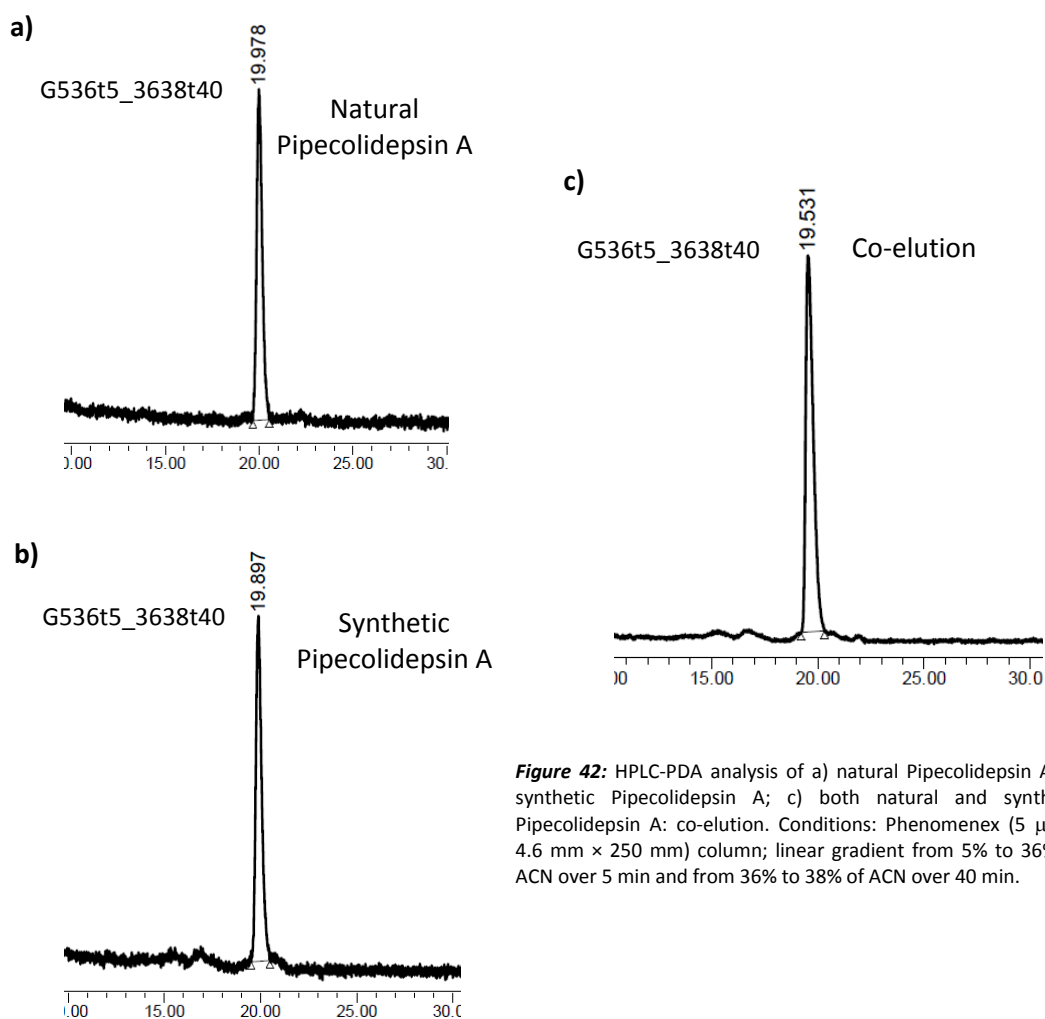
Three samples of natural Pipecolidepsin A, synthetic Pipecolidepsin A' (Figure 41) and synthetic Pipecolidepsin A (Figure 42) were dissolved in H<sub>2</sub>O-ACN (1:1) and analyzed by reversed-phase HPLC by means of an extremely long C18 analytical column. Then, each sample of synthetic compound was co-eluted, one by one, with the natural sample using an extremely plane gradient. HRMS data for the three samples matched perfectly.

#### Validation of synthetic Pipecolidepsin A'



**Figure 41:** HPLC-PDA analysis of a) natural Pipecolidepsin A; b) synthetic Pipecolidepsin A'; c) both natural Pipecolidepsin A and synthetic Pipecolidepsin A': co-elution. Conditions: Zorbax (5  $\mu$ m  $\times$  4.6 mm  $\times$  150 mm) column; linear gradient from 30% to 45% of ACN over 40 min, and from 45% to 100% of ACN over 10 min.

## Validation of synthetic Pipecolidepsin A



**Figure 42:** HPLC-PDA analysis of a) natural Pipecolidepsin A; b) synthetic Pipecolidepsin A; c) both natural and synthetic Pipecolidepsin A: co-elution. Conditions: Phenomenex (5  $\mu\text{m}$   $\times$  4.6 mm  $\times$  250 mm) column; linear gradient from 5% to 36% of ACN over 5 min and from 36% to 38% of ACN over 40 min.

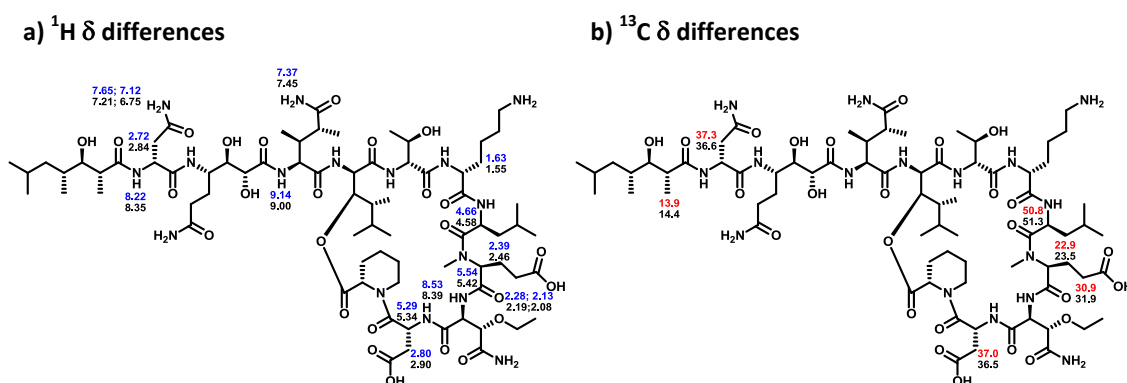
These analyses were unambiguously conclusive. While synthetic Pipecolidepsin A' showed an earlier retention time (0.807 min of difference) than the natural compound, synthetic Pipecolidepsin A perfectly co-eluted with natural Pipecolidepsin A. Thus, this single co-elution peak was validating the synthetic strategy and confirming the chemical identity of both natural and synthetic Pipecolidepsin A.

### 1.5.5.2. Spectral validation

Spectral equivalence was validated by comparison of monodimensional and bidimensional NMR data of the two synthetic compounds with regard to the natural product. The complete  $^1\text{H}$  and  $^{13}\text{C}$  assignment in  $\text{CD}_3\text{OH}$  for synthetic Pipecolidepsin A' and synthetic Pipecolidepsin A is detailed in the experimental section. Herein we try to reflect the more significant differences in  $^1\text{H}$  and  $^{13}\text{C}$  of each synthetic compound regarding the values reported in the patent WO 2010/070078 A1 for natural Pipecolidepsin A.

### Pipecolidepsin A' (NMe-Glu and D-Asn)

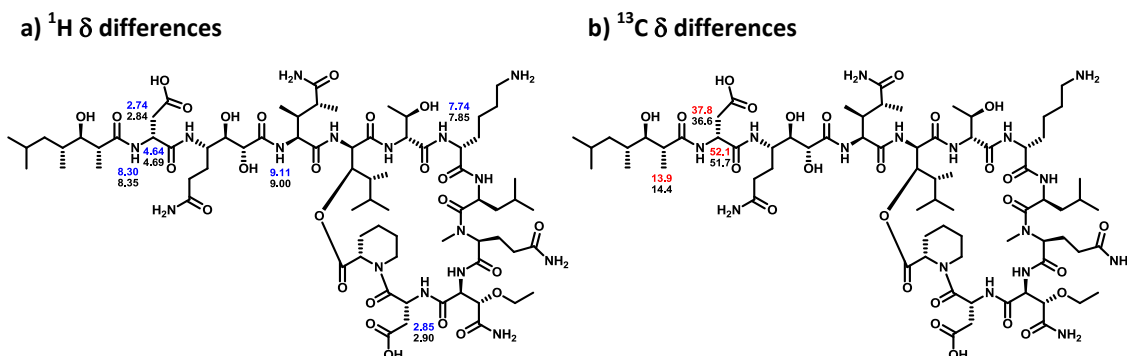
2.3 mg of synthetic Pipecolidepsin A' with purity above 95% determined by HPLC-PDA analysis at 220 nm were dissolved in 650  $\mu\text{L}$  of  $\text{CD}_3\text{OH}$ . WaterGate and PreSat  $^1\text{H}$ , gCOSY, TOCSY (mixing time = 80 ms), NOESY (mixing time = 400 ms) and  $^{13}\text{C}$  experiments were recorded on a Bruker 600 Avance III Ultrashielded spectrometer provided with a cryoprobe TCI (600 MHz for  $^1\text{H}$  NMR, 150 MHz for  $^{13}\text{C}$  NMR). Differences of  $^1\text{H}$  above 0.05 ppm and of  $^{13}\text{C}$  above 0.4 ppm are highlighted in Figure 43.



**Figure 43:** a)  $^1\text{H}$  chemical shifts of synthetic Pipecolidepsin A' (in blue) and natural Pipecolidepsin A (in black); b)  $^{13}\text{C}$  chemical shifts of synthetic Pipecolidepsin A' (in red) and natural Pipecolidepsin A (in black).

### Pipecolidepsin A (NMe-Gln and D-Asp)

2.9 mg of Pipecolidepsin A with purity above 95% determined by HPLC-PDA analysis at 220 nm were dissolved in 650  $\mu\text{L}$  of  $\text{CD}_3\text{OH}$ . WaterGate and PreSat  $^1\text{H}$ , gCOSY, TOCSY (mixing time = 80 ms), NOESY (mixing time = 600 ms), gHMBC and  $^{13}\text{C}$  experiments were recorded on a Bruker 600 Avance III Ultrashielded spectrometer provided with a cryoprobe TCI (600 MHz for  $^1\text{H}$  NMR, 150 MHz for  $^{13}\text{C}$  NMR). Differences of  $^1\text{H}$  above 0.05 ppm and of  $^{13}\text{C}$  above 0.4 ppm are highlighted in Figure 44.

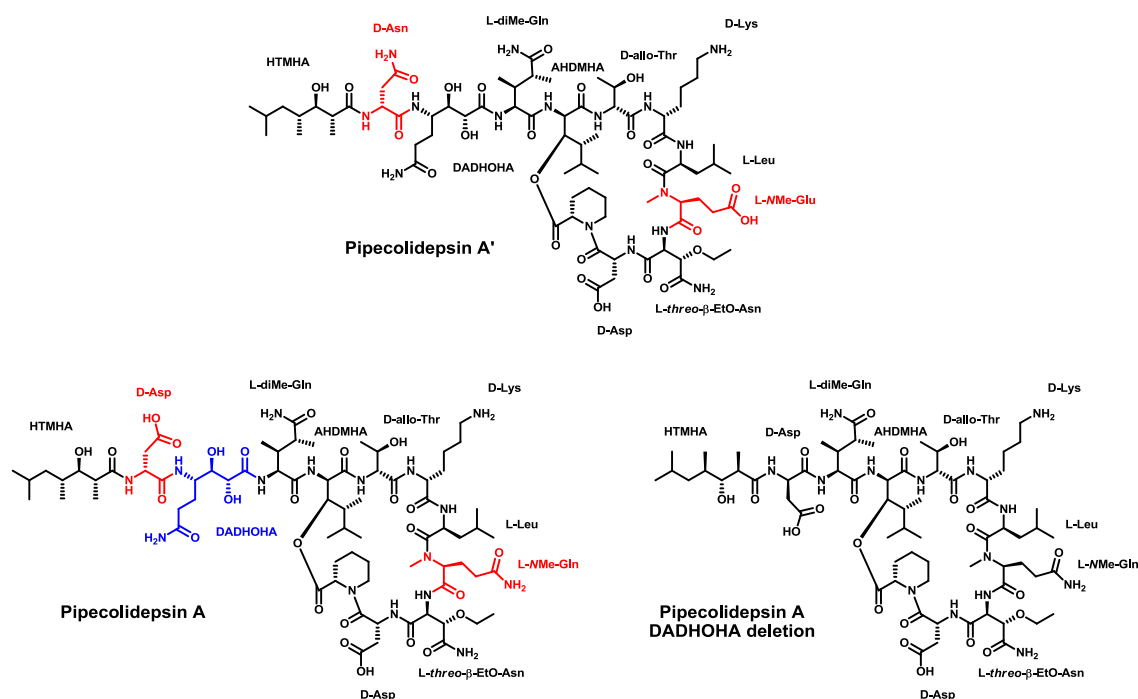


**Figure 44:** a)  $^1\text{H}$  chemical shifts of synthetic Pipecolidepsin A (in blue) and natural Pipecolidepsin A (in black); b)  $^{13}\text{C}$  chemical shifts of synthetic Pipecolidepsin A (in red) and natural Pipecolidepsin A (in black).

Differences are significantly bigger and abundant for synthetic Pipecolidepsin A' than for synthetic Pipecolidepsin A, thus supporting the results from the chemical validation. However, the variations in  $^{13}\text{C}$   $\delta$  of the exocyclic D-Asp residue made us suspect of a massive and unexpected epimerization during the incorporation of the last two moieties as a single unit, which is one of the most sensitive synthetic steps to this side reaction. In order to check the occurrence of racemization, Marfey's analysis was undertaken. Thus, a synthetic sample of synthetic Pipecolidepsin A was hydrolyzed with 6 M aqueous HCl for 12 h at 110 °C and derivatized with FDAA. Then, the derivatized moieties were injected into the HPLC and compared with the corresponding standards to check the configuration of the residues in the final synthetic peptide. No epimerization was detected at any residue.

### 1.5.5.3. Biological validation

Synthetic Pipecolidepsin A', synthetic Pipecolidepsin A and Pipecolidepsin A with DADHOHA deletion (Figure 45) were evaluated against three human cancer cell lines: lung (A549), colon (HT-29) and breast (MDA-MB-231). A colorimetric assay, using sulforhodamine B (SRB) reaction, has been adapted to provide a quantitative measurement of cell growth and viability. Analysis of the dose-response data obtained from the assays, afforded the  $\text{GI}_{50}$ ,  $\text{LC}_{50}$  and TGI values detailed in Table 4.



**Figure 45:** Chemical structures of Pipecolidepsin A', Pipecolidepsin A and Pipecolidepsin A DADHOHA deletion. Differences between Pipecolidepsin A' and Pipecolidepsin A are shown in red; and between Pipecolidepsin A and DADHOHA deletion, in blue.

Peptide		Lung-NSCLC A549		Colon HT-29		Breast MDA-MB-231	
		$\mu\text{g/mL}$	Molar	$\mu\text{g/mL}$	Molar	$\mu\text{g/mL}$	Molar
		Natural	GI <sub>50</sub>	4.6E-01	2.78E-07	1.3E+00	7.85E-07
Pipecolidepsin	TGI	6.9E-01	4.17E-07	1.8E+00	1.09E-06	4.0E-01	2.42E-07
A	LC <sub>50</sub>	1.0E+00	6.04E-07	2.4E+00	1.45E-06	8.5E-01	5.13E-07
Synthetic	GI <sub>50</sub>	5.1E-01	3.08E-07	9.7E-01	5.86E-07	2.3E-01	1.39E-07
Pipecolidepsin	TGI	7.1E-01	4.29E-07	1.3E+00	7.85E-07	4.0E-01	2.42E-07
A'	LC <sub>50</sub>	1.0E+00	6.04E-07	1.7E+00	1.03E-06	7.2E-01	4.35E-07
Synthetic	GI <sub>50</sub>	2.3E-01	1.39E-07	6.1E-01	3.68E-07	9.0E-02	5.44E-08
Pipecolidepsin	TGI	3.7E-01	2.23E-07	1.2E+00	7.25E-07	2.1E-01	1.27E-07
A	LC <sub>50</sub>	6.0E-01	3.62E-07	2.0E+00	1.21E-06	4.7E-01	2.84E-07
Synthetic	GI <sub>50</sub>	4.7E+00	3.20E-06	>1.0E+01	>6.81E-06	4.0E+00	2.73E-06
Pipecolidepsin	TGI	>1.0E+01	>6.81E-06	>1.0E+01	>6.81E-06	4.1E+00	2.79E-06
A DADHOHA deletion	LC <sub>50</sub>	>1.0E+01	>6.81E-06	>1.0E+01	>6.81E-06	>1.0E+01	>6.81E-06

**Table 4:** Biological evaluation of natural Pipecolidepsin A, synthetic Pipecolidepsin A', synthetic Pipecolidepsin A, and Pipecolidepsin A DADHOHA deletion against three cancer cell lines.

Natural Pipecolidepsin A and synthetic Pipecolidepsin A showed similar GI<sub>50</sub>, LC<sub>50</sub> and TGI values for the three cancer cell lines assayed. These data were consistent with the chemical validation previously done by reversed-phase HPLC co-elution and NMR comparison, and confirmed synthetic Pipecolidepsin A identity. Furthermore, deletion of the DADHOHA moiety caused a dramatic decrease in the biological activity, thus showing that this  $\gamma$ -amino acid plays an important role in Pipecolidepsin A cytotoxicity.

Synthetic Pipecolidepsin A' and natural Pipecolidepsin A also exhibited extremely close GI<sub>50</sub>, LC<sub>50</sub> and TGI values. The structures of the two compounds only differ in two moieties. Natural Pipecolidepsin A residues NMe-Gln<sup>4</sup> (placed in the macrocyclic region) and D-Asp<sup>11</sup> (placed in the exocyclic arm), are replaced by NMe-Glu<sup>4</sup> and D-Asn<sup>11</sup> in synthetic Pipecolidepsin A'. These substitutions may not substantially modify the hydrogen-bond pattern of the two compounds, as both COOH and CONH<sub>2</sub> functions own hydrogen bond donors and acceptors. Assuming no significant differences in their stability in serum, the small variations observed in their cytotoxicities can be explained if both compounds share a really close hydrogen-bond pattern that does not affect the 3D structure of the two peptides.

**References**

- (1) Banker, R.; Carmeli, S. *Tetrahedron* **1999**, *55*, 10835–10844.
- (2) Reshef, V.; Carmeli, S. *Tetrahedron* **2001**, *57*, 2885–2894.
- (3) Martin, C.; Oberer, L.; Ino, T.; König, W. A.; Busch, M.; Weckesser, J. *The Journal of Antibiotics* **1993**, *46*, 1550–1556.
- (4) Jakobi, C.; Oberer, L.; Quiquerez, C.; König, W. A.; Weckesser, J. *FEMS Microbiol. Lett.* **1995**, *129*, 129–133.
- (5) Itou, Y.; Ishida, K.; Shin, H. J.; Murakami, M. *Tetrahedron* **1999**, *55*, 6871–6882.
- (6) Fujii, K.; Sivonen, K.; Naganawa, E.; Harada, K. *Tetrahedron* **2000**, *56*, 725–733.
- (7) Ploutno, A.; Carmeli, S. *Tetrahedron* **2002**, *58*, 9949–9957.
- (8) von Elert, E.; Oberer, L.; Merkel, P.; Huhn, T.; Blom, J. F. *J. Nat. Prod.* **2005**, *68*, 1324–1327.
- (9) Harada, K.; Mayumi, T.; Shimada, T.; Fujii, K.; Kondo, F.; Watanabe, M. F. *Tetrahedron Lett.* **1993**, *34*, 6091–6094.
- (10) Harada, K.; Mayumi, T.; Shimada, T.; Fujii, K.; Kondo, F.; Park, H. D.; Watanabe, M. F. *Environ. Toxicol.* **2001**, *16*, 298–305.
- (11) Plaza, A.; Bewley, C. A. *J. Org. Chem.* **2006**, *71*, 6898–6907.
- (12) Matthew, S.; Ross, C.; Rocca, J. R.; Paul, V. J.; Luesch, H. *J. Nat. Prod.* **2007**, *70*, 124–127.
- (13) Taori, K.; Matthew, S.; Rocca, J. R.; Paul, V. J.; Luesch, H. *J. Nat. Prod.* **2007**, *70*, 1593–1600.
- (14) Lee, A. Y.; Smitka, T. A.; Bonjouklian, R.; Clardy, J. *Chem. Biol.* **1994**, *1*, 113–117.
- (15) Matern, U.; Oberer, L.; Falchetto, R. a; Erhard, M.; König, W. a; Herdman, M.; Weckesser, J. *Phytochemistry* **2001**, *58*, 1087–95.
- (16) Yamaki, H.; Sitachitta, N.; Sano, T.; Kaya, K. *J. Nat. Prod.* **2005**, *68*, 14–18.
- (17) Nakanishi, I.; Kinoshita, T.; Sato, A.; Tada, T. *Biopolymers* **2000**, *53*, 434–445.
- (18) Matern, U.; Schleberger, C.; Jelakovic, S.; Weckesser, J.; Schulz, G. E. *Chem. Biol.* **2003**, *10*, 997–1001.
- (19) Linington, R. G.; Edwards, D. J.; Shuman, C. F.; McPhail, K. L.; Maitainaho, T.; Gerwick, W. H. *J. Nat. Prod.* **2008**, *71*, 22–27.

- (20) Okino, T.; Qi, S.; Matsuda, H.; Murakami, M.; Yamaguchi, K. *J. Nat. Prod.* **1997**, *60*, 158–161.
- (21) Grach-Pogrebinsky, O.; Sedmak, B.; Carmeli, S. *Tetrahedron* **2003**, *59*, 8329–8336.
- (22) Yokokawa, F.; Shioiri, T. *Tetrahedron Lett.* **2002**, *43*, 8673–8677.
- (23) Stolze, S. C.; Meltzer, M.; Ehrmann, M.; Kaiser, M. *Chem. Commun.* **2010**, *46*, 8857–8859.
- (24) Stolze, S. C.; Meltzer, M.; Ehrmann, M.; Kaiser, M. *Eur. J. Org. Chem.* **2012**, *2012*, 1616–1625.
- (25) von Nussbaum, F.; Anlauf, S.; Benet-Buchholz, J.; Häbich, D.; Köbberling, J.; Musza, L.; Telsler, J.; Rübsamen-Waigmann, H.; Brunner, N. *Angew. Chem. Int. Ed.* **2007**, *46*, 2039–2042.
- (26) Guzman-Martinez, A.; Lamer, R.; VanNieuwenhze, M. S. *J. Am. Chem. Soc.* **2007**, *129*, 6017–6021.
- (27) Hall, E. a; Kuru, E.; VanNieuwenhze, M. S. *Org. Lett.* **2012**, *14*, 2730–2733.
- (28) Cavalleri, B.; Pagani, H.; Volpe, G.; Selva, E.; Parenti, F. *J. Antibiot. (Tokyo)* **1984**, *37*, 309–317.
- (29) Parenti, F.; Ciabatti, R.; Cavalleri, B.; Kettenring, J. *Drugs Exp. Clin. Res.* **1990**, *16*, 451–455.
- (30) Skelton, N. J.; Harding, M. M.; Mortishire-Smith, R. J.; Rahman, S. K.; Williams, D. H.; Rance, M. J.; Ruddock, J. C. *J. Am. Chem. Soc.* **1991**, *113*, 7522–7530.
- (31) Meyers, E.; Weisenborn, F. L.; Pansy, F. E.; Slusarchyk, D. S.; Von Saltza, M. H.; Rathnum, M. L. *J. Antibiot.* **1970**, *23*, 502–507.
- (32) Castiglione, F.; Marazzi, A.; Meli, M.; Colombo, G. *Magn. Reson. Chem.* **2005**, *43*, 603–610.
- (33) Jiang, W.; Wanner, J.; Lee, R. J.; Bounaud, P.-Y.; Boger, D. L. *J. Am. Chem. Soc.* **2002**, *124*, 5288–5290.
- (34) Jiang, W.; Wanner, J.; Lee, R. J.; Bounaud, P.-Y.; Boger, D. L. *J. Am. Chem. Soc.* **2003**, *125*, 1877–1887.
- (35) Shin, D.; Rew, Y.; Boger, D. L. *P. Natl. Acad. Sci. USA* **2004**, *101*, 11977–11979.
- (36) Ciabatti, R.; Maffioli, S. I.; Panzone, G.; Canavesi, A.; Michelucci, E.; Tiseni, P. S.; Marzorati, E.; Checchia, A.; Giannone, M.; Jabes, D.; Romano, G.; Brunati, C.; Candiani, G.; Castiglione, F. *J. Med. Chem.* **2007**, *50*, 3077–3085.
- (37) Hoertz, A. J.; Hamburger, J. B.; Gooden, D. M.; Bednar, M. M.; McCafferty, D. G. *Bioorgan. Med. Chem.* **2012**, *20*, 859–865.



- (38) Hamann, M. T.; Scheuer, P. J. *J. Am. Chem. Soc.* **1993**, *115*, 5825–5826.
- (39) Hamann, M. T.; Otto, C. S.; Scheuer, P. J.; Dunbar, D. C. *J. Org. Chem.* **1996**, *61*, 6594–6600.
- (40) Goetz, G.; Nakao, Y.; Scheuer, P. J. *J. Nat. Prod.* **1997**, *60*, 562–567.
- (41) Horgen, F. D.; delos Santos, D. B.; Goetz, G.; Sakamoto, B.; Kan, Y.; Nagai, H.; Scheuer, P. J. *J. Nat. Prod.* **2000**, *63*, 152–154.
- (42) Ashour, M.; Edrada, R.; Ebel, R.; Wray, V.; Wätjen, W.; Padmakumar, K.; Müller, W. E. G.; Lin, W. H.; Proksch, P. *J. Nat. Prod.* **2006**, *69*, 1547–1553.
- (43) Gao, J.; Caballero-George, C.; Wang, B.; Rao, K. V.; Shilabin, A. G.; Hamann, M. T. *J. Nat. Prod.* **2009**, *72*, 2172–2176.
- (44) Faircloth, G. T.; Elices, M.; Sasak, H.; Avilés Marin, P. M.; Cuevas Marchante, M. D. C. *WO Patent 2004035613* **2004**.
- (45) Cruz, L. J.; Luque-ortega, J. R.; Rivas, L.; Albericio, F. *Mol. Pharm.* **2009**, *6*, 813–824.
- (46) Shilabin, A. G.; Kasanah, N.; Wedge, D. E.; Hamann, M. T. *J. Med. Chem.* **2007**, *50*, 4340–4350.
- (47) Jiménez, J. C.; López-Macià, A.; Gracia, C.; Varón, S.; Carrascal, M.; Caba, J. M.; Royo, M.; Francesch, A. M.; Cuevas, C.; Giralt, E.; Albericio, F. *J. Med. Chem.* **2008**, *51*, 4920–4931.
- (48) Bourel-Bonnet, L.; Rao, K. V.; Hamann, M. T.; Ganesan, A. *J. Med. Chem.* **2005**, *48*, 1330–1335.
- (49) López-Macià, a; Jiménez, J. C.; Royo, M.; Giralt, E.; Albericio, F. *J. Am. Chem. Soc.* **2001**, *123*, 11398–11401.
- (50) López, P. E.; Isidro-Llobet, A.; Gracia, C.; Cruz, L. J.; García-Granados, A.; Parra, A.; Álvarez, M.; Albericio, F. *Tetrahedron Lett.* **2005**, *46*, 7737–7741.
- (51) López-Macià, À.; Jiménez, J. C.; Royo, M.; Giralt, E.; Albericio, F. *Tetrahedron Lett.* **2000**, *41*, 9765–9769.
- (52) Gracia, C.; Isidro-Llobet, A.; Cruz, L. J.; Acosta, G. a; Alvarez, M.; Cuevas, C.; Giralt, E.; Albericio, F. *J. Org. Chem.* **2006**, *71*, 7196–7204.
- (53) Rinehart, K. L.; Gloer, J. B.; Carter Cook, J. *J. Am. Chem. Soc.* **1981**, *103*, 1857–1859.
- (54) Rinehart, K. L. J.; Gloer, J. B.; Hughes, R. G. J.; Renis, H. E.; McGroven, J. P.; Swynenberg, E. B.; Stringfellow, D. A.; Kuentzel, S. L.; Li, L. H. *Science* **1981**, *212*, 933–935.
- (55) Vervoort, H.; Fenical, W.; Epifanio, R. a *J. Org. Chem.* **2000**, *65*, 782–792.

- (56) Rinehart, K. L.; Kishore, V.; Nagarajan, S.; Lake, R. J.; Gloer, J. B.; Bozich, F. A.; Li, K.; Maleczka, R. E.; Todsén, W. L.; Munro, M. H. G.; Sullins, D. W.; Sakai, R. *J. Am. Chem. Soc.* **1987**, *109*, 6846–6848.
- (57) Hamada, Y.; Kondo, Y.; Shibata, M.; Shioiri, T. *J. Am. Chem. Soc.* **1989**, *111*, 669–673.
- (58) Li, W.-R.; Ewing, W. R.; Harris, B. D.; Joullié, M. M. *J. Am. Chem. Soc.* **1990**, *112*, 7659–7672.
- (59) Jouin, P.; Poncet, J.; Dufour, M.-N.; Pantaloni, A.; Castro, B. *J. Org. Chem.* **1989**, *54*, 617–627.
- (60) Jou, G.; González, I.; Albericio, F.; Lloyd-Williams, P.; Giralt, E. *J. Org. Chem.* **1997**, *62*, 354–366.
- (61) Vera, M. D.; Joullié, M. M. *Med. Res. Rev.* **2002**, *22*, 102–145.
- (62) Liang, B.; Portonovo, P.; Vera, M. D.; Xiao, D.; Joullié, M. M. *Org. Lett.* **1999**, *1*, 1319–1322.
- (63) Liang, B.; Richard, D. J.; Portonovo, P. S.; Joullié, M. M. *J. Am. Chem. Soc.* **2001**, *123*, 4469–4474.
- (64) Joullie, M. M.; Portonovo, P.; Liang, B.; Richard, D. J. *Tetrahedron Lett.* **2000**, *41*, 9373–9376.
- (65) Lassen, K. M.; Lee, J.; Joullié, M. M. *J. Org. Chem.* **2010**, *75*, 3027–3036.
- (66) Adrio, J.; Cuevas, C.; Manzanares, I.; Joullié, M. M. *Org. Lett.* **2006**, *8*, 511–514.
- (67) Adrio, J.; Cuevas, C.; Manzanares, I.; Joullié, M. M. *J. Org. Chem.* **2007**, *72*, 5129–5138.
- (68) Sakai, R.; Rinehart, K. L.; Kishore, V.; Kundu, B.; Faircloth, G.; Gloer, J. B.; Carney, J. R.; Namikoshi, M.; Sun, F.; Hughes, R. G.; García Grávalos, D.; de Quesada, T. G.; Wilson, G. R.; Heid, R. M. *J. Med. Chem.* **1996**, *39*, 2819–2834.
- (69) Zampella, A.; D’Auria, M. V.; Gomez Paloma, L.; Casapullo, A.; Minale, L.; Debitus, C.; Henin, Y. *J. Am. Chem. Soc.* **1996**, *118*, 6202–6209.
- (70) D’Auria, M. V.; Zampella, A.; Paloma, L. G.; Minale, L.; Debitus, C.; Roussakis, C.; Le Bert, V. *Tetrahedron* **1996**, *52*, 9589–9596.
- (71) Zampella, A.; Randazzo, A.; Borbone, N.; Luciani, S.; Trevisi, L.; Debitus, C.; D’Auria, M. V. *Tetrahedron Lett.* **2002**, *43*, 6163–6166.
- (72) Sepe, V.; D’Orsi, R.; Borbone, N.; Valeria D’Auria, M.; Bifulco, G.; Monti, M. C.; Catania, A.; Zampella, A. *Tetrahedron* **2006**, *62*, 833–840.
- (73) D’Auria, M. V.; Sepe, V.; D’Orsi, R.; Bellotta, F.; Debitus, C.; Zampella, A. *Tetrahedron* **2007**, *63*, 131–140.

- (74) Krishnamoorthy, R.; Vazquez-Serrano, L. D.; Turk, J. A.; Kowalski, J. A.; Benson, A. G.; Breaux, N. T.; Lipton, M. A. *J. Am. Chem. Soc.* **2006**, *128*, 15392–15393.
- (75) Krishnamoorthy, R.; Richardson, B. L.; Lipton, M. a *Bioorg. Med. Chem. Lett.* **2007**, *17*, 5136–5138.
- (76) Kikuchi, M.; Watanabe, Y.; Tanaka, M.; Akaji, K.; Konno, H. *Bioorg. Med. Chem. Lett.* **2011**, *21*, 4865–4868.
- (77) Oku, N.; Krishnamoorthy, R.; Benson, A. G.; Ferguson, R. L.; Lipton, M. A.; Phillips, L. R.; Gustafson, K. R.; McMahon, J. B. *J. Org. Chem.* **2005**, *70*, 6842–6847.
- (78) Oku, N.; Gustafson, K. R.; Cartner, L. K.; Wilson, J. A.; Shigematsu, N.; Hess, S.; Pannell, L. K.; Boyd, M. R.; McMahon, J. B. *J. Nat. Prod.* **2004**, *67*, 1407–1141.
- (79) Yamano, Y.; Arai, M.; Kobayashi, M. *Bioorg. Med. Chem. Lett.* **2012**, *22*, 4877–4881.
- (80) Tran, T. D.; Pham, N. B.; Fechner, G.; Zencak, D.; Vu, H. T.; Hooper, J. N. a; Quinn, R. J. *J. Nat. Prod.* **2012**, *75*, 2200–2208.
- (81) Ford, P. W.; Gustafson, K. R.; Mckee, T. C.; Shigematsu, N.; Maurizi, L. K.; Pannell, L. K.; Williams, D. E.; Silva, E. D. D.; Lassota, P.; Allen, T. M.; Soest, R. V.; Andersen, R. J.; Boyd, M. R. *J. Am. Chem. Soc.* **1999**, *121*, 5899–5909.
- (82) Prasad, P.; Aalbersberg, W.; Feussner, K.-D.; Van Wagoner, R. M. *Tetrahedron* **2011**, *67*, 8529–8531.
- (83) Xie, W.; Ding, D.; Zi, W.; Li, G.; Ma, D. *Angew. Chem. Int. Ed.* **2008**, *47*, 2844–2848.
- (84) Ratnayake, A. S.; Bugni, T. S.; Feng, X.; Harper, M. K.; Skalicky, J. J.; Mohammed, K. A.; Andjelic, C. D.; Barrows, L. R.; Ireland, C. M. *J. Nat. Prod.* **2006**, *69*, 1582–1586.
- (85) Plaza, A.; Bifulco, G.; Keffer, J. L.; Lloyd, J. R.; Baker, H. L.; Bewley, C. a *J. Org. Chem.* **2009**, *74*, 504–512.
- (86) Plaza, A.; Gustchina, E.; Baker, H. L.; Kelly, M.; Bewley, C. A. *J. Nat. Prod.* **2007**, *70*, 1753–1760.
- (87) Lu, Z.; Wagoner, R. M. V.; Harper, M. K.; Baker, H. L.; Hooper, J. N. A.; Bewley, C. A.; Ireland, C. M. *J. Nat. Prod.* **2011**, *74*, 185–193.
- (88) Zampella, A.; Sepe, V.; Luciano, P.; Bellotta, F.; Monti, M. C.; D’Auria, M. V.; Jepsen, T.; Petek, S.; Adeline, M.-T.; Laprêvôte, O.; Aubertin, A.-M.; Debitus, C.; Poupat, C.; Ahond, A. *J. Org. Chem.* **2008**, *73*, 5319–5327.
- (89) Bellotta, F.; D’Auria, M. V.; Sepe, V.; Zampella, A. *Tetrahedron* **2009**, *65*, 3659–3663.
- (90) Coello, L.; Fernández, R.; Reyes, J. F.; Francesch, A.; Cuevas, M. D. C. WO 2010/070078 A1 **2010**.
- (91) Gisin, B. F.; Merrifield, R. B. *J. Am. Chem. Soc.* **1972**, *94*, 3102–3106.

- (92) Lukenheimer, W.; Zahn, H. *Liebigs Ann. Chem.* **1970**, *740*, 1.
- (93) Barlos, K.; Chatzi, O.; Gatos, D.; Stavropoulos, G. *Int. J. Pept. Prot. Res.* **1991**, *37*, 513–520.
- (94) Barlos, K.; Gatos, D.; Kapolos, S.; Poulos, W. S.; Wenqing, Y. *Int. J. Pept. Prot. Res.* **1991**, *38*, 555–561.
- (95) Carpino, L. A.; El-faham, A.; Minorb, C. A.; Albericio, F. *J. Chem. Soc., Chem. Commun.* **1994**, 201–203.
- (96) Shoji, J.; Hino, H.; Matsumoto, K.; Hattori, T.; Yoshida, T.; Matsuura, S.; Kondo, E.; Kondo, E. *The Journal of antibiotics* **1987**, *XLI*, 713–718.
- (97) Boger, D. L.; Lee, R. J.; Bounaud, P. Y.; Meier, P. *J. Org. Chem.* **2000**, *65*, 6770–6772.
- (98) Hafez, A. M.; Dudding, T.; Wagerle, T. R.; Shah, M. H.; Taggi, A. E.; Lectka, T. *J. Org. Chem.* **2003**, *68*, 5819–5825.
- (99) Guzmán-Martínez, A.; Vannieuwenhze, M. S. *Synlett* **2007**, *10*, 1513–1516.
- (100) Spengler, J.; Pelay, M.; Tulla-Puche, J.; Albericio, F. *Amino acids* **2010**, *39*, 161–165.
- (101) Saito, S.; Komada, K.; Moriwake, T. *Org. Synth.* **1996**, *73*, 184–200.
- (102) Charvillon, F. B.; Amoroux, R. *Synthetic Commun.* **1997**, *27*, 395–403.
- (103) Aikins, J. A.; Haurez, M.; Rizzo, J. R.; Van Hoeck, J.-P.; Brione, W.; Kestemont, J.-P.; Stevens, C.; Lemair, X.; Stephenson, G. A.; Marlot, E.; Forst, M.; Houpis, I. N. *J. Org. Chem.* **2005**, *70*, 4695–4705.
- (104) Parmenon, C.; Guillard, J.; Caignard, D.-H.; Hennuyer, N.; Staels, B.; Audinot-Bouchez, V.; Boutin, J.-A.; Dacquet, C.; Ktorza, A.; Viaud-Massuard, M.-C. *Bioorg. Med. Chem. Lett.* **2008**, *18*, 1617–1622.
- (105) Spengler, J.; Böttcher, C.; Albericio, F.; Burger, K. *Chem. Rev.* **2006**, *106*, 4728–4746.
- (106) Weygand, F.; Steglich, W.; Bjarnason, J. *Chem. Ber.* **1968**, *101*, 3642–3648.
- (107) Albericio, F.; Burger, K.; Cupido, T.; Ruiz, J.; Spengler, J. *Arkivoc* **2005**, *vi*, 191–199.
- (108) Davis, F. A.; Srirajan, V.; Fanelli, D. L.; Portonovo, P. *J. Org. Chem.* **2000**, *65*, 7663–7666.
- (109) Watanabe, B.; Yamamoto, S.; Sasaki, K.; Nakagawa, Y.; Miyagawa, H. *Tetrahedron Lett.* **2004**, *45*, 2767–2769.
- (110) Liang, X.; Andersch, J.; Bols, M. *J. Chem. Soc., Perkin Trans. 1* **2001**, 2136–2157.
- (111) Garner, P. *Tetrahedron Lett.* **1984**, *25*, 5855–5858.

- (112) D'Aniello, F.; Falorni, M.; Mann, A.; Taddei, M. *Tetrahedron-Asymmetr.* **1996**, *7*, 1217–1226.
- (113) Liang, B.; Carroll, P. J.; Joullié, M. M. *Org. Lett.* **2000**, *2*, 4157–4160.
- (114) Acevedo, C. M.; Kogut, E. F.; Lipton, M. A. *Tetrahedron* **2001**, *57*, 6353–6359.
- (115) Okamoto, N.; Hara, O.; Makino, K.; Hamada, Y. *Tetrahedron-Asymmetr.* **2001**, *12*, 1353–1358.
- (116) Çalimsiz, S.; Lipton, M. A. *J. Org. Chem.* **2005**, *70*, 6218–6221.
- (117) Chandrasekhar, S.; Ramachandar, T.; Rao, B. V. *Tetrahedron-Asymmetr.* **2001**, *12*, 2315–2321.
- (118) Ravi Kumar, A.; Rao, B. V. *Tetrahedron Lett.* **2003**, *44*, 5645–5647.
- (119) Thoen, J. C.; Morales-Ramos, A. I.; Lipton, M. a *Org. Lett.* **2002**, *4*, 4455–4458.
- (120) Jeon, J.; Hong, S.-K.; Oh, J. S.; Kim, Y. G. *J. Org. Chem.* **2006**, *71*, 3310–3313.
- (121) Kolb, H. C.; Vannieuwenhze, M. S.; Sharpless, K. B. *Chem. Rev.* **1994**, *94*, 2483–2547.
- (122) Wang, L.; Sharpless, K. B. *J. Am. Chem. Soc.* **1992**, *114*, 7568–7570.
- (123) Wang, Z.-M.; Kakiuchi, K.; Sharpless, K. B. *J. Org. Chem.* **1994**, *59*, 6895–6897.
- (124) Guerlavais, V.; Carroll, P. J.; Joullie, M. M. *Tetrahedron-Asymmetr.* **2002**, *13*, 675–680.
- (125) Zampella, A.; Sorgente, M.; D'Auria, M. V. *Tetrahedron-Asymmetr.* **2002**, *13*, 681–685.
- (126) Sabitha, G.; Yadagiri, K.; Chandrashekhar, G.; Yadav, J. *Synthesis* **2010**, *24*, 4307–4311.
- (127) Zampella, A.; D'Auria, M. V. *Tetrahedron-Asymmetr.* **2002**, *13*, 1237–1239.
- (128) Turk, J. a; Visbal, G. S.; Lipton, M. a *J. Org. Chem.* **2003**, *68*, 7841–7844.
- (129) Çalimsiz, S.; Morales Ramos, A. I.; Lipton, M. A. *J. Org. Chem.* **2006**, *71*, 6351–6356.
- (130) Katagiri, N.; Itakura, K.; Narang, S. A. *J. Chem. Soc., Chem. Commun.* **1974**, 325–326.
- (131) Blankemeyer-Menge, B.; Nimtz, M.; Frank, R. *Tetrahedron Lett.* **1990**, *31*, 1701–1704.
- (132) El-Sagheer, A. H.; Brown, T. *J. Am. Chem. Soc.* **2009**, *131*, 3958–3964.
- (133) Kiburu, I.; Shurer, A.; Yan, L.; Sintim, H. O. *Mol. Biosyst.* **2008**, *4*, 518–520.
- (134) Weik, S.; Luksch, T.; Evers, A.; Böttcher, J.; Sotriffer, C. A.; Hasilik, A.; Löffler, H.-G.; Klebe, G.; Rademann, J. *ChemMedChem* **2006**, *1*, 445–457.
- (135) Harth-Fritschy, E.; Cantacuzène, D. *J. Peptide Res.* **1997**, *50*, 415–420.

- (136) Tulla-Puche, J.; Torres, A.; Calvo, P.; Royo, M.; Albericio, F. *Bioconjugate Chem.* **2008**, *19*, 1968–1971.
- (137) Falb, E.; Yechezkel, T.; Salitra, Y.; Gilon, C. *J. Peptide Res.* **1999**, *53*, 507–517.



## **CHAPTER 2**

**Synthesis, structural elucidation and  
biological evaluation of Phakellistatin 19**





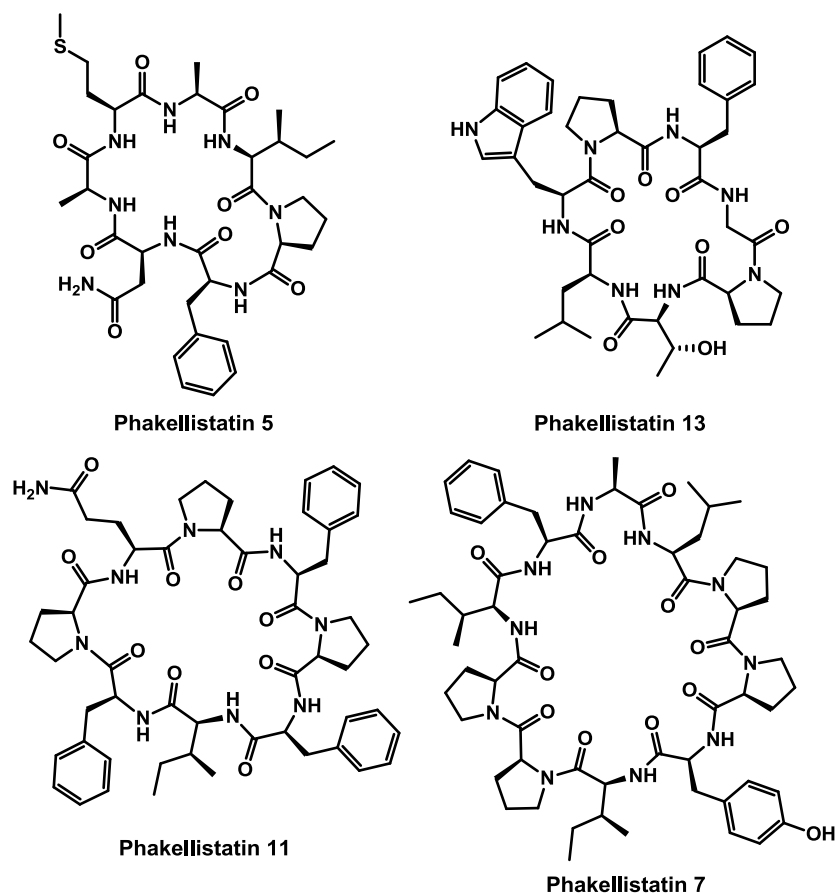
## 2.1. Introduction: Phakellistatins

Homodetic peptides are also an interesting class of secondary metabolites with promising therapeutic profiles. Cyclic peptides have some advantages with regard to their linear counterparts. The absence of ionized C- and N- termini confers them a greater resistance to *in vivo* enzymatic degradation, a higher bioavailability, and a more restricted conformational flexibility. Furthermore, their transport through membranes is also facilitated by the absence of charged terminus.<sup>1</sup>

Several families of proline-rich peptides isolated from marine sponges and displaying significant cytotoxicities, such as Hymenamides,<sup>2,3</sup> Stylopeptides,<sup>4,5</sup> Axinellins,<sup>6,7</sup> Axinastatins<sup>8,9</sup> and Phakellistatins,<sup>10,11</sup> have been described in the literature. All of them share a number of structural features. In general, they comprise homodetic hepta or octapeptides with an unusual percentage of Pro moieties, with high contents of apolar amino acids, including one or two aromatic residues, and with a significant structural analogy.

Phakellistatins will focus our attention in this second chapter. Nineteen different cyclopeptides have been isolated so far from marine sponges of the genus *Phakellia*. They all

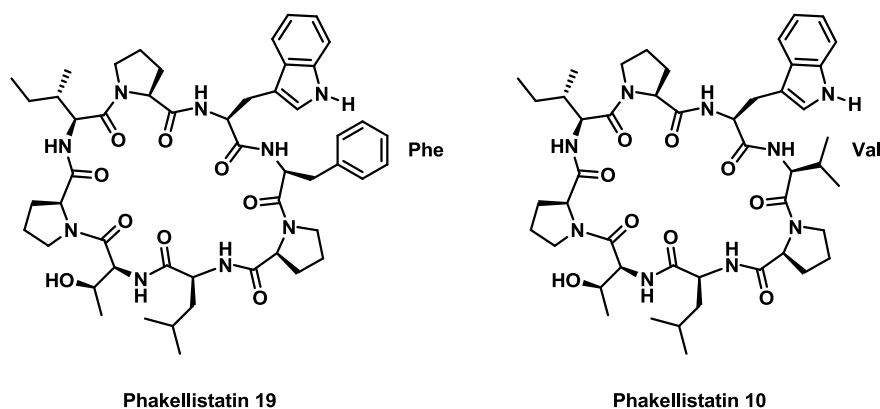
consist of seven to ten amino acids, including at least one proline moiety, and most of them more than one (Figure 46). From the nineteen described peptides, four comprise the distinctive Pro-Pro track,<sup>12,13</sup> which represents a notable synthetic challenge. All described Phakellistatins consist only of coded amino acid residues, with the uncertain exception of Phakellistatin 4. After its isolation and structural elucidation, it was described to contain a D-Thr residue, but once its synthesis was accomplished, NMR comparison with the natural peptide raised doubt about the stereochemical assignment.<sup>14</sup>



**Figure 46:** Chemical structures of Phakellistatin 5 (one proline), Phakellistatin 13 (two prolines), Phakellistatin 11 (three prolines) and Phakellistatin 7 (four prolines).

Synthetic strategies for most of the described Phakellistatins have been developed and reported in the literature. Phakellistatin 1,<sup>15</sup> 2,<sup>14</sup> 3,<sup>16</sup> 4,<sup>14</sup> 5,<sup>17</sup> 7,<sup>18</sup> 8,<sup>18</sup> 9,<sup>18</sup> 10<sup>15</sup> and 13<sup>16</sup> have been accessed by means of a combination of solid and solution-phase techniques. Thus, after fully solid-phase assembly of the linear precursor, its cleavage from the resin was performed to carry out the cyclization and final deprotection steps in solution. The final yield strongly depends on the starting/cyclization point. Conversely, Phakellistatin 11<sup>19</sup> and 12<sup>20</sup> were synthesized using full solid-phase strategies. A solution phase approach to obtain Phakellistatin 11 proved to be unsuccessful owing to spontaneous cleavage of the Fmoc-protecting group at

the heptapeptide stage. Hence, Fmoc-Glu(OH)-OAllyl was side-chain anchored onto PAL resin. The third level of orthogonality, achieved by means of Allyl-protection at the C-terminus, enabled the performance of the cyclization step on solid phase. A safety-catch linker strategy was implemented to accomplish simultaneous cyclization and cleavage of Phakellistatin 12. Finally, Phakellistatin 2 was fully synthesized also in solution,<sup>21</sup> following a combination of stepwise peptide elongation and (4 + 3) segment condensation, rendering the final product with good yields. Phakellistatin 6,<sup>22</sup> 14,<sup>23</sup> and 15-18<sup>24</sup> were isolated and structurally elucidated, but no syntheses have been attempted so far. Herein we describe the synthesis of the last Phakellistatin discovered, Phakellistatin 19 (Figure 47). A combination of solid-phase and solution methodologies will be suggested and evaluated.



**Figure 47:** Chemical structure of Phakellistatin 19 and 10. Differences in the sequence are indicated.

Phakellistatin 19 is an octacyclopeptide containing three proline moieties and a high percentage of apolar residues, including a Leu, an Ile and a Phe. Its amino acid sequence is really close to the one of Phakellistatin 10<sup>25</sup> with one single modification, the Val moiety is replaced by a Phe residue. Biological evaluation of natural Phakellistatin 19 showed promising cytotoxic (Table 5) and anti-mitotic ( $IC_{50} = 4.20 \text{ E-}07\text{-}8.40 \text{ E-}08 \text{ M}$ ) activity.

Compound		Breast	Lung-NSCL	Colon
		MDA-MB-231 (M)	A549 (M)	HT29 (M)
Natural	GI <sub>50</sub>	5.15 E-07	4.41 E-07	4.62 E-07
Phakellistatin 19	TGI	1.47 E-06	1.16 E-06	6.72 E-07

**Table 5:** Cytotoxic activities displayed by natural Phakellistatin 19 againsts a mini-panel of three cancer cell lines.

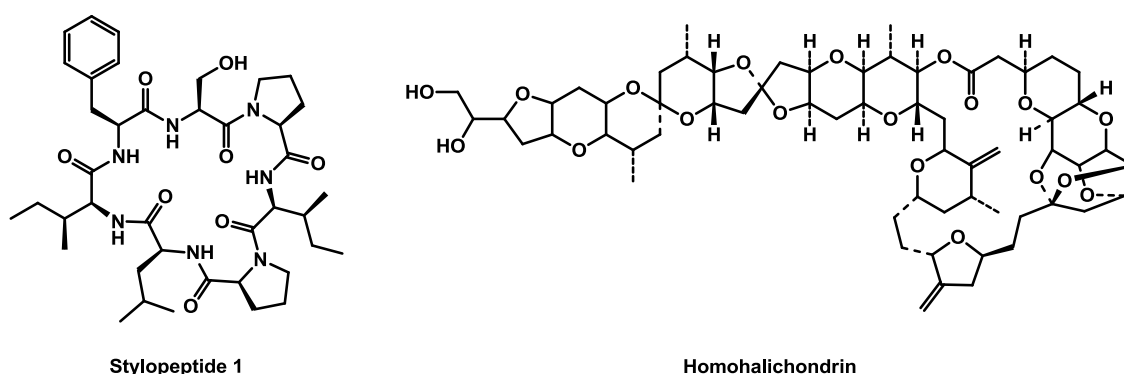
A surprising behavior has been associated with Phakellistatins. After chemical and spectral validation by means of NMR, HPLC, HRMS and Marfey's techniques, biological evaluation of synthetic Phakellistatins has revealed cytotoxicities largely different from those

displayed by their natural counterparts. This phenomenon has been widely reported by several groups working on this field, and has turned into a scientific puzzle to solve.

Two main hypotheses have been suggested so far to explain this biological incongruity. On one hand, a number of authors argue that a likely explanation could be the presence of trace amounts of a highly cytotoxic contaminant that binds noncovalently to natural Phakellistatins. This antineoplastic agent would represent less than a 5% and would thus prevent its detection by NMR spectroscopy.

Pettit and collaborators<sup>19</sup> reported an experiment proving the viability of this working hypothesis. After the synthesis and chemical and spectral validation of Phakellistatin 11, they found that the P388 leukemia ED<sub>50</sub> value was 0.2 µg/mL for the natural peptide, and >10 µg/mL for the synthetic one. HPLC analysis of natural and synthetic Phakellistatin 11 showed that both products had the same retention time. However, a shoulder was detected only in the HPLC peak corresponding to the synthetic compound. Furthermore, the rotation value found for synthetic Phakellistatin 11, significantly differed from the one reported for the natural product, pointing out the presence of an impurity in the natural sample. <sup>1</sup>H NMR studies of the synthetic peptide in ACN-*d*<sub>3</sub> showed two different conformers at 25 °C and one at 100 °C. Chemical shifts in DMSO-*d*<sub>6</sub> were identical for both synthetic and natural peptides. To prove the contamination premise, an experiment was set up.

The described biological incongruity between natural and synthetic Phakellistatins, was also detected for other proline-rich peptides such as axinastins<sup>26,27</sup> and stylopeptides<sup>5,4</sup>. Thus, Pettit et al. finally selected Stylopeptide 1 to prove the viability of the contamination assumption. Stylopeptide 1 is a heptapeptide isolated from the marine sponges *Phakellia costata* and *Stylorella aurantium*, displaying an interesting inhibitory activity, whose synthetic version proved to be 10-fold less active against the same P388 lymphocytic leukemia cell line. Homohalichondrin<sup>8</sup> is a polyether macrolide with an exceptional activity as an antineoplastic agent (Figure 48). This and other related products have been extracted also from marine sponges of several species such as *Phakellia*<sup>28</sup> and *Hymeniacidon*. Biological evaluation of a mixture of synthetic Stylopeptide 1 with decreasing small amounts of Homohalichondrin, proved that high cytotoxicities were obtained when the contamination was almost non-detectable by NMR techniques (Table 6).



**Figure 48:** Chemical structures of Stylopeptide 1 and Homohalichondrin.

Experiment	Homohalichondrin ( $\mu\text{g}$ )	wt (%)	P388 cell line ( $\text{ED}_{50}$ $\mu\text{g}/\text{mL}$ )
1	100.0	10	0.005
2	50.0	5	0.032
3	10.0	1	0.041
4	1.0	0.1	0.51
5	0.1	0.01	4.5

**Table 6:** Biological study of Stylopeptide 1 (1 mg) contaminated with Homohalichondrin.

All this experimentation proved that Phakellistatins, either complexing or carrying out a highly cytotoxic agent, could explain the non-reproducible biological results obtained with the synthetic peptides.

On the other hand, a conformational issue owed to the presence of a high percentage of Pro residues in a quite small cyclopeptide, could be another likely interpretation of the intriguing biological behavior.

Proline is unique among the 20 proteinogenic amino acids because the nitrogen and the  $\alpha$ -carbon are comprised in a cyclic array. It is a rigid residue that reduces peptides' conformational flexibility but, at the same time, enables the equilibrium between the *trans* and the *cis* isomers at the amide bond  $\text{Xaa}^{i-1}\text{-Pro}^i$ . A  $\text{H}_\alpha$  represents a much smaller sterical hindrance than a  $\text{C}_\alpha$ , hence the *trans* isomer is always thermodynamically more stable, and the *cis-trans* equilibrium is always completely shifted to the *trans* isomer. However, Pro residues represent again an exception. The absence of  $\text{H}_\alpha$  causes a small energetic difference between the two isomers ( $\Delta G^\circ < 8.4$  kJ/mol), making real an equilibrium where the proportion of *cis* isomer is not negligible (Figure 49).<sup>29,30</sup>

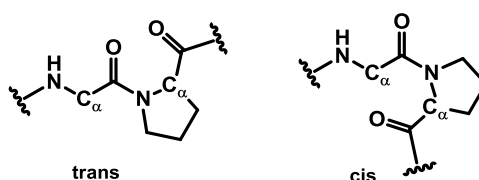


Figure 49: *Trans* and *cis* isomers at the amide bond Xaa<sup>i-1</sup>-Pro<sup>i</sup>.

Despite the small  $\Delta G^\circ$ , the *cis-trans* imide isomerization reaction of the peptide bond is a slow process due to the partial double-bond character of the C-N bond. It requires the migration of the N lone pair to a  $sp^3$  orbital to enable rotation around the peptide bond through a distorted transition state ( $\Delta G^\ddagger = 85 \pm 10$  kJ/mol).<sup>31,32</sup> However, around a 10% of the prolyl peptide bonds found in native proteins adopt the *cis* isomerism, suggesting that the isomerization reaction can be the limiting-rate step of the protein folding process and pointing out the large importance of this isomerism in nature.<sup>33,34,35</sup>

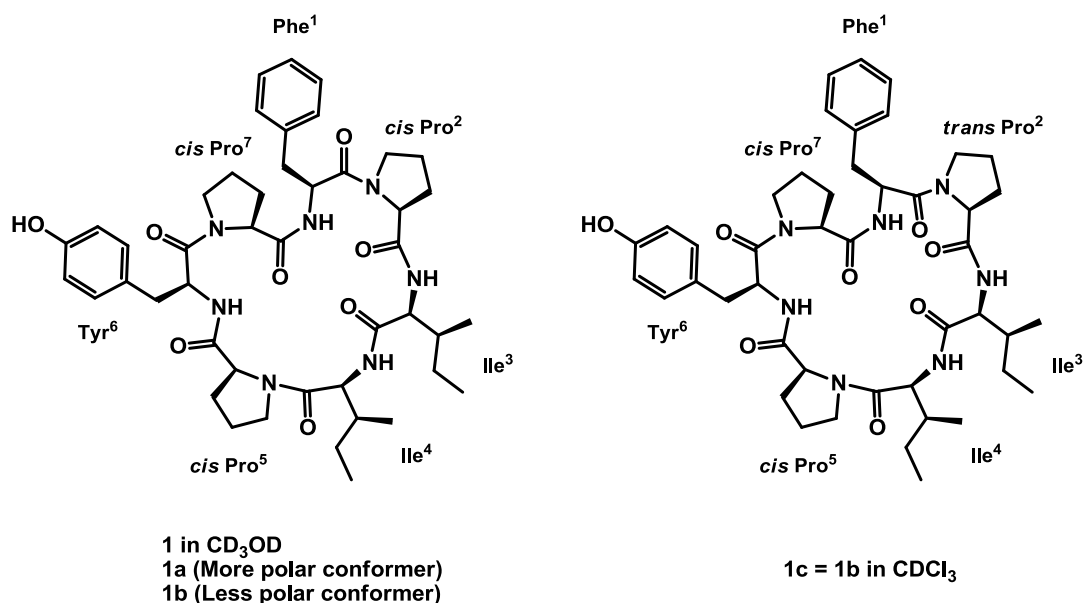
The *cis/trans* conformation of a prolyl peptide bond is important for recognition, stability and reactivity processes of the peptides and proteins comprising them.<sup>36,37,38</sup> From a pharmacological perspective, Pro derivatives are introduced in peptides with therapeutic activity to improve their bioavailability, since the cyclic nature of the Pro moieties hampers the proteases attack.

Considering all this information, it can be concluded that the presence of proline residues in a constrained macrocycle represents a crucial structural feature entailing complex *cis-trans* equilibria, as well as more subtle conformational changes.

The more exhaustive study with regard to this hypothesis was published by Tabudravu and co-workers.<sup>39</sup> Phakellistatin 2 was isolated and elucidated by Pettit and collaborators for the first time. Its biological evaluation revealed a submicromolar ED<sub>50</sub> against P388 cell line. A later re-isolation led to completely different biological results, what motivated its first total synthesis.<sup>14</sup> NMR comparison of synthetic and natural Phakellistatin 2 pointed out a missassignment during the initial isolation of the natural product. Finally, a re-synthesis<sup>21</sup> of the peptide was conducted again confirming its original structure, but concluding that the initial cytotoxicity could not be attributed to Phakellistatin2.

After bioassay-guided fractionation of a Fijian collection of *Stylorella aurantium*, Tabudravu et al. reported the isolation of two compounds with slightly different polarity as judged by HPLC analysis. Detailed NMR, MS and chiral TLC studies revealed that the two

compounds had the same amino acid sequence cyclo-[Phe<sup>1</sup>-Pro<sup>2</sup>-Ile<sup>3</sup>-Ile<sup>4</sup>-Pro<sup>5</sup>-Tyr<sup>6</sup>-Pro<sup>7</sup>] with all the Pro residues adopting the *cis* geometry. However, significant differences in the MS spectra and the <sup>1</sup>H and <sup>13</sup>C NMR spectral assignment were found for both products. Thus, the two HPLC peaks could be attributed to two different conformers of Phakellistatin 2, named conformer 1a, the more polar one, and conformer 1b, the less polar one (Figure 50). When the conformer 1b was dissolved in CDCl<sub>3</sub>, the Phe-Pro<sup>2</sup> bond changed from the *cis* to the *trans* conformation, while conformer 1a could not be studied in this solvent due to the low solubility and the resulting complex spectra.



**Figure 50:** Chemical structures of the two conformers in CD<sub>3</sub>OD and in CDCl<sub>3</sub>.

Deep analysis of the ROE cross-peaks of both conformers led to experimental restraints which were employed in dynamic calculations to find the solution state conformations of the two peptides. The major difference between 1a and 1b was the presence of an extra hydrogen bond between Phe<sup>1</sup>-NH and Ile<sup>3</sup>-CO in the less polar conformer 1b. Bioactivity results are highly dependent on the solvent used to store the sample and to perform the assays, being the MeOH the one providing the best results.

For some other Phakellistatins members, comparison of <sup>1</sup>H and <sup>13</sup>C chemical shifts resulted in minor differences while the biological results showed a big disagreement. However, subtle conformational modifications due to the presence of several proline residues could still account for that behavior. Detailed analysis of NOE and ROE cross-peaks would be mandatory to identify these slightly different arrangements.



In the present thesis, the synthesis, structure elucidation and biological evaluation of Phakellistatin 19 was faced. Some experimental work was done to shed light on the disagreements between natural and synthetic Phakellistatins' cytotoxicities.

## 2.2. Solid-phase synthesis of Phakellistatin 19

Phakellistatin 19's linear precursor was synthesized on solid phase following the Fmoc/<sup>t</sup>Bu protection scheme and using the 2-chlorotrityl resin as the polymeric support. 2-CTC resin was chosen because its steric hindrance minimizes DKPs formation, and the mild acidic conditions required to perform the cleavage step, which enable the performance of the "head-to-tail" cyclization in solution.

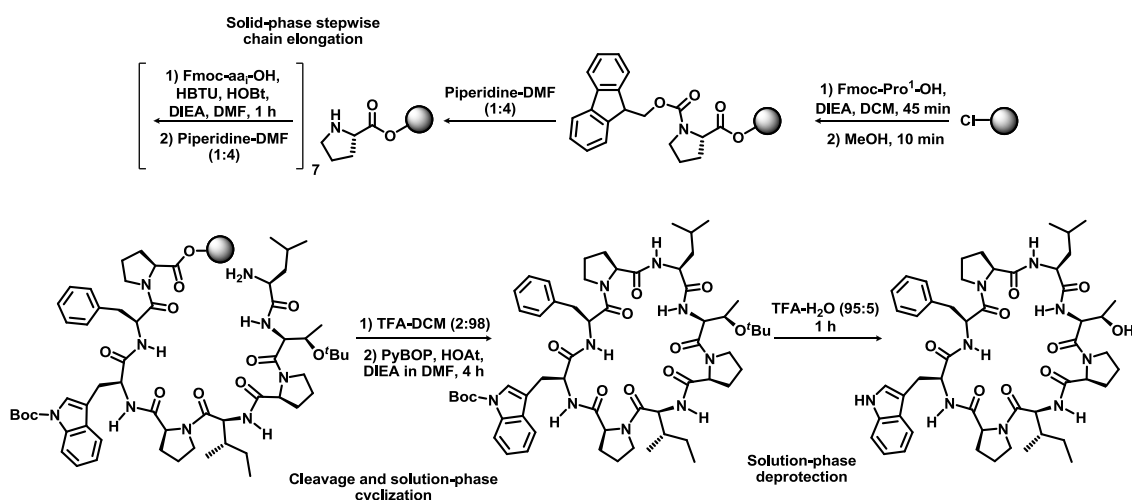
In general, the cyclization step poses the biggest synthetic challenge of an all-L-cyclopeptide's synthesis, and strongly impacts on its final yield. Thus, two different cyclization/starting points were evaluated: Leu(C)-(N)Thr and Pro(C)-(N)Leu. The first amide bond involves a  $\beta$ -branched residue, while the second linkage has a Pro at the C-terminus, which minimizes the racemization during the cyclization step, but increases the risk of DKPs formation during the linear peptide assembly. The two approaches were carefully examined.

HCTU-Cl-HOBt-DIEA was adopted as the coupling system to form the amide bonds. The use of 4 equivalents of aa guaranteed the quantitative coupling over the more hindered prolines. In all cases, after one hour of treatment, the De Clercq test revealed the absence of free secondary amines for Pro. The Fmoc group removal was accomplished by treatment with piperidine-DMF (1:4) (2  $\times$  1 min; 2  $\times$  5 min). Fmoc quantification after amino-deprotection of the second residue incorporated onto the resin, proved the absence of DKP formation.

Once the linear precursor was fully assembled, it was cleaved from the resin by treatment with a solution of DCM-TFA (98:2, 5  $\times$  2 min). All the washes were collected in water to avoid the loss of the side-chain protecting groups (Boc and <sup>t</sup>Bu). The DCM-TFA solution was evaporated, some ACN was added to dissolve the peptide crude and, after checking its purity by HPLC-PDA and HPLC-MS analysis, the solution was lyophilized. Then, the macrolactamization reaction was undertaken by means of PyBOP-HOAt-DIEA (2:1:4) in DCM-DMF (95:5) at pH = 8 and at extremely diluted conditions ( $10^{-4}$  M) to avoid oligomerization. HPLC-PDA analysis showed completion of the cyclization after 3 h of reaction. A work-up including washes with base (5% aqueous NaHCO<sub>3</sub> solution) and acid (saturated aqueous NH<sub>4</sub>Cl) enabled removal of DIEA, DMF and most of the coupling reagents. Finally, all the side-chain

protecting groups were eliminated by treatment with TFA-H<sub>2</sub>O (95:5) for 1 h, and the crude was purified by reversed-phase semi-preparative HPLC (Scheme 31).

The synthetic approach comprising the linkage Pro-Leu as the cyclization point rendered the desired product with better yielding, and thus, all the analogs were synthesized following this synthetic scheme.

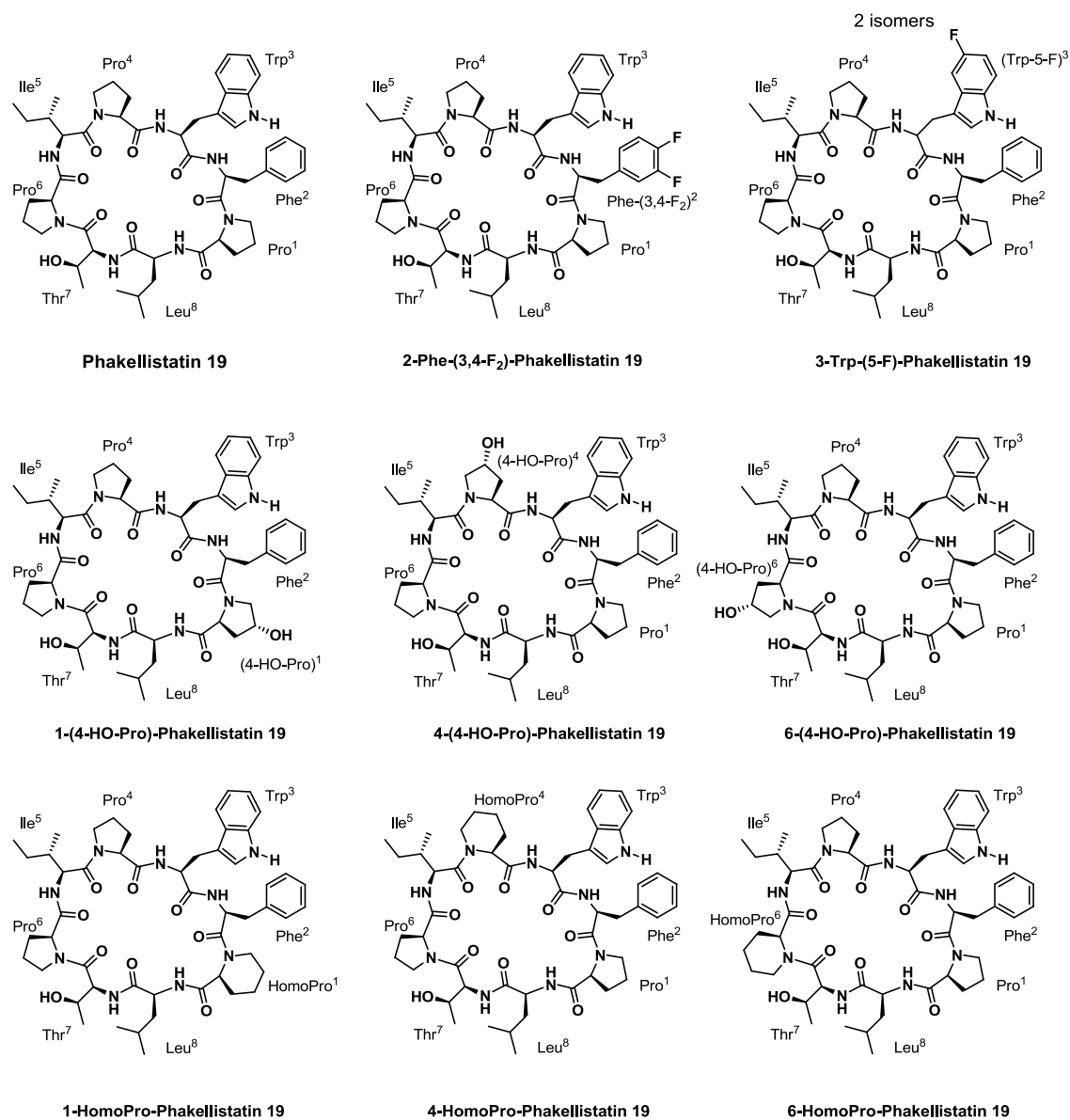


**Scheme 31:** Phakellistatin 19 synthetic strategy. The cyclization point shown is the Leu-Pro<sup>1</sup> amide bond.

The synthesis afforded Phakellistatin 19 in a 22% yield after reversed-phase semi-preparative HPLC purification.

### 2.3. Synthesis of a small library of Phakellistatin 19 analogs

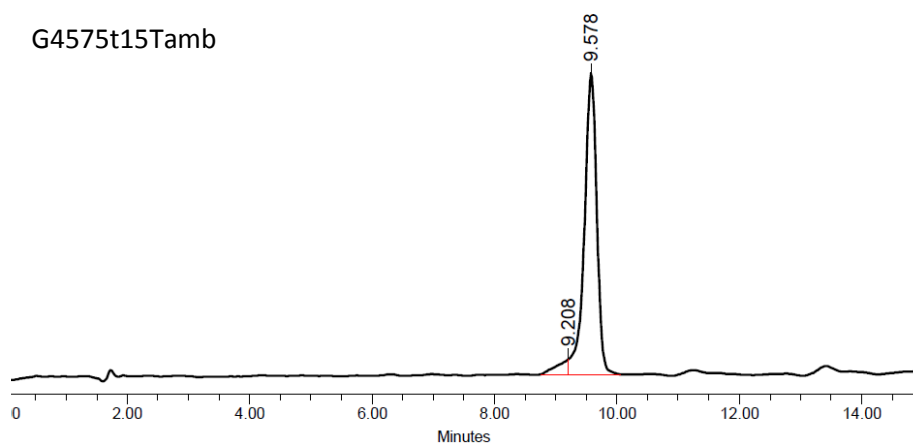
A small library of Phakellistatin 19 (Figure 51) analogs was designed following two different criteria: replacement of the prolines, which are the most relevant structural amino acids, by other proline analogs, and incorporation of residues containing fluorine atoms,<sup>40</sup> trying to improve in both cases the biological properties. Thus, Phe and Trp were replaced by fluorinated derivatives, and prolines were replaced by 4-HO-Pro and by homoprolines, a 6-membered ring amino acid, to fulfill a library of 9 analogs. In all cases, the synthetic strategy developed for Phakellistatin 19, was successfully applied providing the desired peptides with moderate-to-good yields, with one single exception, analog 4-HomoPro, which required double purification and was obtained with a final yield of 1%.



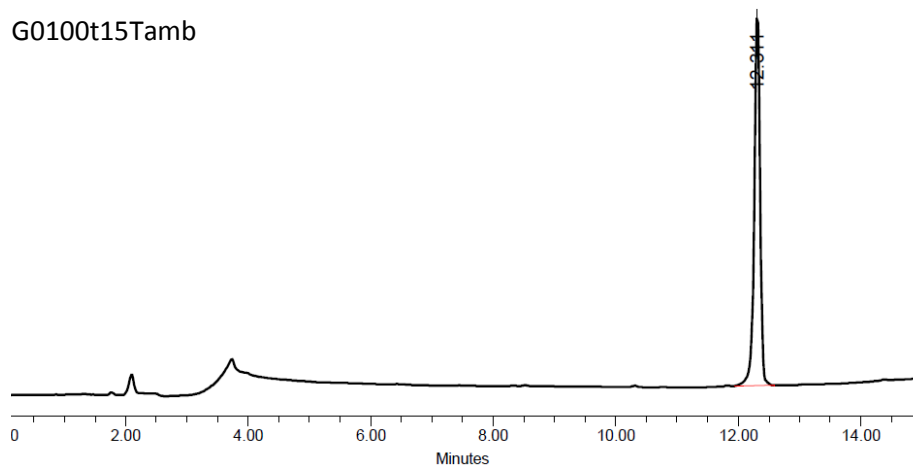
**Figure 51:** Chemical structures of Phakellistatin 19 and the small library of analogs.

In all cases, the purity of the final product was above 95% after reversed-phase semi-preparative HPLC purification (Figure 52).

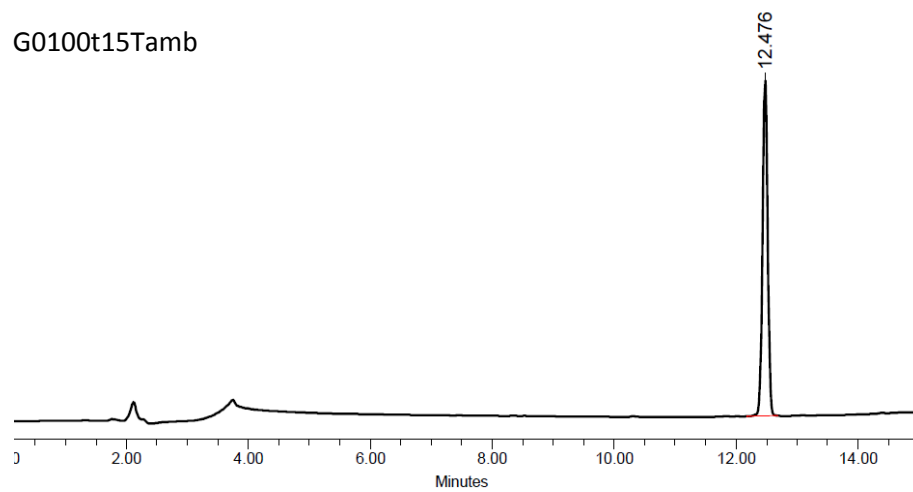
Cyclo-[Leu-Thr-Pro-Ile-Pro-Trp-(Phe-3,4-F<sub>2</sub>)-Pro]



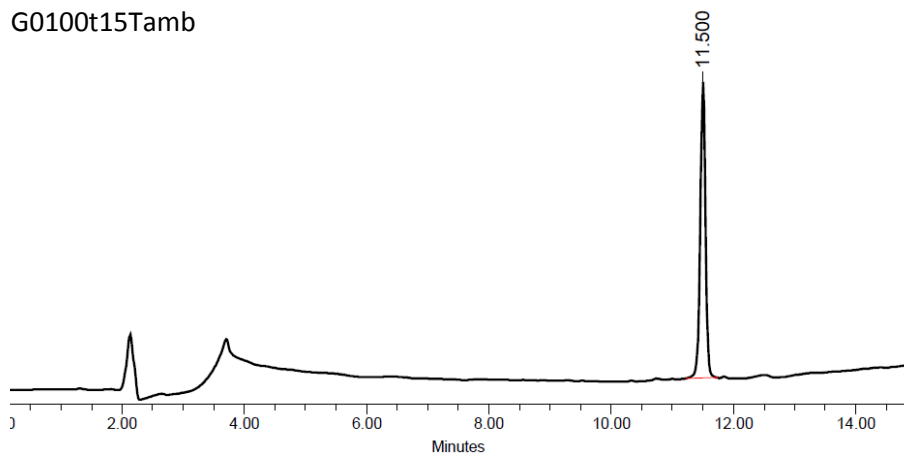
Cyclo-[Leu-Thr-Pro-Ile-Pro-(Trp-5-F)-Phe-Pro] (Peak 1)



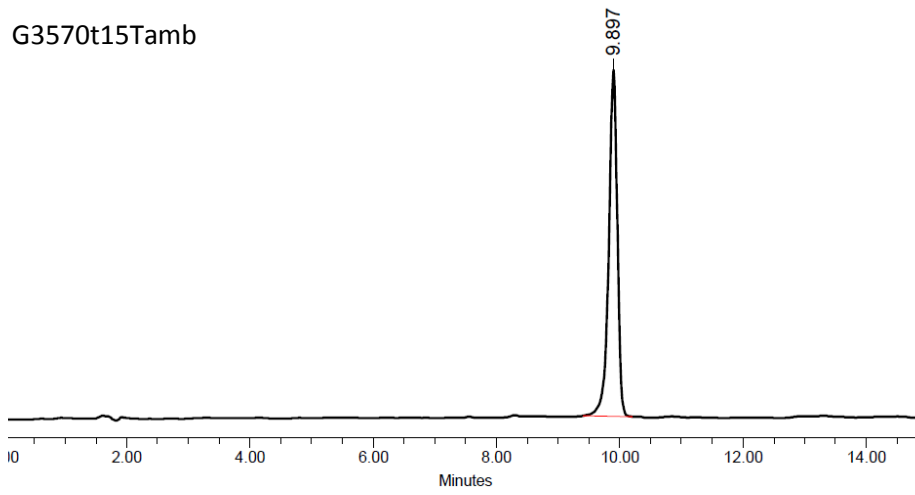
Cyclo-[Leu-Thr-Pro-Ile-Pro-(Trp-5-F)-Phe-Pro] (Peak 2)



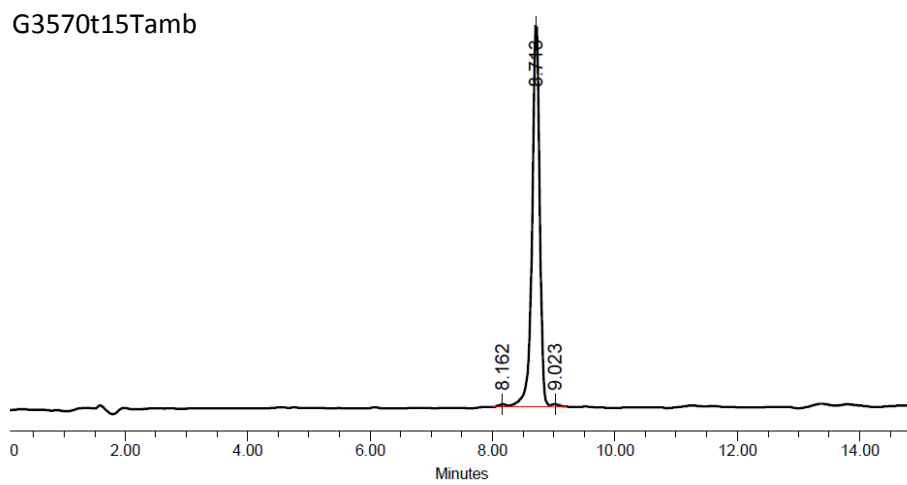
Cyclo-[Leu-Thr-Pro-Ile-Pro-Trp-Phe-(4-HO-Pro)]



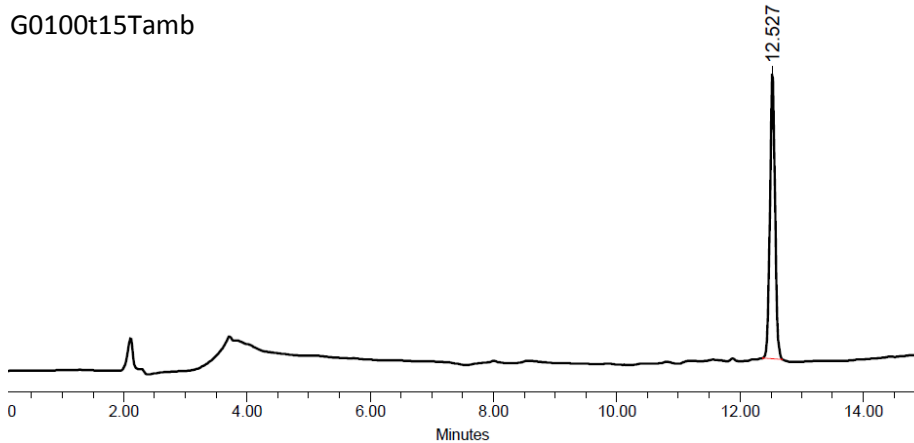
Cyclo-[Leu-Thr-Pro-Ile-(4-HO-Pro)-Trp-Phe-Pro]



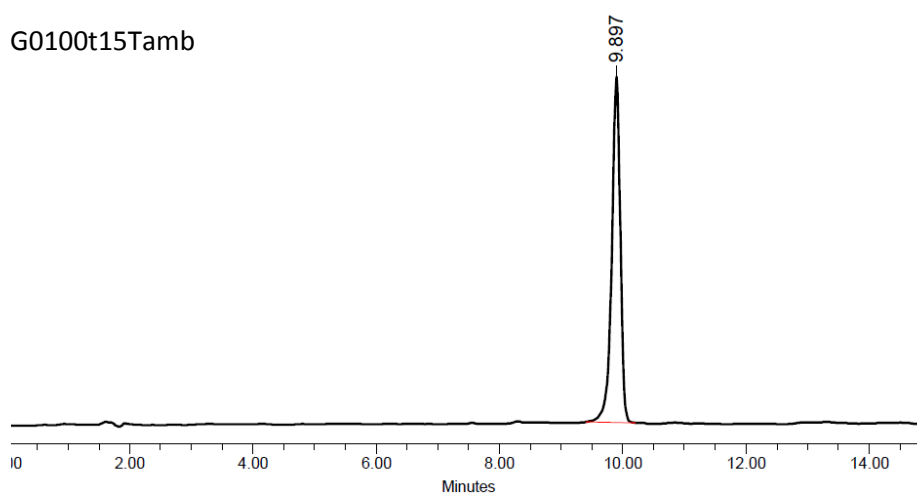
Cyclo-[Leu-Thr-(4-HO-Pro)-Ile-Pro-Trp-Phe-Pro]



Cyclo-[Leu-Thr-Pro-Ile-Pro-Trp-Phe-HomoPro]



Cyclo-[Leu-Thr-Pro-Ile-HomoPro-Trp-Phe-Pro]



Cyclo-[Leu-Thr-HomoPro-Ile-Pro-Trp-Phe-Pro]

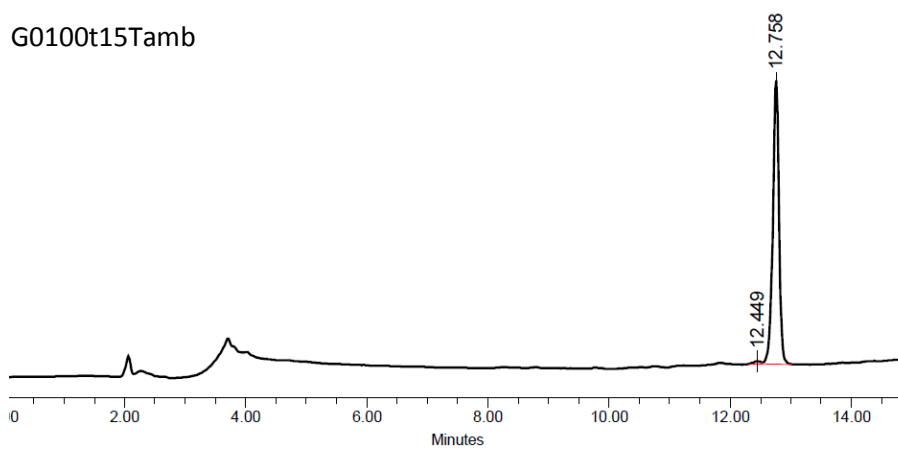
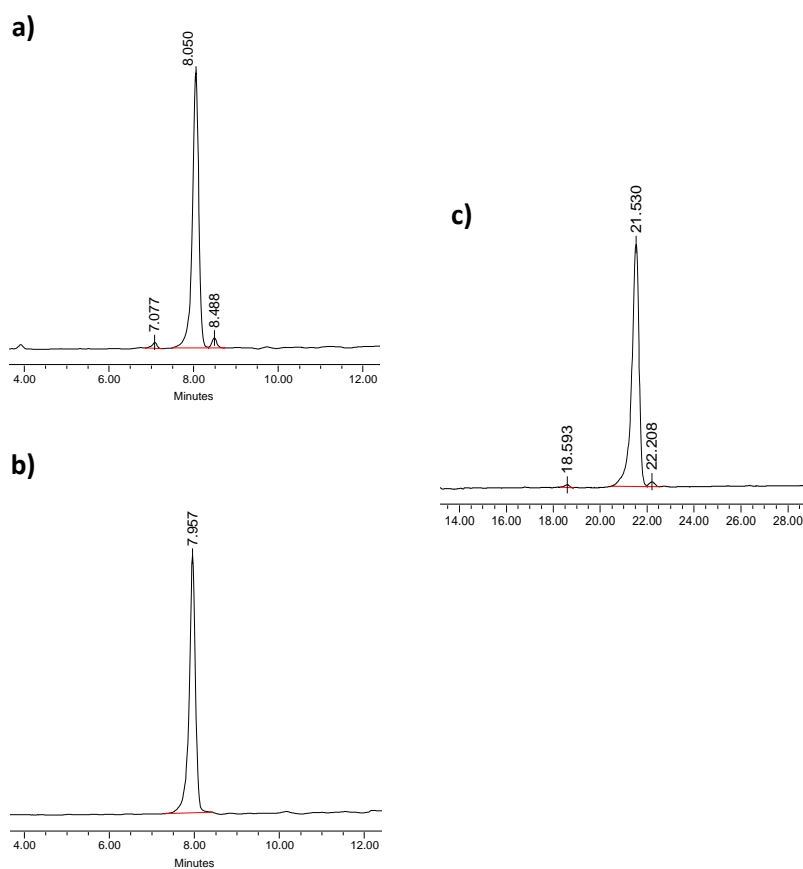


Figure 52: HPLC-PDA chromatograms of the purified analogs of Phakellistatin 19.

## 2.4. Validation of synthetic Phakellistatin 19

### 2.4.1. Chemical validation

To verify the chemical identity of the product obtained, samples of synthetic and natural Phakellistatin 19 were dissolved in H<sub>2</sub>O-ACN (1:1) and analyzed by reversed-phase HPLC-PDA by means of a C18 analytical column. Then, the two samples were co-eluted using a plane and long gradient (Figure 53). HRMS data for the two samples matched perfectly.

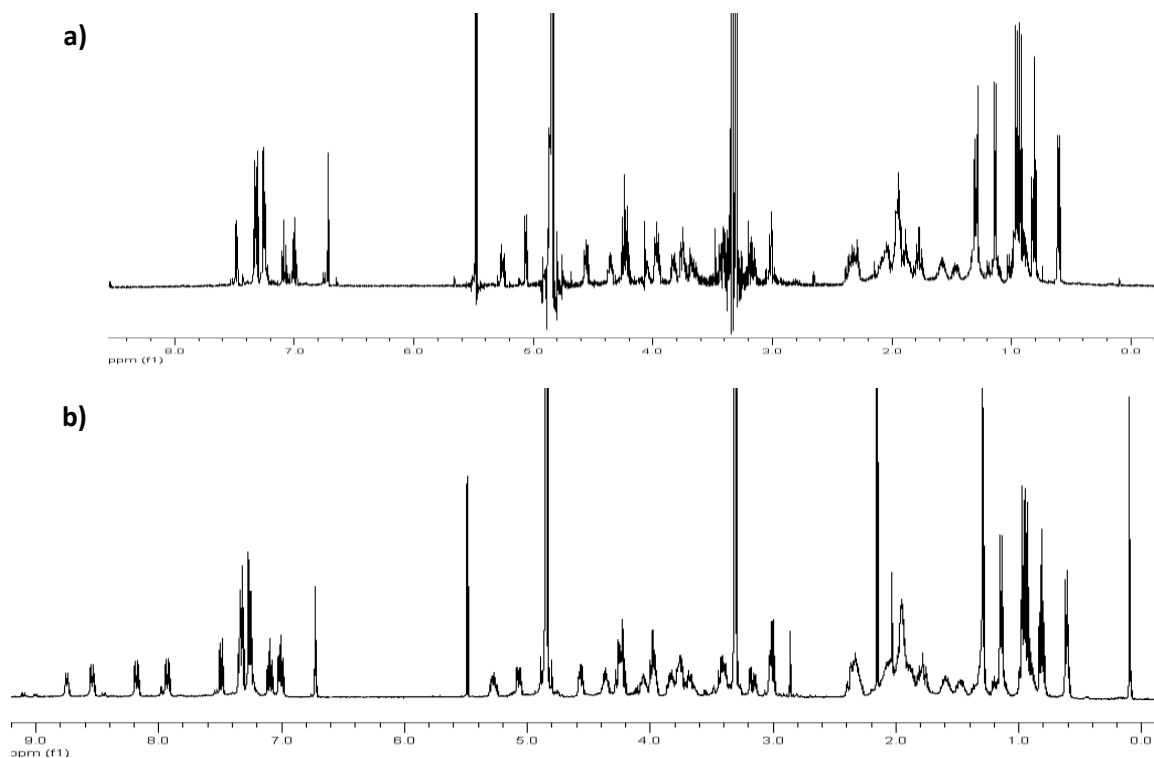


**Figure 53:** HPLC-PDA analysis of a) synthetic Phakellistatin 19; b) natural Phakellistatin 19; c) both natural and synthetic Phakellistatin 19: Co-elution. Conditions: Symmetry C18 reversed-phase analytical column (5  $\mu\text{m}$   $\times$  4.6 mm  $\times$  150 mm); linear gradient from 45% to 75% of ACN over 15 min for a) and b) and from 35% to 55% of ACN over 30 min for the co-elution experiment.

The co-elution experiment showed a single peak pointing out the chemical equivalence between the two samples. Further verifications applying different techniques were made to ensure Phakellistatin 19 chemical identity.

### 2.4.2. Spectral validation

Comparison of monodimensional  $^1\text{H}$  and bidimensional spectra of natural and synthetic Phakellistatin 19 in  $\text{CD}_3\text{OH}$  at 298 K, proved the spectral equivalence between the two peptides. Major differences between both spectra are due to the loss, in the natural sample, of the amide protons, and the consequent loss of multiplicity at the  $\text{H}_\alpha$  protons (Figure 54).



**Figure 54:**  $^1\text{H}$  monodimensional spectra in  $\text{CD}_3\text{OH}$  at 298 K of: a) Natural Phakellistatin 19; b) Synthetic Phakellistatin 19. The amide protons can partially or totally exchange with the solvent. This fact explains the complete absence of amide protons in the spectrum b).

Detailed  $^1\text{H}$  chemical shifts assignment is detailed in Table 7.



	<sup>1</sup> H (ppm) Natural peptide	<sup>1</sup> H (ppm) Synthetic peptide		<sup>1</sup> H (ppm) Natural peptide	<sup>1</sup> H (ppm) Synthetic peptide
<b>Pro<sup>1</sup></b>	-	-	<b>Ile<sup>5</sup> NH</b>	-	8.56 (d, 8.7)
H <sub>α</sub>	4.22	4.23	H <sub>α</sub>	4.25	4.26
H <sub>β</sub>	2.29, 1.89'	2.31, 1.90'	H <sub>β</sub>	2.06	2.06
H <sub>γ</sub>	2.09, 1.94'	2.10, 1.93'	H <sub>γ</sub>	1.46, 1.14'	1.48, 1.12'
H <sub>δ</sub>	3.97, 3.74'	3.97, 3.75'	H <sub>δ</sub>	0.60 (d, 6.8)	0.61 (d, 6.8)
				0.80 (t, 7.4)	0.81 (t, 7.4)
<b>Phe<sup>2</sup> NH</b>	-	8.19 (d, 9.8)	<b>Pro<sup>6</sup></b>	-	-
H <sub>α</sub>	5.26	5.27 (dt, 9.4, 9.3, 5.0)	H <sub>α</sub>	4.56	4.57
H <sub>β</sub>	3.01	3.02	H <sub>β</sub>	2.32	2.34
H <sub>2/6</sub>			H <sub>γ</sub>	1.96	1.96
H <sub>3/5</sub>			H <sub>δ</sub>	3.82, 3.67'	3.82, 3.68'
H <sub>4</sub>			<b>Thr<sup>7</sup> NH</b>	-	7.93 (d, 9.6)
<b>Trp<sup>3</sup> NH</b>	-	6.73 (br s)	H <sub>α</sub>	5.06	5.07 (dd, 9.7, 4.0)
H <sub>α</sub>	4.23	4.23	H <sub>β</sub>	4.35	4.36 (td, 10.8, 6.5)
H <sub>β</sub>	3.42, 3.16'	3.41, 3.17	H <sub>γ</sub>	1.14 (d, 6.3)	1.14 (d, 6.3)
H <sub>2</sub>		(dd, 14.4, 4.8)	OH	-	-
H <sub>4</sub>			<b>Leu<sup>8</sup> NH</b>	-	8.75 (d, 6.7)
H <sub>5</sub>			H <sub>α</sub>	3.75	3.76
H <sub>6</sub>			H <sub>β</sub>	2.36, 1.77'	2.37, 1.79'
H <sub>7</sub>			H <sub>γ</sub>	1.57	1.58
NH <sub>ind</sub>	-	-	H <sub>δ</sub>	0.96 (d, 6.7)	0.97 (d, 6.7)
<b>Pro<sup>4</sup></b>	-	-		0.93' (d, 6.6)	0.93 (d, 6.6)
H <sub>α</sub>	3.97	3.97			
H <sub>β</sub>	2.05, 1.78'	2.05, 1.79'			
H <sub>γ</sub>	1.94, 1.87'	1.96, 1.87'			
H <sub>δ</sub>	4.04, 3.40'	4.06, 3.41'			

**Table 7:** <sup>1</sup>H NMR spectral assignment of natural and synthetic Phakellistatin 19 in CD<sub>3</sub>OD.

### 2.4.3. Biological validation

Synthetic Phakellistatin 19 and the 9 members of the small library were tested against three cancer cell lines by means of MTT assays. According to the rest of Phakellistatins, synthetic Phakellistatin 19 did not show the same cytotoxic activity as its natural counterpart. Additionally, from all the analogs, only 5-HomoPro-Phakellistatin 19 was slightly active (Table 8).

		Breast MDA-MB-231 (M)	Lung-NSCLC A549 (M)	Colon HT29 (M)
Natural	GI <sub>50</sub>	5.15 E-07	4.41 E-07	4.62 E-07
Phakellistatin 19	TGI	1.47 E-06	1.16 E-06	6.72 E-07
Synthetic	GI <sub>50</sub>	n.d.	n.d.	n.d.
Phakellistatin 19	TGI	n.d.	n.d.	n.d.
5-HomoPro- Phakellistatin 19	GI <sub>50</sub>	4.97 E-06	n.d.	9.63 E-06
	TGI	>1.04 E-05	n.d.	>1.04 E-05

**Tabla 8:** Cytotoxic activities displayed by natural and synthetic Phakellistatin 19 and 5-HomoPro-Phakellistatin 19.

As it has been explained before (see Section 2.1.), the same unexpected behavior has been reported in the literature for most of the described Phakellistatins. Herein, the two more recurrent hypotheses and two other different explanations for this surprising behavior are detailed:

- A) Preparations of natural Phakellistatins could contain a spectrally undetectable amount of a contamination, eg. an epimer, which would be responsible for the biological activity. This hypothesis is supported by the presence of two extra peaks only detected in the chromatogram of natural Phakellistatin 19 (see Fig. 53 a).
- B) The presence of several Pro residues capable of *cis-trans* isomerism in a constrained macrocycle provides structures with a complex conformational profile. Individual conformers at Pro linkages bearing different biological properties could be stabilized in different conditions (i.e. solvents).
- C) The contamination discussed above could be due to another compound with a chemical structure totally different to Phakellistatin 19.
- D) Phakellistatins and, particularly, Phakellistatin 19, can be chelating cyclopeptides. The absence of metallic cations in the synthetic sample would account for the decrease in the cytotoxicity.

As this phenomenon of lack of activity is described in the literature for most of the Phakellistatin family, A and B look more plausible causes. Hypothesis C is hard to prove in our hands because we did not have easy access to the natural Phakellistatin 19. Furthermore, the presence of a non-related contaminant in every single member of the big Phakellistatins family seems quite unlikely. Finally, despite the hypothesis D being logical, we decided to focus our efforts in verifying or discarding hypotheses A and B.

## 2.5. Structural elucidation

The Nuclear Magnetic Resonance (NMR) is one of the most used experimental techniques in the structural analysis of all kind of molecules. Chemical shifts, NOE cross peak's intensities and coupling constants depend on the conformation adopted by the target compound, and provide a high amount of structural information.

Before starting a deep investigation regarding the reasons of the disagreement between natural and synthetic Phakellistatin 19, an exhaustive structural study mostly based on NMR techniques was undertaken.

### 2.5.1. Chemical shifts: $^1\text{H}$ and $^{13}\text{C}$ assignment

NMR study of Phakellistatin 19 in DMSO- $d_6$  provided a monodimensional  $^1\text{H}$  spectrum with a single set of sharp peaks corresponding either to a single Phakellistatin 19 conformer, or to a mixture of conformers in a fast equilibrium for the NMR time scale.

Complete  $^1\text{H}$  (500 MHz) and  $^{13}\text{C}$  (125 MHz) spectral assignments were successfully accomplished after registration and exhaustive study of  $^1\text{H}$ , gCOSY, TOCSY, ROESY, HSQC and HMBC experiments (Table 9).

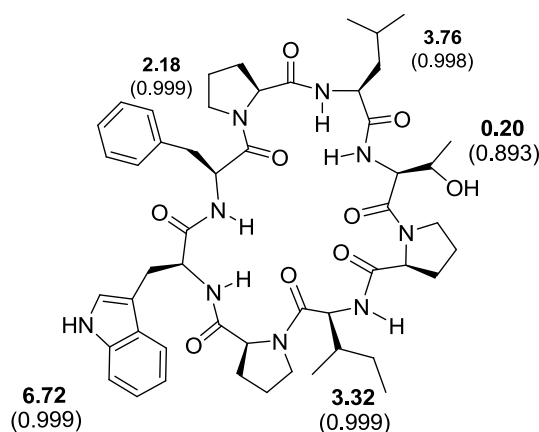
	$^1\text{H}$ (ppm)	$^{13}\text{C}$ (ppm)		$^1\text{H}$ (ppm)	$^{13}\text{C}$ (ppm)
<b>Pro<sup>1</sup></b>	-	-	<b>Ile<sup>5</sup> NH</b>	8.34	-
C/H <sub><math>\alpha</math></sub>	4.05	60.6	C/H <sub><math>\alpha</math></sub>	4.20	54.0
C/H <sub><math>\beta</math></sub>	2.13, 1.98'	29.7	C/H <sub><math>\beta</math></sub>	1.97	35.0
C/H <sub><math>\gamma</math></sub>	1.83, 1.72'	24.6-24.7	C/H <sub><math>\gamma</math></sub>	1.31, 1.04'	24.6-24.7
C/H <sub><math>\delta</math></sub>	3.89, 3.59'	47.8		0.85 <sub>CH<sub>3</sub></sub>	21.0/14.4 <sub>CH<sub>3</sub></sub>
			C/H <sub><math>\delta</math></sub>	0.65	9.7
<b>Phe<sup>2</sup> NH</b>	8.11	-	<b>Pro<sup>6</sup></b>	-	-
C/H <sub><math>\alpha</math></sub>	5.03	51.1	C/H <sub><math>\alpha</math></sub>	4.47	59.3
C/H <sub><math>\beta</math></sub>	2.95, 2.86'	36.5	C/H <sub><math>\beta</math></sub>	2.06, 1.93'	28.4
C <sub>1</sub>		138.2	C/H <sub><math>\gamma</math></sub>	1.83, 1.72'	24.6-24.7
C <sub>2/6</sub>		129.2	C/H <sub><math>\delta</math></sub>	3.69, 3.56'	47.0
C <sub>3/5</sub>		127.8			
C <sub>4</sub>		126.0	<b>Thr<sup>7</sup> NH</b>	7.56	-
<b>Trp<sup>3</sup> NH</b>	8.20		C/H <sub><math>\alpha</math></sub>	4.87	56.2
C/H <sub><math>\alpha</math></sub>	3.70	57.0	C/H <sub><math>\beta</math></sub>	4.13	67.6
C/H <sub><math>\beta</math></sub>	3.61, 3.16'	23.3	C/H <sub><math>\gamma</math></sub>	0.94	18.4
C/H <sub>2</sub>	6.95	123.5	OH	5.54	-
C <sub>3</sub>	-	111.2	<b>Leu<sup>8</sup> NH</b>	8.73	-
C/H <sub>4</sub>	7.40	118.2	C/H <sub><math>\alpha</math></sub>	3.53	53.0
C/H <sub>5</sub>	6.94	117.9	C/H <sub><math>\beta</math></sub>	2.16, 1.68'	36.1
C/H <sub>6</sub>	7.03	120.8	C/H <sub><math>\gamma</math></sub>	1.47	24.6-24.7
C/H <sub>7</sub>	7.30	111.3			

C <sub>8</sub>	-	136.0	C/H <sub>δ</sub>	0.88, 0.85'	23.4,
C <sub>9</sub>	-	127.0			21.0/14.4
NH <sub>ind</sub>	10.76	-			
<b>Pro<sup>4</sup></b>	-	-			
C/H <sub>α</sub>	3.92	61.0			
C/H <sub>β</sub>	1.99, 1.83'	24.6-24.7			
C/H <sub>γ</sub>	1.76, 1.75'	29.0			
C/H <sub>δ</sub>	3.96, 3.52'	47.5			

**Table 9:** <sup>1</sup>H and <sup>13</sup>C NMR spectral assignments for synthetic Phakellistatin 19 in DMSO-*d*<sub>6</sub>. Carbonylic and quaternary carbons have not been assigned because they were not visible at the HMBC experiment. The carbons C<sub>γ</sub>-CH<sub>3</sub>-Ile and C<sub>δ</sub>-Leu, as well as C<sub>γ</sub>-Pro<sup>1</sup>, C<sub>β</sub>-Pro<sup>4</sup>, C<sub>γ</sub>-Ile and C<sub>β</sub>-Leu could not be univocally assigned either using the gHSQC or the HMBC experiments.

### 2.5.2. Chemical shifts and temperature: temperature coefficients

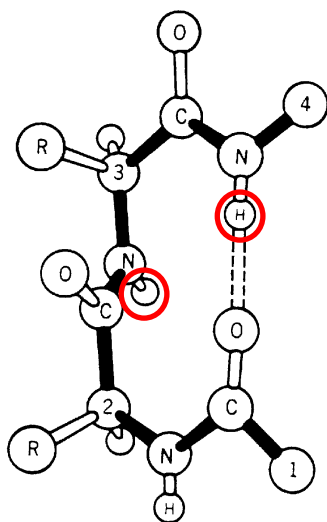
In order to study the hydrogen bonding pattern of Phakellistatin 19, the temperature coefficients ( $\Delta\delta/\Delta T$ ) of its amide protons were calculated (Figure 55). Thus, monodimensional <sup>1</sup>H spectra of Phakellistatin 19 were recorded at five different temperatures between 298 K and 318 K, and the evolution of their chemical shifts analyzed.



**Figure 55:** Chemical structure of Phakellistatin 19. Temperature coefficients are shown in bold (ppb/K) and the linear regression coefficients in brackets.

Although the rather viscous DMSO-*d*<sub>6</sub> was used as a solvent, the temperature coefficients obtained were significantly low for Phe and Thr amide protons, pointing out its likely participation in two intramolecular hydrogen bonds. Moreover, the presence of Pro residues in small cyclic peptides may help in the stabilization of structural elements such as  $\beta$ -turns. On the basis of these two observations, we proposed the existence of two  $\beta$ -turns. The first one involved the residues Pro<sup>1</sup> and Leu at the positions *i*+1 and *i*+2 respectively, while Pro<sup>4</sup> and Trp were placed at the analogous *i*+1 and *i*+2 positions of a second  $\beta$ -turn. The high values of the coupling constant <sup>3</sup>*J*<sub>NH,α</sub> for the residues Thr and Phe (9.3 Hz and 9.9 Hz

respectively), suggested their participation in an extended conformation. On the other side, the smaller values obtained for Leu and Trp (6.6 Hz and 6.3 Hz) would agree with their participation in a more folded conformation. All these experimental data together with the NOE cross-peaks between NH-Leu and NH-Thr, and NH-Trp and NH-Phe detected in the ROESY spectra, supported the existence of the two  $\beta$ -turns (Figure 56).



**Figure 56:** Schematic representation of a  $\beta$ -turn. The hydrogen bond  $\text{CO}_i\text{-HN}_{i+3}$  stabilizing the turn is highlighted with a dashed line. The two amide protons  $\text{NH}_{i+2}$  and  $\text{NH}_{i+3}$  showing a NOE cross peak are indicated with a red circle. The residues  $i$  and  $i+3$  are involved in an extended conformation, while the aa  $i+1$  and  $i+2$  adopt a more folded conformation.

Finally, the linear variation of the chemical shifts regarding the temperature, suggested that there were no drastic conformational changes in the studied range of temperatures.

### 2.5.3. NOE cross peaks

Qualitative and quantitative analysis of NOE experiments, such as NOESY and ROESY, is a potent tool when dealing with the elucidation of molecules' tridimensional structure.

Choosing between NOESY and ROESY experiments depends on the correlation time of the studied molecule ( $\tau_c$ ). When we are close to the condition  $\omega\tau_c = 1$ , where  $\omega$  is the Larmor frequency, then the NOE is zero or approximately zero (Figure 57). In these cases and taking into account that the ROE never reaches the zero, the preferred option is always a ROESY experiment. The correlation time of a molecule mainly depends on three factors: molecular weight, solvent, and working temperature. In general, for small molecules ( $\text{MW} < 600 \text{ g/mol}$ ) NOE is positive, it is zero for middle-sized molecules ( $\text{MW} = 700\text{-}1200\text{g/mol}$ ) and it is negative for large molecules ( $\text{MW} > 1200 \text{ g/mol}$ ). Phakellistatin 19 is a middle weight molecule (952.53 g/mol), that has been solubilized in an extremely viscose solvent and studied in a standard

range of temperatures around 298 K. Under these working conditions, NOE is close to zero, so a ROESY spectrum was required.

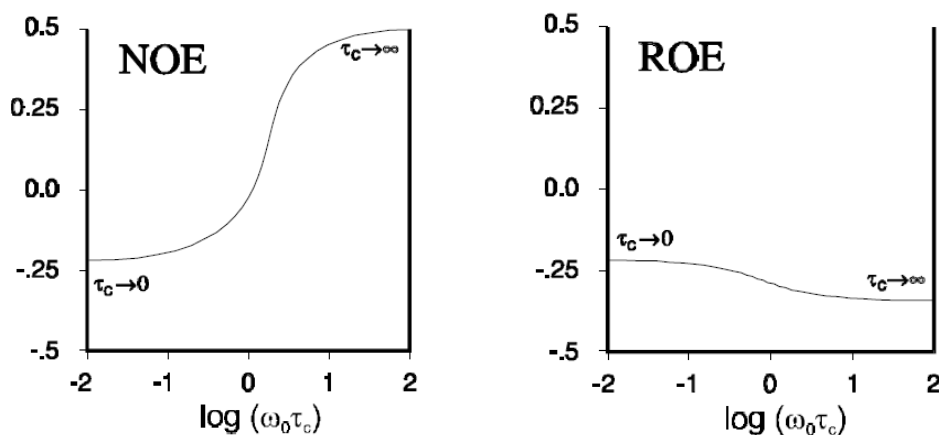


Figure 57: NOE and ROE values regarding to the  $\log(\omega_0\tau_c)$ .

However, the structural information is more reliable when obtained from a NOESY than from a ROESY experiment. Spin diffusion is a more severe phenomenon for NOESY than for ROESY experiments, and may cause false NOE cross-peaks and wrong interatomic distances. If the mixing times are small enough, we are confined to the linearity region, and the artefacts can be easily minimized. On the other side, ROESY experiments present several problems: cross-peaks's intensities depend on their relative distance to the offset, and the TOCSY magnetic transference can partially or totally cancel NOE cross-peaks. Some corrections can be applied to enable the use of the experimental data extracted from a ROESY experiment to obtain reliable interatomic distances.<sup>41</sup>

### 2.5.3.1. Qualitative analysis

ROESY's cross-peaks pattern gives information about the *cis/trans* isomerism of  $Xaa^{i-1}$ - $Pro^i$  linkages. When it is a *cis* peptide bond, a large NOE cross-peak between  $H_\alpha$ - $Pro^i$  and  $H_\alpha$ - $Xaa^{i-1}$  is detected; and when it is a *trans* amide bond, the large NOE cross-peak is observed between  $H_\delta$ - $Pro^i$  and  $H_\alpha$ - $Xaa^{i-1}$ . Analysis of Phakellistatin 19's ROESY spectrum enabled the identification of large NOE cross peaks between the protons:  $H_\alpha$ -Phe and  $H_\delta$ - $Pro^1$ ;  $H_\alpha$ -Ile and  $H_\delta$ - $Pro^4$ ; and  $H_\alpha$ -Thr and  $H_\delta$ - $Pro^6$ . This experimental data proved that the thermodynamically most stable *trans* isomerism is the one adopted by the Phe- $Pro^1$ , Ile- $Pro^4$  and Thr- $Pro^6$  amide bonds. The small differences between the chemical shifts of  $C_\beta$  and  $C_\gamma$  of the proline residues also confirmed the *trans* conformation:  $Pro^1 \Delta\delta_{C\beta-C\gamma} = 5.01$  ppm,  $Pro^4 \Delta\delta_{C\beta-C\gamma} = -4.38$  ppm and  $Pro^6 \Delta\delta_{C\beta-C\gamma} = 3.78$  ppm.<sup>42,43</sup>

Finally, the NOE's cross-peaks between NH-Leu and NH-Thr, and NH-Trp and NH-Phe also supported the existence of the two previously predicted  $\beta$ -turns (see section 2.5.2.).

### 2.5.3.2. Quantitative analysis

A sample of synthetic Phakellistatin 19 (5.0 mg) was dissolved in DMSO- $d_6$  (0.6  $\mu$ L) and a ROESY spectrum was recorded at 298 K using a mixing time of 150 ms. The volumes of the cross-peaks were converted into inter-protonic distances neglecting the effect of the spin diffusion (isolated spin pair approximation: ISPA) but correcting the dependence with regard to the offset. Thus, distances ( $r_{ij}$ ) were calculated using the corrected integrals of the cross-peaks:

$$r_{ij} = r_{\text{ref}} (a_{\text{ref}} \cdot c_{\text{ref}} / a_{ij} \cdot c_{ij})^{1/6}$$

where:  $c_{ij} = 1/(\sin^2\theta_i \cdot \sin^2\theta_j)$  and  $\tan\theta_i = \gamma B_1 / (\omega_i - \omega_0)$

and  $(\omega_i - \omega_0)$  is the difference of chemical shifts between the proton  $H_i$  and the offset expressed in Hz, and  $\gamma B_1$  is the spin-lock potency.

After quantitative analysis of Phakellistatin 19's ROESY spectra, Table 10 shows the interatomic distances experimentally found.

Atom i	Atom j	Cross-peak volume ( $a_{ij}$ )	$r_{ij}$ (Å)	$r_{\text{centroid}}$ (Å)
NH-Ile	$H_{\alpha}$ -Pro <sup>6</sup>	0.04	2.96	-
NH-Trp	NH-Phe	0.04	2.83	-
NH-Ile	$H_{\beta}$ -Thr	0.05	2.83	-
NH-Thr	NH-Leu	0.05	2.83	-
NH-Leu	$H_{\alpha}$ -Pro <sup>1</sup>	0.31	2.06	-
$H_{\alpha}$ -Thr	$H_{\delta}$ -Pro <sup>6</sup>	0.28	2.24	2.42
$H_{\alpha}$ -Thr	$H_{\delta'}$ -Pro <sup>6</sup>	0.06	2.88	-
$H_{\alpha}$ -Phe	$H_{\delta}$ -Pro <sup>1</sup>	0.35	2.17	2.08
$H_{\alpha}$ -Phe	$H_{\delta'}$ -Pro <sup>1</sup>	0.2	2.36	-
$H_{\beta}$ -Ile	$H_{\beta}$ -Phe	0.06	2.64	2.66
$H_{\beta}$ -Ile	$H_{\beta'}$ -Phe	0.03	2.96	-
$H_{\alpha}$ -Ile	$H_{\delta}$ -Pro4	0.42	2.09	2.03
$H_{\alpha}$ -Ile	$H_{\delta'}$ -Pro4	0.2	2.34	-
HO-Thr	$H_{\beta}$ -Phe	0.06	2.84	2.80
HO-Thr	$H_{\beta'}$ -Phe	0.04	3.03	-
HO-Thr	NH-Ile	0.06	2.78	-

**Table 10:** Interatomic distances calculated from the NOE's cross-peaks of a ROESY experiment. The  $H_{\delta}/H_{\delta'}$ -Pro<sup>4</sup> protons were used as a reference. For the methylenic protons, a centroid was defined and the corresponding distance was re-calculated.

These interatomic distances, together with the hydrogen bonds already identified during the temperature coefficients' calculation, were used as experimental restrictions in a

standard protocol of restricted simulated annealing (SA) to find an energetically minimized conformation in solution of Phakellistatin 19.

During this protocol, Phakellistatin 19 was heated to 1000 K in increments of 100 K at a rate of 1 K/ps, to reach a condition where all conformations are equally probable. Every 100 K increment, the sample was allowed to equilibrate for 1000 ps. Once the 1000 K were reached, this temperature was kept for 30000 ps before starting the cooling down, again at a rate of 1 K/ps, in increments of 100 K and allowing the sample to equilibrate for 5000 ps after every 100 K-interval. However, before starting the cooling down, a new parameter was introduced when calculating the total energy of the molecule. Thus, an energetic penalization was charged every time an experimental interatomic distance was ignored. The force constant defining the weight of the experimental restrictions during the cooling down process was re-scaled 3 times by a factor of 0.5 as the temperature was decreased. Hence, the initial penalization was 40 kcal/mol and the last one, applied at 400 K, was 5 kcal/mol. The total energy of every conformation was calculated as follows:

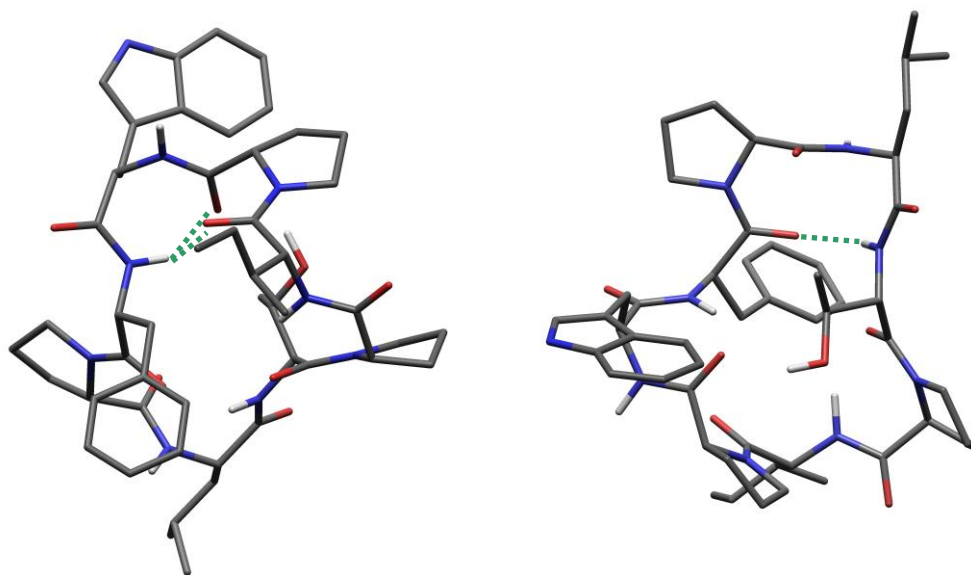
$$E_T = E_{\text{potential}} + E_{\text{restrictions}}$$

$$E_{\text{potential}} = E_{\text{bond component}} + \sum_{1,2} [k' (A/r^{12} - C/r^6) + (q_1 \cdot q_2)/(\epsilon \cdot r)]$$

where:  $\epsilon$  is the medium dielectrical constant (for DMSO  $\epsilon = 48$ ) and  $k'$  is a factor of 0.25 to modulate the Van der Waals forces in order to simulate the solvation effect of an organic solvent.

This heating and restricted cooling down process was repeated 125 times to obtain 125 conformations with minimized energy. The conformation with the lowest energy is shown in Figure 58. Measurement of interatomic distances on this structure proved that all the experimental restrictions were fulfilled (all found values turn to be confined in an acceptable range of  $r_{ij} \pm 20\%$ ).





**Figure 58:** Energetically minimized structure of Phakellistatin 19 obtained after application of a restricted SA protocol. The two checked hydrogen bonds are highlighted in dashed green lines.

Phakellistatin 19 presents a first  $\beta$ -turn stabilized by the hydrogen bond ThrNH-OC<sub>Phe</sub> (the measured distance is 2.06 Å) and with the residues Pro<sup>1</sup> and Leu placed at the positions  $i+1$  and  $i+2$  respectively. The second predicted  $\beta$ -turn is not clearly defined. The expected hydrogen bond (see section 2.5.2.) PheNH-OC<sub>Ile</sub> (3.07 Å) seems to have been replaced by another one, PheNH-OC<sub>Pro4</sub> (1.95 Å), that would stabilize a  $\gamma$ -turn involving the residues Phe, Trp and Pro<sup>4</sup> in the positions  $i$ ,  $i+1$  and  $i+2$  respectively. The  $\phi_{i+1}$  and  $\psi_{i+1}$  angles measure 78° and -56° respectively on the minimized structure. These values perfectly match with the ones established for a  $\gamma$ -turn: 70-95 for  $\phi_{i+1}$  and (-75)-(-45) for  $\psi_{i+1}$ . All these observations pointed out the more likely existence of a  $\beta$ -turn and a  $\gamma$ -turn rather than two  $\beta$ -turns.

The region around the  $\gamma$ -turn resembles a hairpin motif. It comprises two antiparallel strands linked by means of hydrogen bonds and orienting the hydrophobic side chains of the Phe and Ile residues into the same direction. Van der Waals interactions between these two side chains help to stabilize the structural motif. Furthermore, Trp's side chain points to the upper region of the  $\gamma$ -turn and is completely exposed to the solvent, suggesting its possible participation in the pharmacophore. The whole structure is highly folded and, somehow, draws a characteristic chair-shape.

### 2.5.3. Coupling constants: dihedral angles

The minimized structure obtained after applying a restricted SA protocol must respect not only the interatomic distances calculated using the ROESY cross-peaks information, but also other experimental parameters such as the dihedral angles. The angles formed by the atoms H-N-C<sub>α</sub>-H<sub>α</sub> can be calculated (Table 11) using the coupling constants and the Karplus-Bystrov equation:<sup>44</sup>

$${}^3J_{\text{NH},\alpha} = 9.4 \cos^2(60 - \phi) - \cos(60 - \phi) + 0.4$$

Aa	<sup>3</sup> J <sub>NH-Hα</sub> (Hz)		Dihedral angles φ <sup>1</sup>			Dihedral angles φ <sup>2</sup>
Phe	9.9	-	162	-	-162 <sup>3</sup>	-176
Trp	6.3	31 <sup>3</sup>	138	-31	-138	14
Ile	8.9	-	153	-	-153 <sup>3</sup>	-173
Thr	9.3	-	157 <sup>3</sup>	-	-157	156
Leu	6.6	29	139	-29 <sup>3</sup>	-139	-4

**Table 11:**<sup>1</sup> Dihedral angles calculated by means of the Karplus-Bystrov equation.

<sup>2</sup> Dihedral angles measured on the Phakellistatin 19's minimized structure.

<sup>3</sup> From all the possible dihedral angles calculated by means of the Karplus-Bystrov equation, these values are the closest to the ones measured on the structure.

The differences between calculated and measured dihedral angles are significant for the Trp and the Thr residues, but acceptable for the other residues.

## 2.6. Finding an explanation for biological activity discrepancies between synthetic and natural Phakellistatin 19.

As it has already been exposed, all the Phakellistatins described in the literature present a strong disagreement between the biological properties of the natural and the synthetic peptides. In rough outlines, two are the hypothesis suggested so far to explain this surprising behavior: a minor but highly cytotoxic impurity or a conformational issue. In the present thesis, some experimentation has been done to try to shed light on this issue.

### 2.6.1. An epimer being responsible of the biological activity?

The presence of two minor peaks in the HPLC-PDA chromatogram of natural Phakellistatin 19 which were not detected in the synthetic sample, took relevance after biological evaluation of synthetic Phakellistatin 19. Firstly, it was hypothesized that one or both of them could be attributed to a highly cytotoxic epimer of Phakellistatin 19, present in

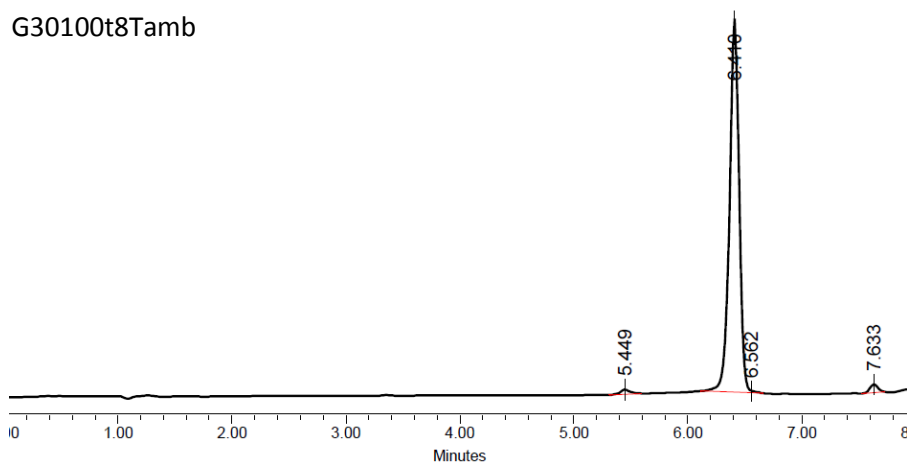
the natural sample in really small amounts and responsible of the detected bioactivity. Although a bit unlikely, it was a logical hypothesis rather easy to be demonstrated. Thus, the ten possible epimers (Table 12) were synthesized using the established synthetic strategy, and biologically tested against the same three cancer cell lines.

Epimer
Cyclo-(Leu-Thr-Pro <sup>6</sup> -Ile-Pro <sup>4</sup> -Trp-Phe- <b>D-Pro</b> <sup>1</sup> )
Cyclo-(Leu-Thr-Pro <sup>6</sup> -Ile-Pro <sup>4</sup> -Trp- <b>D-Phe</b> -Pro <sup>1</sup> )
Cyclo-(Leu-Thr-Pro <sup>6</sup> -Ile-Pro <sup>4</sup> - <b>D-Trp</b> -Phe-Pro <sup>1</sup> )
Cyclo-(Leu-Thr-Pro <sup>6</sup> -Ile- <b>D-Pro</b> <sup>4</sup> -Trp-Phe-Pro <sup>1</sup> )
Cyclo-(Leu-Thr-Pro <sup>6</sup> - <b>D-Ile</b> -Pro <sup>4</sup> -Trp-Phe-Pro <sup>1</sup> )
Cyclo-(Leu-Thr- <b>D-Pro</b> <sup>6</sup> -Ile-Pro <sup>4</sup> -Trp-Phe-Pro <sup>1</sup> )
Cyclo-(Leu- <b>D-Thr</b> -Pro <sup>6</sup> -Ile-Pro <sup>4</sup> -Trp-Phe-Pro <sup>1</sup> )
Cyclo-( <b>D-Leu</b> -Thr-Pro <sup>6</sup> -Ile-Pro <sup>4</sup> -Trp-Phe-Pro <sup>1</sup> )
Cyclo-(Leu-Thr-Pro <sup>6</sup> - <b>allo-Ile</b> -Pro <sup>4</sup> -Trp-Phe-Pro <sup>1</sup> )
Cyclo-(Leu- <b>allo-Thr</b> -Pro <sup>6</sup> -Ile-Pro <sup>4</sup> -Trp-Phe-Pro <sup>1</sup> )

**Table 12:** Peptidic sequence of all the synthesized epimers.

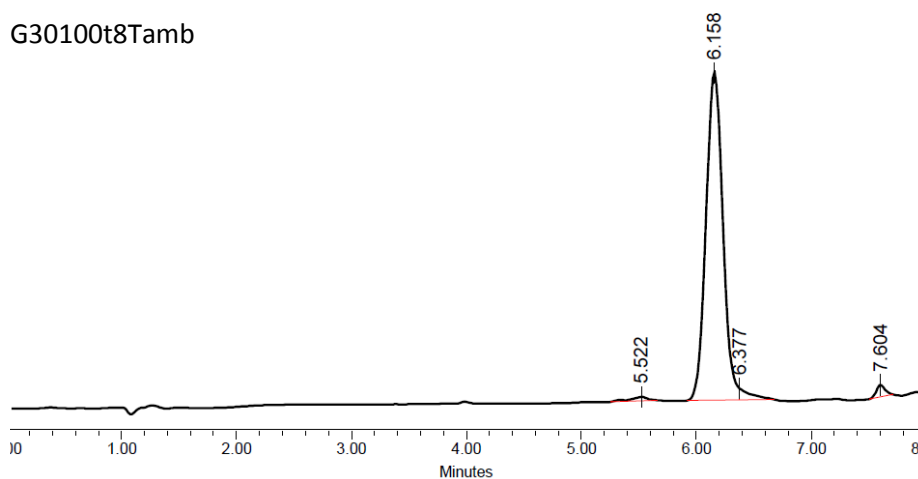
After semi-preparative HPLC purification, all epimers were obtained with purities above 95% (Figure 59).

Cyclo-[Leu-Thr-Pro<sup>6</sup>-Ile-Pro<sup>4</sup>-Trp-Phe-D-Pro<sup>1</sup>]



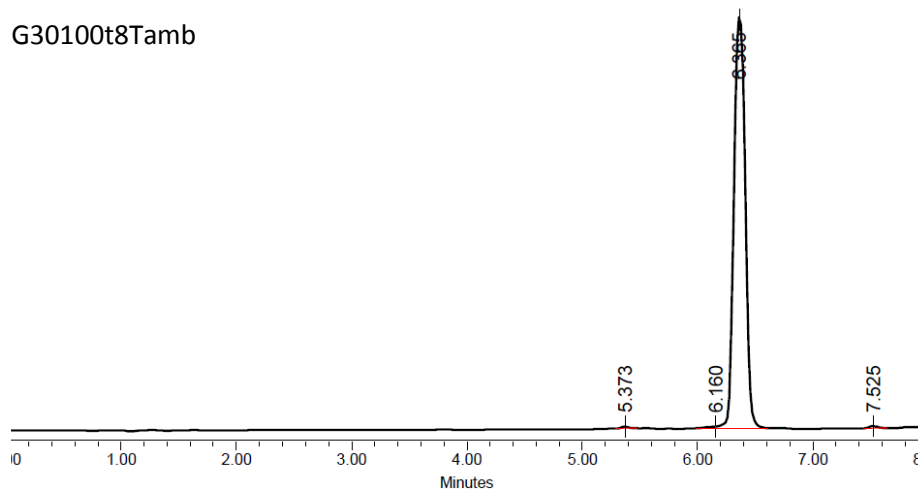
Cyclo-[Leu-Thr-Pro<sup>6</sup>-Ile-Pro<sup>4</sup>-Trp-D-Phe-Pro<sup>1</sup>]

G30100t8Tamb



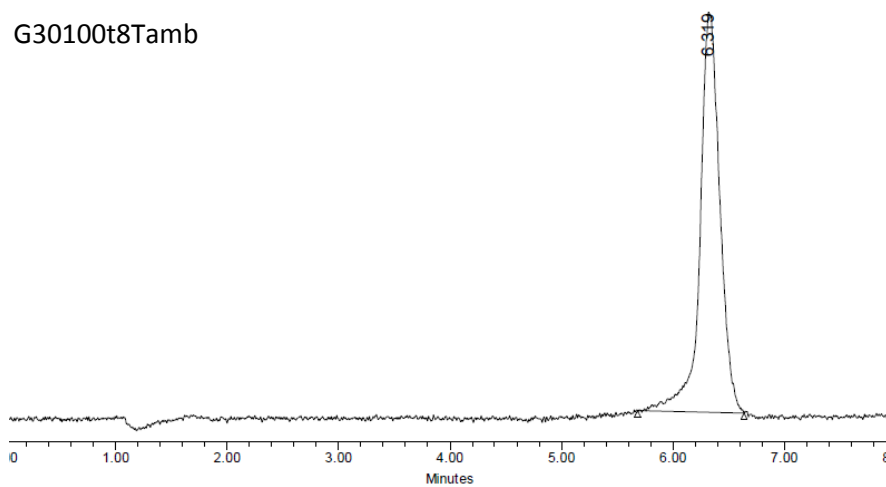
Cyclo-[Leu-Thr-Pro<sup>6</sup>-Ile-Pro<sup>4</sup>-D-Trp-Phe-Pro<sup>1</sup>]

G30100t8Tamb



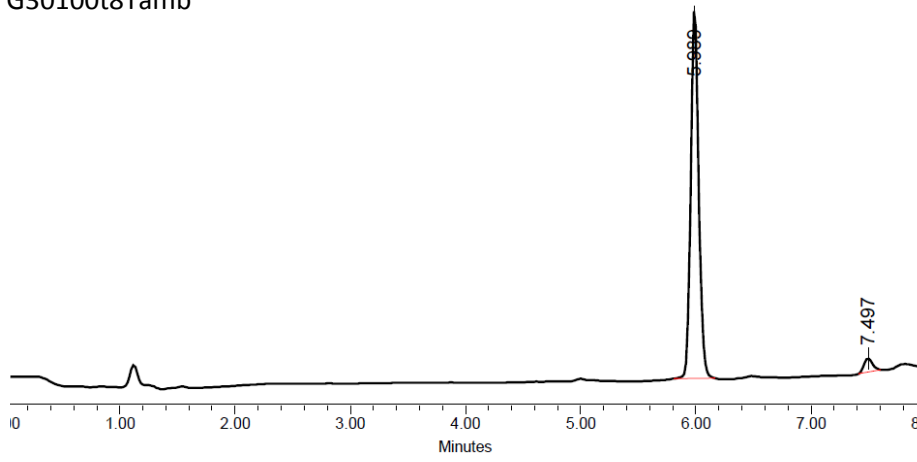
Cyclo-[Leu-Thr-Pro<sup>6</sup>-Ile-D-Pro<sup>4</sup>-Trp-Phe-Pro<sup>1</sup>]

G30100t8Tamb



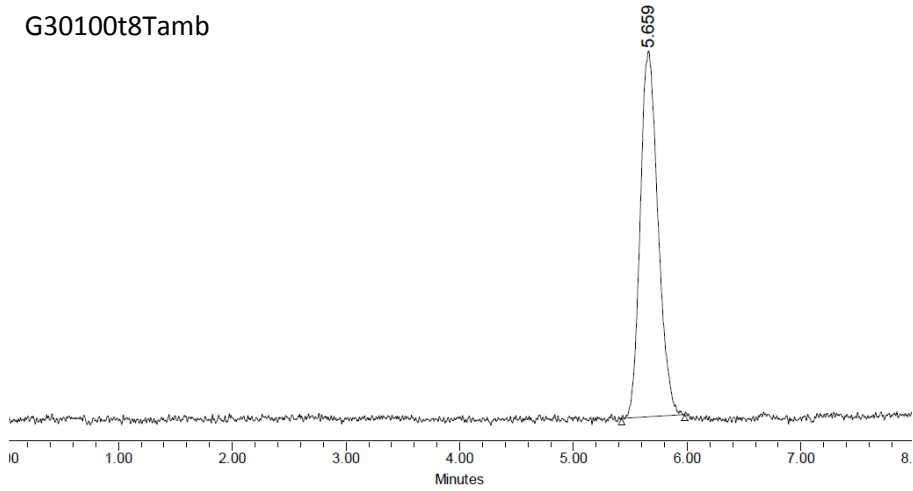
Cyclo-[Leu-Thr-Pro<sup>6</sup>-D-Ile-Pro<sup>4</sup>-Trp-Phe-Pro<sup>1</sup>]

G30100t8Tamb



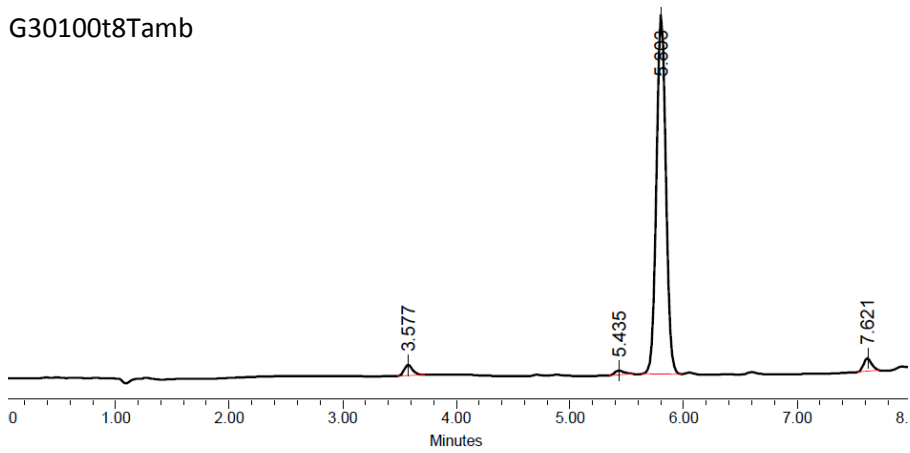
Cyclo-[Leu-Thr-D-Pro<sup>6</sup>-Ile-Pro<sup>4</sup>-Trp-Phe-Pro<sup>1</sup>]

G30100t8Tamb



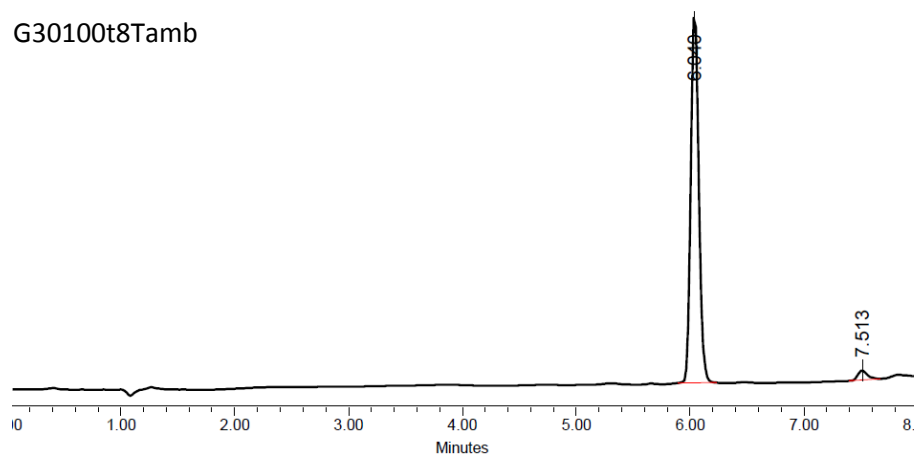
Cyclo-[Leu-D-Thr-Pro<sup>6</sup>-Ile-Pro<sup>4</sup>-Trp-Phe-Pro<sup>1</sup>]

G30100t8Tamb



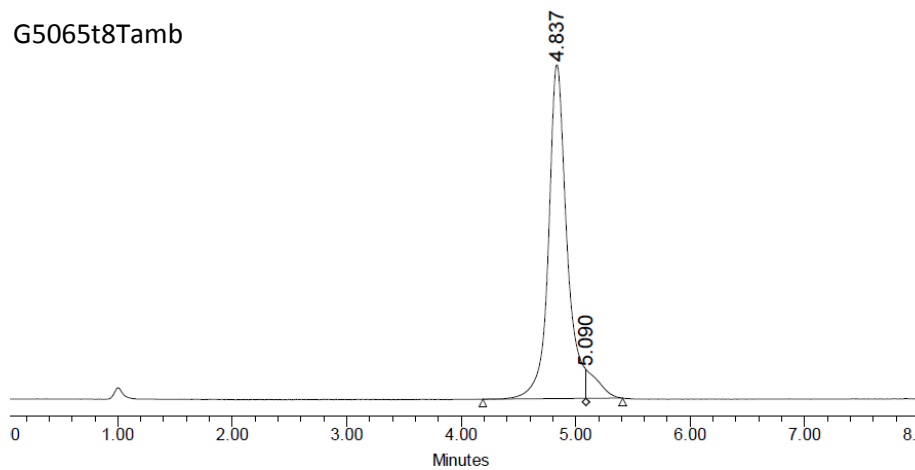
Cyclo-[D-Leu-Thr-Pro<sup>6</sup>-Ile-Pro<sup>4</sup>-Trp-Phe-Pro<sup>1</sup>]

G30100t8Tamb



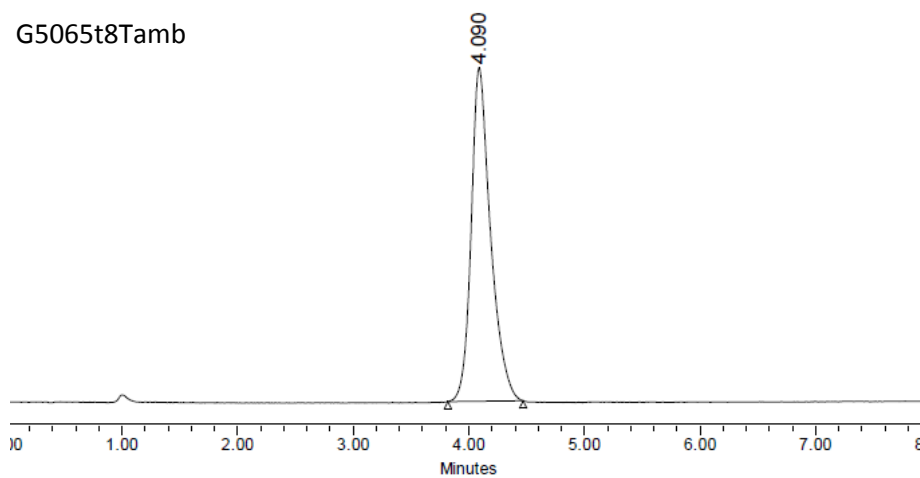
Cyclo-[Leu-Thr-Pro<sup>6</sup>-*allo*-Ile-Pro<sup>4</sup>-Trp-Phe-Pro<sup>1</sup>]

G5065t8Tamb



Cyclo-[Leu-*allo*-Thr-Pro<sup>6</sup>-Ile-Pro<sup>4</sup>-Trp-Phe-Pro<sup>1</sup>]

G5065t8Tamb



**Figure 59:** HPLC-PDA chromatograms of the purified epimers of Phakellistatin 19.

Biological assays revealed no GI<sub>50</sub> under 10<sup>-6</sup> M for any of the epimers, excluding then this first hypothesis.

### 2.6.2. *Cis-trans* isomerism at the Pro linkages responsible of the activity?

The presence of up to three Pro moieties in a constrained macrocycle, such as in Phakellistatins, can lead to complex *cis-trans* isomerism equilibria around the Pro linkages. It is assumed that different conformations would own different biological properties. Thus, the synthetic process would provide a non-cytotoxic but thermodynamically most stable conformation, while marine sponges would produce a cytotoxic but less stable conformation.

#### 2.6.2.1. Thermodynamic studies of the *cis-trans* equilibrium at Pro linkages: Biological evaluation

It was plausible to think that pre-treating synthetic Pipecolidepsin A samples with different solvents, at different temperatures or at a different pH, would have an effect on the thermodynamic equilibrium between Phakellistatin 19's conformers also altering the bioactivity results.

In order to evaluate this hypothesis, four samples of synthetic Phakellistatin 19 were subjected to different treatments and then biologically assayed (Table 13). In all cases, residual TFA from the purification step was replaced by HCl, a less hygroscopic acid showing fewer interactions with biological systems.

Treatment	Lung-NSCLC A549 GI <sub>50</sub> (M)	Colon HT29 GI <sub>50</sub> (M)	Breast MDA-MB-231 GI <sub>50</sub> (M)
TFA exchange by HCl	n.d.	n.d.	n.d.
TFA exchange by HCl + MeOH	n.d.	n.d.	n.d.
TFA exchange by HCl + H <sub>2</sub> O a 45.4 °C	n.d.	n.d.	n.d.
TFA exchange by HCl + phosphate buffer 200 mM at pH = 8.1	8.61 E-08	9.35 E-08	2.63 E-08

**Table 13:** GI<sub>50</sub> values for the four pre-treated samples of synthetic Phakellistatin 19. All treatments lasted 8 days.

The positive results obtained after treatment with 200 mM phosphate buffer at pH= 8.1 required corroboration in order to discard any false positive due to the high phosphate salts concentration. Thus, three new samples of synthetic Phakellistatin 19 were pre-treated

and bio-assayed. We used 200 mM phosphate buffer at pH = 8.04; 20 mM phosphate buffer at pH = 8.10; and 20 mM tris buffer at pH = 8.18. A blank for all the buffers and a new parameter, the time, were included in this second biological evaluation (Table 14).

Buffer	Treatment	Lung-NSCLC A549 GI <sub>50</sub> (M)	Colon HT29 GI <sub>50</sub> (M)	Breast MDA-MB-231 GI <sub>50</sub> (M)
Phosphate 200 mM, pH = 8.04	Blank	3.68 E-06	1.89 E-06	2.52 E-06
	2 h	4.10 E-07	2.52 E-07	2.42 E-07
	8 d	2.31 E-08	1.47 E-08	1.47 E-08
Phosphate 20 mM, pH = 8.10	Blank	n.d.	n.d.	n.d.
	1 d	3.78 E-07	1.26 E-07	4.37 E-07
	2 d	n.d.	n.d.	n.d.
Tris 20 mM, pH = 8.18	5.5 d	1.89 E-06	9.66 E-07	2.84 E-06
	Blank	n.d.	n.d.	n.d.
	2 h	n.d.	n.d.	n.d.
	2 d	n.d.	n.d.	n.d.
	4 d	n.d.	n.d.	n.d.

**Table 14:** GI<sub>50</sub> values for the three new samples of pre-treated synthetic Phakellistatin 19.

The values of cytotoxicity obtained were difficult to interpret. Pre-treatment with two buffers at the same pH and salt concentration, one based on organic compounds and the other on inorganic salts, had completely different effects. Moreover, there was a substantial difference in the results obtained for the 200 mM and the 20 mM phosphate buffer. These experimental observations may point out a more direct influence of the sodium and phosphate ions in the cytotoxicity exerted by synthetic Phakellistatin 19. Finally, the behavior respect to the parameter time was also incoherent.

Our second hypothesis explained the different biological behavior on the basis of an equilibrium between conformers with different *cis-trans* isomerism at the Pro linkages. Thus, and taking into account the poorly concluding biological results, it was decided to perform an exhaustive structural study of the pre-treated samples of synthetic Phakellistatin 19 to check the existence of any conformational variation.

#### 2.6.2.2. Thermodynamic studies of the *cis-trans* equilibrium at Pro linkages: Structural study

Six out of the eight constitutive residues of Phakellistatin 19 are hydrophobic amino acids or Pro. Therefore, Phakellistatin 19 is a highly lipophilic peptide with poor solubility in H<sub>2</sub>O. In order to study its conformation in basic and acid media, the synthesis of a spectrally comparable and H<sub>2</sub>O-soluble analog was required.



Analysis of Phakellistatin 19's minimized structure obtained after application of the restricted SA protocol, revealed a number of important structural features. Phe and Ile's side-chains proved to play an important structural role in the  $\gamma$ -turn stabilization, while Trp and Leu's side-chains remained quite isolated and exposed. Moreover, we must consider the presence of the structurally crucial prolines, and a last amino acid, a Thr, bearing a rather polar uncharged side-chain. Considering all these structural features and the minor presence of Trp than Leu in nature, the H<sub>2</sub>O-soluble analog was designed with a positively charged Orn at the Leu's position. Its synthesis was successfully achieved following the synthetic strategy developed for Phakellistatin 19, and the biological assays revealed no significant cytotoxic properties.

Once the Orn-analog was proven to be H<sub>2</sub>O-soluble, its spectral equivalence with Phakellistatin 19 was checked by comparison of <sup>1</sup>H NMR spectral assignments of the two peptides in DMSO-*d*<sub>6</sub>. The small differences found, validated the use of the Orn-analog in the structural study as an appropriate model for Phakellistatin 19.

To study whether or not a conformational change at the Pro linkages occurred, a sample of 5 mg of analog was treated with a 20 mM phosphate buffer at a pH of 5.95 for 12 h. Then, a full set of NMR experiments were registered in a Bruker 500 MHz spectrophotometer at 273 K. The same analysis at 298 K was undertaken with a second sample of 5 mg of Orn-analog after treatment for 4 days with a 100 mM phosphate buffer at pH = 8.12. Complete <sup>1</sup>H NMR spectral assignment is shown in Table 15.

	$\delta^1\text{H}$ (ppm) DMSO- <i>d</i> <sub>6</sub>	$\delta^1\text{H}$ (ppm) H <sub>2</sub> O:D <sub>2</sub> O (pH = 5.95)	$\delta^1\text{H}$ (ppm) H <sub>2</sub> O:D <sub>2</sub> O (pH = 8.12)		$\delta^1\text{H}$ (ppm) DMSO- <i>d</i> <sub>6</sub>	$\delta^1\text{H}$ (ppm) H <sub>2</sub> O:D <sub>2</sub> O (pH = 5.95)	$\delta^1\text{H}$ (ppm) H <sub>2</sub> O:D <sub>2</sub> O (pH = 8.12)
<b>Pro</b> <sup>1</sup>	-	-	-	<b>Ile</b> <sup>5</sup> NH	8.33	8.41	8.29
H <sub><math>\alpha</math></sub>	4.09	4.41	4.34	H <sub><math>\alpha</math></sub>	4.21	4.22	4.12
H <sub><math>\beta</math></sub>	2.18, 2.00'	2.44, 1.97'	2.38, 1.91'	H <sub><math>\beta</math></sub>	1.97	1.89	1.81
H <sub><math>\gamma</math></sub>	1.86, 1.82'	2.16, 2.08'	2.08, 2.00'	H <sub><math>\gamma</math></sub>	1.32, 1.06'	1.42, 1.11'	1.31, 0.99'
H <sub><math>\delta</math></sub>	3.91, 3.61'	3.86	3.84, 3.75'		0.86 <sub>CH3</sub>	0.30 <sub>CH3</sub>	0.19 <sub>CH3</sub>
				H <sub><math>\delta</math></sub>	0.66	0.80	0.72
<b>Phe</b> <sup>2</sup> NH	8.12	7.92	7.77				
H <sub><math>\alpha</math></sub>	5.06	5.35	5.31	<b>Pro</b> <sup>6</sup>	-	-	-
H <sub><math>\beta</math></sub>	2.93, 2.90'	3.09, 2.87'	3.05, 2.79'	H <sub><math>\alpha</math></sub>	4.48	4.58	4.51
H <sub>2/6</sub>				H <sub><math>\beta</math></sub>	2.14, 2.09'	2.46, 1.89'	2.38, 1.78'
H <sub>3/5</sub>				H <sub><math>\gamma</math></sub>	1.83, 1.73'	1.97	1.85
H <sub>4</sub>				H <sub><math>\delta</math></sub>	3.70, 3.56'	3.89, 3.61'	3.76, 3.43'
<b>Trp</b> <sup>3</sup> NH	8.18	6.74	6.36	<b>Thr</b> <sup>7</sup> NH	7.54	7.92	7.81
H <sub><math>\alpha</math></sub>	3.70	4.51	4.46	H <sub><math>\alpha</math></sub>	4.88	5.12	5.04
H <sub><math>\beta</math></sub>	3.61, 3.17'	3.29, 3.10'	3.10, 3.03'	H <sub><math>\beta</math></sub>	4.15	4.45	4.28
H <sub>2</sub>	6.96			H <sub><math>\gamma</math></sub>	0.94	1.13	1.04
H <sub>4</sub>	7.41			OH	5.54	5.92	5.65

H <sub>5</sub>	6.96							
H <sub>6</sub>	7.05				Orn <sup>8</sup> NH	8.82	9.10	8.90
H <sub>7</sub>	7.32				H <sub>α</sub>	3.55	4.01	3.94
HN <sub>ind</sub>	10.79	10.22	10.10		H <sub>β</sub>	2.16, 2.02'	2.31, 2.17'	2.26, 2.10'
					H <sub>γ</sub>	1.49	1.73	1.68
<b>Pro<sup>4</sup></b>	-	-	-		H <sub>δ</sub>	2.79	3.09, 2.87'	3.04
H <sub>α</sub>	3.91	4.12	4.07		NH <sub>2</sub>	7.68	7.75	-
H <sub>β</sub>	2.18, 2.00'	2.20, 1.81'	2.12, 1.64'					
H <sub>γ</sub>	1.86, 1.77'	1.96	1.78					
H <sub>δ</sub>	3.96, 3.54'	3.89, 3.26'	3.77					

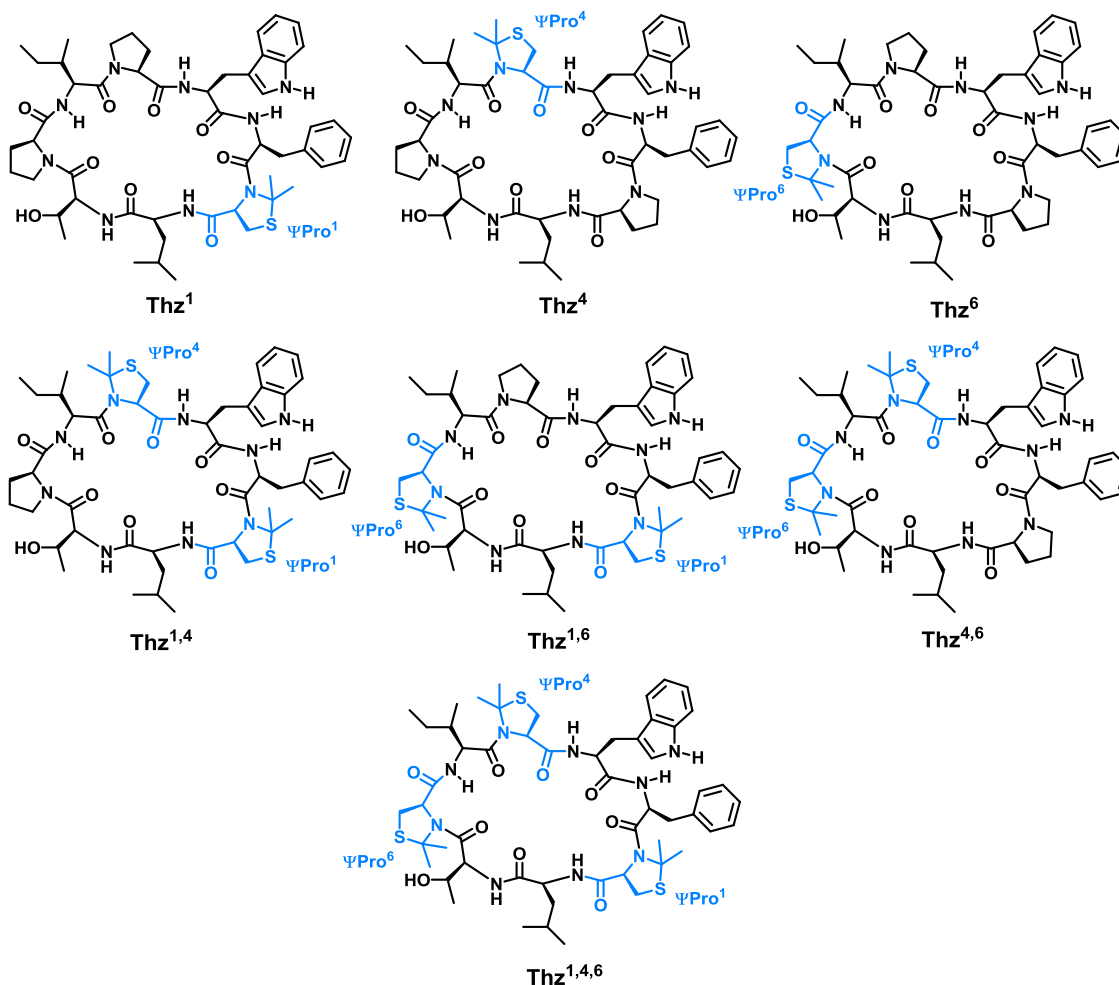
**Table 15:** <sup>1</sup>H NMR spectral assignment of Orn-analog in DMSO-*d*<sub>6</sub>, in acid aqueous media and in basic aqueous media. For the samples in H<sub>2</sub>O-D<sub>2</sub>O (9:1), dioxane was used as a reference. Assignment at pH = 8.12 is less accurate due to the inferior quality of the spectra.

The cross-peaks pattern of the ROESY (pH = 8.12 and T = 298 K) and NOESY (pH = 5.95 and T = 273 K) experiments showed the *trans* isomerism of the three prolines in DMSO-*d*<sub>6</sub> and in acid and basic water. This experimental verification refuted the initial hypothesis: the cytotoxicity observed after treatment with phosphate buffer cannot be explained by arguing a *cis-trans* isomerism at the Pro linkages. A hypothetical co-responsibility of the sodium and/or phosphate ions in the detected bioactivity is coherent with the NMR results and the cytotoxicity values found after treatment with tris buffer. The incoherent behavior regarding the parameter time still remains unclear.

### 2.6.3. Enhancing the *cis* isomerism: Pro replacement by Ψ<sup>Me,Me</sup>Pro

#### 2.6.3.1. Synthesis of a small library of Ψ<sup>Me,Me</sup>Pro-containing Phakellistatin 19 analogs

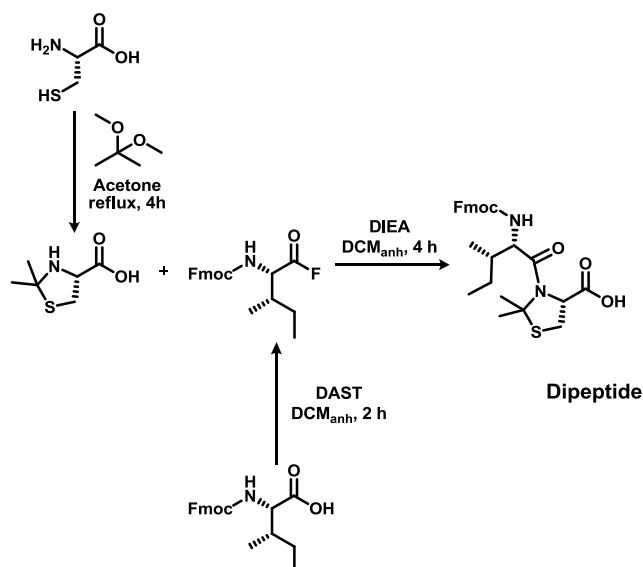
A small library of 7 peptides with the Pro moieties replaced by Ψ<sup>Me,Me</sup>Pro covering all the possibilities was designed (Figure 60).



**Figure 60:** Chemical structure of  $\Psi^{\text{Me,Me}}\text{Pro}$ -analogs of Phakellistatin 19. The residues  $\Psi^{\text{Me,Me}}\text{Pro}$  are highlighted in blue.

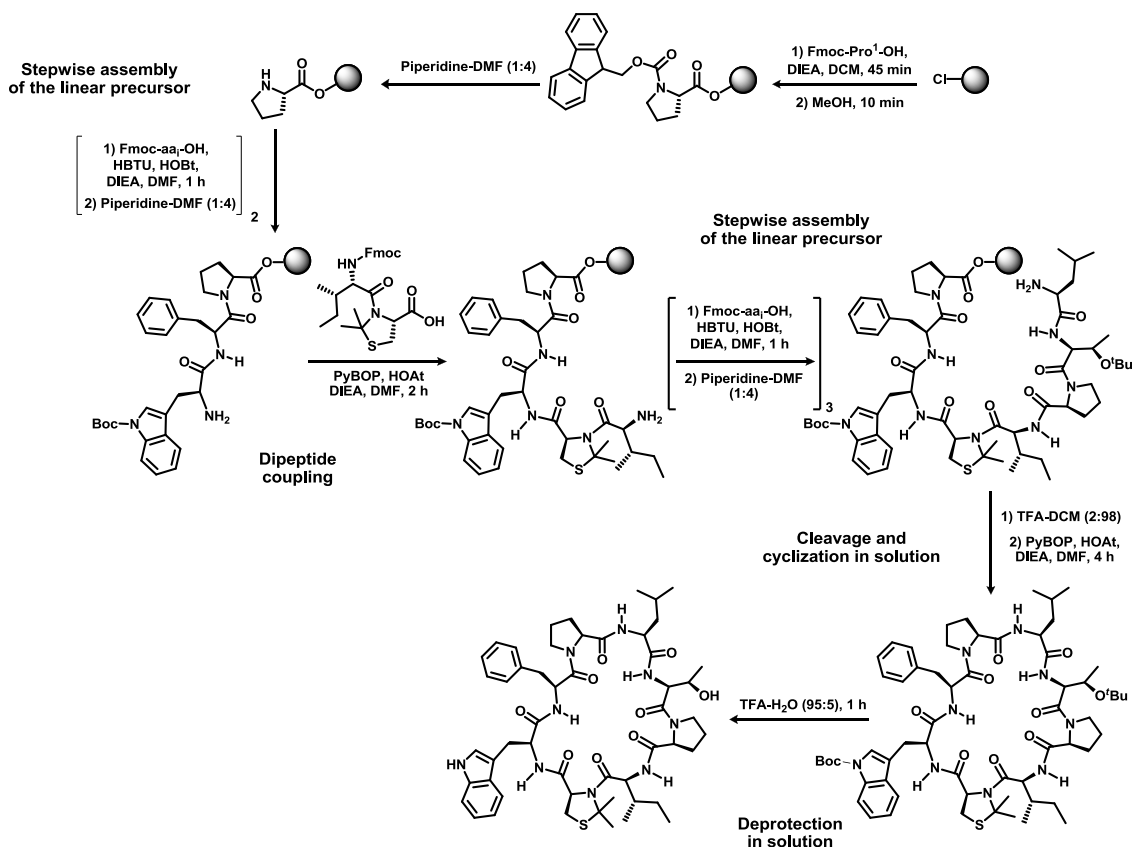
The synthetic strategy previously developed and validated for Phakellistatin 19 (see Scheme 31), could not be directly applied to obtain the pseudoproline-containing analogs since the extremely hindered  $\Psi^{\text{Me,Me}}\text{Pro}$  was not acylated under any conditions: DIPCDI-HOBT, COMU-Oxyma-DIEA, HATU-HOAt-DIEA, PyBOP-HOAt-DIEA, TCFH-HOAt-DIEA, Fmoc-aa-F, applying MW and other reagents and techniques. Taking this into consideration, it was decided to completely change the synthetic approach. All approaches including a solid-phase acylation of  $\Psi^{\text{Me,Me}}\text{Pro}$  were discarded, and the synthesis in solution of a dipeptide containing the  $\Psi^{\text{Me,Me}}\text{Pro}$  at the C-terminus was faced.

Although coupling of Fmoc-aa-F on  $\Psi^{\text{Me,Me}}\text{Pro}$  was not achieved on solid phase, it did work in solution to form the dipeptide (Scheme 32).



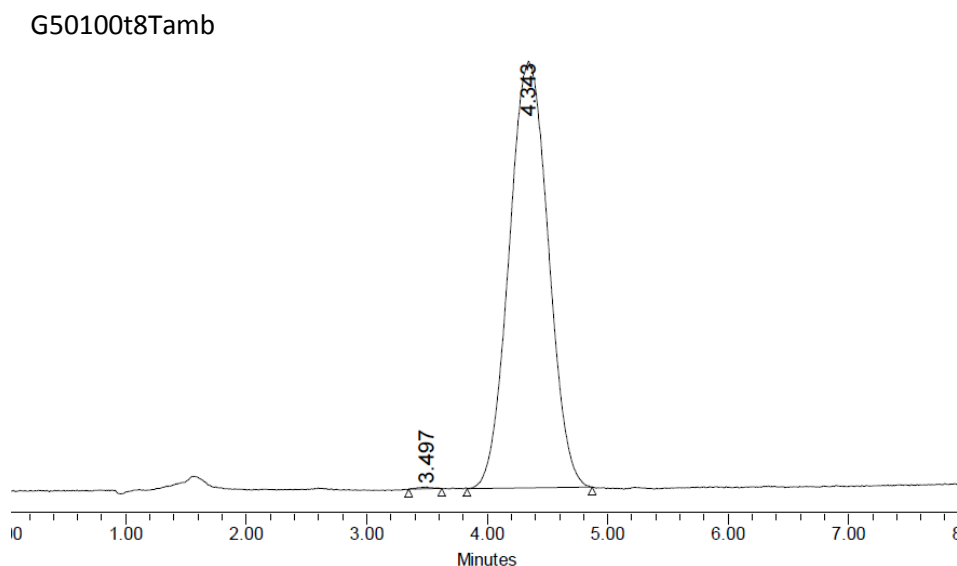
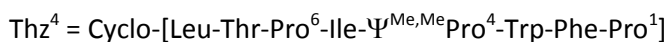
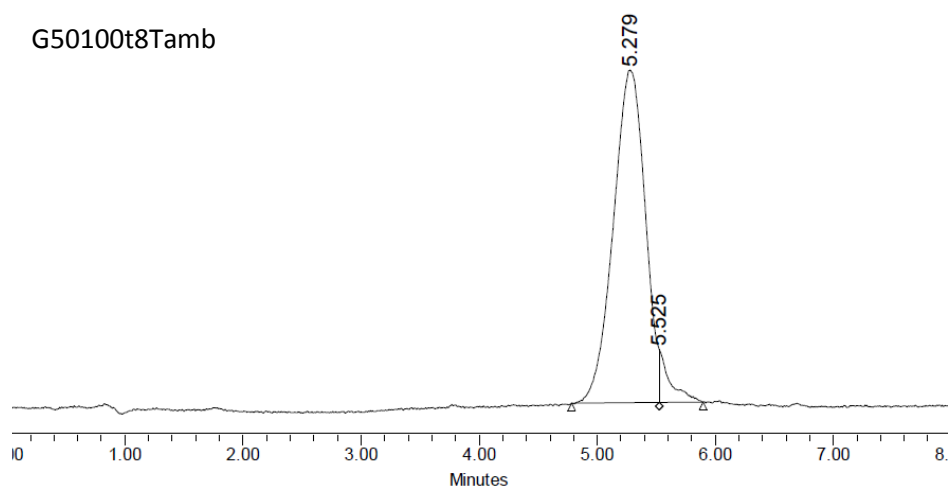
**Scheme 32:** Synthetic strategy to obtain  $\Psi^{\text{Me,Me}}$ Pro-containing dipeptides.

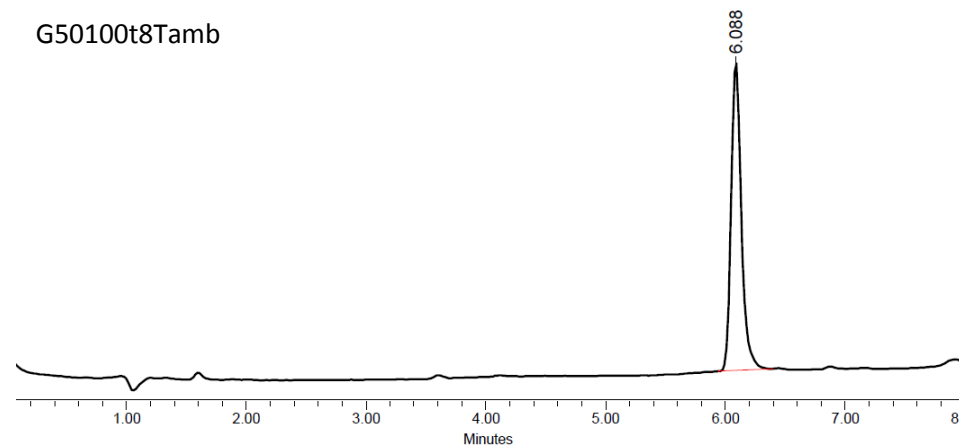
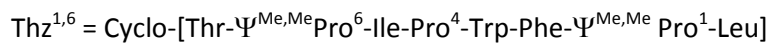
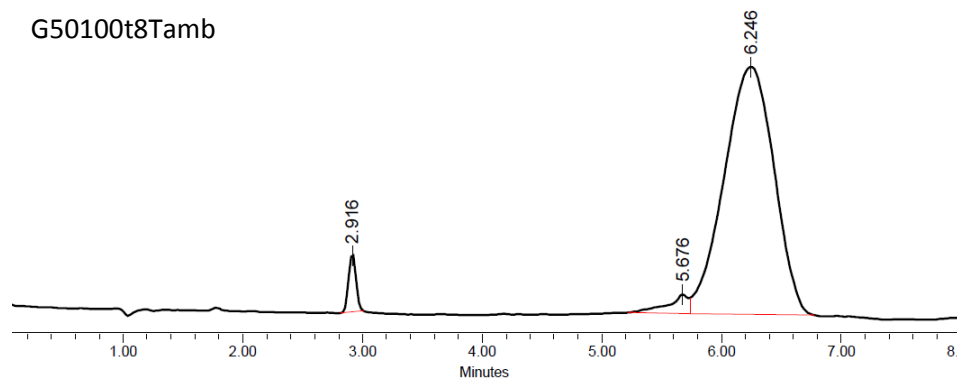
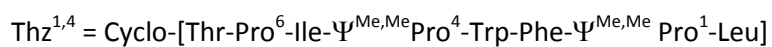
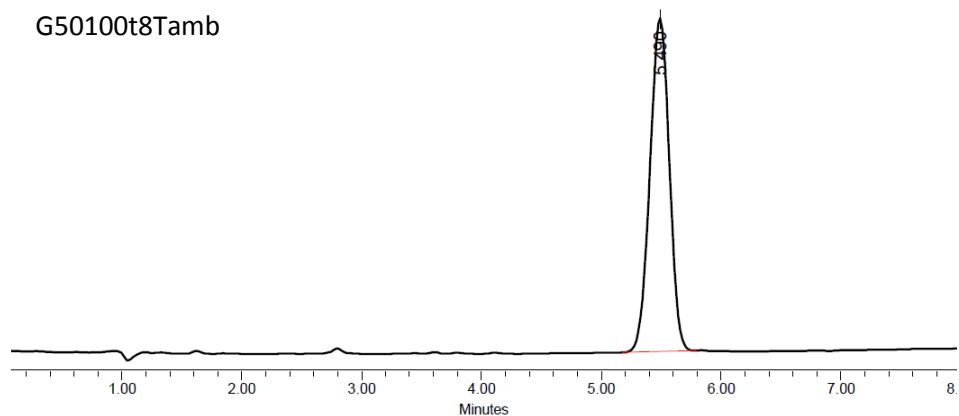
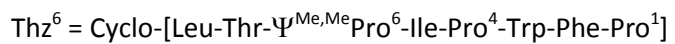
With all dipeptides on hand, a modified synthetic scheme on solid phase was successfully attempted to access all the  $\Psi^{\text{Me,Me}}$ Pro-containing analogs (Scheme 33).

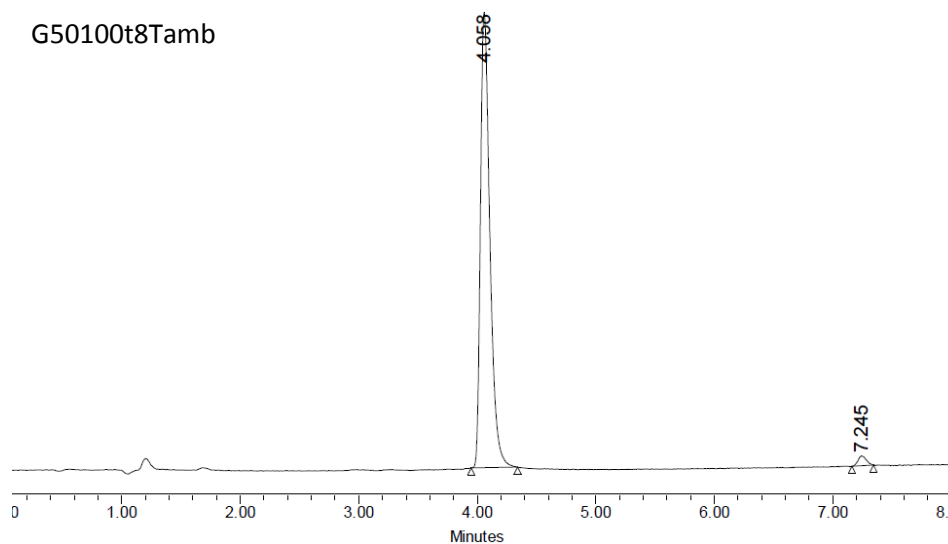
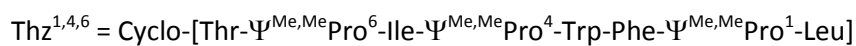
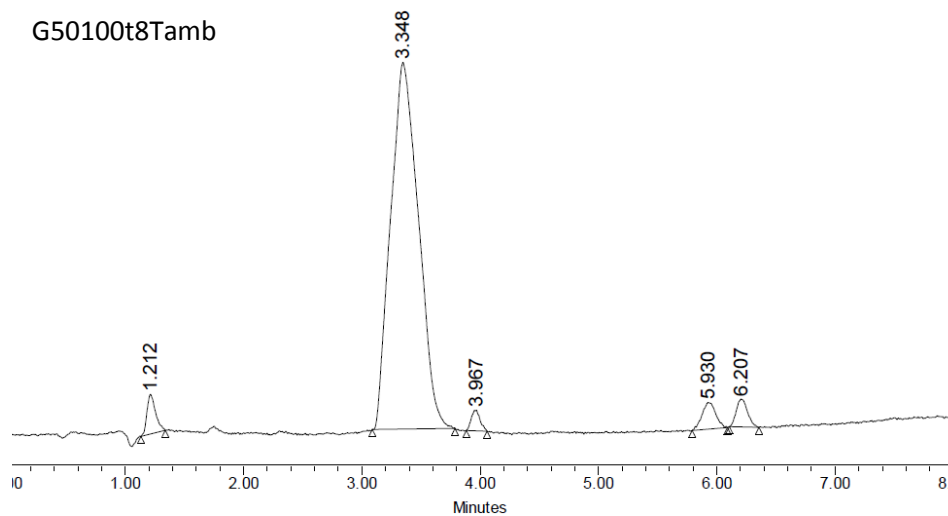


**Scheme 33:** Thz<sup>4</sup> analog synthetic strategy.

For the synthesis of Thz<sup>1</sup>, Thz<sup>1,4</sup>, Thz<sup>1,6</sup> and Thz<sup>1,4,6</sup> analogs, the starting and cyclization point was modified to avoid direct incorporation of the dipeptide onto the resin. For these analogs, the linear precursor's assembly started with incorporation of Fmoc-Leu-OH onto 2-CTC resin. The synthesis of all the  $\Psi^{\text{Me,Me}}$ Pro-containing analogs was successfully achieved. Chromatograms of all the members of the library after reversed-phase semi-preparative HPLC purification are shown in Figure X.







**Figure 61:** HPLC-PDA chromatograms of the purified  $\Psi^{\text{Me,Me}}$ Pro-containing analogs of Phakellistatin 19.

### 2.6.3.2. Biological evaluation of a small library of $\Psi^{\text{Me,Me}}$ Pro-containing Phakellistatin 19 analogs

All the members of the small library of  $\Psi^{\text{Me,Me}}$ Pro-containing Phakellistatin 19 analogs were tested against three cancer cell lines by means of a MTT assay (Table 16).

Compound		Lung-NSCLC A549		Colon HT-29		Breast MDA-MB-231	
		$\mu\text{g/mL}$	Molar	$\mu\text{g/mL}$	Molar	$\mu\text{g/mL}$	Molar
Thz <sup>1</sup>	GI <sub>50</sub>	>1.0E+01	>1.00E-05	5.7E+00	5.71E-06	6.1E+00	6.11E-06
	TGI	>1.0E+01	>1.00E-05	>1.0E+01	>1.00E-05	>1.0E+01	>1.00E-05
	LC <sub>50</sub>	>1.0E+01	>1.00E-05	>1.0E+01	>1.00E-05	>1.0E+01	>1.00E-05
Thz <sup>4</sup>	GI <sub>50</sub>	>1.0E+01	>1.00E-05	>1.0E+01	>1.00E-05	>1.0E+01	>1.00E-05
	TGI	>1.0E+01	>1.00E-05	>1.0E+01	>1.00E-05	>1.0E+01	>1.00E-05
	LC <sub>50</sub>	>1.0E+01	>1.00E-05	>1.0E+01	>1.00E-05	>1.0E+01	>1.00E-05
Thz <sup>6</sup>	GI <sub>50</sub>	>1.0E+01	>1.00E-05	4.0E+00	4.01E-06	2.7E+00	2.70E-06
	TGI	>1.0E+01	>1.00E-05	4.2E+00	4.21E-06	4.1E+00	4.11E-06
	LC <sub>50</sub>	>1.0E+01	>1.00E-05	4.6E+00	4.61E-06	6.0E+00	6.01E-06
Thz <sup>1,4</sup>	GI <sub>50</sub>	>1.0E+01	>9.58E-06	3.3E+00	3.16E-06	5.9E+00	5.65E-06
	TGI	>1.0E+01	>9.58E-06	6.9E+00	6.61E-06	>1.0E+01	>9.58E-06
	LC <sub>50</sub>	>1.0E+01	>9.58E-06	>1.0E+01	>9.58E-06	>1.0E+01	>9.58E-06
Thz <sup>1,6</sup>	GI <sub>50</sub>	3.6E+00	3.45E-06	1.9E+00	1.82E-06	1.8E+00	1.72E-06
	TGI	8.2E+00	7.85E-06	2.3E+00	2.20E-06	2.1E+00	2.01E-06
	LC <sub>50</sub>	>1.0E+01	>9.58E-06	2.8E+00	2.68E-06	2.4E+00	2.30E-06
Thz <sup>4,6</sup>	GI <sub>50</sub>	3.8E+00	3.64E-06	1.9E+00	1.82E-06	2.3E+00	2.20E-06
	TGI	>1.0E+01	>9.58E-06	2.2E+00	2.11E-06	3.5E+00	3.35E-06
	LC <sub>50</sub>	>1.0E+01	>9.58E-06	2.5E+00	2.39E-06	5.3E+00	5.08E-06
Thz <sup>1,4,6</sup>	GI <sub>50</sub>	1.6E+00	1.47E-06	1.5E+00	1.38E-06	1.8E+00	1.65E-06
	TGI	1.8E+00	1.65E-06	1.9E+00	1.74E-06	2.1E+00	1.93E-06
	LC <sub>50</sub>	2.0E+00	1.83E-06	2.3E+00	2.11E-06	2.4E+00	2.20E-06

**Table 16:** Cytotoxicity results for the small library of  $\Psi^{\text{Me,Me}}$ Pro-containing Phakellistatin 19 analogs.

Data obtained from the MTT experiments showed that replacement of Pro<sup>6</sup> by a  $\Psi^{\text{Me,Me}}$ Pro was translated into a significant increase in cytotoxicity. Moreover, a more rigid structure due to the presence of an increasing number of  $\Psi^{\text{Me,Me}}$ Pro residues, also rose the bioactivity results. For a better comprehension of these results, a structural study of the library by means of NMR technique was carried out.

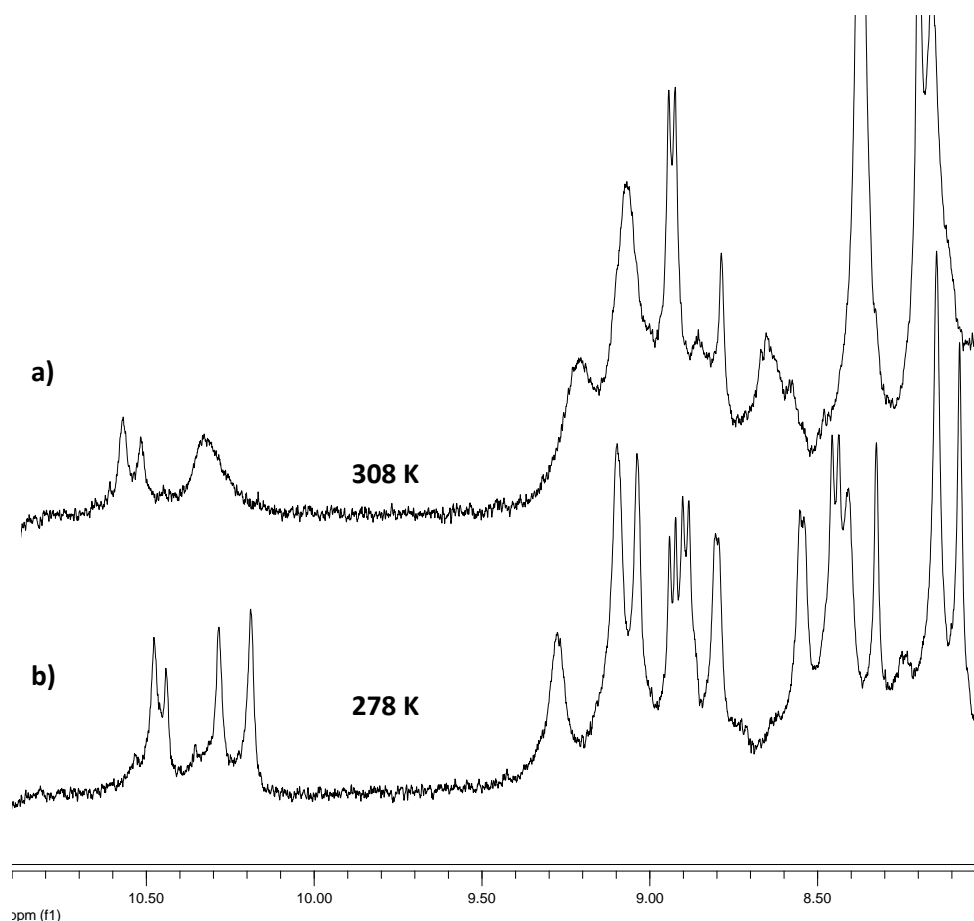
#### 2.6.3.3. Structural study of a small library of $\Psi^{\text{Me,Me}}$ Pro-containing Phakellistatin 19 analogs

From the three analogs containing one single  $\Psi^{\text{Me,Me}}$ Pro residue (Thz<sup>1</sup>, Thz<sup>4</sup> and Thz<sup>6</sup>), we decided to study by NMR the most active one Thz<sup>6</sup>. Comparison of two <sup>1</sup>H NMR spectra at 298 K, one in CDCl<sub>3</sub> and the other in CD<sub>3</sub>OH, revealed that chloroform strongly favored the existence of numerous conformers. Consequently, CD<sub>3</sub>OH was finally chosen as the solvent when performing the structural study.



Thz<sup>6</sup>

Monodimensional spectra of Thz<sup>6</sup> in CD<sub>3</sub>OH were then recorded at two other temperatures: 278 K and 308 K. Analysis of the region between 10 and 11 ppm, where the indolic proton of the Trp moiety is found, provided an idea of the complex conformational equilibrium in which Thz<sup>6</sup> analog was involved (Figure 62).



**Figure 62:** <sup>1</sup>H NMR spectra of Thz<sup>6</sup> analog in CD<sub>3</sub>OH: a) at 308 K; b) at 278 K. The region between 8 and 11 ppm is shown.

Replacement of one single Pro residue by a Ψ<sup>Me,Me</sup>Pro dramatically modified the *cis-trans* isomerism at the Pro linkages completely altering the conformational panorama. Phakellistatin 19 appeared, in DMSO-*d*<sub>6</sub> at 298 K, as a single conformer with all Pro in *trans*, while Thz<sup>6</sup> presented, at least, 7 conformers (5 major conformers and 2 minor conformers) at 278 K, and at least 4 conformers (2 of them in a fast equilibrium) at 308 K. Any attempt of <sup>1</sup>H assignment for the numerous conformers appeared extremely challenging. Thus, two presumably less flexible analogs were examined, Thz<sup>1,4</sup> and Thz<sup>1,6</sup>.

Thz<sup>1,4</sup>

As detected by NMR, Thz<sup>1,4</sup> in CD<sub>3</sub>OH at 298 K, presented two major conformers in a proportion conformer 1-conformer 2 (58:42). Exhaustive analysis of <sup>1</sup>H, gCOSY, TOCSY, NOESY, ROESY and gHSQC experiments enabled <sup>1</sup>H NMR spectral assignment of both conformers (Table 17).

	<sup>1</sup> H (ppm) (1)	<sup>1</sup> H (ppm) (2)		<sup>1</sup> H (ppm) (1)	<sup>1</sup> H (ppm) (2)
<b>Ψ<sup>Me,Me</sup>Pro<sup>1</sup></b>	-	-	<b>Ile<sup>5</sup> NH</b>	8.13	7.60
C/H <sub>α</sub>	3.97	3.90	C/H <sub>α</sub>	4.12	4.14
C/H <sub>β</sub>	2.35	1.92	C/H <sub>β</sub>	1.76	1.91
C/CH <sub>3</sub>			C/H <sub>γ</sub>	1.31	1.61
				1.07 <sub>CH<sub>3</sub></sub>	0.99 <sub>CH<sub>3</sub></sub>
<b>Phe<sup>2</sup> NH</b>	7.69	7.80	C/H <sub>δ</sub>	0.98	0.98
C/H <sub>α</sub>	4.59	5.24			
C/H <sub>β</sub>	3.09, 2.98'	3.24, 2.94'	<b>Pro<sup>6</sup></b>	-	-
C <sub>1</sub>			C/H <sub>α</sub>	4.92	4.50
C <sub>2/6</sub>			C/H <sub>β</sub>	2.45, 2.31'	2.45, 1.93
C <sub>3/5</sub>			C/H <sub>γ</sub>	1.89, 1.83'	2.16, 2.02'
C <sub>4</sub>			C/H <sub>δ</sub>	3.79, 3.51'	3.84, 3.74'
<b>Trp<sup>3</sup> NH</b>	9.00	7.73	<b>Thr<sup>7</sup> NH</b>	7.33	7.60
C/H <sub>α</sub>	4.92	5.07	C/H <sub>α</sub>	4.51	4.68
C/H <sub>β</sub>	3.39, 3.18'	3.53, 3.37'	C/H <sub>β</sub>	4.07	4.46
C/H <sub>2</sub>			C/H <sub>γ</sub>	1.19	1.21
C <sub>3</sub>			OH	-	-
C/H <sub>4</sub>					
C/H <sub>5</sub>			<b>Leu<sup>8</sup> NH</b>	8.88	8.66
C/H <sub>6</sub>			C/H <sub>α</sub>	4.59	4.13
C/H <sub>7</sub>			C/H <sub>β</sub>	2.02, 1.73'	2.11, 1.68'
C <sub>8</sub>			C/H <sub>γ</sub>	1.79	1.78
C <sub>9</sub>			C/H <sub>δ</sub>	0.93, ?	0.88, ?
NH <sub>ind</sub>					
<b>Ψ<sup>Me,Me</sup>Pro<sup>4</sup></b>	-	-			
C/H <sub>α</sub>	4.93	5.01			
C/H <sub>β</sub>	3.56, 3.01'	3.15, 2.91'			
C/CH <sub>3</sub>					

**Table 17:** <sup>1</sup>H NMR spectral assignment of the two major conformers of Thz<sup>1,4</sup> analog in CD<sub>3</sub>OH at 298 K.

gHSQC experiment enabled the assignment of the key Pro's carbons C<sub>β</sub> and C<sub>γ</sub>. For Pro<sup>6</sup> of conformer 1, it was found that δ<sub>Cβ</sub> = 33.095 ppm and δ<sub>Cγ</sub> = 22.643 ppm, meaning that Δδ<sub>Cβ-Cγ</sub> = 10.452 ppm; while for Pro<sup>6</sup> of conformer 2, δ<sub>Cβ</sub> = 29.943 ppm and δ<sub>Cγ</sub> = 26.791 ppm, meaning that Δδ<sub>Cβ-Cγ</sub> = 3.152 ppm. According to these data, Pro<sup>6</sup> adopted *cis* isomerism in conformer 1 and *trans* isomerism in conformer 2. Large NOE's cross peak between H<sub>α</sub>-Thr and

$H_{\delta}$ -Pro<sup>6</sup> in conformer 2 and ROE's cross-peak between  $H_{\alpha}$ -Thr and  $H_{\alpha}$ -Pro<sup>6</sup> in conformer 1, also supported the assigned isomerism at the Thr-Pro<sup>6</sup> linkage for both conformers.

As expected, both  $\Psi^{\text{Me,Me}}\text{Pro}^1$  and  $\Psi^{\text{Me,Me}}\text{Pro}^4$  adopt *cis* isomerism in all conformers. Large NOE's cross-peaks between  $H_{\alpha}$ -Phe and  $H_{\alpha}$ - $\Psi^{\text{Me,Me}}\text{Pro}^1$ , and  $H_{\alpha}$ -Ile and  $H_{\alpha}$ - $\Psi^{\text{Me,Me}}\text{Pro}^4$  served as confirmation.

### Thz<sup>1,6</sup>

Thz<sup>1,6</sup> analog showed a more confusing spectroscopic data. Again, two major different conformers were detected. <sup>1</sup>H and <sup>13</sup>C NMR spectral assignment of the 16 residues was accomplished, but the cross-peaks of the ROESY spectra did not provide enough information to perform complete sequential assignment for the two conformers. However, the two Pro moieties were fully assigned and its geometry was identified (Table 18).

Conformer 1			Conformer 2		
Ile <sup>1</sup> H (ppm)	Pro <sup>4</sup> <sup>1</sup> H (ppm) <sup>13</sup> C (ppm)		Ile' <sup>1</sup> H (ppm)	Pro <sup>4'</sup> <sup>1</sup> H(ppm) <sup>13</sup> C (ppm)	
7.63	-		8.15	-	-
4.36	4.44	61.87	4.50	4.41	64.21
1.69	1.80, 1.74'	31.08	2.05	2.26, 1.47'	28.73
0.99	1.36	21.54	1.06	1.88	26.70
1.53, 1.22'	3.23, 3.15'	47.49	1.77, 1.44'	3.82, 3.76'	48.27
0.89			1.03		

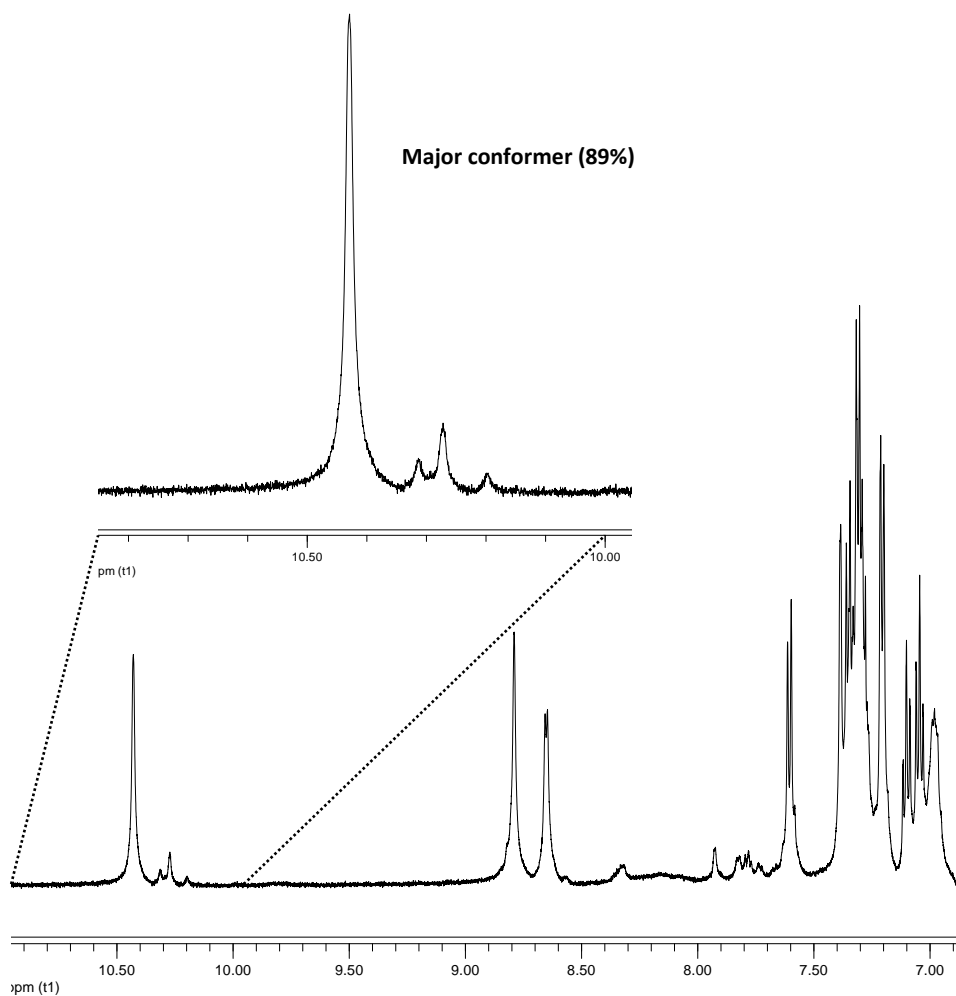
**Table 18:** <sup>1</sup>H NMR spectral assignment of Ile and <sup>1</sup>H and <sup>13</sup>C NMR spectral assignment of Pro<sup>4</sup> for both conformers.

For conformer 1, it was found that  $\Delta\delta_{\text{C}\beta\text{-C}\gamma} = 9.54$  ppm, suggesting a *cis* geometry of the amide bond Ile-Pro<sup>4</sup>. On the contrary, for conformer 2,  $\Delta\delta_{\text{C}\beta\text{-C}\gamma} = 2.03$  ppm strongly pointed out a *trans* prolyl peptide bond. The ROESY cross-peaks detected between  $H_{\alpha}$ -Ile' and  $H_{\delta}/H_{\delta'}$ -Pro<sup>4'</sup> for conformer 2, also supported the *trans* isomerism. For conformer 1, no ROE cross-peak between  $H_{\alpha}$ -Ile and  $H_{\alpha}$ -Pro<sup>4</sup> was detected, probably due to the low quality of the ROESY spectra. The *cis* geometry of the Xaa- $\Psi^{\text{Me,Me}}\text{Pro}$  was confirmed by the cross-peaks between  $H_{\alpha}$ -Thr and  $H_{\alpha}$ - $\Psi^{\text{Me,Me}}\text{Pro}$ , and  $H_{\alpha}$ -Phe and  $H_{\alpha}$ - $\Psi^{\text{Me,Me}}\text{Pro}$ .

All the NMR experiments were recorded in CD<sub>3</sub>OH at 273 K. The bad quality of the spectra and the partial assignment, prevent from finding the ratio between the *cis* and the *trans* conformers.

Thz<sup>1,4,6</sup>

Finally, Thz<sup>1,4,6</sup> analog, with the three prolines replaced by  $\Psi^{\text{Me,Me}}\text{Pro}$ , was the most conformationally restricted analog, as it was confirmed by the presence of one major conformer (89%) and 3 minor conformers (Figure 63). NMR studies showed that all  $\Psi^{\text{Me,Me}}\text{Pro}$  adopted *cis* isomerism, as proved by the NOE's cross peaks detected between the protons H<sub>α</sub>-Phe and H<sub>α</sub>- $\Psi^{\text{Me,Me}}\text{Pro}^1$ , H<sub>α</sub>-Ile and H<sub>α</sub>- $\Psi^{\text{Me,Me}}\text{Pro}^4$ , H<sub>α</sub>-Thr and H<sub>α</sub>- $\Psi^{\text{Me,Me}}\text{Pro}^6$ , H<sub>β</sub>-Phe and H<sub>α</sub>- $\Psi^{\text{Me,Me}}\text{Pro}^1$ , H<sub>β</sub>-Ile and H<sub>α</sub>- $\Psi^{\text{Me,Me}}\text{Pro}^4$  and H<sub>β</sub>-Thr and H<sub>α</sub>- $\Psi^{\text{Me,Me}}\text{Pro}^6$ .



**Figure 63:** <sup>1</sup>H NMR spectral assignment of Thz<sup>1,4,6</sup> analog in CD<sub>3</sub>OH at 298 K. The region between 10 and 11 ppm is enlarged.

Complete  $^1\text{H}$  assignment is detailed in Table 19.

	$^1\text{H}$ (ppm)		$^1\text{H}$ (ppm)
$\Psi^{\text{Me,Me}}\text{Pro}^1$	-	Ile <sup>5</sup> NH	6.98
H <sub>α</sub>	4.28	H <sub>α</sub>	4.16
H <sub>β</sub>	2.95 (5.4)	H <sub>β</sub>	1.75
S <sub>γ</sub>	-	H <sub>γ</sub>	1.58, 1.15'
H <sub>δ</sub>	1.69, 1.60'		0.97 <sub>CH3</sub> (6.8)
		H <sub>δ</sub>	0.93 (7.2)
Phe <sup>2</sup> NH	6.98		
H <sub>α</sub>	4.54	$\Psi^{\text{Me,Me}}\text{Pro}^6$	-
H <sub>β</sub>	2.74 (12.8, 9.6)	H <sub>α</sub>	4.99
	2.58' (12.2, 5.1)	H <sub>β</sub>	3.62 (13.0, 7.0)
H <sub>2/6</sub>	7.21 (6.6)		3.21 (12.9)
H <sub>3/5</sub>	7.31	S <sub>γ</sub>	-
H <sub>4</sub>	?	H <sub>δ</sub>	2.11, 1.84'
Trp <sup>3</sup> NH	8.65 (5.2)	Thr <sup>7</sup> NH	?
H <sub>α</sub>	4.58	H <sub>α</sub>	4.15
H <sub>β</sub>	3.28 (6.6)	H <sub>β</sub>	5.36
H <sub>2</sub>	7.39 (1.5)	H <sub>γ</sub>	1.33 (6.6)
H <sub>4</sub>	7.61 (7.8)	OH	-
H <sub>5</sub>	7.05 (7.4, 0.8)		
H <sub>6</sub>	7.10 (7.5, 1.0)	Leu <sup>8</sup> NH	8.79
H <sub>7</sub>	7.35	H <sub>α</sub>	4.30
NH <sub>ind</sub>	10.4	H <sub>β</sub>	1.67
		H <sub>γ</sub>	
$\Psi^{\text{Me,Me}}\text{Pro}^4$	-	H <sub>δ</sub>	1.06 (5.8)
H <sub>α</sub>	5.09		1.02 (5.8)
H <sub>β</sub>	3.50		
S <sub>γ</sub>	-		
H <sub>δ</sub>	1.80, 1.68'		

**Table 19:**  $^1\text{H}$  NMR spectral assignment of the major conformer of Thz<sup>1,4,6</sup> in CD<sub>3</sub>OH at 298 K.

The biological and the structural data all together, suggest that Pro<sup>6</sup> plays a crucial role in Phakellistatin 19's structure with direct influence on the bioactivity exerted by this peptide. Although Pro replacement by  $\Psi^{\text{Me,Me}}\text{Pro}$  represents a notable gain of sterical hindrance and also an alteration of the hydrogen donors and acceptors pattern, the bioactivity results showed a significant difference between Thz<sup>6</sup> analog and Thz<sup>1,6</sup>, Thz<sup>4,6</sup> and Thz<sup>1,4,6</sup>. Thus, we are able to affirm that a more likely explanation relies on a structural issue rather than the aa<sup>6</sup> being the pharmacophore of Phakellistatin 19.

NMR analysis confirmed that an increasing number of  $\Psi^{\text{Me,Me}}\text{Pro}$  on Phakellistatin 19's structure, entailed a gain of structural rigidity. Thz<sup>1,4,6</sup> analog, with all the Xaa<sup>i-1</sup>- $\Psi^{\text{Me,Me}}\text{Pro}^i$  linkages adopting the *cis* isomerism, was the most active one, and also the most rigid one, as its major conformer represented a 89% of the mixture. A whole *cis* Phakellistatin 19's

conformer being significantly more active, strongly suggests that *cis-trans* isomerism at the Pro linkages may have a crucial role in the bioactivity displayed by Phakellistatins.

## References

- (1) Wipf, P. *Chem. Rev.* **1995**, *95*, 2115–2134.
- (2) Peris, Á.; Napolitano, A.; Bruno, I.; Rovero, P.; Lucas, R.; Paya, M.; Gomez-Paloma, L.; Riccio, R. *Tetrahedron* **2001**, *57*, 6249–6255.
- (3) Kobayashi, J.; Nakamura, T.; Tsuda, M. *Tetrahedron* **1996**, *52*, 6355–6360.
- (4) Pettit, G. R.; Srirangam, J. K.; Herald, D. L.; Xu, J.; Boyd, M. R.; Cichacz, Z.; Kamano, Y.; Schmidt, J. M.; Erickson, K. L. *J. Org. Chem.* **1995**, *60*, 8257–8261.
- (5) Pettit, G. R.; Taylor, S. R. *J. Org. Chem.* **1996**, *61*, 2322–2325.
- (6) Randazzo, A.; Dal, F.; Orru, S.; Gomez-paloma, L. *Eur. J. Org. Chem.* **1998**, *3*, 2659–2665.
- (7) Tabudravu, J. N.; Morris, L. a.; Jantina Kettenes-van den Bosch, J.; Jaspars, M. *Tetrahedron* **2002**, *58*, 7863–7868.
- (8) Pettit, G. R.; Herald, C. L.; Boyd, M. R.; Leet, J. E.; Dufresne, C.; Doubek, D. L.; Schmidt, J. M.; Cerny, R. L.; Hooper, J. N.; Rutzler, K. C. *J. Med. Chem.* **1991**, *34*, 3339–3340.
- (9) Pettit, G. R.; Gao, F.; Schmidt, J. M.; Chapuis, J.; Cerny, R. L. *Bioorg. Med. Chem. Lett.* **1994**, *4*, 2935–2940.
- (10) Pettit, G. R.; Tan, R.; Williams, M. D.; Tackett, L.; Schmidt, J. M.; Cerny, R. L.; Hooper, J. N. A. *Bioorg. Med. Chem. Lett.* **1993**, *3*, 2869–2874.
- (11) Pettit, G. R.; Cichacz, Z.; Barkoczy, J.; Dorsaz, A.-C.; Herald, D. L.; Williams, M. D.; Doubek, D. L.; Schmidt, J. M.; Tackett, L. P.; Brune, D. C.; Cerny, R. L.; Hooper, J. N. A.; Bakus, G. J. *J. Nat. Prod.* **1993**, *56*, 260–267.
- (12) Pettit, G. R.; Xu, J.; Dorsaz, A.-C.; Williams, M. D.; Boyd, M. R.; Cerny, R. L. *Bioorg. Med. Chem. Lett.* **1995**, *5*, 1339–1344.
- (13) Pettit, G. R.; Tan, R. *Bioorg. Med. Chem. Lett.* **2003**, *13*, 685–688.
- (14) Mechnich, O.; Kessler, H. *Lett. Pept. Sci.* **1997**, *4*, 21–28.
- (15) Napolitano, A.; Rodriguez, M.; Bruno, I.; Marzocco, S.; Autore, G.; Riccio, R.; Gomez-Paloma, L. *Tetrahedron* **2003**, *59*, 10203–10211.
- (16) Greenman, K. L.; Hach, D. M.; Van Vranken, D. L. *Organic letters* **2004**, *6*, 1713–1716.
- (17) Pettit, G. R.; Toki, B. E.; Xu, J. P.; Brune, D. C. *J. Nat. Prod.* **2000**, *63*, 22–28.
- (18) Napolitano, A.; Bruno, I.; Riccio, R.; Gomez-Paloma, L. *Tetrahedron* **2005**, *61*, 6808–6815.
- (19) Pettit, G. R.; Iij, J. W. L.; Taylor, S. R.; Tan, R.; Williams, M. D. *J. Nat. Prod.* **2001**, *64*, 883–891.

- (20) Ali, L.; Musharraf, S. G.; Shaheen, F. *J. Nat. Prod.* **2008**, *71*, 1059–1062.
- (21) Pettit, G. R.; Rhodes, M. R.; Tan, R. *J. Nat. Prod.* **1999**, *62*, 409–414.
- (22) Pettit, G. R.; Xu, J.-P.; Cichacz, Z. A.; Williams, M. D.; Chapuis, J. C.; Cerny, R. L. *Bioorg. Med. Chem. Lett.* **1994**, *4*, 2677–2682.
- (23) Pettit, G. R.; Tan, R. *J. Nat. Prod.* **2005**, *68*, 60–63.
- (24) Zhang, H.-J.; Yi, Y.-H.; Yang, G.-J.; Hu, M.-Y.; Cao, G.-D.; Yang, F.; Lin, H.-W. *J. Nat. Prod.* **2010**, *73*, 650–655.
- (25) Pettit, G. R.; Tan, R.; Ichihara, Y.; Williams, M. D.; Doubek, D. L.; Tackett, L. P.; Schmidt, J. M.; Cerny, R. L.; Boyd, M. R.; Hooper, J. N. A. *J. Nat. Prod.* **1995**, *58*, 961–965.
- (26) Bates, R. B.; Caldera, S.; Ruane, M. D. *J. Nat. Prod.* **1998**, *61*, 405.
- (27) Mechnich, O.; Hessler, G.; Kessler, H.; Bernd, M.; Kutscher, B. *Helv. Chim. Acta* **1997**, *80*, 1338–1354.
- (28) Pettit, G. R.; Ichihara, Y.; Wurzel, G.; Williams, M. D.; Schmidt, J. M.; Chapuis, J. C. *J. Chem. Soc., Chem. Commun.* **1995**, 383–385.
- (29) Wüthrich, K.; Grathwohl, C. *FEBS Lett.* **1974**, *43*, 337–340.
- (30) Zimmerman, S. S.; Scheraga, H. a *Macromolecules* **1975**, *9*, 408–16.
- (31) Fischer, S.; Dunbrack, R. L.; Karplus, M. *J. Am. Chem. Soc.* **1994**, *116*, 11931–11937.
- (32) Eberhardt, E. S.; Loh, S. N.; Hinck, A. P.; Raines, R. T. *J. Am. Chem. Soc.* **1992**, *114*, 5437–5439.
- (33) Brandts, J. F.; Halvorson, H. R.; Brennan, M. *Biochemistry* **1975**, *14*, 4953–63.
- (34) Schmid, F. X.; Baldwin, R. L. *Proc. Natl. Acad. Sci. USA* **1978**, *75*, 4764–4768.
- (35) Balbach, J.; Steegborn, C.; Schindler, T.; Schmid, F. X. *J. Mol. Biol.* **1999**, *285*, 829–842.
- (36) Yamazaki, T.; Ro, S.; Goodman, M.; Chung, N. N.; Schiller, P. W. *J. Med. Chem.* **1993**, *36*, 708–719.
- (37) Larive, C. K.; Guerra, L.; Rabenstein, D. L. *J. Am. Chem. Soc.* **1992**, *114*, 4879–4880.
- (38) Williams, K. A.; Deber, C. M. *Biochemistry* **1991**, *30*, 8919–8923.
- (39) Tabudravu, J. N.; Jaspars, M.; Morris, L. A.; Bosch, J. J. K. D.; Smith, N. *J. Org. Chem.* **2002**, *67*, 8593–8601.
- (40) Park, B. K.; Kitteringham, N. R.; O'Neill, P. M. *Annu. Rev. Pharmacol. Toxicol.* **2001**, *41*, 443–470.



- (41) Ämmälähti, E.; Bardet, M.; Molko, D.; Cadet, J. *J. Magn. Reson.* **1996**, *122*, 230–232.
- (42) Bax, A.; Griffey, R. H.; Hawkins, B. L. *J. Magn. Reson.* **1983**, *55*, 301–315.
- (43) Dorman, D. E.; Bovey, F. A. *J. Org. Chem.* **1978**, *38*, 2379–2383.
- (44) Bystrov, V. F.; Ivanov, V. T.; Portnova, S. L.; Balashova, T. A.; Ovchinnikov, Y. A. *Tetrahedron* **1973**, *29*, 873–882.

## **CONCLUSIONS**



## Conclusions

1. The synthesis of complex peptides cannot be approached using conventional strategies. In this sense, a robust and reproducible synthetic strategy to obtain the marine cytotoxic cyclodepsipeptide Pipecolidepsin A has been developed for the first time. Pipecolidepsin A represents a paradigm of structural complexity in the “head-to-side-chain” depsipeptides family due to the presence at the branching position of the extremely bulky *D-allo*-AHDMHA amino acid. To the best of our knowledge, Pipecolidepsin A’s ester bond is the most challenging ester linkage successfully assembled so far in the cyclodepsipeptides field.
2. Development of a synthetic strategy, that provides easy access to optically pure non natural amino acids at a preparative scale, was required to synthesize Pipecolidepsin A. Thus, the syntheses of suitable protected derivatives of the new building blocks *L-threo*- $\beta$ -EtO-Asn and DADHOHA have been successfully achieved. These amino acids, and/or closely related ones, are constitutive residues of a number of natural cyclodepsipeptides with promising therapeutic profiles.

3. Coupling of Fmoc-diMe-Gln-OH moiety before ester bond formation and applying temperature when constructing the ester bond turned out to be crucial to achieve Pipecolidepsin A's synthesis. General use (with exceptions) of HATU-HOAt-DIEA as a coupling system with 1 min of pre-activation is necessary to minimize side reactions. Introduction of the last two moieties of the exocyclic arm as a single unit is also mandatory.
4. Extensive synthetic work was required to validate the proposed chemical structure for Pipecolidepsin A. Chemical, spectral and biological equivalence of synthetic Pipecolidepsin A have been satisfactory proved by means of HPLC-PDA co-elution, NMR analysis and SRB assays resolving any structural uncertainty.
5. *In vivo* assays require always large amounts of natural products for exhaustive evaluations. As Pipecolidepsin A is produced by a marine sponge, its extraction is a highly demanding task. Therefore, the establishment of a solid synthetic route that provides ready access to Pipecolidepsin A is crucial to enable its evaluation as a viable and valuable therapeutic agent.
6. The set up synthetic scheme has been proved useful to provide straightforward access to analogs. Their study will facilitate valuable structure-activity relationships (SARs) that will enable the design of related products displaying similar or improved anticancer properties but bearing a lower synthetic complexity.
7. The synthesis of Phakellistatin 19, an all-L-cyclooctapeptide with a high percentage of proline residues and a promising activity as an antineoplastic agent, has been successfully achieved. The synthetic scheme is robust and has been applied to synthesize several analogs of the natural peptide.
8. All described Phakellistatins have shown severe disagreements between synthetic and natural peptides in terms of cytotoxicity. In our hands, Phakellistatin 19 also proved to display the same surprising biological behavior.
9. Natural samples of Phakellistatin 19 being contaminated with a highly cytotoxic epimer responsible of the bioactivity, has been ruled out.

10. Exhaustive NMR study of synthetic Phakellistatin 19 in CD<sub>3</sub>OD, CDCl<sub>3</sub>, DMSO-*d*<sub>6</sub>, and of a water-soluble analog in H<sub>2</sub>O-D<sub>2</sub>O (9:1) at pH = 5.95 and 8.12, proved the all-*trans* geometry for the three Pro residues in all solvents and pH conditions. Natural Phakellistatin 19 also showed the all-*trans* geometry in CD<sub>3</sub>OD. Thus, a difference in the *cis-trans* isomerism at the prolyl peptide bonds does not account for the positive cytotoxicity results obtained with the samples of synthetic Phakellistatin 19 treated phosphate buffer.
11. A new synthetic strategy to access  $\Psi^{\text{Me,Me}}$ Pro-containing analogs of Phakellistatin 19 has been successfully developed. The presence of the extremely bulky  $\Psi^{\text{Me,Me}}$ Pro amino acid poses a severe synthetic challenge. Since all attempted conditions of  $\Psi^{\text{Me,Me}}$ Pro's solid-phase acylation failed badly, the synthesis of Xaa- $\Psi^{\text{Me,Me}}$ Pro dipeptides in solution was mandatory.
12. Biological evaluation and structural analysis of  $\Psi^{\text{Me,Me}}$ Pro-containing analogs revealed that Pro<sup>6</sup> plays a key structural role in Phakellistatin 19, with direct influence on its cytotoxic activity. The most rigid analog containing the all-*cis*  $\Psi^{\text{Me,Me}}$ Pro moieties displayed the highest bioactivity.



# **MATERIALS AND METHODS**





---

<b>1. Materials and methods for peptide synthesis and purification</b>	<b>173</b>
1.1. Solvents and reagents	173
1.1.1. Solvents	173
1.1.2. Reagents	173
1.2. Instrumentation	173
1.2.1. General basic instrumentation	173
1.2.2. High-performance liquid chromatography	174
1.2.2.1. Analytical HPLC	174
1.2.2.2. Semi-analytical HPLC	174
1.2.2.3. Semi-preparative HPLC	174
1.2.2.4. HPLC-MS	175
1.2.3. MALDI-TOF	175
1.2.4. Amino acids analysis	175
1.2.5. Nuclear Magnetic Resonance	175
1.3. Solid Phase Peptide Synthesis (SPPS)	176
1.3.1. General considerations	176
1.3.2. Colorimetric test	176
1.3.2.1. Kaiser test	176
1.3.2.2. Chloranil test	177
1.3.2.3. De Clerq test	177
1.3.3. Conditioning of the resin and incorporation of the first amino acid	178
1.3.4. Elimination and quantification of the Fmoc group	179
1.3.5. Peptide chain elongation	180
1.3.6. Allyl and Alloc groups elimination	181
1.3.7. Cleavage of the peptide from the resin	181
1.3.8. Peptide purification	182
1.3.9. Peptide characterization	182
1.4. Phakellistatins	183
1.4.1. Synthesis of building blocks	183
1.4.2. Phakellistatin 19	188
1.4.2.1. Synthesis of Phakellistatin 19	188
1.4.2.2. Characterization of Phakellistatin 19	188
1.4.3. Libraries of epimers and analogs	190
1.4.3.1. Synthesis of epimers and analogs	190
1.4.3.2. Characterization of epimers and analogs	190

1.5. Pipecolidepsins	204
1.5.1. Synthesis of building blocks	204
1.5.1.1. Synthesis of Fmoc-L- <i>threo</i> - $\beta$ -EtO-Asn(Trt)-OH	204
1.5.1.2. Synthesis of Alloc-Pipecolic-OH	208
1.5.1.3. Synthesis of Fmoc-DADHOHA(Acetonide,Trt)-OH	209
1.5.1.4. Synthesis of (2 <i>R</i> ,3 <i>R</i> ,4 <i>R</i> )-3-hydroxy-2,4,6-trimethylheptanoic acid (HTMHA)	225
1.5.1.5. Synthesis of HTMHA-D-Asp( <sup>t</sup> Bu)-OH	228
1.5.2. Synthetic Pipecolidepsin A	231
1.5.2.1. Synthesis of Pipecolidepsin A	231
1.5.2.2. Characterization of synthetic Pipecolidepsin A	234
1.5.3. Pipecolidepsin A'	237
1.5.3.1. Synthesis of Pipecolidepsin A'	237
1.5.3.2. Characterization of Pipecolidepsin A'	237
1.5.4. Analog of Pipecolidepsin A': Analog 1A	239
1.5.4.1. Synthesis of an analog of Pipecolidepsin A': Analog 1A	239
1.5.4.2. Characterization on an analog of Pipecolidepsin A': Analog 1A	240

## 1. Materials and methods for peptide synthesis and purification

### 1.1. Solvents and reagents

#### 1.1.1. Solvents

All the solvents used in the present thesis have been purchased to the suppliers Panreac, Scharlau, SDS and Sigma-Aldrich.

#### 1.1.2. Reagents

All the reagents employed in the present thesis have been purchased to the suppliers Alfa Aesar, Bachem AG, Fluka, Iris Biotech, Luxemburg Industries, Novabiochem, Panreac, and Sigma-Aldrich.

### 1.2. Instrumentation

#### 1.2.1. General basic instrumentation

<b>Balances</b>	METTLER TOLEDO MS 303-S. 3 significant figures AB 204-S. 4 significant figures AT 261 DeltaRange®. 5 significant figures MX5. 6 significant figures
<b>Lyophilizers</b>	Freezemobile 25 EL, VirTis
<b>Orbital shakers</b>	Unimax 1010, Heidolph
<b>Rotary evaporators</b>	Laborota 4003 Control, Heidolph
<b>Ultrasonic bath</b>	BRANSON
<b>UV-Vis spectrophotometer</b>	UV-2501PC, Shimadzu
<b>Vortex mixers</b>	MERCK® eurolab

## 1.2.2. High-performance liquid chromatography

### 1.2.2.1. Analytical HPLC

Analytical HPLC was performed on a Waters instrument comprising a Waters 2695 (Waters, MA, USA) separation module, an automatic injector, a photodiode array detector (Waters 996 or Waters 2998), and a Millenium<sup>32</sup> login system controller. The columns used were a Xbridge<sup>TM</sup> C18 reversed-phase analytical column (2.5  $\mu\text{m}$   $\times$  4.6 mm  $\times$  75 mm), a Xbridge<sup>TM</sup> BEH130 C18 reversed-phase analytical column (3.5  $\mu\text{m}$   $\times$  4.6 mm  $\times$  100 mm) and a SunFire<sup>TM</sup> C18 reversed-phase analytical column (3.5  $\mu\text{m}$   $\times$  4.6 mm  $\times$  100 mm) run with linear gradients of ACN (0.036% TFA) into H<sub>2</sub>O (0.045% TFA) over 8 min or a Symmetry C18 reversed-phase analytical column (5  $\mu\text{m}$   $\times$  4.6 mm  $\times$  150 mm) run with linear gradients over 15 min. UV detection was at 220 and 254 nm and the system was run at a flow rate of 1.0 mL/min.

### 1.2.2.2. Semi-analytical HPLC

Semi-analytical HPLC was performed on a Waters instrument comprising two solvent delivery pumps (Waters 1525), an automatic injector (Waters 717 autosampler), a Waters 2487 dual wavelength detector, a Breeze v3.20 system controller, a Symmetry<sup>®</sup> C18 reversed-phase column (5  $\mu\text{m}$   $\times$  7.8 mm  $\times$  100 mm) or a XBridge<sup>TM</sup> Prep BEH130 C18 reversed-phase column (5  $\mu\text{m}$   $\times$  10 mm  $\times$  100 mm) and linear gradients of ACN (0.036% TFA) into H<sub>2</sub>O (0.045% TFA) over 20 min. The system was run at a flow rate of 3 mL/min. UV detection was at 220 or 254 nm.

### 1.2.2.3. Semi-preparative HPLC

Semi-preparative RP-HPLC was carried on a Waters instrument comprising two solvent delivery pumps (Waters Delta 600), an automatic injector (Waters 2700 Sample Manager), a Waters 2487 dual wavelength absorbance detector, an automatic sample collector (Waters Fraction Collector II), a Masslunx v3.5 system controller and three different columns, obtained also from Waters: a Symmetry<sup>®</sup> C8 reversed-phase column (5  $\mu\text{m}$   $\times$  30 mm  $\times$  100 mm), a Symmetry<sup>®</sup> C18 reversed-phase column (5  $\mu\text{m}$   $\times$  30 mm  $\times$  100 mm) and a SunFire<sup>TM</sup> Prep C18 OBD<sup>TM</sup> reversed-phase column (5  $\mu\text{m}$   $\times$  19 mm  $\times$  100 mm). Linear gradients of ACN (0.5% TFA) into H<sub>2</sub>O (1% TFA) with a flow rate of 10 mL/min or 15 mL/min were used.

#### 1.2.2.4. HPLC-MS

HPLC-MS analysis was performed on two different instruments provided with two different columns. The first of them was a Waters instrument comprising a Waters 2695 separation module, an automatic injector, a Waters 2998 photodiode array detector, a Waters ESI-MS Micromass ZQ spectrometer, a Masslynx v4.1 system controller and a Sunfire™ C18 reversed-phase analytical column (3.5 mm × 2.1 mm × 100 mm). UV detection was at 220 and 254 nm, and linear gradients of ACN (0.07% Formic acid) into H<sub>2</sub>O (0.1% Formic acid) were run at a 0.3 mL/min flow rate over 8 min. The second instrument comprised a Waters Alliance 2795 separation module, a Waters 2487 Dual λ Absorbance Detector, a MassLynx V4.0 system controller, a Waters ESI-MS Micromass ZQ spectrometer and a Symmetry® C18 reversed-phase analytical column (5 μm × 4.6 mm × 150 mm) run with linear gradients over 15 min and a flow rate of 1 mL/min.

#### 1.2.3. MALDI-TOF

Mass spectra were recorded on a MALDI-TOF Applied Biosystem 4700 with a N<sub>2</sub> laser of 337 nm using ACH matrix (10 mg/mL of ACH in ACN-H<sub>2</sub>O-TFA (1:1:0.1)).

Sample preparation: a mixture of sample solution (1 μL) and matrix (1 μL) is prepared, placed on a MALDI-TOF plate and dried by air.

#### 1.2.4. Amino acids analysis

After hydrolysis and derivatization (AccQ-Tag™ Chemistry Kit, Waters) of the peptidic sample, the concentration of each amino acid was found using a Waters 600 instrument provided with a delta 600 pump, a Waters 717 automatic injector, a Waters 2487 UV detector, a Masslynx system controller and a Waters AccQ-Tag™ amino acid analysis Nova-pak C18 column (4 μm × 3.9 mm × 150 mm). Linear gradients of AccQ-Tag™ eluent A (Waters) and ACN at a flow rate of 1 mL/min were used.

#### 1.2.5. Nuclear Magnetic Resonance

<sup>1</sup>H and <sup>13</sup>C NMR spectra were recorded on a Varian MERCURY 400 (400 MHz for <sup>1</sup>H NMR, 100 MHz for <sup>13</sup>C NMR) spectrometer for organic small molecules and on a Bruker DMX 500 MHz or a Bruker 600 Avance III Ultrashielded, provided with a cryoprobe TCI (600 MHz for <sup>1</sup>H NMR, 150 MHz for <sup>13</sup>C NMR), spectrometers for the peptidic samples. Chemical shifts (δ) are

expressed in parts per million downfield from tetramethylsilyl chloride. Coupling constants are expressed in Hertz.

### 1.3. Solid Phase Peptide Synthesis (SPPS)

#### 1.3.1. General considerations

Solid phase syntheses were undertaken manually in polypropylene syringes fitted with two polyethylene filter discs. All solvents and soluble reagents were removed by suction. Washings between deprotection, coupling and cyclization steps were carried out with DMF (3 × 1 min) and DCM (3 × 1 min) using 4 mL solvent/g resin for each wash. When not specified, all transformations and washes were performed at 25 °C. Short treatments were carried out with manual stirring while longer transformations took place in orbital shakers. All the peptides were synthesized in solid phase using the Fmoc/<sup>t</sup>Bu protection strategy.<sup>1</sup>

#### 1.3.2. Colorimetric tests

##### 1.3.2.1. Kaiser test<sup>2</sup>

The Kaiser or ninhydrin test is a colorimetric test that enables qualitative detection of free primary amines. It is commonly used in SPPS to monitor coupling and deprotection treatments.

The peptide-resin is washed with DCM and the solvent removed by suction. A small amount of resin beads are transferred to a glass tube and 6 drops of solution A and 2 drops of solution B are added. Then, the tube is incubated at 110 °C for three minutes. A dark blue color (in the supernatant and/or in the resin beads) reveals the presence of free primary amines, thus, pointing out that the deprotection is taken place or the coupling is incomplete, while a yellow coloration ensures 99.5% of coupling rate.

· *Solution A*: A solution of phenol (400 g) in absolute EtOH (100 mL) is prepared. Some heating is needed for complete dissolution of the phenol. 20 mL of a 10 mM aqueous KCN solution (65 mg of KCN in 100 mL of H<sub>2</sub>O) are added to freshly distilled pyridine (1000 mL). The two solutions are stirred with the ion exchange resin Amberlite MB-3 (40 g) for 45 min, then filtered and combined to obtain Solution A for the Kaiser test.

· *Solution B*: Ninhydrin (2.5 g) is dissolved in absolute EtOH (50 mL). The ninhydrin reagent is light sensitive, thus, Solution B is kept in a flask protected from light.

### 1.3.2.2. Chloranil test<sup>3</sup>

The chloranil test is a colorimetric test used in SPPS that enables qualitative detection of free secondary amines. It is commonly used to monitor couplings onto proline or N-alkyl residues.

The peptide-resin is washed with DCM and the solvent removed by suction. A small amount of resin beads are transferred to a glass tube and 5 drops of saturated chloranil solution (2,3,5,6-tetrachloro-1,4-benzoquinone in toluene) and 20 drops of acetone are added. The resulting solution is shaken in a vortex mixer for 5 min at room temperature. The resin beads which are stained green/The resin beads staining green indicate the presence of free secondary amines and it is considered a positive test. A negative test keeps the yellow color in the supernatant and in the beads.

### 1.3.2.3. De Clercq test<sup>4</sup>

The De Clercq test, also known as the *p*-nitrophenyl ester test, is a colorimetric test used in SPPS that enables qualitative detection of free secondary and primary amines with a higher sensitivity than the Chloranil test (see section 1.3.2.2.).

The peptide-resin is washed with DCM and the solvent removed by suction. A small amount of resin beads are transferred to a glass tube and 5 drops of the De Clercq reagent are added. Then, the tube is incubated at 70 °C for 10 minutes. The supernatant is removed with a Pasteur pipette and the resin beads washed with MeOH (× 3), DMF (× 3) and DCM (× 1). The resin beads which are stained red indicate the presence of free amines and it is considered a positive test. The absence of coloration ensures a quantitative coupling.

· *De Clercq reagent*: A three-step synthesis enables ready access to the *p*-nitrophenyl ester of red disperse 1 with high yields. To a solution of disperse red 1 (6.28 mg, 20 μmol) and Rh<sub>2</sub>(OAc)<sub>4</sub> (150 mg, 0.34 μmol) in DCM-toluene (1:1, 200 mL) another solution of ethyl diazoacetate (8.4 mL, 80 μmol) in toluene (40 mL) is added at 40 °C over 1 h. The reaction mixture is stirred overnight at room temperature and purified by flash chromatography. The product obtained (5 g, 12.5 μmol) and KOH (4.062 g, 62.5 μmol) are dissolved in MeOH-toluene (4.3:1, 370 mL) and the resulting mixture is refluxed under N<sub>2</sub> for 1.5 h. The product is purified by extractions. Finally, the purified product (2.322 g, 6 μmol) and *p*-nitrophenol (0.834 g, 6 μmol) are dissolved in pyridine-DCM (1:1.2, 220 mL), the resulting mixture cooled down to -15 °C and a solution of POCl<sub>3</sub> in DCM (1.006 mL in 10 mL of DCM) slowly added over 1



h. The final *p*-nitrophenyl ester of red disperse 1 is purified by extractions. It is used as a 0.02 M solution in ACN.

### 1.3.3. Conditioning of the resin and incorporation of the first amino acid

Two different resins were used to synthesize all the peptides described in the present thesis: 2-chlorotrytil chloride resin (2-CTC) and aminomethyl resin functionalized with the 3-(4-hydroxymethylphenoxy)propionic acid (AB linker). Peptide cleavage from both resins provides the peptide with an acid function at the C-terminal. In all cases the Fmoc/<sup>t</sup>Bu protection strategy was used.

Conditioning of the two resins consist on washes with DMF (5 × 1 min) to eliminate hydrochloric acid traces (especially critical for the extremely labile 2-CTC resin) and with DCM (5 × 1 min) to obtain an optimal swollen of the resin before incorporation of the first amino acid.

#### · *2-Chlorotrytil chloride resin (2-CTC)*

Incorporation of the first amino acid into 2-CTC resin is achieved through a nucleophilic attack of the carboxylate form of the corresponding Fmoc-protected amino acid to form an ester bond. Decreasing the loading of commercial 2-CTC resin (1.6 mmol/g) is necessary to avoid aggregation problems when growing the peptidic chains. Thus, to achieve a common loading of 0.8 mmol/g resin, 0.5 equiv of Fmoc-AA-OH and 3.3 equiv of DIEA are dissolved in DCM and the solution is added into the resin. After 5 min of manual stirring, 1.7 equiv more of DIEA are added, and the resulting mixture is shaken for 40 more min. To terminate the excess of reactive positions, 800 µL of MeOH/g resin are added and the reaction is shaken for 10 more min. Then, the solvents are removed by suction, and the resin washed with DCM (3 × 1 min), DMF (3 × 1 min) and DCM (3 × 1 min).

When cyclization is carried out in solid phase, the loading is decreased to 0.4-0.6 mmol/g resin. Some batches of 2-CTC resin can need a bigger excess of Fmoc-AA-OH to achieve the desired loading.

#### · *Aminomethyl resin*

A number of conditions to decrease the loading of a commercially available aminomethyl resin (0.93 mmol/g) have been unsuccessfully attempted. Thus, a 0.36 mmol/g resin was finally chosen in order to easily perform cyclizations in solid phase with minimized

side reactions. First of all, the AB linker is attached to the resin through an amide bond using the coupling conditions linker-HBTU-HOBt-DIEA (3:3:3:6) in DMF and in pre-activation mode. The AB linker, the HOBt and the DIEA are dissolved in DMF and then HBTU is added. After 1 min of vortex mixing (pre-activation), the mixture is added into the resin and shaken for 1.5 h. The solvents are removed by suction and the resin is washed with DMF (3 × 1 min) and DCM (3 × 1 min). A Kaiser test is performed to check the coupling conversion.

The incorporation of the first amino acid is carried out forming an ester bond under the conditions Fmoc-AA-OH-DIPCDI-HOAt-DMAP (5:5:5:0.5) in DCM-DMF(3:2) for 3 h. Then, the solvents are removed, the resin washed with DCM (3 × 1 min), DMF (3 × 1 min) and DCM (3 × 1 min), and the amino acid re-coupled under the same conditions. The excess of reactive sites of the AB linker are quenched by reaction with a solution of DIEA (50 equiv) and Ac<sub>2</sub>O (50 equiv) in DMF for 16 min. Then, the reagents are filtered under *vacuo* and the resin washed with DMF (3 × 1 min) and DCM (3 × 1 min).

#### 1.3.4. Elimination and quantification of the Fmoc group

The Fmoc group is removed by treatment with a solution of piperidine-DMF (1:4). When the Fmoc group is protecting a primary amine, the resin is treated four times (2 × 1 min, 2 × 5 min), while if it is a secondary amine, a longer treatment is needed (2 × 1 min, 2 × 5 min, 1 × 10 min).

The loading capacity of the resin can be found by quantifying the Fmoc group from the first amino acid anchored into the resin. Thus, when deprotecting, all the treatments with piperidine-DMF and the washes with DMF (3 × 1 min) are collected in a volumetric flask, and the UV absorbance at 290 nm of the resulting solution is measured. The loading capacity is calculated as follows:

$$Z = \frac{A \cdot X}{\varepsilon \cdot Y \cdot l}$$

Where:

A Absorbance

X Volume of the solvent (mL)

ε Molar absorbance coefficient (5800 L · mol<sup>-1</sup> · cm<sup>-1</sup>)

- Y Resin weight (g)  
 l Length of the cell (cm)  
 Z Loading of the resin

### 1.3.5. Peptide chain elongation

The assembly of the peptidic chain can be achieved by using several different coupling conditions. In the present thesis, all the peptides have been synthesized using one or a combination of the following protocols:

#### *Protocol A:*

<i>Step</i>	<i>Treatment</i>	<i>Conditions</i>
1	Washes	DCM (3 × 1 min)
2	Deprotection	Piperidine:DMF (1:4) (2 × 1 min, 2 × 5 min)
3	Washes	DMF (3 × 1 min), DCM (3 × 1 min)
4	Coupling	Fmoc-AA-OH-HBTU-HOBt-DIEA (4:4:4:8) in DMF (1 h)
5	Washes	DMF (3 × 1 min), DCM (3 × 1 min)
6	Colorimetric test	Kaiser test, chloranil test or De Clercq test, as needed

#### *Protocol B:*

<i>Step</i>	<i>Treatment</i>	<i>Conditions</i>
1	Washes	DCM (3 × 1 min)
2	Deprotection	Piperidine:DMF (1:4) (2 × 1 min, 2 × 5 min)
3	Washes	DMF (3 × 1 min), DCM (3 × 1 min)
4	Coupling	Fmoc-AA-OH-DIPCDI-HOBt (3:3:3) in DMF (1 h)
5	Washes	DMF (3 × 1 min), DCM (3 × 1 min)
6	Colorimetric test	Kaiser test, chloranil test or De Clercq test, as needed

*Protocol C:*

<i>Step</i>	<i>Treatment</i>	<i>Conditions</i>
1	Washes	DCM (3 × 1 min)
2	Deprotection	Piperidine:DMF (1:4) (2 × 1 min, 2 × 5 min, 1 × 10 min)
3	Washes	DMF (3 × 1 min), DCM (3 × 1 min)
4	Coupling	Fmoc-AA-OH-HATU-HOAt-DIEA (x:x:x:2x) in DMF (1 h)
5	Washes	DMF (3 × 1 min), DCM (3 × 1 min)
6	Colorimetric test	Kaiser test, chloranil test or De Clercq test, as needed

All the coupling treatments were performed at 25 °C and lasted 1 h. After 3 min of manual stirring, they were kept in an orbital shaker. Coupling conversion was checked by means of the appropriate colorimetric test (see section 1.3.2.) and re-couplings were performed when needed.

### 1.3.6. Allyl and Alloc groups elimination

The allyl ester and the alloc- group are removed by treatment with catalytic amount of [Pd(PPh<sub>3</sub>)<sub>4</sub>] (0.1 equiv) in the presence of the scavenger PhSiH<sub>3</sub> (10 equiv) in DCM and under N<sub>2</sub> atmosphere (3 × 15 min). After the treatments, the resin is washed with DCM (3 × 1 min), DMF (3 × 1 min) and DCM (3 × 1 min). Additional washes with a 0.02 M solution of sodium diethylthiocarbamate in DMF may be needed to remove all palladium traces.

### 1.3.7. Cleavage of the peptide from the resin

#### · 2-Chlorotrytil chloride resin (2-CTC)

Cleavage from 2-CTC resin is achieved by acidolytic treatment in very mild TFA conditions to furnish the completely protected linear peptide, therefore enabling cyclizations in solution. After washing the resin with DCM (3 × 1 min), it is treated with a TFA-DCM (2:98) solution (5 × 2 min) and then washed again with DCM until the resin colour changes from red to the original yellow. All washes are collected in a H<sub>2</sub>O-containing flask (15 mL H<sub>2</sub>O/200 mg resin) and the TFA and DCM removed by means of a N<sub>2</sub> stream or under *vacuo*. ACN is added and the resulting solution is lyophilized.

Cleavage from the resin and complete side-chain deprotection could be performed in one step increasing the TFA percentage and using the appropriate scavengers according to the

peptide sequence. Nevertheless, is better recommended carrying out the two treatments stepwise to obtain cleaner crudes.

· *Aminomethyl resin*

Cleavage from the aminomethyl resin functionalized with the AB linker requires harsh acidic conditions and furnishes the completely unprotected peptide. The cleavage cocktail is chosen according to the sensitiveness of the residues present in the peptide sequence and their protecting groups. For all the synthesis performed in the present thesis using this resin, after washes with DCM (3 × 1 min), the polymeric support was treated with a TFA-H<sub>2</sub>O-Tis (95:2.5:2.5) solution (1 × 1.5 h, 3 × 2 min). All the filtrates were collected in a round-bottom flask, evaporated to dryness under reduced pressure and lyophilized in H<sub>2</sub>O-ACN (3:2).

### **1.3.8. Peptide purification**

All peptides were purified using a reversed-phase HPLC equipment. The instrument and the column (see section 5.2.2.) were chosen depending on the amount of crude, the degree of purity and the complexity of the chromatographic profile of the crude. All the samples were dissolved in the minimum amount of a H<sub>2</sub>O-ACN solution, whose ACN percentage depended on the solubility of the peptide crude, and filtered through a 0.45 mm nylon filter. The fractions were analyzed by HPLC-PDA, combined and lyophilized.

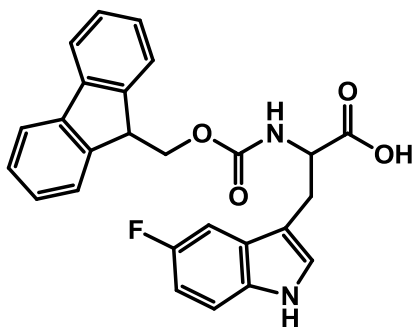
### **1.3.9. Peptide characterization**

Peptides identity was confirmed by MALDI-TOF, HPLC-MS and/or HRMS analysis, and their purity was checked by HPLC-PDA.

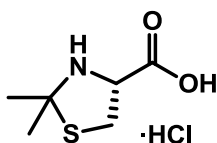
## 1.4. Phakellistatins

### 1.4.1. Synthesis of building blocks

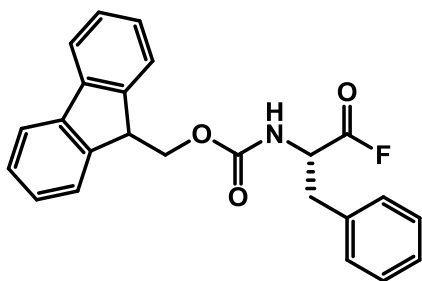
#### Fmoc-DL-Trp-(5-F)-OH



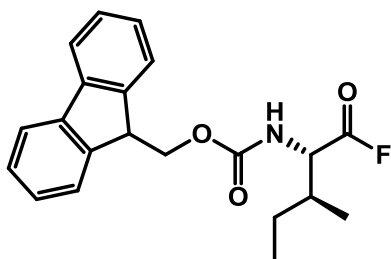
Fmoc-Cl (1164.2 mg, 4.50 mmol, 1 equiv) and  $\text{NaN}_3$  (351.1 mg, 5.40 mmol, 1.2 equiv) were dissolved in dioxane- $\text{H}_2\text{O}$  (1:1; 4.4 mL) and stirred for 2.5 hours at 25 °C. Then, a solution of H-LD-Trp-(5-F)-OH (1000 mg, 4.50 mmol, 1 equiv) in dioxane-aqueous solution of  $\text{Na}_2\text{CO}_3$  at 2% (1:1; 19 mL) was added dropwise. More dioxane was added (4.3 mL) and after adjusting to pH = 10, the mixture was stirred for 48 hours. The reaction was monitored by TLC. After quantitative conversion,  $\text{H}_2\text{O}$  (50 mL) was added and the resultant aqueous solution was washed with  $\text{Et}_2\text{O}$  ( $\times 3$ ), acidified to pH 3 by the addition of 1 M aqueous HCl and extracted with  $\text{EtOAc}$  ( $\times 3$ ). The combined organic layer was washed with brine, dried over  $\text{MgSO}_4$ , filtrated and concentrated under *vacuo* to give 1012.1 mg (51%) of Fmoc-DL-Trp(5-F)-OH as a white solid, which was used in the next reaction without further purification.  $^1\text{H}$  NMR (400 MHz,  $\text{CD}_3\text{OD}$ )  $\delta$  3.13 (1H, dd,  $J = 14.7, 8.4$  Hz,  $\text{CH}_2^\beta$ ), 3.31 (1H, dd,  $J = 14.6, 5.0$  Hz,  $\text{CH}_2^\beta$ ), 4.15 (1H, t,  $J = 7.0, 7.0$  Hz, CH, Fmoc), 4.22 (1H, dd,  $J = 10.2, 7.1$  Hz,  $\text{CH}_2$ , Fmoc), 4.31 (1H, dd,  $J = 10.3, 7.1$  Hz,  $\text{CH}_2$ , Fmoc), 4.47 (1H, dd,  $J = 8.2, 5.0$  Hz,  $\text{CH}^\alpha$ ), 6.85 (1H, dt,  $J = 2.4, 9.2, 9.1$  Hz, CH, Ar, Trp), 7.14 (1H, s, CH, Ar, Trp), 7.22-7.30 (4H, m, CH, Ar, Fmoc, Trp), 7.36 (2H, t,  $J = 7.5, 7.5$  Hz, CH, Ar, Fmoc), 7.57 (2H, dd,  $J = 7.4, 3.7$  Hz, CH, Ar, Fmoc), 7.77 (2H, d,  $J = 7.6$  Hz, CH, Ar, Fmoc);  $^{13}\text{C}$  NMR (400 MHz,  $\text{CD}_3\text{OD}$ )  $\delta$  28.70 ( $\text{CH}_2^\beta$ ), 48.16 (CH, Fmoc), 56.42 ( $\text{CH}^\alpha$ ), 68.06 ( $\text{CH}_2$ , Fmoc), 103.89 (CH, Ar, Trp), 104.12 (Cq, Trp), 110.36 (CH, Ar, Trp), 110.62 (Cq, Trp), 113.00 (CH, Ar, Trp), 113.10 (Cq, Trp), 120.88 (CH, Ar, Fmoc), 120.90 (CH, Ar, Fmoc), 126.25 (CH, Ar, Fmoc), 126.36 (CH, Ar, Fmoc), 126.54 (CH, Ar, Trp), 128.18 (CH, Ar, Fmoc), 128.76 (CH, Ar, Fmoc), 134.62 (Cq, Fmoc), 142.55 (Cq, Fmoc), 142.57 (Cq, Fmoc), 145.27 (Cq, Fmoc), 157.86 (OCONH), 158.43 (Cq, Trp), 160.17 (COOH). Analytical HPLC-PDA (Symmetry C18 column (5  $\mu\text{m}$   $\times$  4.6 mm  $\times$  150 mm);  $t_r = 4.21$  min, from 30% to 90% ACN over 15 min, purity > 95%). HPLC-ESMS(+) analysis showed:  $m/z$  calcd for  $\text{C}_{26}\text{H}_{21}\text{FN}_2\text{O}_4$   $[\text{M}+\text{H}]^+$  444.5, found 446.2.

**H-Cys( $\psi^{\text{Me,Me}}$ pro)-OH\*HCl**

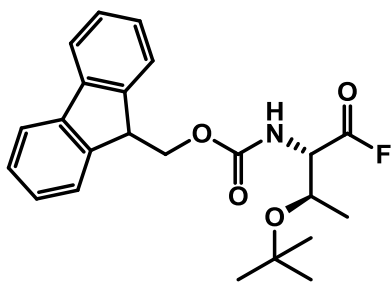
A solution of H-Cys-OH\*HCl (438.0 mg, 2.78 mmol, 1 equiv) and acetone dimethyl acetal (6.3 mL, 51.01 mmol, 18.4 equiv) in acetone (30 mL) was placed in a round bottomed flask equipped with a condenser and the mixture was heated at 57 °C for 2 h. Then, the reaction suspension was allowed to cool down to 25 °C, filtered and the solid washed with cold acetone and dried under *vacuo* to give 298 mg (54%) of H-Cys( $\psi^{\text{Me,Me}}$ pro)-OH\*HCl as a white solid which was used in the next reaction without further purification.

**Fmoc-Phe-F**

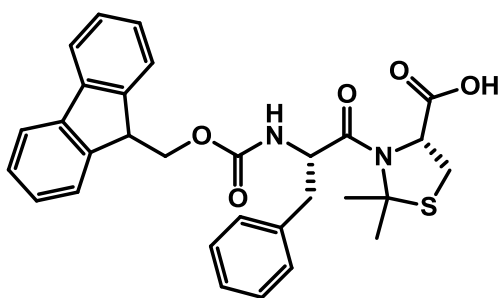
To a solution of Fmoc-Phe-OH (500.0 mg, 1.29 mmol, 1 equiv) in dry DCM (400 mL) at 0 °C, DAST (203  $\mu\text{L}$ , 1.55 mmol, 1.2 equiv) was added and the mixture was stirred for 1 h. Then, after monitoring the reaction by TLC, more DAST was added (203  $\mu\text{L}$ , 1.55 mmol, 1.2 equiv) and the resulting mixture was reacted for 1 h more. The reaction was quenched by adding  $\text{H}_2\text{O}$ , and the organic layer was washed with brine ( $\times 1$ ), dried over  $\text{Na}_2\text{SO}_4$ , filtrated and concentrated under *vacuo* to give 410.0 mg (82%) of crude Fmoc-Phe-F as an orange solid, which was used in the next step without further purification.

**Fmoc-Ile-F**

To a solution of Fmoc-Ile-OH (500.0 mg, 1.41 mmol, 1 equiv) in dry DCM (70 mL) at 0 °C, DAST (222  $\mu\text{L}$ , 1.70 mmol, 1.2 equiv) was added and the mixture was stirred for 2 h. Then, after monitoring the reaction by TLC, more DAST was added (222  $\mu\text{L}$ , 1.70 mmol, 1.2 equiv) and the resulting mixture reacted for 1.5 h more. The reaction was quenched by adding  $\text{H}_2\text{O}$ , and the organic layer was washed with brine ( $\times 1$ ), dried over  $\text{Na}_2\text{SO}_4$ , filtrated and concentrated under *vacuo* to give 493.7 mg (98%) of crude Fmoc-Ile-F as an orange solid, which was used in the next step without further purification.

**Fmoc-Thr(<sup>t</sup>Bu)-F**

To a solution of Fmoc-Thr(<sup>t</sup>Bu)-OH (500.0 mg, 1.26 mmol, 1 equiv) in dry DCM (70 mL) at 0 °C, DAST (198  $\mu$ L, 1.51 mmol, 1.2 equiv) was added and the mixture was stirred for 2 h. Then, after monitoring the reaction by TLC, more DAST was added (198  $\mu$ L, 1.51 mmol, 1.2 equiv) and the resulting mixture reacted for 2 h more. The reaction was quenched by adding H<sub>2</sub>O, and the organic layer was washed with brine ( $\times$  1), dried over Na<sub>2</sub>SO<sub>4</sub>, filtrated and concentrated under *vacuo* to give 483.0 mg (96%) of crude Fmoc-Thr(<sup>t</sup>Bu)-F as an orange solid, which was used in the next step without further purification.

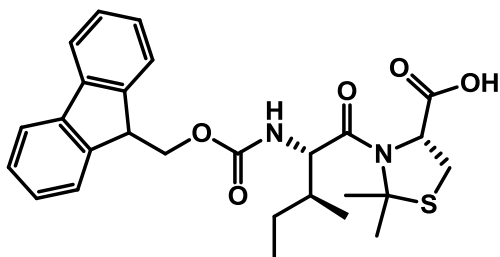
**Fmoc-Phe-Cys( $\psi^{\text{Me,Me}}$ pro)-OH**

To a solution of H-Cys( $\psi^{\text{Me,Me}}$ pro)-OH\*HCl (310.6 mg, 1.57 mmol, 1.5 equiv) in dry DCM (35 mL), Fmoc-Phe-F (410.0 mg, 1.05 mmol, 1 equiv) and DIEA (602  $\mu$ L, 3.46 mmol, 3.3 equiv) were added and the resulting mixture was stirred for 3.5 h at room temperature under a N<sub>2</sub> atmosphere. Then, the organic layer was washed with a 5% aqueous solution of citric acid ( $\times$  1) and with brine ( $\times$  1), dried over Na<sub>2</sub>SO<sub>4</sub>, filtrated and concentrated under *vacuo* to give 510.7 mg (91%) of crude dipeptide Fmoc-Phe-Cys( $\psi^{\text{Me,Me}}$ pro)-OH as a white solid, which was used in the SPPS without further purification. <sup>1</sup>H NMR (400 MHz, CDCl<sub>3</sub>)  $\delta$  1.74 (3H, s, CH<sub>3</sub>, Cys( $\psi^{\text{Me,Me}}$ pro)), 1.83 (3H, s, CH<sub>3</sub>, Cys( $\psi^{\text{Me,Me}}$ pro)), 2.36 (1H, m, CH<sub>2</sub> <sup>$\beta$</sup> , Cys( $\psi^{\text{Me,Me}}$ pro)), 2.90 (1H, m, CH<sub>2</sub> <sup>$\beta$</sup> , Cys( $\psi^{\text{Me,Me}}$ pro)), 3.05 (2H, m, CH<sub>2</sub> <sup>$\beta$</sup> , Phe), 4.08 (1H, t,  $J$  = 6.9, 6.9 Hz, CH, Fmoc), 4.17 (2H, m, CH<sub>2</sub>, Fmoc), 4.30 (1H, dd,  $J$  = 10.3, 7.4 Hz, CH <sup>$\alpha$</sup> , Cys( $\psi^{\text{Me,Me}}$ pro)), 4.72 (1H, dt,  $J$  = 5.2, 9.6, 9.6 Hz, CH <sup>$\alpha$</sup> , Phe), 5.87 (1H, d,  $J$  = 8.7 Hz, OCONH), 7.23-7.31 (7H, m, CH, Ar, Fmoc, Phe), 7.37 (2H, br dd,  $J$  = 12.8, 7.2 Hz, CH, Ar, Fmoc), 7.45 (1H, d,  $J$  = 7.4 Hz, CH, Ar, Fmoc), 7.51 (1H, d,  $J$  = 7.5 Hz, CH, Ar, Fmoc), 7.72 (2H, dd,  $J$  = 7.4, 2.1 Hz, CH, Ar, Fmoc). <sup>13</sup>C NMR (400 MHz, CDCl<sub>3</sub>)  $\delta$  27.66 (CH<sub>3</sub>, Cys( $\psi^{\text{Me,Me}}$ pro)), 29.29 (CH<sub>3</sub>, Cys( $\psi^{\text{Me,Me}}$ pro)), 30.41 (CH<sub>2</sub> <sup>$\beta$</sup> , Cys( $\psi^{\text{Me,Me}}$ pro)), 41.22 (CH<sub>2</sub> <sup>$\beta$</sup> , Phe), 47.00 (CH, Fmoc), 54.89 (CH <sup>$\alpha$</sup> , Phe), 65.34 (CH<sub>2</sub>, Fmoc), 67.37 (C <sup>$\delta$</sup> , Cys( $\psi^{\text{Me,Me}}$ pro)), 73.93 (CH <sup>$\alpha$</sup> , Cys( $\psi^{\text{Me,Me}}$ pro)), 119.93 (CH, Ar, Fmoc), 119.96 (CH, Ar, Fmoc), 125.09 (CH, Ar, Fmoc), 125.12 (CH, Ar, Fmoc), 127.08 (CH, Ar, Fmoc), 127.39 (CH, Ar, Phe), 127.72 (CH, Ar, Fmoc), 128.65 (CH, Ar, Phe), 129.92 (CH, Ar, Phe), 135.38 (Cq, Phe), 141.22 (Cq, Fmoc), 141.24 (Cq, Fmoc), 143.43 (Cq, Fmoc), 143.77 (Cq, Fmoc),



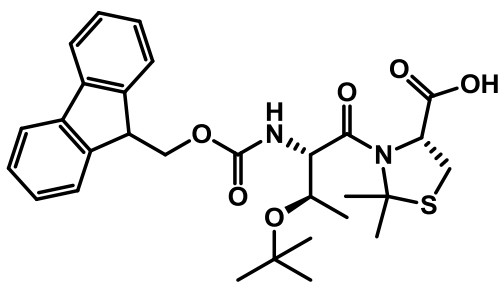
155.79 (CONH), 169.58 (CO). Analytical HPLC-PDA (SunFire™ C18 column (3.5  $\mu\text{m}$   $\times$  4.6 mm  $\times$  100 mm);  $t_{\text{R}}$  = 3.77 min, from 70% to 100% ACN over 8 min, purity > 88%). HPLC-ESMS(+):  $m/z$  calculated for  $\text{C}_{30}\text{H}_{30}\text{N}_2\text{O}_5\text{S}$  530.63, found 531.28  $[\text{M}+\text{H}]^+$ .

### Fmoc-Ile-Cys( $\psi^{\text{Me,Me}}$ pro)-OH



To a solution of H-Cys( $\psi^{\text{Me,Me}}$ pro)-OH $\cdot\text{HCl}$  (500.9 mg, 2.53 mmol, 1.5 equiv) in dry DCM (50 mL), Fmoc-Ile-F (603.5 mg, 1.70 mmol, 1 equiv) and DIEA (971  $\mu\text{L}$ , 5.57 mmol, 3.3 equiv) were added and the resulting mixture was stirred for 4 h at room temperature under a  $\text{N}_2$  atmosphere.

Then, the organic layer was washed with a 5% aqueous solution of citric acid ( $\times$  1) and with brine ( $\times$  1), dried over  $\text{Na}_2\text{SO}_4$ , filtrated and concentrated under *vacuo*. The residue was purified by semi-preparative RP-HPLC to give 132.4 mg (16%) of dipeptide Fmoc-Ile-Cys( $\psi^{\text{Me,Me}}$ pro)-OH as a white solid. Conditions: SunFire™ Prep C18 OBD™ column (5  $\mu\text{m}$   $\times$  19 mm  $\times$  100 mm); linear gradient (5% to 60%) of ACN over 5 min and (60% to 90%) over 20 min, with a flow rate of 15 mL/min.  $^1\text{H}$  NMR (400 MHz,  $\text{CDCl}_3$ )  $\delta$  0.88 (3H, t,  $J$  = 7.4, 7.4 Hz,  $\text{CH}_3^\delta$ , Ile), 0.96 (3H, d,  $J$  = 6.7 Hz,  $\text{CH}_3^\gamma$ , Ile), 1.09 (1H, m,  $\text{CH}_2^\gamma$ , Ile), 1.51 (1H, m,  $\text{CH}_2^\gamma$ , Ile), 1.64 (1H, m,  $\text{CH}^\beta$ , Ile), 1.84 (3H, s,  $\text{CH}_3$ , Cys( $\psi^{\text{Me,Me}}$ pro)), 1.93 (3H, s,  $\text{CH}_3$ , Cys( $\psi^{\text{Me,Me}}$ pro)), 3.22 (1H, dd,  $J$  = 11.9, 5.7 Hz,  $\text{CH}_2^\beta$ , Cys( $\psi^{\text{Me,Me}}$ pro)), 3.40 (1H, d,  $J$  = 11.9 Hz,  $\text{CH}_2^\beta$ , Cys( $\psi^{\text{Me,Me}}$ pro)), 4.10 (2H, m,  $\text{CH}_2$ , Fmoc), 4.26 (1H, dd,  $J$  = 10.1, 7.2 Hz, CH, Fmoc), 4.51 (1H, dd,  $J$  = 9.4, 7.1 Hz,  $\text{CH}^\alpha$ , Ile), 5.03 (1H, d,  $J$  = 5.4 Hz,  $\text{CH}^\alpha$ , Cys( $\psi^{\text{Me,Me}}$ pro)), 5.85 (1H, d,  $J$  = 9.6 Hz, CONH), 7.25 (2H, m, CH, Ar, Fmoc), 7.35 (2H, q,  $J$  = 7.7, 7.7, 7.7 Hz, CH, Ar, Fmoc), 7.44 (1H, d,  $J$  = 7.5 Hz, CH, Ar, Fmoc), 7.50 (1H, d,  $J$  = 7.5 Hz, CH, Ar, Fmoc), 7.69 (2H, dd,  $J$  = 6.8, 6.2 Hz, CH, Ar, Fmoc).  $^{13}\text{C}$  NMR (400 MHz,  $\text{CDCl}_3$ )  $\delta$  11.56 ( $\text{CH}_3^\delta$ , Ile), 14.88 ( $\text{CH}_3^\gamma$ , Ile), 23.89 ( $\text{CH}_2^\gamma$ , Ile), 27.86 ( $\text{CH}_3$ , Cys( $\psi^{\text{Me,Me}}$ pro)), 29.24 ( $\text{CH}_3$ , Cys( $\psi^{\text{Me,Me}}$ pro)), 30.77 ( $\text{CH}_2^\beta$ , Cys( $\psi^{\text{Me,Me}}$ pro)), 39.34 ( $\text{CH}_2^\beta$ , Ile), 47.03 (CH, Fmoc), 58.14 ( $\text{CH}^\alpha$ , Ile), 65.40 ( $\text{CH}_2$ , Fmoc), 67.38 ( $\text{C}^\delta$ , Cys( $\psi^{\text{Me,Me}}$ pro)), 73.83 ( $\text{CH}^\alpha$ , Cys( $\psi^{\text{Me,Me}}$ pro)), 119.85 (CH, Ar, Fmoc), 119.90 (CH, Ar, Fmoc), 125.12 (CH, Ar, Fmoc), 125.17 (CH, Ar, Fmoc), 127.06 (CH, Ar, Fmoc), 127.67 (CH, Ar, Fmoc), 141.18 (Cq, Fmoc), 141.20 (Cq, Fmoc), 143.38 (Cq, Fmoc), 143.81 (Cq, Fmoc), 156.58 (CONH), 170.63 (CO), 171.62 (CO). Analytical HPLC-PDA (SunFire™ C18 column (3.5  $\mu\text{m}$   $\times$  4.6 mm  $\times$  100 mm);  $t_{\text{R}}$  = 3.97 min, from 70% to 100% ACN over 8 min, purity > 98%). HPLC-ESMS(+):  $m/z$  calculated for  $\text{C}_{27}\text{H}_{32}\text{N}_2\text{O}_5\text{S}$  496.62, found 497.14  $[\text{M}+\text{H}]^+$ .

**Fmoc-Thr(<sup>t</sup>Bu)-Cys( $\psi^{\text{Me,Me}}$ pro)-OH**

To a solution of H-Cys( $\psi^{\text{Me,Me}}$ pro)-OH\*HCl (370.8 mg, 1.88 mmol, 1.5 equiv) in dry DCM (40 mL), Fmoc-Thr(<sup>t</sup>Bu)-F (502.0 mg, 1.26 mmol, 1 equiv) and DIEA (719  $\mu$ L, 4.13 mmol, 3.3 equiv) were added and the resulting mixture was stirred for 4 h at room temperature under a N<sub>2</sub>

atmosphere. Then, the organic layer was washed with a 5% aqueous solution of citric acid ( $\times$  1) and with brine ( $\times$  1), dried over Na<sub>2</sub>SO<sub>4</sub>, filtrated and concentrated under *vacuo*. The residue was purified by semi-preparative RP-HPLC to give 54.4 mg (8%) of dipeptide Fmoc-Thr(<sup>t</sup>Bu)-Cys( $\psi^{\text{Me,Me}}$ pro)-OH as a white solid. Conditions: SunFire™ Prep C18 OBD™ column (5  $\mu$ m  $\times$  19 mm  $\times$  100 mm); linear gradient (5% to 50%) of ACN over 5 min and (50% to 90%) over 20 min, with a flow rate of 15 mL/min. <sup>1</sup>H NMR (400 MHz, CDCl<sub>3</sub>)  $\delta$  1.06 (3H, d,  $J$  = 6.3 Hz, CH<sub>3</sub> <sup>$\gamma$</sup> , Thr), 1.23 (9H, s, CH<sub>3</sub>, <sup>t</sup>Bu), 1.86 (3H, s, CH<sub>3</sub>, Cys( $\psi^{\text{Me,Me}}$ pro)), 1.90 (3H, s, CH<sub>3</sub>, Cys( $\psi^{\text{Me,Me}}$ pro)), 3.25 (1H, dd,  $J$  = 11.9, 5.7 Hz, CH<sub>2</sub> <sup>$\beta$</sup> , Cys( $\psi^{\text{Me,Me}}$ pro)), 3.33 (1H, d,  $J$  = 11.8 Hz, CH<sub>2</sub> <sup>$\beta$</sup> , Cys( $\psi^{\text{Me,Me}}$ pro)), 3.88 (1H, m, CH <sup>$\beta$</sup> , Thr), 4.18 (1H, t,  $J$  = 7.1, 7.1 Hz, CH, Fmoc), 4.33 (2H, m, CH<sub>2</sub>, Fmoc), 4.46 (1H, dd,  $J$  = 7.3, 3.7 Hz, CH <sup>$\alpha$</sup> , Thr), 6.03 (1H, d,  $J$  = 5.4 Hz, CH <sup>$\alpha$</sup> , Cys( $\psi^{\text{Me,Me}}$ pro)), 6.12 (1H, d,  $J$  = 7.4 Hz, OCONH), 7.30 (2H, dt,  $J$  = 3.0, 7.4, 7.4 Hz, CH, Ar, Fmoc), 7.39 (2H, br t,  $J$  = 7.4, 7.4 Hz, CH, Ar, Fmoc), 7.56 (1H, d,  $J$  = 7.5 Hz, CH, Ar, Fmoc), 7.60 (1H, d,  $J$  = 7.5 Hz, CH, Ar, Fmoc), 7.74 (2H, d,  $J$  = 7.5 Hz, CH, Ar, Fmoc). <sup>13</sup>C NMR (400 MHz, CDCl<sub>3</sub>)  $\delta$  17.55 (CH<sub>3</sub> <sup>$\gamma$</sup> , Thr), 27.77 (CH<sub>3</sub>, Cys( $\psi^{\text{Me,Me}}$ pro)), 28.00 (CH<sub>3</sub>, <sup>t</sup>Bu, Thr), 29.44 (CH<sub>3</sub>, Cys( $\psi^{\text{Me,Me}}$ pro)), 30.70 (CH<sub>2</sub> <sup>$\beta$</sup> , Cys( $\psi^{\text{Me,Me}}$ pro)), 47.03 (CH, Fmoc), 58.13 (CH <sup>$\alpha$</sup> , Cys( $\psi^{\text{Me,Me}}$ pro)), 65.67 (CH<sub>2</sub>, Fmoc), 67.33 (C <sup>$\delta$</sup> , Cys( $\psi^{\text{Me,Me}}$ pro)), 69.47 (CH<sub>2</sub> <sup>$\beta$</sup> , Cys( $\psi^{\text{Me,Me}}$ pro)), 74.12 (CH <sup>$\alpha$</sup> , Cys( $\psi^{\text{Me,Me}}$ pro)), 75.24 (Cq, <sup>t</sup>Bu), 119.91 (CH, Ar, Fmoc), 119.93 (CH, Ar, Fmoc), 125.21 (CH, Ar, Fmoc), 125.28 (CH, Ar, Fmoc), 127.05 (CH, Ar, Fmoc), 127.69 (CH, Ar, Fmoc), 127.70 (CH, Ar, Fmoc), 141.23 (Cq, Fmoc), 141.30 (Cq, Fmoc), 143.45 (Cq, Fmoc), 143.95 (Cq, Fmoc), 155.88 (OCONH), 167.64 (CO), 172.81 (CO). Analytical HPLC-PDA (SunFire™ C18 3.5  $\mu$ m  $\times$  4.6 mm  $\times$  100 mm column;  $t_r$  = 5.11 min, from 70% to 100% ACN over 8 min, purity > 98%). HPLC-ESMS(+):  $m/z$  calculated for C<sub>29</sub>H<sub>36</sub>N<sub>2</sub>O<sub>6</sub>S 540.67, found 541.29 [M+H]<sup>+</sup>.

## 1.4.2. Phakellistatin 19

### 1.4.2.1. Synthesis of Phakellistatin 19

2-CTC resin (100 mg, 1.60 mmol/g) was placed in a 10 mL-polypropylene syringe fitted with two polyethylene filter discs. The resin was then washed, the first amino acid (Fmoc-Pro-OH) coupled and the excess of reactive positions terminated as it has been described in the general procedures (see section 1.3.). The peptide elongation was carried out under the conditions described for protocol A and the resulting protected linear peptide cleaved using the conditions specified in the section 1.3.7.

The protected lyophilized peptide (91.2 mg, 81  $\mu$ mol, 1 equiv) and a solution of HOAt (11.1 mg, 81  $\mu$ mol, 1 equiv) in the minimum amount of DMF (0.5 mL) were dissolved in DCM (163 mL; 0.5 mM). Then, solid PyBOP (84.9 mg, 163  $\mu$ mol, 2 equiv) first and DIEA (56  $\mu$ L, 329  $\mu$ mol, 4 equiv) second were added. After adjusting to basic pH = 8 with more DIEA, the solution was stirred for 4 hours at 25 °C. The reaction was monitored by HPLC-PDA. After the completion of the cyclization, the DCM was partly evaporated under reduced pressure, and washed with 5% aqueous NaHCO<sub>3</sub> solution ( $\times$  3), saturated aqueous NH<sub>4</sub>Cl solution ( $\times$  3) and brine ( $\times$  1), dried over Na<sub>2</sub>SO<sub>4</sub>, filtrated and concentrated under *vacuo*. To fully remove the side-chain protecting groups, the protected cyclopeptide was treated with a TFA-H<sub>2</sub>O solution (95:5; 5 mL) for 1 hour at 25 °C. The HPLC-PDA showed completion of the deprotection. The TFA was removed under reduced pressure and the resulting aqueous suspension was re-dissolved adding H<sub>2</sub>O-ACN (7:3; 15 mL) and lyophilized. The product was then purified by semi-preparative RP-HPLC. Conditions: Symmetry® semi-preparative C18 column (5  $\mu$ m  $\times$  30 mm  $\times$  100 mm); linear gradient (30% to 100%) of ACN over 45 min, with a flow rate of 10 mL/min;  $t_R$  = 32.4 min.

### 1.4.2.2. Characterization of Phakellistatin 19

#### Linear precursor

Column: Symmetry C18 5  $\mu$ m  $\times$  4.6 mm  $\times$  150 mm

HPLC-PDA,  $t_R$  (0% to 100% of ACN over 15 min): 10.10 min

m/z calculated for C<sub>60</sub>H<sub>88</sub>N<sub>9</sub>O<sub>12</sub> [M+H]<sup>+</sup>: 1127.39 Da

HPLC-ESMS(+), [M+H]<sup>+</sup>: 1127.37 Da

Phakellistatin 19Analytical column: Symmetry C18 5  $\mu\text{m}$   $\times$  4.6 mm  $\times$  150 mm

Yield: 22%

HPLC-PDA,  $t_R$  (45% to 75% of ACN over 15 min): 7.96 minPurity ( $\lambda = 220$  nm): 95%m/z calculated for  $\text{C}_{51}\text{H}_{70}\text{N}_9\text{O}_9$   $[\text{M}+\text{H}]^+$ : 952.5291 DaHRMS (NanoESI),  $[\text{M}+\text{H}]^+$ : 952.5293 Da $^1\text{H}$  and  $^{13}\text{C}$  NMR (Bruker DMX 500 MHz,  $\text{DMSO}-d_6$ ):

	$^1\text{H}$ (ppm)	$^{13}\text{C}$ (ppm)		$^1\text{H}$ (ppm)	$^{13}\text{C}$ (ppm)
<b>Leu<sup>1</sup> NH</b>	8.73	-	<b>Pro<sup>5</sup></b>	-	-
C/H $\alpha$	3.53	52.97	C/H $\alpha$	3.92	60.95
C/H $\beta$	2.16, 1.68'	36.10	C/H $\alpha$	1.99, 1.83'	24.57-24.71
C/H $\gamma$	1.47	24.57-24.71	C/H $\beta$	1.76, 1.75'	29.02
C/H $\delta$	0.88, 0.85'	23.39	C/H $\gamma$	3.96, 3.52'	47.51
		20.95/14.43'	C/H $\delta$		
<b>Thr<sup>2</sup> NH</b>	7.56	-	<b>Trp<sup>6</sup> NH</b>	8.20	-
C/H $\alpha$	4.87	56.23	C/H $\alpha$	3.70	56.95
C/H $\beta$	4.13	67.60	C/H $\beta$	3.61, 3.16'	23.34
OH	5.54	-	C/H $_2$	6.95	123.54
C/H $\gamma$	0.94	18.43	C $_3$	-	111.18
			C/H $_4$	7.40	118.16
			C/H $_5$	6.94	117.94
			C/H $_6$	7.03	120.79
			C/H $_7$	7.30	111.34
			C $_8$	-	136.04
			C $_9$	-	126.97
			HN <sub>ind</sub>	10.76	-
<b>Pro<sup>3</sup></b>	-	-	<b>Phe<sup>7</sup> NH</b>	8.11	-
C/H $\alpha$	4.47	59.26	C/H $\alpha$	5.03	51.07
C/H $\beta$	2.06, 1.93'	28.42	C/H $\beta$	2.95, 2.86'	36.46
C/H $\gamma$	1.83, 1.72'	24.57-24.71	C $_1$	-	138.17
C/H $\delta$	3.69, 3.56'	46.98	C/H $_{2/6}$		129.21
			C/H $_{3/5}$		127.77
			C/H $_4$		125.96
<b>Ile<sup>4</sup> NH</b>	8.34	-	<b>Pro<sup>8</sup></b>	-	-
C/H $\alpha$	4.20	53.98	C/H $\alpha$	4.05	60.57
C/H $\beta$	1.97	35.03	C/H $\beta$	2.13, 1.98'	29.65
C/H $\gamma$	1.31, 1.04'	24.57-24.71	C/H $\gamma$	1.83, 1.72'	24.57-24.71
	0.85 <sub>Me</sub>	20.95/14.43 <sub>Me</sub>	C/H $\delta$	3.89, 3.59'	47.78
C/H $\delta$	0.65	9.71			

**Table 20:** Chemical shifts of  $^1\text{H}$  and  $^{13}\text{C}$  for synthetic Phakellistatin 19 in  $\text{DMSO}-d_6$ . Carbonylic C weren't visible in the HMBC experiment. Carbons  $\text{C}_{\gamma\text{CH}_3\text{-Ile}}$  and  $\text{C}\delta\text{-Leu}$  as well as  $\text{C}_{\gamma\text{-Pro}^8}$ ,  $\text{C}\beta\text{-Pro}^5$ ,  $\text{C}_{\gamma\text{-Ile}}$  and  $\text{C}\beta\text{-Leu}$  couldn't be univocally assigned.

### 1.4.3. Libraries of epimers and analogs

#### 1.4.3.1. Synthesis of epimers and analogs

All epimers were synthesized following the same procedure described for Phakellistatin 19 with one variation: the peptide chain assembly was achieved using protocol B instead of protocol A. All the amino acids were incorporated in pre-activation mode.

The first library of analogs was synthesized as it has been detailed for Phakellistatin 19. The main differences are found in the purification step. Nevertheless, for the second library of analogs, its structural design demanded the implementation of some modifications with regard to the general synthetic protocol of Phakellistatin 19: the additive HOBt (protocol A) was replaced by HOAt; the Cys( $\psi^{\text{Me,Me}}$ pro) residues were incorporated as the corresponding dipeptides Fmoc-Phe-Cys( $\psi^{\text{Me,Me}}$ pro)-OH, Fmoc-Ile-Cys( $\psi^{\text{Me,Me}}$ pro)-OH or Fmoc-Thr(<sup>t</sup>Bu)-Cys( $\psi^{\text{Me,Me}}$ pro)-OH under the conditions dipeptide-PyBOP-HOAt-DIEA (2:2:2:4) in DMF (1 mL) for 2 h and in pre-activation mode; and the final deprotection step was carried out under the conditions TFA-MeOH-TIS-H<sub>2</sub>O solution (80:15:2.5:2.5; 20 mL) for 15 min at 25 °C. After checking by HPLC-PDA analysis completion of the deprotection, the mixture of solvents was co-evaporated with toluene (× 2, 20 mL) first and DCM (× 2, 20 mL) second.

#### 1.4.3.2. Characterization of epimers and analogs

##### Library of epimers

##### **Cyclo-[Leu-Thr-Pro-Ile-Pro-Trp-Phe-D-Pro]**

Linear precursor

Column: SunFire™ C18 (3.5  $\mu\text{m}$  × 4.6 mm × 100 mm)

HPLC-PDA,  $t_R$  (5% to 100% of ACN over 8 min): 6.36 min

$m/z$  calculated for C<sub>60</sub>H<sub>88</sub>N<sub>9</sub>O<sub>12</sub> [M+H]<sup>+</sup>: 1127.39 Da

HPLC-ESMS(+), [M+H]<sup>+</sup>: 1127.73 Da

Cyclic unprotected peptide

Purification column: SunFire™ Prep C18 OBD™ (5  $\mu\text{m}$  × 19 mm × 100 mm)

Purification gradient: 30% to 100% of ACN over 40 min with a flow of 15 mL/min

Yield: 12%

Analytical column: SunFire™ C18 (3.5  $\mu\text{m}$  × 4.6 mm × 100 mm)

HPLC-PDA,  $t_R$  (30% to 100% of ACN over 8 min): 6.41 min

Purity ( $\lambda = 220$  nm): 97%

$m/z$  calculated for  $C_{51}H_{70}N_9O_9$   $[M+H]^+$ : 952.5291 Da

HRMS (NanoESI),  $[M+H]^+$ : 952.5266 Da

#### **Cyclo-[Leu-Thr-Pro-Ile-Pro-Trp-D-Phe-Pro]**

Linear precursor

Column: SunFire™ C18 (3.5  $\mu$ m  $\times$  4.6 mm  $\times$  100 mm)

HPLC-PDA,  $t_R$  (5% to 100% of ACN over 8 min): 6.37 min

$m/z$  calculated for  $C_{60}H_{88}N_9O_{12}$   $[M+H]^+$ : 1127.39 Da

HPLC-ESMS(+),  $[M+H]^+$ : 1127.54 Da

Cyclic unprotected peptide

Purification column: SunFire™ Prep C18 OBD™ (5  $\mu$ m  $\times$  19 mm  $\times$  100 mm)

Purification gradient: 30% to 100% of ACN over 40 min with a flow of 15 mL/min

Yield: 7%

Analytical column: SunFire™ C18 (3.5  $\mu$ m  $\times$  4.6 mm  $\times$  100 mm)

HPLC-PDA,  $t_R$  (30% to 100% of ACN over 8 min): 6.16 min

Purity ( $\lambda = 220$  nm): 95%

$m/z$  calculated for  $C_{51}H_{70}N_9O_9$   $[M+H]^+$ : 952.5291 Da

HRMS (NanoESI),  $[M+H]^+$ : 952.5288 Da

#### **Cyclo-[Leu-Thr-Pro-Ile-Pro-D-Trp-Phe-Pro]**

Linear precursor

Column: SunFire™ C18 (3.5  $\mu$ m  $\times$  4.6 mm  $\times$  100 mm)

HPLC-PDA,  $t_R$  (5% to 100% of ACN over 8 min): 4.65 min

$m/z$  calculated for  $C_{60}H_{88}N_9O_{12}$   $[M+H]^+$ : 1127.39 Da

HPLC-ESMS(+),  $[M+H]^+$ : 1127.73 Da

Cyclic unprotected peptide

Purification column: SunFire™ Prep C18 OBD™ (5  $\mu$ m  $\times$  19 mm  $\times$  100 mm)

Purification gradient: 30% to 100% of ACN over 40 min with a flow of 15 mL/min

Yield: 31%

Analytical column: SunFire™ C18 (3.5  $\mu$ m  $\times$  4.6 mm  $\times$  100 mm)

HPLC-PDA,  $t_R$  (30% to 100% of ACN over 8 min): 6.37 min

Purity ( $\lambda = 220$  nm): 99%

$m/z$  calculated for  $C_{51}H_{70}N_9O_9$   $[M+H]^+$ : 952.5291 Da

HRMS (NanoESI),  $[M+H]^+$ : 952.5294 Da

### **Cyclo-[Leu-Thr-Pro-Ile-D-Pro-Trp-Phe-Pro]**

Linear precursor

Column: SunFire™ C18 (3.5  $\mu$ m  $\times$  4.6 mm  $\times$  100 mm)

HPLC-PDA,  $t_R$  (5% to 100% of ACN over 8 min): 6.27 min

$m/z$  calculated for  $C_{60}H_{88}N_9O_{12}$   $[M+H]^+$ : 1127.39 Da

HPLC-ESMS(+),  $[M+H]^+$ : 1127.91 Da

Cyclic unprotected peptide

Purification column: SunFire™ Prep C18 OBD™ (5  $\mu$ m  $\times$  19 mm  $\times$  100 mm)

Purification gradient: 30% to 100% of ACN over 40 min with a flow of 15 mL/min

Yield: 14%

Analytical column: SunFire™ C18 (3.5  $\mu$ m  $\times$  4.6 mm  $\times$  100 mm)

HPLC-PDA,  $t_R$  (30% to 100% of ACN over 8 min): 6.32 min

Purity ( $\lambda = 220$  nm): 100%

$m/z$  calculated for  $C_{51}H_{70}N_9O_9$   $[M+H]^+$ : 952.5291 Da

HRMS (NanoESI),  $[M+H]^+$ : 952.5295 Da

### **Cyclo-[Leu-Thr-Pro-D-Ile-Pro-Trp-Phe-Pro]**

Linear precursor

Column: SunFire™ C18 (3.5  $\mu$ m  $\times$  4.6 mm  $\times$  100 mm)

HPLC-PDA,  $t_R$  (5% to 100% of ACN over 8 min): 4.39 min

$m/z$  calculated for  $C_{60}H_{88}N_9O_{12}$   $[M+H]^+$ : 1127.39 Da

HPLC-ESMS(+),  $[M+H]^+$ : 1127.54 Da

Cyclic unprotected peptide

Purification column: SunFire™ Prep C18 OBD™ (5  $\mu$ m  $\times$  19 mm  $\times$  100 mm)

Purification gradient: 30% to 100% of ACN over 40 min with a flow of 15 mL/min

Yield: 15%

Analytical column: SunFire™ C18 (3.5  $\mu$ m  $\times$  4.6 mm  $\times$  100 mm)

HPLC-PDA,  $t_R$  (30% to 100% of ACN over 8 min): 6.04 min

Purity ( $\lambda = 220$  nm): 98%

$m/z$  calculated for  $C_{51}H_{70}N_9O_9$   $[M+H]^+$ : 952.5291 Da

HRMS (NanoESI),  $[M+H]^+$ : 952.5288 Da

#### **Cyclo-[Leu-Thr-Pro-L-*allo*-Ile-Pro-Trp-Phe-Pro]**

Linear precursor

Column: SunFire™ C18 (3.5  $\mu$ m  $\times$  4.6 mm  $\times$  100 mm)

HPLC-PDA,  $t_R$  (5% to 100% of ACN over 8 min): 6.40 min

$m/z$  calculated for  $C_{60}H_{88}N_9O_{12}$   $[M+H]^+$ : 1127.39 Da

HPLC-ESMS(+),  $[M+H]^+$ : 1126.74 Da

Cyclic unprotected peptide

Purification column: SunFire™ Prep C18 OBD™ (5  $\mu$ m  $\times$  19 mm  $\times$  100 mm)

Purification gradient: 52% to 60% of ACN over 20 min with a flow of 15 mL/min

Yield: 28%

Analytical column: SunFire™ C18 (3.5  $\mu$ m  $\times$  4.6 mm  $\times$  100 mm)

HPLC-PDA,  $t_R$  (50% to 65% of ACN over 8 min): 4.84 min

Purity ( $\lambda = 220$  nm): 95%

$m/z$  calculated for  $C_{51}H_{70}N_9O_9$   $[M+H]^+$ : 952.5291 Da

HRMS (NanoESI),  $[M+H]^+$ : 952.5306 Da

#### **Cyclo-[Leu-Thr-D-Pro-Ile-Pro-Trp-Phe-Pro]**

Linear precursor

Column: SunFire™ C18 (3.5  $\mu$ m  $\times$  4.6 mm  $\times$  100 mm)

HPLC-PDA,  $t_R$  (5% to 100% of ACN over 8 min): 4.82 min

$m/z$  calculated for  $C_{60}H_{88}N_9O_{12}$   $[M+H]^+$ : 1127.39 Da

HPLC-ESMS(+),  $[M+H]^+$ : 1127.76 Da

Cyclic unprotected peptide

Purification column: SunFire™ Prep C18 OBD™ (5  $\mu$ m  $\times$  19 mm  $\times$  100 mm)

Purification gradient: 25% to 80% of ACN over 40 min with a flow of 15 mL/min

Yield: 5%

Analytical column: SunFire™ C18 (3.5  $\mu$ m  $\times$  4.6 mm  $\times$  100 mm)

HPLC-PDA,  $t_R$  (30% to 100% of ACN over 8 min): 5.66 min



Purity ( $\lambda = 220$  nm): 100%

$m/z$  calculated for  $C_{51}H_{70}N_9O_9$   $[M+H]^+$ : 952.5291 Da

HRMS (NanoESI),  $[M+H]^+$ : 952.5287 Da

### **Cyclo-[Leu-D-Thr-Pro-Ile-Pro-Trp-Phe-Pro]**

Linear precursor

Column: SunFire™ C18 (3.5  $\mu$ m  $\times$  4.6 mm  $\times$  100 mm)

HPLC-PDA,  $t_R$  (5% to 100% of ACN over 8 min): 6.54 min

$m/z$  calculated for  $C_{60}H_{88}N_9O_{12}$   $[M+H]^+$ : 1127.39 Da

HPLC-ESMS(+),  $[M+H]^+$ : 1127.45 Da

Cyclic unprotected peptide

Purification column: SunFire™ Prep C18 OBD™ (5  $\mu$ m  $\times$  19 mm  $\times$  100 mm)

Purification gradient: 30% to 100% of ACN over 40 min with a flow of 15 mL/min

Yield: 2%

Analytical column: SunFire™ C18 (3.5  $\mu$ m  $\times$  4.6 mm  $\times$  100 mm)

HPLC-PDA,  $t_R$  (30% to 100% of ACN over 8 min): 5.80 min

Purity ( $\lambda = 220$  nm): 94%

$m/z$  calculated for  $C_{51}H_{70}N_9O_9$   $[M+H]^+$ : 952.5291 Da

HRMS (NanoESI),  $[M+H]^+$ : 952.5294 Da

### **Cyclo-[Leu-L-*allo*-Thr-Pro-Ile-Pro-Trp-Phe-Pro]**

Linear precursor

Column: SunFire™ C18 (3.5  $\mu$ m  $\times$  4.6 mm  $\times$  100 mm)

HPLC-PDA,  $t_R$  (35% to 100% of ACN over 8 min): 4.05 min

$m/z$  calculated for  $C_{60}H_{88}N_9O_{12}$   $[M+H]^+$ : 1127.39 Da

HPLC-ESMS(+),  $[M+H]^+$ : 1127.74 Da

Cyclic unprotected peptide

Purification column: SunFire™ Prep C18 OBD™ (5  $\mu$ m  $\times$  19 mm  $\times$  100 mm)

Purification gradient: 50% to 54% of ACN over 20 min with a flow of 15 mL/min

Yield: 21%

Analytical column: SunFire™ C18 (3.5  $\mu$ m  $\times$  4.6 mm  $\times$  100 mm)

HPLC-PDA,  $t_R$  (50% to 65% of ACN over 8 min): 4.09 min

Purity ( $\lambda = 220$  nm): 100%

$m/z$  calculated for  $C_{51}H_{70}N_9O_9$   $[M+H]^+$ : 952.5291 Da

HRMS (NanoESI),  $[M+H]^+$ : 952.5309 Da

### **Cyclo-[D-Leu-Thr-Pro-Ile-Pro-Trp-Phe-Pro]**

Linear precursor

Column: SunFire™ C18 (3.5  $\mu$ m  $\times$  4.6 mm  $\times$  100 mm)

HPLC-PDA,  $t_R$  (5% to 100% of ACN over 8 min): 6.46 min

$m/z$  calculated for  $C_{60}H_{88}N_9O_{12}$   $[M+H]^+$ : 1127.39 Da

HPLC-ESMS(+),  $[M+H]^+$ : 1127.63 Da

Cyclic unprotected peptide

Purification column: SunFire™ Prep C18 OBD™ (5  $\mu$ m  $\times$  19 mm  $\times$  100 mm)

Purification gradient: 30% to 100% of ACN over 20 min with a flow of 15 mL/min

Yield: 4%

Analytical column: SunFire™ C18 (3.5  $\mu$ m  $\times$  4.6 mm  $\times$  100 mm)

HPLC-PDA,  $t_R$  (30% to 100% of ACN over 8 min): 6.04 min

Purity ( $\lambda = 220$  nm): 97%

$m/z$  calculated for  $C_{51}H_{70}N_9O_9$   $[M+H]^+$ : 952.5291 Da

HRMS (NanoESI),  $[M+H]^+$ : 952.5290 Da

### Library of analogs I

### **Cyclo-[Leu-Thr-Pro-Ile-Pro-Trp-Phe-(4-HO-Pro)]**

Linear precursor

Column: Symmetry C18 (5  $\mu$ m  $\times$  4.6 mm  $\times$  150 mm)

HPLC-PDA,  $t_R$  (0% to 100% of ACN over 15 min): 10.10 min

$m/z$  calculated for  $C_{60}H_{88}N_9O_{13}$   $[M+H]^+$ : 1143.39 Da

HPLC-ESMS(+),  $[M+H]^+$ : 1144.03 Da

Cyclic unprotected peptide

Purification column: Symmetry semi-preparative C18 (5  $\mu$ m  $\times$  30 mm  $\times$  100 mm) and Symmetry semi-analytical C18 (5  $\mu$ m  $\times$  7.8 mm  $\times$  100 mm)

Purification gradient: 40% to 100% of ACN over 45 min with a flow of 10 mL/min and 35% to 60% of ACN over 20 min with a flow of 3 mL/min

Yield: 8%

Analytical column: Symmetry C18 (5  $\mu$ m  $\times$  4.6 mm  $\times$  150 mm)

HPLC-PDA,  $t_R$  (0% to 100% of ACN over 15 min): 11.53 min

Purity ( $\lambda = 220$  nm): 100%

$m/z$  calculated for  $C_{51}H_{70}N_9O_{10}$   $[M+H]^+$ : 968.5240 Da

HRMS (NanoESI),  $[M+H]^+$ : 968.5253 Da

#### **Cyclo-[Leu-Thr-Pro-Ile-(4-HO-Pro)-Trp-Phe-Pro]**

Linear precursor

Column: Symmetry C18 (5  $\mu$ m  $\times$  4.6 mm  $\times$  150 mm)

HPLC-PDA,  $t_R$  (0% to 100% of ACN over 15 min): 9.41 min

$m/z$  calculated for  $C_{60}H_{88}N_9O_{13}$   $[M+H]^+$ : 1143.39 Da

HPLC-ESMS(+),  $[M+H]^+$ : 1143.49 Da

Cyclic unprotected peptide

Purification column: Symmetry semi-preparative C8 (5  $\mu$ m  $\times$  30 mm  $\times$  100 mm)

Purification gradient: 30% to 100% of ACN over 30 min with a flow of 15 mL/min

Yield: 34%

Analytical column: Symmetry C18 (5  $\mu$ m  $\times$  4.6 mm  $\times$  150 mm)

HPLC-PDA,  $t_R$  (35% to 70% of ACN over 15 min): 9.90 min

Purity ( $\lambda = 220$  nm): 100%

$m/z$  calculated for  $C_{51}H_{70}N_9O_{10}$   $[M+H]^+$ : 968.5240 Da

HRMS (NanoESI),  $[M+H]^+$ : 968.5242 Da

#### **Cyclo-[Leu-Thr-(4-HO-Pro)-Ile-Pro-Trp-Phe-Pro]**

Linear precursor

Column: Symmetry C18 (5  $\mu$ m  $\times$  4.6 mm  $\times$  150 mm)

HPLC-PDA,  $t_R$  (0% to 100% of ACN over 15 min): 8.68 min

$m/z$  calculated for  $C_{60}H_{88}N_9O_{13}$   $[M+H]^+$ : 1143.39 Da

HPLC-ESMS(+),  $[M+H]^+$ : 1143.42 Da

## Cyclic unprotected peptide

Purification column: Symmetry semi-preparative C18 (5  $\mu\text{m}$   $\times$  30 mm  $\times$  100 mm)

Purification gradient: 30% to 100% of ACN over 45 min with a flow of 10 mL/min

Yield: 29%

Analytical column: Symmetry C18 (5  $\mu\text{m}$   $\times$  4.6 mm  $\times$  150 mm)

HPLC-PDA,  $t_R$  (35% to 70% of ACN over 15 min): 8.71 min

Purity ( $\lambda = 220$  nm): 99%

$m/z$  calculated for  $\text{C}_{51}\text{H}_{70}\text{N}_9\text{O}_{10}$   $[\text{M}+\text{H}]^+$ : 968.5240 Da

HRMS (NanoESI),  $[\text{M}+\text{H}]^+$ : 968.5248 Da

**Cyclo-[Leu-Thr-Pro-Ile-Pro-Trp-Phe-HomoPro]**

## Linear precursor

Column: Symmetry C18 (5  $\mu\text{m}$   $\times$  4.6 mm  $\times$  150 mm)

HPLC-PDA,  $t_R$  (0% to 100% of ACN over 15 min): 10.99 min

$m/z$  calculated for  $\text{C}_{61}\text{H}_{90}\text{N}_9\text{O}_{12}$   $[\text{M}+\text{H}]^+$ : 1141.42 Da

HPLC-ESMS(+),  $[\text{M}+\text{H}]^+$ : 1142.20 Da

## Cyclic unprotected peptide

Purification column: Symmetry semi-preparative C18 (5  $\mu\text{m}$   $\times$  30 mm  $\times$  100 mm)

Purification gradient: 40% to 100% of ACN over 45 min with a flow of 10 mL/min

Yield: 7%

Analytical column: Symmetry C18 (5  $\mu\text{m}$   $\times$  4.6 mm  $\times$  150 mm)

HPLC-PDA,  $t_R$  (45% to 75% of ACN over 15 min): 9.21 min

Purity ( $\lambda = 220$  nm): 100%

$m/z$  calculated for  $\text{C}_{52}\text{H}_{72}\text{N}_9\text{O}_9$   $[\text{M}+\text{H}]^+$ : 966.5448 Da

HRMS (NanoESI),  $[\text{M}+\text{H}]^+$ : 966.5462 Da

**Cyclo-[Leu-Thr-Pro-Ile-HomoPro-Trp-Phe-Pro]**

## Linear precursor

Column: Symmetry C18 (5  $\mu\text{m}$   $\times$  4.6 mm  $\times$  150 mm)

HPLC-PDA,  $t_R$  (0% to 100% of ACN over 15 min): 10.89 min

$m/z$  calculated for  $\text{C}_{61}\text{H}_{90}\text{N}_9\text{O}_{12}$   $[\text{M}+\text{H}]^+$ : 1141.42 Da

HPLC-ESMS(+),  $[\text{M}+\text{H}]^+$ : 1142.13 Da

#### Cyclic unprotected peptide

Purification column: Symmetry semi-preparative C18 (5  $\mu\text{m}$   $\times$  30 mm  $\times$  100 mm) and Symmetry semi-analytical C18 (5  $\mu\text{m}$   $\times$  7.8 mm  $\times$  100 mm)

Purification gradient: 30% to 100% of ACN over 40 min with a flow of 10 mL/min and 40% to 45% of ACN over 30 min with a flow of 3 mL/min

Yield: 1%

Analytical column: Symmetry C18 (5  $\mu\text{m}$   $\times$  4.6 mm  $\times$  150 mm)

HPLC-PDA,  $t_R$  (45% to 75% of ACN over 15 min): 7.73 min

Purity ( $\lambda = 220$  nm): > 80%

$m/z$  calculated for  $\text{C}_{52}\text{H}_{72}\text{N}_9\text{O}_9$   $[\text{M}+\text{H}]^+$ : 966.5448 Da

HRMS (NanoESI),  $[\text{M}+\text{H}]^+$ : 966.5463 Da

#### **Cyclo-[Leu-Thr-HomoPro-Ile-Pro-Trp-Phe-Pro]**

Linear precursor

Column: Symmetry C18 (5  $\mu\text{m}$   $\times$  4.6 mm  $\times$  150 mm)

HPLC-PDA,  $t_R$  (0% to 100% of ACN over 15 min): elutes at 100% of ACN

$m/z$  calculated for  $\text{C}_{61}\text{H}_{90}\text{N}_9\text{O}_{12}$   $[\text{M}+\text{H}]^+$ : 1141.42 Da

HPLC-ESMS(+),  $[\text{M}+\text{H}]^+$ : 1142.00 Da

Cyclic unprotected peptide

Purification column: Symmetry semi-preparative C18 (5  $\mu\text{m}$   $\times$  30 mm  $\times$  100 mm)

Purification gradient: 40% to 100% of ACN over 45 min with a flow of 10 mL/min

Yield: 6%

Analytical column: Symmetry C18 (5  $\mu\text{m}$   $\times$  4.6 mm  $\times$  150 mm)

HPLC-PDA,  $t_R$  (0% to 100% of ACN over 15 min): 12.53 min

Purity ( $\lambda = 220$  nm): 99%

$m/z$  calculated for  $\text{C}_{52}\text{H}_{72}\text{N}_9\text{O}_9$   $[\text{M}+\text{H}]^+$ : 966.5448 Da

HRMS (NanoESI),  $[\text{M}+\text{H}]^+$ : 966.5466 Da

#### **Cyclo-[Leu-Thr-Pro-Ile-Pro-Trp-(Phe-3,4-F<sub>2</sub>)-Pro]**

Linear precursor

Column: Symmetry C18 (5  $\mu\text{m}$   $\times$  4.6 mm  $\times$  150 mm)

HPLC-PDA,  $t_R$  (0% to 100% of ACN over 15 min): 11.49 min

$m/z$  calculated for  $C_{60}H_{86}F_2N_9O_{12}$   $[M+H]^+$ : 1163.37 Da

HPLC-ESMS(+),  $[M+H]^+$ : 1163.27 Da

Cyclic unprotected peptide

Purification column: Symmetry semi-preparative C8 (5  $\mu$ m  $\times$  30 mm  $\times$  100 mm)

Purification gradient: 30% to 100% of ACN over 30 min with a flow of 15 mL/min

Yield: 6%

Analytical column: Symmetry C18 (5  $\mu$ m  $\times$  4.6 mm  $\times$  150 mm)

HPLC-PDA,  $t_R$  (45% to 75% of ACN over 15 min): 9.58 min

Purity ( $\lambda$  = 220 nm): 96%

$m/z$  calculated for  $C_{51}H_{68}F_2N_9O_9$   $[M+H]^+$ : 988.5103 Da

HRMS (NanoESI),  $[M+H]^+$ : 988.5120 Da

### **Cyclo-[Leu-Thr-Pro-Ile-Pro-(Trp-5-F)-Phe-Pro]**

Linear precursor

Column: Symmetry C18 (5  $\mu$ m  $\times$  4.6 mm  $\times$  150 mm)

HPLC-PDA,  $t_R$  (0% to 100% of ACN over 15 min): 9.48 min and 9.72 min

$m/z$  calculated for  $C_{55}H_{79}FN_9O_{10}$   $[M+H]^+$ : 1045.27 Da

HPLC-ESMS(+),  $[M+H]^+$ : 1043.31 Da

Cyclic unprotected peptide

Purification column: Symmetry semi-preparative C18 (5  $\mu$ m  $\times$  30 mm  $\times$  100 mm) and Symmetry semi-analytical C18 (5  $\mu$ m  $\times$  7.8 mm  $\times$  100 mm)

Purification gradient: 5% to 100% of ACN over 30 min with a flow of 10 mL/min and 45% to 50% of ACN over 30 min with a flow of 3 mL/min

Yield: 9% and 10%

Analytical column: Symmetry C18 (5  $\mu$ m  $\times$  4.6 mm  $\times$  150 mm)

HPLC-PDA,  $t_R$  (0% to 100% of ACN over 15 min): 12.29 min and 12.44 min

Purity ( $\lambda$  = 220 nm): > 95%

$m/z$  calculated for  $C_{51}H_{69}FN_9O_9$   $[M+H]^+$ : 970.5197 Da

HRMS (NanoESI),  $[M+H]^+$ : 970.5198 Da

### **Cyclo-[Orn-Thr-Pro-Ile-Pro-Trp-Phe-Pro]**

Cyclic unprotected peptide

Purification column: Symmetry semi-preparative C8 (5  $\mu\text{m}$   $\times$  30 mm  $\times$  100 mm)

Purification gradient: 30% to 100% of ACN over 30 min with a flow of 15 mL/min

Yield: 60%

Analytical column: SunFire™ C18 (3.5  $\mu\text{m}$   $\times$  4.6 mm  $\times$  100 mm)

HPLC-PDA,  $t_R$  (20% to 80% of ACN over 8 min): 5.07 min

Purity ( $\lambda = 220$  nm): 98%

$m/z$  calculated for  $\text{C}_{50}\text{H}_{69}\text{N}_{10}\text{O}_9$   $[\text{M}+\text{H}]^+$ : 953.5244 Da

HRMS (NanoESI),  $[\text{M}+\text{H}]^+$ : 953.5246 Da

### Library of analogs II

### **Cyclo-[Thr-Pro-Ile-Pro-Trp-Phe-Cys( $\psi^{\text{Me,Me}}$ pro)-Leu]**

Linear precursor

Column: SunFire™ C18 (3.5  $\mu\text{m}$   $\times$  4.6 mm  $\times$  100 mm)

HPLC-PDA,  $t_R$  (5% to 100% of ACN over 8 min): 7.09 min

$m/z$  calculated for  $\text{C}_{61}\text{H}_{90}\text{N}_9\text{O}_{12}\text{S}$   $[\text{M}+\text{H}]^+$ : 1173.49 Da

HPLC-ESMS(+),  $[\text{M}+\text{H}]^+$ : 1173.71 Da

Cyclic unprotected peptide

Purification column: SunFire™ Prep C18 OBD™ (5  $\mu\text{m}$   $\times$  19 mm  $\times$  100 mm)

Purification gradient: 5% to 65% of ACN over 5 min and 65% to 100% of ACN over 20 min with a flow of 15 mL/min

Yield: 17%

Analytical column: SunFire™ C18 (3.5  $\mu\text{m}$   $\times$  4.6 mm  $\times$  100 mm)

HPLC-PDA,  $t_R$  (50% to 100% of ACN over 8 min): 5.28 min

Purity ( $\lambda = 220$  nm): 95%

$m/z$  calculated for  $\text{C}_{52}\text{H}_{72}\text{N}_9\text{O}_9\text{S}$   $[\text{M}+\text{H}]^+$ : 998.5168 Da

HRMS (NanoESI),  $[\text{M}+\text{H}]^+$ : 998.5150 Da

**Cyclo-[Leu-Thr-Pro-Ile-Cys( $\psi^{\text{Me,Me}}$ pro)-Trp-Phe-Pro]**

Linear precursor

Column: SunFire™ C18 (3.5  $\mu\text{m}$   $\times$  4.6 mm  $\times$  100 mm)

HPLC-PDA,  $t_R$  (5% to 100% of ACN over 8 min): 6.59 min

$m/z$  calculated for  $\text{C}_{61}\text{H}_{90}\text{N}_9\text{O}_{12}\text{S}$   $[\text{M}+\text{H}]^+$ : 1173.49 Da

HPLC-ESMS(+),  $[\text{M}+\text{H}]^+$ : 1173.57 Da

Cyclic unprotected peptide

Purification column: SunFire™ Prep C18 OBD™ (5  $\mu\text{m}$   $\times$  19 mm  $\times$  100 mm)

Purification gradient: 5% to 65% of ACN over 5 min and 65% to 100% of ACN over 20 min with a flow of 15 mL/min

Yield: 2%

Analytical column: SunFire™ C18 (3.5  $\mu\text{m}$   $\times$  4.6 mm  $\times$  100 mm)

HPLC-PDA,  $t_R$  (50% to 100% of ACN over 8 min): 4.34 min

Purity ( $\lambda = 220$  nm): 100%

$m/z$  calculated for  $\text{C}_{52}\text{H}_{72}\text{N}_9\text{O}_9\text{S}$   $[\text{M}+\text{H}]^+$ : 998.5168 Da

HRMS (NanoESI),  $[\text{M}+\text{H}]^+$ : 998.5161 Da

**Cyclo-[Leu-Thr-Cys( $\psi^{\text{Me,Me}}$ pro)-Ile-Pro-Trp-Phe-Pro]**

Linear precursor

Column: SunFire™ C18 (3.5  $\mu\text{m}$   $\times$  4.6 mm  $\times$  100 mm)

HPLC-PDA,  $t_R$  (5% to 100% of ACN over 8 min): 7.15 min

$m/z$  calculated for  $\text{C}_{61}\text{H}_{90}\text{N}_9\text{O}_{12}\text{S}$   $[\text{M}+\text{H}]^+$ : 1173.49 Da

HPLC-ESMS(+),  $[\text{M}+\text{H}]^+$ : 1172.70 Da

Cyclic unprotected peptide

Purification column: SunFire™ Prep C18 OBD™ (5  $\mu\text{m}$   $\times$  19 mm  $\times$  100 mm)

Purification gradient: 5% to 65% of ACN over 5 min and 65% to 100% of ACN over 20 min with a flow of 15 mL/min

Yield: 10%

Analytical column: SunFire™ C18 (3.5  $\mu\text{m}$   $\times$  4.6 mm  $\times$  100 mm)

HPLC-PDA,  $t_R$  (50% to 100% of ACN over 8 min): 5.49 min

Purity ( $\lambda = 220$  nm): 100%

$m/z$  calculated for  $\text{C}_{52}\text{H}_{72}\text{N}_9\text{O}_9\text{S}$   $[\text{M}+\text{H}]^+$ : 998.5168 Da



HRMS (NanoESI), [M+H]<sup>+</sup>: 998.5170 Da

**Cyclo-[Thr-Pro-Ile-Cys( $\psi^{\text{Me,Me}}$ pro)-Trp-Phe-Cys( $\psi^{\text{Me,Me}}$ pro)-Leu]**

Linear precursor

Column: SunFire™ C18 (3.5  $\mu\text{m}$   $\times$  4.6 mm  $\times$  100 mm)

HPLC-PDA,  $t_{\text{R}}$  (5% to 100% of ACN over 8 min): 7.68 min

$m/z$  calculated for C<sub>62</sub>H<sub>92</sub>N<sub>9</sub>O<sub>12</sub>S<sub>2</sub> [M+H]<sup>+</sup>: 1219.58 Da

HPLC-ESMS(+), [M+H]<sup>+</sup>: 1219.60 Da

Cyclic unprotected peptide

Purification column: SunFire™ Prep C18 OBD™ (5  $\mu\text{m}$   $\times$  19 mm  $\times$  100 mm)

Purification gradient: 5% to 60% of ACN over 5 min and 60% to 90% of ACN over 20 min with a flow of 15 mL/min

Yield: 16%

Analytical column: SunFire™ C18 (3.5  $\mu\text{m}$   $\times$  4.6 mm  $\times$  100 mm)

HPLC-PDA,  $t_{\text{R}}$  (50% to 100% of ACN over 8 min): 6.24 min

Purity ( $\lambda$  = 220 nm): 94%

$m/z$  calculated for C<sub>53</sub>H<sub>74</sub>N<sub>9</sub>O<sub>9</sub>S<sub>2</sub> [M+H]<sup>+</sup>: 1044.5045 Da

HRMS (NanoESI), [M+H]<sup>+</sup>: 1044.5029 Da

**Cyclo-[Thr-Cys( $\psi^{\text{Me,Me}}$ pro)-Ile-Pro-Trp-Phe-Cys( $\psi^{\text{Me,Me}}$ pro)-Leu]**

Linear precursor

Column: SunFire™ C18 (3.5  $\mu\text{m}$   $\times$  4.6 mm  $\times$  100 mm)

HPLC-PDA,  $t_{\text{R}}$  (20% to 100% of ACN over 8 min): 7.84 min

$m/z$  calculated for C<sub>62</sub>H<sub>92</sub>N<sub>9</sub>O<sub>12</sub>S<sub>2</sub> [M+H]<sup>+</sup>: 1219.58 Da

HPLC-ESMS(+), [M+H]<sup>+</sup>: 1219.36 Da

Cyclic unprotected peptide

Purification column: SunFire™ Prep C18 OBD™ (5  $\mu\text{m}$   $\times$  19 mm  $\times$  100 mm)

Purification gradient: 5% to 50% of ACN over 5 min and 50% to 90% of ACN over 20 min with a flow of 15 mL/min

Yield: 18%

Analytical column: SunFire™ C18 (3.5  $\mu\text{m}$   $\times$  4.6 mm  $\times$  100 mm)

HPLC-PDA,  $t_{\text{R}}$  (50% to 100% of ACN over 8 min): 6.09 min

Purity ( $\lambda = 220$  nm): 100%

$m/z$  calculated for  $C_{53}H_{74}N_9O_9S_2$   $[M+H]^+$ : 1044.5045 Da

HRMS (NanoESI),  $[M+H]^+$ : 1044.5029 Da

**Cyclo-[Leu-Thr-Cys( $\psi^{Me,Me}$ pro)-Ile-Cys( $\psi^{Me,Me}$ pro)-Trp-Phe-Pro]**

Linear precursor

Column: SunFire™ C18 (3.5  $\mu$ m  $\times$  4.6 mm  $\times$  100 mm)

HPLC-PDA,  $t_R$  (5% to 100% of ACN over 8 min): 7.37 min

$m/z$  calculated for  $C_{62}H_{92}N_9O_{12}S_2$   $[M+H]^+$ : 1219.58 Da

HPLC-ESMS(+),  $[M+H]^+$ : 1219.23 Da

Cyclic unprotected peptide

Purification column: SunFire™ Prep C18 OBD™ (5  $\mu$ m  $\times$  19 mm  $\times$  100 mm)

Purification gradient: 5% to 50% of ACN over 5 min and 50% to 90% of ACN over 20 min with a flow of 15 mL/min

Yield: 34%

Analytical column: SunFire™ C18 (3.5  $\mu$ m  $\times$  4.6 mm  $\times$  100 mm)

HPLC-PDA,  $t_R$  (50% to 100% of ACN over 8 min): 3.35 min

Purity ( $\lambda = 220$  nm): 92%

$m/z$  calculated for  $C_{53}H_{74}N_9O_9S_2$   $[M+H]^+$ : 1044.5045 Da

HRMS (NanoESI),  $[M+H]^+$ : 1044.5051 Da

**Cyclo-[Thr-Cys( $\psi^{Me,Me}$ pro)-Ile-Cys( $\psi^{Me,Me}$ pro)-Trp-Phe-Cys( $\psi^{Me,Me}$ pro)-Leu]**

Linear precursor

Column: SunFire™ C18 (3.5  $\mu$ m  $\times$  4.6 mm  $\times$  100 mm)

HPLC-PDA,  $t_R$  (5% to 100% of ACN over 8 min): 7.37 min

$m/z$  calculated for  $C_{63}H_{94}N_9O_{12}S_3$   $[M+H]^+$ : 1265.67 Da

HPLC-ESMS(+),  $[M+H]^+$ : 1267.30 Da

Cyclic unprotected peptide

Purification column: SunFire™ Prep C18 OBD™ (5  $\mu$ m  $\times$  19 mm  $\times$  100 mm)

Purification gradient: 5% to 50% of ACN over 5 min and 50% to 90% of ACN over 20 min with a flow of 15 mL/min

Yield: 32%

Analytical column: SunFire™ C18 (3.5  $\mu\text{m}$   $\times$  4.6 mm  $\times$  100 mm)

HPLC-PDA,  $t_{\text{R}}$  (50% to 100% of ACN over 8 min): 4.06 min

Purity ( $\lambda = 220$  nm): 98%

$m/z$  calculated for  $\text{C}_{54}\text{H}_{76}\text{N}_9\text{O}_9\text{S}_3$   $[\text{M}+\text{H}]^+$ : 1090.4923 Da

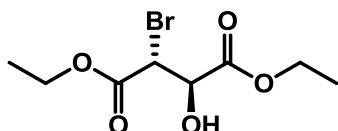
HRMS (NanoESI),  $[\text{M}+\text{H}]^+$ : 1090.4937 Da

## 1.5. Pipecolidepsins

### 1.5.1. Synthesis of building blocks

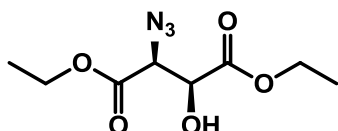
#### 1.5.1.1. Synthesis of Fmoc-L-threo-EtO-Asn(Trt)-OH

##### Diethyl (2R,3R)-2-hydroxy-3-bromosuccinate (1)



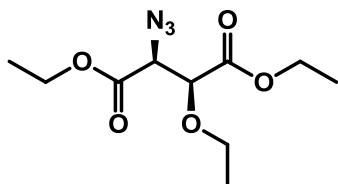
For experimental procedure and chemical characterization, check article: Mori, K., Iwasawa, H. *Tetrahedron* **1980**, 36 (1), 87-90.

##### Diethyl (2S,3S)-2-azido-3-hydroxysuccinate (2)

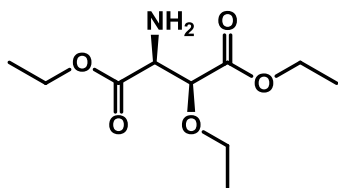


For experimental procedure and chemical characterization, check article: Charvillon, F. B., Amouroux, R. *Synthetic Commun.* **1997**, 27(3), 395-403.

##### Diethyl (2S,3S)-2-azido-3-ethoxysuccinate (3) (as a diastereomeric mixture)

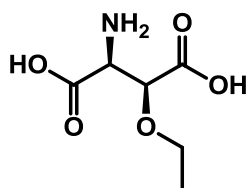


A solution of (2S,3S)-2-azido-3-hydroxysuccinate **2** (10.02 g, 43.34 mmol, 1 equiv) and iodoethane (35.1 g, 18 mL, 225.04 mmol, 5.2 equiv) in  $\text{Et}_2\text{O}$  (200 mL) was placed in a round bottomed flask equipped with a condenser and stirred with a mixture of  $\text{Ag}_2\text{O}$  (13 g, 56.10 mmol, 1.3 equiv) and sand (50 g) at 37  $^\circ\text{C}$  for 15 h (the sand was added to prevent that the  $\text{Ag}_2\text{O}$  sticks together). When TLC analysis revealed complete conversion, the solution was filtered and concentrated under *vacuo*. The residue was purified by flash column chromatography (isocratic hexane-EtOAc = 2:1) to give 10.0 g (89%) of the product **3** as a yellow oil. The product was a mixture of diastereomers and some side products were also present. It was used in the next step without further purification.  $^1\text{H}$  NMR (400 MHz,  $\text{CDCl}_3$ )  $\delta$  1.16-1.40 (24H, m, ca.), 3.39-3.59 (2H, m, ca.), 3.66 (1H, m, ca.), 3.79-3.91 (2H, m, ca.), 4.17-4.39 (14H, m), 4.43 (1H, d,  $J = 3.6$  Hz).

**Diethyl (2S,3S)-2-amino-3-ethoxysuccinate (4)**

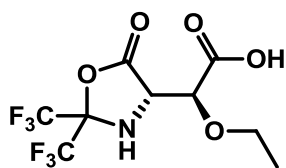
A solution of **3** (as a diastereomeric mixture) (10.0 g, 38.57 mmol) in EtOAc (150 mL) was stirred with Pd-C (5% Pd, 0.5 g) under an atmosphere of H<sub>2</sub> (air pressure) for 15 h. When TLC revealed complete conversion, it was filtered through celite and concentrated under *vacuo*. The diastereomers were partially separated by flash column chromatography (isocratic DCM-MeOH-AcOH = 10:1:0.5). The fractions with product were sampled and concentrated under *vacuo*. HOAc was removed by co-evaporations with toluene to give 7.85 g (87%) of the product **4** as a yellow oil with ca. 10% of the (2*R*,3*S*)-diastereomer (detected by NMR). <sup>1</sup>H NMR (400 MHz, CDCl<sub>3</sub>) δ 1.17 (3H, m, CH<sub>3</sub>, EtO), 1.29 (6H, m, CH<sub>3</sub>, COOEt), 3.40 (1H, m, CH<sub>2</sub>, EtO), 3.76 (1H, m, CH<sub>2</sub>, EtO), 3.89 (1H, d, *J* = 3.0 Hz, CH<sup>2</sup>), 4.18-4.27 (4H, m, CH<sub>2</sub>, COOEt), 4.33 (1H, d, *J* = 3.0 Hz, CH<sup>3</sup>); <sup>13</sup>C NMR (100 MHz, CDCl<sub>3</sub>) δ 14.1 (CH<sub>3</sub>, COOEt), 14.8 (CH<sub>3</sub>, EtO), 56.8 (CH<sup>2</sup>), 61.3 (CH<sub>2</sub>, COOEt), 61.5 (CH<sub>2</sub>, COOEt), 67.0 (CH<sub>2</sub>, EtO), 79.1 (CH<sup>3</sup>), 170.3 (COO); HRMS (ES<sup>+</sup>) *m/z* calculated for C<sub>10</sub>H<sub>19</sub>NNaO<sub>5</sub> [M+Na]<sup>+</sup> 256.1161, found 256.1154.

**Diethyl (2*R*,3*S*)-2-amino-3-ethoxysuccinate:** <sup>1</sup>H NMR (400 MHz, CDCl<sub>3</sub>) δ 1.19-1.32 (9H, m, CH<sub>3</sub>, EtO, COOEt), 3.49 (1H, m, CH<sub>2</sub>, EtO), 3.80 (1H, m, CH<sub>2</sub>, EtO), 3.98 (1H, d, *J* = 3.0 Hz, CH<sup>2</sup>), 4.14-4.28 (5H, m, CH<sub>2</sub>, COOEt, CH<sup>3</sup>).

**(2S,3S)-2-amino-3-ethoxysuccinic acid (5)**

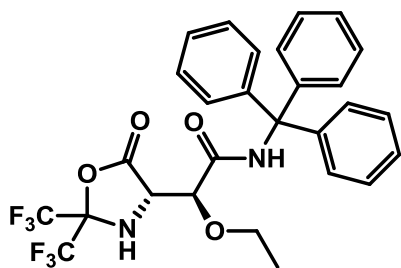
Diethyl (2*S*,3*S*)-2-amino-3-ethoxysuccinate **4** (7.85 g, 33.65 mmol) was refluxed with stirring in 5 M aqueous HCl (100 mL) for 5 h. When TLC revealed complete conversion, the solution was concentrated under *vacuo* at 70 °C. The residue was dissolved in THF (30 mL) and propylene oxide (10 mL) was added dropwise. The supernatant was removed by suction and the precipitate was dried under *vacuo* to give 5.01 g (84%) of the acid **5** as a white solid. The <sup>1</sup>H and <sup>13</sup>C NMR spectra showed approx. 10% contamination with the (2*R*,3*S*)-diastereomer. <sup>1</sup>H NMR (400 MHz, DMSO-*d*<sub>6</sub>) δ 1.13 (3H, m, CH<sub>3</sub>, EtO), 3.42 (1H, m, CH<sub>2</sub>, EtO), 3.72 (1H, d, *J* = 9.2 Hz, CH<sup>2</sup>), 3.79 (1H, m, CH<sub>2</sub>, EtO), 3.92 (1H, d, *J* = 9.2 Hz, CH<sup>4</sup>); <sup>13</sup>C NMR (400 MHz, DMSO-*d*<sub>6</sub>) δ 14.9 (CH<sub>3</sub>, EtO), 53.4 (CH<sup>2</sup>), 66.4 (CH<sub>2</sub>, EtO), 75.2 (CH<sup>3</sup>), 168.4 (COOH), 170.9 (COOH); HRMS (ES<sup>-</sup>) *m/z* calculated for C<sub>6</sub>H<sub>10</sub>NO<sub>5</sub> [M-H]<sup>-</sup> 176.0559, found 176.0562.

**(2*R*,3*S*)-2-amino-3-ethoxysuccinic acid:** <sup>13</sup>C NMR (400 MHz, DMSO-*d*<sub>6</sub>) δ 14.7 (CH<sub>3</sub>, EtO), 53.8 (CH<sup>2</sup>), 65.5 (CH<sub>2</sub>, EtO), 79.7 (CH<sup>3</sup>), 167.9 (COOH), 170.1 (COOH).

**(2S)-2-Ethoxy-2-[(4S)-5-oxo-2,2-bis-trifluoromethyl-oxazolidin-4-yl]-acetic acid (6)**

A solution of **5** (3.73 g, 21.05 mmol) in DMF (20 mL) was stirred under an atmosphere of dry hexafluoroacetone for 22 h (uptake of 8.8 g). DMF was removed at 1 mm Hg at 55 °C and the residue was purified by flash column chromatography (isocratic hexane-EtOAc-HOAc = 1:1:0.05). The fractions with product were pooled and concentrated under *vacuo*. HOAc was removed by co-evaporations with toluene to give 5.65 g (83%) of **6** as a yellow oil. The  $^1\text{H}$  and  $^{13}\text{C}$  NMR spectra showed ca. 10% contamination with the (2*R*,3*S*-diastereomer).  $^1\text{H}$  NMR (400 MHz, acetone- $d_6$ )  $\delta$  1.15 (3H, t,  $J = 7.0, 7.0$  Hz,  $\text{CH}_3$ , EtO), 3.52 (1H, m,  $\text{CH}_2$ , EtO), 3.85 (1H, m,  $\text{CH}_2$ , EtO), 4.32 (1H, d,  $J = 2.6$  Hz,  $\text{CH}^2$ ), 4.66 (1H, dd,  $J = 7.0, 2.4$  Hz,  $\text{CH}^{4'}$ ), 5.09 (1H, d,  $J = 6.8$  Hz, NH);  $^{19}\text{F}$  NMR (400 MHz, acetone- $d_6$ )  $\delta$  -80.14 (3F, q,  $J = 9.0$  Hz,  $\text{CF}_3$ ), -80.31 (3F, q,  $J = 9.2$  Hz,  $\text{CF}_3$ );  $^{13}\text{C}$  NMR (400 MHz,  $\text{CDCl}_3$ )  $\delta$  14.6 ( $\text{CH}_3$ , EtO), 58.1 ( $\text{CH}^{4'}$ ), 63.3 ( $\text{CH}_2$ , EtO), 75.2 ( $\text{CH}^2$ ), 89.4 (m, Cq), 119.95 (q,  $J = 285.7$  Hz,  $\text{CF}_3$ ), 120.99 (q,  $J = 287.5$  Hz,  $\text{CF}_3$ ), 169.2 (COO), 174.3 (COO); HRMS (ES-)  $m/z$  calculated for  $\text{C}_9\text{H}_8\text{F}_6\text{NO}_5$  [ $\text{M}-\text{H}$ ] $^-$  325.0307, found 325.0309.

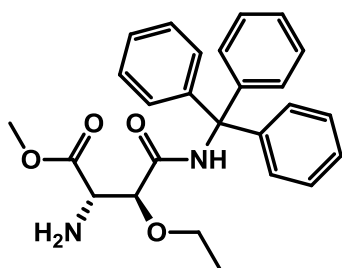
**(2R)-2-Ethoxy-2-[(4S)-5-oxo-2,2-bis-trifluoromethyl-oxazolidin-4-yl]-acetic acid:**  $^{19}\text{F}$  NMR (400 MHz, acetone- $d_6$ )  $\delta$  -80.31 (0.3F approx., q,  $J = 9.0$  Hz,  $\text{CF}_3$ ), -80.31 (0.3F approx., q,  $J = 9.2$  Hz,  $\text{CF}_3$ ).

**(2S)-2-Ethoxy-2-[(4S)-5-oxo-2,2-bis-trifluoromethyl-oxazolidin-4-yl]-*N*-trityl-acetamide (7)**

Oxazolidinone **6** (2.28 mg, 7.01 mmol, 1 equiv) was dissolved in oxalyl chloride (10 mL) and five drops of DMF were added. The mixture was stirred for 30 min. The excess of oxalyl chloride was removed under *vacuo* and the residue was co-evaporated with dry toluene (20 mL). The resulting acid chloride was directly converted without further purification.  $^1\text{H}$  NMR (400 MHz,  $\text{CDCl}_3$ )  $\delta$  1.22 (3H, t,  $J = 6.7$  Hz,  $\text{CH}_3$ ), 3.39 (1H, br d,  $J = 8.5$  Hz, NH), 3.59 (1H, m,  $\text{CH}_2$ , EtO), 3.88 (1H, m,  $\text{CH}_2$ , EtO), 4.42 (1H, m,  $\text{CH}^{4'}$ ), 4.52 (1H, d,  $J = 2.0$  Hz,  $\text{CH}^2$ );  $^{19}\text{F}$  NMR (400 MHz,  $\text{CDCl}_3$ )  $\delta$  -79.07 (3F, q,  $J = 8.4$  Hz,  $\text{CF}_3$ ), -80.78 (3F, q,  $J = 8.5$  Hz,  $\text{CF}_3$ ); **(2R)-Diastereomer:**  $^{19}\text{F}$  NMR (400 MHz,  $\text{CDCl}_3$ )  $\delta$  -79.87 (0.3F approx., q,  $J = 8.5$  Hz,  $\text{CF}_3$ ), -80.53 (0.3F approx., q,  $J = 8.5$  Hz,  $\text{CF}_3$ ). The acid chloride of **6** was dissolved in dry toluene (10 mL) and dropped into a solution of tritylamine (3.82 g, 14.72 mmol, 2.1 equiv) in dry toluene (30 mL) at 0 °C. After 1 h of stirring at this temperature, the suspension was filtered and the precipitate washed with toluene (4  $\times$  10 mL). The combined layers were concentrated under

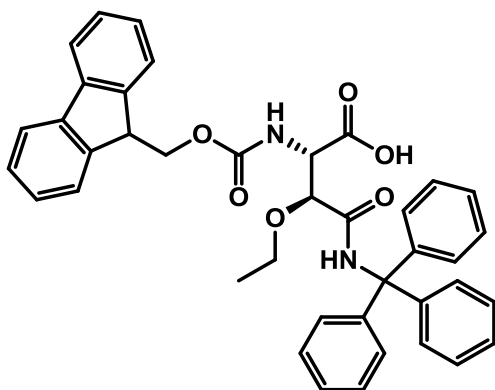
*vacuo* and the residue purified by flash column chromatography (isocratic hexane-EtOAc = 2:1). The undesired diastereomer was completely separated and eluted in a mixture with tritylamine. After the column, the product was dissolved in H<sub>2</sub>O-ACN and lyophilized to give 2.36 g (59%) of diastereomerically pure product **7**. <sup>1</sup>H NMR (400 MHz, CDCl<sub>3</sub>) δ 1.26 (3H, t, *J* = 7.0 Hz, CH<sub>3</sub>, EtO), 2.76 (1H, d, *J* = 7.9 Hz, NH), 3.78 (2H, m, CH<sub>2</sub>, EtO), 4.23 (1H, d, *J* = 2.1 Hz, CH<sup>2</sup>), 4.48 (1H, dd, *J* = 7.8, 1.8 Hz, CH<sup>4</sup>), 7.22-7.33 (15H, CH, Ar, Trt), 8.08 (1H, br s, CONH); <sup>19</sup>F NMR (400 MHz, acetone-*d*<sub>6</sub>) δ -80.16 (3F, q, *J* = 8.6 Hz, CF<sub>3</sub>), -80.79 (3F, q, *J* = 8.5 Hz, CF<sub>3</sub>); <sup>13</sup>C NMR (400 MHz, CDCl<sub>3</sub>) δ 15.2 (CH<sub>3</sub>, EtO), 57.9 (CH<sup>4</sup>), 69.4 (CH<sub>2</sub>, EtO), 70.4 (Cq, Trt), 78.7 (CH<sup>2</sup>), 89.5 (m, Cq), 120.0 (q, *J* = 284.6 Hz, CF<sub>3</sub>), 121.0 (q, *J* = 287.4 Hz, CF<sub>3</sub>), 127.3 (CH, Ar, Trt), 128.1 (CH, Ar, Trt), 128.4 (CH, Ar, Trt), 144.0 (Cq, Ar, Trt), 168.0 (COO), 169.2 (COO); HRMS (ES+) *m/z* calculated for C<sub>28</sub>H<sub>25</sub>F<sub>6</sub>N<sub>2</sub>O<sub>4</sub> [M+H]<sup>+</sup> 567.1719, found 567.1712.

#### (2*S*,3*S*)-2-Amino-3-ethoxy-*N*-trityl-succinamic acid methyl ester hydrochloride (**8**)

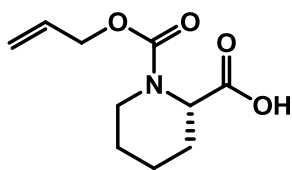


A solution of dry HCl 4 M in dioxane (60 mL) was added to a solution of the acetamide **7** (2.98 g, 4.72 mmol) in MeOH (60 mL) at 0 °C, and the resulting mixture was stirred (closed flask) for 15 h. After checking complete conversion by HPLC-PDA, the volatiles were removed under *vacuo* and the residue was treated with Et<sub>2</sub>O (30 mL). The solid precipitate was dried

under *vacuo* to give 2.1 g (95%) of **8** as a hygroscopic acid. <sup>1</sup>H NMR (400 MHz, DMSO-*d*<sub>6</sub>) δ 1.08 (3H, t, *J* = 7.0 Hz, CH<sub>3</sub>, EtO), 3.51 (2H, m, CH<sub>2</sub>, EtO), 3.70 (3H, s, COOMe), 4.36 (1H, d, *J* = 5.9 Hz, CH<sup>2</sup>), 4.49 (1H, d, *J* = 5.9 Hz, CH<sup>3</sup>), 7.18-7.33 (15H, CH, Ar, Trt), 8.99 (1H, s, CONH); <sup>13</sup>C NMR (400 MHz, DMSO-*d*<sub>6</sub>) δ 14.9 (CH<sub>3</sub>, EtO), 52.4 (COOMe), 54.3 (CH<sup>2</sup>), 66.3 (CH<sub>2</sub>, EtO), 69.5 (Cq, Trt), 78.4 (CH<sup>3</sup>), 126.7 (CH, Ar, Trt), 127.6 (CH, Ar, Trt), 128.3 (CH, Ar, Trt), 144.2 (Cq, Ar, Trt), 167.9 (CO), 171.9 (CO); HRMS (ES+) *m/z* calculated for C<sub>26</sub>H<sub>29</sub>N<sub>2</sub>O<sub>4</sub> [M+H]<sup>+</sup> 433.2127, found 433.2119.

**(2S,3S)-2-(9H-Fluoren-9-yl)methoxycarbonylamino-3-ethoxy-N-trityl-succinic acid (9)**

A solution of KOH (1.22 g, 21.85 mmol, 5 equiv) in H<sub>2</sub>O (20 mL) was added to a solution of **8** (1.89 g, 4.37 mmol, 1 equiv) in dioxane (40 mL) at 0 °C. After 1 h of stirring, TLC revealed complete conversion. Glacial HOAc (1.25 mL) was added and the solution was cooled down to 0 °C. After addition of Fmoc-OSu (2.21 g, 6.55 mmol, 1.5 equiv), DIEA was dropped into the milky suspension until pH 9 was reached (ca. 2 mL). After 1 h of stirring, dioxane was removed under *vacuo* and 1 M aqueous HCl (100 mL) was added. The product was extracted with EtOAc (× 3) and the combined organic layers were dried over MgSO<sub>4</sub>, filtered and concentrated under *vacuo*. The residue was purified by flash column chromatography (hexane-EtOAc = 3:2 to elute the Fmoc-OSu and hexane-EtOAc-AcOH = 1:1:0.05 to elute the product). The HOAc was removed by co-evaporations with toluene to give 1.98 g (70%) of **9** as a foamy white solid. <sup>1</sup>H NMR (400 MHz, DMSO-*d*<sub>6</sub>) δ 1.17 (3H, t, *J* = 7.0 Hz, CH<sub>3</sub>, EtO), 3.57 (1H, m, CH<sub>2</sub>, EtO), 3.72 (1H, m, CH<sub>2</sub>, EtO), 4.07 (1H, m, CH, Fmoc), 4.19 (1H, m, CH<sup>2</sup>), 4.34 (1H, d, *J* = 2.9 Hz, CH<sup>3</sup>), 4.39 (2H, m, CH<sub>2</sub>, Fmoc), 7.14-7.33 (17H, CH, Ar, Fmoc, Trt), 7.37-7.44 (2H, CH, Ar, Fmoc), 7.81 (1H, d, *J* = 7.5 Hz, CH, Ar, Fmoc), 7.86-7.91 (3H, m, CH, Ar, Fmoc), 7.99 (1H, d, *J* = 9.3 Hz, CONH), 8.40 (1H, s, CONH); <sup>13</sup>C NMR (400 MHz, DMSO-*d*<sub>6</sub>) δ 15.0 (CH<sub>3</sub>, EtO), 46.5 (CH, Fmoc), 55.9 (CH<sup>2</sup>), 66.2 (CH<sub>2</sub>, EtO), 67.1 (CH<sub>2</sub>, Fmoc), 69.3 (Cq, Trt), 80.1 (CH<sup>3</sup>), 119.9 (CH, Ar, Fmoc), 120.0 (CH, Ar, Fmoc), 125.4 (CH, Ar, Fmoc), 125.8 (CH, Ar, Fmoc), 126.5 (CH, Ar, Fmoc), 126.9 (CH, Ar, Trt), 127.0 (CH, Ar, Fmoc), 127.5 (CH, Ar, Fmoc), 127.6 (CH, Ar, Fmoc), 127.6 (CH, Ar, Trt), 128.4 (CH, Ar, Trt), 140.6 (Cq, Ar, Fmoc), 140.8 (Cq, Ar, Fmoc), 143.5 (Cq, Ar, Fmoc), 143.7 (Cq, Ar, Fmoc), 144.3 (Cq, Ar, Trt), 156.3 (OCONH), 167.9 (CO), 171.3 (CO); HRMS (ES<sup>+</sup>) *m/z* calculated for C<sub>40</sub>H<sub>37</sub>N<sub>2</sub>O<sub>6</sub> [M+H]<sup>+</sup> 641.2652, found 641.2649.

**1.5.1.2. Synthesis of Alloc-pipecolic-OH (10)**

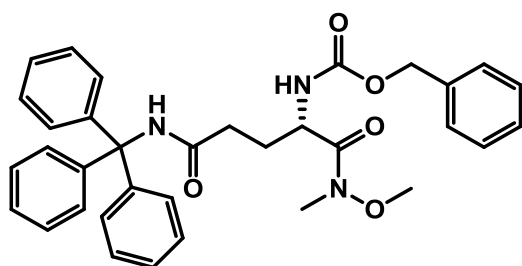
To a solution of H-pipecolic-OH (500 mg, 3.87 mmol) in 2% aqueous Na<sub>2</sub>CO<sub>3</sub>-dioxane (1:1, 20 mL), Alloc-Cl (823 μL, 7.74 mmol) was dropped and the pH re-adjusted to 8-9 by addition of 3 M aqueous NaOH solution. The reaction mixture was stirred overnight at room temperature. The pH was re-adjusted again to 8-9, the dioxane was eliminated under reduced pressure, and the aqueous layer was washed with TBME (× 3), acidified to pH 2 by

adding 4 M aqueous HCl and extracted with EtOAc ( $\times 3$ ). The combined organic layer was washed with brine, dried over  $\text{Na}_2\text{SO}_4$ , filtrated and concentrated under *vacuo*. The residue was purified by flash column chromatography (DCM-MeOH = 100:0 to 95:5) to give 775.2 mg (94%) of Alloc-pipecolic-OH **10** as a yellowish oil.  $^1\text{H}$  NMR (400 MHz,  $\text{CDCl}_3$ )  $\delta$  1.34 (1H, m,  $\text{CH}_2^\gamma$ ), 1.42 (1H, m,  $\text{CH}_2^\delta$ ), 1.67 (1H, m,  $\text{CH}_2^\delta$ ), 1.71 (1H, m,  $\text{CH}_2^\beta$ ), 1.73 (1H, m,  $\text{CH}_2^\gamma$ ), 2.26 (1H, m,  $\text{CH}_2^\beta$ ), 3.02 (1H, m,  $\text{CH}_2^\epsilon$ ), 4.07 (1H, dd,  $J = 26.8, 12.8$  Hz,  $\text{CH}_2^\epsilon$ ), 4.62 (2H, m,  $\text{CH}_2$ , Allyl), 4.94 (1H, dd,  $J = 34.6, 4.1$  Hz,  $\text{CH}^\alpha$ ), 5.22 (1H, dd,  $J = 18.9, 9.0$  Hz,  $\text{CH}_2$ ,  $\text{H}_{trans}$ , Allyl), 5.31 (1H, d,  $J = 16.5$  Hz,  $\text{CH}_2$ ,  $\text{H}_{cis}$ , Allyl), 5.93 (1H, m, CH, Allyl);  $^{13}\text{C}$  NMR (400 MHz,  $\text{CDCl}_3$ )  $\delta$  20.67 ( $\text{CH}_2^\gamma$ ), 24.63 ( $\text{CH}_2^\delta$ ), 26.53 ( $\text{CH}_2^\beta$ ), 41.83 ( $\text{CH}_2^\epsilon$ ), 54.07 ( $\text{CH}^\alpha$ ), 66.42 ( $\text{CH}_2$ , Allyl), 117, 44 ( $\text{CH}_2$ , Allyl), 132.76 (CH, Allyl), 156.53 (OCONH), 176.95 (COO).

### 1.5.1.3. Synthesis of Fmoc-DADHOHA(Acetonide, Trt)-OH

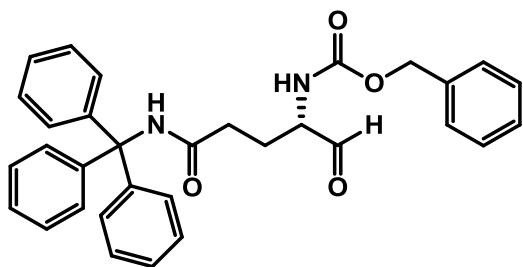
#### Route A

#### [(S)-*N*<sup>1</sup>-methoxy-*N*<sup>1</sup>-methyl-2-(2-phenylacetamido)-*N*<sup>5</sup>-tritylpentanediamide] (**11**)

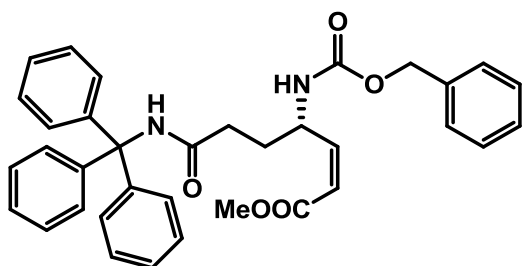


To a solution of Z-L-Gln(Trt)-OH (5 g, 9.57 mmol, 1 equiv) in dry DMF (15 mL), HOBT $\cdot$ H $_2$ O (1.758 g, 11.48 mmol, 1.2 equiv) and EDC (2.201 g, 11.48 mmol, 1.2 equiv) were added at room temperature. After 30 min of stirring under Ar, a solution of N,O-dimethylhydroxylamine hydrochloride (1.213 g, 12.44 mmol, 1.3 equiv) and DIEA (2.17 mL, 12.43 mmol, 1.3 equiv) in dry DMF (10 mL) was added dropwise and the reaction mixture was reacted for 3 h. Saturated aqueous  $\text{NaHCO}_3$  was added and the aqueous layer was extracted with EtOAc ( $\times 3$ ). The combined organic layer was washed twice with 0.1 M aqueous HCl, once with brine, dried over  $\text{Na}_2\text{SO}_4$ , filtrated and concentrated under *vacuo* to give 5.20 g of the Weinreb amide **11** (96%) as a white solid which was used in the next reaction without further purification.  $^1\text{H}$  NMR (400 MHz,  $\text{CDCl}_3$ )  $\delta$  1.83 (1H, m,  $\text{CH}_2^3$ ), 2.14 (1H, m,  $\text{CH}_2^3$ ), 2.37 (2H, m,  $\text{CH}_2^4$ ), 3.17 (3H, s, N- $\text{CH}_3$ ), 3.65 (3H, s, O- $\text{CH}_3$ ), 4.75 (1H, m,  $\text{CH}^2$ ), 5.08 (2H, m, Z), 5.66 (1H, d,  $J = 8.4$  Hz, OCONH), 6.93 (1H, s, CONH), 7.19-7.36 (20H, m, Trt, Z);  $^{13}\text{C}$  NMR (400 MHz,  $\text{CDCl}_3$ )  $\delta$  29.20 ( $\text{CH}_2^3$ ), 32.34 (N- $\text{CH}_3$ ), 33.63 ( $\text{CH}_2^4$ ), 50.86 ( $\text{CH}^2$ ), 61.77 (O- $\text{CH}_3$ ), 67.18, ( $\text{CH}_2$ , Z), 70.81 (Cq, Trt), 127.15 (CH, Ar, Trt), 128.12 (CH, Ar, Trt), 128.38 (CH, Ar, Z), 128.71 (CH, Ar, Z), 128.98 (CH, Ar, Trt), 136.50 (Cq, Z), 144.97 (Cq, Ar, Trt), 156.66 (OCONH), 171.03 (CO), 172.29 (CO); HRMS (NanoESI)  $m/z$  calculated for  $\text{C}_{34}\text{H}_{36}\text{N}_3\text{O}_5$  [ $\text{M}+\text{H}$ ] $^+$  566.2650, found 566.2651.



**(S)-5-oxo-4-(2-phenylacetamido)-N-tritylpentanamide (12)**

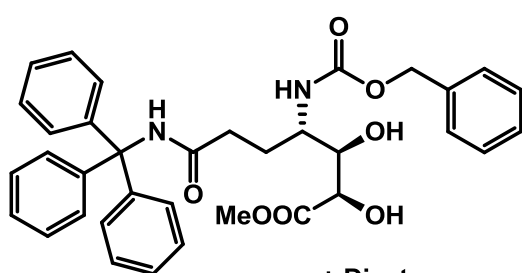
To a solution of Weinreb amide **11** (1.54 g, 1.66 mmol, 1 equiv) in dry THF (10 mL) at 0 °C, a pre-cooled suspension of LiAlH<sub>4</sub> (164.9 mg, 4.35 mmol, 2.6 equiv) in dry THF (5 mL) was added dropwise. After 30 min of stirring at 0 °C, the reaction was quenched with a 5% aqueous KHSO<sub>4</sub> solution keeping the ice bath. The aqueous layer was extracted with EtOAc (× 3) and the combined organic layer was washed once with brine, dried over Na<sub>2</sub>SO<sub>4</sub>, filtrated and concentrated under *vacuo* to give 1.34 g of crude aldehyde **12** (97%) as a white solid, which was used in the next reaction without further purification. <sup>1</sup>H NMR (400 MHz, CDCl<sub>3</sub>) δ 1.84 (1H, m, CH<sub>2</sub><sup>3</sup>), 2.22 (1H, m, CH<sub>2</sub><sup>3</sup>), 2.37 (1H, m, CH<sub>2</sub><sup>4</sup>), 2.48 (1H, m, CH<sub>2</sub><sup>4</sup>), 4.17 (1H, m, CH<sup>2</sup>), 5.10 (2H, d, *J* = 2.5 Hz, Z), 5.71 (1H, d, *J* = 6.1 Hz, OCONH), 6.86 (1H, s, CONH), 7.16-7.37 (20H, m, Trt, Z), 9.46 (1H, s, CHO); <sup>13</sup>C NMR (400 MHz, CDCl<sub>3</sub>) δ 24.64 (CH<sub>2</sub><sup>3</sup>), 32.72 (CH<sub>2</sub><sup>4</sup>), 59.68 (CH<sup>2</sup>), 67.17 (CH<sub>2</sub>, Z), 70.72 (Cq, Trt), 127.07 (CH, Ar, Trt), 127.96 (CH, Ar, Trt), 128.21 (CH, Ar, Z), 128.26 (CH, Ar, Z), 128.53 (CH, Ar, Z), 128.61 (CH, Ar, Trt), 136.07 (Cq, Z), 144.46 (Cq, Ar, Trt), 156.51 (OCONH), 170.85 (CONH), 198.84 (CHO); HRMS (NanoESI) *m/z* calculated for C<sub>32</sub>H<sub>31</sub>N<sub>2</sub>O<sub>4</sub> [M+H]<sup>+</sup> 507.2278, found 507.2281.

**[(S,Z)-methyl 7-oxo-4-(2-phenylacetamido)-7-(tritylamino)hept-2-enoate] (13)**

To a solution of 18-Crown-6 (3.07 g, 11.60 mmol, 4.4 equiv) and methyl *P,P*-bis(2,2,2-trifluoroethyl)phosphonoacetate (1.5 mL, 6.85 mmol, 2.6 equiv) in dry THF (40 mL) cooled down at -78 °C and under Ar, a solution 0.5 M of KHMDS in dry toluene (13.7 mL, 6.85 mmol, 2.6 equiv) was added dropwise. After 30 min of stirring at -78 °C, a solution of aldehyde **12** (1.34 g, 2.64 mmol, 1 equiv) in dry THF (40 mL) was cannulated into the reaction mixture and allowed to react for 3 h. Saturated aqueous NH<sub>4</sub>Cl was used to quench the reaction that didn't reach completion. The aqueous layer was extracted with EtOAc (× 3) and the combined organic layer was washed with brine, dried over Na<sub>2</sub>SO<sub>4</sub>, filtrated and concentrated under *vacuo*. The residue was purified by flash column chromatography (hexane-TBME = 7:3 to 1:1; isocratic hexane-EtOAc = 6:4) to give 1.02 g of the Z-alkene **13** (67%) as a yellowish solid. <sup>1</sup>H NMR (400 MHz, CDCl<sub>3</sub>) δ 1.93 (2H, m, CH<sub>2</sub><sup>5</sup>), 2.42 (2H, m, CH<sub>2</sub><sup>6</sup>), 3.70 (3H, s, COOCH<sub>3</sub>), 5.07 (2H, s, Z), 5.15

(1H, m, CH<sup>4</sup>), 5.56 (1H, d, *J* = 6.2 Hz, OCONH), 5.82 (1H, d, *J* = 11.5 Hz, CH<sup>2</sup>), 6.04 (1H, dd, *J* = 10.8, 9.2 Hz, CH<sup>3</sup>), 6.73 (1H, s, CONH), 7.15-7.38 (20H, m, Trt, Z); <sup>13</sup>C NMR (400 MHz, CDCl<sub>3</sub>) δ 28.89 (CH<sub>2</sub><sup>5</sup>), 33.78 (CH<sub>2</sub><sup>6</sup>), 49.76 (CH<sup>4</sup>), 51.46 (COOCH<sub>3</sub>), 66.68 (CH<sub>2</sub>, Z), 70.66 (Cq, Trt), 119.97 (CH<sup>2</sup>), 127.00 (CH, Ar, Trt), 127.93 (CH, Ar, Trt), 128.04 (CH, Ar, Z), 128.17 (CH, Ar, Z), 128.44 (CH, Ar, Z), 128.64 (CH, Ar, Trt), 136.46 (Cq, Z), 144.56 (Cq, Ar, Trt), 149.75 (CH<sup>3</sup>), 156.04 (OCONH), 166.21 (COO), 171.47 (CONH); HRMS (NanoESI) *m/z* calculated for C<sub>35</sub>H<sub>35</sub>N<sub>2</sub>O<sub>5</sub> [M+H]<sup>+</sup> 563.2541, found 563.2527.

**[(2*R*,3*R*,4*S*)-methyl 2,3-dihydroxy-7-oxo-4-(2-phenylacetamido)-7-(tritylamino)heptanoate] (14) and its (2*S*,3*S*,4*S*) diastereomer (14b)**

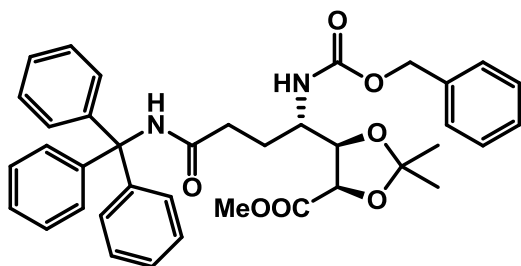


4-Methylmorpholine *N*-oxide (780.0 mg, 5.77 mmol, 3.1 equiv) and OsO<sub>4</sub> (cat.) were added to a solution of alkene **13** (1.05 g, 1.86 mmol, 1 equiv) in THF-H<sub>2</sub>O (9:1, 30 mL) at room temperature, and the resulting reaction mixture was stirred for 10 days at room temperature.

Dihydroxylation completion was monitored by HPLC-PDA and HPLC-ESMS analysis. The reaction was quenched with a 40% aqueous NaHSO<sub>3</sub> solution, and the resulting mixture was stirred further for 30 min. The aqueous layer was extracted with EtOAc (× 3) and the combined organic layer was washed with brine, dried over Na<sub>2</sub>SO<sub>4</sub>, filtrated and concentrated under *vacuo*. The residue was purified by flash column chromatography (DCM-EtOAc = 1:1 to 2:8) to give 418.1 mg of the diastereomer (2*R*,3*R*,4*S*) **14** (75%) and 432.7 mg of the diastereomer (2*S*,3*S*,4*S*) **14b** (77%). Diastereomer (2*R*,3*R*,4*S*) **14**: <sup>1</sup>H NMR (400 MHz, CDCl<sub>3</sub>) δ 1.92 (2H, ddd, *J* = 7.1, 7.1, 6.9 Hz, CH<sub>2</sub><sup>5</sup>), 2.39 (2H, m, CH<sub>2</sub><sup>6</sup>), 3.66 (1H, d, *J* = 8.2 Hz, CH<sup>3</sup>), 3.78 (3H, s, COOCH<sub>3</sub>), 3.95 (1H, m, CH<sup>4</sup>), 3.96 (1H, m, CH<sup>2</sup>), 5.08 (2H, s, Z), 5.28 (1H, d, *J* = 9.4 Hz, OCONH), 6.78 (1H, s, CONH), 7.15-7.35 (20H, m, Trt, Z); <sup>13</sup>C NMR (400 MHz, CDCl<sub>3</sub>) δ 26.95 (CH<sub>2</sub><sup>5</sup>), 33.63 (CH<sub>2</sub><sup>6</sup>), 51.17 (CH<sup>4</sup>), 52.64 (COOCH<sub>3</sub>), 67.29 (CH<sub>2</sub>, Z), 70.72 (Cq, Trt), 71.11 (CH<sup>2</sup>), 73.22 (CH<sup>3</sup>), 127.05 (CH, Ar, Trt), 127.97 (CH, Ar, Trt), 128.15 (CH, Ar, Z), 128.26 (CH, Ar, Z), 128.55 (CH, Ar, Z), 128.63 (CH, Ar, Trt), 136.05 (Cq, Z), 144.48 (Cq, Ar, Trt), 157.63 (OCONH), 171.59 (COO), 173.71 (CONH); HRMS (NanoESI) *m/z* calculated for C<sub>35</sub>H<sub>37</sub>N<sub>2</sub>O<sub>7</sub> [M+H]<sup>+</sup> 597.2595, found 597.2601. Diastereomer (2*S*,3*S*,4*S*) **14b**: <sup>1</sup>H NMR (400 MHz, CDCl<sub>3</sub>) δ 1.71 (1H, m, CH<sub>2</sub><sup>5</sup>), 2.08 (1H, m, CH<sub>2</sub><sup>5</sup>), 2.37 (2H, m, CH<sub>2</sub><sup>6</sup>), 3.68 (3H, s, COOCH<sub>3</sub>), 3.81 (1H, m, CH<sup>3</sup>), 3.85 (1H, m, CH<sup>4</sup>), 4.20 (1H, m, CH<sup>2</sup>), 5.06 (1H, d, *J* = 12.1 Hz, Z), 5.11 (1H, d, *J* = 12.2 Hz, Z), 5.24 (1H, d, *J* = 9.0 Hz, OCONH), 6.87 (1H, s, CONH), 7.16-7.36 (20H, m, Trt, Z); <sup>13</sup>C NMR (400 MHz, CDCl<sub>3</sub>) δ 25.63 (CH<sub>2</sub><sup>5</sup>), 33.37

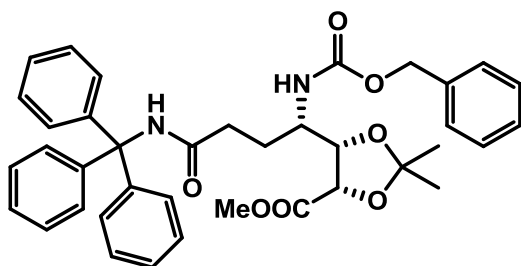
(CH<sub>2</sub><sup>6</sup>), 51.93 (CH<sup>4</sup>), 52.58 (COOCH<sub>3</sub>), 67.17 (CH<sub>2</sub>, Z), 70.72 (Cq, Trt), 72.41 (CH<sup>2</sup>), 74.86 (CH<sup>3</sup>), 127.01 (CH, Ar, Trt), 127.93 (CH, Ar, Trt), 128.20 (CH, Ar, Z), 128.25 (CH, Ar, Z), 128.49 (CH, Ar, Z), 128.68 (CH, Ar, Trt), 136.20 (Cq, Z), 144.50 (Cq, Ar, Trt), 156.97 (OCONH), 172.00 (CO), 173.10 (CO); HRMS (NanoESI) *m/z* calculated for C<sub>35</sub>H<sub>37</sub>N<sub>2</sub>O<sub>7</sub> [M+H]<sup>+</sup> 597.2595, found 597.2593.

**[(4*R*,5*R*)-methyl 2,2-dimethyl-5-((*S*)-4-oxo-1-(2-phenylacetamido)-4-(tritylamino)butyl)1,3-diolcolane-4-carboxylate] (15)**



A solution of (2*R*,3*R*,4*S*) diol **14** (746.6 mg, 1.25 mmol) and acetone dimethyl acetal (15 mL) in dry toluene (30 mL) was placed in a round bottomed flask equipped with a condenser and, after addition of catalytic PPTS, the mixture was heated at 60 °C for 36 h. The toluene was removed under reduced pressure, the residue re-dissolved in EtOAc and the organic layer washed with saturated aqueous NH<sub>4</sub>Cl and brine, dried over Na<sub>2</sub>SO<sub>4</sub>, filtrated and concentrated under *vacuo*. The residue was purified by flash column chromatography (DCM-EtOAc = 97.5:2.5 to 9:1) to give 579.4 mg of acetal **15** (77%) as a white solid: <sup>1</sup>H NMR (400 MHz, CDCl<sub>3</sub>) δ 1.34 (3H, s, CH<sub>3</sub>, acetal), 1.60 (3H, s, CH<sub>3</sub>, acetal), 1.83 (1H, m, CH<sub>2</sub><sup>5</sup>), 1.91 (1H, m, CH<sub>2</sub><sup>5</sup>), 2.29 (2H, m, CH<sub>2</sub><sup>6</sup>), 3.40 (3H, s, COOCH<sub>3</sub>), 4.04 (1H, td, *J* = 10.3, 10.1, 2.5 Hz, CH<sup>4</sup>), 4.34 (1H, d, *J* = 7.8 Hz, CH<sup>3</sup>), 4.57 (1H, d, *J* = 7.8 Hz, CH<sup>2</sup>), 4.97 (1H, d, *J* = 9.4 Hz, OCONH), 5.02 (1H, d, *J* = 12.2 Hz, Z), 5.09 (1H, d, *J* = 12.2 Hz, Z), 7.21-7.39 (20H, m, Trt, Z); <sup>13</sup>C NMR (400 MHz, CDCl<sub>3</sub>) δ 24.50 (CH<sub>3</sub>, acetal), 26.39 (CH<sub>3</sub>, acetal), 31.90 (CH<sub>2</sub><sup>5</sup>), 33.86 (CH<sub>2</sub><sup>6</sup>), 48.50 (CH<sup>4</sup>), 51.99 (COOCH<sub>3</sub>), 67.00 (CH<sub>2</sub>, Z), 70.51 (Cq, Trt), 75.08 (CH<sup>2</sup>), 79.19 (CH<sup>3</sup>), 110.29 (Cq, acetal), 126.81 (CH, Ar, Trt), 127.78 (CH, Ar, Trt), 128.19 (CH, Ar, Z), 128.40 (CH, Ar, Z), 128.44 (CH, Ar, Z), 128.79 (CH, Ar, Trt), 136.26 (Cq, Z), 144.82 (Cq, Ar, Trt), 156.58 (OCONH), 169.59 (COO), 171.48 (CONH); HRMS (NanoESI) *m/z* calculated for C<sub>38</sub>H<sub>41</sub>N<sub>2</sub>O<sub>7</sub> [M+H]<sup>+</sup> 637.2908, found 637.2921.

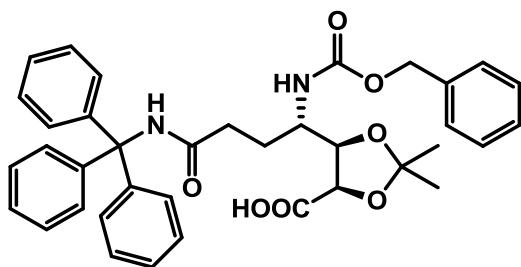
**[(4*S*,5*S*)-methyl 2,2-dimethyl-5-((*S*)-4-oxo-1-(2-phenylacetamido)-4-(tritylamino)butyl)1,3-diolcolane-4-carboxylate] (15b)**



A solution of (2*S*,3*S*,4*S*) diol **14b** (774.4 mg, 1.30 mmol) and acetone dimethyl acetal (15 mL) in dry toluene (30 mL) was placed in a round bottomed flask equipped with a condenser and, after addition of catalytic PPTS, the mixture was

heated at 60 °C for 36 h. The toluene was removed under reduced pressure, the residue re-dissolved in EtOAc and the organic layer washed with saturated aqueous NH<sub>4</sub>Cl and brine, dried over Na<sub>2</sub>SO<sub>4</sub>, filtrated and concentrated under *vacuo* to give 795.6 mg of the acetal **15b** (96%) as a white solid which was used in the next reaction without further purification: <sup>1</sup>H NMR (400 MHz, CDCl<sub>3</sub>) δ 1.33 (3H, s, CH<sub>3</sub>, acetal), 1.54 (3H, s, CH<sub>3</sub>, acetal), 1.71 (1H, m, CH<sub>2</sub><sup>5</sup>), 2.01 (1H, m, CH<sub>2</sub><sup>5</sup>), 2.31 (2H, m, CH<sub>2</sub><sup>6</sup>), 3.54 (3H, s, COOCH<sub>3</sub>), 3.80 (1H, m, CH<sup>4</sup>), 4.30 (1H, dd, *J* = 6.8, 6.8 Hz, CH<sup>3</sup>), 4.63 (1H, d, *J* = 6.8 Hz, CH<sup>2</sup>), 4.97 (1H, d, *J* = 9.4 Hz, OCONH), 5.02 (1H, d, *J* = 12.3 Hz, Z), 5.10 (1H, d, *J* = 12.3 Hz, Z), 6.89 (1H, s, CONH), 7.16-7.35 (20H, m, Trt, Z); <sup>13</sup>C NMR (400 MHz, CDCl<sub>3</sub>) δ 25.29 (CH<sub>3</sub>, acetal), 26.55 (CH<sub>3</sub>, acetal), 27.68 (CH<sub>2</sub><sup>5</sup>), 33.76 (CH<sub>2</sub><sup>6</sup>), 51.20 (CH<sup>4</sup>), 52.41 (COOCH<sub>3</sub>), 66.89 (CH<sub>2</sub>, Z), 70.56 (Cq, Trt), 75.99 (CH<sup>2</sup>), 79.46 (CH<sup>3</sup>), 110.93 (Cq, acetal), 126.92 (CH, Ar, Trt), 127.88 (CH, Ar, Trt), 128.14 (CH, Ar, Z), 128.17 (CH, Ar, Z), 128.47 (CH, Ar, Z), 128.72 (CH, Ar, Trt), 136.33 (Cq, Z), 144.71 (Cq, Ar, Trt), 156.23 (OCONH), 170.05 (COO), 171.26 (CONH); HRMS (NanoESI) *m/z* calculated for C<sub>38</sub>H<sub>41</sub>N<sub>2</sub>O<sub>7</sub> [M+H]<sup>+</sup> 637.2908, found 637.2913.

**[(4*R*,5*R*)-2,2-dimethyl-5-((*S*)-4-oxo-1-(2-phenylacetamido)-4-(tritylamino)butyl)-1,3-dioxolane-4-carboxylic acid] (**16**)**

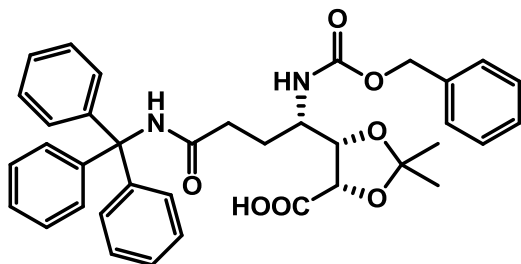


To a solution of acetal **15** (529.4 mg, 0.83 mmol, 1 equiv) in THF-H<sub>2</sub>O (7:3, 8 mL) at 0 °C, LiOH·H<sub>2</sub>O (55.8 mg, 1.33 mmol, 1.6 equiv) was added and the resulting mixture was stirred for 2 h at 0 °C. The reaction was allowed to warm to room temperature and acidified to pH 5

by the addition of 1 M aqueous HCl. The aqueous layer was extracted with EtOAc (x 3) and the combined organic layer was washed with brine, dried over Na<sub>2</sub>SO<sub>4</sub>, filtrated and concentrated under *vacuo* to give 507.4 mg of crude acid **16** (98%) as a white solid, which was used in the next reaction without further purification. <sup>1</sup>H NMR (400 MHz, CD<sub>3</sub>OD) δ 1.34 (3H, s, CH<sub>3</sub>, acetal), 1.53 (3H, s, CH<sub>3</sub>, acetal), 1.75 (1H, m, CH<sub>2</sub><sup>5</sup>), 1.90 (1H, m, CH<sub>2</sub><sup>5</sup>), 2.32 (2H, m, CH<sub>2</sub><sup>6</sup>), 4.00 (1H, ddd, *J* = 9.6, 3.7, 3.7 Hz, CH<sup>4</sup>), 4.40 (1H, dd, *J* = 7.6, 3.6 Hz, CH<sup>3</sup>), 4.62 (1H, d, *J* = 7.7 Hz, CH<sup>2</sup>), 5.01 (1H, d, *J* = 12.4, Z), 5.11 (1H, d, *J* = 12.4 H, Z), 7.17-7.39 (20H, m, Trt, Z); <sup>13</sup>C NMR (400 MHz, CD<sub>3</sub>OD) δ 24.76 (CH<sub>3</sub>, acetal), 26.80 (CH<sub>3</sub>, acetal), 30.67 (CH<sub>2</sub><sup>5</sup>), 34.73 (CH<sub>2</sub><sup>6</sup>), 51.85 (CH<sup>4</sup>), 67.69 (CH<sub>2</sub>, Z), 71.59 (Cq, Trt), 77.26 (CH<sup>2</sup>), 80.11 (CH<sup>3</sup>), 110.46 (Cq, acetal), 127.73 (CH, Ar), 128.69 (CH, Ar), 128.93 (CH, Ar), 129.45 (CH, Ar), 130.09 (CH, Ar), 138.42 (Cq, Z), 146.11 (Cq,

Ar, Trt), 158.64 (CONH), 174.98 (CO); HRMS (NanoESI)  $m/z$  calculated for  $C_{37}H_{38}N_2NaO_7$   $[M+Na]^+$  645.2571, found 645.2586.

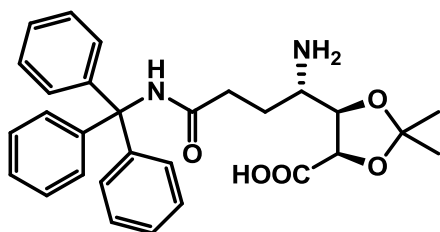
**[(4*S*,5*S*)-2,2-dimethyl-5-((*S*)-4-oxo-1-(2-phenylacetamido)-4-(tritylamino)butyl)-1,3-dioxolane-4-carboxylic acid] (**16b**)**



To a solution of acetal **15b** (745.6 mg 1.17 mmol, 1 equiv) in THF-H<sub>2</sub>O (7:3, 10 mL) at 0 °C, LiOH·H<sub>2</sub>O (78.6 mg, 1.87 mmol, 1.6 equiv) was added and the resulting mixture was stirred for 2 h at 0 °C. The reaction was allowed to warm to room temperature and acidified to pH 5

by the addition of 1 M aqueous HCl. The aqueous layer was extracted with EtOAc (x 3) and the combined organic layer was washed with brine, dried over Na<sub>2</sub>SO<sub>4</sub>, filtrated and concentrated under *vacuo* to give 698.4 mg of crude acid **16b** (96%) as a white solid, which was used in the next reaction without further purification. <sup>1</sup>H NMR (400 MHz, CD<sub>3</sub>OD) δ 1.32 (3H, s, CH<sub>3</sub>, acetal), 1.48 (3H, s, CH<sub>3</sub>, acetal), 1.66 (1H, m, CH<sub>2</sub><sup>5</sup>), 1.94 (1H, m, CH<sub>2</sub><sup>5</sup>), 2.23 (1H, m, CH<sub>2</sub><sup>6</sup>), 2.36 (1H, m, CH<sub>2</sub><sup>6</sup>), 3.88 (1H, m, CH<sup>4</sup>), 4.36 (1H, dd, *J* = 7.3, 4.9 Hz, CH<sup>3</sup>), 4.61 (1H, d, *J* = 7.3 Hz, CH<sup>2</sup>), 5.05 (2H, s, Z), 7.16-7.38 (20H, m, Trt, Z); <sup>13</sup>C NMR (400 MHz, CD<sub>3</sub>OD) δ 25.35 (CH<sub>3</sub>, acetal), 26.94 (CH<sub>3</sub>, acetal), 28.88 (CH<sub>2</sub><sup>5</sup>), 34.93 (CH<sub>2</sub><sup>6</sup>), 53.65 (CH<sup>4</sup>), 67.52 (CH<sub>2</sub>, Z), 71.58 (Cq, Trt), 78.29 (CH<sup>2</sup>), 80.61 (CH<sup>3</sup>), 110.73 (Cq, acetal), 127.70 (CH, Ar, Trt), 128.69 (CH, Ar, Trt), 128.94 (CH, Ar, Z), 129.45 (CH, Ar, Z), 130.10 (CH, Ar, Trt), 138.46 (Cq, Ar, Z), 146.11 (Cq, Ar, Trt), 158.62 (CONH), 175.19 (CO); HRMS (NanoESI)  $m/z$  calculated for  $C_{37}H_{38}N_2NaO_7$   $[M+Na]^+$  645.2571, found 645.2586.

**[(4*R*,5*R*)-5-((*S*)-1-amino-4-oxo-4-(tritylamino)butyl)-2,2-dimethyl-1,3-dioxolane-4-carboxylic acid] (**17**)**

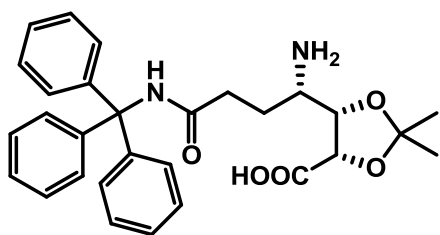


A solution of acid **16** (413.0 mg, 0.66 mmol) in dry MeOH (7 mL) was stirred with a catalytic amount of Pd-C (10%) under an atmosphere of H<sub>2</sub> (atmospheric pressure) for 5 h. EtOAc was added and the mixture was filtrated through celite and concentrated under

*vacuo* to give 304.6 mg of crude amina **17** (94%) as a yellow solid which was used in the next reaction without further purification. <sup>1</sup>H NMR (400 MHz, CD<sub>3</sub>OD) δ 1.36 (3H, s, CH<sub>3</sub>, acetal), 1.54 (3H, s, CH<sub>3</sub>, acetal), 1.75 (1H, m, CH<sub>2</sub><sup>5</sup>), 1.89 (1H, m, CH<sub>2</sub><sup>5</sup>), 2.50 (2H, m, CH<sub>2</sub><sup>6</sup>), 3.05 (1H, m,

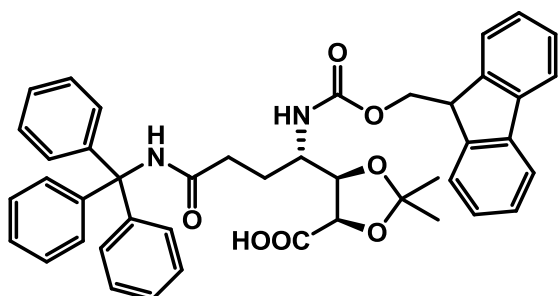
CH<sup>4</sup>), 4.34 (1H, dd,  $J = 7.5, 1.8$  Hz, CH<sup>3</sup>), 4.63 (1H, d,  $J = 7.6$  Hz, CH<sup>2</sup>), 7.19-7.30 (15H, m, Trt); <sup>13</sup>C NMR (400 MHz, CD<sub>3</sub>OD)  $\delta$  24.69 (CH<sub>3</sub>, acetal), 26.56 (CH<sub>3</sub>, acetal), 28.90 (CH<sub>2</sub><sup>5</sup>), 34.19 (CH<sub>2</sub><sup>6</sup>), 53.32 (CH<sup>4</sup>), 71.69 (Cq, Trt), 77.83 (CH<sup>3</sup>), 79.63 (CH<sup>2</sup>), 110.86 (Cq, acetal), 127.86 (CH, Ar, Trt), 128.76 (CH, Ar, Trt), 130.05 (CH, Ar, Trt), 145.96 (Cq, Ar, Trt), 174.51 (CO); HRMS (NanoESI)  $m/z$  calculated for C<sub>29</sub>H<sub>33</sub>N<sub>2</sub>O<sub>5</sub> [M+H]<sup>+</sup> 489.2384, found 489.2393.

**[[4*S*,5*S*]-5-((*S*)-1-amino-4-oxo-4-(tritylamino)butyl)-2,2-dimethyl-1,3-dioxolane-4-carboxylic acid] (17b)**



A solution of acid **16b** (633.6 mg, 1.02 mmol) in dry MeOH (15 mL) was stirred with a catalytic amount of Pd-C (10%) under an atmosphere of H<sub>2</sub> (atmospheric pressure) for 24 h. EtOAc was added and the mixture was filtrated through celite and concentrated under *vacuo* to give 462.8 mg of crude amina **17b** (93%) as a yellow solid which was used in the next reaction without further purification. <sup>1</sup>H NMR (400 MHz, CD<sub>3</sub>OD)  $\delta$  1.34 (3H, s, CH<sub>3</sub>, acetal), 1.50 (3H, s, CH<sub>3</sub>, acetal), 1.65 (1H, m, CH<sub>2</sub><sup>5</sup>), 2.04 (1H, m, CH<sub>2</sub><sup>5</sup>), 2.51 (2H, m, CH<sub>2</sub><sup>6</sup>), 3.02 (1H, m, CH<sup>4</sup>), 4.19 (1H, dd,  $J = 7.0, 7.0$  Hz, CH<sup>3</sup>), 4.57 (1H, d,  $J = 7.2$  Hz, CH<sup>2</sup>), 7.18-7.30 (15H, m, Trt); <sup>13</sup>C NMR (400 MHz, CD<sub>3</sub>OD)  $\delta$  25.41 (CH<sub>3</sub>, acetal), 27.12 (CH<sub>3</sub>, acetal), 28.66 (CH<sub>2</sub><sup>5</sup>), 34.51 (CH<sub>2</sub><sup>6</sup>), 53.47 (CH<sup>4</sup>), 71.65 (Cq, Trt), 79.15 (CH<sup>3</sup>), 80.44 (CH<sup>2</sup>), 110.68 (Cq, acetal), 127.82 (CH, Ar, Trt), 128.74 (CH, Ar, Trt), 130.06 (CH, Ar, Trt), 146.00 (Cq, Ar, Trt), 175.22 (CO); HRMS (NanoESI)  $m/z$  calculated for C<sub>29</sub>H<sub>33</sub>N<sub>2</sub>O<sub>5</sub> [M+H]<sup>+</sup> 489.2384, found 489.2394.

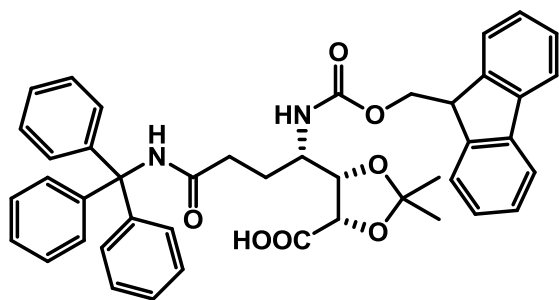
**(4*R*,5*R*)-5-(((9*H*-fluoren-9-yl)methoxy)carbonylamino)-4-oxo-4-(tritylamino)butyl)-2,2-dimethyl-1,3-dioxolane-4-carboxylic acid (18)**



To a pre-cooled solution of NaN<sub>3</sub> (93.0 mg, 1.43 mmol, 3 equiv) in H<sub>2</sub>O (2 mL) Fmoc-Cl (246.6 mg, 0.95 mmol, 2 equiv) dissolved in dioxane (2.5 mL) was added dropwise at 0 °C and the resulting mixture was stirred for 2 h at 0 °C. This solution was then dropped at 0 °C into a solution of amina **17** (232.9 mg, 0.48 mmol, 1 equiv) in H<sub>2</sub>O-2% Na<sub>2</sub>CO<sub>3</sub> (1:1, 4 mL). Some more dioxane (3 mL) was needed for complete solubilisation of the reagents, and the pH was re-adjusted to 9 by addition of 0.1 M aqueous HCl. The reaction mixture was allowed to react for 6 days at room

temperature. The solution was acidified to pH 5 by the addition of 1 M aqueous HCl, the aqueous layer was extracted with EtOAc (x 3) and the combined organic layer was washed with brine, dried over Na<sub>2</sub>SO<sub>4</sub>, filtrated and concentrated under *vacuo*. The residue was purified by flash column chromatography (DCM-hexane = 1:1 to DCM-MeOH 9:1) to give 156.0 mg of the Fmoc-protected diol moiety **18** (46%) as a white solid. <sup>1</sup>H NMR (400 MHz, CD<sub>3</sub>OD) δ 1.35 (3H, s, CH<sub>3</sub>, acetal), 1.57 (3H, s, CH<sub>3</sub>, acetal), 1.76 (1H, m, CH<sub>2</sub><sup>5</sup>), 1.88 (1H, m, CH<sub>2</sub><sup>5</sup>), 2.29 (2H, m, CH<sub>2</sub><sup>6</sup>), 4.01 (1H, m, CH<sup>4</sup>), 4.24 (1H, dd, *J* = 6.9, 6.9 Hz, CH, Fmoc), 4.33 (2H, m, CH<sub>2</sub>, Fmoc), 4.38 (1H, m, CH<sup>3</sup>), 4.62 (1H, d, *J* = 7.6 Hz, CH<sup>2</sup>), 7.16-7.31 (17H, m, Fmoc, Trt), 7.37 (2H, dt, *J* = 7.4, 7.4, 3.3 Hz, CH, Ar, Fmoc), 7.64 (1H, d, *J* = 7.3 Hz, CH, Ar, Fmoc), 7.69 (1H, d, *J* = 7.4 Hz, CH, Ar, Fmoc), 7.78 (2H, d, *J* = 7.5 Hz, CH, Ar, Fmoc); <sup>13</sup>C NMR (400 MHz, CD<sub>3</sub>OD) δ 24.86 (CH<sub>3</sub>, acetal), 26.82 (CH<sub>3</sub>, acetal), 30.99 (CH<sub>2</sub><sup>5</sup>), 34.67 (CH<sub>2</sub><sup>6</sup>), 49.33 (CH, Fmoc), 51.53 (CH<sup>4</sup>), 67.95 (CH<sub>2</sub>, Fmoc), 71.61 (Cq, Trt), 77.00 (CH<sup>2</sup>), 80.43 (CH<sup>3</sup>), 110.73 (Cq, acetal), 120.92 (CH, Ar, Fmoc), 126.37 (CH, Ar, Fmoc), 126.59 (CH, Ar, Fmoc), 127.74 (CH, Ar, Trt), 128.19 (CH, Ar, Fmoc), 128.70 (CH, Ar, Trt), 128.75 (CH, Ar, Fmoc), 128.82 (CH, Ar, Fmoc), 130.08 (CH, Ar, Trt), 142.55 (Cq, Fmoc), 142.70 (Cq, Fmoc), 145.11 (Cq, Fmoc), 145.83 (Cq, Fmoc), 146.09 (Cq, Ar, Trt), 158.71 (OCONH), 174.92 (CO); HRMS (NanoESI) *m/z* calculated for C<sub>44</sub>H<sub>43</sub>N<sub>2</sub>O<sub>7</sub> [M+H]<sup>+</sup> 711.3065, found 711.3077.

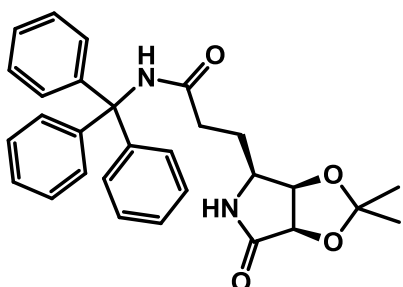
**(4*S*,5*S*)-5-(((9H-fluoren-9-yl)methoxy)carbonylamino)-4-oxo-4-(tritylamino)butyl)-2,2-dimethyl-1,3-dioxolane-4-carboxylic acid (**18b**)**



To a pre-cooled solution of NaN<sub>3</sub> (99.8 mg, 1.54 mmol, 3 equiv) in H<sub>2</sub>O (2.5 mL) Fmoc-Cl (264.7 mg, 1.02 mmol, 2 equiv) dissolved in dioxane (3 mL) was added dropwise at 0 °C and the resulting mixture was stirred for 2 h at 0 °C. This solution was then dropped at 0 °C into a solution of amina **17b** (250.0 mg, 0.51 mmol, 1 equiv) in H<sub>2</sub>O-2% Na<sub>2</sub>CO<sub>3</sub> (1:1, 4 mL). Some more dioxane (3 mL) was needed for complete solubilisation of the reagents, and the pH was re-adjusted to 9 by addition of 0.1 M aqueous HCl. The reaction mixture was allowed to react for 6 days at room temperature. The solution was acidified to pH 5 by the addition of 1 M aqueous HCl, the aqueous layer was extracted with EtOAc (x 3) and the combined organic layer was washed with brine, dried over Na<sub>2</sub>SO<sub>4</sub>, filtrated and concentrated under *vacuo*. The residue was purified by flash column chromatography (DCM-hexane = 1:1 to DCM-MeOH 9:1) to give 165.4 mg of the

Fmoc-protected diol moiety **18b** (45%) as a white solid.  $^1\text{H}$  NMR (400 MHz,  $\text{CD}_3\text{OD}$ )  $\delta$  1.35 (3H, s,  $\text{CH}_3$ , acetal), 1.53 (3H, s,  $\text{CH}_3$ , acetal), 1.59 (1H, m,  $\text{CH}_2^5$ ), 2.02 (1H, m,  $\text{CH}_2^5$ ), 2.26 (2H, m,  $\text{CH}_2^6$ ), 3.84 (1H, ddd,  $J = 10.7, 8.4, 2.7$  Hz,  $\text{CH}^4$ ), 4.21 (1H, dd,  $J = 6.8, 6.8$  Hz, CH, Fmoc), 4.31 (1H, m,  $\text{CH}^3$ ), 4.37 (2H, dd,  $J = 6.8, 2.2$  Hz,  $\text{CH}_2$ , Fmoc), 4.63 (1H, d,  $J = 6.8$  Hz,  $\text{CH}^2$ ), 7.16-7.32 (17H, m, Fmoc, Trt), 7.37 (2H, dt,  $J = 7.5, 7.4, 2.1$  Hz, CH, Ar, Fmoc), 7.63 (1H, d,  $J = 7.5$  Hz, CH, Ar, Fmoc), 7.67 (1H, d,  $J = 7.4$  Hz, CH, Ar, Fmoc), 7.78 (2H, d,  $J = 7.4$  Hz, CH, Ar, Fmoc);  $^{13}\text{C}$  NMR (400 MHz,  $\text{CD}_3\text{OD}$ )  $\delta$  25.65 ( $\text{CH}_3$ , acetal), 27.14 ( $\text{CH}_3$ , acetal), 30.33 ( $\text{CH}_2^5$ ), 34.33 ( $\text{CH}_2^6$ ), 48.69 (CH, Fmoc), 52.26 ( $\text{CH}^4$ ), 67.61 ( $\text{CH}_2$ , Fmoc), 71.62 (Cq, Trt), 77.67 ( $\text{CH}^2$ ), 80.80 ( $\text{CH}^3$ ), 111.92 (Cq, acetal), 120.95 (CH, Ar, Fmoc), 126.30 (CH, Ar, Fmoc), 126.40 (CH, Ar, Fmoc), 127.73 (CH, Ar, Trt), 128.15 (CH, Ar, Fmoc), 128.17 (CH, Ar, Fmoc), 128.72 (CH, Ar, Trt), 128.74 (CH, Ar, Fmoc), 128.82 (CH, Ar, Fmoc), 130.08 (CH, Ar, Trt), 142.62 (Cq, Fmoc), 142.73 (Cq, Fmoc), 145.15 (Cq, Fmoc), 145.75 (Cq, Fmoc), 146.07 (Cq, Ar, Trt), 158.60 (CONH), 173.07 (CO), 174.95 (CO); HRMS (NanoESI)  $m/z$  calculated for  $\text{C}_{44}\text{H}_{43}\text{N}_2\text{O}_7$   $[\text{M}+\text{H}]^+$  711.3065, found 711.3082.

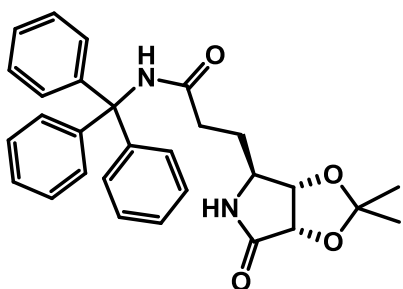
### 3-((3aR,4S,6aR)-2,2-dimethyl-6-oxotetrahydro-3aH-[1,3]dioxolo[4,5-c]pyrrol-4-yl)-N-tritylpropionamide (**19**)



To a suspension of amina **17** (49.5 mg, 0.10 mmol, 1 equiv) in dry DMF (5 mL), HOBT\* $\text{H}_2\text{O}$  (31.0 mg, 0.20 mmol, 2 equiv) and EDC\*HCl (38.8 mg, 0.20 mmol, 2 equiv) were added at room temperature. The pH was re-adjusted to 6 and the resulting mixture was stirred for 6 h. EtOAc was added and the organic layer was washed with 0.1 M aqueous HCl ( $\times 2$ ), with 5% aqueous  $\text{NaHCO}_3$  solution ( $\times 2$ ) and once with brine, dried over  $\text{Na}_2\text{SO}_4$ , filtrated and concentrated under *vacuo*. The residue was purified by flash column chromatography (hexane-EtOAc = 10:0 to 1:1) to give 25 mg of bicycle **19** (52%) as a yellowish oil.  $^1\text{H}$  NMR (400 MHz,  $\text{CDCl}_3$ )  $\delta$  1.32 (3H, s,  $\text{CH}_3$ , acetal), 1.43 (3H, s,  $\text{CH}_3$ , acetal), 1.75 (1H, tdd,  $J = 15.2, 10.2, 5.1, 5.1$  Hz,  $\text{CH}_2^5$ ), 1.91 (1H, m,  $\text{CH}_2^5$ ), 2.48 (2H, m,  $\text{CH}_2^6$ ), 2.67 (1H, m,  $\text{CH}^4$ ), 3.98 (1H, d,  $J = 5.7$  Hz,  $\text{CH}^2$ ), 4.27 (1H, t,  $J = 5.1, 5.1$  Hz,  $\text{CH}^3$ ), 7.17-7.33 (15H, m, Trt), 7.78 (1H, s, CONH), 8.32 (1H, s, CONH);  $^{13}\text{C}$  NMR (400 MHz,  $\text{CDCl}_3$ )  $\delta$  25.30 ( $\text{CH}_3$ , acetal), 25.73 ( $\text{CH}_3$ , acetal), 26.96 ( $\text{CH}_2^5$ ), 32.78 ( $\text{CH}_2^6$ ), 53.13 ( $\text{CH}^4$ ), 70.45 (Cq, Trt), 76.12 ( $\text{CH}^3$ ), 77.67 ( $\text{CH}^2$ ), 112.59 (Cq, acetal), 126.64 (CH, Ar, Trt), 127.73 (CH, Ar, Trt), 128.60 (CH, Ar, Trt), 144.67 (Cq, Ar, Trt), 171.53 (CONH), 174.98 (CONH); HRMS (NanoESI)  $m/z$  calculated for  $\text{C}_{58}\text{H}_{61}\text{N}_4\text{O}_8$   $[\text{2M}+\text{H}]^+$  941.4484, found 941.4504.



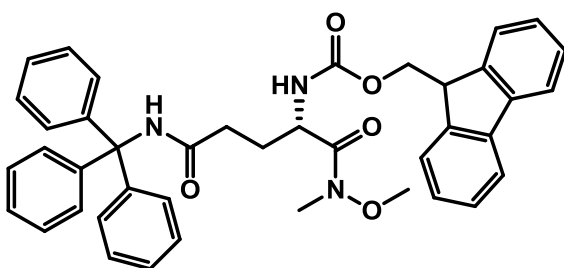
**3-((3a*S*,4*S*,6a*S*)-2,2-dimethyl-6-oxotetrahydro-3a*H*-[1,3]dioxolo[4,5-*c*]pyrrol-4-yl)-*N*-tritylpropionamide (19b)**



To a suspension of amina **17b** (70.5 mg, 0.14 mmol, 1 equiv) in dry DMF (5 mL), HOBt\*H<sub>2</sub>O (44.2 mg, 0.29 mmol, 2 equiv) and EDC\*HCl (55.3 mg, 0.29 mmol, 2 equiv) were added at room temperature. The pH was re-adjusted to 6 and the resulting mixture was stirred for 6 h. EtOAc was added and the organic layer was washed with 0.1 M aqueous HCl (× 2), with 5% aqueous NaHCO<sub>3</sub> solution (× 2) and once with brine, dried over Na<sub>2</sub>SO<sub>4</sub>, filtrated and concentrated under *vacuo*. The residue was purified by flash column chromatography (hexane-EtOAc = 10:0 to 0:10) to give 41.1 mg of bicycle **19b** (61%) as a yellowish solid. <sup>1</sup>H NMR (400 MHz, CDCl<sub>3</sub>) δ 1.33 (3H, s, CH<sub>3</sub>, acetal), 1.41 (3H, s, CH<sub>3</sub>, acetal), 1.55 (1H, m, CH<sub>2</sub><sup>5</sup>), 1.95 (1H, m, CH<sub>2</sub><sup>5</sup>), 2.38 (2H, t, *J* = 7.2, 7.2 Hz, CH<sub>2</sub><sup>6</sup>), 3.49 (1H, dd, *J* = 9.2, 5.0 Hz, CH<sup>4</sup>), 4.32 (1H, d, *J* = 5.9 Hz, CH<sup>2</sup>), 4.44 (1H, d, *J* = 5.9 Hz, CH<sup>3</sup>), 7.12 (1H, s, CONH), 7.19-7.30 (15H, m, Trt), 7.72 (1H, s, CONH); <sup>13</sup>C NMR (400 MHz, CDCl<sub>3</sub>) δ 25.58 (CH<sub>3</sub>, acetal), 26.93 (CH<sub>3</sub>, acetal), 30.39 (CH<sub>2</sub><sup>5</sup>), 32.89 (CH<sub>2</sub><sup>6</sup>), 57.69 (CH<sup>4</sup>), 70.57 (Cq, Trt), 76.50 (CH<sup>3</sup>), 79.58 (CH<sup>2</sup>), 112.54 (Cq, acetal), 126.93 (CH, Ar, Trt), 127.87 (CH, Ar, Trt), 128.62 (CH, Ar, Trt), 144.55 (Cq, Ar, Trt), 170.53 (CONH), 174.33 (CONH); HRMS (NanoESI) *m/z* calculated for C<sub>29</sub>H<sub>31</sub>N<sub>2</sub>O<sub>4</sub> [M+H]<sup>+</sup> 471.2284, found 471.2286.

Route B

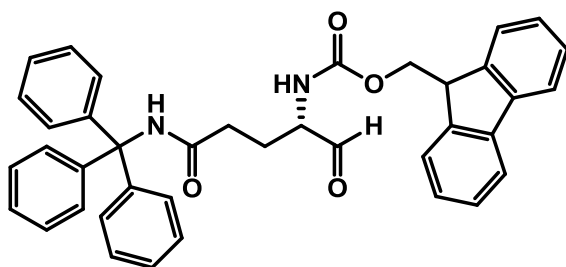
**[(*S*)-(9*H*-fluoren-9-yl)methyl 1-(methoxy(methyl)amino)-1,5-dioxo-5-(tritylamino)pentan-2-yl]carbamate (20)**



To a solution of Fmoc-L-Gln(Trt)-OH (5 g, 8.19 mmol, 1 equiv) in dry DMF (20 mL), HOBt\*H<sub>2</sub>O (1.505 g, 9.82 mmol, 1.2 equiv) and EDC (1.883 g, 9.82 mmol, 1.2 equiv) were added at room temperature. After 30 min of stirring under Ar, a solution of *N*,*O*-dimethylhydroxylamine hydrochloride (1.038 g, 10.64 mmol, 1.3 equiv) and DIEA (1.82 mL, 10.64 mmol, 1.3 equiv) in dry DMF (10 mL) was added dropwise and the reaction mixture was reacted for 3 h. Saturated aqueous NaHCO<sub>3</sub> was added and the aqueous layer was extracted with EtOAc (× 3). The combined organic layer was washed twice with 0.1 M aqueous HCl, once with brine, dried over Na<sub>2</sub>SO<sub>4</sub>, filtrated and concentrated under *vacuo*. The residue was

purified by flash column chromatography (hexane-EtOAc = 10:0 to 2:8) to give 5.249 g of the Weinreb amide **20** (98%) as a white solid.  $^1\text{H}$  NMR (400 MHz,  $\text{CDCl}_3$ )  $\delta$  1.83 (1H, m,  $\text{CH}_2^3$ ), 2.16 (1H, m,  $\text{CH}_2^3$ ), 2.36 (2H, m,  $\text{CH}_2^4$ ), 3.18 (3H, s, N- $\text{CH}_3$ ), 3.64 (3H, s, O- $\text{CH}_3$ ), 4.20 (1H, dd,  $J = 6.9$ , 6.9 Hz, CH, Fmoc), 4.38 (2H, d,  $J = 7.0$  Hz,  $\text{CH}_2$ , Fmoc), 4.77 (1H, m,  $\text{CH}^2$ ), 5.69 (1H, d,  $J = 8.3$  Hz, OCONH), 6.95 (1H, s, CONH), 7.19-7.34 (17H, m, Trt, Fmoc), 7.38 (2H, dd,  $J = 7.3$ , 7.3 Hz, CH, Ar, Fmoc), 7.58 (2H,  $J = 7.5$ , 7.5 Hz, CH, Ar, Fmoc), 7.76 (2H, d,  $J = 7.6$  Hz, CH, Ar, Fmoc);  $^{13}\text{C}$  NMR (400 MHz,  $\text{CDCl}_3$ )  $\delta$  29.16 ( $\text{CH}_2^3$ ), 32.13 (N- $\text{CH}_3$ ), 33.39 ( $\text{CH}_2^4$ ), 47.22 (CH, Fmoc), 50.53 ( $\text{CH}^2$ ), 61.59 (O- $\text{CH}_3$ ), 66.91 ( $\text{CH}_2$ , Fmoc), 70.58 (Cq, Trt), 119.95 (CH, Ar, Fmoc), 119.98 (CH, Ar, Fmoc), 125.12 (CH, Ar, Fmoc), 126.92 (CH, Ar, Trt), 127.02 (CH, Ar, Fmoc), 127.05 (CH, Ar, Fmoc), 127.69 (CH, Ar, Fmoc), 127.87 (CH, Ar, Trt), 128.75 (CH, Ar, Trt), 141.26 (Cq, Fmoc), 141.33 (Cq, Fmoc), 143.68 (Cq, Fmoc), 143.92 (Cq, Fmoc), 144.73 (Cq, Ar, Trt), 156.45 (OCONH), 170.80 (CO), 171.13 (CO); HRMS (NanoESI)  $m/z$  calculated for  $\text{C}_{41}\text{H}_{40}\text{N}_3\text{O}_5$   $[\text{M}+\text{H}]^+$  654.2968, found 654.2974.

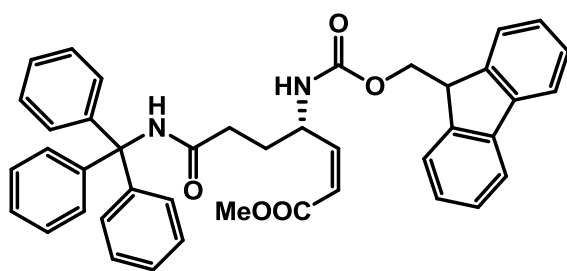
**[(S)-(9H-fluoren-9-yl)methyl 1,5-dioxo-5-(tritylamino)pentan-2-ylcarbamate] (**21**)**



To a solution of Weinreb amide **20** (1.896 g, 2.90 mmol, 1 equiv) in dry THF (10 mL) at 0 °C, a pre-cooled 1M solution of  $\text{LiAlH}_4$  in dry THF (3.77 mL, 3.77 mmol, 1.3 equiv) was added dropwise. After 30 min of stirring at 0 °C, the reaction was quenched

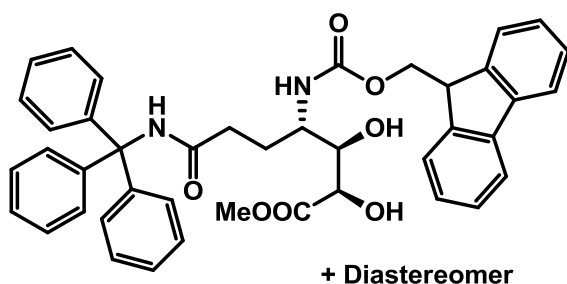
with a 5% aqueous  $\text{KHSO}_4$  solution keeping the ice bath. The aqueous layer was extracted with EtOAc ( $\times 3$ ) and the combined organic layer was washed once with brine, dried over  $\text{Na}_2\text{SO}_4$ , filtrated and concentrated under *vacuo* to give 1.654 g of crude aldehyde **21** (96%) as a white solid, which was used in the next reaction without further purification.  $^1\text{H}$  NMR (400 MHz,  $\text{CDCl}_3$ )  $\delta$  1.83 (1H, m,  $\text{CH}_2^3$ ), 2.24 (1H, m,  $\text{CH}_2^3$ ), 2.37 (2H, m,  $\text{CH}_2^4$ ), 4.13 (1H, m,  $\text{CH}^2$ ), 4.21 (1H, t,  $J = 6.5$ , 6.5 Hz, CH, Fmoc), 4.46 (2H, m,  $\text{CH}_2$ , Fmoc), 5.57 (1H, d,  $J = 6.2$  Hz, OCONH), 6.80 (1H, s, CONH), 7.16-7.42 (19H, m, Trt, Fmoc), 7.58 (2H, d,  $J = 7.3$  Hz, CH, Ar, Fmoc), 7.71 (2H, t,  $J = 7.0$ , 7.0 Hz, CH, Ar, Fmoc), 9.44 (1H, s, CHO);  $^{13}\text{C}$  NMR (400 MHz,  $\text{CDCl}_3$ )  $\delta$  24.59 ( $\text{CH}_2^3$ ), 32.46 ( $\text{CH}_2^4$ ), 47.30 (CH, Fmoc), 59.44 ( $\text{CH}^2$ ), 66.73 ( $\text{CH}_2$ , Fmoc), 70.71 (Cq, Trt), 119.98 (CH, Ar, Fmoc), 125.03 (CH, Ar, Fmoc), 127.08 (CH, Ar, Trt), 127.73 (CH, Ar, Fmoc), 127.96 (CH, Ar, Trt), 128.62 (CH, Ar, Trt), 141.33 (Cq, Fmoc), 141.36 (Cq, Fmoc), 143.64 (Cq, Fmoc), 143.76 (Cq, Fmoc), 144.47 (Cq, Ar, Trt), 156.44 (OCONH), 170.88 (CONH), 198.56 (CHO); HRMS (NanoESI)  $m/z$  calculated for  $\text{C}_{39}\text{H}_{35}\text{N}_2\text{O}_4$   $[\text{M}+\text{H}]^+$  595.2591, found 595.2600.

**[(*S,Z*)-methyl 4-(((9*H*-fluoren-9-yl)methoxy)carbonylamino)-7-oxo-7-(tritylamino)hept-2-enoate] (**22**)**



To a solution of 18-Crown-6 (4.432 g, 16.77 mmol, 4.4 equiv) and methyl *P,P*-bis(2,2,2-trifluoroethyl)phosphonoacetate (2.1 mL, 9.91 mmol, 2.6 equiv) in dry THF (65 mL) cooled down at -78 °C and under Ar, a solution 0.5 M of KHMDS in toluene (19.8 mL, 9.91 mmol, 2.6 equiv) was added dropwise. After 30 min of stirring at -78 °C, a solution of aldehyde **21** (2.266 g, 3.81 mmol, 1 equiv) in dry THF (65 mL) was cannulated into the reaction mixture and allowed to react for 3.5 h. Saturated aqueous NH<sub>4</sub>Cl was used to quench the reaction that didn't reach completion. The aqueous layer was extracted with EtOAc (× 3) and the combined organic layer was washed with brine, dried over Na<sub>2</sub>SO<sub>4</sub>, filtrated and concentrated under *vacuo*. The residue was purified by flash column chromatography (isocratic DCM-EtOAc-hexane = 7:2:1) to give 1.817 g of the *Z*-alkene **22** (72%) as a yellowish solid. <sup>1</sup>H NMR (400 MHz, CDCl<sub>3</sub>) δ 1.65 (2H, m, CH<sub>2</sub><sup>5</sup>), 2.28 (2H, m, CH<sub>2</sub><sup>6</sup>), 3.64 (3H, s, CH<sub>3</sub>), 4.21 (1H, t, *J* = 6.8, 6.8 Hz, CH, Fmoc), 4.30 (2H, dd, *J* = 6.7, 3.5 Hz, CH<sub>2</sub>, Fmoc), 5.08 (1H, m, CH<sup>4</sup>), 5.81 (1H, d, *J* = 11.7 Hz, CH<sup>2</sup>), 6.08 (1H, dd, *J* = 11.5, 9.1 Hz, CH<sup>3</sup>), 7.14-7.47 (19H, m, Trt, Fmoc), 7.68 (2H, d, *J* = 7.3 Hz, CH, Ar, Fmoc), 7.89 (2H, d, *J* = 7.5 Hz, CH, Ar, Fmoc), 8.57 (1H, s, CONH); <sup>13</sup>C NMR (400 MHz, CDCl<sub>3</sub>) δ 29.96 (CH<sub>2</sub><sup>5</sup>), 32.47 (CH<sub>2</sub><sup>6</sup>), 46.64 (CH, Fmoc), 48.51 (CH<sup>4</sup>), 51.05 (CH<sub>3</sub>), 65.15 (CH<sub>2</sub>, Fmoc), 69.06 (Cq, Trt), 118.60 (CH<sup>2</sup>), 120.03 (CH, Ar, Fmoc), 124.99 (CH, Ar, Fmoc), 125.03 (CH, Ar, Fmoc), 126.16 (CH, Ar, Trt), 126.94 (CH, Ar, Fmoc), 127.31 (CH, Ar, Trt), 127.50 (CH, Ar, Fmoc), 128.41 (CH, Ar, Trt), 140.62 (Cq, Fmoc), 143.74 (Cq, Fmoc), 144.82 (Cq, Ar, Trt), 155.38 (OCONH), 165.36 (COO), 171.30 (CONH); HRMS (NanoESI) *m/z* calculated for C<sub>42</sub>H<sub>39</sub>N<sub>2</sub>O<sub>5</sub> [M+H]<sup>+</sup> 651.2854, found 651.2853.

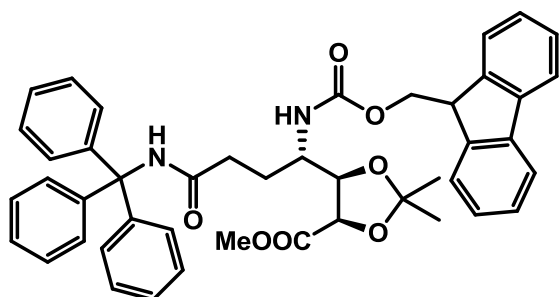
**[(*2R,3R,4S*)-methyl 4-(((9*H*-fluoren-9-yl)methoxy)carbonylamino)-2,3-dihydroxy-7-oxo-7-(tritylamino)heptanoate] (**23**) and its (*2S,3S,4S*) diastereomer (**23b**)**



4-Methylmorpholine *N*-oxide (225.2 mg, 1.67 mmol, 3.1 equiv) and OsO<sub>4</sub> (cat.) were added to a solution of alkene **22** (349.8 mg, 0.54 mmol, 1 equiv) in THF-H<sub>2</sub>O (9:1, 10 mL) at room temperature, and the resulting reaction mixture was stirred for 7 days at

room temperature. Dihydroxylation completion was monitored by HPLC-PDA and HPLC-ESMS analysis. The reaction was quenched with a 40% aqueous NaHSO<sub>3</sub> solution, and the resulting mixture was stirred further for 30 min. The aqueous layer was extracted with EtOAc (× 3) and the combined organic layer was washed with brine, dried over Na<sub>2</sub>SO<sub>4</sub>, filtrated and concentrated under *vacuo*. The residue was purified by flash column chromatography (isocratic DCM-EtOAc = 8:2) to give 282.3 mg of the diastereomer **23** (2*R*,3*R*,4*S*) (76%) and 259.0 mg of the diastereomer **23b** (2*S*,3*S*,4*S*) (70%). Diastereomer **23** (2*R*,3*R*,4*S*): <sup>1</sup>H NMR (400 MHz, CDCl<sub>3</sub>) δ 1.91 (2H, m, CH<sub>2</sub><sup>5</sup>), 2.34 (2H, m, CH<sub>2</sub><sup>6</sup>), 3.55 (1H, br s, OH), 3.64 (1H, d, *J* = 8.5 Hz, CH<sup>3</sup>), 3.79 (3H, s, OCH<sub>3</sub>), 3.85 (1H, d, *J* = 8.7 Hz, CH<sup>2</sup>), 3.92 (1H, m, CH<sup>4</sup>), 3.92 (1H, br s, OH), 4.17 (1H, t, *J* = 6.5, 6.5 Hz, CH, Fmoc), 4.43 (1H, dd, *J* = 10.7, 6.5 Hz, CH<sub>2</sub>, Fmoc), 4.50 (1H, dd, *J* = 10.7, 6.6 Hz, CH<sub>2</sub>, Fmoc), 5.23 (1H, d, *J* = 9.3 Hz, OCONH), 6.78 (1H, s, CONH), 7.15-7.34 (17H, m, Trt, Fmoc), 7.38 (2H, t, *J* = 7.4, 7.4 Hz, CH, Ar, Fmoc), 7.57 (2H, d, *J* = 7.4 Hz, CH, Ar, Fmoc), 7.75 (2H, d, *J* = 7.5 Hz, CH, Ar, Fmoc); <sup>13</sup>C NMR (400 MHz, CDCl<sub>3</sub>) δ 27.12 (CH<sub>2</sub><sup>5</sup>), 33.62 (CH<sub>2</sub><sup>6</sup>), 47.34 (CH, Fmoc), 51.03 (CH<sup>4</sup>), 52.66 (OCH<sub>3</sub>), 66.71 (CH<sub>2</sub>, Fmoc), 70.71 (Cq, Trt), 71.00 (CH<sup>2</sup>), 73.22 (CH<sup>3</sup>), 120.00 (CH, Ar, Fmoc), 120.01 (CH, Ar, Fmoc), 124.94 (CH, Ar, Fmoc), 124.99 (CH, Ar, Fmoc), 127.04 (CH, Ar, Trt), 127.71 (CH, Ar, Fmoc), 127.72 (CH, Ar, Fmoc), 127.96 (CH, Ar, Trt), 128.64 (CH, Ar, Trt), 141.34 (Cq, Fmoc), 141.36 (Cq, Fmoc), 143.61 (Cq, Fmoc), 143.67 (Cq, Fmoc), 144.47 (Cq, Ar, Trt), 157.58 (OCONH), 171.62 (COO), 173.81 (CONH); HRMS (NanoESI) *m/z* calculated for C<sub>42</sub>H<sub>41</sub>N<sub>2</sub>O<sub>7</sub> [M+H]<sup>+</sup> 685.2908, found 685.2929. Diastereomer **23b** (2*S*,3*S*,4*S*): <sup>1</sup>H NMR (400 MHz, CDCl<sub>3</sub>) δ 1.67 (1H, m, CH<sub>2</sub><sup>5</sup>), 2.07 (1H, m, CH<sub>2</sub><sup>5</sup>), 2.31 (2H, m, CH<sub>2</sub><sup>6</sup>), 3.66 (3H, s, OCH<sub>3</sub>), 3.78 (1H, m, CH<sup>3</sup>), 3.82 (1H, m, CH<sup>4</sup>), 4.17 (1H, m, CH<sup>2</sup>), 4.19 (1H, m, CH, Fmoc), 4.45 (2H, d, *J* = 6.5 Hz, CH<sub>2</sub>, Fmoc), 5.19 (1H, d, *J* = 8.9 Hz, OCONH), 6.89 (1H, s, CONH), 7.15-7.32 (17H, m, Trt, Fmoc), 7.38 (2H, dt, *J* = 7.2, 7.2, 7.3 Hz, CH, Ar, Fmoc), 7.57 (2H, dd, *J* = 7.3, 3.0 Hz, CH, Ar, Fmoc), 7.74 (2H, d, *J* = 7.5 Hz, CH, Ar, Fmoc); <sup>13</sup>C NMR (400 MHz, CDCl<sub>3</sub>) δ 25.69 (CH<sub>2</sub><sup>5</sup>), 33.32 (CH<sub>2</sub><sup>6</sup>), 47.31 (CH, Fmoc), 51.74 (CH<sup>4</sup>), 52.56 (OCH<sub>3</sub>), 66.54 (CH<sub>2</sub>, Fmoc), 70.71 (Cq, Trt), 72.29 (CH<sup>2</sup>), 74.84 (CH<sup>3</sup>), 119.96 (CH, Ar, Fmoc), 125.00 (CH, Ar, Fmoc), 125.04 (CH, Ar, Fmoc), 127.00 (CH, Ar, Trt), 127.04 (CH, Ar, Fmoc), 127.66 (CH, Ar, Fmoc), 127.69 (CH, Ar, Fmoc), 127.92 (CH, Ar, Trt), 128.68 (CH, Ar, Trt), 141.31 (Cq, Fmoc), 141.36 (Cq, Fmoc), 143.66 (Cq, Fmoc), 143.92 (Cq, Fmoc), 144.49 (Cq, Ar, Trt), 156.93 (OCONH), 172.03 (COO), 173.14 (CONH); HRMS (NanoESI) *m/z* calculated for C<sub>42</sub>H<sub>41</sub>N<sub>2</sub>O<sub>7</sub> [M+H]<sup>+</sup> 685.2908, found 685.2911.

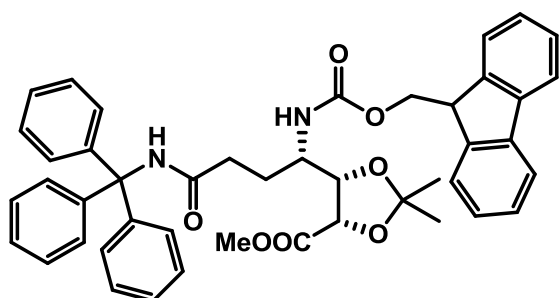
**[(4*R*,5*R*)-methyl 5-((*S*)-1-(((9*H*-fluoren-9-yl)methoxy)carbonylamino)-4-oxo-4-(tritylamino)butyl)-2,2-dimethyl-1,3-dioxolane-4-carboxylate] (24)**



A solution of (2*R*,3*R*,4*S*) diol **23** (916.4 mg, 1.34 mmol) and acetone dimethyl acetal (18 mL) in dry toluene (36 mL) was placed in a round bottomed flask equipped with a condenser and, after addition of catalytic PPTS, the mixture was heated at 60 °C for 24 h. The toluene was removed under reduced

pressure, the residue re-dissolved in EtOAc and the organic layer washed with saturated aqueous NH<sub>4</sub>Cl and brine, dried over Na<sub>2</sub>SO<sub>4</sub>, filtrated and concentrated under *vacuo*. The residue was purified by flash column chromatography (DCM-EtOAc = 97.5:2.5 to 9:1) to give 746.6 mg of acetal **24** (77%) as a white solid. <sup>1</sup>H NMR (400 MHz, CDCl<sub>3</sub>) δ 1.37 (3H, s, CH<sub>3</sub>, acetal), 1.66 (3H, s, CH<sub>3</sub>, acetal), 1.84 (1H, m, CH<sub>2</sub><sup>5</sup>), 1.93 (1H, m, CH<sub>2</sub><sup>5</sup>), 2.26 (2H, m, CH<sub>2</sub><sup>6</sup>), 3.50 (3H, s, OCH<sub>3</sub>), 4.06 (1H, td, *J* = 10.1, 10.1, 2.4 Hz, CH<sup>4</sup>), 4.23 (1H, t, *J* = 7.0, CH, Fmoc), 4.37 (2H, m, CH<sub>2</sub>, Fmoc), 4.37 (1H, m, CH<sup>3</sup>), 4.61 (1H, d, *J* = 7.8 Hz, CH<sup>2</sup>), 4.99 (1H, d, *J* = 9.4 Hz, OCONH), 7.18-7.43 (17H, m, Trt, Fmoc), 7.61 (2H, d, *J* = 7.4 Hz, CH, Ar, Fmoc), 7.63 (2H, d, *J* = 7.5 Hz, CH, Ar, Fmoc), 7.76 (2H, d, *J* = 7.5 Hz, CH, Ar, Fmoc); <sup>13</sup>C NMR (400 MHz, CDCl<sub>3</sub>) δ 24.53 (CH<sub>3</sub>, acetal), 26.44 (CH<sub>3</sub>, acetal), 31.87 (CH<sub>2</sub><sup>5</sup>), 33.80 (CH<sub>2</sub><sup>6</sup>), 47.27 (CH, Fmoc), 48.53 (CH<sup>4</sup>), 52.18 (OCH<sub>3</sub>), 66.90 (CH<sub>2</sub>, Fmoc), 70.53 (Cq, Trt), 75.16 (CH<sup>2</sup>), 79.25 (CH<sup>3</sup>), 110.37 (Cq, acetal), 119.95 (CH, Ar, Fmoc), 119.99 (CH, Ar, Fmoc), 125.19 (CH, Ar, Fmoc), 126.82 (CH, Ar, Trt), 127.06 (CH, Ar, Fmoc), 127.07 (CH, Ar, Fmoc), 127.70 (CH, Ar, Fmoc), 127.75 (CH, Ar, Fmoc), 127.78 (CH, Ar, Trt), 128.77 (CH, Ar, Trt), 141.25 (Cq, Fmoc), 141.35 (Cq, Fmoc), 143.54 (Cq, Fmoc), 144.03 (Cq, Fmoc), 144.79 (Cq, Ar, Trt), 156.60 (OCONH), 169.58 (COO), 171.43 (CONH); HRMS (NanoESI) *m/z* calculated for C<sub>45</sub>H<sub>45</sub>N<sub>2</sub>O<sub>7</sub> [M+H]<sup>+</sup> 725.3221, found 725.3213.

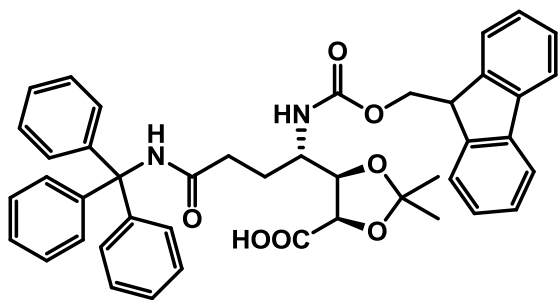
**[(4*S*,5*S*)-methyl 5-((*S*)-1-(((9*H*-fluoren-9-yl)methoxy)carbonylamino)-4-oxo-4-(tritylamino)butyl)-2,2-dimethyl-1,3-dioxolane-4-carboxylate] (24b)**



A solution of (2*S*,3*S*,4*S*) diol **23b** (847.0 mg, 1.24 mmol) and acetone dimethyl acetal (17 mL) in dry toluene (34 mL) was placed in a round bottomed flask and, after addition of catalytic PPTS, the mixture was stirred for 36 h. The toluene was removed

under reduced pressure, the residue re-dissolved in EtOAc and the organic layer washed with saturated aqueous  $\text{NH}_4\text{Cl}$  and brine, dried over  $\text{Na}_2\text{SO}_4$ , filtrated and concentrated under *vacuo* to give 893.9 mg of the acetal **24b** (quantitative) as a white solid which was used in the next reaction without further purification.  $^1\text{H}$  NMR (400 MHz,  $\text{CDCl}_3$ )  $\delta$  1.34 (3H, s,  $\text{CH}_3$ , acetal), 1.56 (3H, s,  $\text{CH}_3$ , acetal), 1.70 (1H, m,  $\text{CH}_2^5$ ), 2.02 (1H, m,  $\text{CH}_2^5$ ), 2.24 (2H, m,  $\text{CH}_2^6$ ), 3.57 (3H, s,  $\text{OCH}_3$ ), 3.77 (1H, m,  $\text{CH}^4$ ), 4.19 (1H, t,  $J = 6.5, 6.5$  Hz, CH, Fmoc), 4.31 (1H, t,  $J = 6.8, 6.8$  Hz,  $\text{CH}^3$ ), 4.42 (2H, dd,  $J = 13.1, 6.7$  Hz,  $\text{CH}_2$ , Fmoc), 4.63 (1H, d,  $J = 6.6$  Hz,  $\text{CH}^2$ ), 4.93 (1H, d,  $J = 9.2$  Hz,  $\text{CONH}$ ), 6.86 (1H, s,  $\text{CONH}$ ), 7.13-7.33 (17H, m, Trt, Fmoc), 7.37 (2H, t,  $J = 7.2, 7.2$  Hz, CH, Ar, Fmoc), 7.58 (2H, d,  $J = 7.4$  Hz, CH, Ar, Fmoc), 7.73 (2H, dd,  $J = 7.5, 4.0$  Hz, CH, Ar, Fmoc);  $^{13}\text{C}$  NMR (400 MHz,  $\text{CDCl}_3$ )  $\delta$  25.31 ( $\text{CH}_3$ , acetal), 26.56 ( $\text{CH}_3$ , acetal), 27.61 ( $\text{CH}_2^5$ ), 33.62 ( $\text{CH}_2^6$ ), 47.33 (CH, Fmoc), 51.06 ( $\text{CH}^4$ ), 52.45 ( $\text{OCH}_3$ ), 66.48 ( $\text{CH}_2$ , Fmoc), 70.57 (Cq, Trt), 76.05 ( $\text{CH}^2$ ), 79.40 ( $\text{CH}^3$ ), 110.96 (Cq, acetal), 119.97 (CH, Ar, Fmoc), 124.99 (CH, Ar, Fmoc), 125.01 (CH, Ar, Fmoc), 126.93 (CH, Ar, Trt), 127.03 (CH, Ar, Fmoc), 127.05 (CH, Ar, Fmoc), 127.70 (CH, Ar, Fmoc), 127.72 (CH, Ar, Fmoc), 127.88 (CH, Ar, Trt), 128.72 (CH, Ar, Trt), 141.34 (Cq, Fmoc), 143.66 (Cq, Fmoc), 143.86 (Cq, Fmoc), 144.70 (Cq, Ar, Trt), 156.20 ( $\text{OCONH}$ ), 170.12 ( $\text{COO}$ ), 171.26 ( $\text{CONH}$ ); HRMS (NanoESI)  $m/z$  calculated for  $\text{C}_{45}\text{H}_{45}\text{N}_2\text{O}_7$   $[\text{M}+\text{H}]^+$  725.3221, found 725.3214.

**[(4*R*,5*R*)-5-(((9*H*-fluoren-9-yl)methoxy)carbonylamino)-4-oxo-4-(tritylamino)butyl)-2,2-dimethyl-1,3-dioxolane-4-carboxylic acid] (**18**)**

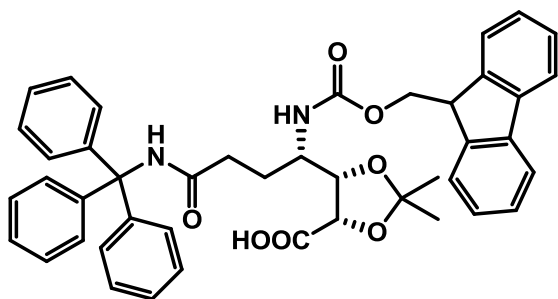


To a solution of acetal **24** (717.6 mg, 0.99 mmol, 1 equiv) in THF- $\text{H}_2\text{O}$  (7:3, 10 mL) at 0 °C,  $\text{LiOH}\cdot\text{H}_2\text{O}$  (45.7 mg, 1.09 mmol, 1.1 equiv) was added and the resulting mixture was stirred for 1 h at 0 °C. After analyzing the reaction crude by TLC, more  $\text{LiOH}\cdot\text{H}_2\text{O}$  (20.8 mg, 0.49 mmol, 0.5 equiv) was added and the

mixture was allowed to react for another hour at 0 °C. Then, after checking complete conversion of the starting material, the reaction mixture was acidified to pH 8 by the addition of 0.1 M aqueous HCl and Fmoc-OSu (667.9 mg, 1.98 mmol, 2 equiv) was added. The solution was allowed to react at room temperature and pH = 8 overnight. After analyzing the crude by HPLC-PDA and HPLC-ESMS to find that there wasn't any unprotected product, the solution was acidified to pH = 5 with 1 M aqueous HCl and extracted with EtOAc ( $\times 3$ ). The combined organic layer was washed with brine, dried over  $\text{Na}_2\text{SO}_4$ , filtrated and concentrated under

*vacuo*. The residue was washed with cold hexane, purified by reverse phase using a C18 Porapak Rxn RP 60 cc (Waters) column and then lyophilized to give 401.4 mg (57%) of the Fmoc-protected diol moiety **18** as a white solid.  $^1\text{H}$  NMR (400 MHz,  $\text{CD}_3\text{OD}$ )  $\delta$  1.35 (3H, s,  $\text{CH}_3$ , acetal), 1.57 (3H, s,  $\text{CH}_3$ , acetal), 1.76 (1H, m,  $\text{CH}_2^5$ ), 1.88 (1H, m,  $\text{CH}_2^5$ ), 2.29 (2H, m,  $\text{CH}_2^6$ ), 4.01 (1H, m,  $\text{CH}^4$ ), 4.24 (1H, dd,  $J = 6.9, 6.9$  Hz, CH, Fmoc), 4.32 (2H, m,  $\text{CH}_2$ , Fmoc), 4.38 (1H, m,  $\text{CH}^3$ ), 4.62 (1H, d,  $J = 7.6$  Hz,  $\text{CH}^2$ ), 7.16-7.31 (17H, m, Fmoc, Trt), 7.37 (2H, dt,  $J = 7.4, 7.4, 3.3$  Hz, CH, Ar, Fmoc), 7.64 (1H, d,  $J = 7.3$  Hz, CH, Ar, Fmoc), 7.69 (1H, d,  $J = 7.4$  Hz, CH, Ar, Fmoc), 7.78 (2H, d,  $J = 7.5$  Hz, CH, Ar, Fmoc);  $^{13}\text{C}$  NMR (400 MHz,  $\text{CD}_3\text{OD}$ )  $\delta$  24.86 ( $\text{CH}_3$ , acetal), 26.82 ( $\text{CH}_3$ , acetal), 30.99 ( $\text{CH}_2^5$ ), 34.67 ( $\text{CH}_2^6$ ), 49.33 (CH, Fmoc), 51.53 ( $\text{CH}^4$ ), 67.95 ( $\text{CH}_2$ , Fmoc), 71.61 (Cq, Trt), 77.00 ( $\text{CH}^2$ ), 80.43 ( $\text{CH}^3$ ), 110.73 (Cq, acetal), 120.92 (CH, Ar, Fmoc), 126.37 (CH, Ar, Fmoc), 126.59 (CH, Ar, Fmoc), 127.74 (CH, Ar, Trt), 128.19 (CH, Ar, Fmoc), 128.70 (CH, Ar, Trt), 128.75 (CH, Ar, Fmoc), 128.82 (CH, Ar, Fmoc), 130.08 (CH, Ar, Trt), 142.55 (Cq, Fmoc), 142.70 (Cq, Fmoc), 145.11 (Cq, Fmoc), 145.83 (Cq, Fmoc), 146.09 (Cq, Ar, Trt), 158.71 (OCONH), 174.92 (CO); HRMS (NanoESI)  $m/z$  calculated for  $\text{C}_{44}\text{H}_{43}\text{N}_2\text{O}_7$   $[\text{M}+\text{H}]^+$  711.3065, found 711.3077.

**[[4S,5S]-5-(((9H-fluoren-9-yl)methoxy)carbonylamino)-4-oxo-4-(tritylamino)butyl)-2,2-dimethyl-1,3-dioxolane-4-carboxylic acid] (18b)**



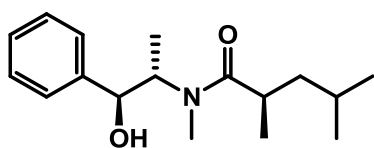
To a solution of acetal **24b** (721.4 mg, 1.00 mmol, 1 equiv) in THF- $\text{H}_2\text{O}$  (7:3, 10 mL) at 0 °C,  $\text{LiOH}\cdot\text{H}_2\text{O}$  (45.9 mg, 1.09 mmol, 1.1 equiv) was added and the resulting mixture was stirred for 1 h at 0 °C. After analyzing the reaction crude by TLC, more  $\text{LiOH}\cdot\text{H}_2\text{O}$  (20.9 mg, 0.50 mmol, 0.5 equiv) was added and the

mixture was allowed to react for another hour at 0 °C. Then, after checking complete conversion of the starting material, the reaction mixture was acidified to pH 8 by the addition of 0.1 M aqueous HCl and Fmoc-OSu (671.4 mg, 1.99 mmol, 2 equiv) was added. The solution was allowed to react at room temperature and pH = 8 overnight. After analyzing the crude by HPLC-PDA and HPLC-ESMS to find that there wasn't any unprotected product, the solution was acidified to pH = 5 with 1 M aqueous HCl and extracted with EtOAc ( $\times 3$ ). The combined organic layer was washed with brine, dried over  $\text{Na}_2\text{SO}_4$ , filtrated and concentrated under *vacuo*. The residue was washed with cold hexane, purified by reverse phase using a C18 Porapak Rxn RP 60 cc (Waters) column and then lyophilized to give 477.6 mg (60%) of the

Fmoc-protected diol moiety **18b** as a white solid.  $^1\text{H}$  NMR (400 MHz,  $\text{CD}_3\text{OD}$ )  $\delta$  1.35 (3H, s,  $\text{CH}_3$ , acetal), 1.53 (3H, s,  $\text{CH}_3$ , acetal), 1.59 (1H, m,  $\text{CH}_2^5$ ), 2.02 (1H, m,  $\text{CH}_2^5$ ), 2.26 (2H, m,  $\text{CH}_2^6$ ), 3.84 (1H, ddd,  $J = 10.7, 8.4, 2.7$  Hz,  $\text{CH}^4$ ), 4.21 (1H, dd,  $J = 6.8, 6.8$  Hz, CH, Fmoc), 4.31 (1H, m,  $\text{CH}^3$ ), 4.37 (2H, dd,  $J = 6.8, 2.2$  Hz,  $\text{CH}_2$ , Fmoc), 4.63 (1H, d,  $J = 6.8$  Hz,  $\text{CH}^2$ ), 7.16-7.32 (17H, m, Fmoc, Trt), 7.37 (2H, dt,  $J = 7.5, 7.4, 2.1$  Hz, CH, Ar, Fmoc), 7.63 (1H, d,  $J = 7.5$  Hz, CH, Ar, Fmoc), 7.67 (1H, d,  $J = 7.4$  Hz, CH, Ar, Fmoc), 7.78 (2H, d,  $J = 7.4$  Hz, CH, Ar, Fmoc);  $^{13}\text{C}$  NMR (400 MHz,  $\text{CD}_3\text{OD}$ )  $\delta$  25.65 ( $\text{CH}_3$ , acetal), 27.14 ( $\text{CH}_3$ , acetal), 30.33 ( $\text{CH}_2^5$ ), 34.33 ( $\text{CH}_2^6$ ), 48.69 (CH, Fmoc), 52.26 ( $\text{CH}^4$ ), 67.61 ( $\text{CH}_2$ , Fmoc), 71.62 (Cq, Trt), 77.67 ( $\text{CH}^2$ ), 80.80 ( $\text{CH}^3$ ), 111.92 (Cq, acetal), 120.95 (CH, Ar, Fmoc), 126.30 (CH, Ar, Fmoc), 126.40 (CH, Ar, Fmoc), 127.73 (CH, Ar, Trt), 128.15 (CH, Ar, Fmoc), 128.17 (CH, Ar, Fmoc), 128.72 (CH, Ar, Trt), 128.74 (CH, Ar, Fmoc), 128.82 (CH, Ar, Fmoc), 130.08 (CH, Ar, Trt), 142.62 (Cq, Fmoc), 142.73 (Cq, Fmoc), 145.15 (Cq, Fmoc), 145.75 (Cq, Fmoc), 146.07 (Cq, Ar, Trt), 158.60 (CONH), 174.95 (CO); HRMS (NanoESI)  $m/z$  calculated for  $\text{C}_{44}\text{H}_{43}\text{N}_2\text{O}_7$   $[\text{M}+\text{H}]^+$  711.3065, found 711.3082.

#### 1.5.1.4. Synthesis of (2R,3R,4R)-3-hydroxy-2,4,6-trimethylheptanoic acid (HTMHA)

##### (R)-N-((1S,2S)-1-hydroxy-1-phenylpropan-2-yl)-N,2,4-trimethylpentanamide (**25**)



LiCl (4.07 g, 96.02 mmol, 8.5 equiv) was placed in a round bottomed flask and dried with a heater under a  $\text{N}_2$  stream until it looked like a fine powder. Then, dry THF (30 mL) and DIPA (5.2 mL, 36.71 mmol, 3.2 equiv) were added, and the resulting suspension was cooled down to  $-78$  °C.  $n\text{-BuLi}$  (2.5 M in hexane, 13.6 mL, 34.00 mmol, 3 equiv) was added dropwise and after 5 min, the reaction mixture was warm up to  $0$  °C for 5 min and then cooled down again to  $-78$  °C. The (*S,S*)-pseudoephedrine propionamide (2.50 g, 11.30 mmol, 1 equiv) dissolved in dry THF (30 mL) was then slowly dropped via cannula at  $-78$  °C and kept under stirring at this temperature. After 1 h, the mixture was first warm up to  $0$  °C for 15 min, and then to room temperature for 5 more min, to be finally cooled down to  $0$  °C. At this point, 1-iodo-2-methylpropane (5.2 mL, 45.19 mmol, 4 equiv) was added, then the ice bath removed and the reaction mixture stirred for 3.5 h. HPLC-PDA analysis revealed complete conversion and the reaction was quenched by slow addition of saturated aqueous  $\text{NH}_4\text{Cl}$  (50 mL) at  $0$  °C. Then, brine (50 mL) was also added and the aqueous layer was extracted with EtOAc ( $\times 3$ ). The combined organic layer was washed with brine, dried over  $\text{MgSO}_4$ , filtrated and concentrated under *vacuo*. The residue was purified by flash column chromatography (hexane-EtOAc = 9:1 to 1:1) to give 3.00 g (96%) of product **26** as a white solid:  $^1\text{H}$  NMR (400 MHz,  $\text{CDCl}_3$ )  $\delta$  0.821 (3H, d,  $J = 6.4$  Hz,  $\text{CH}_3^4$ ), 0.851



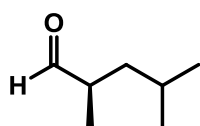
(3H, d,  $J = 6.2$  Hz, CH<sub>3</sub><sup>4</sup>), 1.069 (3H, d,  $J = 6.7$  Hz, CH<sub>3</sub><sup>2</sup>), 1.143 (3H, br d,  $J = 7.1$  Hz, CH<sub>3</sub><sup>3'</sup>), 1.148 (1H, m, CH<sub>2</sub><sup>3</sup>), 1.511 (1H, m, CH<sub>2</sub><sup>3</sup>), 1.511 (1H, m, CH<sup>4</sup>), 2.674 (1H, m, CH<sup>2</sup>), 4.118 (1H, q,  $J = 7.1, 7.1, 7.1$  Hz, CH<sup>2</sup>), 4.615 (1H, d,  $J = 7.5$  Hz, CH<sup>1</sup>); <sup>13</sup>C NMR (400 MHz, CDCl<sub>3</sub>)  $\delta$  14.44 (CH<sub>3</sub><sup>3'</sup>), 17.43 (CH<sub>3</sub><sup>2</sup>), 22.57 (CH<sub>3</sub><sup>4</sup>), 22.69 (CH<sub>3</sub><sup>4</sup>), 25.65 (CH<sup>4</sup>), 33.51 (NMe), 34.41 (CH<sup>2</sup>), 43.06 (CH<sub>2</sub><sup>3</sup>), 58.10 (CH<sup>2</sup>), 76.54 (CH<sup>1</sup>), 126.26 (CH, Ar), 127.49 (CH, Ar), 128.28 (CH, Ar), 142.59 (Cq, Ar), 179.36 (CONH).

### (*R*)-2,4-Dimethylpentanol (**26**)



To a solution of DIPA (6.3 mL, 44.81 mmol, 4.2 equiv) in dry THF (50 mL) cooled down to  $-78$  °C, *n*-BuLi (2.5 M in hexane, 16.7 mL, 41.75 mmol, 4 equiv) was slowly dropped. After 10 min, the mixture was warmed up to  $0$  °C for 5 min and then cooled down again to  $-78$  °C. At this point, H<sub>3</sub>B-NH<sub>3</sub> complex (1.47 g, 42.68 mmol, 4 equiv) was added and the resulting solution was warm up to  $0$  °C for 20 min, then to room temperature for 10 more min and finally cooled down to  $0$  °C again for 10 min. A solution of the amide **25** (2.96 g, 10.67 mmol, 1 equiv) in dry THF (50 mL) was added dropwise and, after the addition, the reaction was allowed to reach room temperature and was stirred for 2.5 h. The TLC revealed complete conversion, thus, the reaction was quenched by addition of 3 M aqueous HCl at  $0$  °C until pH = 3 was reached (approx. 30 mL were needed). Then, brine was added (30 mL) and the aqueous layer was extracted with Et<sub>2</sub>O ( $\times$  3). The combined organic layers were washed with 3 M aqueous HCl ( $\times$  1), 3 M aqueous NaOH ( $\times$  1) and brine ( $\times$  1), dried over MgSO<sub>4</sub>, filtrated and concentrated under *vacuo* at a temperature below  $20$  °C to obtain 1.24 g (quantitative) of the alcohol **26** as a yellowish oil. <sup>1</sup>H NMR (300 MHz, CDCl<sub>3</sub>)  $\delta$  0.86 (3H, d,  $J = 6.5$  Hz, CH<sub>3</sub><sup>2</sup>), 0.89 (3H, d,  $J = 6.6$  Hz, CH<sub>3</sub><sup>4</sup>), 0.90 (3H, d,  $J = 6.6$  Hz, CH<sub>3</sub><sup>4</sup>), 1.00 (1H, ddd,  $J = 13.6, 8.6, 6.1$  Hz, CH<sub>2</sub><sup>3</sup>), 1.13-1.36 (1H, m, CH<sub>2</sub><sup>3</sup>), 1.57-1.78 (2H, m, CH<sup>2</sup>, CH<sup>4</sup>), 3.37 (1H, dd,  $J = 10.5, 6.6$  Hz, CH<sub>2</sub><sup>1</sup>), 3.50 (1H, dd,  $J = 10.5, 5.5$  Hz, CH<sub>2</sub><sup>1</sup>); <sup>13</sup>C NMR (100 MHz, CDCl<sub>3</sub>)  $\delta$  16.8 (CH<sub>3</sub><sup>2</sup>), 22.2 (CH<sub>3</sub><sup>4</sup>), 23.6 (CH<sub>3</sub><sup>4</sup>), 25.3 (CH<sup>4</sup>), 33.5 (CH<sup>2</sup>), 42.7 (CH<sub>2</sub><sup>3</sup>), 68.9 (CH<sub>2</sub><sup>1</sup>).

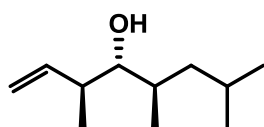
### (*R*)-2,4-Dimethylpentanal (**27**)



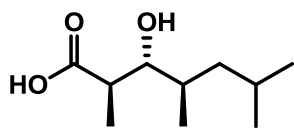
To a solution of (*R*)-2,4-dimethylpentanol **26** (1.24 g, 10.67 mmol, 1 equiv) in dry DCM (55 mL) in the presence of 4 Å MS, Dess-Martin reagent (5.11 g, 12.06 mmol, 1.13 equiv) was added, and the resulting milky mixture allowed to stir at room temperature for 30 min. The reaction was filtered and the solid washed with abundant pentane. The combined organic layers were washed with saturated aqueous NaHCO<sub>3</sub>-saturated aqueous Na<sub>2</sub>S<sub>2</sub>O<sub>3</sub> (1:1,  $\times$  2), brine ( $\times$  1), dried over MgSO<sub>4</sub>, filtrated and

concentrated under *vacuo* at temperatures below 20 °C. The residue was filtered through silica with pentane-Et<sub>2</sub>O (9:1) and concentrated under *vacuo* again (at temperatures below 20 °C) to give 1.142 g (83%-94%) of aldehyde **27** as a yellowish oil. <sup>1</sup>H NMR (500 MHz, CDCl<sub>3</sub>) δ 0.90 (3H, d, *J* = 6.5 Hz, CH<sub>3</sub><sup>4</sup>), 0.93 (3H, d, *J* = 6.5 Hz, CH<sub>3</sub><sup>4</sup>), 1.08 (3H, d, *J* = 6.9 Hz, CH<sub>3</sub><sup>2</sup>), 1.20 (1H, m, CH<sub>2</sub><sup>3</sup>), 1.59 (1H, m, CH<sub>2</sub><sup>3</sup>), 1.63 (1H, m, CH<sup>4</sup>), 2.41 (1H, ddq, *J* = 4.2, 4.2, 4.2 Hz, CH<sup>2</sup>), 9.60 (1H, d, *J* = 1.9 Hz, CHO); <sup>13</sup>C NMR (500 MHz, CDCl<sub>3</sub>) δ 20.6 (CH<sub>3</sub><sup>2</sup>), 22.2 (CH<sub>3</sub><sup>4</sup>), 22.9 (CH<sub>3</sub><sup>4</sup>), 25.5 (CH<sup>4</sup>), 39.7 (CH<sub>2</sub><sup>3</sup>), 44.4 (CH<sup>2</sup>), 205.4 (CHO).

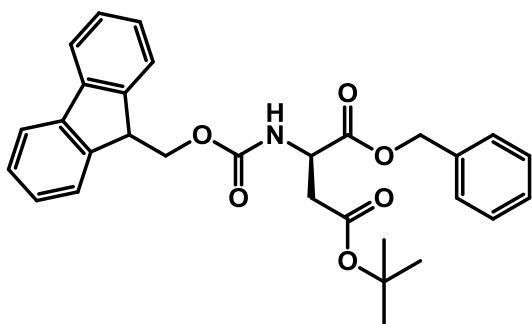
#### (3*S*,4*R*,5*R*)-3,5,7-Trimethylocten-4-ol (**28**)



A 1 M solution of <sup>t</sup>BuOK in dry THF (28 mL, 28.00 mmol, 2.8 equiv) was placed in a round bottomed flask provided with a cold finger and submerged in a cold bath at -78 °C. Then, *trans*-butene (3.7 mL, 40.00 mmol, 4 equiv) was condensed into the solution, followed by slow addition of *n*-BuLi (2.5 M in hexane, 11.2 mL, 28 mmol, 2.8 equiv). The resulting bright yellow mixture was stirred at -78 °C for 15 min, then warm up to -57 °C for 20 more min and finally cooled down again to -78 °C. At this point, a solution of IPc<sub>2</sub>BOMe (10.12 g, 32.00 mmol, 3.2 equiv) in dry THF (20 mL) was added dropwise, and the resulting mixture was stirred for 40 min, before adding the BF<sub>3</sub>·OEt<sub>2</sub> (3.95 mL, 32.00 mmol, 3.2 equiv) first and a solution of the aldehyde **27** (1.14 g, 10.00 mmol, 1 equiv) in dry THF (15 mL) second. The resulting cloudy solution was stirred at -78 °C for 4 h. Then the reaction was quenched by slow addition of 3 M aqueous NaOH (6.4 mL) and 30% aqueous H<sub>2</sub>O<sub>2</sub> (3.2 mL). The cold bath was removed and the resulting mixture was stirred 18 h at room temperature. The reaction was then diluted with H<sub>2</sub>O and extracted with Et<sub>2</sub>O (× 3), and all the combined organic layers were washed with brine, dried over MgSO<sub>4</sub>, filtrated and concentrated under *vacuo*. The residue was purified twice by flash column chromatography (hexane-EtOAc = 10:0 to 8:2) to give 1.28 g (75%) of product **28** as a colorless oil. <sup>1</sup>H NMR (500 MHz, CDCl<sub>3</sub>) δ 0.86 (3H, d, *J* = 6.6 Hz, CH<sub>3</sub><sup>7</sup>), 0.91 (3H, d, *J* = 6.5 Hz, CH<sub>3</sub><sup>7</sup>), 0.92 (3H, d, *J* = 6.7 Hz, CH<sub>3</sub><sup>5</sup>), 1.00 (3H, d, *J* = 6.9 Hz, CH<sub>3</sub><sup>3</sup>), 1.13 (1H, m, CH<sup>7</sup>), 1.26 (1H, m, CH<sup>5</sup>), 1.65 (2H, m, CH<sub>2</sub><sup>6</sup>), 2.37 (1H, ddq, *J* = 7.0, 7.0, 7.0 Hz, CH<sup>3</sup>), 3.13 (1H, t, *J* = 6.0, 6.0 Hz, CH<sup>4</sup>), 5.12 (2H, m, CH<sub>2</sub><sup>1</sup>), 5.76 (1H, m, CH<sup>2</sup>); <sup>13</sup>C NMR (500 MHz, CDCl<sub>3</sub>) δ 16.8 (CH<sub>3</sub><sup>3</sup>), 16.9 (CH<sub>3</sub><sup>5</sup>), 21.3 (CH<sub>3</sub><sup>7</sup>), 24.4 (CH<sub>3</sub><sup>7</sup>), 25.3 (CH<sup>7</sup>), 33.0 (CH<sup>5</sup>), 39.5 (CH<sub>2</sub><sup>6</sup>), 41.2 (CH<sup>3</sup>), 79.5 (CH<sup>4</sup>), 116.2 (CH<sub>2</sub><sup>1</sup>), 140.7 (CH<sup>2</sup>).

**(2R,3R,4R)-3-Hydroxy-2,4,6-trimethylheptanoic acid (29)**

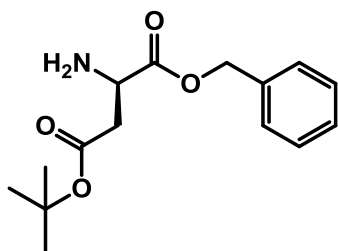
To a solution of the alkene **28** (139.6 mg, 0.82 mmol, 1 equiv) in H<sub>2</sub>O-dioxane (1:1, 8 mL), 4-methyl-morpholine *N*-oxide (143.9 mg, 1.23 mmol, 1.5 equiv) and OsO<sub>4</sub> (4% in H<sub>2</sub>O, 104 μL, 0.033 mmol, 0.04 equiv) were added. NaIO<sub>4</sub> (263.1 mg, 1.23 mmol, 1.5 equiv) was added after 1 h and the resulting milky suspension was stirred for 2 h more. Then the reaction mixture was cooled down to 0 °C and quenched by adding NaClO<sub>2</sub> (368.9 mg, 3.28 mmol, 4 equiv) and H<sub>2</sub>NSO<sub>3</sub>H (318.1 mg, 3.28 mmol, 4 equiv) to obtain a bright yellow suspension that was stirred for 2 h more at room temperature. Then, 5% aqueous HCl was added and the aqueous layer was extracted with DCM (× 3). The combined organic extracts were washed with 5% aqueous HCl (× 1) and brine, dried over MgSO<sub>4</sub>, filtrated and concentrated under *vacuo* to obtain **29** as a yellowish oil that was used without further purification. <sup>1</sup>H NMR (400 MHz, CDCl<sub>3</sub>) δ 0.83 (3H, d, *J* = 6.5 Hz, CH<sub>3</sub><sup>6</sup>), 0.91 (3H, d, *J* = 6.6 Hz, CH<sub>3</sub><sup>6</sup>), 0.94 (3H, d, *J* = 6.7 Hz, CH<sub>3</sub><sup>4</sup>), 1.13 (1H, m, CH<sub>2</sub><sup>5</sup>), 1.23 (3H, d, *J* = 7.2 Hz, CH<sub>3</sub><sup>2</sup>), 1.24 (1H, m, CH<sub>2</sub><sup>5</sup>), 1.65 (1H, m, CH<sup>6</sup>), 1.69 (1H, m, CH<sup>4</sup>), 2.69 (1H, m, CH<sup>2</sup>), 3.44 (1H, dd, *J* = 6.5, 5.1 Hz, CH<sup>3</sup>); <sup>13</sup>C NMR (400 MHz, CDCl<sub>3</sub>) δ 14.71 (CH<sub>3</sub><sup>2</sup>), 16.56 (CH<sub>3</sub><sup>4</sup>), 21.24 (CH<sub>3</sub><sup>6</sup>), 24.24 (CH<sub>3</sub><sup>6</sup>), 25.16 (CH<sup>6</sup>), 33.55 (CH<sup>4</sup>), 39.51 (CH<sub>2</sub><sup>5</sup>), 41.96 (CH<sup>2</sup>), 78.15 (CH<sup>3</sup>).

**1.5.1.5. Synthesis of HTMHA-D-Asp(<sup>t</sup>Bu)-OH****Fmoc-D-Asp(<sup>t</sup>Bu)-OBzl (30)**

To a solution of Fmoc-D-Asp(<sup>t</sup>Bu)-OH (1.5 g, 3.65 mmol, 1 equiv) in dry MeOH (20 mL) Cs<sub>2</sub>CO<sub>3</sub> (593.8 mg, 1.82 mmol, 0.5 equiv) was added, and the resulting solution was stirred under Ar at room temperature for 20 min. Then, the solvent was removed under reduced pressure to furnish the cesium carboxylate as a white solid. It was re-dissolved in dry DMF (17 mL) and BzlBr (1.3 mL, 10.94 mmol, 3 equiv) was dropped under Ar. The resulting mixture was stirred for 2 h. Saturated aqueous NH<sub>4</sub>Cl was used to quench the reaction. The aqueous layer was extracted with EtOAc (× 3) and the combined organic layer was washed once with brine, dried over Na<sub>2</sub>SO<sub>4</sub>, filtrated and concentrated under *vacuo*. The residue was purified by flash column chromatography (hexane-EtOAc = 10:0 to 8:2) to give 1.75 mg of Fmoc-D-Asp(<sup>t</sup>Bu)-OBzl **30** (95%) as a white solid. <sup>1</sup>H NMR (400 MHz, CDCl<sub>3</sub>) δ 1.42 (9H, s, CH<sub>3</sub>), 2.79 (1H, dd, *J* = 17.0, 4.5 Hz, CH<sub>2</sub><sup>β</sup>), 2.97 (1H, dd, *J* =

17.0, 4.6 Hz, CH<sub>2</sub><sup>β</sup>), 4.23 (1H, t, *J* = 7.2, 7.2 Hz, CH, Fmoc), 4.33 (1H, dd, *J* = 10.4, 7.5 Hz, CH<sub>2</sub>, Fmoc), 4.42 (1H, dd, *J* = 10.5, 7.3 Hz, CH<sub>2</sub>, Fmoc), 4.65 (1H, td, *J* = 8.9, 4.5, 4.5 Hz, CH<sup>α</sup>), 5.17 (1H, d, *J* = 12.3 Hz, CH<sub>2</sub>, Bzl), 5.24 (1H, d, *J* = 12.2 Hz, CH<sub>2</sub>, Bzl), 5.83 (1H, d, *J* = 8.6 Hz, CONH), 7.30 (2H, td, *J* = 7.5, 7.5, 0.9 Hz, CH, Ar, Fmoc), 7.32-7.36 (5H, m, CH, Ar, Bzl), 7.40 (2H, t, *J* = 7.5, 7.5 Hz, CH, Ar, Fmoc), 7.59 (2H, d, *J* = 7.4 Hz, CH, Ar, Fmoc), 7.76 (2H, d, *J* = 7.5 Hz, CH, Ar, Fmoc); <sup>13</sup>C NMR (400 MHz, CDCl<sub>3</sub>) δ 27.99 (CH<sub>3</sub>), 37.73 (CH<sub>2</sub><sup>β</sup>), 47.09 (CH, Fmoc), 50.64 (CH<sup>α</sup>), 67.28 (CH<sub>2</sub>, Fmoc), 67.46 (CH<sub>2</sub>, Bzl), 81.88 (Cq, <sup>t</sup>Bu), 119.96 (CH, Ar, Fmoc), 125.11 (CH, Ar, Fmoc), 125.16 (CH, Ar, Fmoc), 127.06 (CH, Ar, Fmoc), 127.70 (CH, Ar, Fmoc), 128.23 (CH, Ar, Bzl), 128.41 (CH, Ar, Bzl), 128.57 (CH, Ar, Bzl), 135.24 (Cq, Bzl), 141.25 (Cq, Fmoc), 141.27 (Cq, Fmoc), 143.70 (Cq, Fmoc), 143.90 (Cq, Fmoc), 155.97 (OCONH), 169.94 (COO), 170.78 (COO).

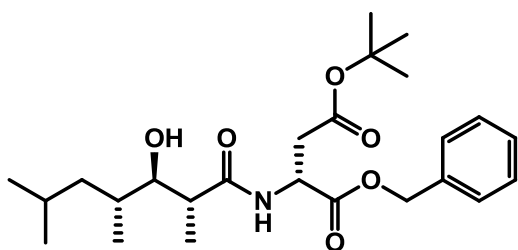
### H-D-Asp(<sup>t</sup>Bu)-OBzl (31)



A solution of piperidine-DCM (1:4, 15 mL) was added to the solid Fmoc-D-Asp(<sup>t</sup>Bu)-OBzl **30** (1.72 g, 3.42 mmol) and the resulting mixture was stirred for 40 min at room temperature. The solvents were removed under reduced pressure and the residue obtained purified by flash column chromatography (hexane-EtOAc = 95:5 to 0:10) to give 765.0 mg (80%) of H-D-

Asp(<sup>t</sup>Bu)-OBzl **31** as a white solid. <sup>1</sup>H NMR (400 MHz, CDCl<sub>3</sub>) δ 1.42 (9H, s, CH<sub>3</sub>), 2.69 (1H, dd, *J* = 16.6, 6.7 Hz, CH<sub>2</sub><sup>β</sup>), 2.77 (1H, dd, *J* = 16.6, 4.7 Hz, CH<sub>2</sub><sup>β</sup>), 3.82 (1H, dd, *J* = 6.6, 4.8 Hz, CH<sup>α</sup>), 5.15 (1H, d, *J* = 12.2 Hz, CH<sub>2</sub>, Bzl), 5.20 (1H, d, *J* = 12.3 Hz, CH<sub>2</sub>, Bzl), 7.32-7.37 (5H, m, Bzl); <sup>13</sup>C NMR (400 MHz, CDCl<sub>3</sub>) δ 28.03 (CH<sub>3</sub>), 39.62 (CH<sub>2</sub><sup>β</sup>), 51.33 (CH<sup>α</sup>), 67.07 (CH<sub>2</sub>, Bzl), 81.41 (Cq, <sup>t</sup>Bu), 128.30 (CH, Ar, Bzl), 128.40 (CH, Ar, Bzl), 128.59 (CH, Ar, Bzl), 135.49 (Cq, Bzl), 170.28 (COO), 173.90 (COO).

### HTMHA-D-Asp(<sup>t</sup>Bu)-OBzl (32)

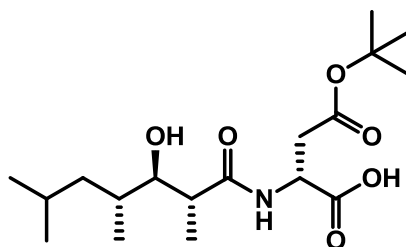


HTMHA **29** (120.0 mg, 0.64 mmol, 1 equiv), H-D-Asp(<sup>t</sup>Bu)-OBzl **31** (359.0 mg, 1.29 mmol, 2 equiv), HOBT\*H<sub>2</sub>O (196.8 mg, 1.29 mmol, 2 equiv) and EDC\*HCl (246.3 mg, 1.29 mmol, 2 equiv) were placed in a round-bottom flask. A mixture of dry DCM:DMF (1:1, 10 mL)

was added and, after checking that the pH of the reaction solution was around 6, it was allowed to react for 8 h at room temperature. DCM was removed under reduced pressure,

AcOEt added and the organic layer washed with saturated aqueous  $\text{NH}_4\text{Cl}$  solution ( $\times 3$ ), saturated aqueous  $\text{NaHCO}_3$  solution ( $\times 3$ ) and brine, dried over  $\text{Na}_2\text{SO}_4$ , filtrated and concentrated under *vacuo*. The residue was purified by flash column chromatography (hexane-EtOAc = 95:5 to 80:20) to give 68.9 mg (24%) of HTMHA-D-Asp(<sup>t</sup>Bu)-OBzl **32** as a yellowish oil.  $^1\text{H}$  NMR (400 MHz,  $\text{CDCl}_3$ )  $\delta$  0.83 (3H, d,  $J = 6.5$  Hz,  $\text{CH}_3^{\epsilon 2}$ , HTMHA), 0.91 (3H, d,  $J = 6.7$  Hz,  $\text{CH}_3^{\epsilon 1}$ , HTMHA), 0.91 (3H, d,  $J = 6.6$  Hz,  $\text{CH}_3^{\gamma}$ , HTMHA), 1.12 (2H, m,  $\text{CH}_2^{\delta}$ , HTMHA), 1.19 (3H, d,  $J = 7.0$  Hz,  $\text{CH}_3^{\alpha}$ , HTMHA), 1.39 (9H, s,  $\text{CH}_3$ , <sup>t</sup>Bu, Asp), 1.62 (1H, m,  $\text{CH}^{\epsilon}$ , HTMHA), 1.65 (1H, m,  $\text{CH}^{\gamma}$ , HTMHA), 2.47 (1H, m,  $\text{CH}^{\alpha}$ , HTMHA), 2.73 (1H, dd,  $J = 17.0, 4.4$  Hz,  $\text{CH}_2^{\beta}$ , Asp), 2.95 (1H, dd,  $J = 17.0, 4.8$  Hz,  $\text{CH}_2^{\beta}$ , Asp), 3.36 (1H, m,  $\text{CH}^{\beta}$ , HTMHA), 4.88 (1H, dt,  $J = 8.8, 4.6, 4.6$  Hz,  $\text{CH}^{\alpha}$ , Asp), 5.14 (1H, d,  $J = 12.2$  Hz,  $\text{CH}_2$ , Bzl), 5.22 (1H, d,  $J = 12.2$  Hz,  $\text{CH}_2$ , Bzl), 6.77 (1H, d,  $J = 8.4$  Hz, CONH), 7.31-7.36 (5H, m, Bzl);  $^{13}\text{C}$  NMR (400 MHz,  $\text{CDCl}_3$ )  $\delta$  15.14 ( $\text{CH}_3^{\alpha}$ , HTMHA), 16.70 ( $\text{CH}_3^{\gamma}$ , HTMHA), 21.33 ( $\text{CH}_3^{\epsilon 2}$ , HTMHA), 24.32 ( $\text{CH}_3^{\epsilon 1}$ , HTMHA), 25.20 ( $\text{CH}^{\epsilon}$ , HTMHA), 27.96 ( $\text{CH}_3$ , <sup>t</sup>Bu), 33.78 ( $\text{CH}^{\gamma}$ , HTMHA), 37.06 ( $\text{CH}_2^{\beta}$ , Asp), 43.17 ( $\text{CH}^{\alpha}$ , HTMHA), 48.56 ( $\text{CH}^{\alpha}$ , Asp), 67.60 ( $\text{CH}_2$ , Bzl), 78.71 ( $\text{CH}^{\beta}$ , HTMHA), 81.95 (Cq, <sup>t</sup>Bu), 128.35 (CH, Ar, Bzl), 128.49 (CH, Ar, Bzl), 128.60 (CH, Ar, Bzl), 135.12 (Cq, Bzl), 170.02 (COO), 170.95 (COO), 176.33 (CONH).

### HTMHA-D-Asp(<sup>t</sup>Bu)-OH (**33**)



A solution of HTMHA-D-Asp(<sup>t</sup>Bu)-OBzl **32** (68.9 mg, 0.15 mmol) in dry MeOH (5 mL) was stirred with a catalytic amount of Pd-C (10%) under an atmosphere of  $\text{H}_2$  (air pressure) for 12 h. EtOAc was added and the mixture was filtrated through celite and concentrated under *vacuo* to give 53.7 mg (97%) of crude HTMHA-D-Asp(<sup>t</sup>Bu)-OH **33**

as a yellow oil. By HPLC-PDA [conditions: linear gradient (5% to 100%) of ACN (0.036% TFA) into  $\text{H}_2\text{O}$  (0.045%) over 8 min, with a flow rate of 1.0 mL/min ( $t_R = 6.61$  min), at 220 nm] it had a purity of 60% but was used in the next reaction without further purification.  $^1\text{H}$  NMR (400 MHz,  $\text{CDCl}_3$ )  $\delta$  0.82 (3H, d,  $J = 6.6$  Hz,  $\text{CH}_3^{\epsilon 2}$ , HTMHA), 0.90 (3H, d,  $J = 6.6$  Hz,  $\text{CH}_3^{\epsilon 1}$ , HTMHA), 0.94 (3H, d,  $J = 6.8$  Hz,  $\text{CH}_3^{\gamma}$ , HTMHA), 1.12 (3H, d,  $J = 7.0$  Hz,  $\text{CH}_3^{\alpha}$ , HTMHA), 1.15 (2H, m,  $\text{CH}_2^{\delta}$ , HTMHA), 1.43 (9H, s,  $\text{CH}_3$ , <sup>t</sup>Bu), 1.61 (1H, m,  $\text{CH}^{\epsilon}$ , HTMHA), 1.68 (1H, m,  $\text{CH}^{\gamma}$ , HTMHA), 2.54 (1H, dt,  $J = 15.1, 7.4, 7.4$  Hz,  $\text{CH}^{\alpha}$ , HTMHA), 2.75 (1H, dd,  $J = 16.7, 4.9$  Hz,  $\text{CH}_2^{\beta}$ , Asp), 2.87 (1H, dd,  $J = 16.9, 5.5$  Hz,  $\text{CH}_2^{\beta}$ , Asp), 3.53 (1H, dd,  $J = 7.3, 4.1$  Hz,  $\text{CH}^{\beta}$ , HTMHA), 4.84 (1H, m,  $\text{CH}^{\alpha}$ , Asp), 7.13 (1H, d,  $J = 8.3$  Hz, CONH);  $^{13}\text{C}$  NMR (400 MHz,  $\text{CDCl}_3$ )  $\delta$  14.60 ( $\text{CH}_3^{\alpha}$ , HTMHA), 16.79 ( $\text{CH}_3^{\gamma}$ , HTMHA), 21.19 ( $\text{CH}_3^{\epsilon 2}$ , HTMHA), 24.35 ( $\text{CH}_3^{\epsilon 1}$ , HTMHA), 25.09 ( $\text{CH}^{\epsilon}$ , HTMHA), 27.99 ( $\text{CH}_3$ , <sup>t</sup>Bu),

32.76 (CH<sup>γ</sup>, HTMHA), 37.02 (CH<sub>2</sub><sup>β</sup>, Asp), 38.82 (CH<sub>2</sub><sup>δ</sup>, HTMHA), 43.67 (CH<sup>α</sup>, HTMHA), 48.74 (CH<sup>α</sup>, Asp), 78.66 (CH<sup>β</sup>, HTMHA), 82.01 (Cq, <sup>t</sup>Bu), 170.30 (COO), 173.69 (COO), 176.97 (CONH).

### 1.5.2. Synthetic Pipecolidepsin A

#### 1.5.2.1. Synthesis of Pipecolidepsin A

Aminomethyl resin (75.1 mg, 0.36 mmol/g) was placed in a 5 mL-polypropylene syringe fitted with two polyethylene filter discs. The resin was then washed, the AB linker and the first amino acid (Fmoc-D-Asp(OH)-OAllyl) incorporated and the excess of reactive positions terminated following the general procedures described in section 5.3.3. The loading, as calculated by UV absorbance at 290 nm, was 0.36 mmol/g.

Peptide elongation was achieved by means of different coupling conditions, being the protocol C the most commonly used one. Thus, sequential incorporation of Fmoc-β-EtO-Asn(Trt)-OH (43.2 mg, 0.068 mmol, 2.5 equiv), Fmoc-NMe-Gln-OH (36.1 mg, 0.095 mmol, 3.5 equiv), Fmoc-Leu-OH (42.9 mg, 0.122 mmol, 4.5 equiv), Fmoc-D-Lys(Boc)-OH (44.3 mg, 0.095 mmol, 3.5 equiv), Fmoc-D-*allo*-Thr(<sup>t</sup>Bu)-OH (32.2 mg, 0.081 mmol, 3 equiv) and Fmoc-AHDMHA-OH (26.8 mg, 0.068 mmol, 2.5 equiv) to the previously obtained H-D-Asp(O-Aminomethyl-resin)-OAllyl was accomplished using HATU/HOAt and DIEA (aa-HATU-HOAt-DIEA 1:1:1:2) in DMF (0.3 mL) with 1 min of pre-activation. In all cases, Kaiser's test showed a quantitative coupling after 60 min of treatment. The Fmoc-Leu-OH was re-coupled by default and clorani's test was used to check the completion of the reaction. Fmoc removal was carried out treating the resin with piperidine-DMF (1:4) (2 × 1 min, 2 × 5 min, 1 × 10 min). The heptapeptide H-AHDMHA-D-*allo*-Thr-D-Lys-Leu-NMe-Gln-β-EtO-Asn-D-Asp-OAllyl was obtained with a purity of 91% as checked by HPLC-PDA. Conditions: Xbridge<sup>TM</sup> BEH130 C18 reversed-phase analytical column (3.5 μm × 4.6 mm × 100 mm); linear gradient (20% to 70%) of ACN over 8 min, with a flow rate of 1.0 mL/min (*t*<sub>R</sub> = 3.08 min). HPLC-ESMS(+) analysis showed: *m/z* calcd for C<sub>43</sub>H<sub>76</sub>N<sub>10</sub>O<sub>15</sub> 973.12; [M+H]<sup>+</sup> found, 974.31.

Fmoc-diMeGln-OH (48.2 mg, 0.122 mmol, 4.5 equiv) was coupled using DIPCDI (19.0 μL, 0.122 mmol, 4.5 equiv) and HOBT\*H<sub>2</sub>O (18.6 mg, 0.122 mmol, 4.5 equiv) in DMF (0.6 mL) for 1 h at 25 °C without pre-activation. The solvents were removed and the resin washed with DMF (3 × 1 min) and DCM (3 × 1 min). The Kaiser's test proved quantitative coupling. The Fmoc group was kept in place until ester bond formation. The octapeptide Fmoc-diMeGln-AHDMHA-D-*allo*-Thr-D-Lys-Leu-NMe-Gln-β-EtO-Asn-D-Asp-OAllyl was obtained with a purity of

87% as checked by HPLC-PDA. Conditions: Xbridge™ BEH130 C18 reversed-phase analytical column (3.5  $\mu\text{m}$   $\times$  4.6 mm  $\times$  100 mm); linear gradient (40% to 80%) of ACN over 8 min, with a flow rate of 1.0 mL/min ( $t_{\text{R}}$  = 2.96 min). HPLC-ESMS(+) analysis showed:  $m/z$  calcd for  $\text{C}_{65}\text{H}_{98}\text{N}_{12}\text{O}_{19}$  1351.54;  $[\text{M}+\text{H}]^+$  found, 1352.93.

After washings with DCM (3  $\times$  1 min) the resin was dried under vacuum for 20 min and transferred to a PYREX<sup>R</sup> culture tube provided with a magnetic stirrer. Fresh Alloc-pipecolic-OH (86.4 mg, 0.405 mmol, 15 equiv) was dissolved in dry DCM (1.5 mL) and DIPCDI (63.4 mL, 0.405 mmol, 15 equiv) was added. The mixture was cooled down to 0  $^{\circ}\text{C}$ , filtered through a 0.45  $\mu\text{m}$  filter and added to the resin. DMAP (1.6 mg, 0.014 mmol, 0.5 equiv) dissolved in dry DMF (0.2 mL) was finally added to the tube. The mixture was reacted for 2.3 h at 45  $^{\circ}\text{C}$  with smooth stirring. The reaction mixture was transferred to the syringe, the solvents removed by filtration and the resin washed with DCM (3  $\times$  1 min), DMF (3  $\times$  1 min) and DCM (3  $\times$  1 min). Ester bond formation was monitored by cleavage of an aliquot of resin with TFA- $\text{H}_2\text{O}$ -Tis (95:2.5:2.5) (0.35 mL, 1  $\times$  1 h), followed by analysis of the crude by HPLC-PDA and HPLC-ESMS. The nonapeptide Fmoc-diMeGln-AHDMHA(Alloc-pipecolic)-D-*allo*-Thr-D-Lys-Leu-NMe-Gln- $\beta$ -EtO-Asn-D-Asp-OAllyl was obtained with a purity of 67% as checked by HPLC-PDA. Conditions: Xbridge™ BEH130 C18 reversed-phase analytical column (3.5  $\mu\text{m}$   $\times$  4.6 mm  $\times$  100 mm); linear gradient (40% to 80%) of ACN over 8 min, with a flow rate of 1.0 mL/min ( $t_{\text{R}}$  = 4.85 min). HPLC-ESMS(+) analysis showed:  $m/z$  calcd for  $\text{C}_{75}\text{H}_{111}\text{N}_{13}\text{O}_{22}$  1546.76;  $[\text{M}+\text{H}]^+$  found, 1548.20.

The Fmoc group of diMeGln was then removed following a short deprotection treatment with piperidine-DMF (1:4) (2  $\times$  2 min, 4 mL). The resin was shortly washed with DMF ( $\times$  2) and DCM ( $\times$  1) and the reaction mixture of the next residue Fmoc-DADHOHA(Trt, Acetonide)-OH (48.0 mg, 0.068 mmol, 2.5 equiv) quickly added to the resin. This amino acid was introduced using HATU (25.7 mg, 0.068 mmol, 2.5 equiv), HOAt (9.19 mg, 0.068 mmol, 2.5 equiv) and DIEA (23.5  $\mu\text{L}$ , 0.135 mmol, 5 equiv) dissolved in DMF (0.3 mL) with 1 min of pre-activation (Protocol C). After 1 h of coupling the solvents were removed and the resin was washed with DMF (3  $\times$  1 min) and DCM (3  $\times$  1 min). The Kaiser's test proved quantitative coupling. The resin was then subjected to the following washings/treatments: piperidine-DMF (1:4) (2  $\times$  1 min, 2  $\times$  5 min, 1  $\times$  10 min), DMF (3  $\times$  1 min) and DCM (3  $\times$  1 min). The decapeptide H-DADHOHA-diMeGln-AHDMHA(Alloc-pipecolic)-D-*allo*-Thr-D-Lys-Leu-NMe-Gln- $\beta$ -EtO-Asn-D-Asp-OAllyl was obtained with a purity of 60% (the decapeptide protected with an acetal group was also considered to calculate purity) as checked by HPLC-PDA. Conditions: Xbridge™ BEH130 C18 reversed-phase analytical column (3.5  $\mu\text{m}$   $\times$  4.6 mm  $\times$  100 mm); linear gradient

(30% to 70%) of ACN over 8 min, with a flow rate of 1.0 mL/min ( $t_R = 3.57$  min). HPLC-ESMS(+) analysis showed:  $m/z$  calcd for  $C_{67}H_{113}N_{15}O_{24}$  1512.70;  $[(M+2H^+)/2]$  found, 757.80.

The last two moieties were incorporated to the growing peptide chain as a single unit. HTMHA-D-Asp(<sup>t</sup>Bu)-OH (60% purity, 80.9 mg, 0.135 mmol, 5 equiv) and HOAt (18.4 mg, 0.135 mmol, 5 equiv) were dissolved in DMF (0.3 mL) and DIEA (47.0  $\mu$ L, 0.270 mmol, 10 equiv) was added. The reaction mixture was added to the resin followed by the addition of solid PyBOP (70.3 mg, 0.135 mmol, 5 equiv) and it was allowed to react for 3.5 h at 25 °C. The solvents were removed and the resin washed with DMF (3  $\times$  1 min) and DCM (3  $\times$  1 min). Coupling completion was monitored by cleavage of an aliquot of resin with TFA-H<sub>2</sub>O-Tis (95:2.5:2.5) (0.35 mL, 1  $\times$  1 h) followed by analysis of the crude by HPLC-PDA and HPLC-ESMS, as the Kaiser's test is not reliable at this point of the growing peptide chain. The dodecapeptide HTMHA-D-Asp-DADHOHA-diMeGln-AHDMHA(Alloc-pipecolic)-D-*allo*-Thr-D-Lys-Leu-NMe-Gln- $\beta$ -EtO-Asn-D-Asp-OAllyl was obtained with a purity of 37% as checked by HPLC-PDA. Conditions: Xbridge™ BEH130 C18 reversed-phase analytical column (3.5  $\mu$ m  $\times$  4.6 mm  $\times$  100 mm); linear gradient (30% to 70%) of ACN over 8 min, with a flow rate of 1.0 mL/min ( $t_R = 5.47$  min). HPLC-ESMS(+) analysis showed:  $m/z$  calcd for  $C_{81}H_{136}N_{16}O_{29}$  1798.04;  $[M+H]^+$  found, 1800.73.

Next, to remove the Allyl and Alloc groups the conditions described in section 5.3.6. were used. Thus, the peptide-resin was treated with Pd(PPh<sub>3</sub>)<sub>4</sub> (6.2 mg, 0.005 mmol, 0.2 equiv) and PhSiH<sub>3</sub> (66.6  $\mu$ L, 0.540 mmol, 20 equiv) dissolved in DCM (0.3 mL) under N<sub>2</sub>. After 15 min, the solvents were removed and the resin washed with DCM (1  $\times$  1 min), DMF (1  $\times$  1 min) and DCM (1  $\times$  1 min). The treatment was repeated three times. Deprotection completion was monitored by cleavage of an aliquot of resin with TFA- H<sub>2</sub>O-Tis (95:2.5:2.5) (0.35 mL, 1  $\times$  1 h) followed by analysis of the crude by HPLC-PDA and HPLC-ESMS. The linear precursor was obtained with a purity of 32% as checked by HPLC-PDA. Conditions: Xbridge™ BEH130 C18 reversed-phase analytical column (3.5  $\mu$ m  $\times$  4.6 mm  $\times$  100 mm); linear gradient (20% to 80%) of ACN over 8 min, with a flow rate of 1.0 mL/min ( $t_R = 4.21$  min). HPLC-ESMS(+) analysis showed:  $m/z$  calcd for  $C_{74}H_{128}N_{16}O_{27}$  1672.91;  $[(M+2H^+)/2]$  found, 838.80.

The macrolactamization step was carried out in solid phase. HOAt (14.7 mg, 0.108 mmol, 4 equiv) was dissolved in DMF (0.3 mL) and DIEA (37.6  $\mu$ L, 0.216 mmol, 8 equiv) was added. The reaction mixture was then added to the resin followed by the addition of solid PyBOP (56.2 mg, 0.108 mmol, 4 equiv) and it was allowed to react for 3 h at 25 °C. The solvents were removed and the resin washed with DMF (3  $\times$  1 min) and DCM (3  $\times$  1 min). The



cyclization step was monitored by cleavage of an aliquot of resin with TFA-H<sub>2</sub>O-Tis (95:2.5:2.5) (0.35 mL, 1 × 1 h) followed by analysis of the crude by HPLC-PDA and HPLC-ESMS.

The cleavage of the peptide and the elimination of the side-chain protecting groups were accomplished simultaneously by treating the resin with TFA-H<sub>2</sub>O-Tis (95:2.5:2.5) (4 mL, 1 × 1.5 h, 3 × 2 min). All the filtrates were collected in a round-bottom flask, evaporated to dryness under reduced pressure and lyophilized in H<sub>2</sub>O-ACN (1:1) to give 37.6 mg of crude with a purity of 15% as checked by HPLC-PDA. Conditions: Xbridge™ BEH130 C18 reversed-phase analytical column (3.5 μm × 4.6 mm × 100 mm); linear gradient (20% to 60%) of ACN over 8 min, with a flow rate of 1.0 mL/min (*t<sub>R</sub>* = 6.71 min). HPLC-ESMS(+) analysis showed: *m/z* calcd for C<sub>74</sub>H<sub>126</sub>N<sub>16</sub>O<sub>26</sub> 1655.88; [M+H]<sup>+</sup> found, 1657.84.

The crude was purified by semi-analytical HPLC-PDA using a XBridge™ Prep BEH130 C18 column (5 μm × 10 mm × 100 mm) and a linear gradient (5% to 35% over 5 min and 35% to 37% over 20 min) of ACN with a flow rate of 3.0 mL/min (*t<sub>R</sub>* = 14.13 min) to give 1.46 mg of synthetic Pipecolidepsin A (3.3%) with a purity of > 95%.

#### 1.5.2.2. Characterization of synthetic Pipecolidepsin A

Synthetic Pipecolidepsin A co-eluted by HPLC-PDA with a natural sample. Conditions: Phenomenex C18 reversed-phase analytical column 5 μm × 4.60 mm × 250 mm; linear gradient (36% to 38%) of ACN (0.036% TFA) into H<sub>2</sub>O (0.045%) over 40 min, with a flow rate of 1.0 mL/min (*t<sub>R</sub>* = 19.53 min); purity of XX%. HRMS(NanoESI) analysis showed: *m/z* calculated for C<sub>74</sub>H<sub>126</sub>O<sub>26</sub>N<sub>16</sub> 1654.9029, found 1654.9025 [M]. The <sup>1</sup>H and <sup>13</sup>C NMR (600 MHz, CD<sub>3</sub>OH) spectra of the synthetic peptide perfectly matched with the natural one (see Table 21 and 22).

N°	<sup>1</sup> H (nat.)	<sup>1</sup> H (sin.)	Δδ <sup>1</sup> H	N°	<sup>1</sup> H (nat.)	<sup>1</sup> H (sin.)	Δδ <sup>1</sup> H
<b>Pipecolic</b>				<b>D-allo-Thr</b>			
1	-	-	-	1	8.33 (br s)	8.33 (br s)	0.00
2	5.27 (m)	5.26 (m)	0.01	2	3.82 (br s)	3.83 (br s)	-0.01
3	2.19 (m) 1.64 (m)	2.20 (m) 1.64 (m)	-0.01 0.00	3	4.39 (m)	4.39 (dd, 13.0, 6.0)	0.00
4	1.74 (m) 1.25 (m)	1.75 (m) 1.26 (m)	-0.01 -0.01	4	1.34 (d, 6.0)	1.34 (d, 6.7)	0.00
5	1.61 (m) 1.58 (m)	1.63 (m) 1.51 (m)	-0.02 0.07	<b>AHDMHA</b>			
6	3.70 (m) 3.12 (m)	3.72 (m) 3.11 (m)	-0.02 0.01	1	8.96 (d, 10)	8.95 (m)	0.01
<b>D-Asp</b>				2	5.29 (m)	5.28 (m)	0.01
1	8.39 (d, 9.0)	8.39 (d, 10.1)	0.00	3	5.62 (dd, 11, 2)	5.61 (br d, 12.6)	0.01
2	5.34 (m)	5.31 (m)	0.03	4	1.91 (m)	1.91 (m)	0.00

3	2.90 (dd, 17, 8) 2.46 (dd, 16.5, 4)	2.85 (m) 2.45 (m)	0.05 0.01	Me	0.74 (d, 7.5)	0.74 (d, 7.4)	0.00
4	-	-	-	5	1.93 (m)	1.94 (m)	-0.01
<b>L-threo-β-EtOAsn</b>				Me	0.94 (d, 6.5)	0.94 (d, 6.8)	0.00
1	6.49 (d, 9.0)	6.50 (d 8.9)	-0.01	6	0.73 (d, 7.5)	0.72 (d, 7.1)	0.01
2	4.92	4.92 (m)	0.00	<b>DiMeGln</b>			
3	4.62	4.61 (m)	0.01	1	9.00 (d, 4.5)	9.11 (br s)	-0.11
4	7.53 (br s) 7.31 (br s)	7.52 (br s) 7.30 (br s)	0.01 0.01	2	4.33 (dd, 11, 5.5)	4.32 (dd, 11.3, 5.5)	0.01
CH <sub>2</sub>	3.67 (m) 3.48 (m)	3.67 (m) 3.49 (m)	0.00 -0.01	3	2.30 (m)	2.29 (m)	0.01
CH <sub>3</sub>	1.19 (t, 7.0)	1.19 (t, 7.2)	0.00	Me	1.09	1.09 (d, 7.2)	0.00
<b>NMeGln</b>				4	2.75 (dddd, 7, 2.5)	2.76 (m)	-0.01
1	-	-	-	Me	1.24 (d, 7)	1.24 (d, 7.4)	0.00
2	5.42 (d, 8.0)	5.42 (m)	0.00	5	7.45 (br s) 6.94 (br s)	7.41 (br s) 6.92 (br s)	0.04 0.02
3	2.46 (m) 1.81 (m)	2.48 (m) 1.81 (m)	-0.02 0.00	<b>DADHOHA</b>			
4	2.19 (m) 2.08 (m)	2.20 (m) 2.08 (m)	-0.01 0.00	1	7.66 (d, 9)	7.63 (d, 9.7)	0.03
5	7.21 (br s) 6.75 (br s)	7.23 (br s) 6.78 (br s)	-0.02 -0.03	2	3.84 (m)	3.85 (d, 9.0)	-0.01
NMe	2.96 (s)	2.96 (s)	0.00	3	3.59 (m)	3.58 (m)	0.01
<b>Leu</b>				4	4.10 (m)	4.10 (m)	0.00
1	7.60 (d, 6.0)	7.58 (d, 5.0)	0.02	5	1.92 (m) 1.78 (m)	1.92 (m) 1.78 (m)	0.00 0.00
2	4.58 (m)	4.59 (m)	-0.01	6	2.23 (m)	2.23(m)	0.00
3	2.39 (m) 1.55 (m)	2.38 (m) 1.56 (m)	0.01 -0.01	7	7.53 (br s) 6.83 (br s)	7.54 (br s) 6.81 (br s)	-0.01 0.02
<b>D-Lys</b>				<b>D-Asp</b>			
1	7.85 (br d, 8.5)	7.74 (br s)	0.11	1	8.35 (d, 8)	8.30 (d, 6.7)	0.05
2	4.49 (m)	4.46 (m)	0.03	2	4.69 (dd, 12, 6.5)	4.64 (m)	0.05
3	2.02 (m) 1.55 (m)	2.00 (m) 1.58 (m)	0.02 -0.03	3	2.92 (m) 2.84 (dd, 17, 5)	2.90 (dd, 18.8, 6.5) 2.74 (m)	0.02 0.10
4	1.48 (m) 1.36 (m)	1.48 (m) 1.35 (m)	0.00 0.01	4	-	-	-
5	1.66 (m)	1.61 (m)	0.05	<b>HTMHA</b>			
6	2.95 (m)	2.95 (m)	0.00	1	-	-	-
NH <sub>2</sub>	-	-	-	2	2.62 (dq, 9.5, 7)	2.62 (m)	0.00
				Me	1.07	1.06 (d, 6.8)	0.01
				3	3.57 (m)	3.56 (m)	0.01
				4	1.74 (m)	1.75 (m)	-0.01
				Me	0.99 (d, 6.5)	0.99 (d, 7.1)	0.00
				5	1.16 (m)	1.17 (m)	-0.01
				6	1.66 (m)	1.65 (m)	0.01
				Me	0.87 (d, 6.5)	0.87 (d, 6.7)	0.00
				7	0.94 (d, 6.5)	0.94 (d, 6.8)	0.00

Table 21: <sup>1</sup>H NMR spectral assignment of Pipecolidepsin A in CD<sub>3</sub>OH.

N°	<sup>13</sup> C (nat.)	<sup>13</sup> C (sin.)	Δδ <sup>13</sup> C	N°	<sup>13</sup> C (nat.)	<sup>13</sup> C (sin.)	Δδ <sup>13</sup> C
<b>Pipecolic</b>				<b>D-allo-Thr</b>			
1	170.4, s	170.5	-0.1	1	171.8, s	171.9	-0.1
2	53.9, d	53.9	0.0	2	64.3, d	64.3	0.0
3	27.6, t	27.5	0.1	3	67.6, d	67.5	0.1
4	22.6, t	22.6	0.0	4	20.1, q	20.2	-0.1
5	26.3, t	26.2	0.1	<b>AHDMHA</b>			
6	44.6, t	44.6	0.0	1	174.6, s	173.7	0.9
<b>D-Asp</b>				2	55.6, d	55.7	-0.1
1	170.5, s	170.5	0.0	3	77.2, d	77.2	0.0
2	47.2, d	47.3	-0.1	4	39.1, d	39.1	0.0
3	36.5, t	36.6	-0.1	Me	8.8, q	8.8	0.0
4	173.8, s	170.5	3.2	5	27.8, d	27.8	0.0
<b>L-threo-β-EtO-Asn</b>				Me	21.3, q	21.3	0.0
1	169.7, s	169.7	0.0	6	15.3, q	15.2	0.1
2	56.7, d	56.8	-0.1	<b>diMeGln</b>			
3	78.5, d	78.5	0.0	1	174.6, s	174.1	0.5
4	174.1, s	174.1	0.0	2	59.0, d	59.2	-0.2
CH <sub>2</sub>	68.0, t	68.0	0.0	3	37.2, d	37.3	-0.1
CH <sub>3</sub>	16.0, q	16.0	0.0	Me	14.3, q	14.3	0.0
<b>NMe-Gln</b>				4	42.5, d	42.2	0.3
1	172.2, s	172.2	0.0	Me	14.4, q	14.7	-0.3
2	58.2, d	58.2	0.0	5	180.2, s	180.0	0.2
3	23.5, t	23.3	0.2	<b>DADHOHA</b>			
4	31.9, t	31.8	0.1	1	176.4, s	176.5	-0.1
5	177.8, s	177.8	0.0	2	72.9, d	72.9	0.0
NMe	31.4, q	31.4	0.0	3	75.7, d	75.9	-0.2
<b>Leu</b>	4	174.7, s	174.6	4	51.1, d	51.1	0.0
1	177.0, s	176.9	0.1	5	28.5, t	28.5	0.0
2	51.3, d	51.3	0.0	6	32.6, t	32.7	-0.1
3	38.9, t	38.9	0.0	7	178.6, s	178.6	0.0
4	26.1, d	26.1	0.0	<b>D-Asp</b>			
Me	20.8, q	20.8	0.0	1	174.8, s	174.9	-0.1
5	24.1, q	24.1	0.0	2	51.7, d	52.1	-0.4
<b>D-Lys</b>	Me	17.4, q	17.4	3	36.6, t	37.8	-1.2
1				174.4, s	174.1	0.3	0.1
2	53.1, d	53.3	-0.2	<b>HTMHA</b>			
3	30.4, t	30.4	0.0	1	179.1, s	179.0	0.1
4	23.5, t	23.5	0.0	2	44.9, d	45.1	-0.2
5	27.9, t	28.0	-0.1	Me	14.4, q	13.9	0.5
6	41.0, t	41.0	0.0	3	79.6, d	79.7	-0.1
NH <sub>2</sub>	-	-	-	4	33.5, d,	33.4	0.1
				Me	17.4, q	17.4	0.0
				5	39.3, t	39.2	0.1
				6	26.2, d	26.2	0.0
				Me	21.5, q	21.5	0.0
				7	24.7, q	24.7	0.0

Table 22: <sup>13</sup>C NMR spectral assignment of Pipecolidepsin A in CD<sub>3</sub>OH.

### 1.5.3. Pipecolidepsin A'

#### 1.5.3.1. Synthesis of Pipecolidepsin A'

The procedure described for synthetic Pipecolidepsin A was also followed to accomplish the synthesis of Pipecolidepsin A' with a few changes because of peptidic sequence demands. Instead of Fmoc-NMe-Gln-OH, Fmoc-NMe-Glu(<sup>t</sup>Bu)-OH (3.5 equiv) was incorporated into the resin and the last two moieties were coupled stepwise instead of as a dipeptide. Fmoc-D-Asn(Trt)-OH was coupled following protocol C (Fmoc-AA-OH-HATU-HOAt-DIEA, 3.5:3.5:3.5:7, in DMF, for 1 h, in pre-activation mode (1 min)) and HTMHA was introduced according to protocol B but without pre-activation and a few changes: acid-DIPCDI-HOBt (3:3:3) in DMF for 3 h.

Synthetic Pipecolidepsin A' was purified by semi-analytical HPLC-PDA using a XBridge™ Prep BEH130 C18 column (5 μm × 10 mm × 100 mm) and a linear gradient (5% to 36% over 5 min and 36% to 42% over 20 min) of ACN with a flow rate of 3.0 mL/min ( $t_R$  = 11.69 min) to give 4.2 mg of Pipecolidepsin A' (4.7%) with a purity of 100%.

#### 1.5.3.2. Characterization of synthetic Pipecolidepsin A'

Synthetic Pipecolidepsin A' was analyzed by HPLC-PDA. Conditions: Xbridge™ BEH130 C18 reversed-phase analytical column (3.5 μm × 4.6 mm × 100 mm); linear gradient (30% to 50%) of ACN over 8 min, with a flow rate of 1.0 mL/min ( $t_R$  = 6.36 min); purity of 100%. HRMS(NanoESI) analysis showed:  $m/z$  calculated for  $C_{74}H_{126}O_{26}N_{16}$  1654.9029, found 1654.9046 [M]. The <sup>1</sup>H and <sup>13</sup>C NMR (600 MHz, CD<sub>3</sub>OH) chemical shifts of the synthetic peptide are detailed in Table 23.

N°	<sup>1</sup> H (sin.)	<sup>13</sup> C (sin.)	N°	<sup>1</sup> H (sin.)	<sup>13</sup> C (sin.)
<b>Pipecolic</b>			<b>D-allo-Thr</b>		
1	-		1	8.30 (br s)	n. a.
2	5.27 (m)	53.9	2	3.82 (m)	64.4
3	2.19 (m) 1.65 (m)	27.6	3	4.39 (m)	67.5
4	1.74 (m) 1.25 (m)	22.5	4	1.33 (d, 6.7)	20.1
5	1.61 (m) 1.52 (m)	26.3	<b>D-allo-AHDMHA</b>		
6	3.71 (m) 3.13 (m)	44.6	1	8.93 (d, 9.1)	
<b>D-Asp</b>			2	5.29 (m)	55.5
1	8.53 (br s)	n. a.	3	5.60 (br dd, 10.8, 1.4)	77.4
2	5.29 (m)	47.5	4	1.91 (m)	39.1

3	2.80 (m) 2.45 (br d, 15.4)	37.0	Me	0.74 (d, 7.7)	8.8
4	-	n. a.	5	1.93 (m)	27.8
<b>L-threo-<math>\beta</math>-EtOAsn</b>			Me	0.94 (d, 6.7)	21.3
1	6.50 (d, 8.4)	n. a.	6	0.73 (d, 7.2)	15.3
2	4.95 (m)	56.7	<b>DiMeGln</b>		
3	4.62 (br s)	78.6	1	9.14 (br s)	n. a.
4	7.59 (br s) 7.32 (br s)	n. a.	2	4.32 (dd, 10.7, 5.5)	59.1
CH <sub>2</sub>	3.67 (m) 3.48 (m)	68.1	3	2.29 (m)	37.4
CH <sub>3</sub>	1.19 (t, 9.7)	16.0	Me	1.08 (m)	14.4
<b>NMeGlu</b>			4	2.78 (m)	42.2
1	-	n. a.	Me	1.24 (dd, 7.1, 1.0)	14.7
2	5.54 (m)	58.3	5	7.37 (br s) 6.92 (br s)	n. a.
3	2.39 (m) 1.80 (m)	22.9	<b>DADHOHA</b>		
4	2.28 (m) 2.13 (m)	30.9	1	7.62 (d, 9.6)	n. a.
5	-	n. a.	2	3.86 (d, 8.7)	73.0
NMe	2.96 (s)	31.5	3	3.59 (m)	75.9
<b>Leu</b>			4	4.10 (m)	51.2
1	7.56 (br s)	n. a.	5	1.92 (m) 1.79 (m)	28.6
2	4.66 (m)	50.8	6	2.23 (m)	32.7
3	2.38 (t, 11.9) 1.53 (m)	39.0	7	7.56 (br s) 6.82 (br s)	n. a.
4	2.02 (m)	26.0	<b>D-Asn</b>		
Me	1.01 (d, 6.6)	20.9	1	8.22 (d, 6.6)	n. a.
5	1.07 (m)	24.1	2	4.66 (m)	51.8
<b>D-Lys</b>			3	2.92 (m) 2.72 (dd, 16.2, 5.2)	37.3
1	7.87 (br s)	n. a.	4	7.65 (br s) 7.12 (br s)	n. a.
2	4.46 (br t, 8.3)	53.3	<b>HTMHA</b>		
3	2.00 (m) 1.63 (m)	30.5	1	-	n. a.
4	1.46 (m) 1.36 (m)	23.5	2	2.61 (dq, 13.8, 6.8, 6.8, 6.8)	45.1
5	1.62 (m)	27.9	Me	1.07 (m)	13.9
6	2.96 (m)	41.0	3	3.57 (m)	79.7
NH <sub>2</sub>	-	-	4	1.75 (m)	33.5
			Me	0.98 (d, 6.8)	17.3
			5	1.17 (m)	39.4
			6	1.65 (m)	26.2
			Me	0.87 (m)	21.5
			7	0.94 (m)	24.7

**Table 23:** <sup>1</sup>H and <sup>13</sup>C NMR spectral assignment of Pipecolidepsin A' in CD<sub>3</sub>OH.

#### 1.5.4. Analog of Pipecolidepsin A': Analog 1A

##### 1.5.4.1. Synthesis of an analog of Pipecolidepsin A': Analog 1A

An analog of Pipecolidepsin A', Analog 1A, in which the *D-allo*-Thr residue was replaced by a D-Thr and the *D-allo*-AHDMHA moiety by a *D-allo*-Thr was synthesized using 2-CTC resin and a slightly different protocol.

2-Chlorotrytil chloride resin (101.6 mg, 1.6 mmol/g) was placed in a 5 mL polypropylene syringe fitted with two polyethylene filter discs. The resin was then washed, the first amino acid (Fmoc-D-Asp(OH)-OAllyl) incorporated and the excess of reactive positions terminated following the general procedures described in section 5.3.3. The loading, as calculated by UV absorbance at 290 nm, was 0.58 mmol/g.

The peptide was elongated until incorporation of the residue Fmoc-DADHOHA(Trt, Acetonide)-OH following the protocol C, in pre-activation mode and using 2.25 equiv of each residue except for diMeGln, which was re-coupled using 3 equiv and 1 equiv. The residue Fmoc-Leu-OH was also re-coupled (2.25 equiv + 2.25 equiv). The key step of removing the Fmoc group from the diMeGln residue and coupling of the Fmoc-DADHOHA(Trt, Acetonide)-OH moiety was performed as described for synthetic Pipecolidepsin A.

Then, the ester bond was formed using softer conditions: Alloc-pipecolic-OH-DIPCDI-DMAP (8:8:0.5, 98.9 mg-72.7  $\mu$ L-3.5 mg, 3 h + on + 2 h) in DCM (0.8 mL) at room temperature. When HPLC-PDA and HPLC-ESMS analysis confirmed complete conversion, the linear precursor was terminated. The last two residues were incorporated using the conditions described for protocol B (aa-DIPCDI-HOBt, X:X:X, 1 h, in DMF) and several re-couplings were needed. Fmoc-D-Asn(Trt)-OH was re-coupled once (4.5 equiv + 2.25 equiv) while the poliketide moiety HTMHA was re-coupled twice (2.25 equiv + 2.25 equiv + 2.25 equiv, 30 min + 1 h + 1 h). As the last Kaiser test wasn't completely negative, a capping treatment was performed using Boc<sub>2</sub>O-DIEA (2:1, 25.3 mg-10.1  $\mu$ L) in DMF (0.3 mL) for 20 min.

Then, the allyl and alloc groups were removed as described in the section 5.3.6. and the macrolactamization carried out under the conditions PyBOP-HOAt-DIEA (4:4:8, 120.7 mg-31.6 mg-81  $\mu$ L) in DMF (0.3 mL) at pH = 8 for 2.5 h. Finally, the cleavage was performed following the protocol described in the section 5.3.7. and the side-chain protecting groups removed by acidolytic treatment with a TFA-TIS-H<sub>2</sub>O (95:2.5:2.5, 16 mL) solution for 1 h.

After lyophilization, the crude was purified by semi-analytical HPLC-PDA using a XBridge™ Prep BEH130 C18 column (5 µm × 10 mm × 100 mm) and a linear gradient (5% to 29% over 5 min and 29% to 31% over 20 min) of ACN with a flow rate of 3.0 mL/min ( $t_R$  = 5.68 min) to give 2.9 mg of the analog of Pipecolidepsin A' (3.1%) with a purity of 94%.

#### 1.5.4.2. Characterization of an analog of Pipecolidepsin A'

The analog of Pipecolidepsin A' was analyzed by HPLC-PDA. Conditions: SunFire™ C18 reversed-phase analytical column (3.5 µm × 4.6 mm × 100 mm); linear gradient (30% to 35%) of ACN over 8 min, with a flow rate of 1.0 mL/min ( $t_R$  = 5.22 min); purity of 94%. HPLC-ESMS(+) analysis showed:  $m/z$  calculated for C<sub>70</sub>H<sub>119</sub>O<sub>26</sub>N<sub>16</sub> 1600.79, found 1599.90 [M+H]<sup>+</sup>. The <sup>1</sup>H and <sup>13</sup>C NMR (600 MHz, CD<sub>3</sub>OH) chemical shifts of the synthetic peptide are detailed in Table 24.

N°	<sup>1</sup> H (sin.)	<sup>13</sup> C (sin.)	N°	<sup>1</sup> H (sin.)	<sup>13</sup> C (sin.)
<b>Pipecolic</b>			<b>D-Thr</b>		
1	-	n. a.	1	8.13	n. a.
2	5.26	53.6	2	3.94	64.0
3	2.22 1.64	27.1	3	4.26	67.9
4	1.71 1.23	21.8	4	1.46	20.6
5	1.51	25.7	<b>D-allo-Thr</b>		
6	3.76 3.08	44.4	1		
<b>D-Asp</b>			2		
1	8.19	n. a.	3		
2	5.35	46.9	4		
3	2.89 2.49	36.4	<b>DiMeGln</b>		
4	-	n. a.	1	9.09	n. a.
<b>L-threo-β-EtOAsn</b>			2	4.23	58.8
1	6.52		3	2.27	37.8
2	4.96	56.4	Me	1.10	14.1
3	4.59	78.1	4	2.70	42.5
4	7.43 7.36	n. a.	Me	1.24	15.0
CH <sub>2</sub>	3.66 3.49	67.8	5	7.53 6.95	n. a.
CH <sub>3</sub>	1.18	15.6	<b>DADHOHA</b>		
<b>NMe-Glu</b>			1	7.60	n. a.
1	-	n. a.	2	3.96	72.9
2	5.46	57.7	3	3.64	75.4
3	2.29 1.84	22.6	4	4.10	51.0
4	2.28 2.14	30.6	5	1.84	28.4
5	-	n. a.	6	2.21	32.4
NMe	2.93	31.0	7	7.48 6.85	n. a.

Leu			D-Asn		
1	7.47	n. a.	1	8.24	n. a.
2	4.70	50.2	2	4.66	51.5
3	2.23 1.58	39.1	3	2.90 2.74	36.7
4	1.95	25.7	4	7.59 7.04	n. a.
Me	0.99	20.7	<b>HTMHA</b>		
5	1.03	23.6	1	-	n. a.
<b>D-Lys</b>			2	2.61	44.9
1	-	n. a.	Me	1.06	14.1
2	4.51	52.9	3	3.55	79.5
3	2.05 1.56	30.4	4	1.75	33.3
4	1.42 1.34	23.5	Me	0.99	17.1
5	1.63	27.8	5	1.18	39.1
6	2.92	40.7	6	1.65	26.1
NH <sub>2</sub>	-	-	Me	0.87	21.3
			7	0.95	24.6

**Table 24:** <sup>1</sup>H and <sup>13</sup>C NMR spectral assignments of Pipecolidepsin A' analog, Analog 1A in CD<sub>3</sub>OH.

## References



- (1) Lloyd-Williams, P., Albericio, F., Giralt, E. (1997). Chemical approaches to the synthesis of peptides and proteins (Boca Raton: CRC Press).
- (2) Kaiser, E., Colescott, R. L., Bossinger, C. D., Cook, P. I. *Anal. Biochem.* **1970**, *34*, 595-598.
- (3) Christensen, T. *Acta Chem. Scand. B* **1979**, *33*, 763-766.
- (4) Madder, A., Farcy, N., Hosten, N. G. C., De Muynck, H., De Clercq, P. J., Barry, J., Davis, A. P. *Eur. J. Org. Chem.* **1999**, 2787-2791.

**RESUM**

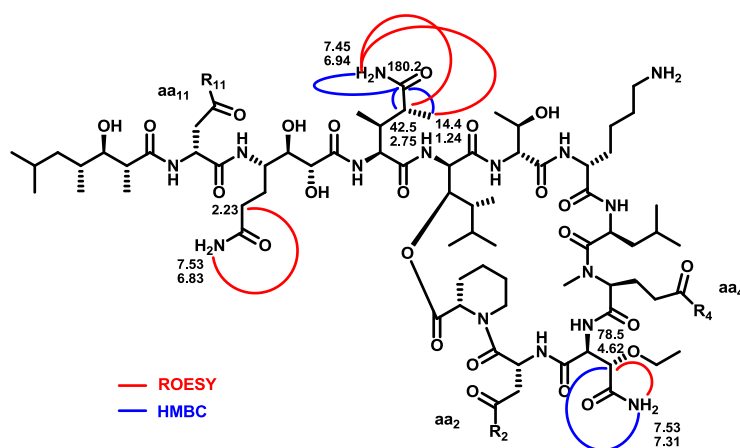


## Resum

Des de principis dels anys 90, l'ús de productes naturals en programes de desenvolupament de nous fàrmacs ha disminuït exponencialment, i la majoria de les grans empreses farmacèutiques, ha redirigit els immensos esforços antigament dedicats a l'aïllament, purificació, caracterització i avaluació de productes naturals, cap a la generació de grans llibreries purament sintètiques. No obstant aquesta tendència, la preponderància de les estructures naturals en l'àrea de la biomedicina és encara una realitat, tal i com reflecteixen les últimes estadístiques publicades l'any 2012. Des del 1981 fins a l'actualitat, el 60% dels fàrmacs aprovats pels organismes oficials FDA i EMA, són o bé productes naturals, o bé en deriven directament. Aquest percentatge és encara més gran (fins a un 70%), quan ens referim a drogues específiques per al tractament de càncer. Aquestes dades justifiquen àmpliament la tasca dels químics sintètics que, malgrat tot, continuen afrontant síntesis totals de productes naturals cada vegada més complexos. El nou repte: els ecosistemes marins.

En aquest context, la present tesi doctoral versa sobre la síntesi, elucidació estructural i avaluació biològica de dos productes naturals fabricats per esponges marines, que tenen un gran potencial com a agents terapèutics.

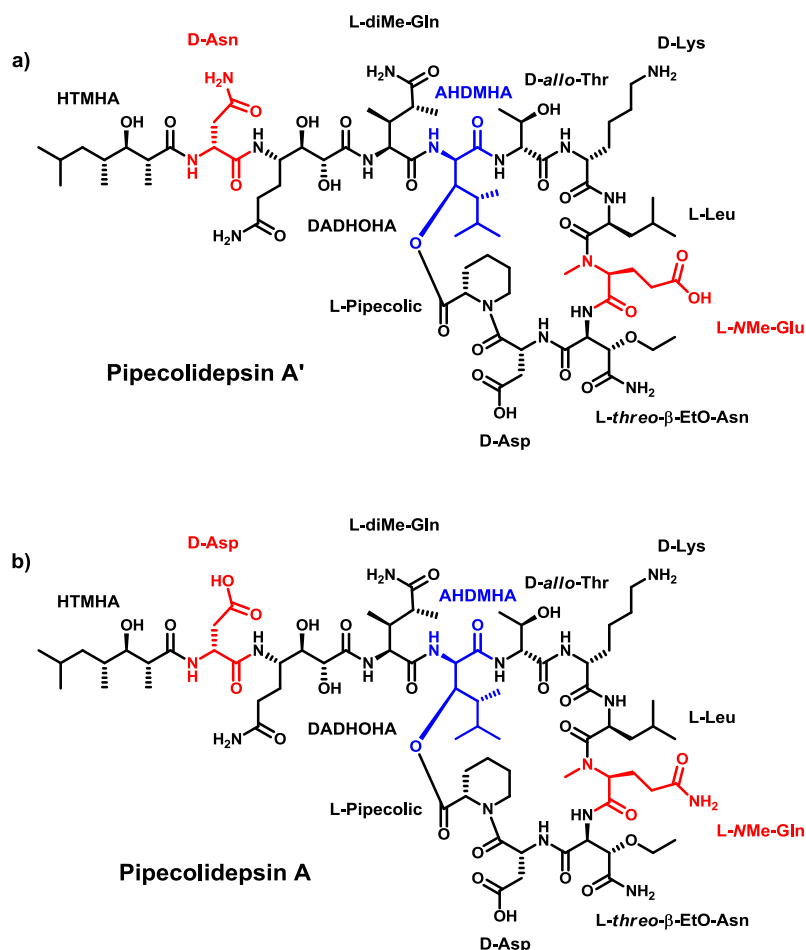
El Pipecolidepsin A és un ciclodepsipèptid aïllat per la companyia farmacèutica PharmaMar, a partir d'extractes d'una esponja marina pertanyent a l'espècie *Homophymia lamellosa*. La seva avaluació biològica va mostrar una activitat citotòxica en el rang del  $10^{-7}$  M en diferents línees cel·lulars cancerígenes (colon, mama, pulmó, pancrees...), convertint-lo en un candidat a fàrmac molt atractiu. Un estudi exhaustiu del pèptid natural emprant les tècniques de RMN i HPLC-MS, va permetre la proposta d'una estructura química preliminar (Pipecolidepsin A'). Quedaven però, incerteses estructurals per resoldre. El pèptid contenia quatre grups amida a les cadenes laterals, però només tres d'elles estaven perfectament identificades mitjançant pics de correlació d'experiments ROESY i HMBC (Figura 64).



**Figura 64:** Pics de correlació d'experiments ROESY i HMBC per als protons amida de cadena lateral del Pipecolidepsin A natural. Els àcids carboxílics i l'amida no assignats apareixen com a grups  $R_i$ .

Un estudi de MS-MS no conclouent, va permetre col·locar la quarta amida en una de les tres posicions factibles, tal i com es mostra a l'estructura preliminar Pipecolidepsin A' (Figura 65). La síntesi i assignació completa de  $^1\text{H}$  i  $^{13}\text{C}$  d'un anàleg simplificat, va forçar la revisió dels espectres de RMN del producte natural, emprant aquesta vegada un nou programa de processat. D'aquesta manera es van descobrir dos nous pics de correlació a l'espectre de ROESY que havien passat desapercebuts inicialment, i que permetien situar la quarta amida amb total seguretat. Teníem doncs, l'estructura química definitiva del Pipecolidepsin A (Figura 65). Finalment, es va decidir dur a terme la síntesi d'ambdues estructures. La comparació de

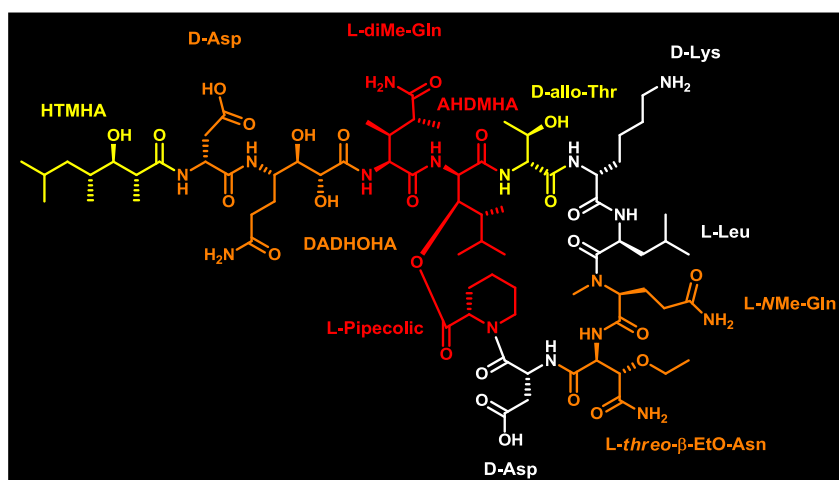
les assignacions completes de  $^1\text{H}$  i  $^{13}\text{C}$  dels tres pèptids (Pipecolidepsin A sintètic i natural i Pipecolidepsin A'), i la co-elució amb el producte natural, va donar la confirmació absoluta que la segona proposta corresponia a l'estructura real del Pipecolidepsin A natural.



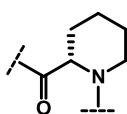
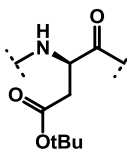
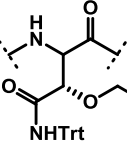
**Figura 65:** a) Estructura química preliminar del Pipecolidepsin A (Pipecolidepsin A'); b) Estructura química corregida del Pipecolidepsin A.

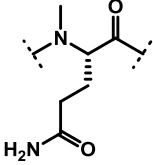
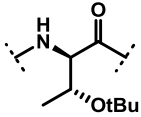
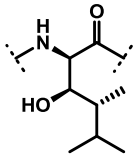
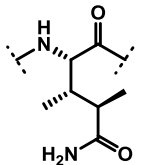
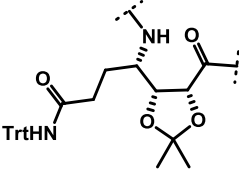
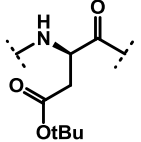
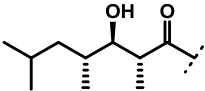
Des d'un punt de vista estructural, el Pipecolidepsin A és un depsipèptid cíclic "cap-cadena lateral". Un depsipèptid és un pèptid on, almenys un enllaç amida ha estat substituït per un enllaç èster. En aquest cas particular i de manera molt significativa, l'enllaç èster uneix l'extrem carboxil-terminal amb la cadena lateral de l'aminoàcid AHDMHA. Aquesta unió genera una estructura molt característica: una regió macrocíclica tancada a través de l'esmentat enllaç èster, i un braç peptídic exocíclic acabat amb un  $\beta$ -hidroxiàcid. Aquesta disposició particular és comú a una sèrie de depsipèptids d'origen marí, amb activitats biològiques molt interessants, que han proliferat a la literatura i als programes de química mèdica en els últims anys.

Una altra característica destacable del Pipecolidepsin A és la presència de fins a sis residus sintètics en la seva estructura, incloent-hi aa's  $\beta$ -ramificats, *N*Me-aa,  $\gamma$ -aa i  $\beta$ -hidroxiàcids. A més a més, dels 6 aminoàcids restants només un és proteínogènic (Leu), quatre són D-aa, i el residu restant és un *N*-alquil aminoàcid (àcid pipecòlic), que dona nom al pèptid. En aquest context doncs, són moltes les reaccions secundàries associades a la síntesi del Pipecolidepsin A. La figura 66 il·lustra la creixent complexitat sintètica associada a cada un dels residus constituents del depsipèptid, mentre la taula 25 detalla totes les possibles reaccions secundàries.



**Figura 66:** Estructura química del Pipecolidepsin A. Els colors indiquen el grau de dificultat associat a l'acoblament de cada aminoàcid.

Residu	Reaccions secundàries i reptes sintètics
	Racemització Estabilitat de l'enllaç èster en les condicions de síntesi Transacilació $O \rightarrow N$
	Formació d'aspartimides
	Eliminació del grup EtO- Baix índex d'acoblament degut a una qüestió d'impediment estèric Aminoàcid sintètic no comercial

	<p>Deshidratació de l'amida de la cadena lateral a grup nitril Lactamització intramolecular Baix índex d'acoblament degut al grup NMe Aminoàcid sintètic no comercial</p>
	<p>Baix índex d'acoblament degut a un qüestió d'impediment estèric</p>
	<p>Acilació del grup hidroxil desprotegit Formació de l'enllaç èster sobre un alcohol secundari extremadament impedit Transacilació <math>O \rightarrow N</math> Elongació de la cadena peptídica en dues direccions: <math>N</math> i <math>O</math> Formació de DKP a nivell de cadena Baix índex d'acoblament degut a una qüestió d'impediment estèric Aminoàcid sintètic no comercial</p>
	<p>Lactamització intramolecular Deshidratació de l'amida de la cadena lateral a grup nitril Baix índex d'acoblament degut a una qüestió d'impediment estèric Aminoàcid sintètic no comercial</p>
	<p>Baix índex d'acoblament degut a un qüestió d'impediment estèric Aminoàcid sintètic no comercial</p>
	<p>Formació d'aspartimides</p>
	<p>Acilació del grup hidroxil desprotegit Baix índex d'acoblament degut a una qüestió d'impediment estèric Aminoàcid sintètic no comercial</p>

Taula 25: Reaccions secundàries associades als aminoàcids presents al Pipecolidepsin A.



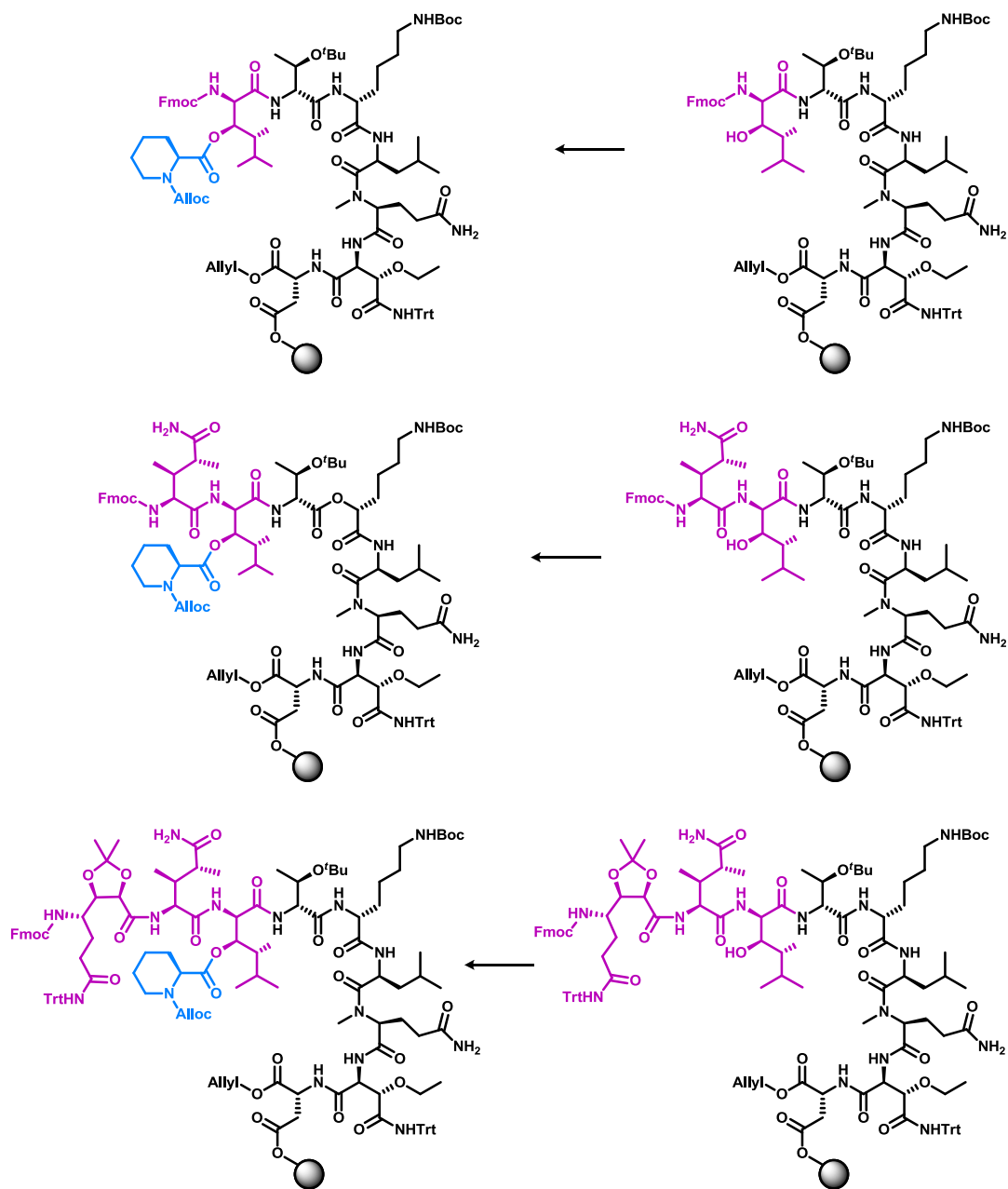
La pèrdua d'informació quiral dels  $C_{\alpha}$  durant les reaccions d'acoblament i ciclació, i la formació de DKP en desprotegir l'amino grup del segon residu incorporat a la resina, se sumen al llista de reaccions secundàries detallades a la Taula 25.

Tenint en compte l'enorme complexitat sintètica descrita prèviament, es va afrontar l'estimulant tasca de dissenyar l'estratègia de síntesi més idònia per al Pipecolidepsin A. Entre els dos esquemes de protecció habituals de la SPPS, es va escollir l'Fmoc/<sup>t</sup>Bu perquè permetia operar sota condicions àcides menys dràstiques. Aquest punt resulta clau a l'hora d'encarar la síntesi d'un depsipèptid d'estabilitat desconeguda que, a més a més, presenta un alt contingut d'aa's sintètics extremadament complexos. La resina 2-CTC va ser seleccionada com a grup protector permanent de l'extrem carboxil-terminal, ja que el seu impediment estèric minimitza el risc de formació de DKP, i les condicions mínimament àcides requerides per a efectuar l'escissió de l'enllaç pèptid-resina, permetent dur a terme la reacció de macrolactamització en fase sòlida i en solució. Finalment, la naturalesa "cap-cadena lateral" del Pipecolidepsin A, requeria la introducció d'un tercer grau d'ortogonalitat en l'esquema de protecció. Així doncs, els extrems carboxil i amino-terminal dels dos aa's involucrats en la reacció de ciclació, es van protegir amb els grups Al·lil i Al·loc respectivament.

L'eficaç sistema d'acoblament HATU-HOAt-DIEA es va seleccionar per a formar els enllaços amida, i només en aquells acoblaments sensibles que requerien condicions especials, va ser substituït pel sistema neutre DIPCDI-HOBt. El sistema PyBOP-HOAt-DIEA es va fer servir per a tractaments més llargs com la macrolactamització.

Com a punt d'inici/ciclació es va triar el residu D-Asp del cicle. La majoria dels enllaços amida de la regió macrocíclica involucren residus  $\beta$ -ramificats o *N*-substituïts que, en qualsevol cas, no representen el millor entorn per dur a terme una reacció de macrolactamització. Hi ha una excepció, l'enllaç D-Lys-Leu. Iniciar l'elongació de la cadena peptídica per l'aa D-Lys però, implicaria la construcció de l'enllaç èster en una etapa de creixement de la cadena massa inicial, l'elongació peptídica en dues direccions diferents, i la formació de dicetopiperazines a nivell de l'èster. L'enllaç D-Asp-Pip en canvi, minimitza tota aquesta problemàtica sintètica. Així doncs, la síntesi del precursor lineal s'iniciaria incorporant el residu D-Asp pel grup  $\alpha$ -COOH si l'etapa de ciclació s'efectua en solució, o pel grup  $\gamma$ -COOH si aquesta es du a terme en fase sòlida.

Finalment, la formació de l'enllaç èster representa el repte sintètic més gran, així doncs, es va decidir avaluar la seva construcció després d'incorporar els residus Fmoc-AHDMHA-OH, Fmoc-diMe-Gln-OH i Fmoc-DADHOHA(Acetal,Trt)-OH (Figura 67).

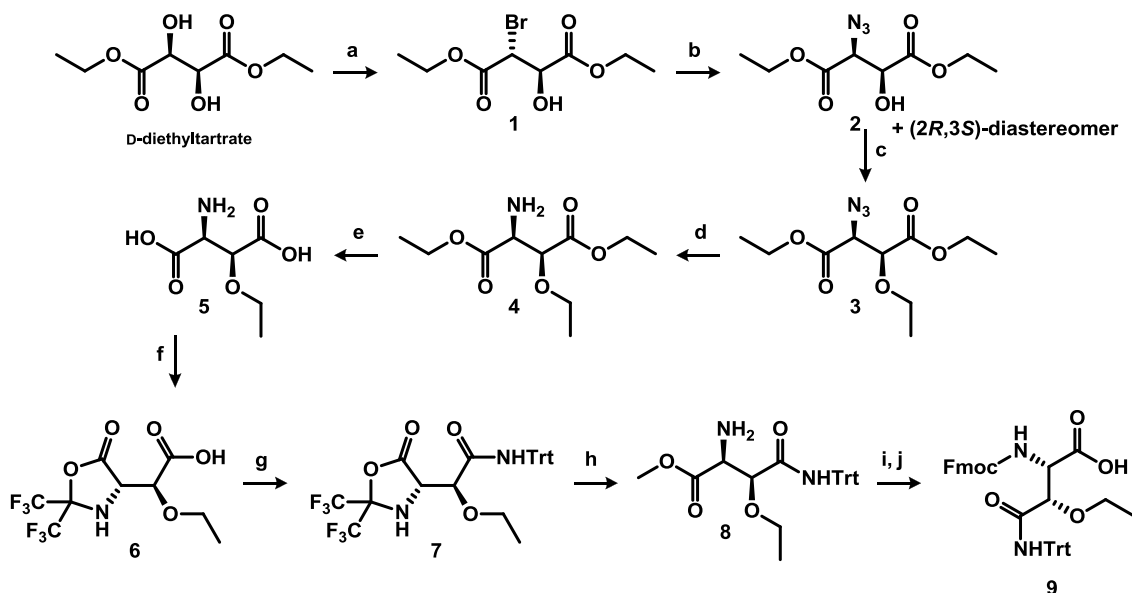


**Figura 67:** Formació de l'enllaç èster després d'acoblar els residus Fmoc-AHDMHA-OH, Fmoc-diMe-Gln-OH i Fmoc-DADHOHA(Acetal,Trt)-OH.

Abans d'iniciar la síntesi en fase sòlida del Pipecolidepsin A, era necessari fabricar els aminoàcids sintètics no comercials que trobem en la seva estructura. A continuació es detallen els esquemes sintètics desenvolupats per als residus Fmoc-*threo*- $\beta$ -EtO-Asn(Trt)-OH, Fmoc-

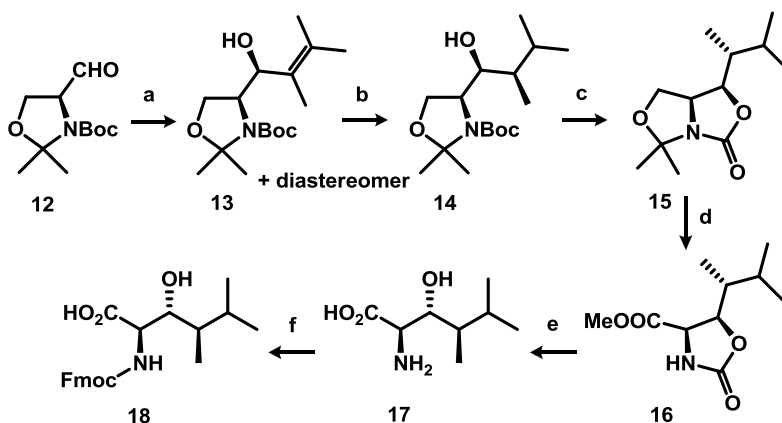
AHDMHA-OH, Fmoc-DADHOHA(Acetal,Trt)-OH i HTMHA. Els residus Fmoc-NMe-Gln-OH i Fmoc-diMe-Gln-OH van ser subministrats per l'empresa PharmaMar.

### Fmoc-threo- $\beta$ -EtO-Asn(Trt)-OH



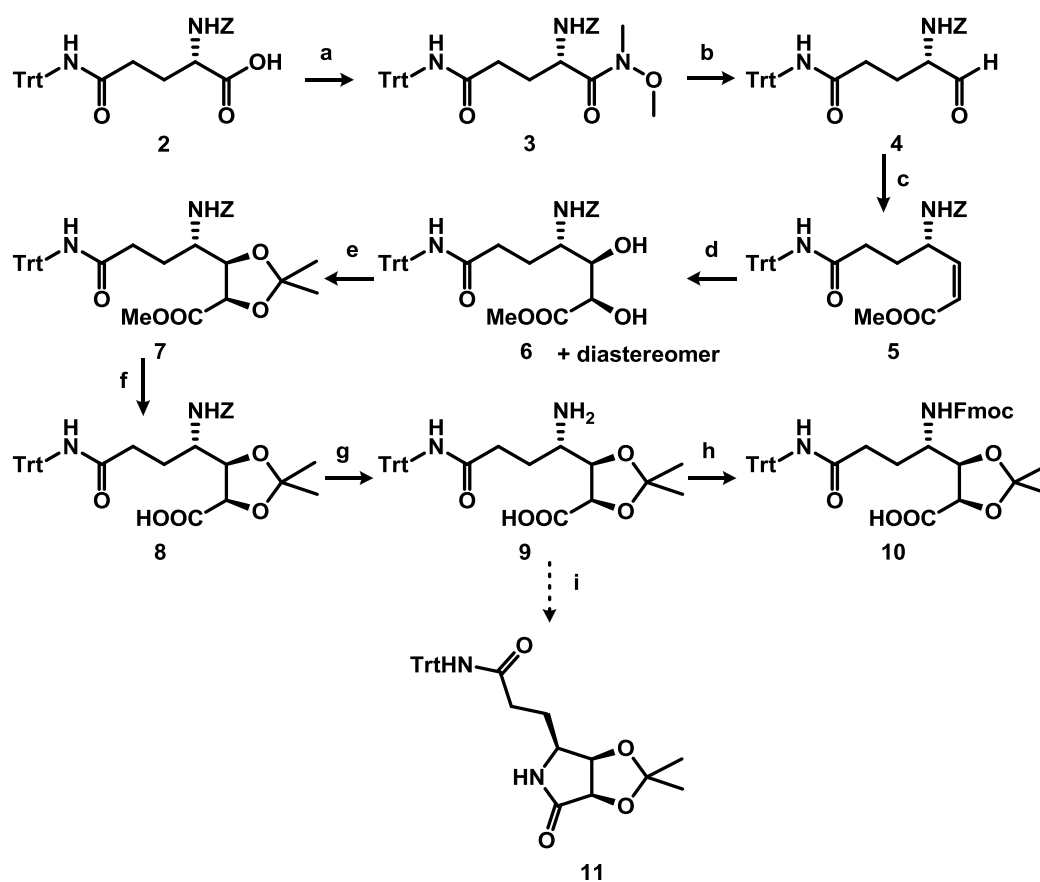
**Esquema 34:** Síntesi del residu Fmoc-L-threo- $\beta$ -EtO-Asn(Trt)-OH (9). a) HBr (30 % en AcOH), 0  $\rightarrow$  25  $^{\circ}$ C, 12 h; CH<sub>3</sub>COCl, EtOH, reflux, 8 h, 90%; b) NaN<sub>3</sub>, 15-Crown-5, DMF<sub>anh</sub>, 36 h, 90%; c) Ag<sub>2</sub>O/EtI, Et<sub>2</sub>O<sub>anh</sub>, reflux, 15 h, 89%; d) H<sub>2</sub>, Pd/C, EtOAc, 25  $^{\circ}$ C, 15 h, 87%; e) Solució aquosa 5 M d'HCl, reflux, 5 h; òxid de propilè, 25  $^{\circ}$ C, 84%; f) hexafluoroacetona, DMF<sub>anh</sub>, 25  $^{\circ}$ C, 22 h, 83%; g) Clorur d'oxal·lil, DMF<sub>anh</sub>, 25  $^{\circ}$ C, 30 min; tritilamina, toluè<sub>anh</sub>, 0  $^{\circ}$ C, 1 h, 59%; h) MeOH/ 4 M HCl en dioxà<sub>anh</sub>, 0  $^{\circ}$ C, 15 h, 95%; i) KOH, dioxà-H<sub>2</sub>O (2:1), 25  $^{\circ}$ C, 1 h; j) Fmoc-OSu, dioxà-H<sub>2</sub>O (2:1), pH = 9, 25  $^{\circ}$ C, 1 h, 70% (dos passos).

### Fmoc-AHDMHA-OH



**Esquema 35:** Síntesi del residu Fmoc-D-allo-AHDMHA-OH. a) i. 2-bromo-3-metil-2-butè, tBuLi, Et<sub>2</sub>O, -78  $^{\circ}$ C, 3.3 h; ii. Aldehid de Garner, Et<sub>2</sub>O, -78  $\rightarrow$  25  $^{\circ}$ C, 1.2 h, 34%; b) H<sub>2</sub> (4 atm), Pd(C), MeOH, -78  $^{\circ}$ C, 2 d, 78%; c) 2,6-di-*tert*-butil piridina, Tf<sub>2</sub>O, DCM, 0  $^{\circ}$ C, 10 min, 90%; d) Reactiu de Jones, acetona, 0  $^{\circ}$ C, 15 h, 67%; e) HCl conc., reflux, 72 h, 100%; f) Fmoc-OSu, 0.5% Na<sub>2</sub>CO<sub>3</sub>-dioxà (1:1), 25  $^{\circ}$ C, 15 h, 91%.

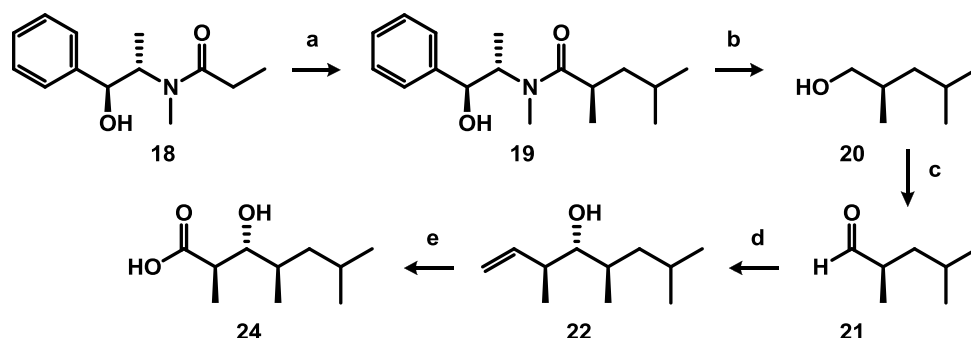
## Fmoc-DADHOHA(Acetal,Trt)-OH



**Esquema 36.** Síntesi del residu Fmoc-DADHOHA(Acetal, Trt)-OH. a) *N,O*-dimetilhidroxilamina, EDC, HOBT, DIEA, DMF<sub>anhv</sub>, 25 °C, 3 h, 96%; b) LiAlH<sub>4</sub>, THF<sub>anhv</sub>, 0 °C, 30 min; c) (CF<sub>3</sub>CH<sub>2</sub>O)<sub>2</sub>P(O)CH<sub>2</sub>COOMe, KHMDS, 18-crown-6, THF<sub>anhv</sub>, -78 °C, 2 h, 67%; d) cat. OsO<sub>4</sub>, NMO, THF-H<sub>2</sub>O (9:1), 25 °C, 10 dies, 75% (**6**) i 77% (diastereòmer); e) (CH<sub>3</sub>)<sub>2</sub>C(OCH<sub>3</sub>)<sub>2</sub>, cat. PPTS, toluè<sub>anhv</sub>, 25 → 50 °C, 36 h, 77% (**7**) i 96% (diastereòmer); f) LiOH, THF-H<sub>2</sub>O (9:1), 0 °C, 2 h, 98% (**8**) i 96% (diastereòmer); g) H<sub>2</sub> (1 atm), Pd(C), MeOH<sub>anhv</sub>, 25 °C, 5 h, 94% (**9**) i 93% (diastereòmer); h) Fmoc-Cl, NaN<sub>3</sub>, dioxà-H<sub>2</sub>O (1:1), pH 9, 0 °C, 5 d, 46% (**10**) i 45% (diastereòmer); i) EDC, HOBT, DMF, 25 °C, 6 h, 61% (**11**) i 52% (diastereòmer).

Un segon esquema sintètic amb Fmoc-Gln(Trt)-OH com a material de partida va ser desenvolupat i verificat. És una estratègia més curta (només 6 passos) i dona millors rendiments finals per a ambdós diastereòmers, però obliga a re-protecte el grup amino.

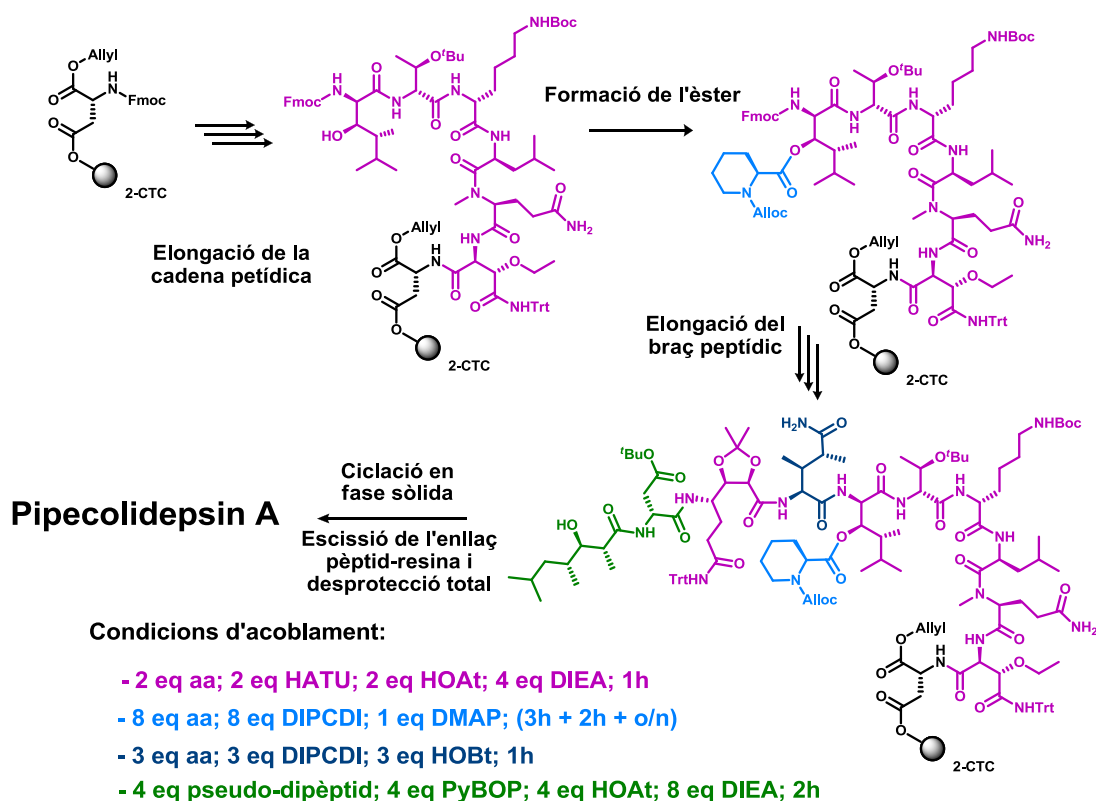
## HTMHA



**Esquema 37:** Síntesi de l'àcid (2*R*,3*R*,4*R*)-3-hidroxi-2,4,6-trimetilheptanoic. a) DIPA, *n*-BuLi, LiCl, THF<sub>anh</sub>, -78 °C, 1 h; 1-iodo-2-metilpropà, -78 °C, 3.5 h, 96%; b) DIPA, *n*-BuLi, H<sub>3</sub>B-NH<sub>3</sub>, THF<sub>anh</sub>, -78 → 25 °C, 2 h; c) Dess-Martin, DCM<sub>anh</sub>, 25 °C, 30 min; d) <sup>t</sup>BuOK, *trans*-2-butè, *n*-BuLi, -78 → -57 °C; (-)-*B*-metoxidiisopinocampfeilborà; BF<sub>3</sub>·Et<sub>2</sub>O, **21**, -78 °C; e) cat. OsO<sub>4</sub>, NaIO<sub>4</sub>, NMO, dioxà-H<sub>2</sub>O, 25 °C, 3 h; NaClO<sub>2</sub>, H<sub>2</sub>NSO<sub>3</sub>H, 0 → 25 °C, 2 h.

## Primera estratègia: AHDMHA + èster

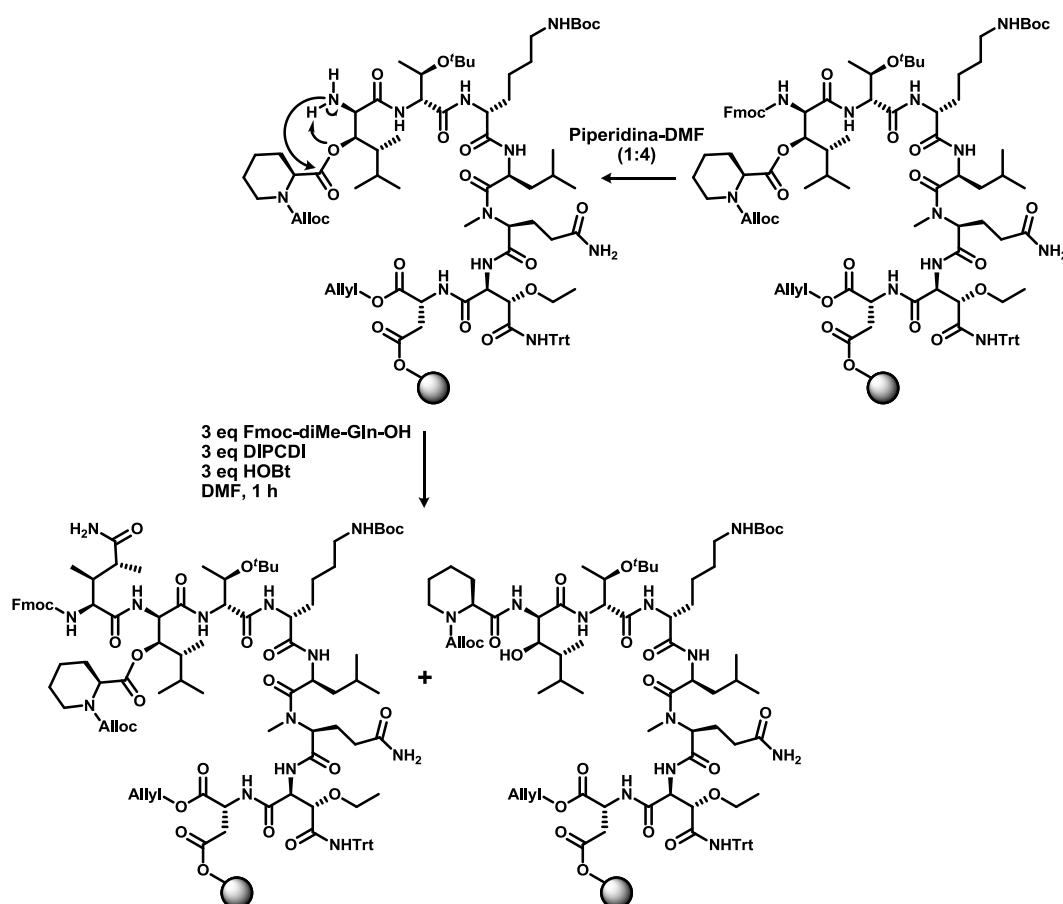
En una primera aproximació, l'enllaç èster es va formar en l'entorn de menys impediment estèric, és a dir, després d'incorporar l'aa Fmoc-AHDMHA-OH (Esquema 38).



**Esquema 38:** Primera estratègia sintètica per al Pipecolidepsin A: Incorporació del residu AHDMHA + formació de l'enllaç èster. Les condicions d'acoblament es troben indicades en colors.

El precursor lineal es va fer créixer fins a incorporar la super-treonina i, mantenint el grup protector Fmoc, es va acoblar l'Al-loc-pipecolic-OH. Les condicions habituals de formació d'enllaços èster van ser suficients per, després de tres tractaments, proporcionar l'intermedi èster de manera quantitativa i neta. A continuació, es preveia eliminar el grup Fmoc, i construir completament el braç peptídic. Els dos últims residus s'incorporarien simultàniament per evitar la formació d'aspartimides que donen lloc a un cru extremadament brut. Per últim i després d'eliminar els grups protectors Al-lil i Al-loc, la ciclació es duria a terme en fase sòlida.

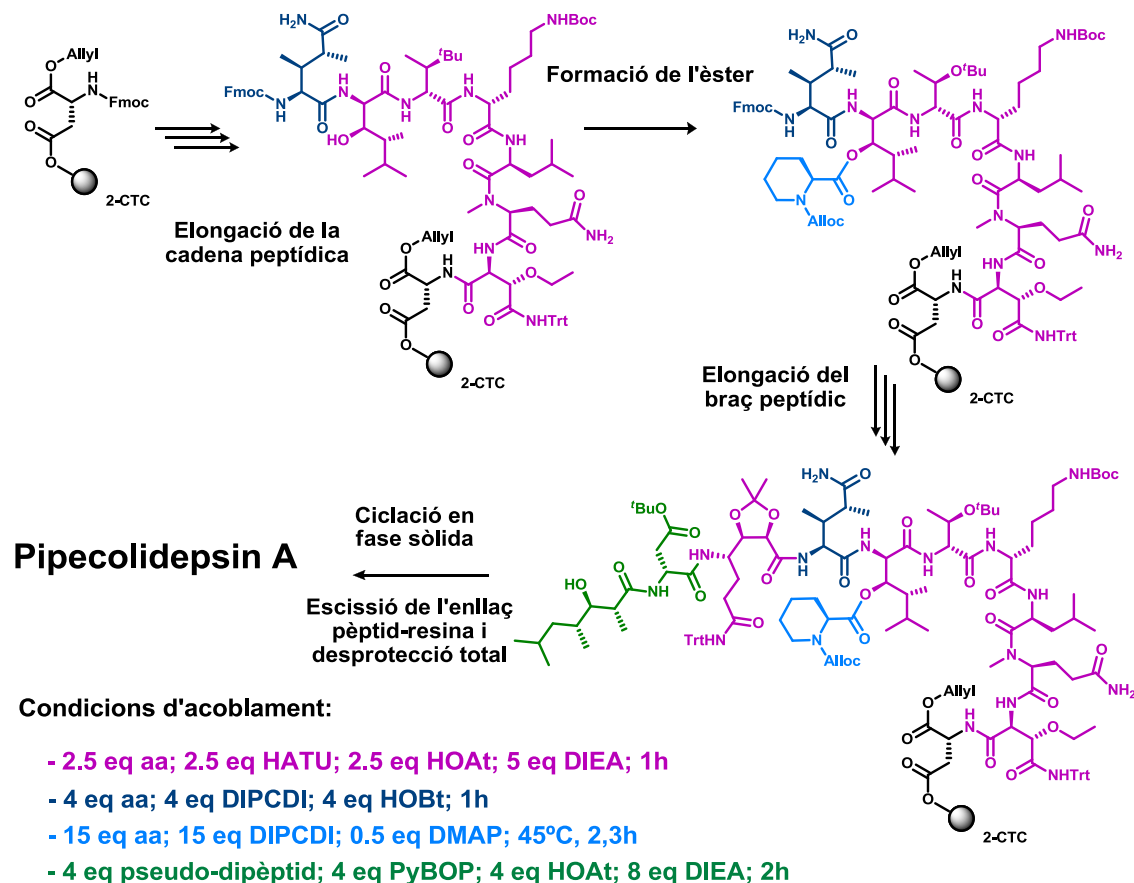
En eliminar el grup Fmoc del residu AHDMHA, va tenir lloc una reacció secundària de transacilació  $N \rightarrow O$  (Esquema 39). El producte secundari es formava en una proporció 1 a 1 respecte el producte desitjat. Reduir el tractament d'eliminació del grup Fmoc, i restringir la llibertat conformacional del pèptid en creixement duent a terme primer la ciclació, no van evitar ni minimitzar la reacció secundària de transacilació. Arribats aquest punt, l'estratègia va ser completament descartada.



**Esquema 39:** Acoblament de l'aa Fmoc-diMe-Gln-OH i la reacció secundària de transacilació  $N \rightarrow O$  que té lloc de manera espontània en eliminar el grup Fmoc del residu AHDMHA.

## Segona estratègia: diMe-Gln + èster

En un segon enfocament, es va decidir acoblar primer el residu diMe-Gln, per evitar la persistent reacció de transacilació (Esquema 40).

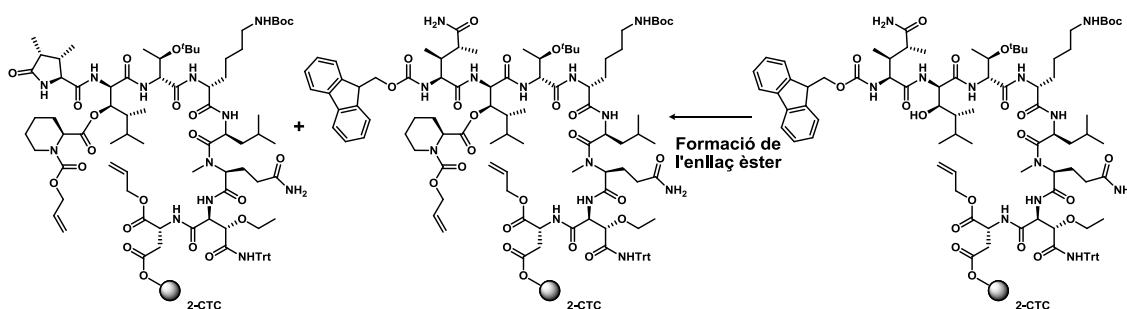


**Esquema 40:** Segona estratègia sintètica per al Pipecolidepsin A: Incorporació del residu diMe-Gln + formació de l'enllaç èster. Les condicions d'acoblament es troben indicades en colors.

L'aa Fmoc-diMe-Gln-OH es va acoblar amb conversions quantitatives i mínima deshidratació (9 %), en un únic tractament d'una hora, fent ús de les condicions neutres aa-DIPCDI-HOBt (4:4:4) en DMF, a alta concentració i sense pre-activació. Tractaments més llargs o altres sistemes d'acoblaments més potents donaven lloc a un percentatge de deshidratació excessivament alt.

L'increment d'impediment estèric al voltant del grup hidroxil del residu AHDMHA però, va convertir la formació de l'enllaç èster en l'etapa crítica d'aquesta segona estratègia. Després de provar fins a 12 condicions diferents (clorurs d'àcid, fluorurs d'àcid, MSNT, anhídrid simètric...), només es van obtenir resultats satisfactoris en aplicar temperatura elevada en

presència de DIPCDI i DMAP catalítica. No obstant les bones conversions, es tracta de condicions molt rigoroses que van afavorir l'eliminació parcial del grup Fmoc de l'intermedi sintètic. Quan l'aminoàcid diMe-Gln té el grup amino lliure, dona lloc de manera espontània i tant en condicions àcides com bàsiques, a una reacció de lactamització intramolecular, generant el derivat peptídic capat pel pirodimetilglutàmic (Figura 41). Aquest reacció secundària era tant important, que en el cru peptídic el producte desitjat i la impuresa es van detectar en una proporció de 6 a 4. L'etapa de formació de l'èster no admetia més optimització que la de reduir al mínim (2.3 h) el temps de reacció. Així doncs, per tal de minimitzar el percentatge de sub-producte obtingut, caldria jugar amb altres factors. L'eliminació del grup Fmoc del residu diMe-Gln amb un únic tractament de 3 min, i l'acoblament del  $\gamma$ -aa DADHOHA fent ús del potent sistema HATU-HOAt-DIEA amb 1 min de pre-activació, van permetre minimitzar fins a un acceptable 18% la formació de pirodimetilglutàmic.

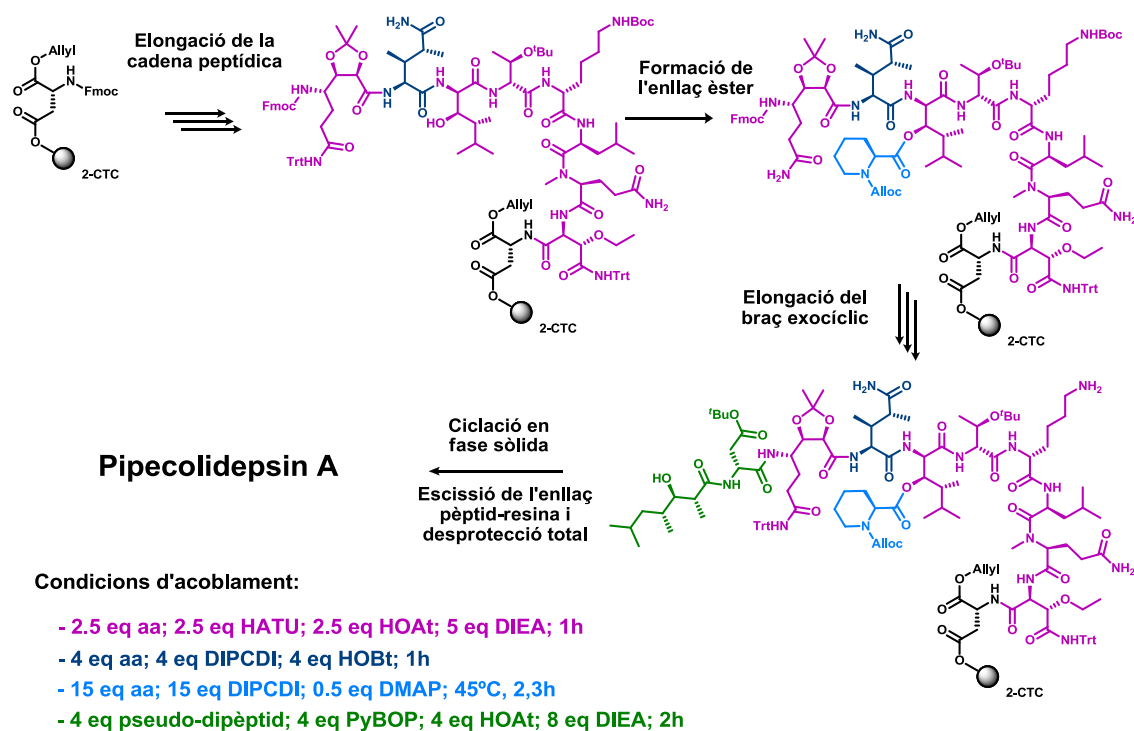


**Esquema 41:** Formació del pèptid capat pel pirodimetilglutàmic durant l'etapa de formació de l'enllaç èster. Aquesta reacció secundària també té lloc durant l'eliminació del grup Fmoc del residu diMe-Gln i durant l'acoblament de l'aa DADHOHA.

Desafortunadament, en procedir amb l'escalat de la síntesi (200 mg de resina 2-CTC), es va detectar l'escissió espontània de l'enllaç pèptid-resina durant l'etapa de formació de l'èster. Les condicions eren massa rigoroses per a la resina i es va decidir investigar una tercera estratègia sintètica. Es plantejava la formació de l'enllaç èster un cop el diol ja estava acoblat (Esquema 42). Amb aquest enfocament, el perill de formació del derivat capat pel pirodimetilglutàmic durant la formació de l'èster deixava de ser un problema.



### Tercera estratègia: DADHOHA + èster



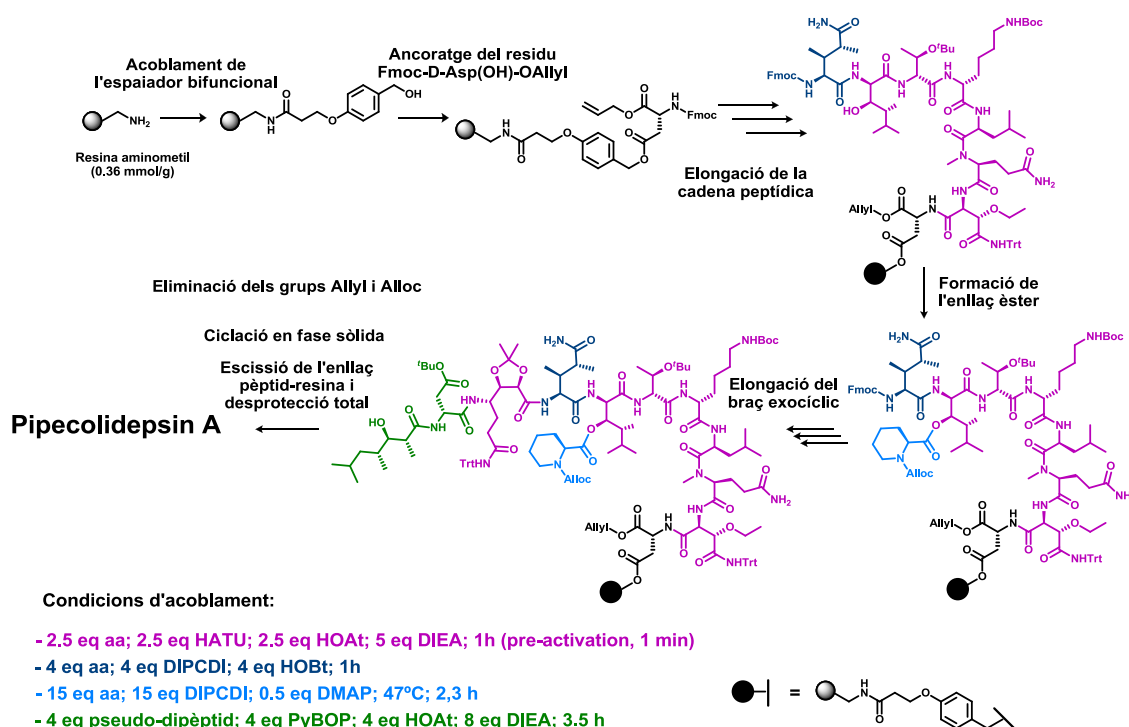
**Esquema 42:** Tercera estratègia sintètica per al Pipecolidepsin A: Incorporació del residu DADHOHA + formació de l'enllaç èster. Les condicions d'acoblament es troben indicades en colors.

La formació de l'enllaç èster no es va aconseguir sota cap condició de reacció. Temperatures extremadament elevades (75 °C) o l'ús de les microones, van mostrar-se totalment ineficaces per a superar el gran impediment estèric al voltant del grup hidroxil de l'AHDMA.

### Quarta estratègia: diMe-Gln + èster. Implementació d'un nou suport polimèric.

Després d'haver estudiat els tres entorns peptídics en els que es podia formar l'enllaç èster, i coneixent els problemes sintètics associats a cada una d'aquestes tres aproximacions, es va decidir intentar solucionar la qüestió de l'escissió de l'enllaç pèptid-resina detectat per a la segona estratègia. Així doncs, la resina 2-CTC va ser substituïda per una resina molt més resistent, la resina aminometil derivatitzada amb l'espaiador bifuncional AB (Esquema 43). Aquest canvi obligava també a modificar parcialment l'estratègia, ja que la possibilitat de realitzar la ciclació en solució quedava totalment descartada. Així doncs i per tal de facilitar

l'etapa de macrolactamització, ara obligatòriament en fase sòlida, es va triar una resina aminometil de baixa funcionalització (0.36 mmol/g).



**Esquema 43:** Quarta estratègia sintètica per al Pipecolidepsin A: Incorporació del residu diMe-Gln + formació enllaç èster. Implementació de la resina aminometil derivatitzada amb l'espaiador bifuncional AB. Les condicions d'acoblament es troben indicades en colors.

L'esquema sintètic dissenyat per a la 2-CTC es va implementar a la nova resina, i un exhaustiu monitoratge de la síntesi va permetre avaluar si les reaccions secundàries detectades i minimitzades en el suport polimèric inicial, experimentaven canvis importants. Així doncs, el seguiment efectuat mitjançant l'HPLC-PDA i l'HPLC-MS, va permetre comprovar que les reaccions no desitjades es produïen en la mateixa extensió que abans del canvi de resina. A més a més, el càlcul de la funcionalització de la resina a nivell de tripèptid, va dictaminar que no es formaven dicetopiperazines en desprotegir el grup  $\alpha$ -amino del residu *threo*- $\beta$ -EtO-Asn. Teníem via lliure per intentar de nou l'escalat de la síntesi.

Amb el nou suport polimèric, la síntesi a una escala de 150 mg de resina no va donar cap problema d'escissió espontània de l'enllaç peptíd-resina. A més a més, els percentatges dels productes secundaris van ser totalment reproduïbles a gran escala amb una única excepció. L'anàlisi per HPLC-PDA i HPLC-MS del cru peptídic, revelava l'aparició d'una nova impuresa no detectada a petita escala en cap de les dues resines emprades. La nova massa

corresponia a la deleció del residu DADHOHA. Un tractament d'eliminació del grup Fmoc del residu diMe-Gln més llarg (enlloc de 1 × 3 min, 2 × 2 min), va permetre confirmar la identitat química del producte secundari i disminuir-ne substancialment la formació.

Seguint aquesta quarta estratègia es van sintetitzar 4.2 mg de Pipecolidepsin A amb un rendiment global del 3.3%. Això va permetre la seva avaluació biològica i caracterització per RMN, i la validació de l'estratègia sintètica.

El compost Pipecolidepsin A' (veure Figura 65) també es va poder sintetitzar sense grans alteracions emprant aquest esquema sintètic. La presència en aquesta estructura d'un residu NMe-Glu en el lloc de la NMe-Gln, va comportar la desaparició de la impuresa corresponent a la deshidratació del nostre cru peptídic. A més a més, la substitució del residu D-Asp del braç exocíclic per una D-Asn, va permetre la incorporació seqüencial dels últims dos residus sense afectar significativament la puresa del cru peptídic, ja que la formació d'aspartimides no era un perill.

La co-elució per HPLC-PDA del Pipecolidepsin A sintètic i natural, així com la comparació dels desplaçaments químics de  $^1\text{H}$  i  $^{13}\text{C}$ ; i la no co-elució entre el Pipecolidepsin A' i el Pipecolidepsin A natural, això com unes majors divergències en l'assignació de  $^1\text{H}$  i  $^{13}\text{C}$ , van confirmar l'estructura química del Pipecolidepsin A natural.

A més a més, es va dur a terme l'avaluació biològica del Pipecolidepsin A natural i sintètic, de la deleció del residu DADHOHA i del Pipecolidepsin A' sintètic. Les dades obtingudes (Taula 26), permetien: verificar l'equivalència biològica entre Pipecolidepsin A sintètic i natural; establir la importància del  $\gamma$ -aminoàcid en l'activitat del depsipèptid; i concloure que, en no alterar significativament el patró d'acceptors i donadors de ponts d'hidrogen en passar de l'estructura del Pipecolidepsin A al Pipecolidepsin A', obtenim activitats citotòxiques comparables.

Pèptid		Pulmó-NSCLC A549		Colon HT29		Mama MDA-MB-231	
		µg/mL	Molar	µg/mL	Molar	µg/mL	Molar
		Pipecolidepsin A Natural	GI <sub>50</sub>	4.6E-01	2.78E-07	1.3E+00	7.85E-07
	TGI	6.9E-01	4.17E-07	1.8E+00	1.09E-06	4.0E-01	2.42E-07
	LC <sub>50</sub>	1.0E+00	6.04E-07	2.4E+00	1.45E-06	8.5E-01	5.13E-07
Pipecolidepsin A sintètic	GI <sub>50</sub>	2.3E-01	1.39E-07	6.1E-01	3.68E-07	9.0E-02	5.44E-08
	TGI	3.7E-01	2.23E-07	1.2E+00	7.25E-07	2.1E-01	1.27E-07
	LC <sub>50</sub>	6.0E-01	3.62E-07	2.0E+00	1.21E-06	4.7E-01	2.84E-07
Pipecolidepsin A' sintètic	GI <sub>50</sub>	5.1E-01	3.08E-07	9.7E-01	5.86E-07	2.3E-01	1.39E-07
	TGI	7.1E-01	4.29E-07	1.3E+00	7.85E-07	4.0E-01	2.42E-07
	LC <sub>50</sub>	1.0E+00	6.04E-07	1.7E+00	1.03E-06	7.2E-01	4.35E-07
Deleció DADHOHA	GI <sub>50</sub>	4.7E+00	3.20E-06	>1.0E+01	>6.81E-06	4.0E+00	2.73E-06
	TGI	>1.0E+01	>6.81E-06	>1.0E+01	>6.81E-06	4.1E+00	2.79E-06
	LC <sub>50</sub>	>1.0E+01	>6.81E-06	>1.0E+01	>6.81E-06	>1.0E+01	>6.81E-06

**Taula 26:** Avaluació biològica de Pipecolidepsin A natural i sintètic, Pipecolidepsin A' sintètic, i Pipecolidepsin A amb deleció del residu DADHOHA, respecte tres línies cel·lulars de càncer.

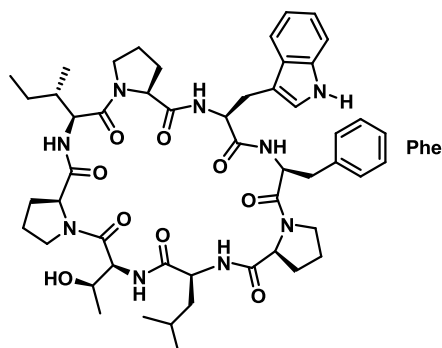
S'obté d'aquesta manera, una estratègia sintètica robusta i reproduïble que dona accés a l'agent antineoplàstic Pipecolidepsin A. Aquest compost representa un paradigma de complexitat estructural dintre dels ciclodepsipèptids "cap-cadena lateral", i conté l'enllaç èster més complicat que s'hagi descrit mai en la literatura. La seva síntesi ha resultat clau per a la validació estructural del producte natural.

A més a més, s'han desenvolupat satisfactòriament els esquemes sintètics que donen accés a dos aminoàcids no naturals altament complexos, presents en almenys un producte natural d'interès terapèutic. Altres derivats podrien ser sintetitzats seguint la mateixa estratègia.

La present tesi obre les portes a la síntesi de molts altres depsipèptids "cap-cadena lateral" que han mostrat unes activitats biològiques molt prometedores, i una complexitat sintètica i estructural comparable al Pipecolidepsin A, i permet l'avaluació *in vivo* d'aquest últim.

Durant la present tesi, es va aconseguir sintetitzar un segon producte natural, també d'origen marí i també citotòxic, anomenat Phakellistatin 19 (Figura 68). Es tracta d'un cicloctapèptid homodètic ric en residus Pro, pertanyent a una família de pèptids amb un comportament biològic peculiar. Malgrat la provada equivalència química i, sovint, espectral dels Phakellistatins sintètics respecte als seus homòlegs naturals, l'activitat biològica no s'aconsegueix reproduir per a la majoria dels membres d'aquesta família. En la literatura es troben dues hipòtesis recurrents: la presència en les mostres naturals d'una impuresa

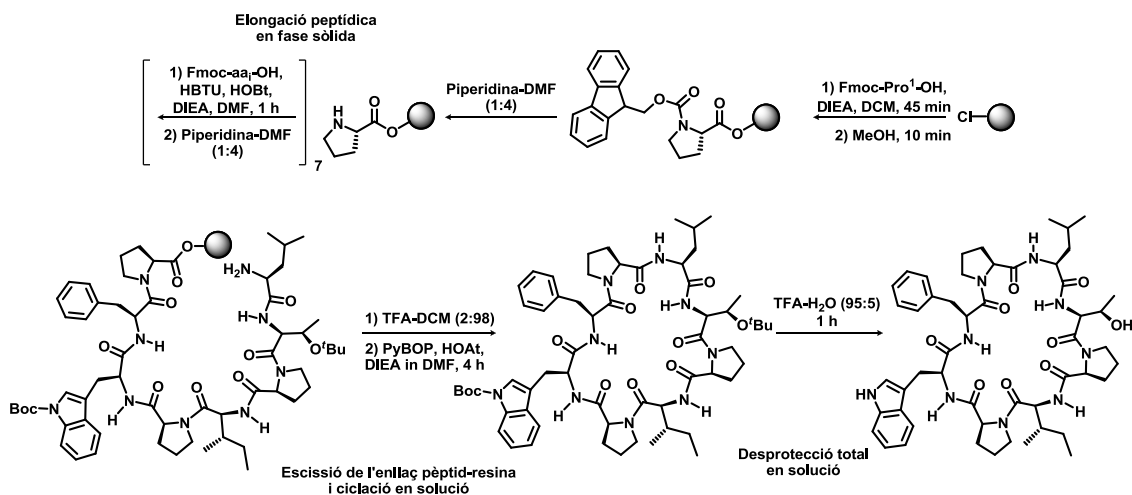
altament citotòxica que seria responsable de l'activitat; o una qüestió de diferències conformacionals, degudes sobretot a la presència de molts residus prolina capaços d'un equilibri real entre els isòmers *cis* i *trans*, en una estructura cíclica relativament poc flexible.



Phakellistatin 19

Figura 68: Estructura química del Phakellistatin 19.

Es va desenvolupar una estratègia de síntesi que combinava química en fase sòlida i en solució (Esquema 44). Seguint aquest esquema es va sintetitzar un Phakellistatin 19 sintètic equivalent al natural químicament (co-elució per HPLC correcte) i espectral (comparació de desplaçaments químics de  $^1\text{H}$  en MeOD correcte), però sense equivalència biològica.



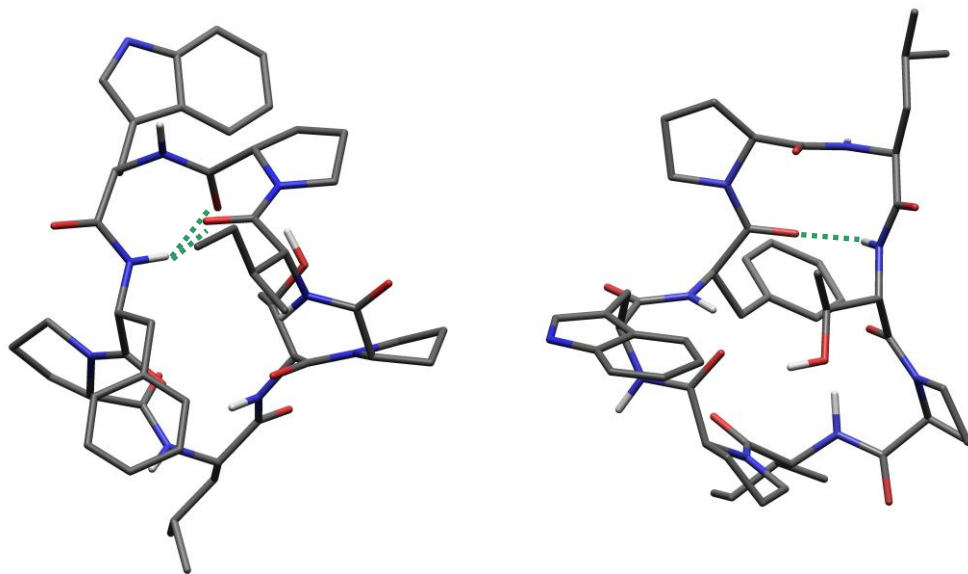
Esquema 44: Estratègia sintètica per al Phakellistatin 19. El punt de ciclació és l'enllaç Leu-Pro<sup>1</sup>.

Arribats a aquest punt, es van proposar 4 hipòtesis que intentaven explicar aquesta incongruència biològica:

- A) Les preparacions de Phakellistatin 19 natural podrien contenir una impuresa, en concret un epímer, que seria la responsable de l'activitat biològica.
- B) La presència de molts residus prolina en un cicle restringit, dóna lloc a un complex equilibri conformacional. Les diferents conformacions tindrien perfils terapèutics diferents.
- C) La contaminació prèviament esmentada correspondria a un compost d'estructura química completament diferent al Phakellistatin 19.
- D) Els Phakellistatins *i*, en concret, el Phakellistatin 19, serien ciclopèptids amb propietats quelants. L'absència de cations metàl·lics en les mostres sintètiques explicarien les discrepàncies en l'activitat biològica.

Finalment, vam decidir centrar els nostres esforços en discutir les hipòtesis A i B.

Abans de verificar o descartar alguna de les premisses anteriors, vam dur a terme un exhaustiu estudi estructural del Phakellistatin 19 emprant la tècnica de RMN. El pèptid es va assignar per complet ( $^1\text{H}$  i  $^{13}\text{C}$ ) en  $\text{DMSO-}d_6$ . Els desplaçaments químics dels  $\text{C}_\beta$  i  $\text{C}_\gamma$  de les tres prolines, així com el patró de pics de correlació del ROESY, van permetre establir la geometria *trans* per als tres residus Pro. A més a més, es va realitzar un estudi de RMN amb temperatura variable (VT-NMR), per tal d'analitzar el patró de ponts d'hidrogen del pèptid. L'existència de dos ponts en els que participaven el protó amida dels residus Phe i Thr, va quedar de manifest. Aquesta informació, juntament amb les distàncies interprotòniques extrems dels pics de correlació de l'experiment ROESY (apropiadament corregides), es van emprar com a restriccions experimentals en un protocol de *restricted-SA* per tal d'obtenir una conformació d'energia minimitzada per al Phakellistatin 19 (Figura 69). L'anàlisi d'aquesta conformació, i la verificació de dades experimentals (distàncies i angles), van permetre proposar l'existència de dos girs: un gir  $\beta$  que involucrava els residus  $\text{Pro}^1$  i Leu a les posicions  $i+1$  i  $i+2$ , i un gir  $\gamma$  en el que participaven els residus Phe, Trp i  $\text{Pro}^4$  en les posicions,  $i$ ,  $i+1$ , i  $i+2$  respectivament.



**Figura 69:** Estructura d'energia minimitzada calculada per al Phakellistatin 19 després d'aplicar un protocol de SA amb restriccions experimentals. Els dos punts d'H detectats s'indiquen en verd.

Per tal de comprovar que cap epímer era responsable de l'activitat biològica mostrada pel Phakellistatin 19 natural, es van sintetitzar, seguint l'esquema sintètic prèviament establert, fins a 10 epímers diferents (Taula 27). La seva avaluació biològica va demostrar que cap d'ells era citotòxic, la qual cosa descartava completament la hipòtesi de treball A.

---

**Epímer**

---

- Ciclo-(Leu-Thr-Pro<sup>6</sup>-Ile-Pro<sup>4</sup>-Trp-Phe-**D-Pro**<sup>1</sup>)
  - Ciclo-(Leu-Thr-Pro<sup>6</sup>-Ile-Pro<sup>4</sup>-Trp-**D-Phe**-Pro<sup>1</sup>)
  - Ciclo-(Leu-Thr-Pro<sup>6</sup>-Ile-Pro<sup>4</sup>-**D-Trp**-Phe-Pro<sup>1</sup>)
  - Ciclo-(Leu-Thr-Pro<sup>6</sup>-Ile-**D-Pro**<sup>4</sup>-Trp-Phe-Pro<sup>1</sup>)
  - Ciclo-(Leu-Thr-Pro<sup>6</sup>-**D-Ile**-Pro<sup>4</sup>-Trp-Phe-Pro<sup>1</sup>)
  - Ciclo-(Leu-Thr-**D-Pro**<sup>6</sup>-Ile-Pro<sup>4</sup>-Trp-Phe-Pro<sup>1</sup>)
  - Ciclo-(Leu-**D-Thr**-Pro<sup>6</sup>-Ile-Pro<sup>4</sup>-Trp-Phe-Pro<sup>1</sup>)
  - Ciclo-(**D-Leu**-Thr-Pro<sup>6</sup>-Ile-Pro<sup>4</sup>-Trp-Phe-Pro<sup>1</sup>)
  - Ciclo-(Leu-Thr-Pro<sup>6</sup>-**allo-Ile**-Pro<sup>4</sup>-Trp-Phe-Pro<sup>1</sup>)
  - Ciclo-(Leu-**allo-Thr**-Pro<sup>6</sup>-Ile-Pro<sup>4</sup>-Trp-Phe-Pro<sup>1</sup>)
- 

**Taula 27:** Seqüència peptídica de tots els epímers sintetitzats.

A continuació, vam centrar-nos en la hipòtesis B: una qüestió conformacional seria responsable de l'estrany comportament biològic.

Canvis de dissolvent, de temperatura i de pH poden afectar l'equilibri entre els isòmers *cis* i *trans* d'un enllaç Xaa<sup>i+1</sup>-Pro<sup>i</sup>. Així doncs, es van prendre 4 mostres de Phakellistatin 19 sintètic i es va bescanviar el TFA residual per HCl. Una mostra es va deixar en MeOH, una altra en H<sub>2</sub>O a 45.4 °C, i la tercera en un tampó fosfat 200 mM a pH = 8.1 durant 8 dies. La quarta no es va sotmetre a cap altre tractament. L'avaluació biològica d'aquestes 4 mostres mostrava una activitat notable només per a la mostra tractada amb tampó fosfat. Per tal de descartar un fals positiu degut a la gran concentració de salts, es van preparar tres mostres més. Una es va tractar amb tampó fosfat 200 mM a pH 8.04 una altra vegada, una altra amb tampó fosfat 20 mM a pH = 8.10, i l'última amb tampó tris 20 mM a pH = 8.18. A més a més, en aquest nou estudi es va introduir la variable temps (Taula 28).

Tampó	Tractament	Pulmó-NSCLC	Colon	Mama
		A549 GI <sub>50</sub> (M)	HT29 GI <sub>50</sub> (M)	MDA-MB-231 GI <sub>50</sub> (M)
Fosfat 200 mM, pH = 8.04	Blanc	3.68 E-06	1.89 E-06	2.52 E-06
	2 h	4.10 E-07	2.52 E-07	2.42 E-07
	8 d	2.31 E-08	1.47 E-08	1.47 E-08
Fosfat 20 mM, pH = 8.10	Blanc	n.d.	n.d.	n.d.
	1 d	3.78 E-07	1.26 E-07	4.37 E-07
	2 d	n.d.	n.d.	n.d.
	5.5 d	1.89 E-06	9.66 E-07	2.84 E-06
Tris 20 mM, pH = 8.18	Blanc	n.d.	n.d.	n.d.
	2 h	n.d.	n.d.	n.d.
	2 d	n.d.	n.d.	n.d.
	4 d	n.d.	n.d.	n.d.

**Taula 28:** Valors de GI<sub>50</sub> per a tres mostres de Phakellistatin 19 pre-tractades.

Els resultats obtinguts són difícils d'interpretar. El comportament respecte la variable temps és completament incoherent. A més a més, hi ha un canvi dràstic de comportament quan canviem el tampó fosfat per un tampó tris.

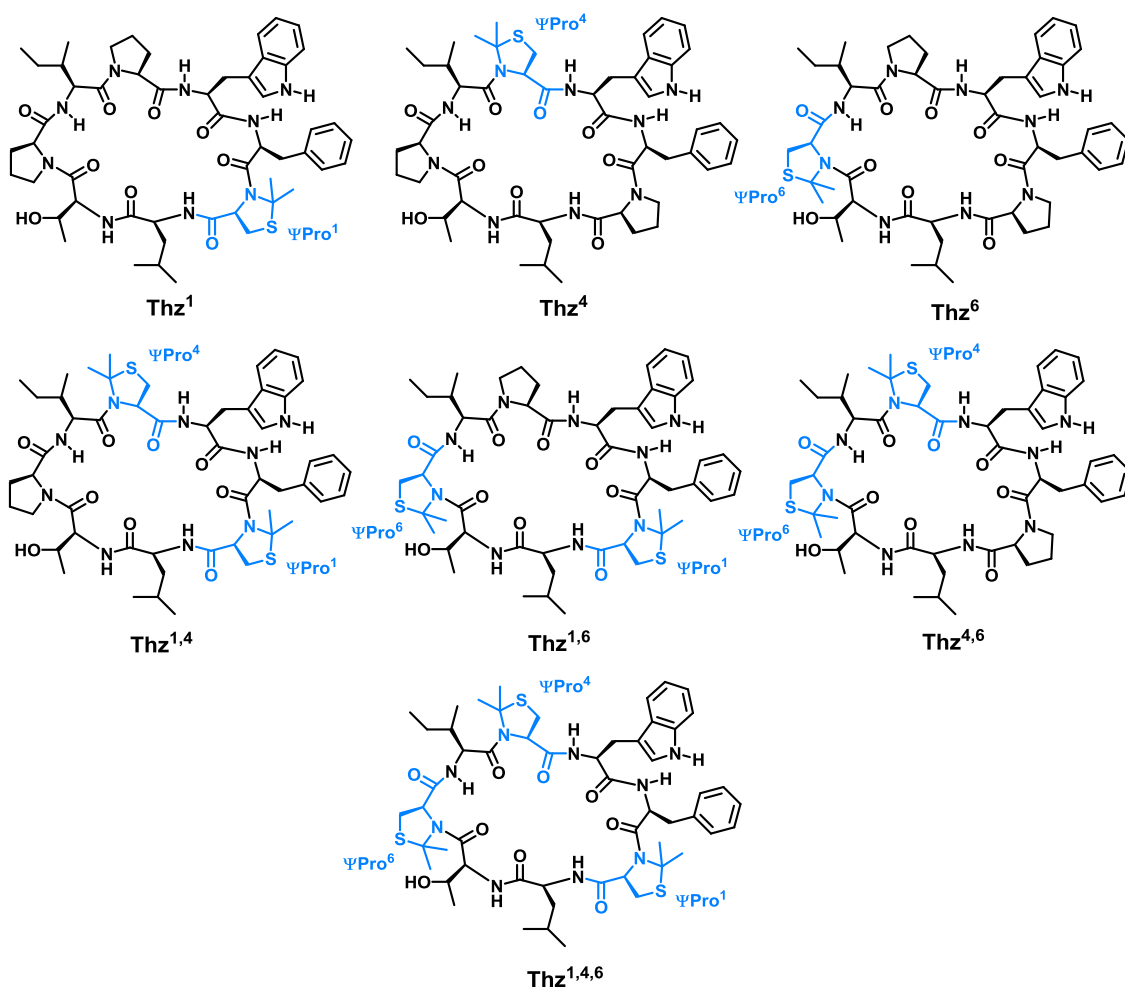
Com la hipòtesi de partida considera que diferent isomeria *cis/trans* de les Pro podria ser la responsable de les diferències en els resultats de citotoxicitat, es va decidir mirar per RMN si la geometria de les prolines podia modificar-se amb un tractament àcid o bàsic, i així intentar comprendre els resultats biològics obtinguts.

El Phakellistatin 19 és un pèptid extremadament apolar, però l'estudi estructural calia fer-lo en medi aquòs. Així doncs, vam decidir reemplaçar el residu Leu per una Orn. La



comparació dels desplaçaments químics de  $^1\text{H}$  en  $\text{DMSO-}d_6$  entre el Phakellistatin 19 sintètic i l'anàleg amb l'Orn, demostrava la validesa d'emprar aquest anàleg com a model en el nostre estudi estructural. D'aquesta manera, vam poder registrar els espectres en  $\text{H}_2\text{O-D}_2\text{O}$  (9:1) a  $\text{pH} = 8.12$  i  $\text{pH} = 5.95$  de l'anàleg soluble en aigua, per trobar que, en qualsevol cas, totes les prolines sempre eren *trans*. Aquesta constatació descarta la hipòtesi inicial. Petites diferències conformacionals queden fora de l'abast de l'estudi. La possibilitat que els cations sodi o els anions fosfats tinguin una responsabilitat més directa en l'activitat del Phakellistatin 19 queda com a possibilitat oberta.

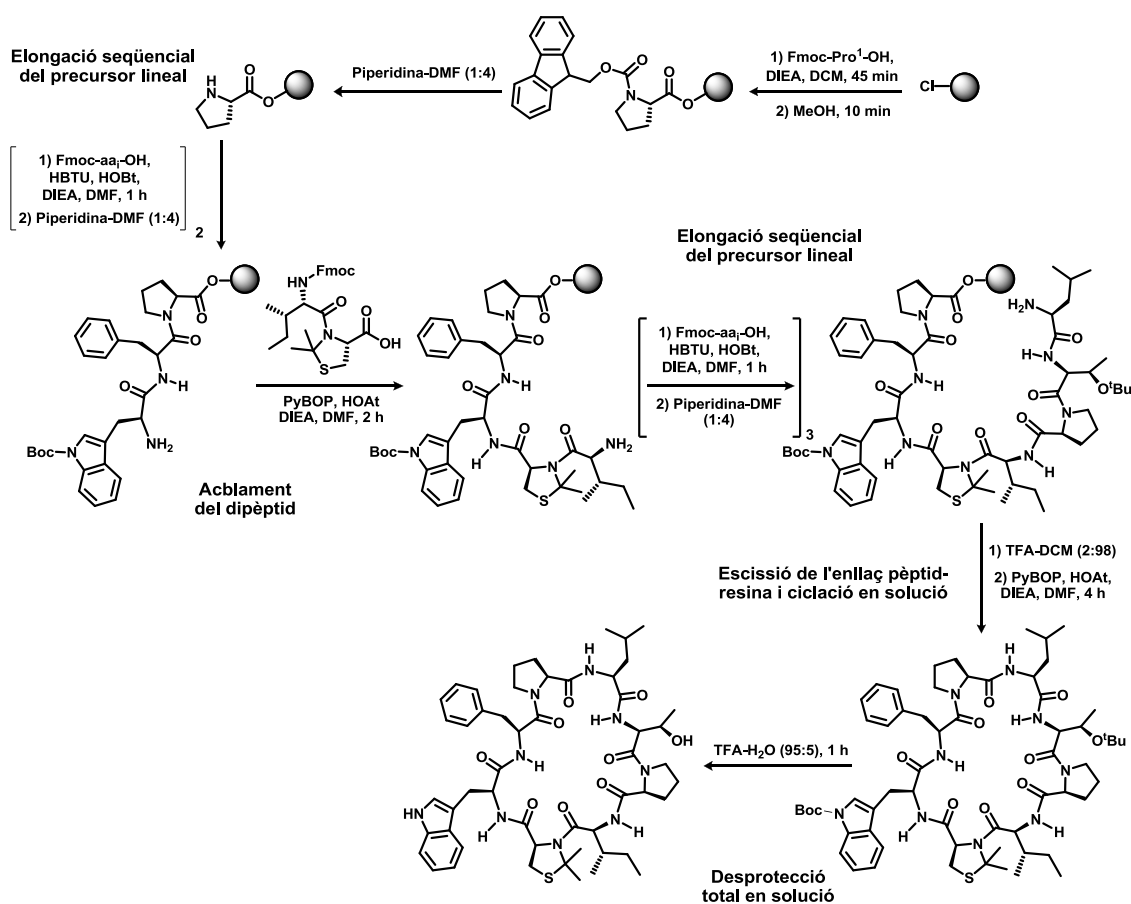
En aquest punt vam decidir que la modificació química de les Pro per tal de forçar la isomeria *cis* ens donaria molta informació. Amb aquest objectiu, es va dissenyar una petita llibreria de 7 pèptids (Figura 70), en la que les Pro eren reemplaçades per residus  $\Psi^{\text{Me,Me}}\text{Pro}$  cobrint totes les possibilitats.



**Figura 70:** Estructura química dels  $\Psi^{\text{Me,Me}}\text{Pro}$ -anàlegs del Phakellistatin 19. Els residus  $\Psi^{\text{Me,Me}}\text{Pro}$  estan indicats en blau.

L'estratègia sintètica desenvolupada per al Phakellistatin 19 no va resultar adequada per a sintetitzar aquests anàlegs. El gran impediment estèric de la  $\Psi^{\text{Me,Me}}\text{Pro}$  feia infructuós l'acoblament en fase sòlida del següent aa en qualsevol de les condicions provades (clorurs d'àcid, fluorurs d'àcid, HATU-HOAt-DIEA, PyBOP-HOAt-DIEA, COMU-Oxyma-DIEA, MW....). Així doncs, per a obtenir la llibreria dissenyada, va caldre primer sintetitzar els dipèptids en solució, i després acoblar-los en fase sòlida (Esquema 45).

Els resultats obtinguts en l'avaluació biològica de la petita llibreria es mostren a la Taula 29.



**Esquema 45:** Estratègia sintètica de l'anàleg Thz<sup>4</sup>.

Anàleg		Pulmó-NSCLC (A549)		Colon (HT29)		Mama (MDA-MB-231)	
		µg/mL	Molar	µg/mL	Molar	µg/mL	Molar
Thz <sup>1</sup>	GI <sub>50</sub>	>1.0E+01	>1.00E-05	5.7E+00	5.71E-06	6.1E+00	6.11E-06
	TGI	>1.0E+01	>1.00E-05	>1.0E+01	>1.00E-05	>1.0E+01	>1.00E-05
	LC <sub>50</sub>	>1.0E+01	>1.00E-05	>1.0E+01	>1.00E-05	>1.0E+01	>1.00E-05
Thz <sup>4</sup>	GI <sub>50</sub>	>1.0E+01	>1.00E-05	>1.0E+01	>1.00E-05	>1.0E+01	>1.00E-05
	TGI	>1.0E+01	>1.00E-05	>1.0E+01	>1.00E-05	>1.0E+01	>1.00E-05
	LC <sub>50</sub>	>1.0E+01	>1.00E-05	>1.0E+01	>1.00E-05	>1.0E+01	>1.00E-05
Thz <sup>6</sup>	GI <sub>50</sub>	>1.0E+01	>1.00E-05	4.0E+00	4.01E-06	2.7E+00	2.70E-06
	TGI	>1.0E+01	>1.00E-05	4.2E+00	4.21E-06	4.1E+00	4.11E-06
	LC <sub>50</sub>	>1.0E+01	>1.00E-05	4.6E+00	4.61E-06	6.0E+00	6.01E-06
Thz <sup>1,4</sup>	GI <sub>50</sub>	>1.0E+01	>9.58E-06	3.3E+00	3.16E-06	5.9E+00	5.65E-06
	TGI	>1.0E+01	>9.58E-06	6.9E+00	6.61E-06	>1.0E+01	>9.58E-06
	LC <sub>50</sub>	>1.0E+01	>9.58E-06	>1.0E+01	>9.58E-06	>1.0E+01	>9.58E-06
Thz <sup>1,6</sup>	GI <sub>50</sub>	3.6E+00	3.45E-06	1.9E+00	1.82E-06	1.8E+00	1.72E-06
	TGI	8.2E+00	7.85E-06	2.3E+00	2.20E-06	2.1E+00	2.01E-06
	LC <sub>50</sub>	>1.0E+01	>9.58E-06	2.8E+00	2.68E-06	2.4E+00	2.30E-06
Thz <sup>4,6</sup>	GI <sub>50</sub>	3.8E+00	3.64E-06	1.9E+00	1.82E-06	2.3E+00	2.20E-06
	TGI	>1.0E+01	>9.58E-06	2.2E+00	2.11E-06	3.5E+00	3.35E-06
	LC <sub>50</sub>	>1.0E+01	>9.58E-06	2.5E+00	2.39E-06	5.3E+00	5.08E-06
Thz <sup>1,4,6</sup>	GI <sub>50</sub>	1.6E+00	1.47E-06	1.5E+00	1.38E-06	1.8E+00	1.65E-06
	TGI	1.8E+00	1.65E-06	1.9E+00	1.74E-06	2.1E+00	1.93E-06
	LC <sub>50</sub>	2.0E+00	1.83E-06	2.3E+00	2.11E-06	2.4E+00	2.20E-06

**Taula 29:** Resultats de l'activitat citotòxica de la llibreria de  $\Psi^{\text{Me,Me}}$ Pro-anàlegs del Phakellistatin 19.

A més a més, els anàlegs Thz<sup>6</sup>, Thz<sup>1,4</sup>, Thz<sup>1,6</sup> i Thz<sup>1,4,6</sup> van ser estudiats per RMN emprant CD<sub>3</sub>OH com a dissolvent. L'anàleg Thz<sup>6</sup> presentava gran quantitat de confòrmers i la seva assignació va resultar impossible. L'anàleg Thz<sup>1,4</sup> presentava dos confòrmers majoritaris en una proporció 58:42, en els que la Pro<sup>6</sup> era *cis* o *trans* respectivament. Els dos residus  $\Psi^{\text{Me,Me}}$ Pro adoptaven sempre la isomeria *cis*. Es va poder realitzar l'assignació completa de <sup>1</sup>H dels dos confòrmers. L'anàleg Thz<sup>1,6</sup> també mostrava dos confòrmers en aquestes condicions, un amb l'enllaç Ile-Pro<sup>4</sup> en *cis*, i l'altre en *trans*. L'assignació de <sup>1</sup>H dels 16 aa es va aconseguir, però no se sap si pertanyien a un o a l'altre confòrmer. Per últim, la Thz<sup>1,4,6</sup> presentava un únic confòrmer majoritari (89 %) en el que totes les  $\Psi^{\text{Me,Me}}$ Pro adoptaven la isomeria *cis*.

Tota aquesta informació estructural i biològica, ens va permetre concloure que la isomeria *cis* o *trans* dels enllaços en els que es veuen involucrades les Pro i les  $\Psi^{\text{Me,Me}}$ Pro, i que determinen l'estructura dels pèptids, representen un factor clau en la seva l'activitat. La Pro<sup>6</sup> té un paper crucial pel que respecta a la citotoxicitat. Creiem que és més una qüestió d'importància estructural, i no tant que en substituir-la per un aa molt més voluminós i amb diferent patró d'acceptors/donadors de ponts d'hidrogen, la interacció amb la diana corresponent sigui més efectiva. De ser així, la introducció de més residus  $\Psi^{\text{Me,Me}}$ Pro no hauria de representar un increment d'activitat tan notable. La rigidesa del pèptid augmenta en

---

incrementar el número de residus Pro substituïts per  $\Psi^{\text{Me,Me}}\text{Pro}$ . Aquest augment de rigidesa va acompanyat d'un augment d'activitat citotòxica. El pèptid més actiu és el més restringit conformacionalment i el que té totes les  $\Psi^{\text{Me,Me}}\text{Pro}$  en *cis*. Aquestes observacions experimentals donen pes a la hipòtesi que hi ha una qüestió estructural al darrera de les incoherències biològiques observades entre Phakellistatins sintètics i naturals.

